University of Wollongong Thesis Collection 1954-2016

University of Wollongong Thesis Collections

2015

Diversity oriented synthesis of fused heterocycles from the cascade reactions of indigo with allylic and propargylic systems

Alireza Shakoori
University of Wollongong

Follow this and additional works at: https://ro.uow.edu.au/theses

Recommended Citation

Diversity Oriented Synthesis of Fused Heterocycles from the Cascade Reactions of Indigo with Allylic and Propargylic Systems

A thesis submitted in fulfilment of the requirements for the award of the degree of

DOCTOR OF PHILOSOPHY

From

University of Wollongong

by

Alireza Shakoori

B.Sc. Chem., M.Sc. Org. Chem.

Supervisor
Prof. Paul A. Keller

SCHOOL OF CHEMISTRY

June 2015

i

Certification

I, Alireza Shakoori, declare that this thesis, submitted in fulfilment of the requirements for the award of Doctor of Philosophy, in the Department of Chemistry, University of Wollongong, is wholly my own work unless otherwise referenced or acknowledged. The document has not been submitted for qualifications at any other academic institution.

This thesis contains the content of the two publications which I had contributed greater than 50% of their content and I am the primary author. These publications have been peer-reviewed and accepted for publication. These publications are primary and report on original research that I conducted during my enrolment.

The biological testing was conducted by Rachada Haritakun at the National Center for Genetic Engineering and Biotechnology (BIOTEC), 113 Phaholyothin Road, Klong 1, Klong Luang in Pathumthani 12120, Thailand.

The entire X-ray crystallography analysis was performed by Dr. Anthony C. Willis at Australian National University Canberra, ACT, Australia.

Alireza Shakoori

June 2015

Citation for the publications

Shakoori, A.; Bremner, J. B.; Willis, A. C.; Haritakun, R.; Keller, P. A., *J. Org. Chem.* **2013,** 78, 7639-7647.

Shakoori, A.; Bremner, J. B.; Abdel-Hamid, M. K.; Willis, A. C.; Haritakun, R.; Keller, P. A., *Beilstein J. Org. Chem.* **2015,** 11, 481–492.

Table of Contents

Acknowledgements

First, I would like to thank my supervisor Prof. Paul A. Keller for his ongoing support and trust throughout this project and for giving me the opportunity to do this work in his research group. I would like to thank Prof. John B. Bremner, for all the input he gave, the brilliant ideas, mechanistic suggestions and knowledge he provided. Also I would like to thank Dr. Chris Hyland for his great suggestions and specially the opportunity of exploring the Gold-catalysed hydroamination.

Many thanks go to the staff for their support and expertise provided to me during the time I was here, especially to Ellen Manning for being always helpful and giving me the opportunity of being a member of the School of Chemistry's safety committee, to Louisa Willdin for her efforts of coordinating the administrative tasks, and also delivering the good news of wining the awards, to Dr. John Korth who introduced me to the MS (ESI) and MS (EI) spectrometers, to Ben Cummings, who solved all the mass spectrometer related problems, to Karin Maxwell who measured numerous HRMS samples for me and to Dr. David Marshal for his input about the special techniques involved with mass spectroscopy. Special thanks go to Dr. Wilford Lie for his help with NMR processing, for solving various occurring NMR problems and for the teaching opportunities he gave me, Peter Sara and Steve Cooper for maintaining the instruments and the equipment in our Lab and School.

Furthermore, I would like to express my very great appreciation to Dr. Tony Willis for solving the X-ray crystallographic structures of the key compounds within this work.

I am also grateful to Dr. Glennys O'Brien, Assoc. Prof. Michael Kelso, Dr. Simon Beford and Prof. Stephen Pyne who provided all the teaching opportunities, to Roza Dimeska, who was there for help all the time, to Roger Kanitz who helped to adapt myself with the teaching lab environment and it was a pleasure to have his company, to Dr. Steve Wales, for providing advice on chemistry and being a good role model, to Nicholas Butler for his great contribution in proof reading of the thesis and more importantly continuing the indigo's adventure.

Abstract

Diversity-oriented synthesis based on the cascade allylation chemistry of indigo, with its 2,2'-bisindolic system, has resulted in rapid access to new examples of the hydroxy-8a,13-dihydroazepino[1,2-*a*:3,4-*b*']diindol-14(8*H*)-one (**248**-**250**) skeleton in up to 51% yield. Additionally the presence of the terminal substituent on the allylic substrates provided selectivity in production of 1-allyl-5'-allyloxy-3',4'-dihydrospiroindoline-pyrido[1,2-*a*]indol-ones systems (**227**-**231**) in up to 69%, where as the absence of the substituent on the terminal position of the allylic systems resulted in production of pyridoindolo-azepino[1,2-*a*]indol-11(7*H*)-ones heterocycles (**232**-**236**) in up to 72% yield. Quantitative generation of *N*-substituted indigo provided the mechanistic insights and preliminary measures to control the outcome of the cascade reactions. The base-induced propargylation of indigo resulted in the rapid one-pot synthesis of three different classes of heterocycles. The pyrazinodiindole **264** in 14%, pyridodiindole **265** in 17% yield and benzoindolonaphthyridinone **266** in 31% yield. The compounds **265** and **266** are possess the same framework of fascaplycin and ring B homologue, respectively. Further optimisation via alteration of the leaving group of the propargylic system from bromine to mesylate resulted in synthesis of the **265** and **266** with higher yields, 28% and 52% respectively. The presence of a phenyl substituent on the terminal alkynic position of the propargyl unit resulted in formation of oxadiazocinodiindole **271** in 62%. Initial biological activity studies with these new heterocyclic derivatives indicated promising *in vitro* antiplasmodial activity as well as good anticancer activity. The chemistry described is new for the indigo moiety and cascade reactions from this readily available and cheap starting material should be more broadly applicable in the synthesis of additional new heterocyclic systems, difficult to access by other means.

xi

List of Abbreviations

^{13}C NMR	carbon nuclear magnetic resonance spectroscopy
^{1}H NMR	proton nuclear magnetic resonance spectroscopy
°C degrees	Celsius
Ac	acetate
ACN	acetonitrile
appt t	apparent triplet
APT	attached proton test (^{13}C NMR)
Ar	aryl
ArC	aromatic carbon
ArH	aromatic proton
BC	before Christ
Bn	benzyl
bs	broad singlet
δ	chemical shift (NMR)
d	doublet (NMR)
dd	doublet of doublets (NMR)
ddd	doublet of doublet of doublets (NMR)
DMF	*N,N*-dimethylformamide
DMSO	dimethylsulfoxide
EC$_{50}$	median effective concentration
e.g.	*exempli gratia* ("for example")
EI	electron impact
eq.	equivalent
ESI	electrospray ionisation
g	gram(s)
gHMBC	gradient heteronuclear multiple bond correlation
gHSQC	gradient heteronuclear single quantum coherence
h	hour(s)
H2BC	heteronuclear 2 bond correlation
HPLC	high performance liquid chromatography
HRMS	high resolution mass spectrometry
Hz	Hertz

IC_{50}	median inhibitory concentration (50%)
ID_{50}	median infective dose
IR	infrared
J	coupling constant
*K*i	inhibition constant
Lit.	literature
μ	micro
m	multiplet (NMR)
m	medium (IR)
M	molar
M^+	molecular ion
MeOH	methanol
mg	milligram
MHz	Megahertz
MIC	minimal inhibitory concentration
min	minutes
mL	millilitre(s)
mmol	millimole(s)
mol	mole(s)
Mp	melting point
MS	mass spectrometry
m/z	mass to charge ratio
2D NOESY	two dimensional nuclear Overhauser effect spectroscopy
nm	nanometre(s)
NMR	nuclear magnetic resonance
Ph	phenyl
ppm	parts per million
q	quartet (NMR)
ROESY	Rotating frame Overhauser effect spectroscopy
s	singlet (NMR)
s	strong (IR)
t	triplet (NMR)
THF	tetrahydrofuran
TLC	thin layer chromatography

TOCSY	total correlation spectroscopy
Ts	tosyl, toluenesulfonyl
TMS	tetramethylsilane
UV/Vis	ultraviolet/visible
w	weak (IR)

Chapter 1: Introduction

Biologically active small molecules represent the basis for chemical biology applications in which they are used as chemical tools to probe biological processes.[1] As an example, the isolation of morphine, and its confirmed biological activity as the key component of opium, attracted the attention of chemists to the synthesis of analogous small molecules with modified biological activity. Drug discovery in its conventional form was based mainly on trial and error, as the principles of drug action were not known.[1] It was only during the second half of the 20th century that the evolution of structural biology and a better understanding of drug-protein interactions delivered a concept of advanced drug discovery.[1]

1.1   Concepts for small molecule synthesis

To define the characteristics and specification of compounds to be synthesized and employed in biochemical or biological screenings is one of the fundamental concerns of chemical biology. Chemical biologists and medicinal chemists have been directed to the synthesis of compound collections or libraries to provide a defined set of compounds for initial screening of various targets, However, the enormous range of plausible chemical substances impedes this approach.[2] Based on calculations, up to 10^{63} different compounds with drug-like properties could exist in chemical space,[3, 4] and therefore a systematic and comprehensive synthesis of this number of compounds is not amenable.[1] In order to address this issue several approaches have been prompted to cover the extended regions of chemical space, or at least estimate the likelihood of the chemical space regions, with suitable biological activity. There are two mainstream approaches for the generation of a chemical library: i.e., biology-oriented synthesis (BIOS) and

diversity-oriented synthesis (DOS). The main concern in BIOS is the production of small molecule compounds based on biologically proved scaffolds, while in DOS the focus is about the generation of libraries of structurally diverse and complex architectures. These approaches rely on individual and specific concepts of design, however the outcome of methods is not exclusive, and identical libraries can be achieved by either of DOS or BIOS methods.[1] Produced scaffold libraries from each method undergo different screenings to evaluate their propensity as a source of biologically active small molecules.[5-7] Other approaches like fragment-based design and computational methods are well-validated and have their own applications.

1.1.1   Biology-oriented synthesis (BIOS)

The long history of natural products in drug discovery and their significant role for synthesis of drug type compounds is undeniable.[8] BIOS focuses mainly on the generation of libraries inspired by natural products compounds. Most of these libraries consist of large molecules while only a tiny portion of nature's small molecules have been disclosed and investigated. Moreover, covering the entire molecular space by organic synthesis is not accessible due to time and matter limitations.[9] Considering the minute knowledge about nature's molecular space and conserved biological function of large molecules, complementary drug discovery methods needed to cover this gap.

1.1.2   Diversity-oriented synthesis (DOS)

Traditionally the synthesis of a defined and particular complex structure involves a multistep and often lengthy, sequential synthesis. This approach was coined target-oriented synthesis (TOS).[10] The generation of compound libraries form TOS is a gradual process, and mostly delivers a series of compounds such as natural products and structurally-similar derivatives, with limited structural diversity. An alternative

perspective is the preparation of a diverse series of structurally complex compounds by facile means from simple and available precursors. This approach is termed diversity-oriented synthesis (DOS).[10] In TOS, a retrosynthetic approach of the target molecule is employed to drive the step-wise process of chemical transformations required to produce the desired compound. In contrast, DOS strategy requires a "forward synthetic plan"[11, 12] to convey simple and similar starting materials to structurally complex and diverse molecules (Figure 1).[13, 14]
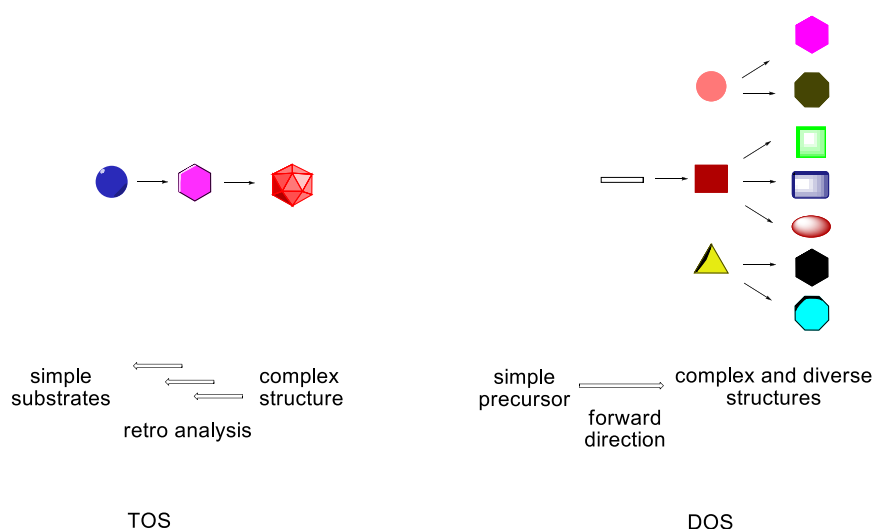
Figure 1: Comparison between TOS and DOS approaches in organic synthesis.[1]

Diversity of a library refers to the variety and differential classes of compounds present[15] and can be established by; (a) synthesis of different architectures, (b) positioning different functional groups on the skeleton of the structures and (c) generating different stereoisomers to maintain diversity of the binding pattern.[1]

To achieve the ultimate efficiency in production of these advances, the synthesis of DOS library members is best not to exceed more than three to five steps reactions.[16] There are three concurrent aims to be considered: complexity, choice of functional groups including correct positioning and three-dimensional stereochemical diversity. Retro-synthetic approaches could not be applied in the production of diverse and

various classes of compounds. A good example of a complexity-generating strategy has been introduced by Ugi in which different combinations of components, involving aldehydes, ketones or carboxylic acids, amines and isocyanides, furnish a large collection of complex structures.[17]

Cascade reactions are the most common shortcuts that can be implemented when the synthesis of complex structures is desired. The ability to design a tandem or domino sequence, in a way that yields the desired compounds with suitable functionality positioning and advanced complexity, is not an easy task and requires significantly more attention.[18] Though part of the knowledge in this field originated from serendipitous discoveries,[19] such designs, yielding novel architectures, are of particular interest for the investigation of new bioactive agents with possible new modes of action, which could be subsequently elaborated in medicinal chemistry projects.[20]

1.2   Cascade reactions

One of the current goals in organic synthesis is the controlled construction of complex molecules, in particular, through the use of cascade reaction sequences.[21, 22] The formation of multiple bonds in a one-pot system without the need to isolate the intermediates, changing conditions or adding various reagents is a suitable pathway to establish complex structures.[23] More than one reaction occurs chronologically in a one-pot process[24]- this means that the product of each sequence is the next step's starting material, resulting in multiple bond breakage with consecutive new bond formation. As a result, molecular complexity builds up quickly.[25] This can dramatically boost the efficiency of synthetic procedures by starting from cheap and ample starting materials and circumventing purification and isolation steps. Due to the application of one solvent, one separation and purification procedure during the cascade synthesis, this

platform is economical and can also be environmental friendly. In contrast, classical methods for the syntheses of complex natural products require multistep pathways, alteration of reaction conditions, multiple reagents different solvents, isolation of intermediates and purification of the isolates with the result of extensive consumption of resources and labour.[26-28] Cascade reactions have been attractive for the organic chemist ever since the formative attempt of a one-pot synthesis of tropinone **4** in 1917.[29] In the original plan, succindialdehyde, methylamine, and acetone were reacted by means of double Mannich reaction to form tropinone in one step, but the yield was too low due to the low acidity of acetone. The application of calcium acetonedicarboxylate **2**, or ethyl acetonedicarboxylate, improved the yield up to 40 % (Scheme 1).
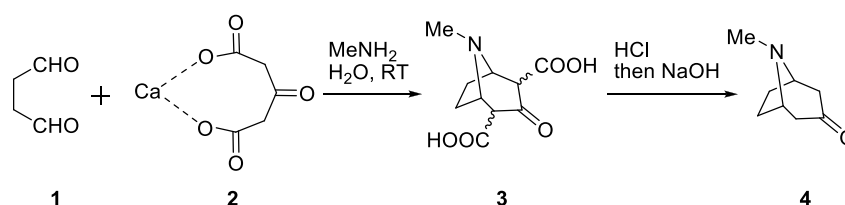
Scheme 1: Robinson's influential total synthesis of tropinone **4**.[29]

The other decisive approach in this field was the synthesis of progesterone **7** by polyolefin cyclization based on the alkyne's utility in exo cyclizations resulting in vinyl cations. The stereospecific cyclization of the trienynol **5** gives rise to intermediate **6** which in turn is readily converted into *dl*-progesterone (Scheme 2).[30]
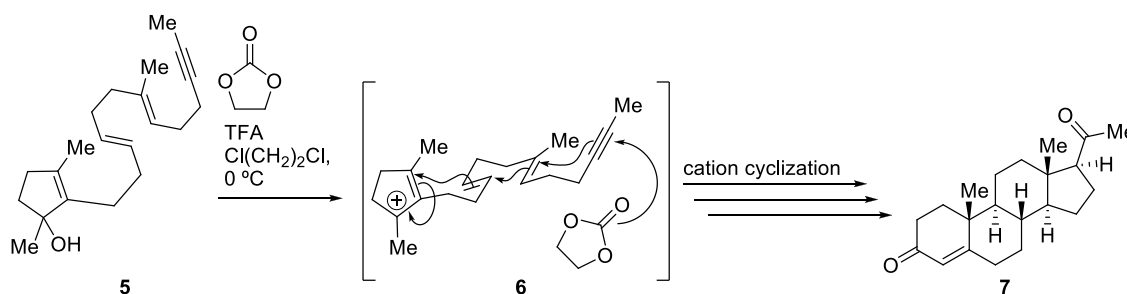
Scheme 2: Synthesis of (±)-progesterone **5** via polyolefin cyclisation cascade.

These cascade sequences were sufficiently influential to pioneer various, and well-designed tandem reactions toward the synthesis of complex structures. To date various applications and different methods of cascade reactions have been reported.[20] Implementation of cascade sequences had a significant impact on synthesis of various natural products (Figure 2).

8
(+)-harziphilone

9
tetronasin

10
(+)-rugulosin

11
alkaloid (-)-205 B

12
(+)-onocerin

13
sclerophytin A

14
bisorbibutenolide

15
trichodimerol

16
hirsutine

17
stenine

18
(-)-spinosyn

19
(-)-FR182877

20
(-)-colombiasin A

21
(+)-elisapterosin B

22
epoxyquinols A

23
(+)-frondosin B

24
(+)-mycotrienin I
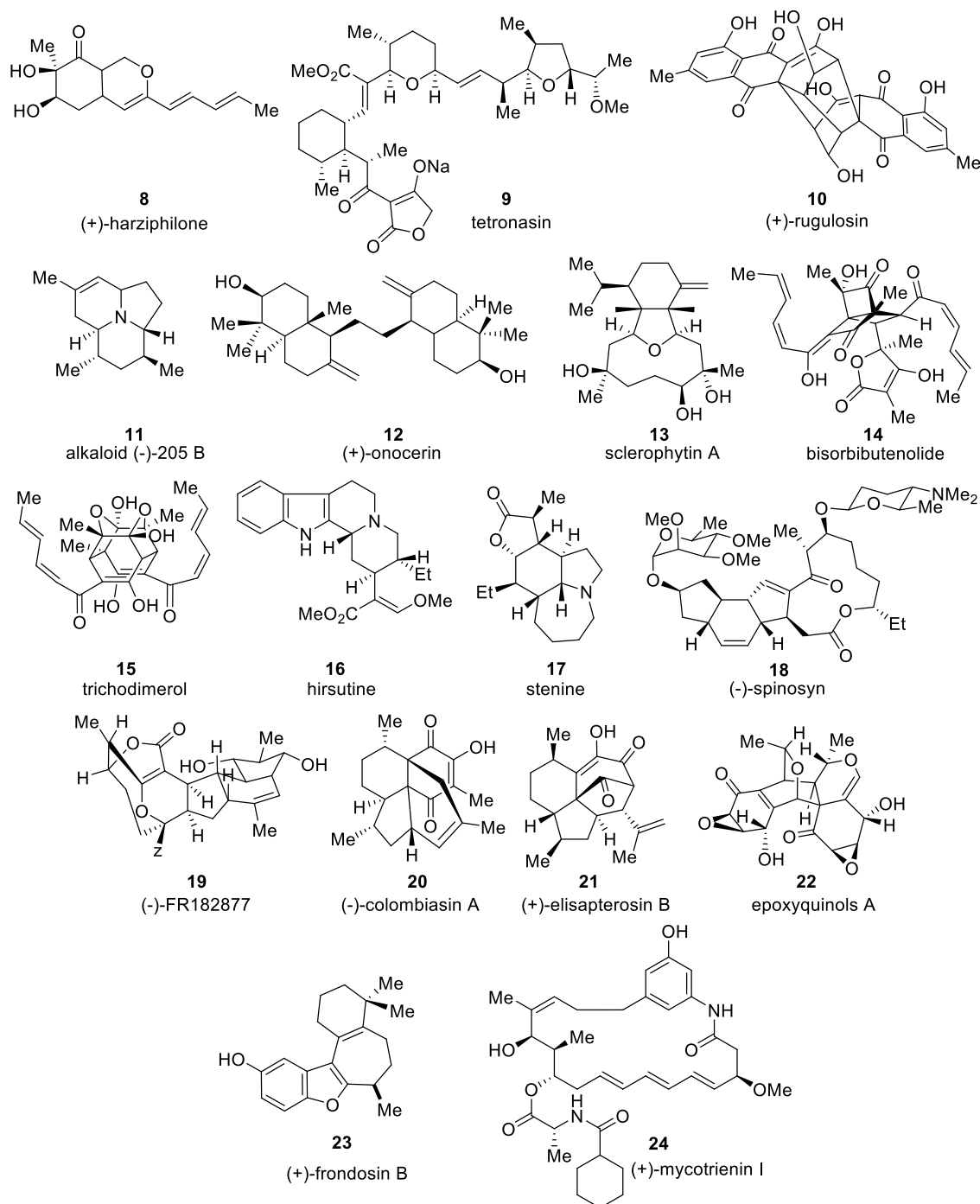
Figure 2: Examples of natural products, synthesised by different cascade reactions

These natural products have been synthesised using cascade reactions and varying key steps such as;

- Nucleophilic cyclisation in the synthesis of harziphilone **8**,[31] and tetronasin **9**.[32]

- Oxidative coupling/Michael reaction in the preparation of (+)-rugulosin **10**.[33]

- Brook rearrangement in the total synthesis of poison frog alkaloid (-)-205 B **11**.[34]

- Epoxy olefin cyclisation cascade for the synthesis of (+)-α-onocerin **12**.[35]

- Electrophilic cascade in the formation of sclerophytin A **13**, synthesis of (+)-bisorbibutenolide **14**,[36] pentacyclic trichodimerol **15**,[37] hirsutine **16**,[38] heterocyclisation of stenine **17**,[39] and total synthesis of (-)-spinosyn A **18**.[40]

- Transannular cyclisation in the production of antitumor polyketide (-)-FR182877 **19**.[41]

- Electrocylisation in the formation of (-)-colombiasin **20**,[42] and oxidative cyclisation in (+)-elisapterosin B **21** formation.[43]

- Pericyclic and Michael reaction cascades in the total synthesis of epoxyquinols A **22**.[44]

- Palladium-catalysed multicomponent coupling approach to benzo[*b*]furan structures in the synthesis of (+)-frondosin B **23**.[45]

- Stille "stitching cyclisation" cascade in the total synthesis of (+)-mycotrienin I **24**.[46]

Electrophile Induced Branching Cascade (EIBC), was introduced as a new technique to produce a variety of biologically important molecular scaffolds. The assumption was the reaction of a common precursor would proceed with scaffold building agents, (SBAs) under the action of a suitable electrophile (E$^+$). Reaction of 2-(alkynyl)benzaldehydes **25** in the presence 2-aminobenzamides **26**, 1,2-diamino benzene **27**, 2-

(aminophenyl)benzimdazoles **28**, 2-aminobenzenesulphonamide **29**, 2-(aminophenyl)imadazole **30**, 2-(aminophenyl)-dihydroquinazolinone **31**, 2-(aminophenyl)pyrrole **32**, aminophenyl indoles **33-34**, 2-aminobenzylalcohols **35** and 5-(2-aminophenyl)-tetrazole **36** as scaffold building agents (SBA) resulted in production of various derivatives of the isoquinoline architecture **37-47** (Figure 3).[47]

Figure 3: Structure of common types of starting materials **25 a-d** and SBAs **26-36**.

As shown in Fig. 4, the common starting material **25** reacted with SBAs **26-36** under certain reaction conditions.[47] Alkyne cyclisation was facilitated through the electrophilicity of the iodonium ions. The iodinated intermediate cross-couples with the nucleophiles in a straightforward manner (Figure 4).[47]

37a, R = Ph, R^1 = H, R^2 = H, R^3 = H   **37d**,R = Ph, R^1 = NHPh, R^2 = H, R^3 = H
37b,R = P h, R^1 = H, R^2 = Br, R^3 = H   **37e**,R = Ph, R^1 = NHPh, R^2 = CH$_3$, R^3 = H
37c,R = Ph, R^1 = H, R^2 = Cl, R^3 = CH$_3$ **37f**,R = 1-Cyclohexenyl, R^1 = NHPh, R^2 = H, R^3 = H

38a,R = Ph, R^1 = H   **39a**,R = Ph   **40a**,R = Ph
38b,R = 1-Cyclohexenyl, R^1 = H   **39b**,R = ^{n}Bu   **40b**,R = p-CNPh
38c,R = Ph, R^1 = F   **39c**,R = 1-Cyclohexenyl,   **40c**,R = 1-Cyclohexenyl,

41a,R = Ph   **43a**,R = Ph, R^1 = H, R^2 = H
41b,R = ^{n}Bu   **43b**,R =PhI, R^1 = H, R^2 = CH$_3$
41c,R = 1-Cyclohexenyl,   **42a**,R = Ph   **43c**,R = Ph, R^1 = H, R^2 = Cl
     42b,R = 1-Cyclohexenyl,
44a,R = Ph   **46a**,R = Ph, R^2 = H
44b,R = ^{n}Bu   **45a**,R = ^{n}Bu   **46b**,R = ^{n}Bu, R^2 = H
44c,R = 1-Cyclohexenyl,   **45b**,R = 1-Cyclohexenyl,   **46c**,R = Ph, R^2 = CH$_3$
47a,R = Ph, R^2 = H
47b,R = p-CNPh, R^2 = H

Figure 4: Series of isoquinolines synthesised by electrophilic cascade sequences under the particular reaction conditions; (a) I$_2$, DCE, rt, 3 hours (N1, N2, N4, N6), (b) I$_2$, CH$_3$CN, rt, 8 hours (N9), (c) I$_2$, K$_2$CO$_3$, CH$_3$CN, rt, 5 hours (N10), (d) I$_2$, K$_2$CO$_3$, DCE, 75 ℃, 5 hours (N8), (e) p-TSA, DCE, rt, 3 hours then K$_2$CO$_3$, I$_2$, rt, 2 hours (N7) and (f) p-TSA, DCE, rt, 6 hours then ICl, 0 ℃, 2 hours (N3, N5, N11).

One of the notable features of a cascade sequence to deliver a diversity-oriented library is an ambient common precursor that positions suitable functionalities. In this research our focus is towards the application of indigo as a cheap, readily available starting material with close functionalities positioned in a conjugated and electronically potent structure.

1.3   The chemistry of indigo

Indigo **98**, an ancient dark blue powder, has been used in dyeing cotton yarn since the 7th century B.C. Traces of this pigment were also identified in cave patterns and old paintings.[48] The original source of the pigment is the plant *Indigofera tinctoria* and related species from which indigo has been extracted through the fermentation of leaves by soaking them in alkaline solution where the structural glycoside indican in the plant hydrolyses to D-glucose and indoxyl; final exposure to air oxidizes indoxyl to indigo. Understanding the mechanism of this ancient process is of interest. In the first instance, 3-oxindole **91** in the presence of a base and suitable oxidant (e.g. PbO_2, $FeCl_3$), will result in the formation of radical **93** and subsequent dimerisation gives the biindoline **94** in high yield, which readily oxidised to indigo by exposure to air (Scheme 3).[49]

B‾= base, Oxidant= PbO_2 or $FeCl_3$
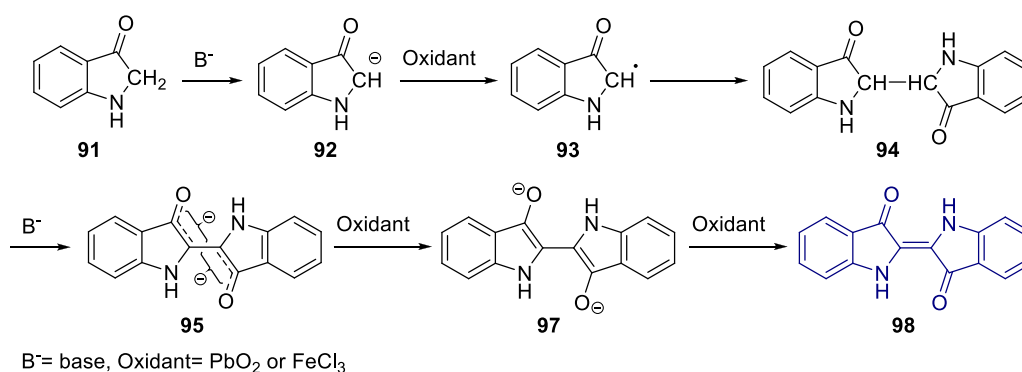
Scheme 3: Mechanism for conversion of oxindole to indigo **98**.[49]

The absorption wavelength for indigo is in the region of 420 and 450 nm of the electromagnetic spectrum, placing it between blue and violet.[50] Indigo refers to the substance which is constructed by two indoxyl unit and named as 2-(3-oxo-1,3-dihydro-2*H*-indol-2-ylidene)-1,2-dihydro-3*H*-indol-3-one or [2,2'-biindolinylidene]-3,3'-dione. It has two isomers; the *E* (*trans*) isomer **98a** is energetically stabilised due to the possibility of hydrogen bonding whereas the *Z* (*cis*) isomer **98b** is less stable as the repulsion of the lone pairs of the carbonyl groups destabilise the structure (Figure 5).[51]
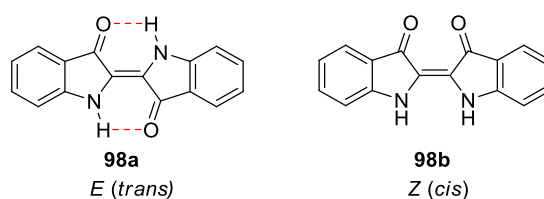
Figure 5: Indigo's two possible isomers.

Indigo is insoluble in water and organic solvents with a few exceptions including hot chloroform, DMF and DMSO.[52] The poor solubility was traced to the H-bonded network, in which each indigo molecule is surrounded by four neighbours where the NH groups are involved in bifurcated intra- and intermolecular H-bond to the O-atoms of carbonyl (Figure 6, a).[52] The blue colour of indigo arises from the extended conjugated system around the central double bond and is independent of the phenyl rings (Figure 6, b).[53] The internal hydrogen bonding between the carbonyl-amine lowers the HOMO/LUMO energy gap and their excited state; therefore it absorbs the higher wavelength of the visible spectrum. The internal hydrogen bonding of indigo is also strong as it forms two 6-membered rings that assist in the overlapping of the orbitals (Figure 6, c).[54]
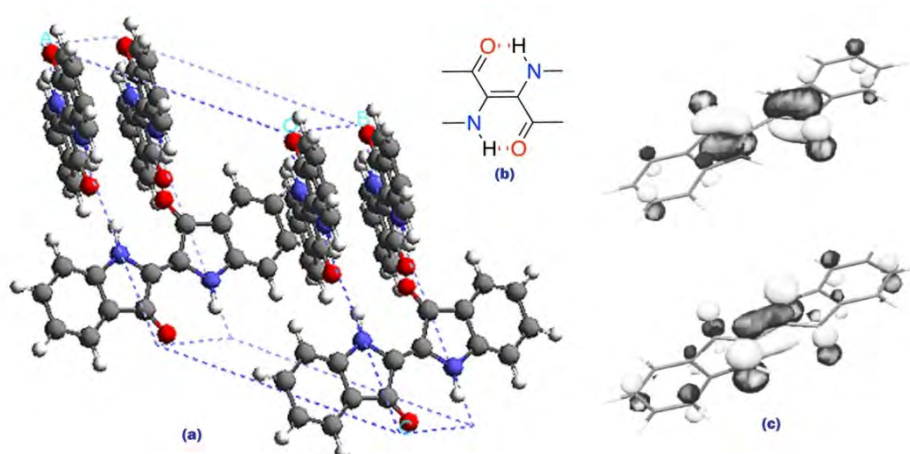
Figure 6: Crystal structure of indigo (a)[52], formation of two six-membered rings around the central double bond due to H-bond (b)[53], HOMO/LUMO orbitals of the indigo (c).[54]

Indigo dissolves in non-polar solvents with range of 10^{-5}-10^{-6} M and the colour of the solution is red to violet. In polar solvents, dissociation of the internal hydrogen bonding

between the carbonyl-amine occurs and the colour is blue.[55] The solubility issue is the instinctive obstacle of any process that involves indigo. As a cheap and available pigment, indigo has captured attention of the textile industry for many centuries and several procedures have been developed to combat the poor solubility of indigo, such as reduction of indigo in alkaline solution, which is normally carried out by treatment of the vat dye with base. More recently, modern applications utilise sodium dithionate as the reducing agent. The result is the generation of the water-soluble indigo-white (leuco indigo) that is able to be applied to textile or yarns and subsequent aerobic oxidation during the drying process restores the characteristic blue colour.

Despite the vast knowledge about dyeing processes with indigo and the significant advantage in starting with a readily available advanced precursor like indigo, its reported chemistry is very limited. The presence of an array of closely positioned functionalities and highly conjugated system make indigo a suitable starting material in synthesis of complex heterocycles carrying a 2,2'-*bis*-indolic system. Moreover, the presence of this system has been shown to be important and appears in several biologically active natural products including the fascaplysins **99-100**,[56-59] iheyamines **101**,[60] rebeccamycin **102**,[61-63] staurosporine **103**,[64] and tjipanazoles **104** (Figure 7).[65]
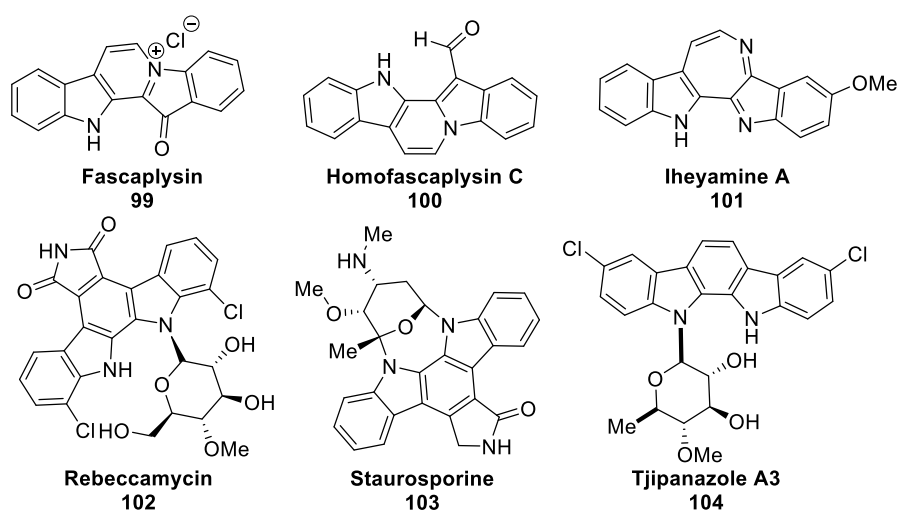
Figure 7: Biologically active natural products carrying 2,2'-*bis*-indolic system.

Tyriverdin **105**, with its high antibacterial activity,[66] and the akashins **106-108**, as potent anti-cancer glycosides,[67] are also promoting the plausible conversion of indigo to versatile and biologically active molecules (Figure 8).
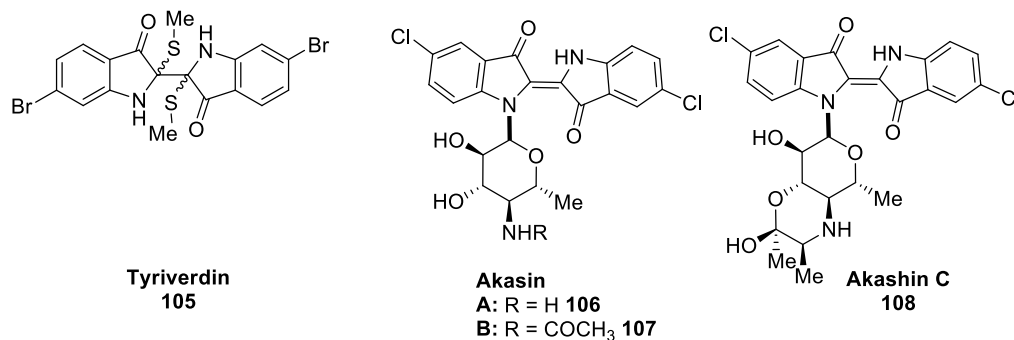
Figure 8: Structure of tyriverdin and akashin A-C.

1.3.1   The synthesis of indigo

Indigo is a unique pigment as it made the transition from natural dye to a high demand industrial pigment.[68] Its first synthetic production was carried out by Adolf von Baeyer from the chlorination of isatin **109** and subsequent acidic-reductive dimerisation.[69] He determined indigo's structure and researched alternative methods for its synthesis.[69*] As isatin was expensive and scarcely available, he developed an alternative method through the nitration of cinnamic acid to afford **113** followed by cyclisation to indoxyl and oxidation to indigo.[70] Both of the procedures failed to accomplish an economical large scale production. A Baeyer and Drewson collaboration led to a new strategy in which the aldol condensation of *o*-nitrobenzaldehyde **114** and acetone resulted in the formation of intermediate **116** followed by formation of **118** which then expelled one molecule of acetic acid after hydrolysis forming the 2-hydroxyindoxyl **119** that was readily converted to indigo (Scheme 4).[71]

---

[*] Baeyer was awarded the Nobel Prize in Chemistry 1905 in recognition of his advancement through his work on organic dyes.
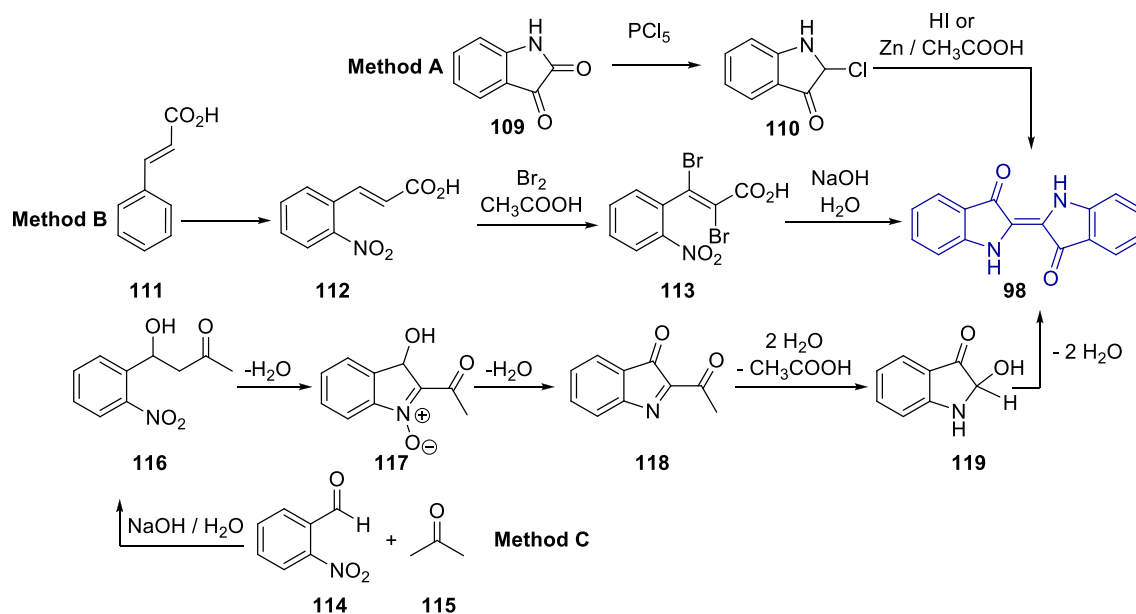
Scheme 4: Baeyer's three different methods of synthesis of indigo **98**.[69-69]

Even the procedure's yield (67%) was gratifying but it did not become an attractive means of mass production due to the expensive synthesis of **114** at that time.[71]

An alternative and also more practical route was carried out by Pfleger in which *N*-phenylglycine **120** was treated with a molten mixture of sodium hydroxide, potassium hydroxide, and sodamide to give indoxyl **121** and subsequent air oxidation formed indigo (Scheme 5).[72]
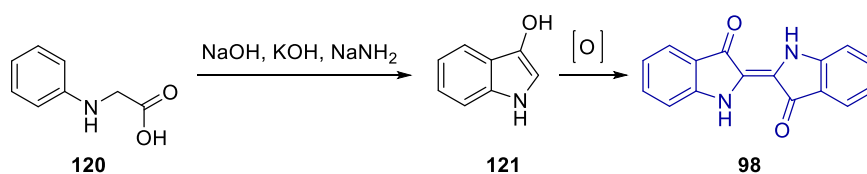
Scheme 5: Synthesis of indigo from *N*-phenylglycine.[72]

A breakthrough in the synthesis of indigo was made by Karl Heumann who oxidised *o*-toluidine **122** to form anthranilic acid **123** and subsequent treatment with chloroacetic acid formed 2-(carboxymethylamino)benzoic acid **124** which was dimerised to indigo under the action of alkaline solution.[73] The procedure was utilised by both BASF and

Hoechst fine chemicals in the production of indigo on an industrial scale. Later, Pfleger discovered that the addition of $NaNH_2$ to the alkaline solution in the last step of the synthesis can dramatically improve the yield (Scheme 6).

BASF: oxidant = Hg, H_2SO_4
Hoechst: oxidant = Cr (III)

* Pfleger modification : OH⁻ and $NaNH_2$
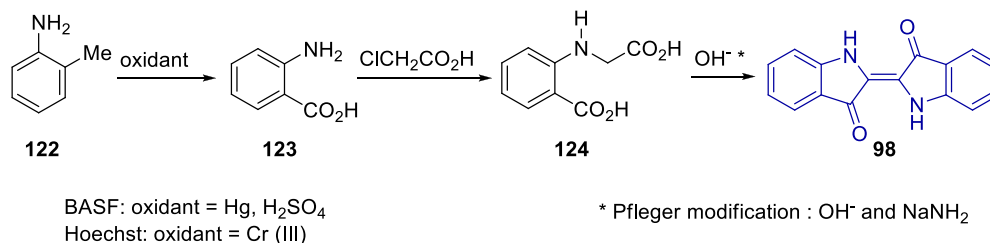
Scheme 6: Heumann method in production of indigo from *o*-toluidine.[73]

A modification by Lucius and Brunning led to invention of a more practical and economical process for synthesis of the dye. The condensation of formaldehyde and hydrogen cyanide generated the imine to react with aniline and formed the corresponding aminophenyl acetonitrile **126**. Hydrolysis of the cyano group delivered the amino acid **120** and subsequent fusion led to the formation of the indoxylate followed by oxidation to furnish indigo. This procedure is the current industrial method for the production of indigo and has been since 1925 (Scheme 7).[74]
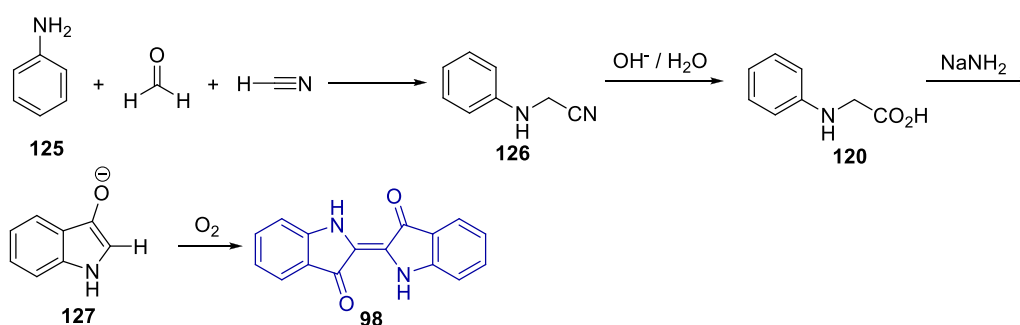
Scheme 7: Synthesis of indigo from aniline.[74]

Recently indigo was obtained from a one-pot synthesis with selective oxidation and dimerization of indole **128** by using a catalytic molybdenum hexacarbonyl complex in the presence of cumene hydroperoxide in *tert*-butyl alcohol at reflux. The procedure deposits pure indigo in high yield and in a practical manner even for large scale production (Scheme 8).[75]
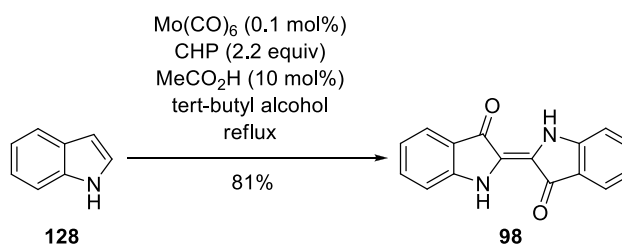
Scheme 8: Metal catalysed oxidation of indole in the synthesis of indigo.[75]

1.4 Reactions of indigo

Records of reactions in which indigo is a starting material are limited. Considerable numbers of these reactions were performed in early decades of the 20th century without access to advanced spectroscopic techniques. Elemental analysis was the only method of structural elucidation and for some of the reactions, percentage yield has not been reported. However, it is essential to review and investigate these records in order to understand its chemistry and behaviour.

1.4.1 Oxidation

The outcomes of the oxidation of indigo depend on the reaction conditions and the type of oxidant. Oxidation with strong mineral acids in the presence of water results in the cleavage of the central double bond and formation of isatin **109**. Oxidation of indigo with different oxidants such as KMnO$_4$ in anhydrous medium generates dehydroindigo **129** (Figure 9).
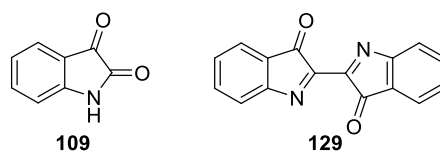
Figure 9: Structure of **109** resulted from oxidation in the presence of water and dehydroindigo produced from oxidation of indigo under anhydrous condition.

Oxidation of the indigo with nitric acid or chromic acid forms **109** as orange-red crystals. This synthesis was performed by Erdman in 1981 and is the current industrial method (Scheme 9).[76] Isatin and its derivatives play a significant role in the synthesis of

various heterocycles such as indoles, indigoids, and quinolones, and have gained recent attention in the cascade synthesis of new heterocycles. Halogenated derivatives of isatin were synthesised by treatment of indigo with bromine or chlorine water.[77]
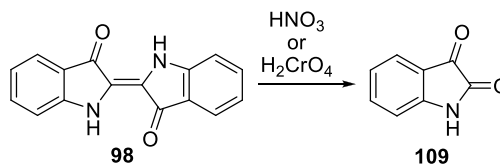
Scheme 9: Oxidative cleavage of indigo to isatin.[76]

Compound **109** also can be produced by the ozonolysis of indigo. The process starts by formation of indigo ozonide **130** and then treatment with water precipitates the product (Scheme 10).[78]
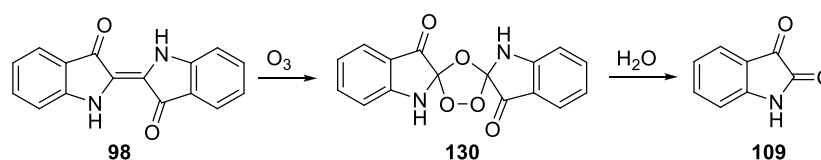
Scheme 10: Ozonolysis of indigo.[78]

Oxidation by chlorine of a suspension of indigo in carbon tetrachloride and subsequent treatment with calcium hydroxide produces dehydroindigo.[79] An alternative method uses a suspension of indigo in dry, boiling benzene oxidised under the action of lead oxide in presence calcium chloride and addition of glacial acetic acid (Scheme 11).[79]
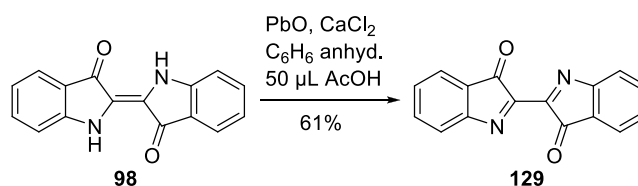
Scheme 11: Kalb's procedure in formation of dehydroindigo.[79]

Reaction of indigo in acetic acid with $KMnO_4$ at 20 °C forms the diacetylindigo **131** which is converted to dehydroindigo by elimination of acetic acid under basic conditions (Scheme 12).[79]
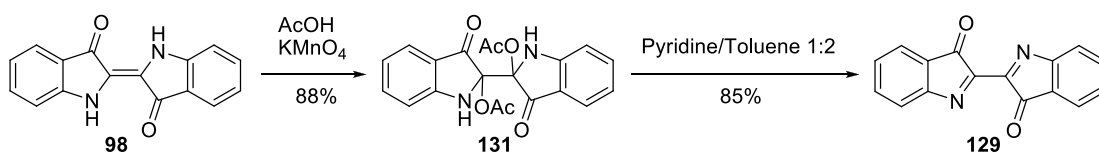
Scheme 12: Oxidative conversion of indigo to dehydroindigo in the presence of $KMnO_4$.[79]

Dehydroindigo appears as yellowish-red crystals[†][79] with increased water solubility compared to indigo. It can be readily reduced to indigo and acts as an oxidizing agent in the conversion of hydroquinone to quinone, and liberates iodine from potassium iodide.[80] Indigo oxidation proceeds analogous to the electrochemical oxidation of indigo carmine, which has been shown to result in the formation of dehydroindigo.[81]

1.4.2   Reduction of indigo

The reduction of indigo is a key feature in the textile industry, especially in the production of jeans. Indigo is reduced by mediation of various reducing agents; methods date back to 10th century Japan where indigo was heated in a culture of anaerobic bacteria. The reduction of indigo by urine, zinc dust, thiourea and arsenic trisulfate has also been recorded. Berzelius used the basic solution of iron sulphate aiming to postpone the reverse oxidation of indigo in presence of Fe^{2+} ions.[82] Treatment of indigo by sodium dithionite ($Na_2S_2O_4$) is the most common method of production of leucoindigo (indigo white), which has been used mostly in the textile industry (Scheme 13).[83] A considerable disadvantage for sodium dithionite is not being recyclable and washing the dyeing bath consumes huge quantities of water and also contaminates water sources.
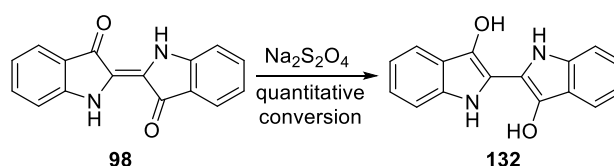
Scheme 13: Reduction of indigo under alkaline condition to leuco indigo.[83]

[†] A purple solid was obtained after recrystallization from benzene.

Leucoindigo has also been obtained from the electrochemical reduction of a 5×10^{-5} M solution of indigo in water while the supporting electrolyte was a mixture of KNO_3 and NaOH 0.7 M and 10^{-2} M respectively. The system is based on a three-electrode system by using Ag | AgCl || 3 M KCl as the reference electrode (green), platinum as auxiliary (blue) and dropping mercury as the working electrode (red) (Figure 10).[84] In an alternative experiment, immobilized microcrystals of indigo on pyrolytic graphite were reduced to leucoindigo in a buffer solution containing NH_4^+ or Na^+ in an Oxford electrodes potentiostat with agency of a thin, gold mini-grid electrode.[85]
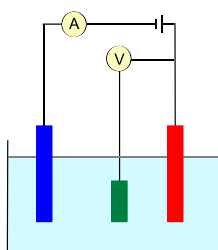
Figure 10: Three-electrode method set up.[84]

Indigo white **132**, under the effects of acetic anhydride, gave diacetylindigo white, **133**. Oxidation of **133** with nitrous acid evidently involved the migration of the acetyl groups to form diacetylindigo (Scheme 14).[86]
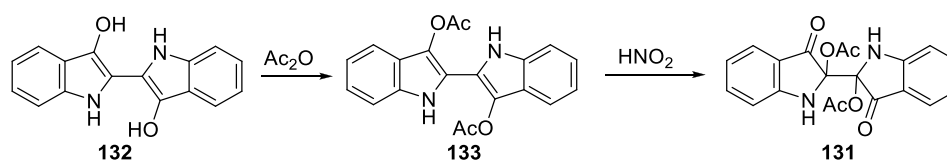
Scheme 14: Diacetylation of indigo white.[86]

Treatment of **132** with zinc dust and barium hydroxide resulted in cleavage to isatic acid **134** and oxindole **91**, followed by condensation and decarboxylation to furnish quindoline **135** (Scheme 15).[87]
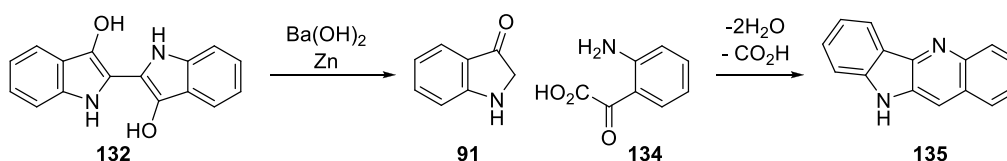
Scheme 15: Formation of quindoline **135** from indigo white.

1.4.3   Formation of salts

Indigo reacts with mineral acids to give indigo salts. Reacting indigo with concentrated sulfuric acid in acetic acid (1:5 V/V), followed by the addition of anhydrous ether, resulted in indigo monosulphate $C_{16}H_{10}O_2N_2.H_2SO_4$ **136** while the prolonged digestion of indigo by sulfuric acid (13.5 M) under the same conditions gave the disulphate salt **137** of indigo.[88-90] Notably, indigo becomes soluble in acetic acid, benzene and chloroform when dry HCl gas passes through the suspension. Addition of ether to the solution precipitates the hydrochloride salt $C_{16}H_{10}O_2N_2.HCl$ **138** (Figure 11).[89] Dissolving these salts in water releases indigo and the corresponding acid.[90]
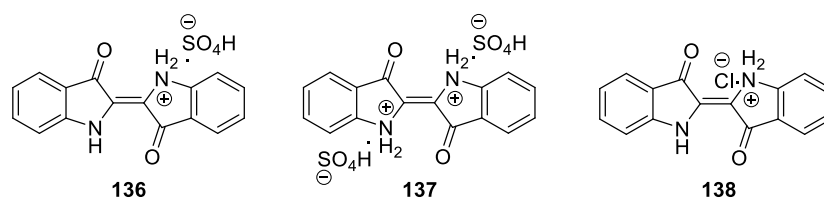
Figure 11: Salts of indigo; monosulphate **136**, disulphate **137** and hydrochloride **138**.[88-90]

When indigo is stirred in a solution of NaOH and ethanol, it gives a green powder with composition of $C_{16}H_{10}O_2N_2.NaOH$ **139**.[88] Heating indigo in concentrated NaOH in 145-150 ºC will result in dissociation to indoxyl aldehyde **140** and anthranilic acid **123** (Scheme 16)[91], whereas fusion of indigo with KOH results in oxindole **91**.
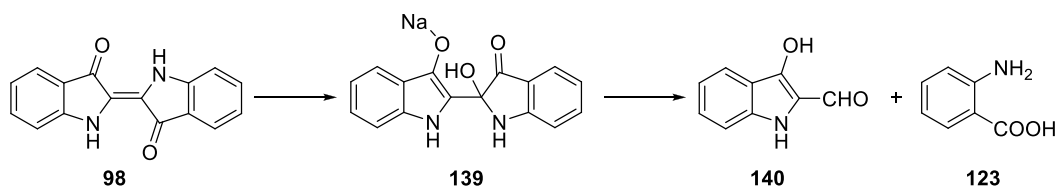
Scheme 16: Sodium salt of indigo **139** and its decomposition to **140** and **123**.

1.4.4   Imines and oximes of indigo

The reaction of the sodium salt of indigo **139** with zinc chloride and ammonia resulted in indigo monoimine **141** while treatment of indigo under the same conditions provided di-imine of indigo **142** as blue needles after recrystallisation from benzene (Figure 12).
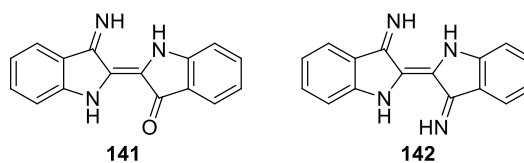
Figure 12: Mono and di-imine of indigo.

Heating indigo in an alkaline alcoholic solution of phenylhydrazine resulted in the Wolff-Kishner product, yielding mono- desoxyindigo **144** (Scheme 17).[92]
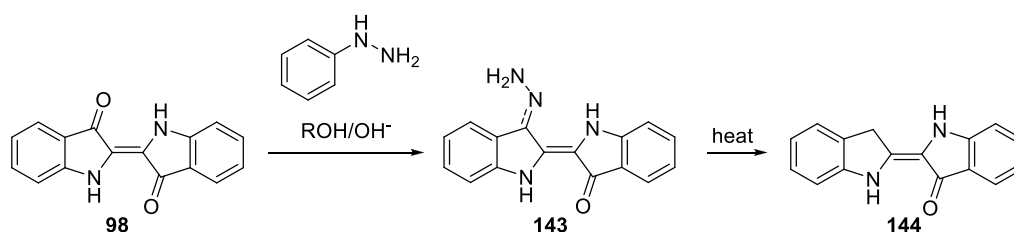
Scheme 17: Desoxyindigo **144** from the heating of indigo with phenylhydrazine.[92]

Indigo oximine **145** is obtained from the reaction of basic solution of indigo with hydroxylamine.[93] Boiling the alkaline solution of **98** in alcoholic mixture of hydroxylamine hydrochloride resulted in the dioxime[94] **146** (Figure 13).
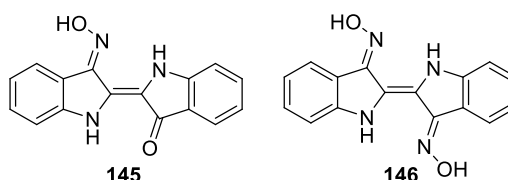
Figure 13: Oxime **145** and dioxime of indigo **146**

1.4.5 Electrophilic substitution of aromatic rings

Electrophilic substitution of indigo, indigo white or dehydroindigo affords sulphonated, halogenated or nitro derivatives. The substituents order is C5 followed by C7 and then C4. Halogenated derivatives of indigo demonstrate a variety of colours mostly based on the number and position of the halogen on the aromatic rings. Ciba blue B (5,5',7,7'-tetrabromo-indigo) **147** is bright blue, 6-bromoindigo **148** is a vibrant violet colour and 6,6′-dibromoindigo **149** is a sharp purple colour (Figure 15).
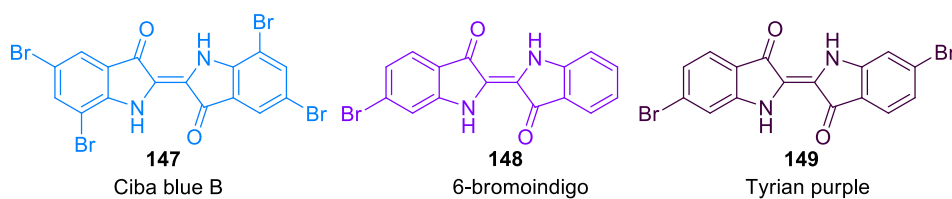
Figure 14: Three different halogenated derivatives of indigo known as ancient pigments.

This was enough to dazzle ancient peoples to apply such pigments to decorate their pottery, clothing and used for cave drawings. Tyrian purple (6,6'-dibromoindigo), also known as Royal Purple, is an ancient pigment believed by some to be the oldest dye, which has been used since the Iron Age by Phoenicians[95], Chinese and Peruvians as a sacred pigment.[96] The roman emperor Nero decreed the exclusive right for the emperor to wear the purple robes.[97] Based on biblical notes, the vestments of high ranked priests are dyed in royal purple. The pigment could only be obtained from exposure of hyperbroncial extract of certain kind of marine *murex* to light.[98] Several mechanisms were proposed to explain the biosynthesis of this pigment (Scheme 18).
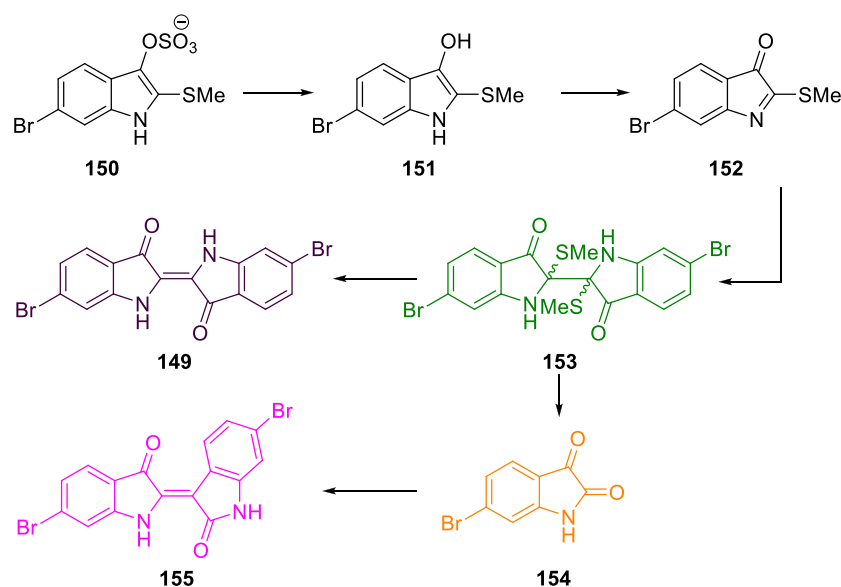
Scheme 18: Biochemical pathway in generation of **149**.

The immediate precursor for Tyrian purple is shown to be photolabile tyriverdin **153**.[99]

The process begins from hydrolysis of the sulphate group of tyrindoxyl sulphate **150** under the action of an enzyme – either purpurase or arylsulfatase. The result is

formation of tyrindoxyl **151** which is oxidised to tyrindoleninone **152**, which dimerises

to form the green tyriverdin **153**. Photolysis of tyriverdin gives rise to dibromoindigo

along with the elimination of odorous dimethyl disulfide.[100] Alternatively, tyriverdin is

also able to undergo homolysis to 6-bromoisatin which reacts with **151** to form 6,6'-

dibromindirubin **155**.[101]

The scarcity of Tyrian purple (secretion of 10,000 marine murexes are required to

produce a gram of the pigment), combined with its political and religious significance,

its value has historically been 10-20 times higher than gold during different periods of

time.[102] Since the early 1900s, chemists sought to establish a process of synthesising

royal purple. A wide variety of synthetic strategies and pathways were reported towards

the synthesis of 6,6'-dibromoindigo such as treatment of 4-bromo-2-nitrobenzaldehyde

the **156** in alkaline acetone (Scheme 19, blue).[103] One of the alternative methods was

starting from *p*-toluidine **159** involved a tandem nitration-diazotization strategy,

followed by diazotization then oxidation in the presence of CrO_3 and subsequent aldol

condensation to afford **149** (Scheme 19, red).[104] Several modifications have been

utilised in order to improve the production of the key intermediate 4-bromo-2-

nitrobenzaldehyde **157**.[105-107] Conversion of 2-amino-4-bromobenzoic acid **163** towards

the diacetylindoxyl **164** and hydrolysis and oxidation furnished **149**. This method

introduced by Friedländer according to Baeyer's method for production of indigo

(Scheme 19, purple).[108] Alternative methods were introduced for the synthesis of **163** in

a more economical manner such as starting from 4-bromo-2-nitrotoluene **160**,[109] 4-

bromo-2-nitroaniline **161**,[110] and phthalic anhydride **162** (Scheme 19).[111] The other

procedure based on the Sandmeyer reaction, involved conversion of dinitroindigo

obtained from 1,3-diacetyl-6-nitroindoxyl (Scheme 19, green).[112] In a different

approach, Majima and Kotake introduced the halogen by bromination of indole-3-

carboxylate **170**, which synthesised by the treatment of indole Grignard with ethylchloroformate. Subsequent saponification and oxidation with ozonised air furnished **149** (Scheme 19, brown).[113] The most recent strategy to the royal purple begins from 6-bromoindole **172** and proceeds 3-acetoxy-6-bromoindole **173**, which can be hydrolysed to deposit **149** (Scheme 19, orange).[114]

Scheme 19: Major procedures in the synthetic production of 6,6'-dibromoindigo **149**.

These are the six major pathways to produce 6,6'-dibromoindigo. Taking into account the modified procedures toward the facile or high yield synthesis of the key intermediates, there have been forty reports towards the synthesis of **149**, however, there have been no reported syntheses of 6,6'-dibromoindigo directly from indigo. 5,5'-Dibromoindigo was obtained from the dropwise addition of bromine to a solution of indigo in nitrobenzene, under microwave-aided condition.[115] The preparation of 5-chloroindigo has been reported by direct halogenation of indigo in glacial acetic acid; this procedure was also found to be amenable to the synthesis of 5,5'- dichloroindigo.[116] 5,5',7,7'-Tetraiodoindigo was prepared from dehydroindigo by the action of iodine monochloride in presence of sodium bisulphate.[117] A quantitative preparation of 5,5',7,7'-tetrabromoindigo from the reaction of indigo with bromine and sodium nitrite in sulfuric acid has also been reported.[118] Direct halogenation of indigo in the presence of water, generally gives the halogenated isatin while halogenation in glacial acetic acid affords mono or di-halogenated indigo.[119] Direct nitration of indigo produces 5,5'-dinitroindigo while other nitrated derivatives of indigo such as 4,4' or 6,6' were synthesised through the conventional methods.[145] Treatment of indigo by concentrated sulfuric acid gives a blue-green compound, named indigo carmine or indigo-5,5'-disulfonic acid. Indigo carmine has various applications as an acid base or redox indicator and also as food colourant.[120, 121] Application of fuming sulfuric acid produces tri or tetra-sulfonic acid indigo as indigo-5,5',7,7'-tetrasulfonic acid.[122] All of these halogenated derivatives of indigo mentioned in this paragraph were reported based on the elemental analysis and with few exceptions, there has been little structural elucidation or no percentage yields reported.

1.4.6   Reaction with Lewis acids

Reaction of the indigo carbonyl moieties with Lewis acids is one of the least explored areas in the chemistry of indigo. Opportunities such as Wittig or other olefination reaction of the carbonyl groups is not yet reported. The only reported example of Lewis acids involved in reactions with indigo was the formation of *N,N'*-diaryldiimines towards the synthesis two *β*-diketimate fused units. In this context indigo reacts with arylamine in presence of $TiCl_4$ and DABCO to yield indigo bis(arylamine) **174-177** known as the Nindigo (Scheme 20).[123]
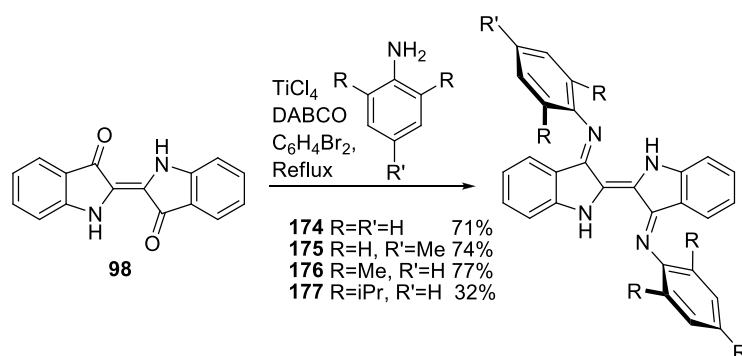
Scheme 20: Reaction of indigo and arylamines in presence of $TiCl_4$.

1.4.7   Nucleophilic substitution

Reaction of indigo with the Grignard reagent (CH_3MgI) in diethyl ether was reported[124] to obtain 3-hydroxy-3-methyl-3'-oxo-2,2'-diindolydene **178**. The yield for this compound was not reported (Figure 15).
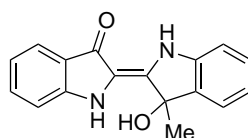
Figure 15: 3-hydroxy-3-methyl indigo **178**.

Early reports for the *N-* and *N,N'*-alkylation of indigo gave the impression that indigo could not be alkylated in such reactions; the given explanations mostly focused on the poor solubility of indigo. This was altered when Kuhn and Trischmann successfully synthesised *N,N'*-dimethylindigo **179** in near to quantitative yield, using iodomethane in

DMF-water with vigorous stirring in the presence of barium oxide as base and under

nitrogen for 18 hours at room temperature. Extraction with chloroform upon workup

resulted in the isolation of a green precipitate of the product (Scheme 21).[125]
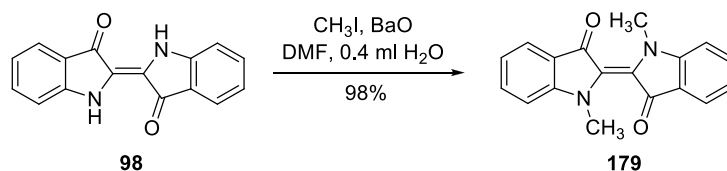
Scheme 21: *N*-Methylation of indigo under action of barium oxide.[125]

Another approach for the production of *N,N'*-dimethylindigo was the reaction of indigo

or 6,6'-di-*tert*-butylindigo **180** with methyl iodide in presence of sodium hydride.[126] *cis-*

N,N'-Bridged indigo derivatives, such as 1,2-ethano and 1,3-propano and 1,4-butane

systems, were synthesized by base-induced (NaH) *N*-alkylation reactions in the

presence of various di-chloroalkanes or 2,3-dichloronaphthoquinone (Scheme 22).[126]
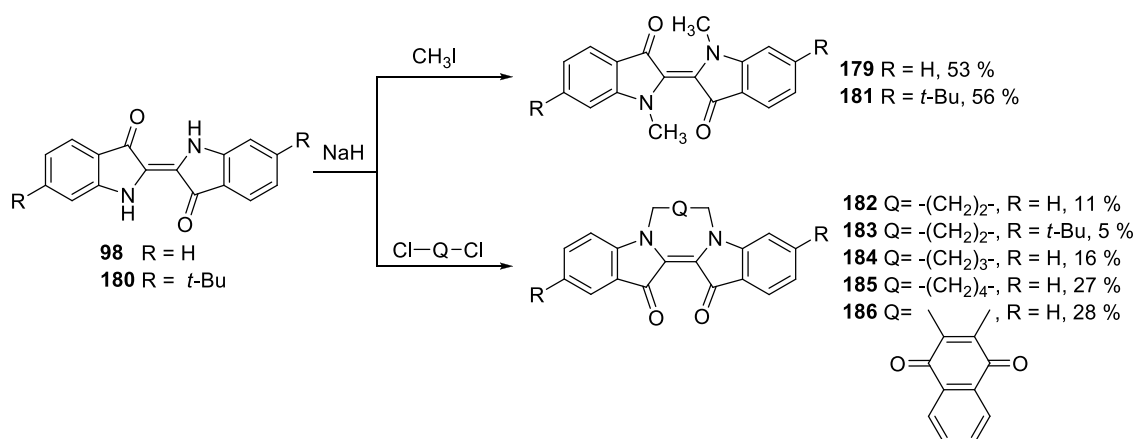
Scheme 22: *N*-Methylation of indigo derivatives in the presence of NaH as base.[126]

cis-N,N'-Bridged oxalyl **187** or malonyl indigoids **188** were synthesised by reaction of

indigo with oxalyl and malonyl dichlorides in nitrobenzene at reflux.[126] Slightly

different conditions were utilised for the reaction of substituted indigos **189**-**190** for the

production of **191**-**193**, where 2,6-lutidine used as base and the solvent was benzene

(Scheme 23).[126]

Scheme 23: Reaction of indigoids with oxalyl or malonyl chlorides.[126]
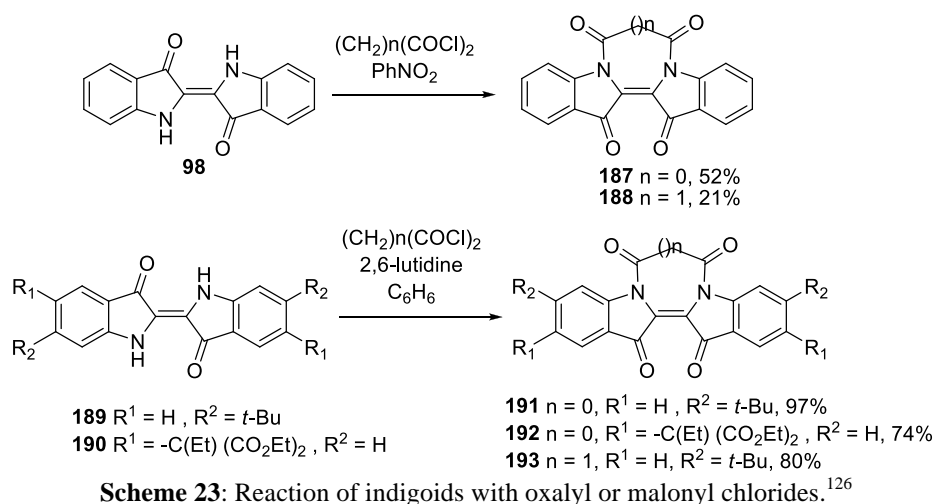
N-Aryl indigoids **194-7 (a-b)** were obtained from the reaction of **98** and aryl halides in *o*-chlorobenzene at reflux, containing K_2CO_3 and catalytic copper powder.[127] The reaction was also carried with naphthalene iodide in excess and only afforded a mono *N*-substituted product **198** (Scheme 24).[127]

	R	X	time (h)	aryl halide/98	a	b
194	H	I	10	2:1	0%	92%
195	OCH₃	I	10	1:1	35%	13%
195	OCH₃	I	10	2:1	0%	74%
196	F	I	10	2:1	43%	17%
197	CN	Br	10	2:1	14%	trace
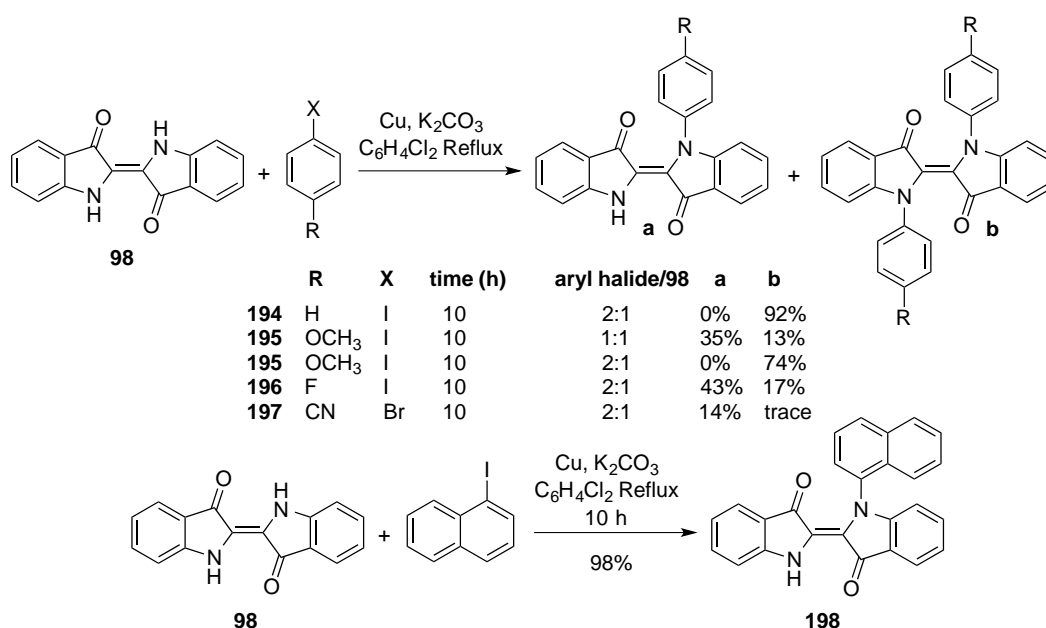
Scheme 24: Reaction of **98** and various aryl halides for production *N*-aryl indigoids.[127]

N,N'-Diacetylindigo **199** was obtained by treatment of indigo with excess acetyl chloride in acetic anhydride at reflux (Scheme 25).[128] The procedure was first reported by Liebermann and Dickhuth in 1891 when they treated indigo with appropriate acyl chlorides in butyl acetate at 100 °C.[129]
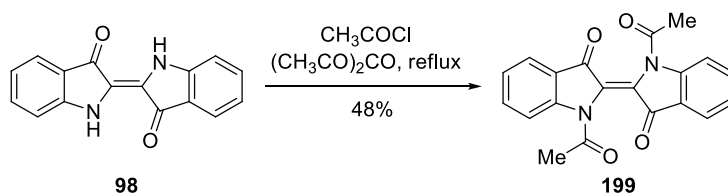
Scheme 25: Formation of *N,N'*-diacetylindigo **199**.[152]

O-Alkylation of indigo white **132** by the addition of ethoxycarbonylacetyl chloride in the presence of zinc furnished *cis-O,O'*-di(ethoxycarbonylacetyl)indigo-white **200**, which underwent the oxidative rearrangement under the effect of DDQ in DMSO and resulted in the production of *trans-O,O'*-di(ethoxycarbonylacetyl)indigo **201** (Scheme 26).[130]
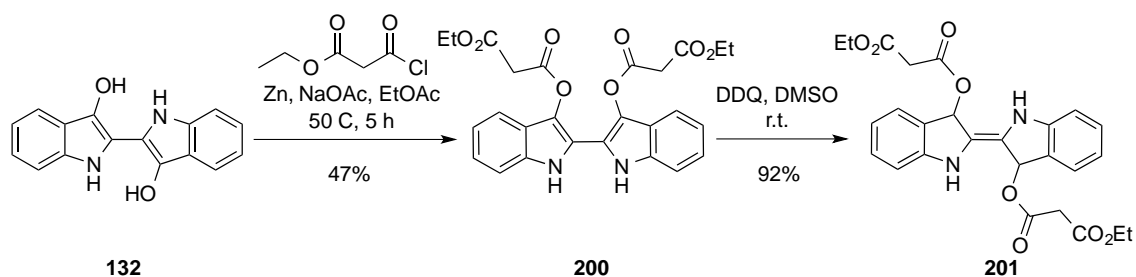
Scheme 26: Preparation of *cis-O,O'*-di(ethoxycarbonylacetyl)indigo-white **200** and its oxidative rearrangement to form **201**.

cis-trans Isomerisation of different *N,N'*-diacylindigoids was observed by Kitao using solutions of *trans-N,N'*-diacylindigoids in benzene, acetonitrile or cyclohexane, and visible light irradiation (>500 nm) resulted in reversible conversion to the *cis*-isomer (Scheme 27). The half-life and the heat released from conversion of thermally unstable *cis* isomer to *trans* were observed and recorded (Table 1).[130]
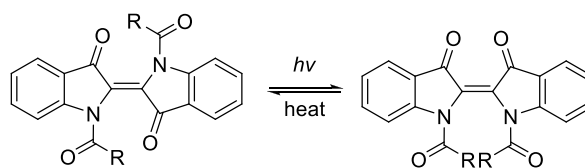
R = Me, Et, Pr, -CH$_2$CO$_2$Et, CH$_2$Ph

Scheme 27: Photochromic isomerisation of *trans-N,N'*-diacylindigoids to the corresponding *cis* isomer.[130]

Table 1: Half-life of the cis *N,N'*-diacylindigoids and the heat released from its conversion to the *trans* isomer.[130]

R		λ_{max}/nm		$t_{1/2}$/min	$-\Delta H$/kcal mol^{-1}
Me	*cis*	438	*trans*	565	186	7.3
Et	*cis*	440	*trans*	573	642	6.6
Pr	*cis*	477	*trans*	581	413	9.8
-CH$_2$CO$_2$Et	*cis*	424	*trans*	556	471	12.2
CH$_2$Ph	*cis*	441	*trans*	575	1264	29.9

Smith and his group investigated the photooxidation of *N,N'*-diacylindigoids. A solution of **201a-f** in toluene at reflux was irradiated with visible light selective and was for photochromic *cis/trans* isomerisation ($\lambda > 530$ nm) while under an oxygen atmosphere, lead to the formation of compounds **207a-f** (Scheme 28).[131]

a R = Me, 95%
b R = -CH$_2$-cyclopropyl, 95%
c R = CH$_2$Cl, 6%
d R = C$_6$H$_5$, 50%
e R = 3,5-(NO$_2$)$_2$C$_6$H$_3$, 50%
f R = *p*-(MeO)C$_6$H$_4$, 50%
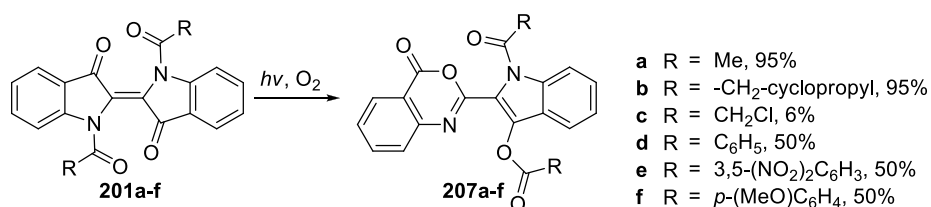
Scheme 28: Photooxidation of *N,N'*-diacylindigoids.

The proposed mechanism suggested the **201** reacted with triplet oxygen to form a peroxy biradical **202**, which was trapped by hydrogen or benzyl to form the peroxide radical **202**. Fission and subsequent rearrangement gives diradical **207**, which undergoes an N to O acyl transfer to provide **207** as stable product (Scheme 29).[131]
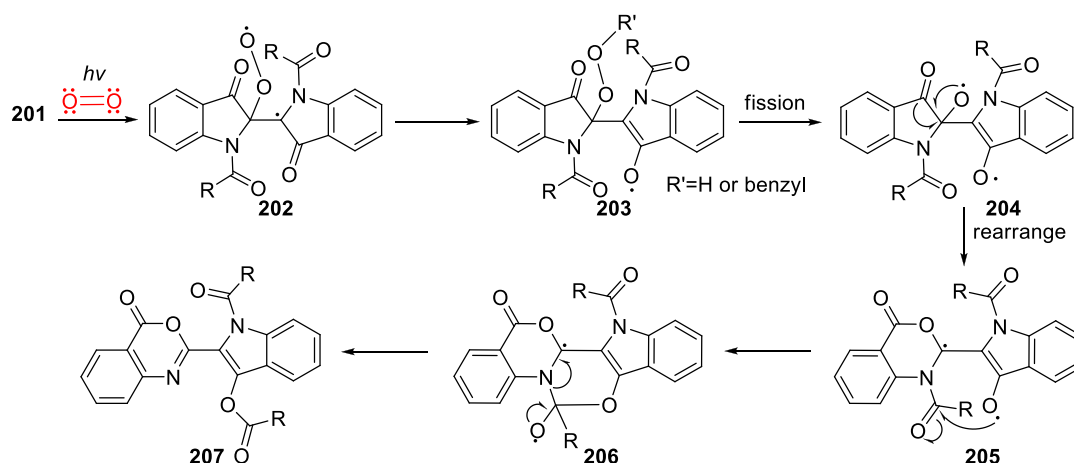
Scheme 29: Photooxidation of *N,N′*-diacylindigoids **201a-f** and tentative mechanism for formation of photoxygenated product **207a-f**.[131]

When dehydroindigo and methylpropionate were stirred in anhydrous benzene, a blue crystalline solid was formed, identified as *N,N′*- vinylidene indigo (Scheme 30).[132] A similar product can be obtained by the slow addition of dehydroindigo to a melt of maleic anhydride followed by extraction with dichloroethane.[133]
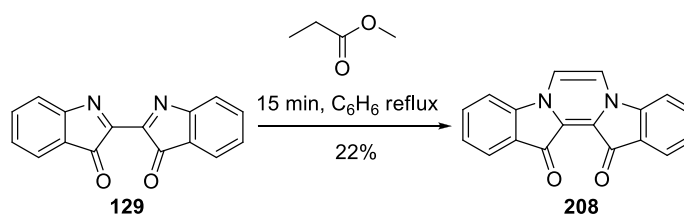
Scheme 30: *N,N′*-Vinylidigo from reaction of the dehydroindigo and methylpropionate.[132]

Heating indigo in the presence of benzoyl chloride in pyridine resulted in the formation of a crystalline violet compound as *N,N′*-dibenzoylindigo **209** (Scheme 31).[134]
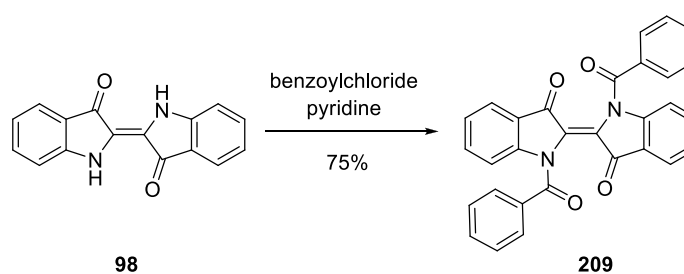
Scheme 31: *N,N′*-Dibenzoylindigo **209** from heating indigo in pyridine in presence of benzoylchloride.

The reaction of indigo in hot benzoylchloride caused one of the long-term disputes in the chemistry of indigo. The synthesis was originally conducted by Schwartz in 1863. He reported a brown amorphous isolate and claimed it as *N,N′*-dibenzoylindigo **209**.[135] Prior to this, acid hydrolysis of **209** was reported to give indigo whereas the same reaction using the product from Schwartz produced different outcomes.[136] Further examination and repetitions revealed that the empirical formula contained chlorine and was assigned as $C_{30}H_{17}O_3N_2Cl$, identical with another reported structure known as Dessoulavy compound **210**, originally synthesised from indigo in excess benzoylchloride at reflux (Scheme 32).[137]
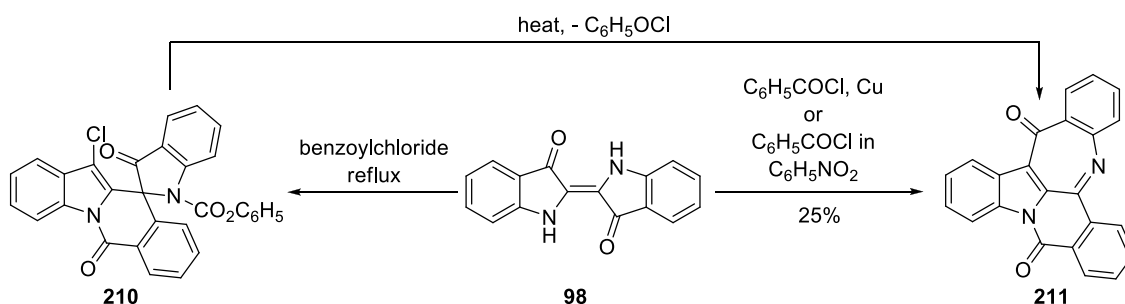
Scheme 32: Synthesis of Dessoulavy compound **210**[137] and its conversion to Ciba Yellow G **211**.[138]

Treatment of **98** with copper or sodium nitrate in benzoylchloride at reflux or reaction of **98** and benzoylchloride in nitrobenzene resulted in production of Ciba Yellow 3G **211** (Scheme 48)[138]; it dyes cotton and wool in a yellowish green colour. Heating (300-380 °C) of Dessoulavy's compound led to the expulsion of benzoylchloride and formation of **211**. Structure elucidation of **211** attracted the attention of organic chemists for decades and during this time a number of structures were proposed, and altered. A preliminary structure suggested by Hofmister in 1926 postulated that the compound was a result of aromatic substitution of benzoyl into one of the benzene rings of indigo **212**, followed by ring closure and rearrangement to give the anthraquinone type structure **214** as proposed structure for Ciba Yellow G (Scheme 33).[139]
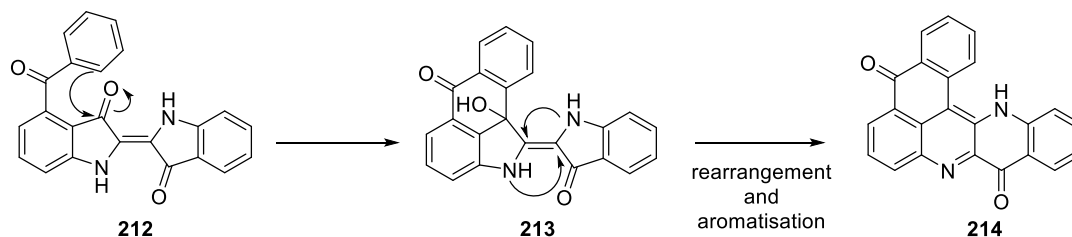
Scheme 33: Proposed mechanism for the formation of anthraquinone structure **214**.

Structure **214** was rejected by Hope and Richter after they heated Ciba Yellow G in 15% NaOH solution and formed a bright yellow precipitate as which they assigned as **216**[‡]. In this regard they proposed **215** structure as the structure of Ciba Yellow G (Scheme 34).[136]
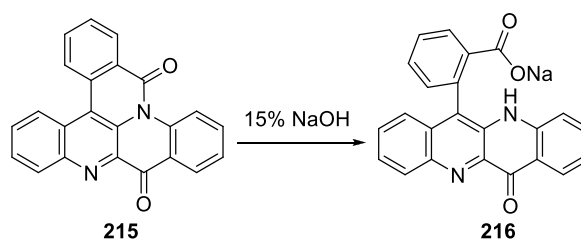
Scheme 34: Proposed structure **215** for Ciba Yellow G by Hope and Richter based on the result from boiling in 15% NaOH solution.

Structure **211** proposed by de Diesbach,[140] was finalised 34 years later by X-ray crystallography (Figure 16).[141]
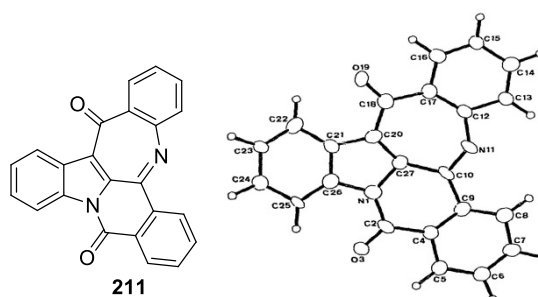
Figure 16: Structure of Ciba Yellow G and its X-ray ORTEP image.[140,141]

[‡] Yield was not reported.

Boiling indigo with zinc chloride in benzoyl chloride yielded Höchst Yellow R **217**.

Heating of **217** with sulphuric acid resulted Höchst Yellow U **218**, an additional isomer

of **211** (Scheme 35).[142]
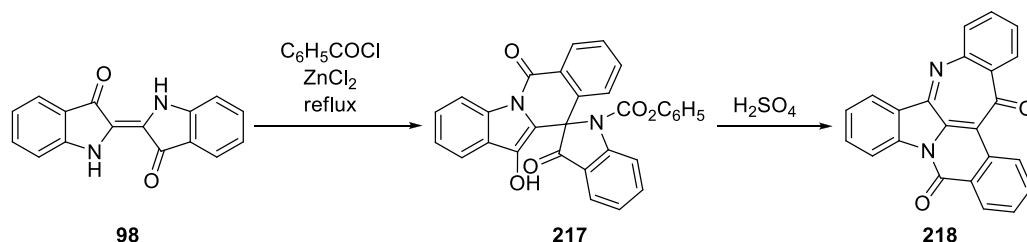
Scheme 35: Formation of Höchst Yellow R **217** and Höchst Yellow U **218**.[142]

Heating of **210** with ammonia in methanol reported to produce a yellow substance

bearing the formula $C_{27}H_{21}N_3O$ (m.p. 247 °C) having structure **219**.[134] However when

the reaction was repeated, a mixture of four different products, **220**-**223** was produced

and none of them had the structure similar to **219** (Scheme 36).[143]
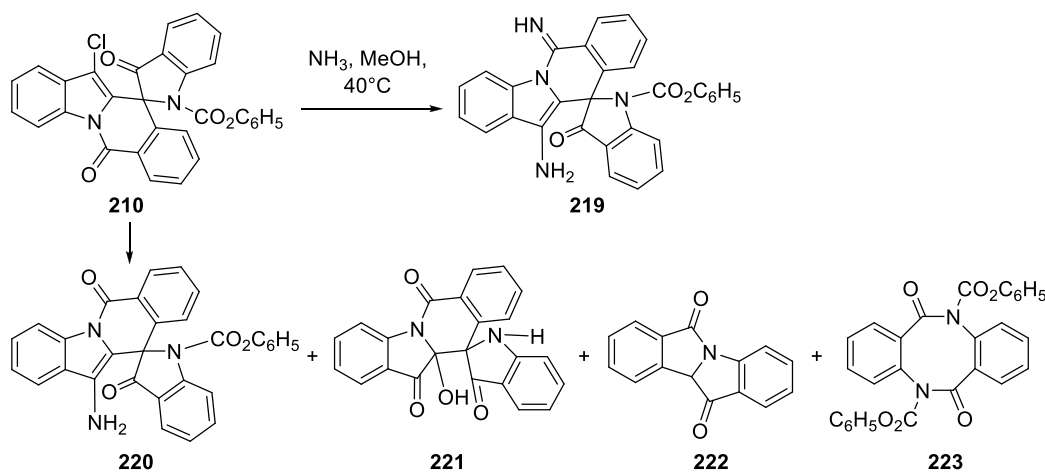
Scheme 36: Treatment of **210** and ammonia and its controversial products.[143]

Reaction of **210** with aniline produced a grey substance, which was believed to have an

empirical formula of $C_{27}H_{21}N_3O$. However, according to subsequent repetition and

supporting experiments, the formula changed to $C_{28}H_{21}N_3O$ and the structure **224** was

suggested (Scheme 37).[143] There is no substantial information to confirm the proposed

structures for **220**-**223**.
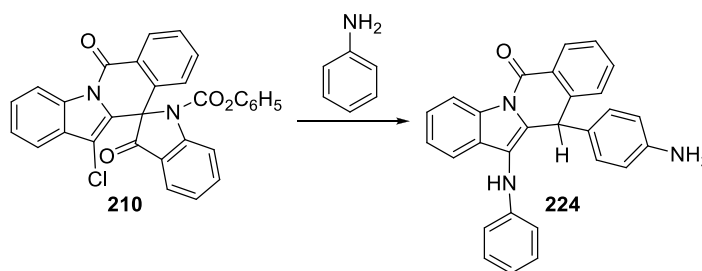
Scheme 37: Reaction of **210** with aniline and the supposed structure of the product **224**.[143]

Heating indigo with an excess of phenylacetyl chloride either alone or in nitrobenzene or neat resulted in the generation of the bright red, crystalline pigment **226**, containing a bay annulated system[144] commonly known as Ciba Lake Red B (Scheme 38).[145]
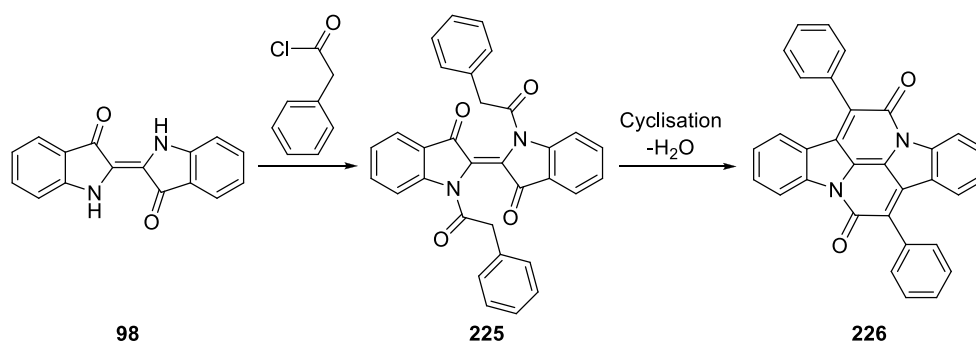
Scheme 38: Formation of Ciba Lake Red B **226** from reaction of **98** and phenylacetyl chloride.[145]

1.4.8 Cascade reactions of indigo

Recent results from Keller research group (KRG) lab revealed that indigo undergoes cascade reactions in the presence of allylic halides.[146] Immediate results of these tandem reactions were rapid, one-pot production of two complex heterocycles; a spiroindoline–pyridoindolone (**Type A**, Scheme 39) arising from the addition of three allylic units, and a fused pyridoindoloazepinoindolone (**Type B**, Scheme 39), generated from the addition and subsequent cyclisation of two allylic moieties. These novel architectures were fully characterised and their structure were assigned by extensive 2D NMR experiments and by X-ray crystallographic techniques (Scheme 39).
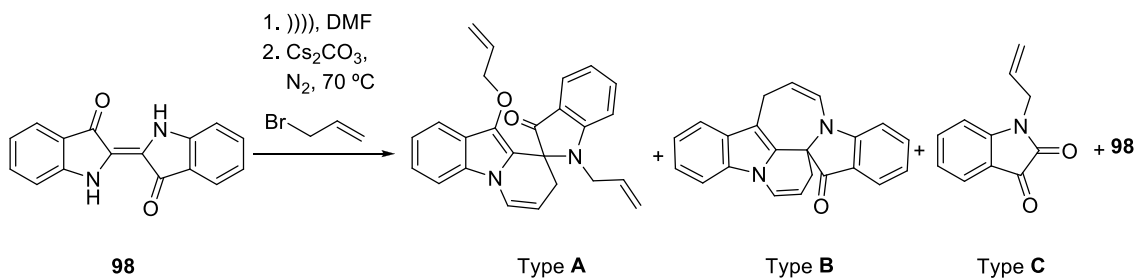
Scheme 39: Formation of two new classes of heterocycles from one-pot cascade reaction of indigo and allylic systems.[146]

Formation of two structurally-diverse heterocycles in a one-pot synthesis gave rise to the possibility of using the structure of indigo scaffold as a suitable platform for further elaboration through cascade reactions.

1.5   Aims

This work designed to explore the cascade reactions of indigo with different π systems in order to produce complex and annulated structure in a short and economic manner.

Therefore the aims of the projects are:

- To improve the yield of the cascade reactions of indigo with allylic systems and the exploration of controlling the cascade process (Chapter 2).
- To explore the effect of the π systems and comparison of the reaction outcome for alkynic and allylic systems (Chapter 3).
- To investigate the impact of the reaction conditions, sequence of the reaction, leaving groups and substituents on the outcome of the reaction (Chapter 2 & 3).
- Mechanistic studies to improve the yield and ability to predict of the outcome of theses cascade reactions.

- To examine indigo as a suitable building block in the generation of the DOS compounds library.

Chapter 2 : Cascade Reactions of Indigo and Allylic Halides

2.1   Screening the reaction of allylic halides and indigo

As it demonstrated in Scheme 39, preliminary results from the reaction of indigo **98** with a series of allylic bromides at 70 °C in the presence of base in dimethyl formamide revealed significant potential for the rapid generation of novel 1-allyl-5'-allyloxy-3',4'-dihydrospiroindoline-pyrido[1,2-*a*]indol-ones (Type **A** up to 32%) and pyridoindolo-azepino[1,2-*a*]indol-11(7*H*)-ones (Type **B** up to 38%) systems, together with isatin-based products (Type **C** up to 25%) resulting from oxidative cleavage process, as well as unreacted indigo **98** (Table 2).[146]
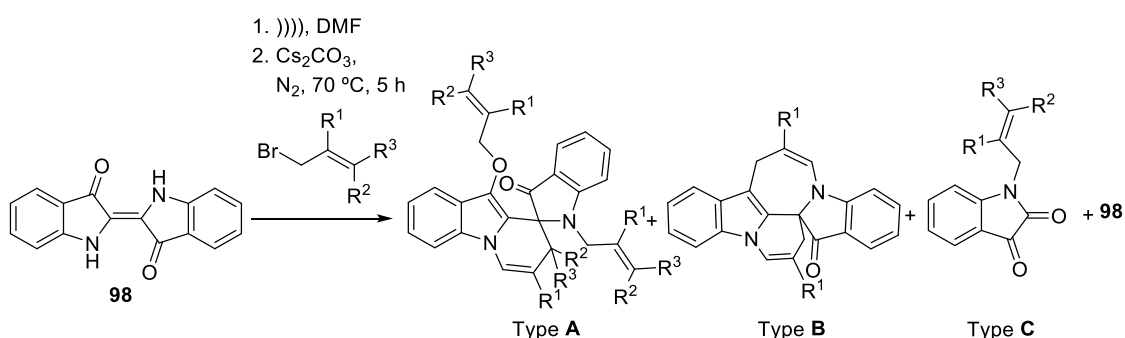
R^1	R^2	R^3		A %		B %		C %	(98) %
H	H	H	**227**	32	**232**	11	**237**	25	23
Me	H	H	**228**	36	**233**	9	**238**	22	18
H	Me	H	**229**	42	**234**	-	**239**	14	6
H	Me	Me	**230**	-	**235**	-	**240**	14	63
H	Ph	H	**231**	12	**236**	-	**241**	-	21

Scheme 40: Products from the reaction of indigo and various allyl bromides.[146]

It was also observed from these early studies that terminal substitutions of the allylic electrophile dramatically reduced the yield of products to the point whereby the use of the disubstituted terminal 3-methyl-1-bromobut-3-ene ($R^2 = R^3 = $ -CH₃) appeared to hamper the generation of spiro-bonded or multi-cyclic products. A proposed mechanism for the formation of type A and B is outlined in Scheme 41. After the initial formation of the monoallylated indigo, intermediate V formed by tautomerisation and subsequent

allylation. This intermediate is a divergence point of the proposed mechanism in which quaternisation of the imine nitrogen is set up for internal nucleophilic attack by the electron-rich alkene on the electron-deficient iminium ion to afford the spiro system VI and then type **A** (Path A). Alternatively, V could form the stabilised allylic zwitterion VII followed by intramolecular nucleophilic addition on the indolone carbonyl. Subsequent loss of water and final cyclisation would realise the azepino-indolone of the type **B**. In alternative route, after formation of monoallylated indigo anion II, deprotonation with subsequent enolisation allows for further *O*-allylation (Path C). A third allylation on the imine nitrogen in II might then take place providing a powerful electrophilic site for internal double bond attack and subsequent proton loss to give the spirocyclic derivative (Type **A**). Formation of the *N*-allylisatin type **C** presumably arises from oxidative cleavage of the *N*-allylindigo intermediate and/or from *N,N'*-diallylindigo which could be readily formed from the former under basic conditions with allyl bromide.[146]

The outcomes were limited with significant quantities of starting material and oxidative degradation products accounting for the majority of the products, despite the interesting spiro and polycyclic structures produced as minor products. These early studies provided a curious insight into the possibilities associated with using indigo as a starting point for chemical synthesis towards the production of more complex architectures in an economical manner, however the consistent high return of unreacted starting material suggested that further optimisation was required to ensure its synthetic utility. Therefore, there was significant motivation to further investigate these cascade reactions with an aim to gain control over reaction pathways, such that these one-pot reactions led to practical yields while minimising the return of unreacted starting material and oxidative products.
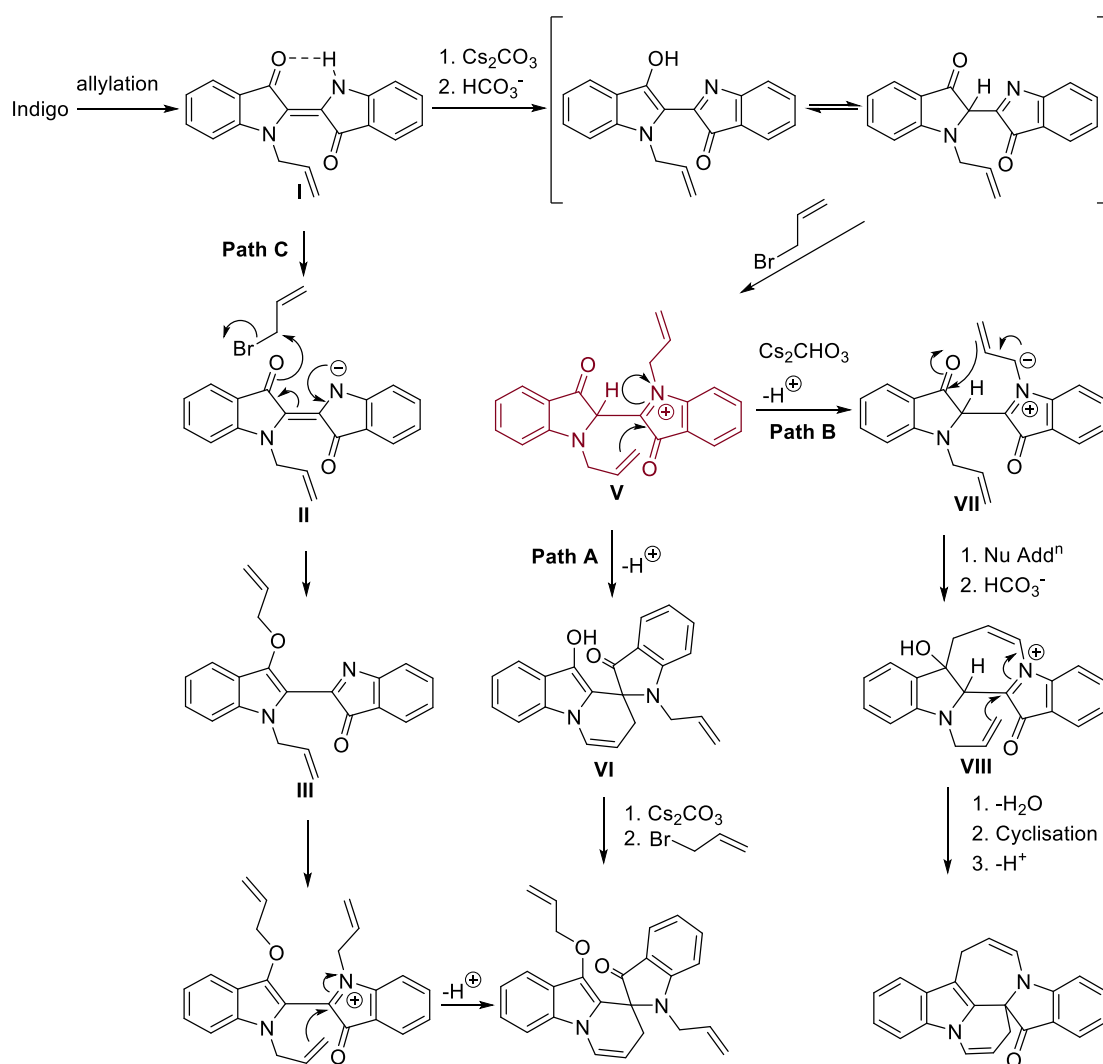
Scheme 41: Proposed mechanism for the formation of type **A** and **B** heterocycles.[146]

Considering the proposed mechanism of the allylation reaction of indigo (Scheme 41), it was reasoned that the water elimination step (VIII→Type B) could be assisted by the application of a static dehydration agent such as molecular sieves to promote better productivity. Furthermore, caesium carbonate is an extremely hygroscopic base, and demands special handling and application techniques. To increase its solubility in DMF and allow for greater solid-liquid phase interaction, ground caesium carbonate in a sealed flask containing 4 Å molecular sieves was heated in *vacuo* to remove the excess moisture. Moreover, in order to minimise exposure of the base to atmospheric moisture,

the reaction sequence was altered such that a sonicated suspension of indigo was transferred by cannula into a septum equipped flask containing the pre-dried caesium carbonate and molecular sieves with a stirrer bar under an inert atmosphere of nitrogen. Increasing the reaction temperature was reasoned to increase the solubility of indigo, though this represented a potential issue as the allyl halides each had boiling points within the range of 70-92 °C, and the use of a flowing inert gas (N_2) would likely diminish the electrophile concentration. To negotiate this incongruity, the mixture of indigo and Cs_2CO_3 mixture was stirred under N_2 for 30 min to stimulate the formation of anion. Then the N_2 gas flow was stopped and the allylic halides were injected into the reaction mixture under a static N_2 blanket. Further an additional 2 eq. of allylic halide were added after 1 hour to ensure the presence of ample allylic halide substrate in the reaction mixture.

The reaction was conducted at different temperatures and the outcomes analysed. It was found that with the modified reaction procedure, there were no significant changes in outcome for the reaction performed at 70-75 °C compared to the original reaction. Prolonged reaction (14 h) at this temperature resulted in the formation of *N*-allylisatin **237** and *N*-allyanthranilic acid **242** as major products, while remaining unreacted indigo (32%) was recovered from the filtration of the hot reaction mixture. The reaction was investigated at elevated temperature (90-100 °C), which similarly resulted in formation of **237** and **242**, though trace quantities of spiroindoline **227** and pyridoindolo-azepinoindolone **232** were found to be present in the crude mixture as detected by TLC analysis (Scheme 42).
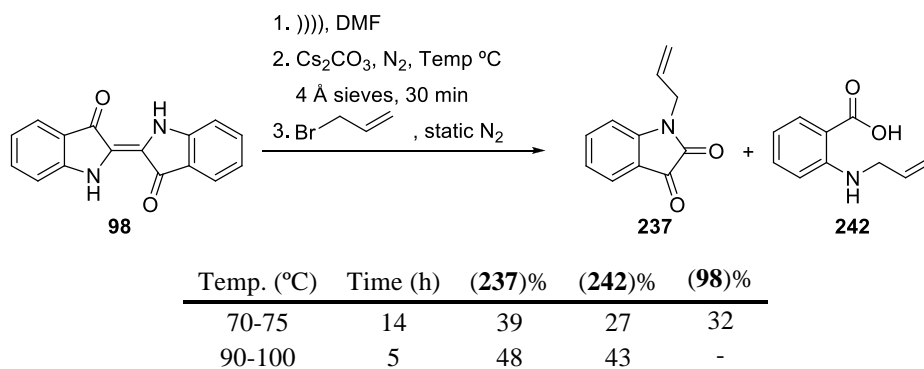
Scheme 42: Reaction of indigo and allylbromide at different temperatures

Temp. (°C)	Time (h)	(237)%	(242)%	(98)%
70-75	14	39	27	32
90-100	5	48	43	-

It was found that by moderating the reaction temperature to 85-88 °C, 5 h after addition

of allylbromide, improved yields in particular for the 7-membered heterocycle **232**

could be obtained (65%), with little or no unreacted indigo remaining. The reaction was

later amended to 3 h, and under these new conditions, the reaction of indigo and

allylbromide resulted in 72% isolated yield of compound **232** by recrystallisation, and

that subjecting the mother liquor to flash column chromatography furnished **227** in 15%

yield. Comprehensive analysis of the mixture revealed the presence of allylic isatin

derivatives in only trace amounts (Scheme 43).
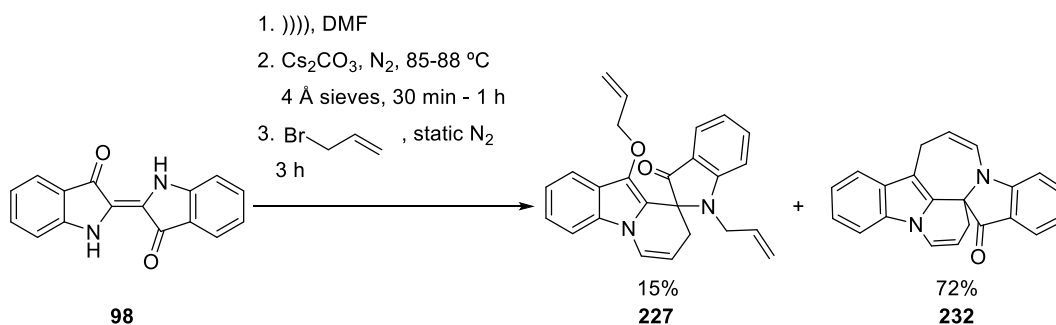
Scheme 43: Modified allylation of indigo.

Furthermore, contrary to the time consuming process for isolation of the products of the

original reaction, compound **232** could be isolated by fractional recrystallisation with a

higher yield under these new conditions (Figure 17). The experiment was also repeated

at 105-110 °C and the result was an inseparable mixture (Table 2).

Table 2: Variation of temperature and its effect on the outcome of the allylation reaction

Temp. ^{o}C	Reaction outcome
75-80	No significant changes compare to the original reaction
85-87	The best result, there was no unreacted indigo, combined isolated yield of 87% for heterocycles **227** and **232**
90-100	Mostly anthranilic acid and allylisatin
105-110	Black tar
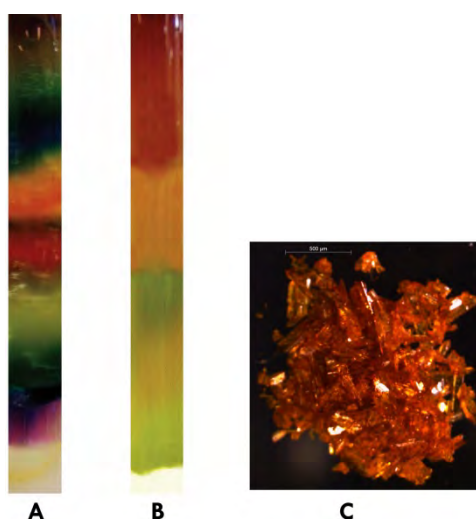
Figure 17: Comparison of purification process of the original reaction and the optimised condition. **A**: Montage of 4 days column chromatography for isolation of the major products formed under the original reaction condition. **B**: Column chromatography of the crude mixture, obtained from the optimised reaction. **C**: Crystals obtained from recrystallisation of the optimised reaction crude to yield compound **232**

The optimised conditions were applied as a generic reaction for the allylation of indigo in presence of different carbonates (Na, K and Cs). The colour change of the reaction mixture from dark navy to amber yellow was considered as a distinctive signature of indigo's consumption. The required reaction times were found to be longer for sodium and potassium carbonate (5 and 7 h respectively), due to the poor solubility of these inorganic bases in DMF. Furthermore, the increasing size of the metal cation is likely to

be involved in destabilising the indigotinide *N*-anion, leading to more reactive anion. Distribution of the products was similar to the reaction with Cs_2CO_3 (Table 3).

Table 3: Effect of different carbonates on the reaction of allylbromide and indigo

Carbonates	Time h	(**227**)%	(**232**)%	(**98**)%
Na	7	9	62	15
K	5	12	65	13
Cs	3	15	72	-

2.2   Variation of time

These modified conditions were used as a new platform from which the effect of longer or shorter reaction times was assessed. The scope of the product outcomes for the cascade process by the addition of different allylic bromides to indigo was investigated at three different reactions times after allylic bromide injection: 5 sec, 1 h and 3 h.

2.2.1   Reaction of indigo and allylic bromides; Five (5) second reaction

When the suspension of indigo in the presence of the base and molecular sieves was heated and stirred under N_2 atmosphere, the colour of the mixture turned to green yellow due to the formation of the anion. It was noted that the colour of the solution was changed instantaneously (from green-yellow to royal blue) with the addition of allylbromides. At this point the reaction was quenched after 5 sec by pouring the mixture into an ice bath. Workup and subsequent recrystallisation of the crude mixture yielded the monoallylated indigos (Type **D**) **243**-**247** in yields of 37-62% as papery blue solids (Scheme 44), however significant quantities of indigo starting material remained at this time. A minor red by-product was also observed (7-10%) in this reaction (see Scheme 46). The *mono*-allylated compounds are a result of the nucleophilic addition of one allyl unit on one of the nitrogen atoms of indigo.

R^1	R^2	R^3		(D) %	(98) %
H	H	H	**243**	54	36
Me	H	H	**244**	62	29
H	Me	H	**245**	57	30
H	Me	Me	**246**	37	41
H	Ph	H	**247**	48	38
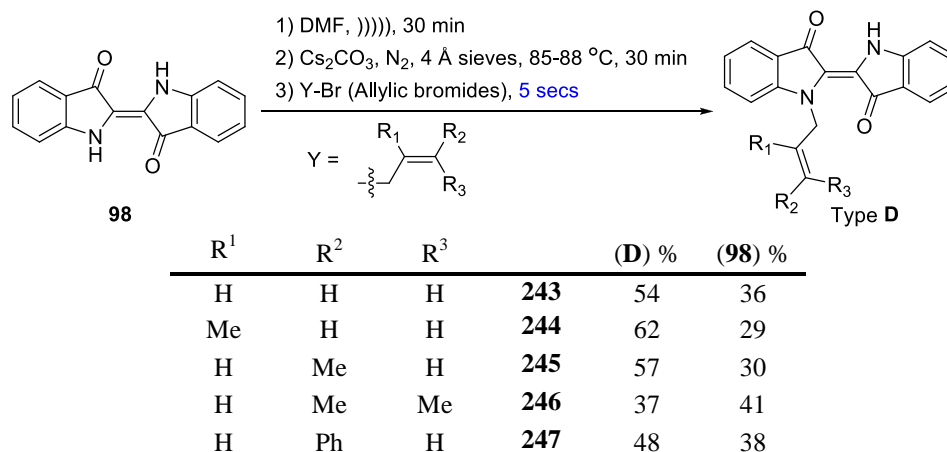
Scheme 44: The synthesis of mono-substituted allylindigo derivatives in 5 seconds reactions.

In the case of *N*-allylindigo **243**, a signal at *m/z* 303 in MS (EI) spectrum was assigned to the molecular ion, confirming the addition of one allylic unit. Analysis of the ^{1}H-NMR spectra showed a peak at 10.71 ppm assigned to the free indolic NH group, as well as two notably deshielded aromatic doublets at 7.64 and 7.72 ppm, assigned to the non-identical H4 and H4' protons, due to the *ortho-para* deshielding effect of the oxoindoline carbonyl moiety. Additionally, analysis of the ^{13}C spectrum confirmed the presence of two carbonyls in the structure assigned, to the peaks at 187.1 and 189.7 ppm. The absence of NOESY correlation between the H1" and NH (H1) along with the X-ray crystallography result confirmed the *trans* conformation of the **243** (Figure 18).
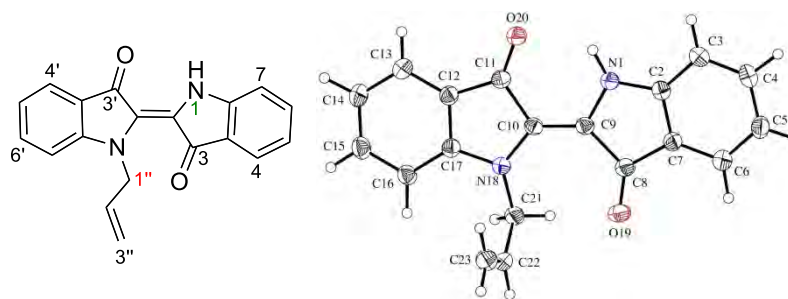
Figure 18: ORTEP file of the compound **243** and its *trans* conformation.

The product trend seen with allyl bromide was evident for most of the substituted allyl bromides used after the 5 sec reaction time with a maximal yield of the monoallylated product and remaining indigo starting material. Allowing the reaction to proceed for

longer in an attempt to increase the yield of *mono*-allylindigo instead led to the immediate formation of multiple products. An alternate optimisation strategy attempted was to firstly generate the indigo anion by heating the mixture of indigo suspension in DMF at 85 ºC with caesium carbonate and then cooling the flask to 40 ºC, and allowing the mixture to equilibrate in the range of 45-50 ºC, prior to the injection of allylbromide. However, when the reaction was quenched after 30 minutes, it was determined that a large quantity of indigo (more than 50%) failed to react and remained unchanged.

Finally, it was found that by increasing the time to one hour to allow a longer period of time for initial deprotonation prior to the addition of electrophile, *mono*-allylindigo products could be isolated after 5 sec in substantially higher yields (Scheme 45).

Reaction conditions:
1) DMF,))))), 30 min
2) Cs_2CO_3, N_2, 4 Å sieves, 85-88 °C, 1 h
3) Y-Br (Allylic bromides), 5 secs

R^1	R^2	R^3		(D) %
H	H	H	**243**	83
Me	H	H	**244**	81
H	Me	H	**245**	89
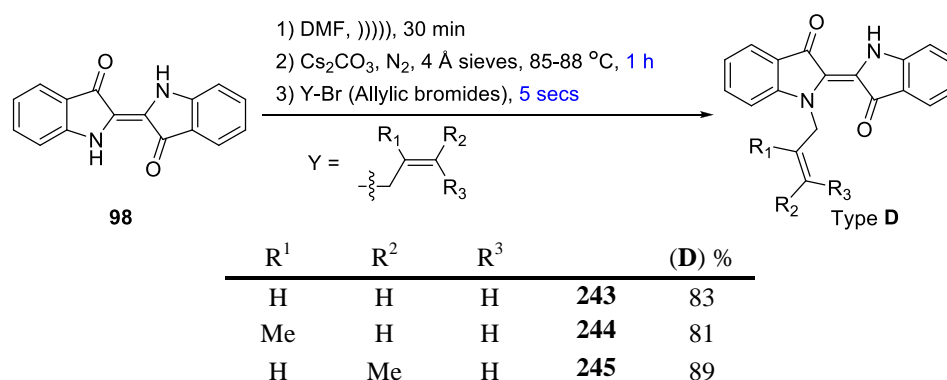
Scheme 45: Optimised reaction for production of *mono*-allylated indigo.

Compared to the characteristically poor solubility of indigo, these *mono*-allylated derivatives are highly soluble in dichloromethane, DMF and DMSO, and moderately soluble in THF, chloroform and ethyl acetate, due to the disruption of intramolecular hydrogen bonding between the adjacent indole and carbonyl groups. This, in turn, allows for simpler manipulation of the scaffold in low boiling point solvents at lower temperatures for further elaboration, quickly providing a solution to the issue of indigo's characteristically poor solubility.

2.2.2   Reaction of indigo and allylic bromides; One (1) hour reaction

These reactions were undertaken using identical conditions to those reported in the previous section, with the exception of a 1 hour reaction time after addition of allyl bromide. In the instance of entry 1 (Scheme 46), one hour after the addition of allylbromide the reaction mixture turned a dark red solution. TLC analysis showed the presence of a polar compound with a red colour close to the base line (CH₂Cl₂ eluent) as the major product. After extraction of the crude reaction mixture with CH₂Cl₂, silica gel as stationary binder was added to the solution to absorb the red compound. The mixture then was filtered and washed with cold CH₂Cl₂ which left the red compound absorbed on silica, and washing the silica with EtOAc furnished 13-allyl-8*a*-hydroxy-8,13*a*-dihydroazepino[1,2-*a*:3,4-*b*']diindol-14(8*H*)-one **248** as a dark red solid. (Type **E**, Scheme 46).

entry	R¹	R²	R³		(E) %	(98) %
1	H	H	H	**248**	41	36
2	Me	H	H	**249**	51	29
3	H	Me	H	**250**	14	30
4	H	Me	Me	**251**	21	41
5	H	Ph	H	**252**	-	38
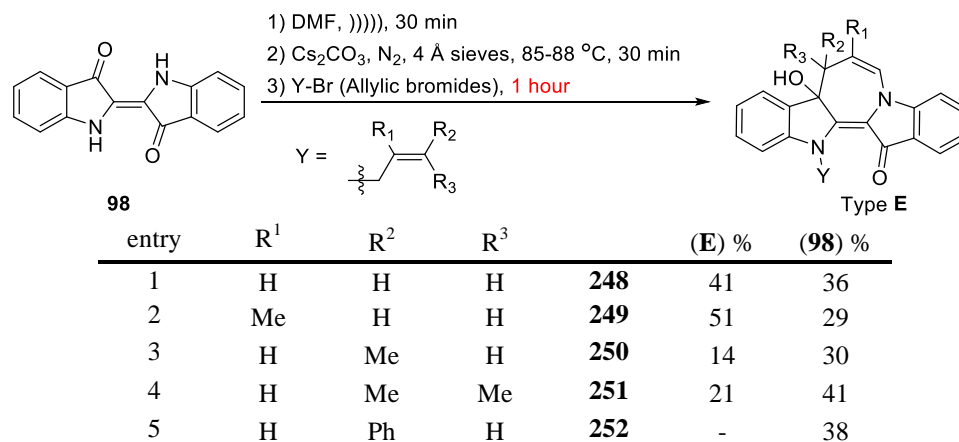
Scheme 46: The synthesis of azepinodiindolo systems by treating indigo with allyl bromides with a 1 hour reaction time.

Mass spectroscopy examination indicated a signal at *m/z* 330 (M⁺) in the EI spectrum, assigned to the molecular weight having the addition of two allylic units to indigo. Analysis of the ¹H NMR spectrum of **248** revealed a set of peaks at δ 4.94-5.03 and δ 5.12 ppm assigned as the terminal alkene with an integration of two protons, implying the other allyl unit has been cyclised. The methylene group at position 8 (Figure 19) was

assigned to the doublet at δ 2.46 ppm and the doublet of doublets centered at δ 2.97 ppm.
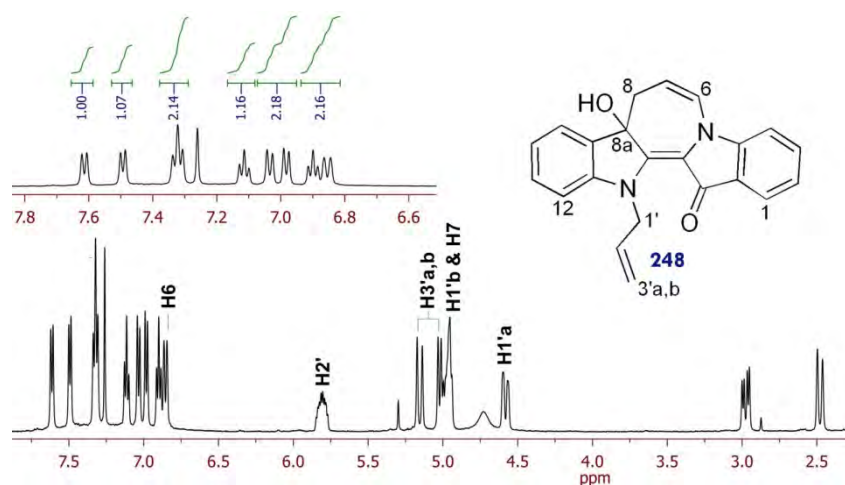
Figure 19: ^{1}H NMR spectrum of **248** and the expansion of the aromatic region

This confirms the existence of a ring as only one of the protons of this methylene can correlate with the olefinic proton of position 7 (Figure 19). This sole correlation was confirmed by analysis of the gCOSY spectrum (Figure 20).
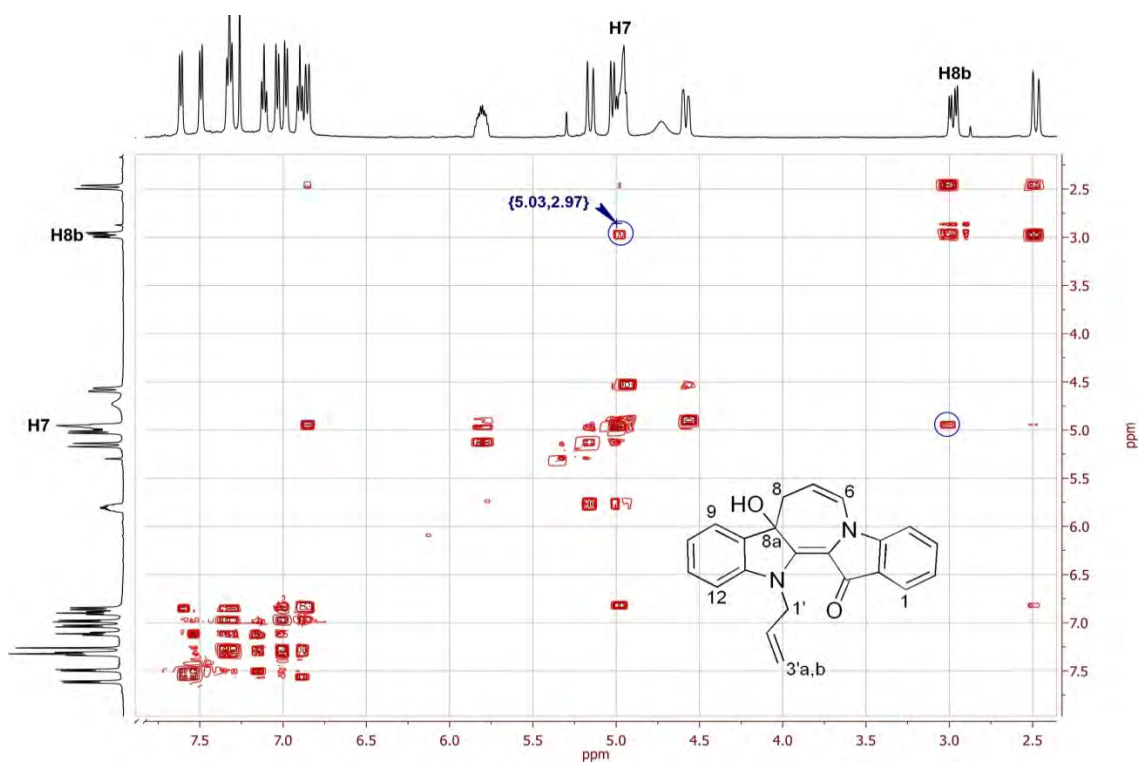
Figure 20: gCOSY spectrum for compound **248**.

A broad singlet at 4.73 ppm was assigned to the alcoholic proton - this peak disappeared upon treatment of the sample with D_2O. The aromatic region was found to contain nine protons, compared to the expected eight aryl protons. The additional doublet corresponded to H6, which was due to the deshielding effects of both the olefin and the adjacent indole nitrogen. (Figure 20, See Appendix 1 for full set of spectra).

The quaternary benzylic C8a was assigned to the peak at 81.3 ppm in the ^{13}C NMR spectrum, and found to be shifted downfield due to the effects of the attached alcohol substituent and its benzylic nature. Additionally the presence of one signal at 178.5 ppm in the carbon spectrum confirmed that the structure contained only one carbonyl group. Analysis of the HMBC spectra revealed strong correlations between H9 and C8a (magenta), H8 and C8a, and a weaker correlation between H6 and C4a (green). Also the other key correlation in HMBC was the three bond correlation between the H1' methylene and quaternary C13a confirmed the position of the uncyclised N-allyl unit (Figure 21, red).
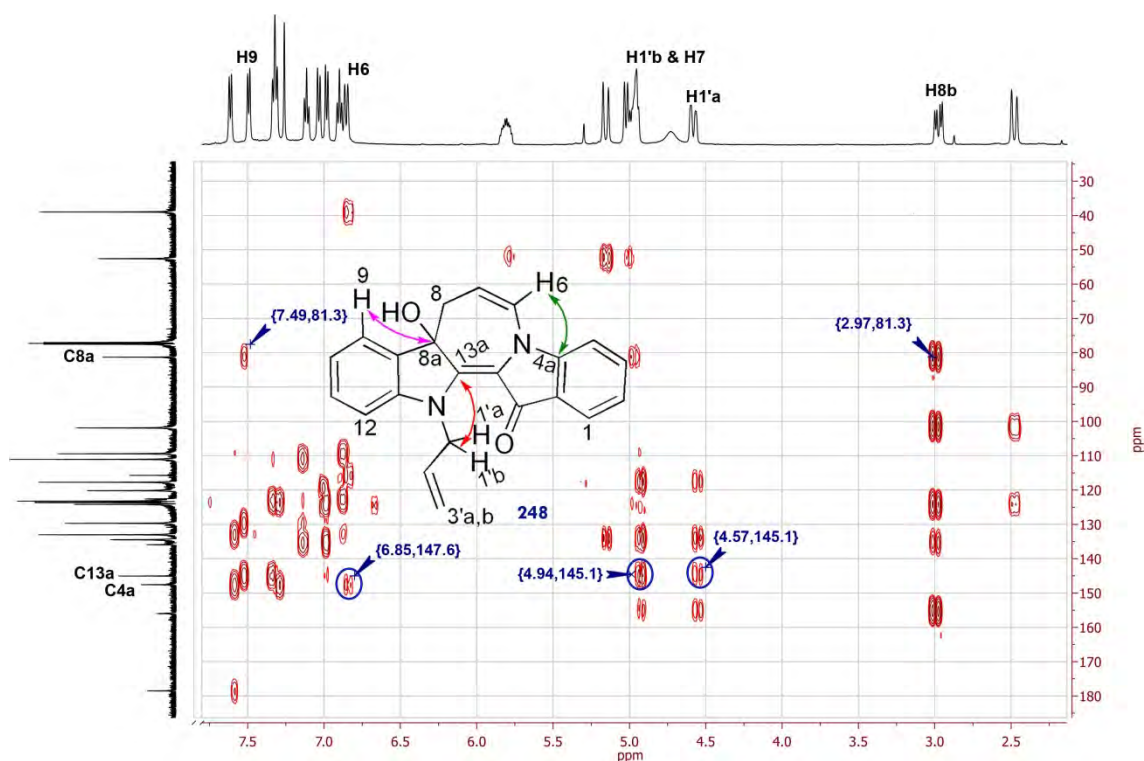
Figure 21: HMBC spectrum for compound **248**.

Interestingly, when 2-methyl-3-bromo propene was used as the allylic substrate, the yield for compound **249** increased to 51%, isolated from two fractional recrystallisations. Conversely, the use of crotyl bromide yielded 14% of the structure **250**, indicating the steric hindrance from the terminal methyl group had hampered the cyclisation to form the dihydro-hydroxyazepine ring. All of these heterocycles exhibited a red colour and formed monoclinic crystals from pet. spirit/EtOAc (9:1).

The structure of compounds **248**-**250** (Type **E)** were characterised by extensive 2D-NMR analysis. Elucidated structures were confirmed by X-ray crystallography analysis (Figure 21).

rel-**248**

rel-**249**

rel-**250**
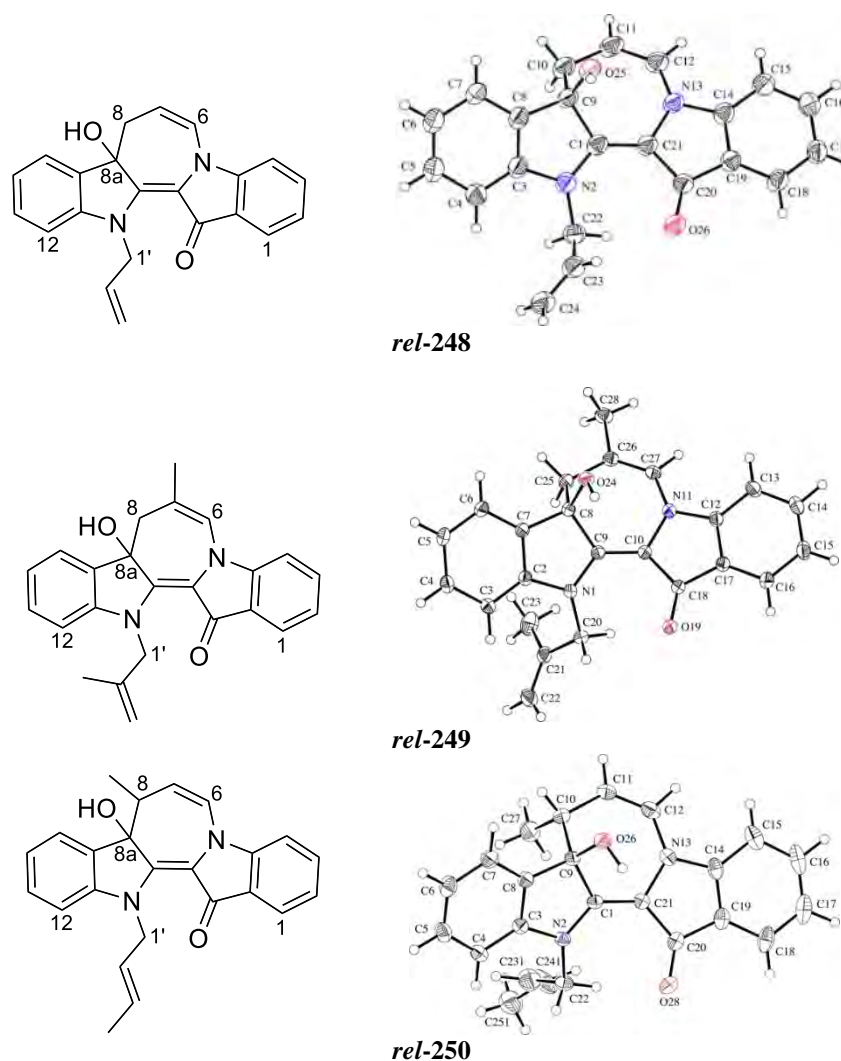
Figure 22: The X-ray crystal structure of **249-251**.

In the case of use of dimethylallyl bromide, a bright orange compound was isolated **251** (21%) with the structure lacking the *N*-allyl substituent. An additional novel heterocyclic derivative **253** was isolated in 26% (Scheme 47).
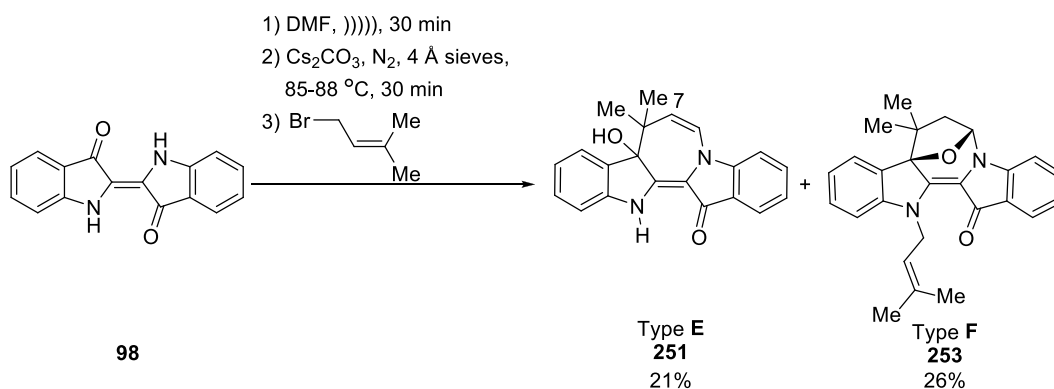
Scheme 47: The synthesis of the bridged tetrahydrofuran heterocycle **253** from indigo and 4-bromo-3-methylbut-2-ene.

Compound **251** was isolated as an orange-red powder with strong fluorescence under the UV light (365 nm). The peak at *m/z* 330 (M+) in the MS (EI) was assigned to the molecular ion which indicated the addition of one dimethyl allyl unit to the indigo core. The ^{1}H NMR spectrum contained one signal for the two CH$_3$ groups with an integration of 6 protons at 0.80 ppm. The absence of the corresponding signal for N-CH$_2$ and presence of the typical shifts of H6 at δ 6.83 ppm (doublet) and H7 at δ 4.84 ppm (doublet) indicated the cyclisation of the dimethyl allyl moiety. (See appendix 1 for the full set of spectra). Slow recrystallisation of **251** from pet. spirit/EtOAc (9:1) deposited X-ray quality crystals. The X-ray structure of compound **251** is shown in Figure 23 (see Appendix 2 for X-ray crystallographic data).
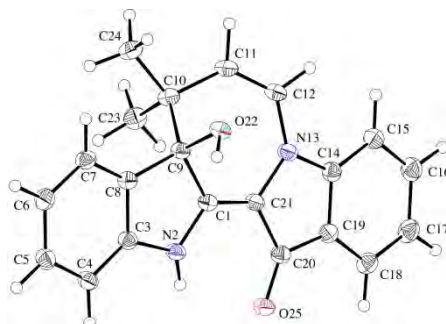
Figure 23: The crystal structure of the dihydroazepinodiindole **251**.

The epoxyazepinodiindole **253** was obtained in 26% yield as a red powder. The peak at *m/z* 398 (M+) in the MS (EI) spectra was assigned to the molecular ion and indicated the addition of two dimethylallyl systems to the indigo scaffold. IR spectrum revealed that the structure lacked OH or free NH groups. The intense colour suggested that the central double bond was intact with the extended conjugation, giving rise to the intense colour. ^{1}H NMR analysis showed a signal at 6.02 ppm which was assigned to the deshielded proton of H6. The ^{1}H spectrum also revealed a total of eight proton signals in the aromatic region. A doublet at 2.07 ppm and the doublet of doublet at 2.36 ppm were assigned to H7a and H7b respectively. From gCOSY spectrum, correlation of H6 with one of the protons of the H7 (annotated in blue) was attributed to the restricted ring system (Figure 25).

The ^{13}C NMR spectrum contained one peak in the region at 177.5 ppm, corresponding to the presence of one carbonyl functionality. Key to the structural elucidation were NOESY experiments which showed correlations between the aromatic H4 proton and the H6 bridgehead proton (Figure 25 and 26, magenta) - the same H6 proton correlated strongly with one H7 and weakly with the second H7 proton suggesting a -CH$_2$-CH-arrangement in a conformationally restricted ring, with the weak correlation assigned to the *transoid* arrangement of protons and the strong correlation to the *cisoid* configuration (Figure 25 and 26, blue). The other significant NOESY correlation was assigned between H1 and H9 of the benzene ring (Figure 25 and 26, green). In addition, significant 3-bond correlations in the HMBC spectrum were observed between H6 and the quaternary C8 and H7 and the benzylic C8a. The downfield shift of the peak at 92.7 ppm, assigned to C8a, is consistent with the benzylic carbon being also attached to an oxygen atom (See appendix 1).
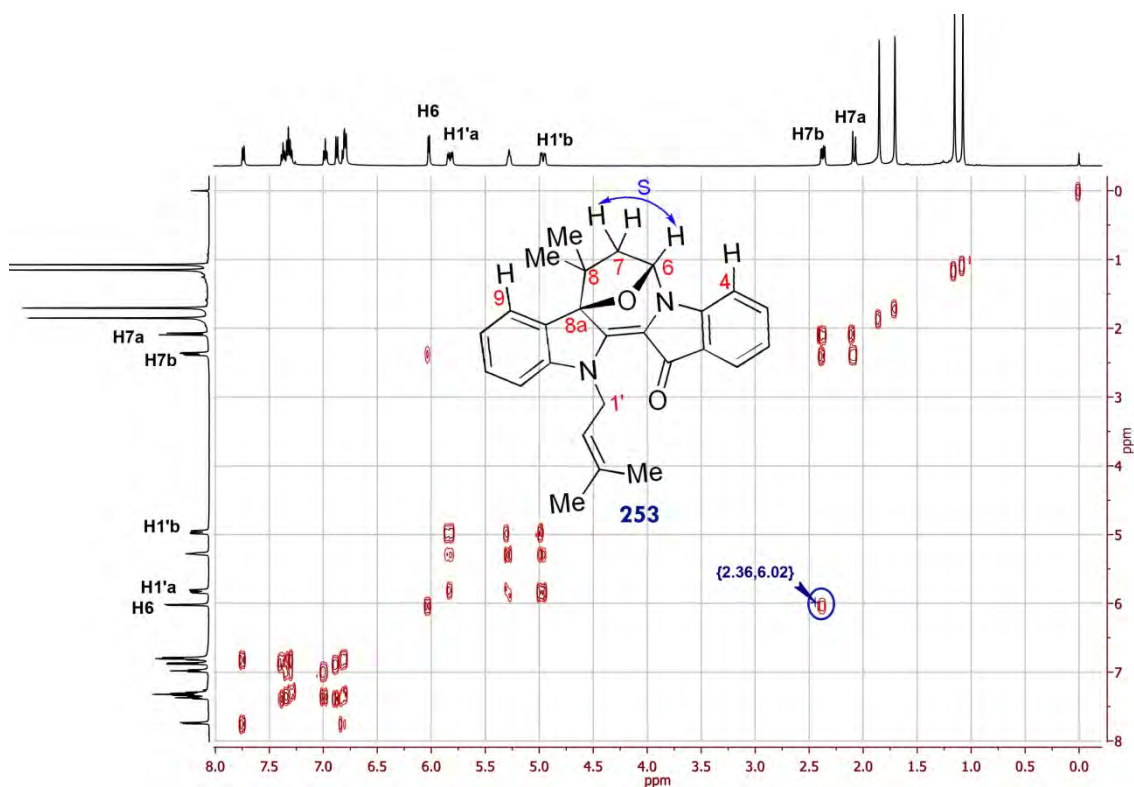
Figure 24: gCOSY spectrum for compound **253**.
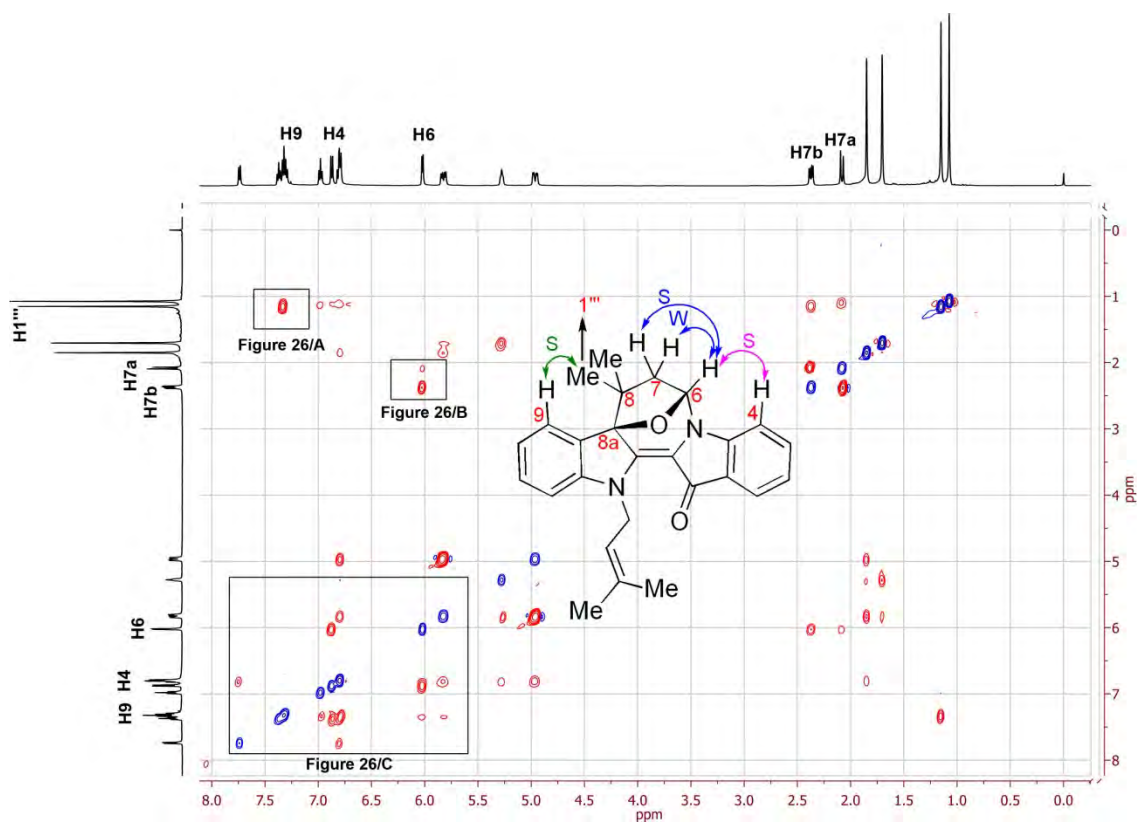
Figure 25: NOESY spectrum for compound **253**.
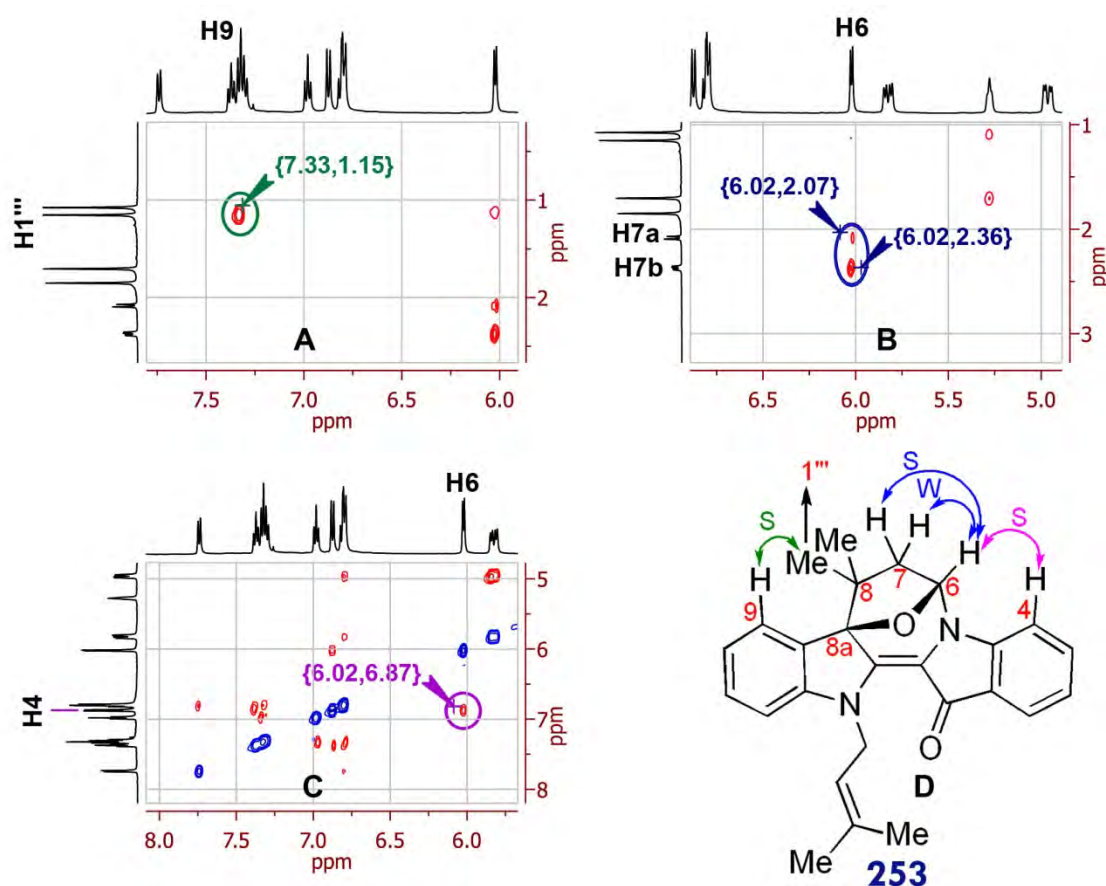
Figure 26: **A**-**C**: Expansion of the NOESY spectrum and **D**: demonstration of the key correlations.

To predict the three-dimensional structure of **253**, the structure was modelled with the aid of Spartan 10, (v1.1.0, Wavefunction Inc software) and the geometry optimisation was performed using Hartree Fock theory at the 6-31G* level. The modelled 3D structure for **253** (Figure 27) showed the two indolic units to be in a slightly bent orientation to each other, with the 7-membered ring in the same curved line. The 5-membered tetrahydrofuryl ring lies in a perpendicular fashion to the curved backbone and is in a puckered conformation, typical of 5-membered aliphatic rings. The heterocycle is stable at room temperature and to air and moisture. This is the first example of the synthesis of such a bridged heterocyclic skeleton.
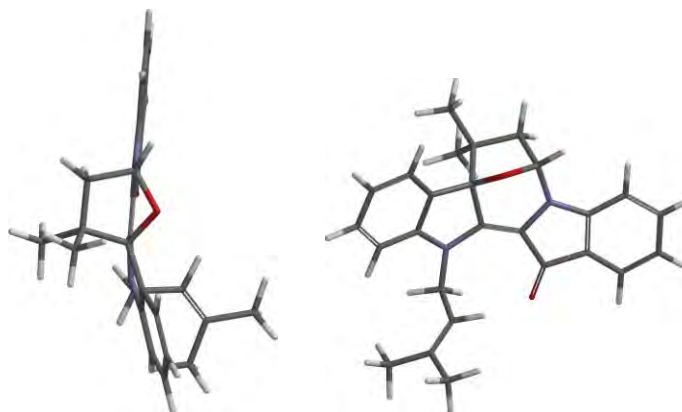
Figure 27: Modelled structure (Spartan 10, v1.1.0, Wavefunction Inc) of bridged indigo-tetrahydrofuran product **253**; Left: top view showing the tetrahydrofuran ring sitting directly over the indigo skeleton (vertical), which is itself twisted from planarity; Right: Front view.

The formation of **253** is an excellent example of the 'gem-dimethyl effect'[147] whereby the presence of that moiety enhances cyclisation.[148] This explains the formation of **253** and the absence of additional examples of such bridged derivatives when using other allyl reagents, as evidenced by the absence of a distinctive red-coloured product by TLC analysis. Interesting in this particular reaction is the induction of the gem-dimethyl effect in producing a bridged product from a cyclic starting material. Further evidence in support of the gem-dimethyl effect in the cyclisation to the bicyclic heterocycle **252** comes from analysis of computational models of the proposed starting materials to cyclisation (i.e. compounds **248**-**250** structures) and the bridged product **253** (Table 5). The ΔH_f of the gem-dimethyl substrate **251** (262.7 kJ/mol) is remarkably similar to the product bicycle **253** (263.0 kJ/mol) whereas the ΔH_f for the corresponding theoretical Type F product (**253**) (295.3 kJ/mol and 351.2 kJ/mol) arising from cyclisation of monomethyl (**250**; 289.2 kJ/mol) and 8-methylene (**248**; 338.3 kJ/mol) Type D starting materials respectively, are of higher energy. Further, the distance between the proposed *O*-nucleophile and C6-imine electrophile in the proposed intermediates to cyclisation (Compound Z, see Scheme 53) is least for the gem dimethyl compound **253** (3.042 Å)

and larger for the monomethyl compound **250** (3.056 Å) and **248** (3.180 Å). Each of these values indicates the *O*-cyclisation to be most favourable in the case where the allyl unit is terminally-substituted with a pair of methyl groups.

Table 4: Calculated values of ΔH$_f$ of Type **E** (**248,250-1**) substrate and Type **F** (**253**) products; the distance between nucleophile (O) and electrophile (C) in the proposed key intermediate of the reaction, structure Z.

C8 substitution pattern	ΔH$_f$ Substrate (Type **E**) kJ/mol	ΔH$_f$ cyclic aminals (Type **F**) kJ/mol	Distance between (C8a) O and C6: (Structure **Z**) (Å)
2 x Me (**251**)	262.715	263.010 (**253**)	3.042
1 x Me, 1 x H (**250**)	289.247	295.266	3.056
2 x H (**248**)	338.331	351.245	3.180

With cinnamyl bromide, an additional deviation in the product outcome (Type **G**) was observed in 16% yield, identified as **254** (Scheme 48) and is a new variation on the spiroheterocycle of Type **A**.
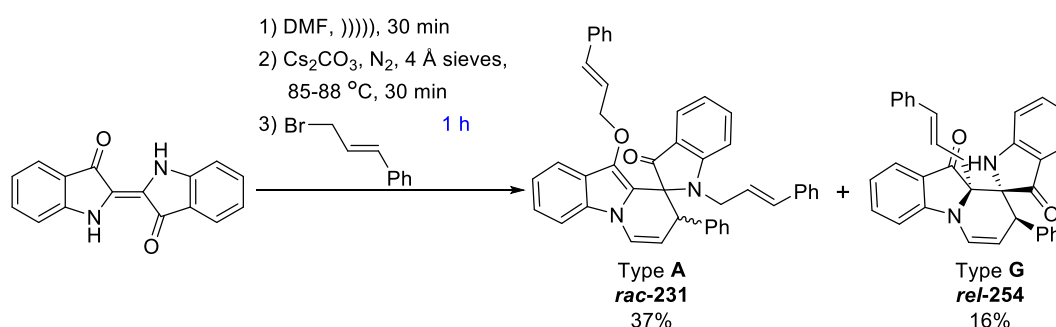
Scheme 48: Reaction of indigo with cinnamyl bromide yielding two spiro-based derivatives.

A signal at *m/z* 494 (M$^+$) in MS (EI) was assigned to the molecular ion, confirming this yellow compound corresponded to the addition of two cinnamyl units. ^{1}H NMR analysis revealed a total of 19 proton signals in the aromatic region whereas the expected number of aromatic protons from this alkylation was 18; eight aromatic protons from

the starting material indigo (**98**), and ten protons from the addition of two cinnamyl

moieties. The additional proton signal with a chemical shift of δ 7.42 ppm was assigned

to the H6', deshielded due to the quaternary amine. A sharp singlet at 7.86 ppm was

assigned to the free NH. A distinctive singlet at 4.12 ppm and a doublet at 4.98 ppm

both with an integration of one proton were assigned to H8' and H7' respectively. This

splitting pattern suggested the presence of a CH-CH-CH unit with restricted rotation

across the carbon-carbon bonds. This confirmed the cyclisation of a cinnamyl unit on

C2'. The upfield multiplet at 2.98-3.10 ppm was assigned to the H1' methylene. The

chemical shift of this methylene group showed a shift around 2.1 ppm compared to the

O-CH$_2$ protons in the spiro product (Figure 28, See appendix 1 for full ^{1}H NMR

spectrum and the full set of spectra for compound **254**). This, and the absence of the

gCOSY correlation to this methylene group, suggested the position of the other

cinnamyl unit on a quaternary carbon (Figure 29).
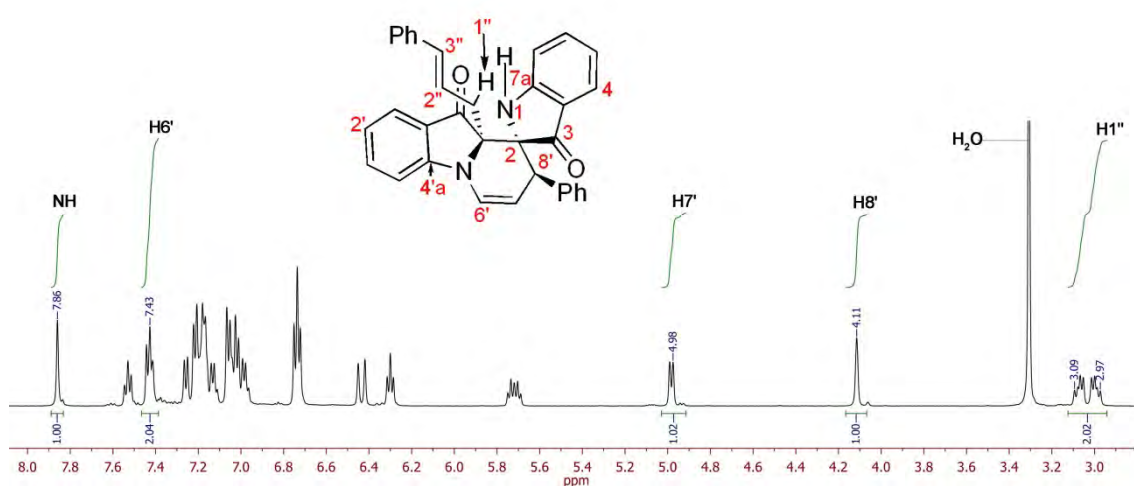
Figure 28: Expansion of ^{1}HNMR for compound **254**.

Analysis of the ^{13}C NMR spectrum showed the appearance of a signal at 68.9 ppm

corresponding to the C2 quaternary carbon. Signals at 122.5 ppm and 164.1 ppm were

assigned to the C4a and C7a quaternary carbons. Also revealed was the presence of two

peaks at 197.5 and 197.8 ppm, assigned to two carbonyl groups. This eliminated the substituent pattern as defined by Type **A** spiro compounds.
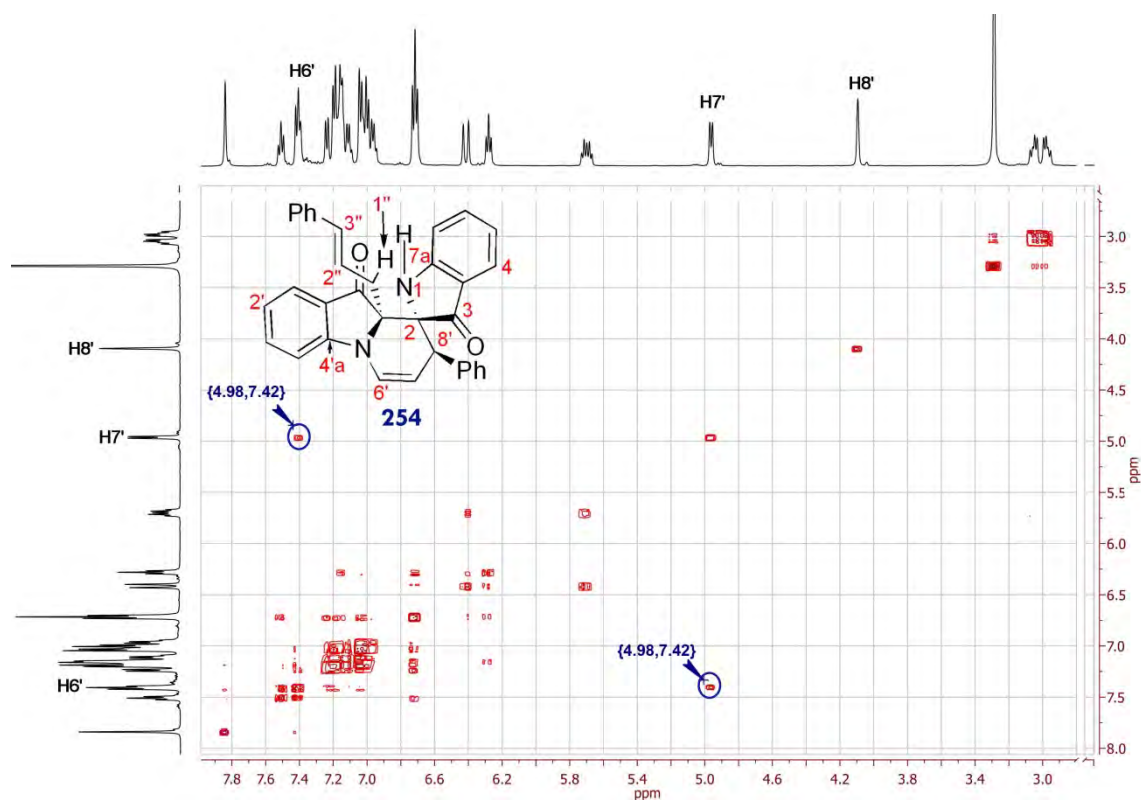
Figure 29: gCOSY spectrum for compound **254**.

Analysis of the HMBC spectrum of the *C*-allylated product **254** revealed a strong 3-bond correlation (Figure 30/A, annotated with red) between the C2 spiro carbon at 68.9 ppm and the cinnamyl methylene H1". The proton of the free NH showed a strong correlation through the three bonds (annotated with blue) with C3 of the carbonyl group and the C7 of the aromatic ring (Figure 30/B). A correlation (annotated with green) between the quaternary carbon C7a and H4 (Figure 30/C) and the strong signal for the correlation (annotated with magenta) of the C4'a and H6' (Figure 30/C) were amongst the information observed from the gHMBC spectrum.
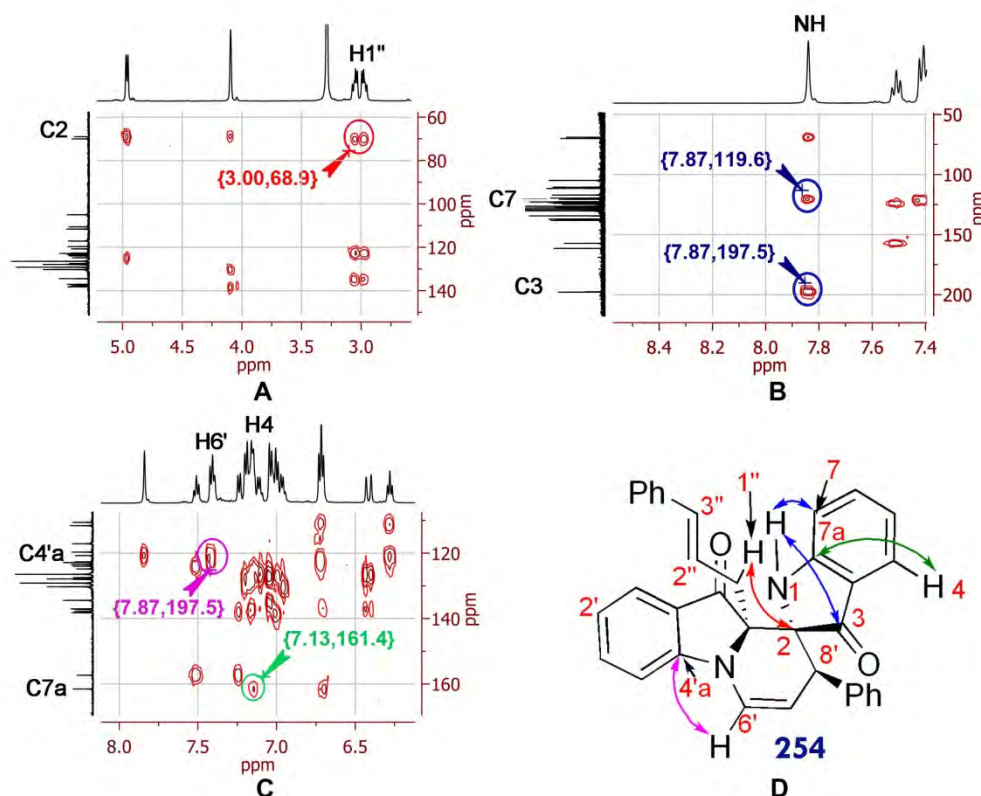
Figure 30: Structural analysis of compound **254**; Key HMBC correlations in support of the proposed structure. **A**: Three bond correlation of C2 and H1. **B**: gHMBC correlations of NH and C3 carbonyl and C7 of the aromatic ring. **C**: Correlation between H6 - C4'a and three bond correlation of the quaternary C7a and H4. D: Compound **254** and selected gHMBC correlations with colour coded arrows.

The presence of one set of peaks in the ^{13}C NMR spectrum indicated the presence of a single enantiomeric pair of isomers, and analysis of the X-ray crystal structure (Figure 31) showed that the relative stereochemistry was either all *R* or all *S*.
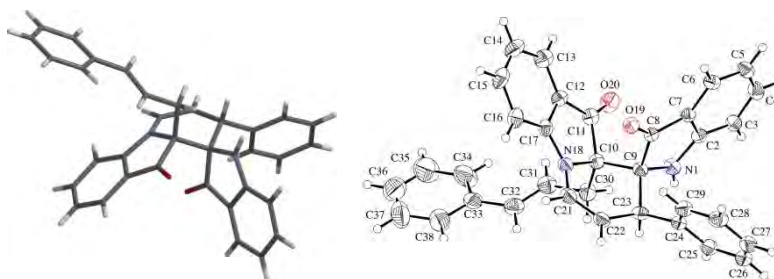
Figure 31: **Left**: Modelled structure of **254** showing *cisoid* configuration of the NH and the cinnamyl substituents; **Right**: X-ray crystal structure of **254** showing the *transoid* NH/C8'-phenyl substituent disposition.

This places the cinnamyl substituent in a *cisoid* orientation to the isooxindolic N-H and a *transoid* configuration with the C8' phenyl substituent. This configuration allows for the bulky cinnamyl substituent to swing away and be on top of the concave structure.

2.2.3   Reaction of indigo and allylic bromides; Three (3) hour reaction

Analysis of the product outcomes of the corresponding 3 hour reactions of indigo with different allyl bromides (Scheme 48) showed the synthesis of the known 8*H*,16*H*-pyrido[1,2,3-*s*,*t*]indolo[1,2-*a*]azepino[3,4-*b*]indol-17-one heterocycles, which arise from the addition of two allyl units with one cyclising to form a 6-membered ring and the other to form a 7-membered ring. By this methodology however, it was possible to enhance the yield for the production of these reasonably complex heterocycles to a consistently repeatable with the approximate yield of 70% for azepinodiindolone **232** and **233**. Notably, the olefinic terminal position remains unsubstituted to achieve these outcomes. The addition of substituents to the terminal positions of the allyl reagents (e.g. crotyl, 1,1-dimethylallyl, cinnamyl) results in an inversion in the major product to the known spiro heterocycles **227**, **228** and **229**, albeit with a decreasing absolute yield (65% to 37%) with increasing steric presence. The yield of 37% for the cinnamyl derivative **231** is a significant improvement on that previously reported of 12%, whereas the corresponding derivative **230** was previously unknown (not synthesised) but in this study, produced a yield of 42% (Scheme 49). The previously reported low yields of these spiro-based heterocycles were accompanied by significant quantities of indigo starting material. Analysis of the mixture also confirmed the new conditions are optimal for complete consumption of indigo as no starting material was recovered.

1) DMF,))))), 30 min
2) Cs$_2$CO$_3$, N$_2$, 4 Å sieves,
   85-88 °C, 30 min
3) Y-Br (Allylic bromides), 3 hours

Y =

Type **A**
227-231

Type **B**
232-236
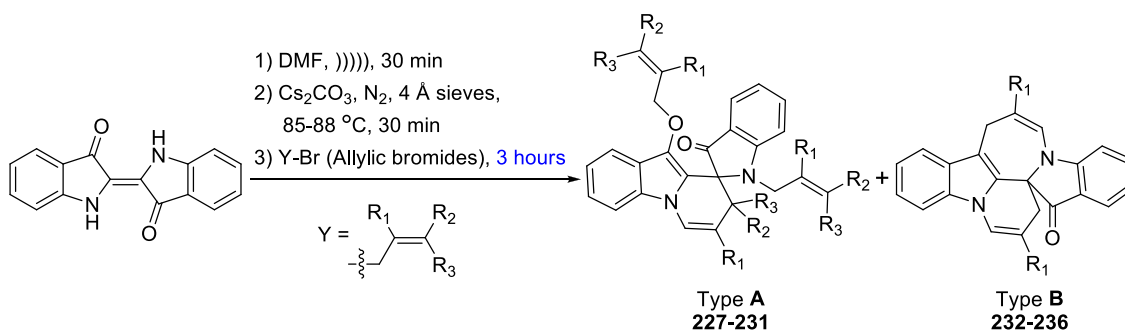
R$_1$	R$_2$	R$_3$		A %		B %
H	H	H	**227**	15	**232**	72
Me	H	H	**228**	15	**233**	69
H	Me	H	**229**	65	**234**	-
H	Me	Me	**230**	42	**235**	-
H	Ph	H	**231**	37	**236**	-

Scheme 49: Distribution of the products of the reaction of indigo and allylic bromides under the modified reaction condition.

2.3   Mechanistic discussion

The proposed mechanism for the formation of Type **A** spiro derivatives is outlined in Scheme 50 using allyl bromide as the allylic reagent. After initial *N*-allylation of indigo **98** to give Type **D** compounds, two possible pathways can be devised to the spiro Type **A** compound. Path A illustrates a proton shift from the indigo N-atom to the indolic C2 position – this structure is stabilised by enolisation to the 3-hydroxyindole moiety. *N*-Allylation of the keto tautomer gives rise to **T**, which undergoes an ene-type reaction producing the spiro unit. The relatively weak nucleophile in this reaction (the alkene) is heavily compensated by the electrophilic carbon which is activated by the iminium cation (red), and additionally by the adjacent carbonyl (red), inducing a highly reactive electrophilic carbon. Final allylation of the 3-hydroxyindole under basic conditions produces the final spiro compound. Path B starts from the *N*-allylindigo and following deprotonation produces the *O*-allylated derivative after electron delocalisation. Ene cyclisation onto the doubly activated (red) C2 position produces the final spiro heterocycle (Scheme 50).
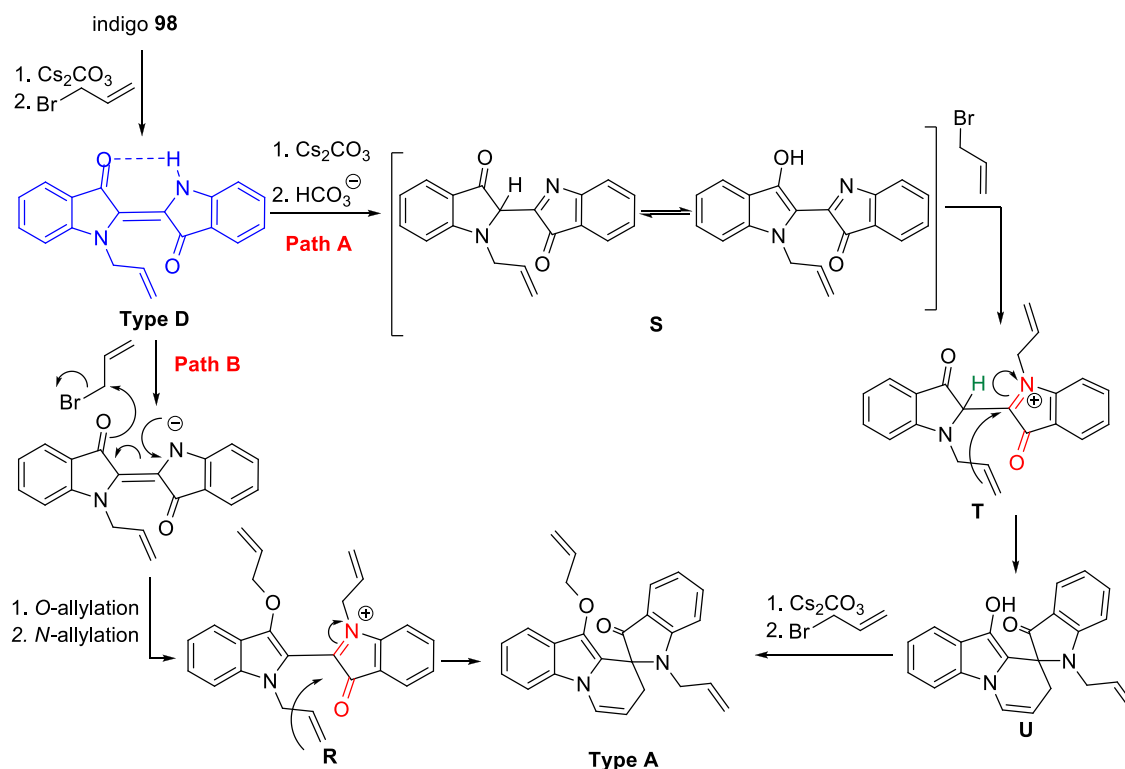
Scheme 50: Proposed mechanism for the synthesis of Type **D** and Type **A** spiro heterocycles.

In the case of the spiro products, an exception is the spirocycle **254** derived from cinnamyl bromide reaction with the intermediate **R**. At the *O*-cinnamyl stage, the formation of two highly stabilised radicals could provide a driving force for thermally-induced homolytic cleavage of the cinnamyl unit and a 1,3-shift leading to the Type **G** structure (Scheme 51).
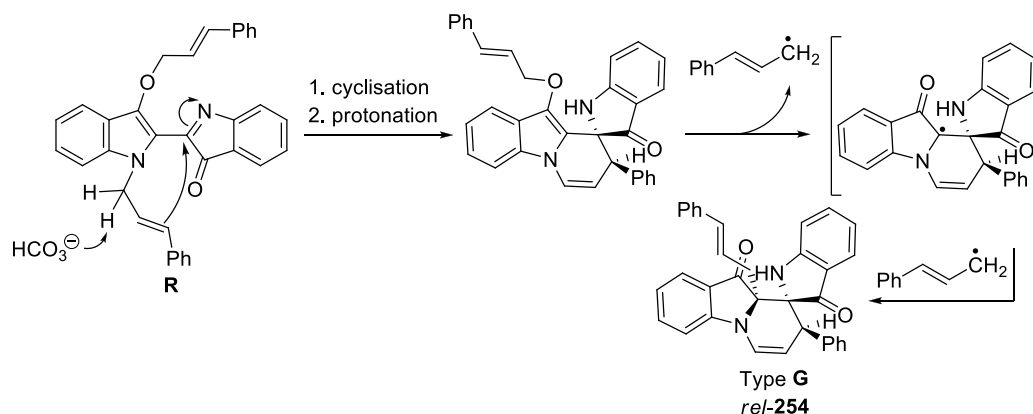
Scheme 51: Proposed mechanism for the formation of **254** from intermediate **R**.

While direct anionic *C*-allylation may also occur (at Step 1 of Path B, Scheme 49), steric considerations and the non-observance of this product with other allylic bromides points to a later intervention of a 1,3-rearrangement process.

Interestingly, it is noted that the C2 proton (green) in **T** should be highly acidic, being flanked by a carbonyl and the iminium moiety – although this acidity plays no role in our proposed mechanism, we might expect H^+ loss to occur – this is not apparent unless the resulting *N,N'*-disubstituted indigo undergoes re-protonation by HCO_3^- to give **T** (Scheme 50).

Scheme 52 illustrates a tentative proposed mechanism for the synthesis of the heterocycles **233** (Type **B**) and **249** (Type **E**). Starting from the intermediate **T**, deprotonation produces an ylid, which stabilises the intermediate and provides a formal negative charge for subsequent cyclisation onto the carbonyl forming the 7-membered ring. Path C illustrates dehydration and cyclisation onto the activated iminium cation to form the heterocycle **233**, supported by a separate experiment (See Scheme 54). Path D describes the base-induced deprotonation to form the neutral product **249** (Scheme 52).
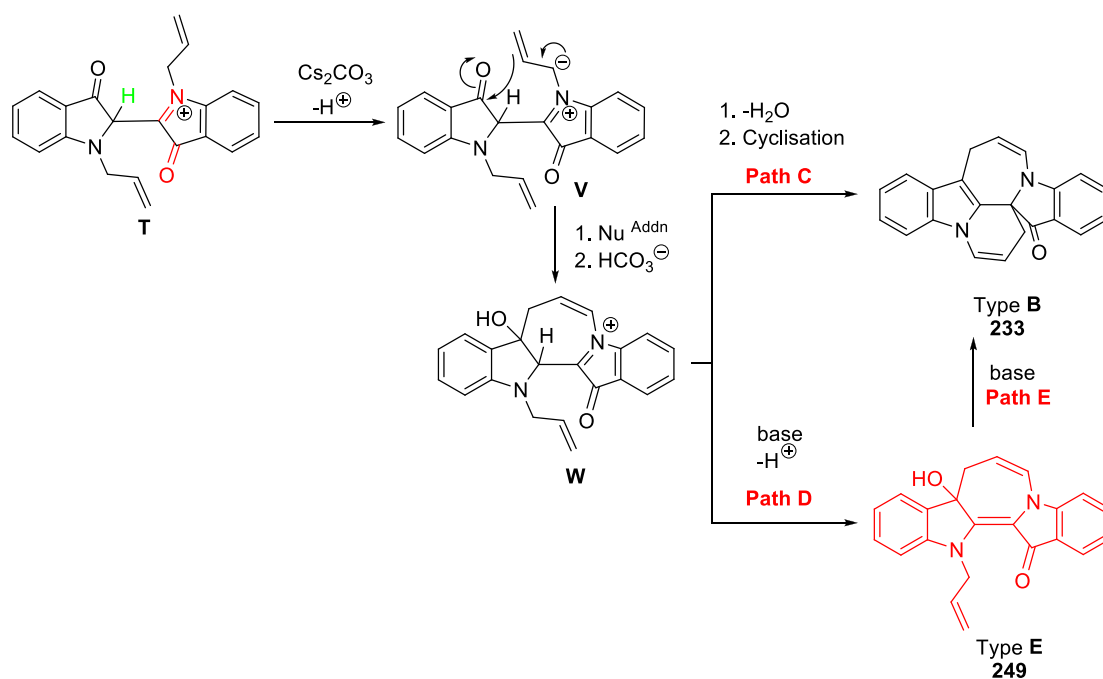
Scheme 52: Proposed mechanism for the synthesis of Types **B** and **E** heterocycles.

In the instance of the dimethyl allyl analogue **251**, reversible protonation (HCO$_3^-$) of the enamine (**Z**, Scheme 52) and deprotonation could occur, leading to intramolecular cyclisation to produce the novel bridged heterocycle **253** with this reaction promoted by the gem-dimethyl effect (Scheme 52).
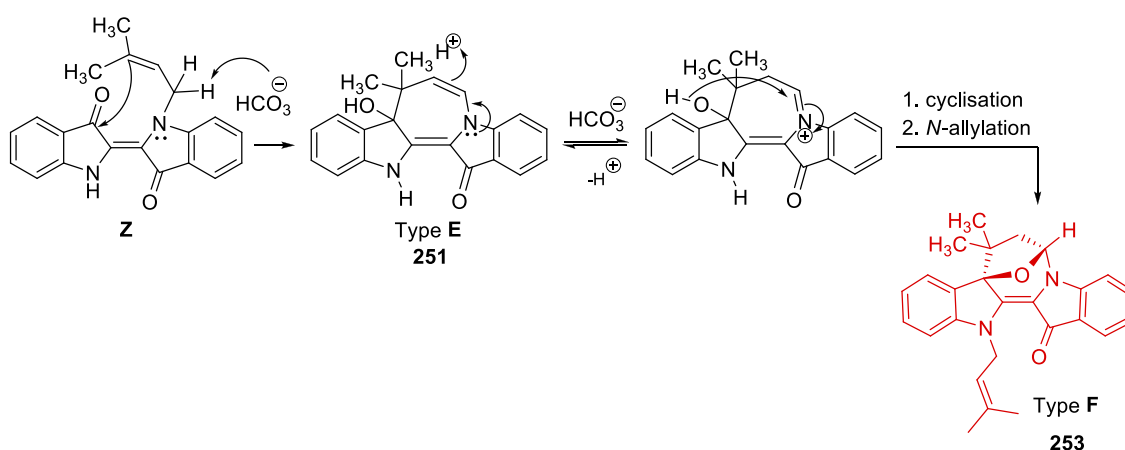
Scheme 53: Proposed mechanism for the formation of **254** (Type F). The order of protonation and allylation is undetermined and the cyclisation is promoted by the gem-dimethyl effect of gem-dimethyl substituted substrates.

While dehydration of **248** could conceivably also occur, no evidence for the expected azepine product was seen. An attempt to separately dehydrate **248**, by reaction with P$_2$O$_5$ resulted in an inseparable mixture. However, the same compound under basic conditions (Cs$_2$CO$_3$) in DMF at 85-87 °C (3 h) produced **232** in 89% yield (Scheme 54), thereby providing evidence that **248** and analogues could also be intermediates in the synthesis of Type **B** compounds as proposed in Scheme 52 (Path E).
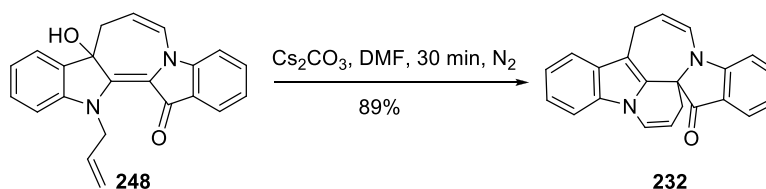
Scheme 54: Conversion of **248** to **232** under the effect of base in DMF.

Additionally, in support of the pathways proposed, the reaction of *N*-allylindigo **243** (Type **D**) under the typical cascade reaction conditions for these compounds gave **232** in 59% yield and the spirocycle **227** in 8% yield (Scheme 55).
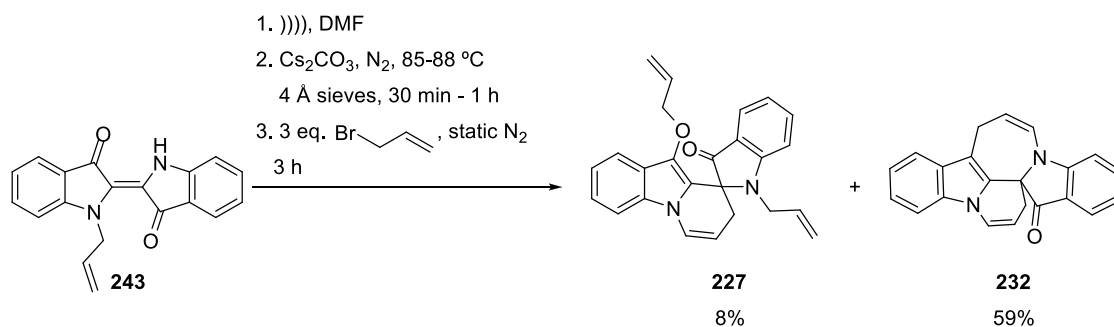
Scheme 55: Supportive reaction to validate the path **D** of the proposed mechanism.

2.3.1 Impact of steric constraints on the product distribution

Considering **T** (Schemes 50 and 52) as key intermediate, there are two possibilities of cyclisation; a nucleophilic addition of alkene to the carbonyl (**a**) or cyclisation of alkene to the iminium ion (**b**). According to the Bürgi–Dunitz modelling,[149] the attack of a nucleophile on a carbonyl group is defined by the Nu-C-O bond angle, and is optimum when the angle of attack is 107º.[149] Facile rotation across the central single bond of **T** provides an arrangement aiding this attack. The presence of the methyl or phenyl substituents hinders the attack on carbonyl group and cyclisation of alkene to the iminium ion becomes more favoured (Scheme 56). Conversely free rotation across the C2-C2' bond (**T**) positions the two indole units in a perpendicular angle which provides enough space for the attack of the nucleophile on the iminium ion with little steric hindrance.
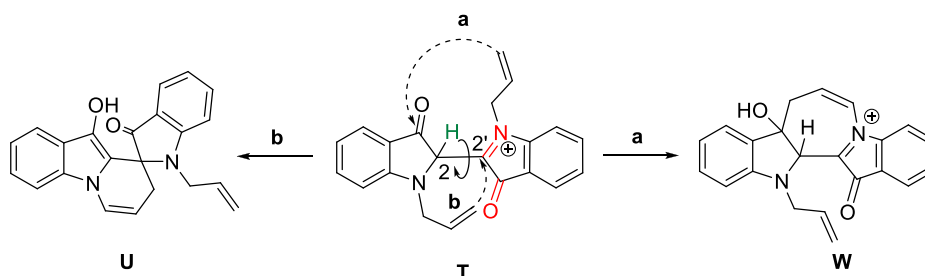
Scheme 56: Qualitative demonstration for two possible cyclisation.

This can be observed by the lower yields in formation of Type **E** products for crotyl and dimethyl and its absence for cinnamyl bromide. In a comparative experiment,

compounds **248** and **250** were reacted with Cs_2CO_3 in DMF for 30 min. Analysis of the

reaction mixture for compound **248** yielded yellow crystals of **232** while the reaction

mixture for **250** showed no change (Scheme 56).
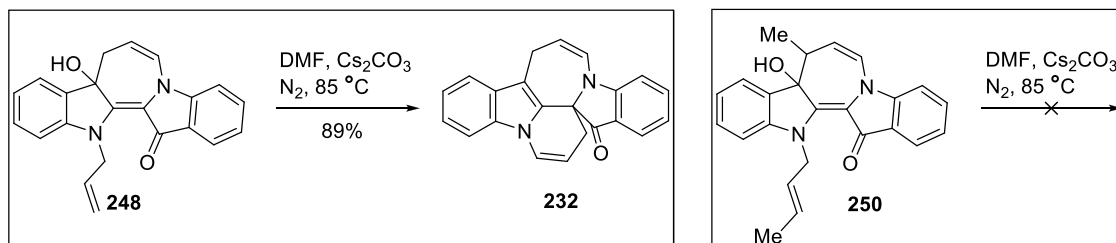
Scheme 57: Comparison of the possibility of the cyclisation of **249** and **251** in order to examine the steric hindrance effect on conversion of Type **E** compounds to Type **B**.

This experiment demonstrated the limitations that exist in Type **E** compounds to

undergo the final cyclisation to realise the azepino-indolone system (Type **B**). After the

first intramolecular nucleophilic attack on the indolone carbonyl and formation of the

seven-membered ring that bridges the two indole units, there is limited space for the

second allylic unit to attack to the iminium ion. To estimate the distance between the

terminal alkene and the carbon of the iminium ion of intermediate **W**, calculations were

performed using Spartan software, at the molecular mechanics level. By analysing

diverse conformations of intermediate **W**, the distance range between the terminal

carbons of the allyl group and iminium carbon (C1" and C2) was determined as 1.23 -

1.82 Å (Figure 32, **W**). This modelling revealed that the presence of any terminal

substituent on C1" hinders the attack and clashes with carbonyl C3 (Figure 32). This

further supports the result of the reaction of **250** and base which failed to produce

azepino-indolone (Type **B**) product. As illustrated in Figure 32, modeling of the diverse

conformers of the spiro cycle showed the angle between the planes of the two indole

units to be 79-85°. This also supports the predominate formation of spiro product in the

instance of the reaction with crotyl bromide.
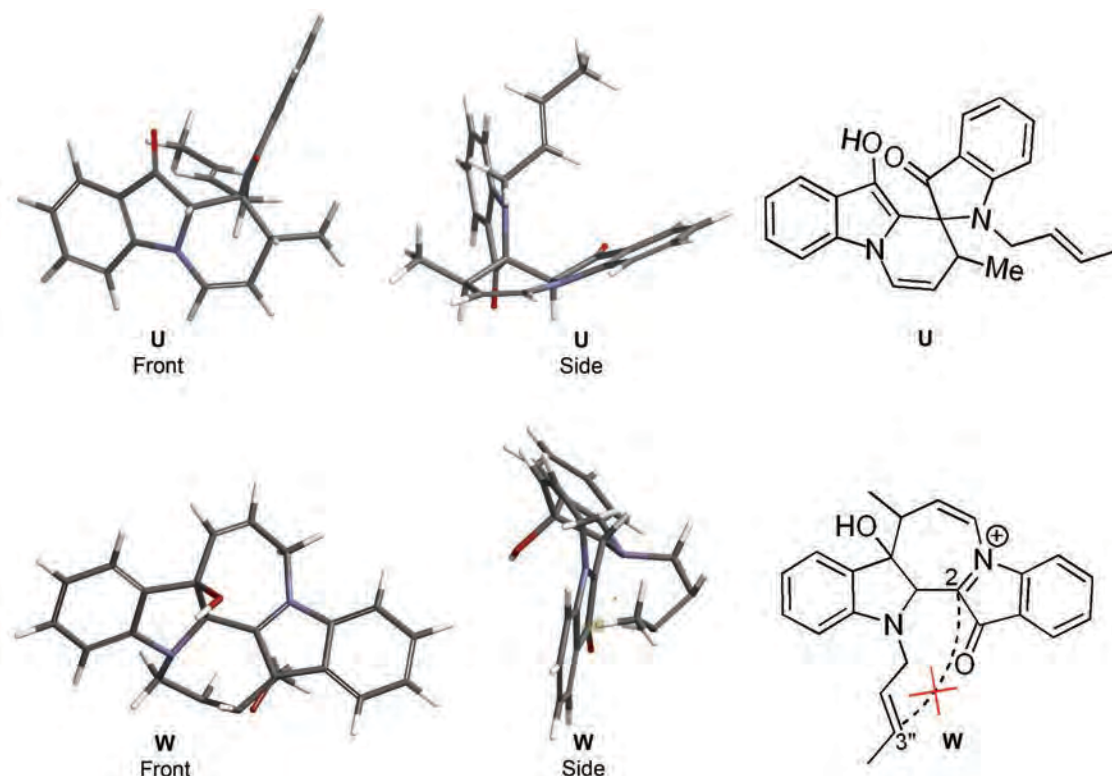
Figure 32: Computer aided modelling for intermediate **U** and **W** to compare the effect of the steric hindrance after formation of the spiro cyclic system or the seven membered rings.

In order to further investigate the effect of steric hindrance on the type of the cyclisation, the indigo substrate was changed to *N*-methylindigo. It was speculated that the limited reaction sites would result in selective formation of a spiro (Type **A**) or a seven membered ring (Type **B**), if the steric hindrance played a substantial role. *N*-Methylindigo was synthesised under analogous conditions as the synthesis of mono allylated indigo. Therefore, a sonicated solution of indigo was added to pre-dried Cs$_2$CO$_3$ and molecular sieves. The resulting mixture was stirred at 85-87 °C for 30 min under an atmosphere of N$_2$. After deprotonation, 1.5 equivalents of methyl iodide were added and after 5 sec the reaction was quenched over ice. TLC analysis showed the formation of two products with no starting material remaining. Fractional recrystallisation of the crude resulted in isolation of (*E*)-1-methyl-[2,2'-biindolinylidene]-3,3'-dione (*N*-methylindigo) **255** (77%) as a blue precipitate. Also

isolated was (*E*)-1,1'-dimethyl-[2,2'-biindolinylidene]-3,3'-dione (*N,N*'-dimethylindigo) **179** in a 12% yield as a dark green precipitate (Scheme 58).

1.)))), DMF, 30 min
2. Cs$_2$CO$_3$, N$_2$, 85 °C, 30 min
3. MeI, 5 sec

98

255
77%

179
12%
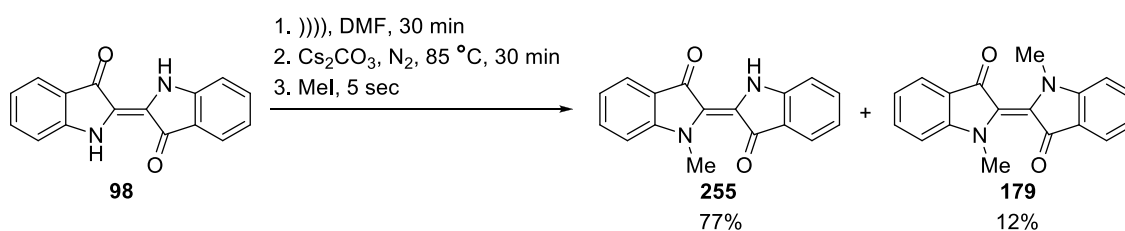
Scheme 58: The synthesis of *N*-methylindigo **255**.

In two different experiments, a solution of *N*-methylindigo was treated with allyl bromide under the identical reaction condition as described above. Purification of the reaction mixture resulted in isolation of **256** whereas the reaction with crotyl bromide yielded spiro type compound **257** as major product (Scheme 59).

DMF, Cs$_2$CO$_3$
N$_2$, 85 °C

255

256 79%

DMF, Cs$_2$CO$_3$
N$_2$, 85 °C

257 78%
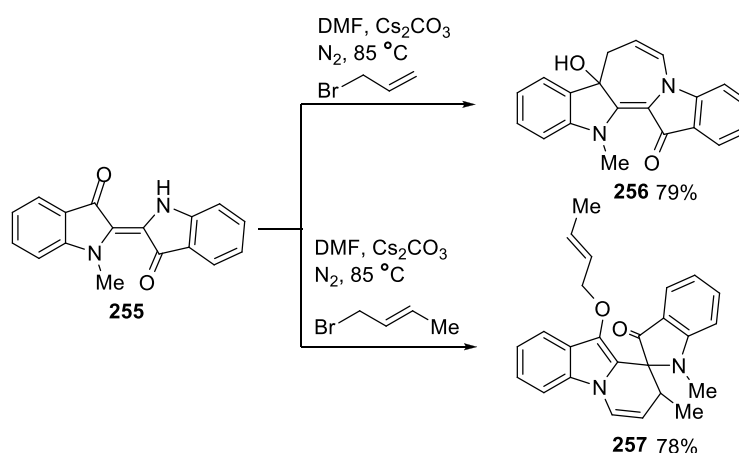
Scheme 59: Comparative experiments to investigate the effect of steric hindrance on the type of cyclisation in reaction of *N*-methylindigo and allyl and crotyl bromides.

Analysis of the mass spectrum of compound **257** showed a signal at *m/z* 316 which was assigned to the molecular ion. A sharp singlet at 3.37 ppm with an integration of three protons was assigned to the methyl group of the *N*-methyl indigo. A set of two doublets at 2.43 and 2.97 ppm were assigned to the H8 methylene group. Analysis of the gHSQC confirms that the both of these signals are attached to one carbon (See appendix 1). The aromatic region of the spectrum showed the presence of nine protons, with eight

assigned to the aromatic protons of the indigo core. The additional signal with the chemical shift of 6.84 ppm, deshielded by the adjacent tertiary nitrogen atom, was assigned as H6. This signal showed a gCOSY correlation to the multiplet at 4.90-4.95 ppm, assigned to H7 (Figure 31, annotated with blue). Interestingly, H7 has a single correlation with one of the H8 methylenes at 2.43 ppm (Figure 33, annotated in green). This proved the restricted rotation as the result of cyclisation of the allyl unit. The ^{13}C NMR showed a signal at 178.0 ppm, indicating the presence of only one carbonyl group.
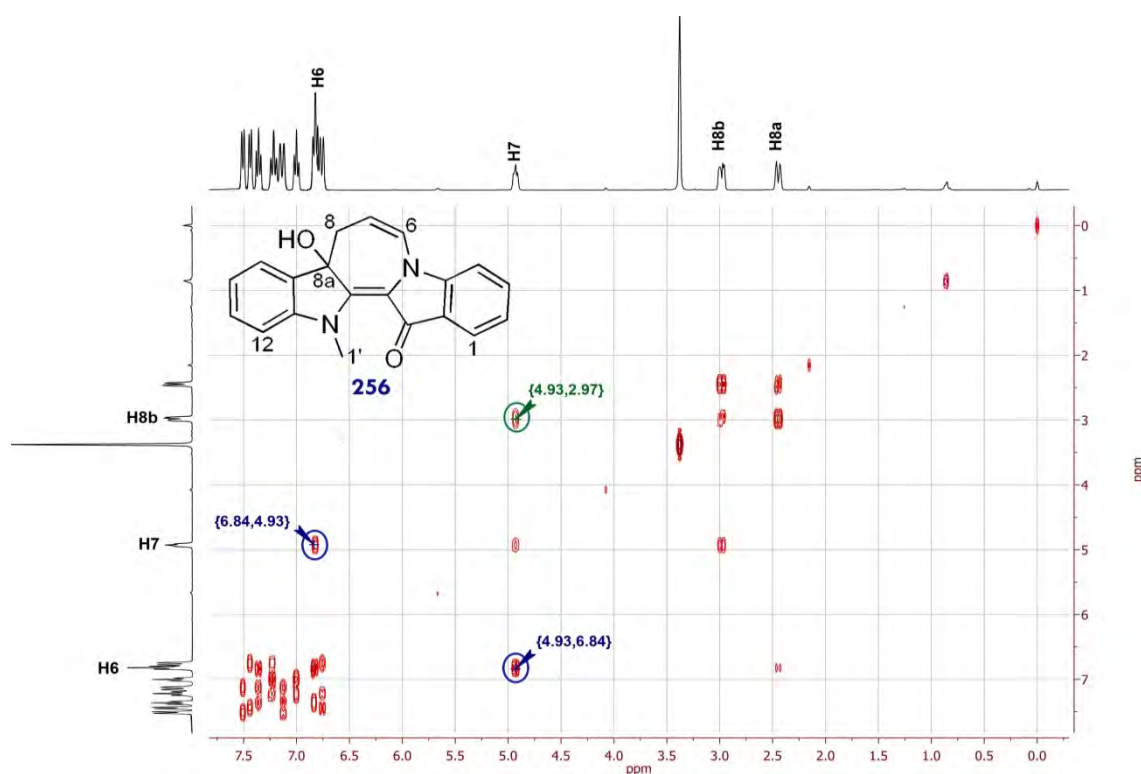
Figure 33: gCOSY spectrum for compound **256**.

In the case of compound **257** a peak at *m/z* 384 in the EI mass spectrum was assigned to the molecular ion which evidenced the addition of two crotyl units to the initial *N*-methyl indigo. Analysis of ^{1}H NMR spectrum showed two doublets at 0.99-1.01 ppm and 1.53-1.54 ppm with an integration of three protons assigned to the methyl groups from the addition of two crotyl units. A doublet at 5.14-5.15 ppm was assigned as the H7' proton. This signal showed a correlation with a proton in the aromatic zone at 7.06

ppm which was assigned to the H6'. Correlation between these two protons in the gCOSY spectrum was noticed whereas there was no signal for the correlation between H7' and H8' suggesting that restriction of rotation as result of being in a ring system. This and the signal at 69.2 ppm for C2 in the ^{13}C NMR spectrum confirmed the typical spiro cyclisation (Figure 34).
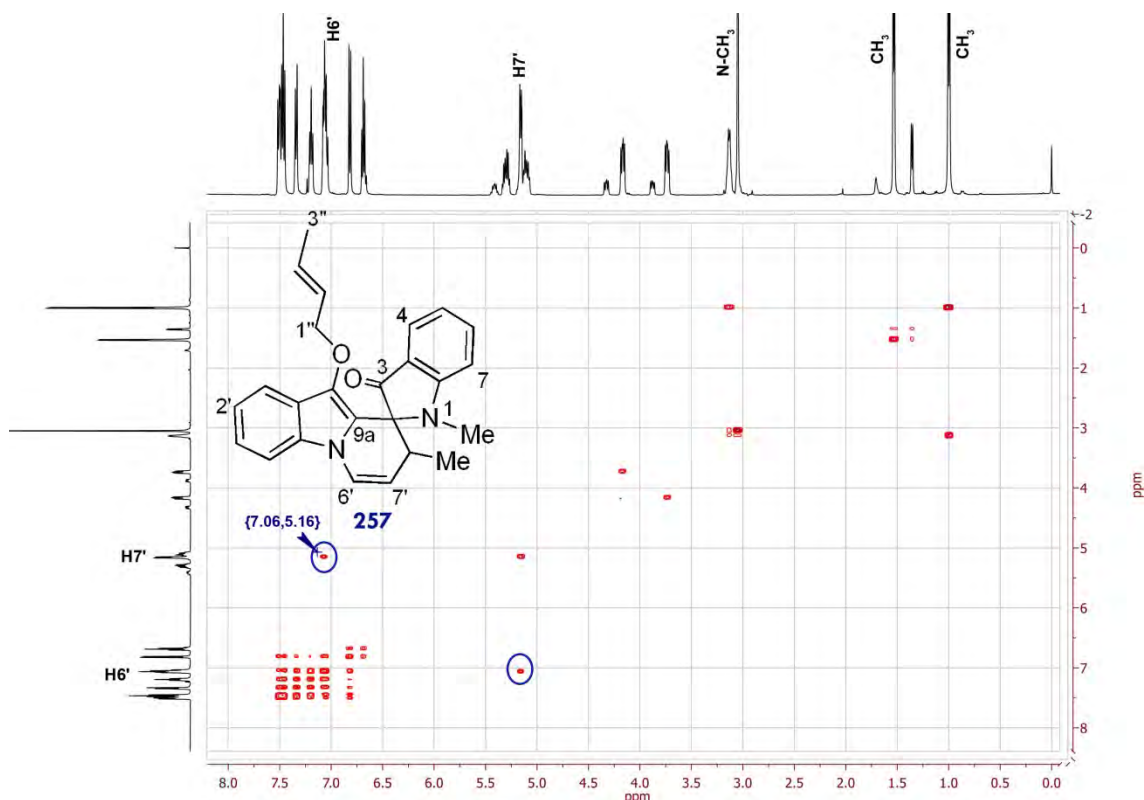
Figure 34: gCOSY spectrum for compound **257**.

To explore the effect of constraining the allylic substituents in a ring, an additional allylation was attempted with 3-bromocyclohexene under typical conditions with a 5 sec reaction time. The major product isolated was the mono-substituted Type **E** derivative **258** in 51% yield (Scheme 60). Only trace amounts of other products were evident from TLC analysis. The peaks at *m/z* 422 and *m/z* 502 in the EI mass spectrum of the crude were assigned to the azepinodiindole and spiroindole products, respectively, however due to the minute quantities (less than 0.5 mg) structural elucidation were not pursued

further. Longer reaction times failed to produce isolable quantities of these additional

products and instead formed base line material.
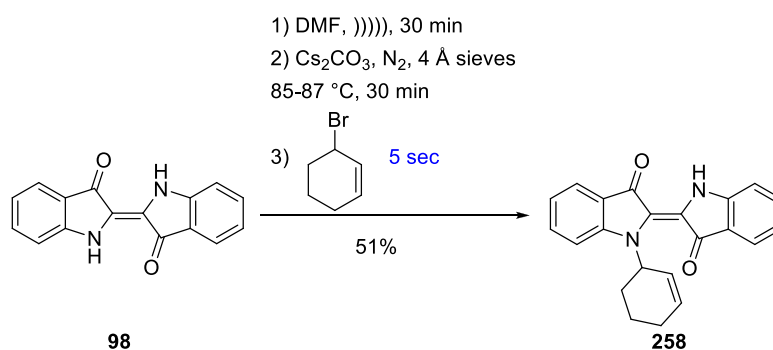
Scheme 60: The reaction of indigo in the presence of base and 3-bromocyclohexene.

2.3.2 Inductive effect of the substituents

Formation of the iminium ions **T** and **W** (Schemes 50 and 52) appeared to be the key

steps in generation of the 7-membered and spiro products from the allylation reaction of

indigo. To validate this assumption, allyl chloroformate used as the allylic substrate to

react with indigo **98**. The reaction was carried under the similar conditions to that

described in the 3 hour allylation reactions. The reaction was monitored by TLC

analysis which revealed the complete consumption of indigo after 3 mins. Then the

reaction was quenched and purified by fractional recrystallisation to afford the dark

magenta crystals of *N,N'*-diallocindigo (71%) **259**. In order to investigate the outcome

of the reaction in longer times, in a separate attempt the reaction mixture was heated and

stirred for 3 h after the addition of allyl chloroformate which yielded **259** (87%) with no

cyclised products isolated (Scheme 61)
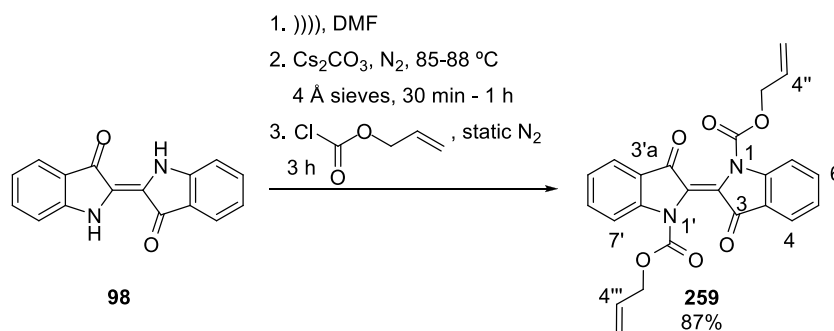
Scheme 61: Reaction of indigo **98** and allyl chloroformate.

The peak at *m/z* 430 (M+H$^+$) in the MS (ESI) spectra was assigned to the molecular ion and confirmed the addition of two allylformates units. ^{1}H NMR analysis revealed four peaks in the aromatic region, with a total integration of eighteen protons. ^{13}C NMR also showed twelve signals. This was compatible with the symmetrical structure of *N,N'*-diallocindigo **259**. From the analysis of the ^{1}H NMR spectrum, the singlet at 4.95 ppm was assigned to the two methylene groups, H3" and H3"'. The two doublets at 5.19-5.21 ppm and 5.27-5.29 ppm were assigned to the terminal olefinic protons H5", H5"' and the multiplet at 5.95-6.01 ppm was assigned to the protons of the alkenes H4" and H4"'. A doublet at 8.16-8.18 ppm, deshielded because of the neighbouring effect of the carbonyl groups, was assigned to the H4 and H4'. From the ^{13}C NMR spectrum the signal at 181.9 ppm was assigned to the carbonyl groups C3 and C3'.

The result of the experiment confirms the effect of the electron lone pair of the nitrogen and their role in these cascades. The presence of the formate group between the tertiary nitrogen and the methylene of hampered the alkene nucleophile from attacking to the activated iminium. Therefore no cyclisation occurred onto the C2 position or the carbonyl group of the indigo.
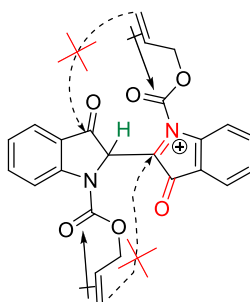
Figure 35: The impact of the electron withdrawing groups on the nucleophilicity of the allylic alkene.

The possibility of production of *N,N'*-diallylindigo from the catalytic decarboxylation of **259** was of interest. This will help to study the suggested divergence point in the suggested mechanisms (Schemes 50 and 52). Therefore, in a separate experiment, **259**

was dissolved in dry CH_2Cl_2 and added to a flask containing $Pd(PPh_3)_4$ under an inert atmosphere of N_2. The reaction was carried at room temperature (27 ºC) and completed in 10 mins followed by the standard protocols for quenching and subsequent workout. A signal at *m/z* 342 EI mass spectroscopy assigned to *N,N'*-diallylindigo. The TLC analysis showed only one product which was a teal-blue colour. The solution was then concentrated under the reduced pressure; surprisingly, the colour of the solution turned to red after being plunged into the rotovap water bath. The filtrate colour was now red with an R_f value of 0.05 (CH_2Cl_2) which was significantly lower than the teal-blue compound (R_f=0.65, CH_2Cl_2). This conversion was quantitative and spectroscopic comparison confirmed the formation of compound **248** (Scheme 62). In an identical separate reaction the solvent removal during the workup was attempted using an inert gas flow to avoid any additional heat, however, under these conditions the colour of the extract turned to red after 2 hours and analysis of the solution confirmed the same conversion.
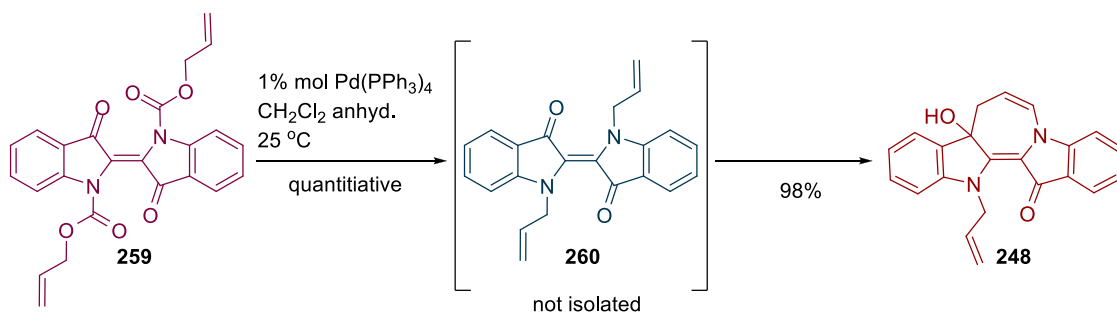
Scheme **62**: The catalytic decarboxylation of the **259** and quantitative formation of **248.**

Formation of the azepinodiindole **248** from **259** in the absence of a base and additional heat highlighted the role of the highly acidic methylene of the *N*-allyl. This experiment also confirms the supportive contribution of the lone of the nitrogen in order to increase the nucleophilicity of the alkene to trigger the cyclisations.

The other advantage of this reaction was to introduce a facile and high yielding procedure towards the formation of azepinodiindolo systems.

2.3.3   The effect of the terminal electron withdrawing substituent

The presence of terminal substituent on the alkene substrate played a significant role by determination of the outcome of the reaction. Until now, these substituents were electron donating groups (Me or Ph, See Scheme 44, 46 and 49). To investigate the effect of an electron withdrawing group at the terminal position of the allyl substrate, the use of methyl 4-bromocrotonate was investigated. The reaction condition was similar to the standard procedure of allylic cascade reactions (3 hours reactions) and resulted in formation of the tetrahydropyrazine **261** in 62% as a dark purple solid (Scheme 63). The pathway suggested by the rearrangement of the *N*-substituted moiety and formation of intermediate **P** which then underwent a Michael conjugate addition **Q** to form compound **261**.
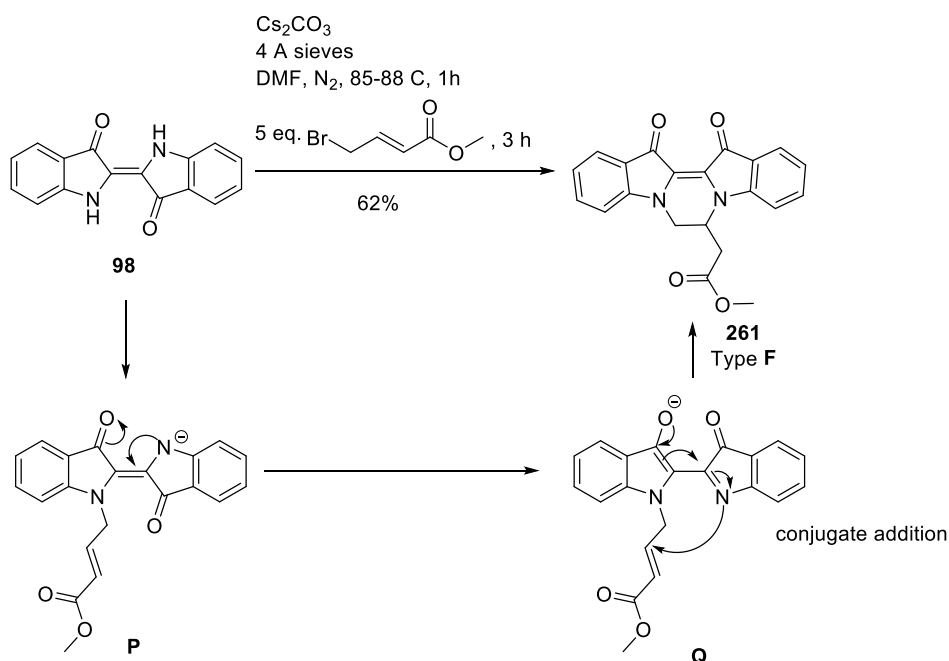
Scheme 63: The reaction of indigo with methyl 4-bromocrotonate and formation of **261**.

Analysis of the ^{1}H NMR spectrum revealed a total of eight proton signals in the aromatic region. A multiplet at 4.83 ppm, deshielded by the adjacent tertiary nitrogen atom, was assigned to proton H6. The gCOSY spectrum revealed the correlation of the

proton H6 to the other deshielded proton H7 as well as to the adjacent methylene substituent (H1') (Figure 36).
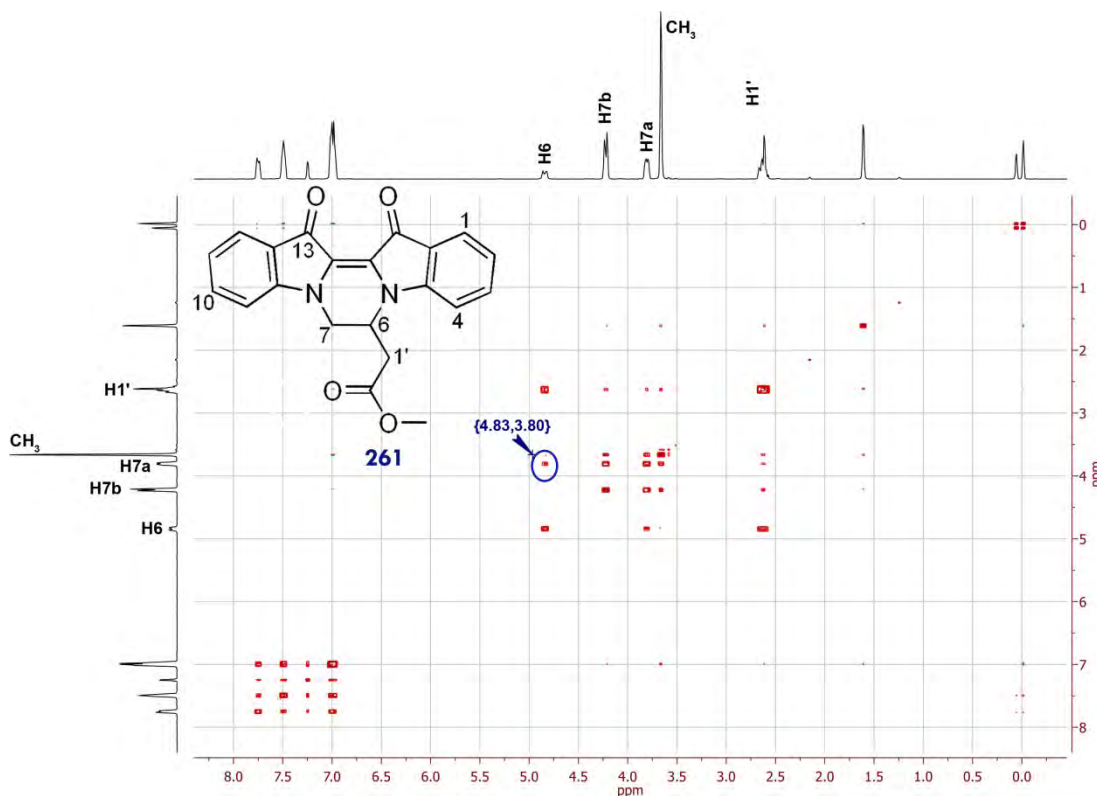
Figure 36: The gCOSY spectrum for **261** with annotated correlation of H7a and H6 in blue.

2.4   Comparative product outcomes

Overall, short reaction times suggest the initial formation of monoallylated products followed by a second *N*-allylation in most cases and cyclisation, although the exact order of these two steps is not apparent. Some evidence for the formation of the *N,N*-diallylated products has been seen (e.g. by mass spectral analysis of reaction mixtures), however, such products have never been isolated. After a 5 second reaction time, heterocycles of the Type **D** system were already produced an indication of the ease of the cascade processes. After 1 hour reaction time, there was no evidence for the presence of the Type **B** compounds and the spiro compounds (Type **A**) were present in minor quantities. Instead, a greater proportion of the red Type **D** compounds were produced. It is only after the 3 hour reaction time that types A and B predominate with a

corresponding loss of formation of the Type **D** and **E** systems – this includes with the use of the more sterically demanding cinnamyl bromide and 1-bromo-2-butene which also gave rise to the Type **A** spiro heterocycles, with the latter reported here for the first time. The products arising from oxidative cleavage, the *N*-allylisatins (Type **C**) are minimised in these optimised conditions, and appear to arise only after longer reaction times. Scheme 64 demonstrates the outcome of the reaction of indigo with allylic bromides in different times and the detailed analysis of each of the reaction mixtures.

R₁	R₂	R₃

R_1	R_2	R_3
H	H	H
Me	H	H
H	Me	H
H	Me	Me
H	Ph	H

Type **A**
Compounds **227**, **228**, **229**, **230**, **231**

Type **B**
Compounds **232**, **233**

Type **C**
Compounds **237**, **241**

Type **E**
Compounds **243**, **244**, **245**, **246**, **247**

Type **D**
Z = Y, Compounds **248**, **249**, **250**
Z = H, Compound **251**

Type **F**
Compound **253**

Type **G**
Compound **254**
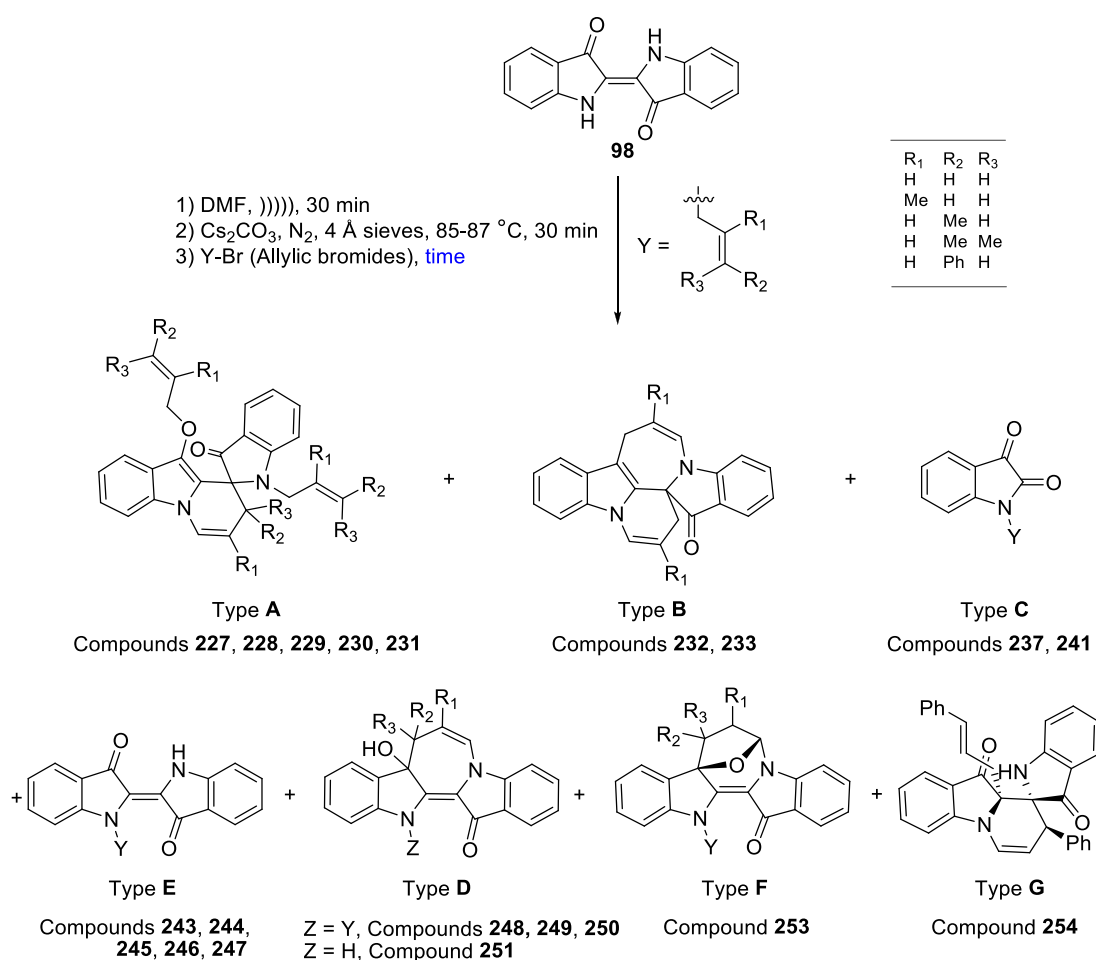
Scheme 64: The outcomes of the cascade reactions of indigo with allyl bromides at three different reaction times.

Chapter 3: Cascade Reactions of Indigo and Propargylic Halides

3.1 Reaction of indigo and propargyl bromide

Complexity and novelty in compound structure is a significant advantage for any drug-like molecule as it therefore has substantial potential to be elaborated in a drug design platform. Therefore the expansion of structural diversity in combination with the economical production of complex architectures is of enormous interest. Facile formation of relatively complex structures from indigo with allylic bromides in a one-pot reaction revealed that indigo is susceptible to cascade reactions. These compounds represent new ring systems with functionalities that are suitable for further elaboration of molecular complexity. In order to expand the mechanistic insight, specifically for reaction directing factors, particularly those modulating nucleophilic-electrophilic reactivities, the base-induced reactions of indigo with the simple alkyne analogue, propargyl bromide were investigated. Previous experience in the allylation of indigo revealed that relatively small changes to reaction conditions could have major impact on the product outcome. Therefore, our attempts at the propargylation of indigo paid particular attention to stringent and repeatable reactions conditions. In this context, all the measures were kept identical to the conditions of allylation reaction. Initially, the propargylation reaction of indigo **98** was performed according to the optimised procedure previously described in allylation section. Thereby, indigo in DMF was sonicated for 30 mins to maximise the solubility and subsequently transferred to a septum equipped flask containing pre-dried caesium carbonate and activated molecular sieves under an inert N_2 atmosphere. The flask was then plunged into a preheated oil-bath (strictly 85-87°C) and stirred for 30 min. At this point the N_2 flow was stopped and propargyl bromide was added under the static inert atmosphere and the mixture was

stirred for 3 h. TLC analysis revealed the formation of two products along with a distinctive base-line residue. Separation by silica gel flash column chromatography afforded an anthranilic acid derivative, as very thick oil with light amber colour **262** (35%) as the major products and pyridodiindole **265** (8%). This was along with a brown polymeric base-line material (42% of the mass of the dry crude filtrate) (Scheme 65).
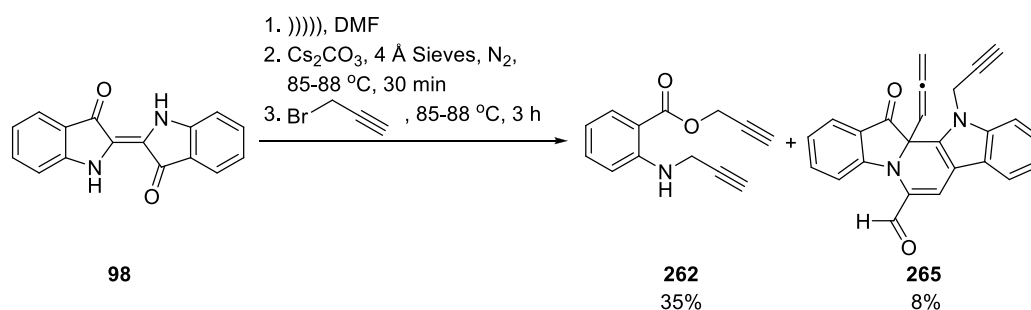
Scheme 65: Preliminary outcome of the propargylation of indigo.

Formation of **262** suggested that the reaction must be altered in order to prevent disintegration of indigo to anthranilic acid. Therefore shorter reaction time was investigated. Reducing the reaction time resulted in a substantial decline in production of the baseline material. Separate reactions were carried with random reaction times; 1.5 h, 30 min and 10 min and 5 min. The optimum result was observed when the solution was heated and stirred for 5 min after the addition of propargyl bromide. Following quenching, a sequence of separations yielded the five new products **263−267** in a combined yield of 81% (Scheme 66).
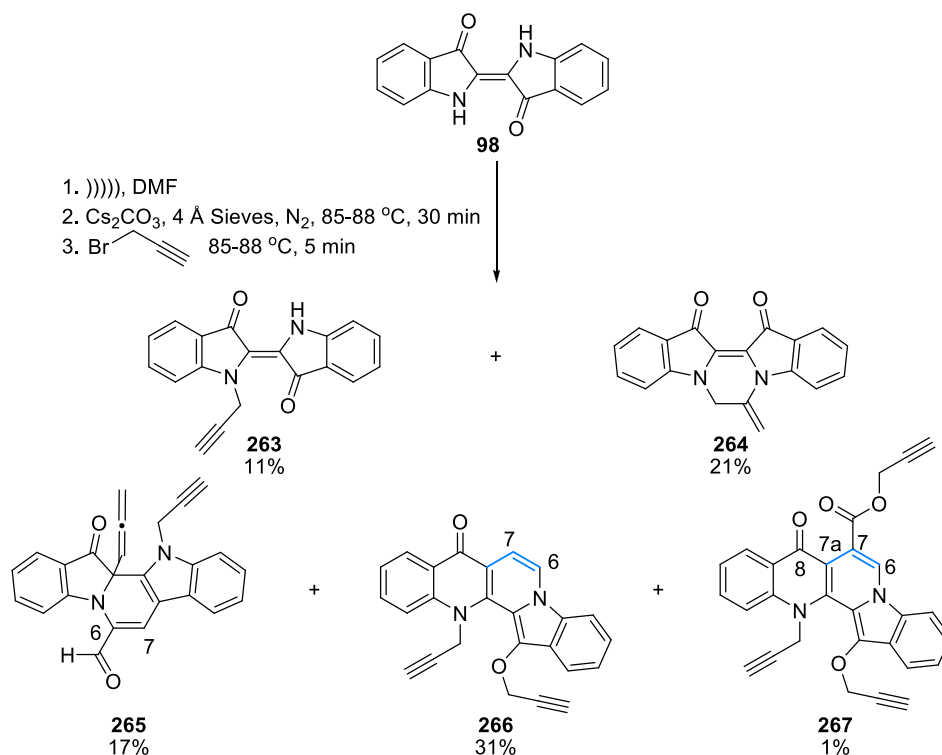
Scheme 66: Base-mediated propargylation of indigo to produce the heterocyclic compounds **263**-**267**.

The reaction mixture was dark brown and initial TLC analysis revealed the presence of 4 distinctive sections (Figure 37/A). Separation attempts including the silica gel column chromatography or Centrifugal Thin-Layer Chromatograph (*Chromatotron*) were not able to fulfil a reasonable mass return. Therefore a strategy of separation was employed that subjected the crude reaction mixture to a short plug of silica gel, collecting four fractions by utilising different solvent mixtures. Fraction (**I**) was isolated by elution with 70:30 CH_2Cl_2/petroleum spirit (250 mL); Fractions (**II**, collected in 3 separate flask), obtained by elution with CH_2Cl_2; Fraction (**III**) was collected from the elution with 50:50 CH_2Cl_2/EtOAc; and Fraction (**IV**) was isolated by the elution with 95:5 EtOAc/MeOH. (See Chapter 7 for the detailed experimental procedure).
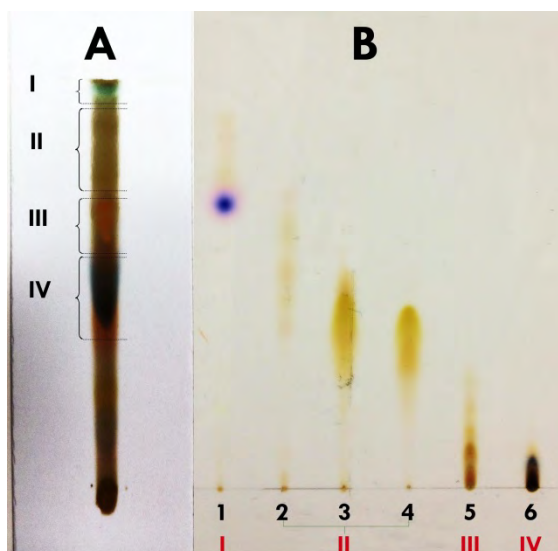
Figure 37: **A**: TLC of the crude mixture of the reaction of **98** with propargyl bromide (95:5, CH_2Cl_2/MeOH). The numbered sections are representing the fractions isolated from the elution of the crude through the short plug of silica by different solvent mixtures. **B**: TLC analysis of the isolated fractions (95:5, CH_2Cl_2/EtOAc).

Concentration of the first fraction (**I**) afforded mono *N*-substituted indigo derivative **263** as a deep blue, papery solid in 11% yield after recrystallisation. The peak at *m/z* 300 (M+H$^+$) in the MS (ESI) spectra was assigned to the molecular ion and was indicative of the addition of one propargyl unit. Analysis of the ^{1}H NMR spectrum revealed a signal at δ 2.17 ppm, assigned to the alkynic proton H3" (Figure 38). The presence of a total of eight proton signals in the aromatic region was compatible with number of the aromatic protons of indigo core. A singlet at δ 10.60 ppm was assigned to the NH proton. This was also confirmed by analysis of the IR spectrum which showed the presence of a broad signal at υ_{max} 3278 (m). A strong NOESY correlation between H7 of the aromatic ring at 7.22 ppm and the methylene group of the propargyl unit H1" confirmed the *trans* configuration for **263** (Figure 37, annotated in blue). This was also validated by the absence of any NOESY correlation between H1" and the free NH.
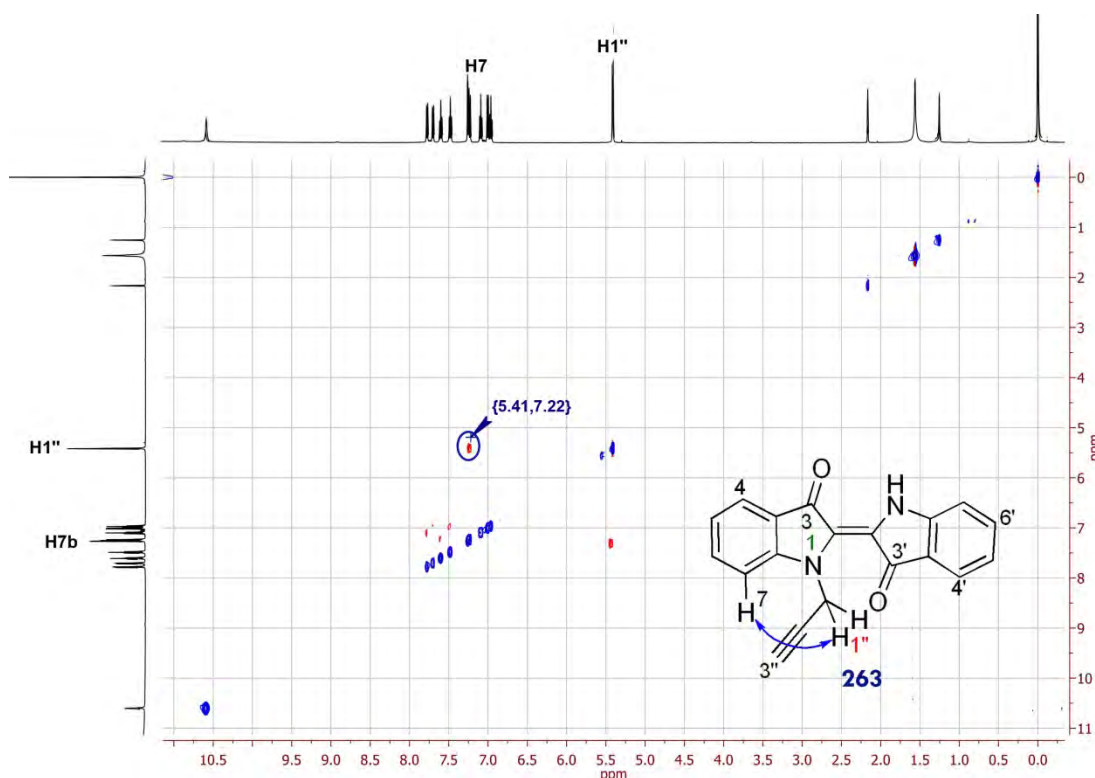
Figure 38: The NOESY spectrum for the compound **263** and the key correlation between H7 and H1''.

The pyrazinodiindole **264** was isolated in 21% yield as a dark eggplant coloured solid from the last fraction (**IV**) after concentration and purification with preparative TLC. Its solution in EtOAc is red-burgundy. A signal at m/z 300 (M+H$^+$) in the MS (ESI) spectra was assigned to the molecular ion. Data from the HRESI mass spectrum was supportive of the molecular formula of **264** and was indicative of the addition of one propargyl unit. The ^{1}H NMR spectrum lacked a signal corresponding terminal alkynic proton at δ 2.17 ppm. The presence of the eight aromatic protons in the range 6.92-7.84 ppm suggested a cyclised alkyne without any extended conjugation.[§] Singlets at δ 5.04 ppm and δ 5.38 ppm were assigned to the exocyclic methylene protons (H1'a,b). A sharp singlet at δ 4.41 ppm was assigned to H7, and showed no correlation in the gCOSY spectrum, indicating the neighbouring atom should be a quaternary carbon or a hetero atom (Figure 39). Analysis of the gHSQC spectrum showed signals with positive phasing (highlighted in blue) corresponding to two methylene groups (Figure 40). The

---

[§] The N-CH of the six-membered pyridine ring in **227** or **232** shifted downfield to the aromatic region

^{13}C NMR spectrum showed 2 peaks at 179.7 and 180.8 ppm, assigned to two non-equivalent carbonyls (See appendix 1 for the full set of spectra).
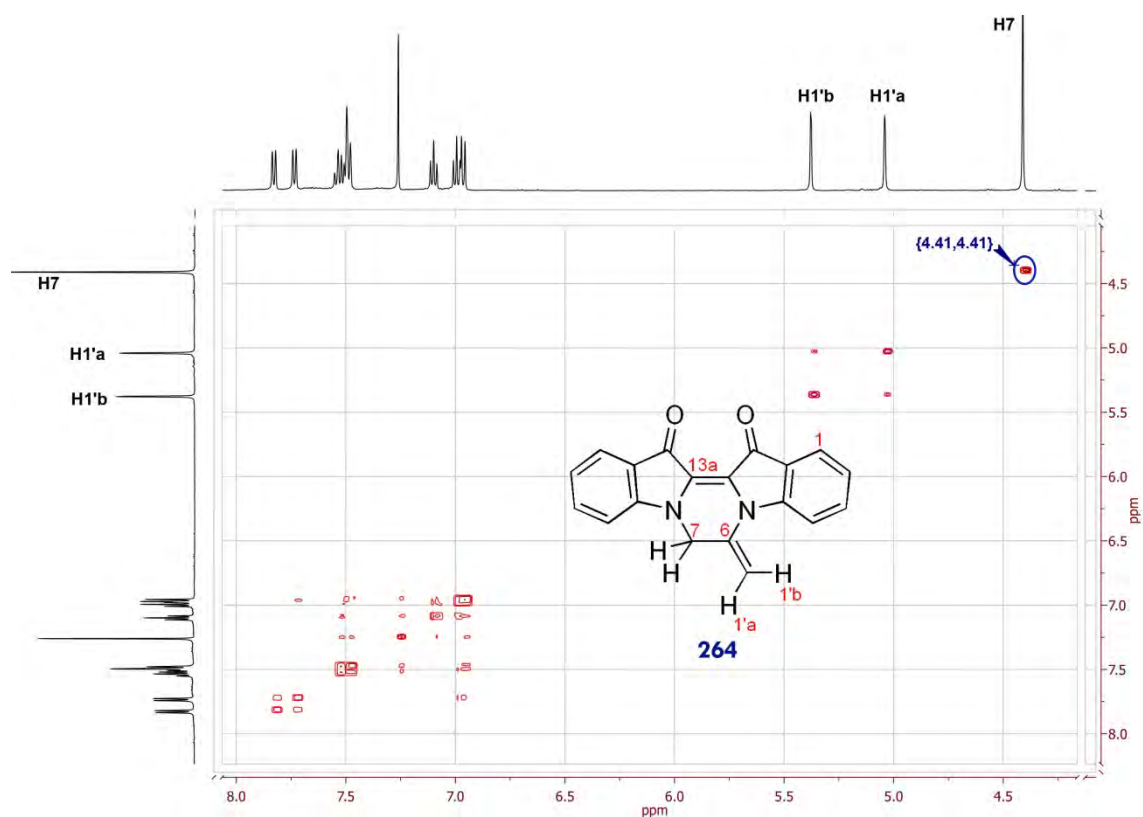
Figure 39: The gCOSY spectrum for the compound **264**, H7 highlighted showing no correlation with any other proton.
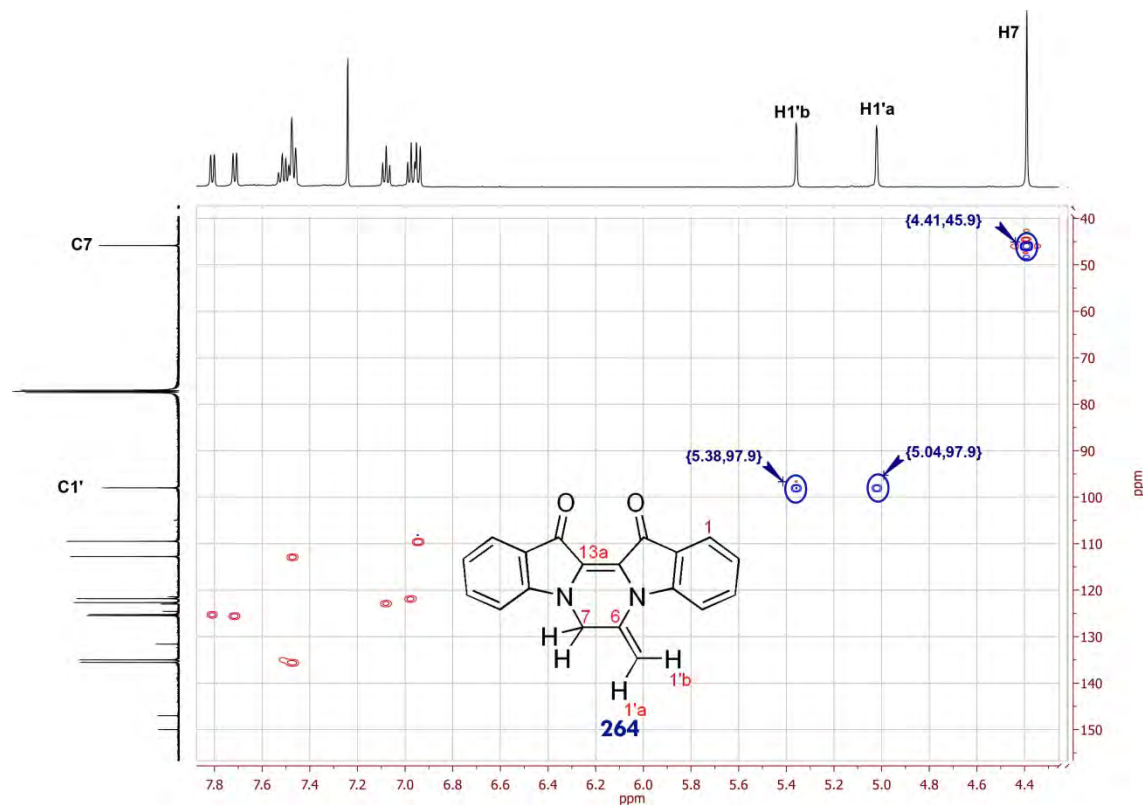
Figure 40: The gHSQC spectrum for the compound **264**.

Furthermore, analysis of the gHMBC spectrum (Figure 41) revealed a strong three bonds correlation of C7 at 45.9 ppm to H1'a,b confirming the pyrazine ring with an exocyclic methylene group (blue). This was also supported by the strong three bond correlation of C1' at 97.9 ppm and H7 (green). The other key correlation observed between the C13a at 121.4 ppm with H7 (red). The three bond correlation between the deshielded H1 at δ 7.82 ppm and the quaternary carbon C4a at 147.0 ppm was also observed from this spectrum. The same holds between H12 at δ 7.73 ppm and C8a at 150.0 ppm (magenta).
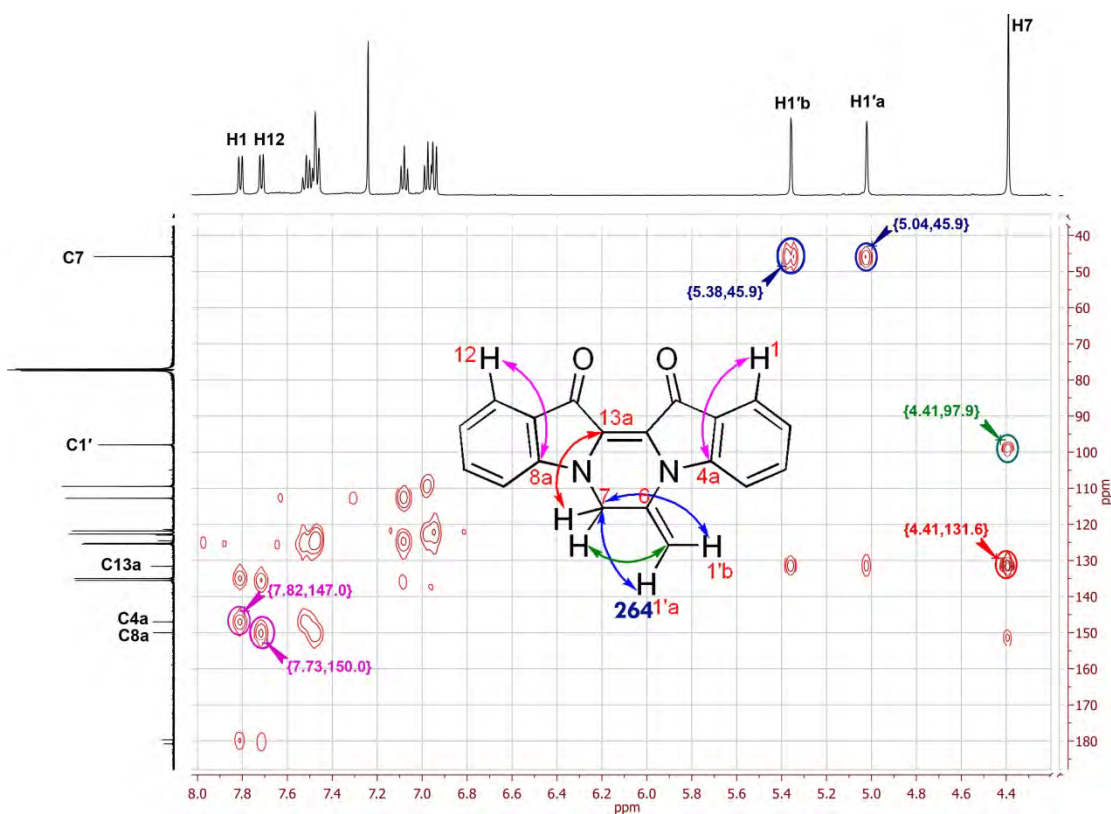
Figure 41: The gHMBC spectrum for **264**. Correlations correspond to the annotation with similar colour.

The UV-vis spectrum of **264** had a strong adsorption band with a maximum at 324 nm (ε = 13,088). The burgundy colour suggested that the central double bond of indigo remained intact, with all other indigo derivatives in which this bond had been converted to a single bond appearing as yellow compounds. Simple modelling studies (Spartan, Wavefunction) indicated that compound **264,** while planar through the indigo moiety,

positioned the hydrogen atoms of the endocyclic methylene group above and below the plane of the molecule with the exocyclic methylene twisted out of the molecule plane. This modelling was performed by using Hartree Fock theory after optimisation at the 6-31G level (Figure 42).
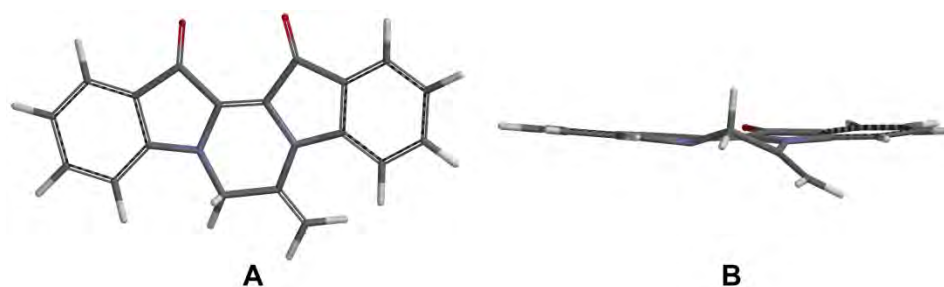
Figure 42: Modelling for the position of the hydrogen atoms of the cyclic methylene and the exocyclic methylene in **264**.

The mother liquors from fraction **I** were combined with fraction **II** and then subjected to a silica gel column and elution with 7:3 CH_2Cl_2/pet. spirit gave the previously mentioned pyridodiindole **265** in 17% yield as yellow-orange crystals. The peak at *m/z* 376 (M^+) in the MS (EI) spectra was assigned to the molecular ion. This was consistent with a molecular formula of $C_{25}H_{16}N_2O_2$ which was a result of the addition of three propargyl units. Analysis of the ^{1}H NMR indicated a peak at 9.62 ppm assigned to the aldehyde proton H1'''. A triplet at 5.42 ppm assigned to the H1'' proton of the allene moiety and a singlet at 2.33 ppm assigned to the terminal alkyne proton H3'. Analysis of the ^{1}H NMR revealed a total of nine proton signals in the aromatic region. In comparison to the starting material indigo **98** (eight aromatic protons), the additional proton signal with a chemical shift of δ 7.65 ppm, deshielded by the extended conjugation of the pyrido ring and the aldehyde group, was assigned as H7. The gCOSY spectrum revealed that the H7 has no correlation with any other proton (Figure 43). The presence of a doublet at 4.79 ppm and an AB quartet between 5.15-5.56 ppm were assigned respectively to the terminal methylene of the allene group H3'' and the methylene of the propargyl unit H1'. This was confirmed by analysis of the gHSQC

spectrum where the presence of the two positively phased signals (shown in blue) correlate H3" and H1' to their corresponding carbon (Figure 44).
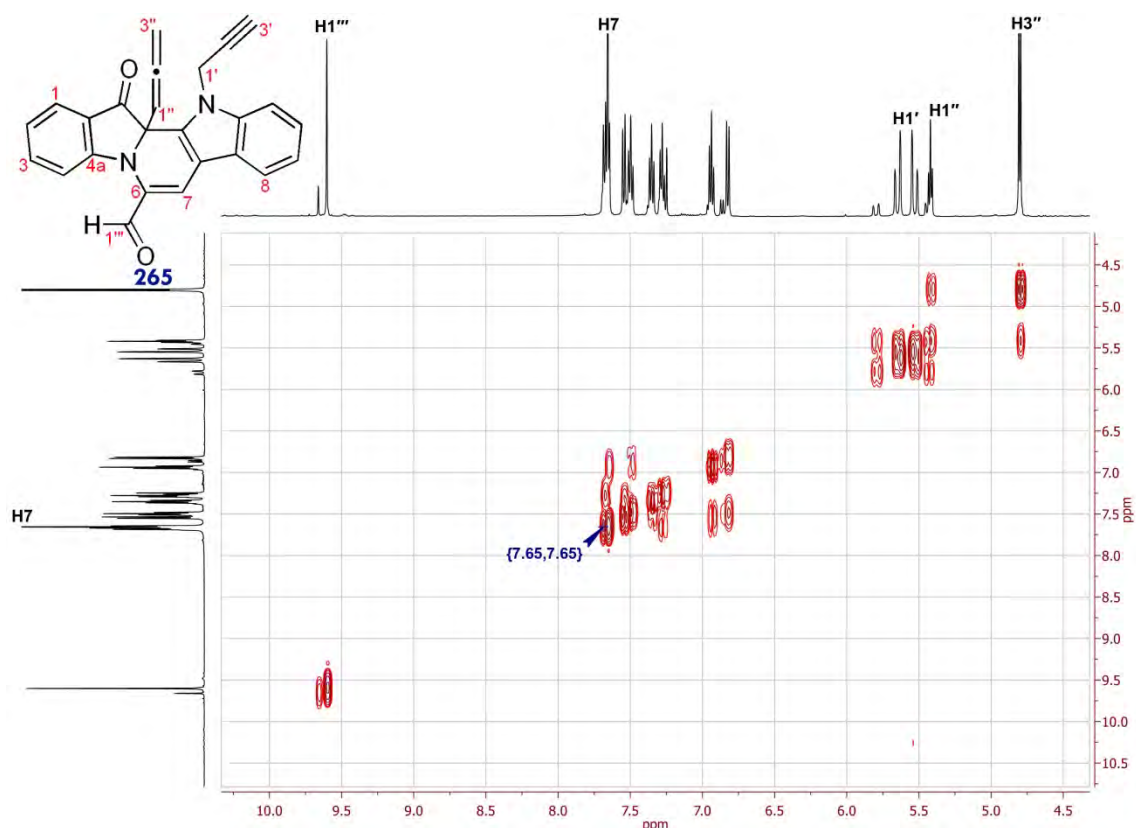
Figure 43: The gCOSY spectrum of pyridodiindole **265**.
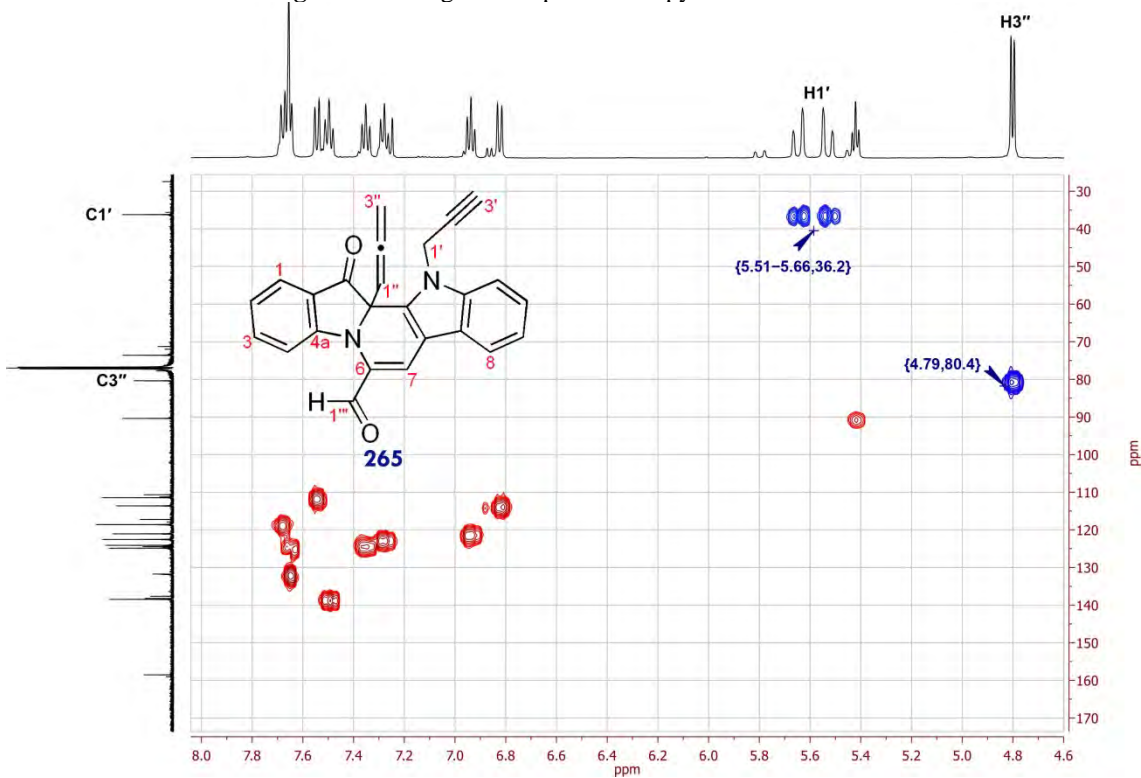
Figure 44: The gHSQC spectrum of pyridodiindole **265** with the CH_2 groups highlighted in blue.

The ^{13}C NMR spectrum showed peaks at 90.4, 208.4 and 80.4 ppm, assigned sequentially to the three allene carbons from the C1''. A peak at 195.7 ppm was assigned to the carbonyl.

From the HMBC spectrum (Figure 44), a key correlation between the H7 and C1''' at 185.3 ppm of the aldehyde further supported the formation of cyclised structure with the formyl pendant (A, annotated in blue). Evidence for presence of *C*-allene was found from the strong signal for three bond correlation of H3'' and C1'' (B, annotated in brown). This was also confirmed by the two bonds correlation between allenic quaternary C2'' at 208.4 ppm and H1'' (C, annotated in brown). A three bond correlation between the H1'' and the carbonyl at 195.7 was further evidence to confirm the position of the allenic moiety (C, annotated in magenta). The other key evidence was the three bond correlation between the quaternary carbon of the aromatic ring C4a at 158.6 ppm and H3 at 7.36 ppm and H1 at 7.64 ppm (A, annotated in black). The C4a also showed a correlation through four bonds with H7 proton (A, black). A complementary three bond correlation was noted between the C13 of the carbonyl and H1 and H4 protons of the aromatic ring (A, annotated in magenta). The quaternary carbon C11a at 138.2 ppm showed a three bond correlation with the protons of the methylene H1' (D, annotated in red). Other significant correlations were observed between the H8 at 7.48 and the C7a at 124.5 ppm (E, annotated in orange). Moreover the quaternary carbon was assigned as C7b at 137.7 ppm showed a three bond correlation with the H7 proton (E, annotated in green). All the arrows on the structure (F) are related to the similar colour of the annotations on spectrum (See Appendix 1 for expansions and detailed spectra)
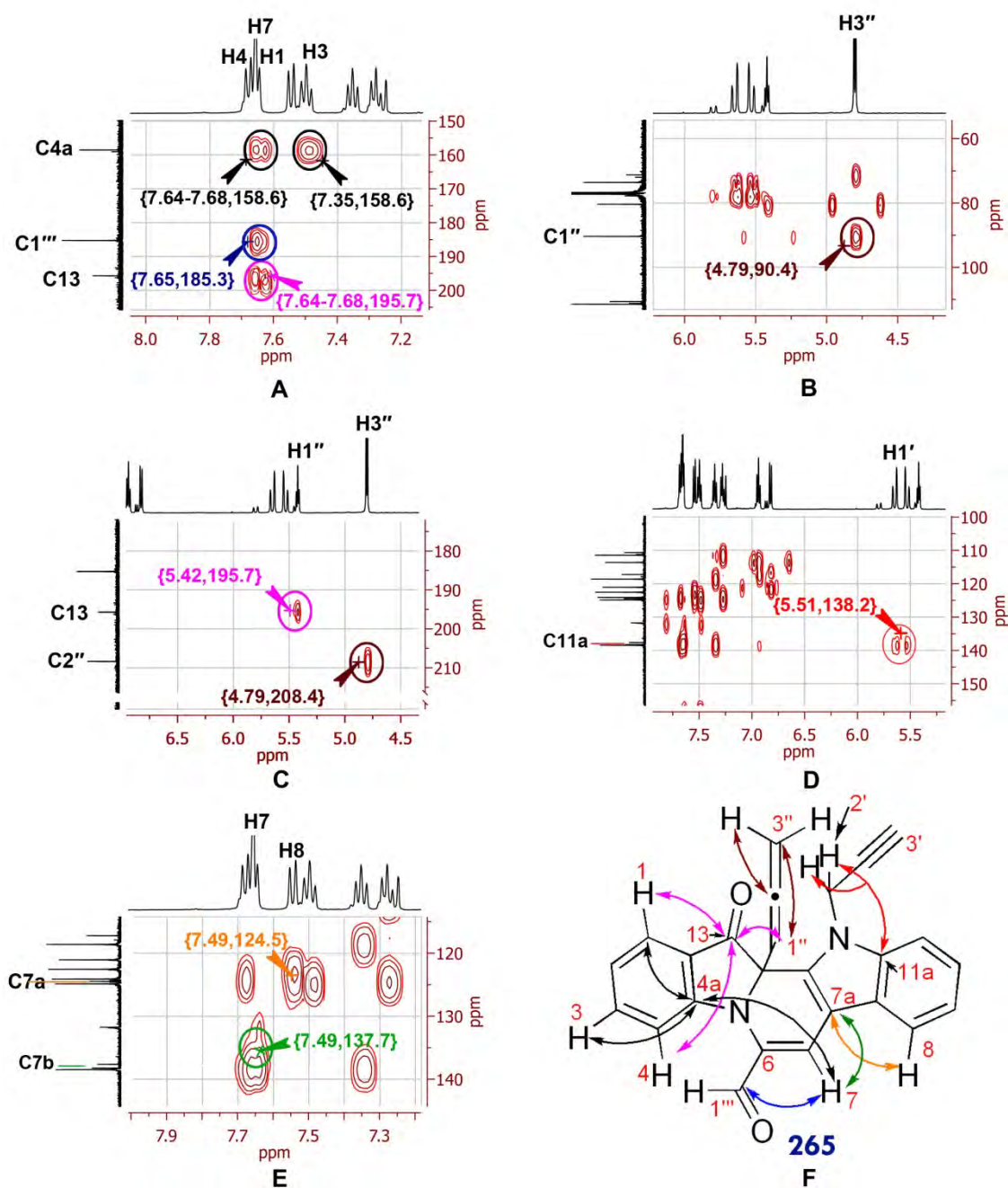
Figure 45: The gHMBC spectrum of pyridodiindole **265**.

Slow recrystallisation of the **265** from a mixture of ethyl acetate and petroleum spirit yielded X-ray quality crystals, analysis of which confirmed the molecular structure together with the disposition of the allene group over the pyrido ring rather than pointing away from it (Figure 45).
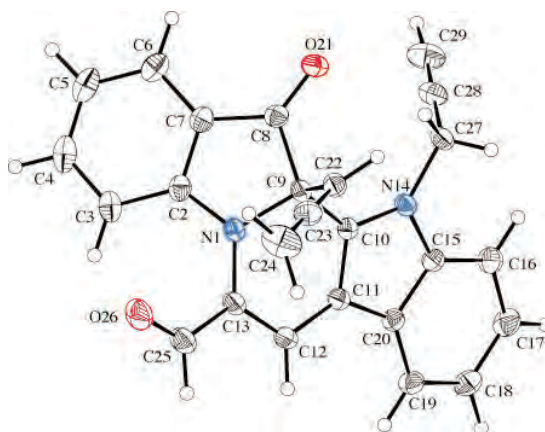
Figure 46: The crystal structure of the pyridodiindole **265**.

There is one stereogenic carbon present at C12a, but in the absence of any chiral element during the reaction, the stereochemical outcome was a racemic mixture, as confirmed by optical rotation analysis of zero. The structure of **265** poses interesting mechanistic questions. The addition of three propargyl units is evidenced by the presence of the allene, the N-propargyl unit and the three carbon moiety encompassing the aldehyde, and C6 and C7. Interestingly, this three carbon unit is attached to the indigoyl N at the propargyl C2 carbon, and not through the terminal methylene or the terminal alkynic positions.

The major product of the reaction was the benzoindolonaphthyridinone **266** which was isolated by the fractional recrystallisation of the fraction **III** from CH_2Cl_2/petroleum spirit (1:9). This heterocycle was obtained in 31% yield as a yellow solid which was highly fluorescent in CH_2Cl_2 solution with a brilliant yellow colour under UV light (365 nm). The peak at *m/z* 376 (M$^+$) in the MS (EI) spectra was assigned to the molecular ion. This was indicative for the addition of three propargyl units to the indigo core. The base peak at 337 is a loss of 39 Da from the molecular ion, which could correspond to the loss of a one propargyl unit. In addition the base peak at 298 Da corresponds to the loss of the second propargyl unit, suggesting that the structure possessed two propargylic pendants. Moreover from the [1]H

NMR spectrum the signals at 2.14 ppm and 2.30 ppm were assigned to the terminal acetylenic protons, H3' and H3" respectively. The doublets at 4.74 ppm was assigned to the methylene of *O*-propargyl (H1') and the other doublet at and 5.49 ppm (J = 2.4 Hz) was identified as methylene of the *N*-propargyl (H1") protons (Figure 47). The aromatic region of the ^{1}H spectrum of the naphthyridine **266** showed the total of ten protons, in comparison with the eight protons of the indigo core, the additional two aromatic protons were identified as two pairs of doublets at 8.01 and 7.33 ppm (J = 7.4 Hz) assigned to H6 and H7 respectively. The chemical shift for these two protons was suggesting the possibility of the incorporation of the third propargyl unit to a ring system in a manner which forms an aromatic ring current. This was also supported the fluorescent property of **266** suggesting the cyclised unit with extended conjugation (Scheme 66, blue). A doublet at 8.48 ppm was assigned to H9 deshielded due to the adjacent carbonyl group C8. Analysis of the ^{13}C spectrum revealed a signal at 175.8 ppm which was assigned to the C8 carbon. The presence of this sole signal at the carbonyl region validated the presence of one carbonyl group in the structure. The gCOSY spectrum showed the correlation between H6 and H7 proton (Figure 47). These two protons did not show any correlation with any other proton, which suggested a positioning between a quaternary carbon and a tertiary amine with an extended conjugation (Figure 47, annotated in blue). The analysis of the gHSQC spectrum confirmed the presence of two signals with positive phasing (blue) correlating the protons of the methylene groups of propargyl pendants (H1' and H1") to their corresponding carbons C1' and C1" at 63.7 and 44.0 ppm respectively (Figure 48, green). The other significant correlations observed from

gHSQC were between the H6 - C6 at 110.9 ppm and between H7 - C7 at 104.0 ppm (Figure 48, magenta).
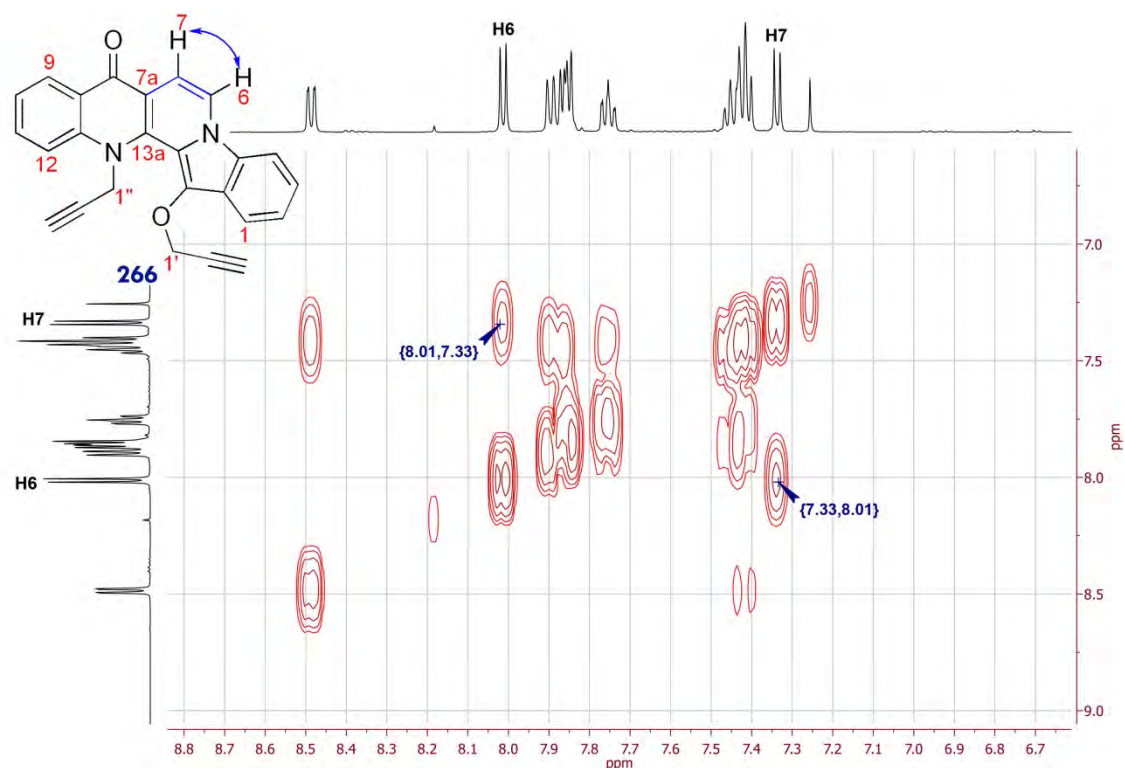
Figure 47: The gCOSY spectrum for compound **266**, correlation of the H6 and H7 annotated with blue pointers.
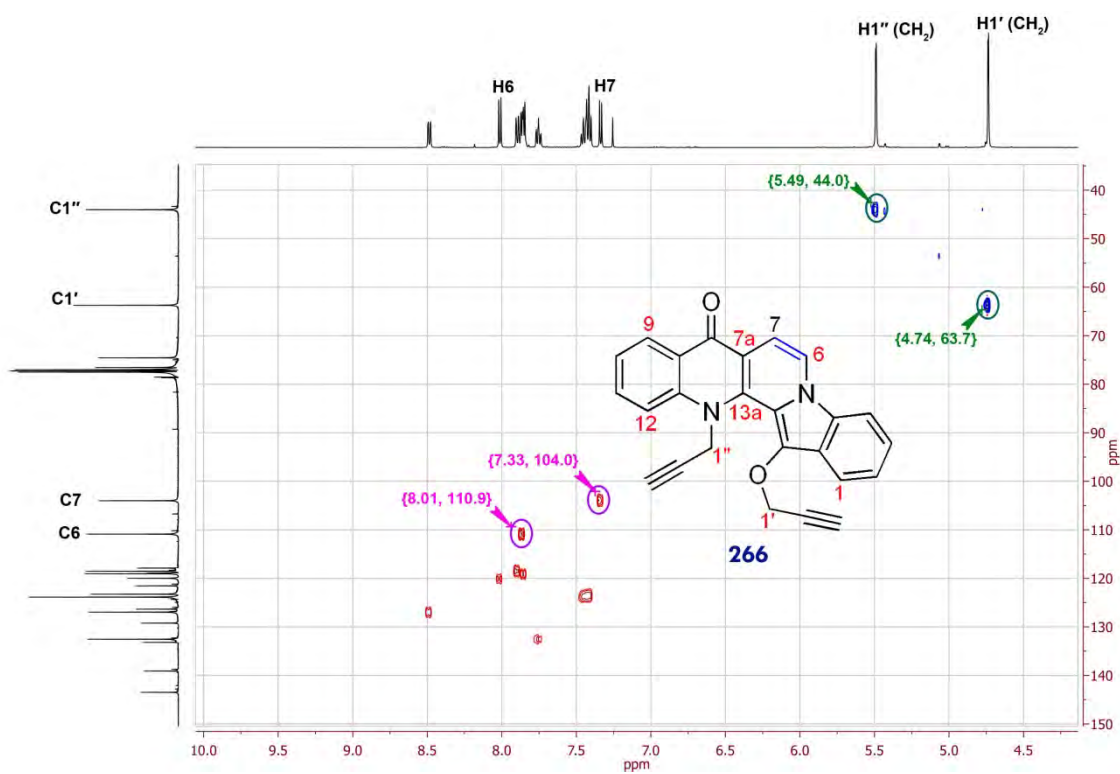
Figure 48: The expanded gHSQC spectrum for compound **266**.

Analysis of the HMBC spectrum indicated a strong three bonds correlation between H7 and the quaternary carbon C13a at 139.1 ppm and a three bond correlation between H7 and C8 (Figure 49, blue pointer). The other key three bond correlation was between the quaternary C13b at 118.9 ppm and H6. This was stronger in comparison to the signal from the four bond correlation between the quaternary C14a at 129.3 ppm and H6 (Figure 49, orange pointer). The H1" protons of the methylene showed three bond correlation with C12a at 143.5 ppm and C13a at 139.1 ppm (Figure 49, green pointer). The correlation of the H1' and C14 at 133.2 ppm (brown) and also between the H9 at 8.71 ppm and C8 were also observed from the gHMBC spectrum (Figure 49, magenta). See the appendix 1 for ^{1}H and ^{13}C NMR spectra and detailed gCOSY, gHSQC and gHMBC NMR spectra.
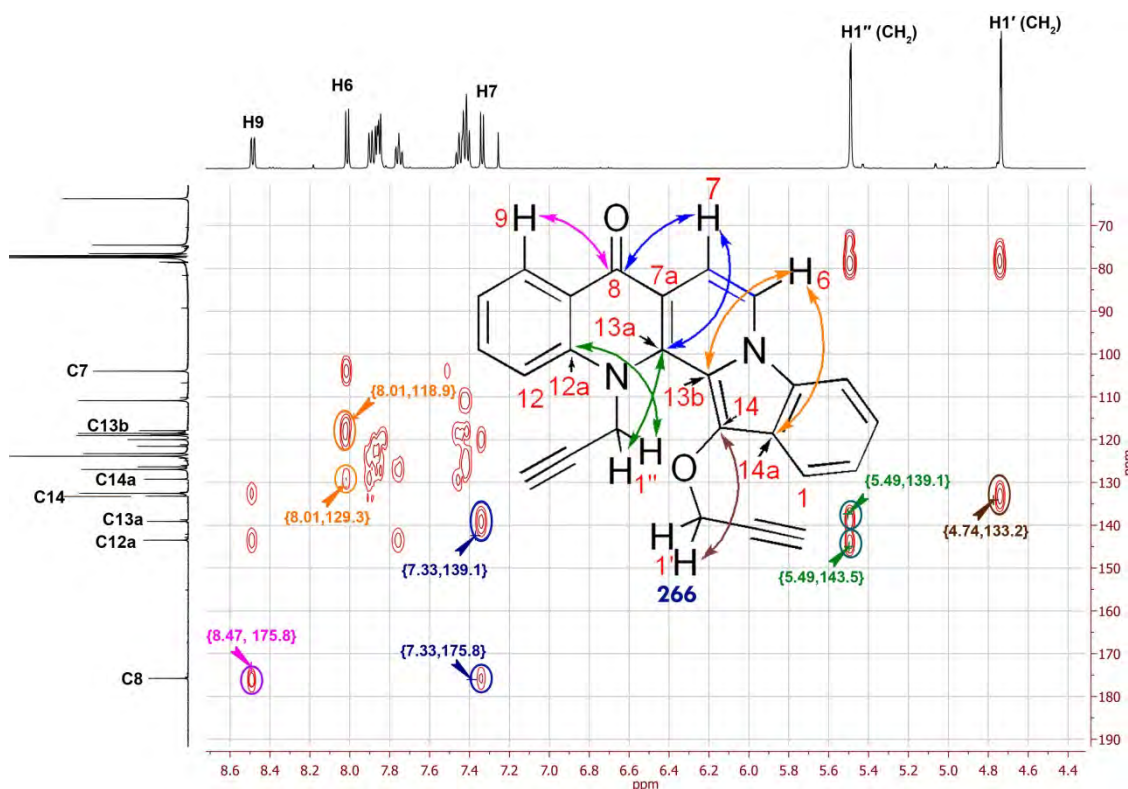
Figure 49: HMBC spectrum expansion for compound **266**.

Slow recrystallisation of compound **266** from a mixture of ethyl acetate and petroleum spirit yielded crystals from which an X-ray crystallographic structure could be solved.
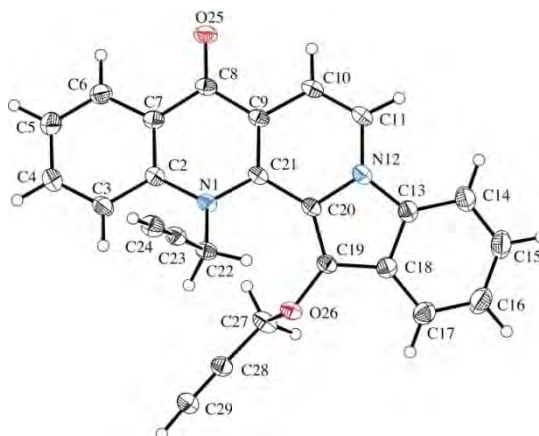
Figure 50: The crystal structure of the pyridodiindole **266**.

The ring expansion of the indigo 5-membered ring into a 6-membered ring is new chemistry, with the three additional carbons of the indolo[1,2-*h*][1,7]naphthyridine parent structure being sourced from the additional propargyl unit. Retrosynthetically, sourcing the C6-C7-C7a moiety of **266** from a propargyl unit with the remaining skeleton from indigo is not intuitive and highlights the novelty of this new chemistry of indigo.

The final product, isolated in very low yield (1%), was the yellow propargyl ester benzoindolonaphthyridinone **267**. Analysis of the mass spectrum (EI+) indicated a peak at *m/z* 458 assigned to the M+H$^+$ ion, and fragment ions at *m/z* 419 and *m/z* 375, corresponding to the loss of a HC≡C-CH$_2$, and then CO$_2$ fragments, respectively. ^{1}H NMR spectrum showed three singlets at 2.14 (H3"), 2.30 (H3"') and 2.53 (H3') ppm, assigned to the three terminal acetylenic protons, with the corresponding propargyl methylene moieties assigned to the three pairs of doublets at 4.76 (H1"), 5.06 (H1"'), and 5.43 (H1") ppm. Expansion of the aromatic region showed the presence of nine aromatic protons, of which the additional proton was assigned as the deshielded singlet H6 at 8.19 ppm due to the adjacent tertiary nitrogen. The comparison with the spectrum of **266** showed the spectrum for **267** lacked one aromatic proton, relative to the ten aromatic protons of **266.** The ^{13}C NMR spectrum revealed a peak at 174.5 ppm,

assigned to the C8 carbonyl and a peak at 167.1 ppm assigned as belonging to the propargyl ester carbonyl (C1'''). The ring-expanded structure was confirmed by single-crystal X-ray analysis as the indigo-ring-expanded product **267** (Figure 51).
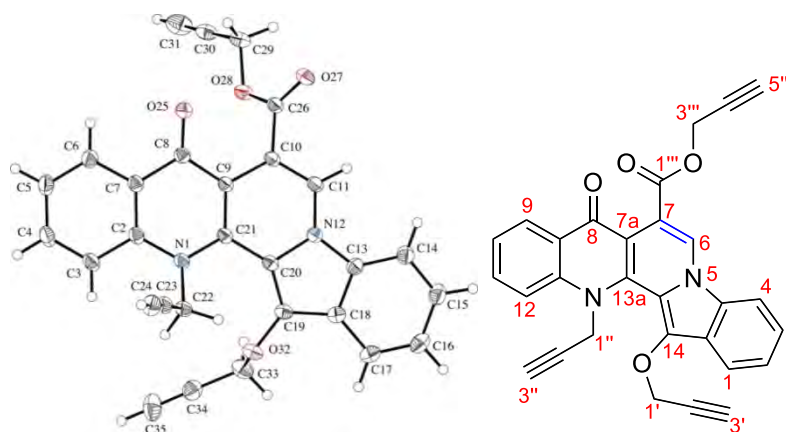
Figure 51: The crystal structure of the pyridodiindole **267**.

3.1.1　Optimisation for the synthesis of *N*-propargyl indigo 263 and pyrazinodiindole 264

In a separate reaction, under analogous conditions but with a very short reaction time (<1 min) and a stoichiometric quantity of propargyl bromide, compound **263** could be isolated in a much improved 93% yield (Scheme 67, Step **A**). The increased solubility in a range of organic solvents (e.g. THF, CH$_2$Cl$_2$) enabled this *mono*-propargylated scaffold to be used as a starting material for subsequent reactions, including cyclisation. This increased flexibility in the use of solvents allowed for a greater variation in reaction conditions to be used. Compound **264** could be synthesized in high yield (98%) by a 6-*exo*-dig hydroamination of **263** in DMF, in the presence of Cs$_2$CO$_3$ (Scheme 67, Step **B**).
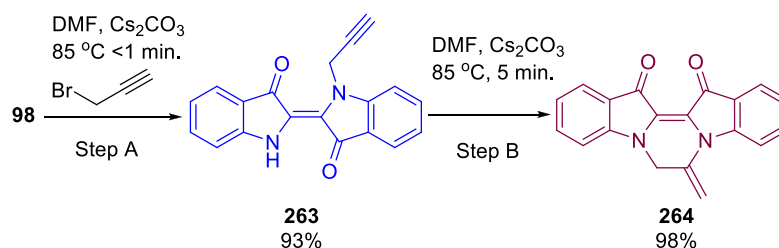
Scheme 67: Synthesis of **263** and subsequent conversion to **264**.

3.2 Reaction of indigo and 1-bromo-2-butyne

In order to understand the mechanism of the reaction of indigo and alkyne moieties and explore the effect of terminal substituents on the outcome of the reaction, indigo and 1-bromo-2-butyne were reacted under the identical conditions to those described earlier. The reaction was monitored by TLC analysis, which demonstrated the complete consumption of indigo after 30 min from the addition of the alkyne. After the purification by silica gel column chromatography The *N*-alkylated derivative of indigo **268** (62%) and the ring-expanded methylbenzonaphthyridine **269** (31%) were isolated (Scheme 68)
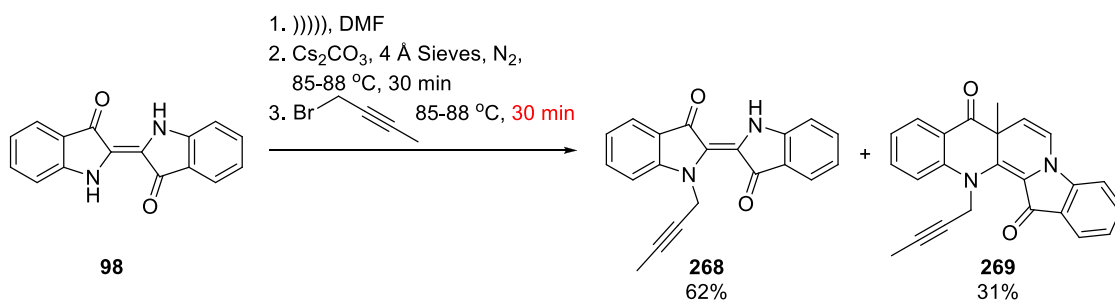
Scheme 68: The reaction of **98** and 1-bromo-2-butyne and formation of **268** and **269** compounds.

Compound **268** appeared as a fluffy solid with navy colour after recrystallisation from methanol/CH$_2$Cl$_2$. The peak at *m/z* 314 (M$^+$) in the MS (EI+) spectra was assigned to the molecular ion, confirming the addition of one methylpropargyl unit. Analysis of the ^{1}H NMR data confirmed the absence of the terminal alkyne at 2.17 ppm in comparison with the ^{1}H NMR spectrum of the **263**. A triplet at 1.69 ppm with integration of three protons was assigned to H4", the terminal methyl substituent. A doublet at 5.32 ppm was assigned to H1" of the methylene and a sharp downfield singlet at 10.60 ppm was assigned to the free NH proton. From the ^{13}C NMR two signals at 187.3 and 189.5 ppm were assigned to the carbonyl groups as C3 and C3' (Figure 52).
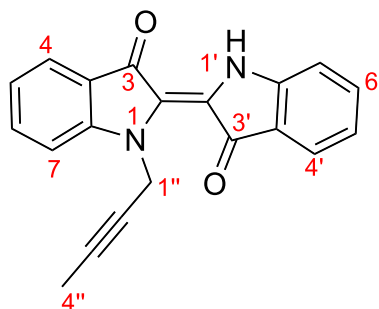
Figure 52: Structure of compound **268**

Methylbenzonaphthyridine **269** was obtained as dark red powder. The peak at *m/z* 366 (M$^+$) in the MS (EI+) spectra was assigned to the molecular ion, indicating the addition of two methyl-propargyl units to the original structure of indigo. Analysis of the ^{1}H NMR spectrum showed two singlets with an integration of three protons. The first signal at 1.65 ppm was assigned to the H1" and the second at 1.74 ppm was assigned to the terminal of the butyne H1' (Figure 53). A doublet at 4.67-5.01 ppm was assigned to the methylene of the butyne pendant. The aromatic region revealed the presence of nine protons, of which the additional proton was assigned as the deshielded H6 at 6.82 ppm due to the neighbouring effect of the tertiary amine. The gCOSY spectrum showed a correlation between H6 and a doublet at 5.44 ppm, which was assigned as H7 (Figure 53). It was also observed both H6 and H7 moved more upfield compared to the chemical shift of the equivalent protons in compound **266** (8.01 and 7.33 ppm). This was suggested that the cyclised section lacked the conjugation previously observed with compound **266**. This was attributed to the presence of the terminal methyl group, which prevents proton abstraction (See mechanistic discussion, Scheme 74). Analysis of the gHSQC spectrum revealed a signal with positive phasing (annotated in blue) assigned to the protons of the methylene and their correlation with the corresponding carbon (C1') at 44.0 ppm (Figure 54).
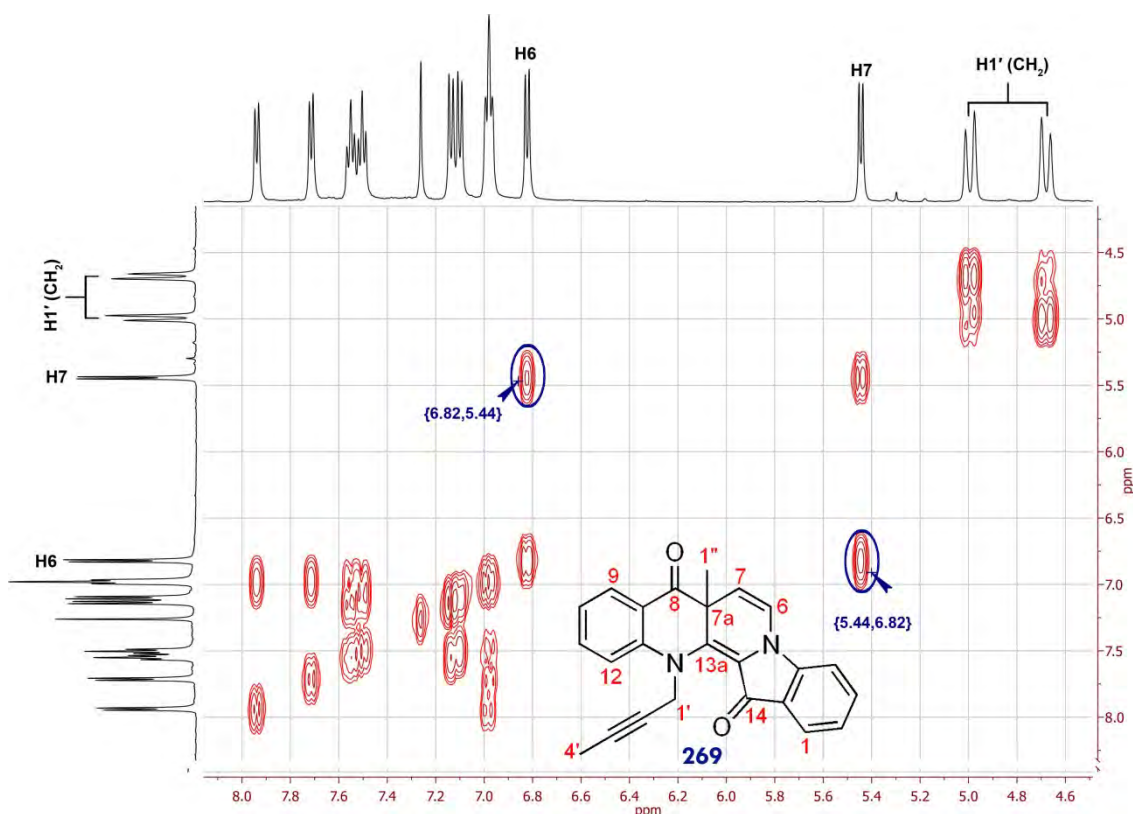
Figure 53: gCOSY spectrum for compound **269** and key correlation between H7and H6.
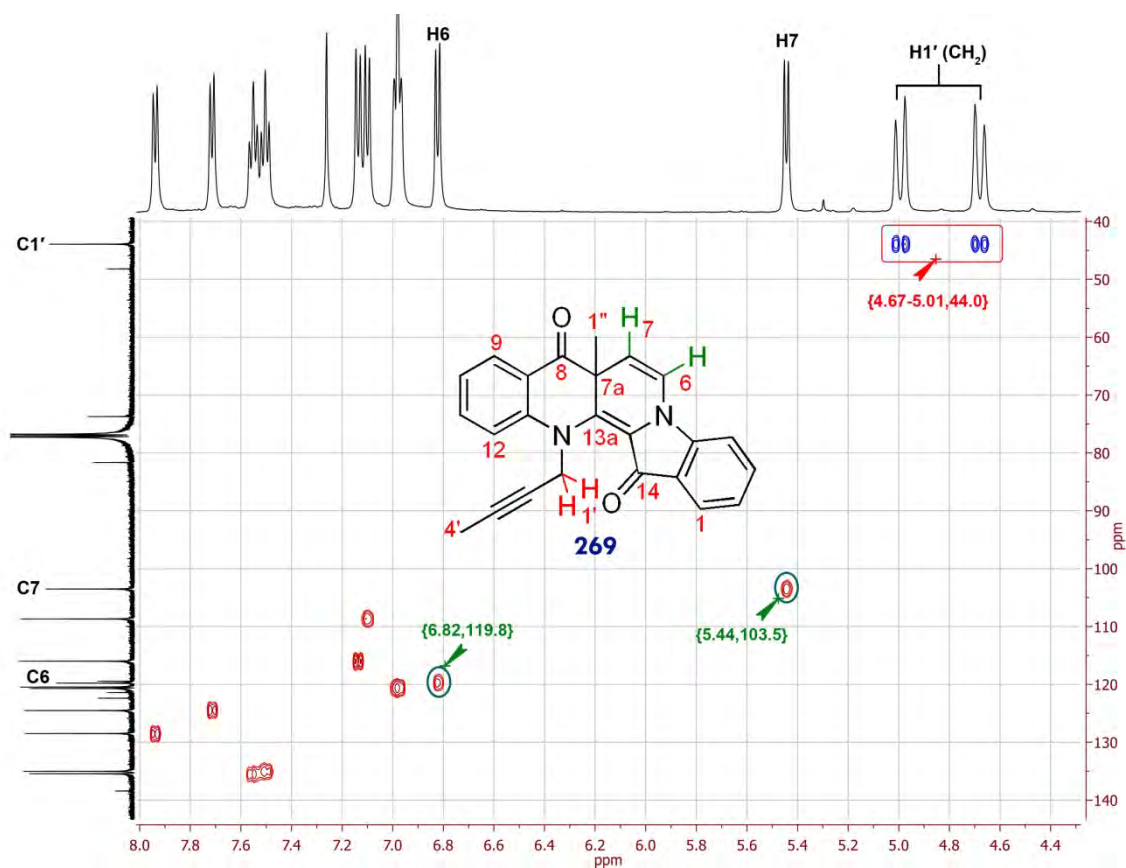
Figure 54: The gHSQC spectrum for **270** illustrated the presence of one CH$_2$ (red) and correlations of H6 and H7 with their corresponding carbons (green).

Analysis of the ^{13}C NMR spectrum confirmed the presence of two carbonyl groups as C14 and C8 (178.4 and 193.6 ppm respectively). Figure 55 illustrates the gHMBC spectrum for compound **269** which revealed a key correlation between H6 and the quaternary carbon C7a at 48.2 ppm through three bonds (green). Another important correlation was observed between C13a at 138.4 ppm and H7 (orange). A three bond correlation between C14 (178.4 ppm) and the aromatic proton H1 (7.71 ppm), as well as a signal assigned to the correlation between H9 (7.94 ppm) and C8 (193.6 ppm) were observed from the analysis of this spectrum (magenta).
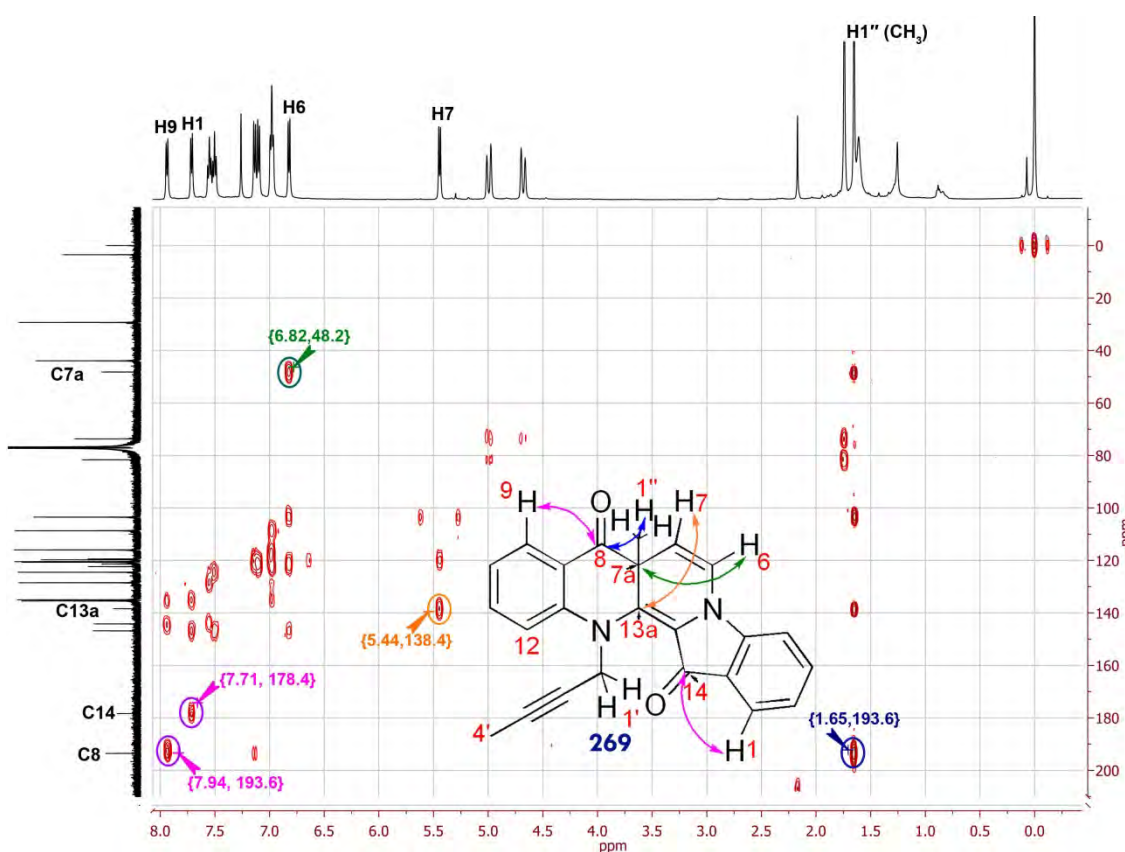
Figure 55: The gHSQC spectrum for **269**, arrows on structure are representing the same colour pointers on the spectrum.

Slow recrystallisation of compound **269** from a mixture of ethyl acetate and petroleum spirit yielded crystals from which an X-ray crystallographic structure could be solved (Figure 55, see Appendix 2 for X-ray crystallographic data).
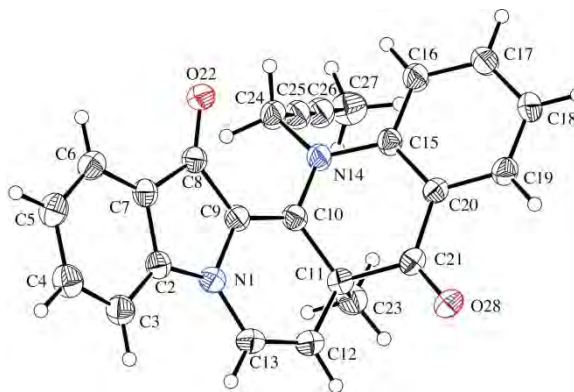
Figure 56: Crystal structure for compound **269**.

3.3   Reaction of indigo and 3-chloro-1-phenyl-1-propyne

To further explore the effect of a larger terminal substituent, indigo was reacted with 3-chloro-1-phenyl-1-propyne under the identical reaction conditions as explained for propargylation reaction. The reaction mixture was stirred and heated at 85 °C under the static inert atmosphere for one hour, and then the reaction mixture was filtered hot in to an ice bath. Upon leaving to stand overnight, the colloidal lumps of the products sank to the bottom of the flask. The clear aqueous layer was decanted out and the remaining crude mixture was partitioned between water and CH_2Cl_2. After the extraction the organic layer was dried and concentrated under the *vacuo*. The remaining filtrate was subjected to a 10 cm plug of silica and celite (50:50 W/W) and eluted with a mixture CH_2Cl_2 and petroleum spirit (70:30) to afforded a fraction with dark amber colour (Fraction **1**). The plug was eluted for the second round but this time with a mixture of CH_2Cl_2 and EtOAc (50:50) and afforded a fraction with dark purple colour (Fraction **2**). Column chromatography of fraction **1** was resulted in the isolation of compound **270** (27%) as an orange-yellow solid. Fraction **2** was also subjected to flash column chromatography which afforded **271** (35%) as a dark blue powder (Scheme 69).
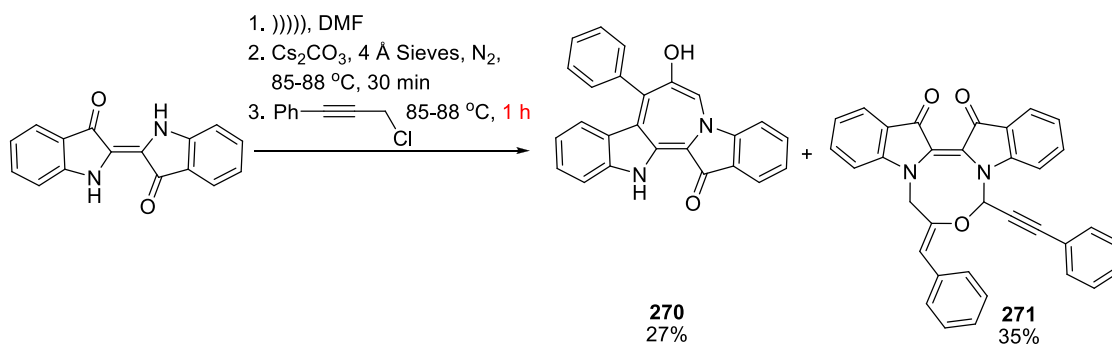
Scheme 69: Reaction of indigo and 3-chloro-1-phenyl-1-propyne.

The phenylazepino diindole **270** was assigned as a result of the addition one phenyl propargyl unit. Analysis of the EI+ mass spectrum revealed a peak at *m/z* 376 corresponding to the molecular ion. Furthermore the ^{1}H NMR spectrum revealed the presence of ten signals in the aromatic region with an integration of fourteen protons in comparison with the expected thirteen protons (eight from indigo core and five from the phenyl ring). The additional proton was assigned to the H6 at 6.90 ppm which is deshielded because of the extended conjugation and adjacent tertiary amine. The doublet at 8.72 ppm was assigned to an aromatic proton H9 moved further downfield due to the shielding effect of the phenyl ring (Ar') hanging over the top. The two doublets at 8.22 ppm and 8.09 ppm were assigned to H12 and H4 respectively. This suggested the presence of an extended resonance in this structure. A doublet at 8.03 ppm was assigned to H1 (Figure 57).
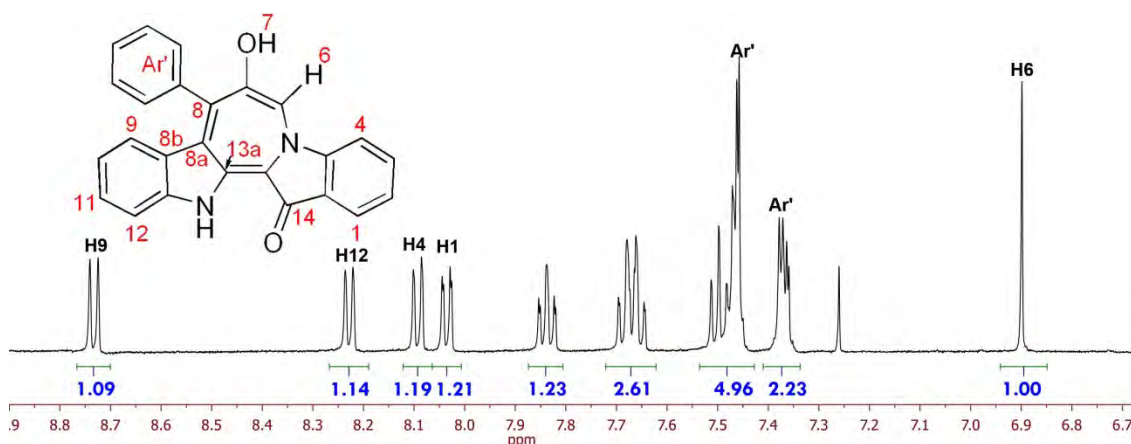
Figure 57: The expansion of the ^{1}H NMR spectrum for the phenylazepino diindole **270**.

The gCOSY spectrum showed that the H6 has no coupling with any other spin and confirmed the position of this proton between a heteroatom and a quaternary olefinic carbon (Figure 58).
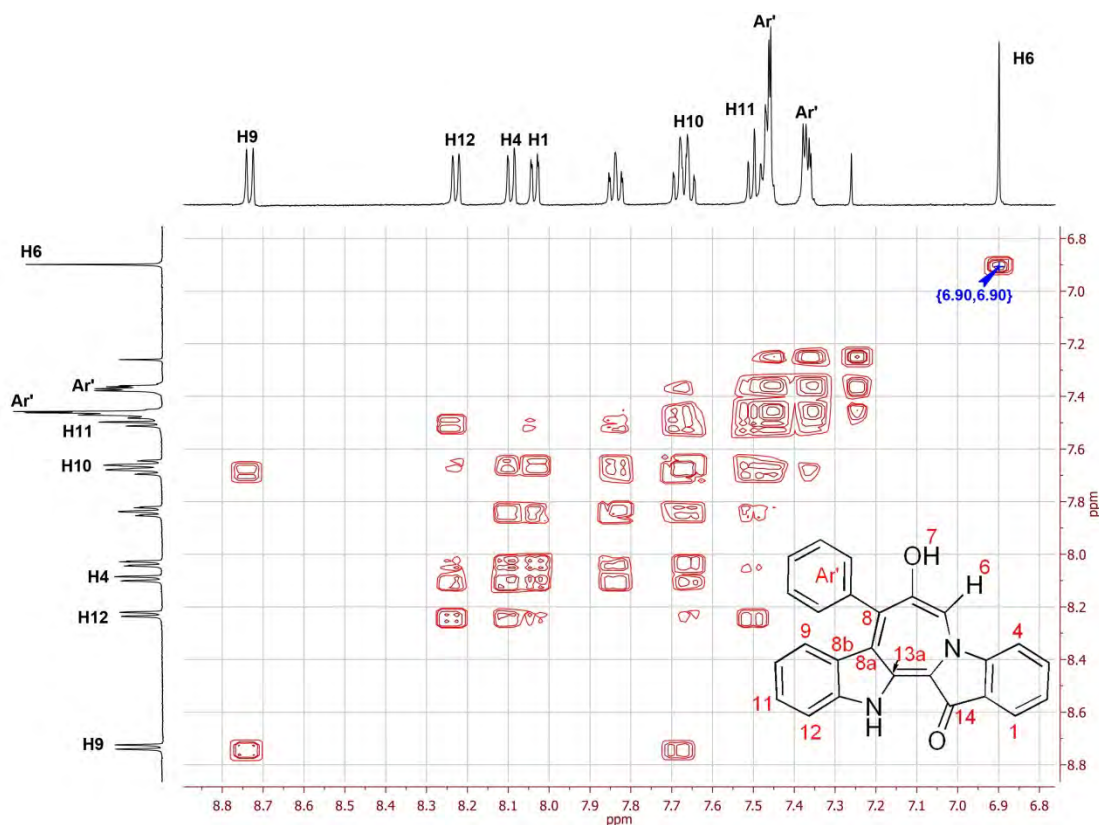
Figure 58: The gCOSY spectrum for **270**.

Analysis of the NOESY spectrum showed weak signals which were assigned to the correlation between the H6 and H4 and also correlation through the space between H9 and one of the aromatic protons of the phenyl pendant HAr' (Figure 59). The gHSQC spectrum revealed that there is no signal with positive phasing indicating the structure has no methylene group. The attached proton test (APT) NMR spectrum showed the presence of twenty five carbons, of which fourteen peaks assigned to the methine signals and eleven negative signals for the quaternary carbons. A peak at 184.6 ppm was assigned to C14 of the carbonyl group. The ^{13}C NMR spectrum revealed a shift for the quaternary carbon C7 at 159.30 ppm.
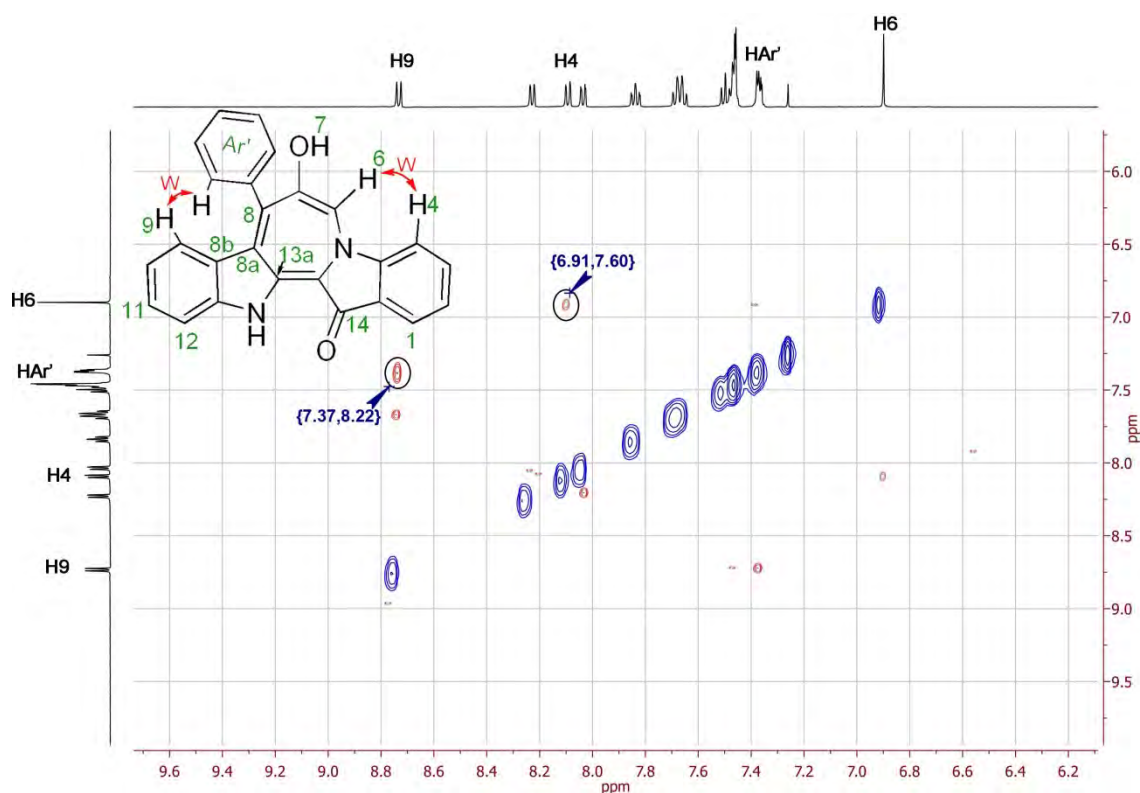
Figure 59: The NOESY spectrum for compound **270** and annotated correlations for H9 and HAr' as well as NOE between H4 and H6.

The correlations in the gHMBC spectrum of H6 to carbon C8 at 135.7 ppm (Figure 60, green) and C13b at 121.8 ppm (Figure 60, orange) further supported the presence of a cyclised structure. The weaker coupling of H6 to carbon C8a at 137.8 ppm (Figure 60, blue) and C4 at 123.1 ppm (Figure 60, black) suggested a four-bond proton to carbon coupling distance. Evidence for the presence of the phenyl group was found through the strong three bonds correlation peaks of ArH2' and ArH6' to C8. The other complementary couplings between C8a and H12 (Figure 60, aqua) and C14 and H1 (Figure 60, magenta) are illustrated on the spectrum.
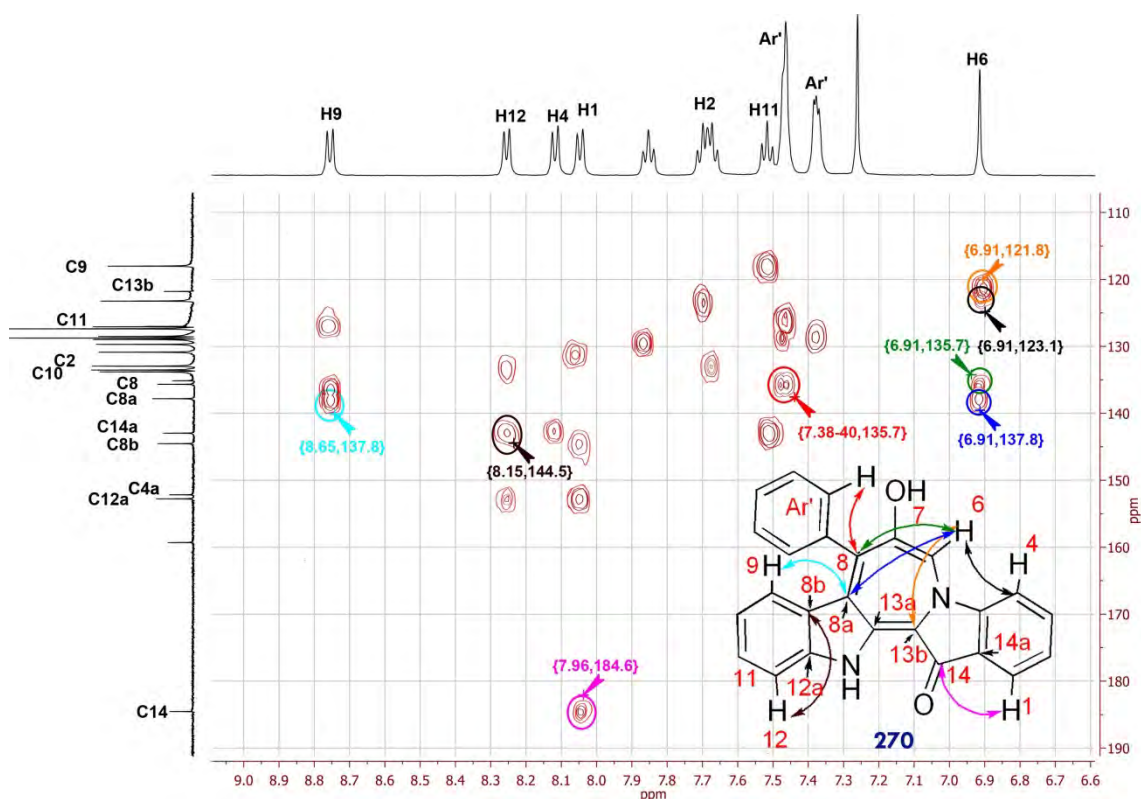
Figure 60: The gHMBC spectrum for the phenylazepinodiindole **270**.

In the case of oxadiazocinodiindole **271**, analysis of the sample with EI-MS showed a *m/z* 506 which was unexpected and was 16 units higher than the expected mass from the addition of the two phenylpropargyl units to the deprotonated indigo skeleton. This was likely to be the result of oxygen insertion. To ascertain the degree of alkylation molecular mass ESI-MS was employed with the same sample and a strong $[M+H]^+$ peak at 507 was observed. Doping the sample with sodium acetate revealed a signal at 529 $[M+Na^+]^+$. Replacing the MeOH solvent with MeOD confirmed that the structure has no exchangeable protons. The analysis of the HRMS (ESI) mass spectrum showed a signal at 507.5154 $[M+H]^+$ which was confirmed the molecular formula as $C_{34}H_{22}N_2O_3$. Analysis of the ^{1}H NMR spectrum showed an AB quartet (ABq) peak at 4.75-4.86 ppm with an integration of two protons which was assigned to the H9 methylene. A singlet at 5.67 ppm was assigned to the H6 of the oxadiazocin ring system. The more downfield singlet at 6.72 ppm was assigned to the H1" proton (Figure 59).
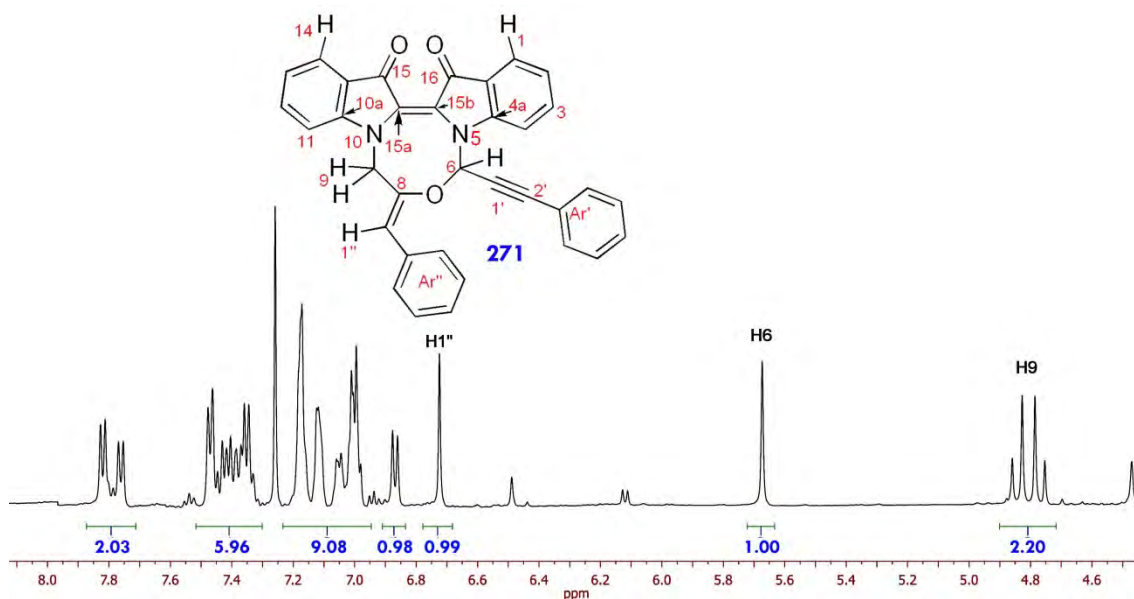
Figure 61: Expansion of the ^{1}H NMR spectrum for **271** and the elucidated structure.

The ^{13}C NMR spectrum confirmed the presence of two peaks in the carbonyl region which were assigned to C15 at 180.9 ppm and C16 at 180.2 ppm confirming the carbonyl groups of indigo core remained unsubstituted. Analysis of the gCOSY spectrum revealed that the H9 has no correlation with any other proton. Therefore splitting of this signal to an AB quartet was attributed to a conformationally restricted ring system. It was also observed that the H6 and H1" protons were not illustrating a correlation with any other protons, suggesting H6 to be an aliphatic proton, deshielded due to the neighbouring effects of the oxygen and tertiary amine. The other downfield singlet (H1") was assigned as styrenic proton (Figure 62). Analysis of the gHSQC spectrum showed one signal with positive phasing (blue) and confirmed the presence of the H9 as protons of a methylene group. This showed the direct correlation of H9 and C9 at 61.2 ppm. From this spectrum, C6 at 56.9 ppm and C1" at 134.5 ppm were assigned as corresponding carbons of H6 and H1" respectively (Figure 63).
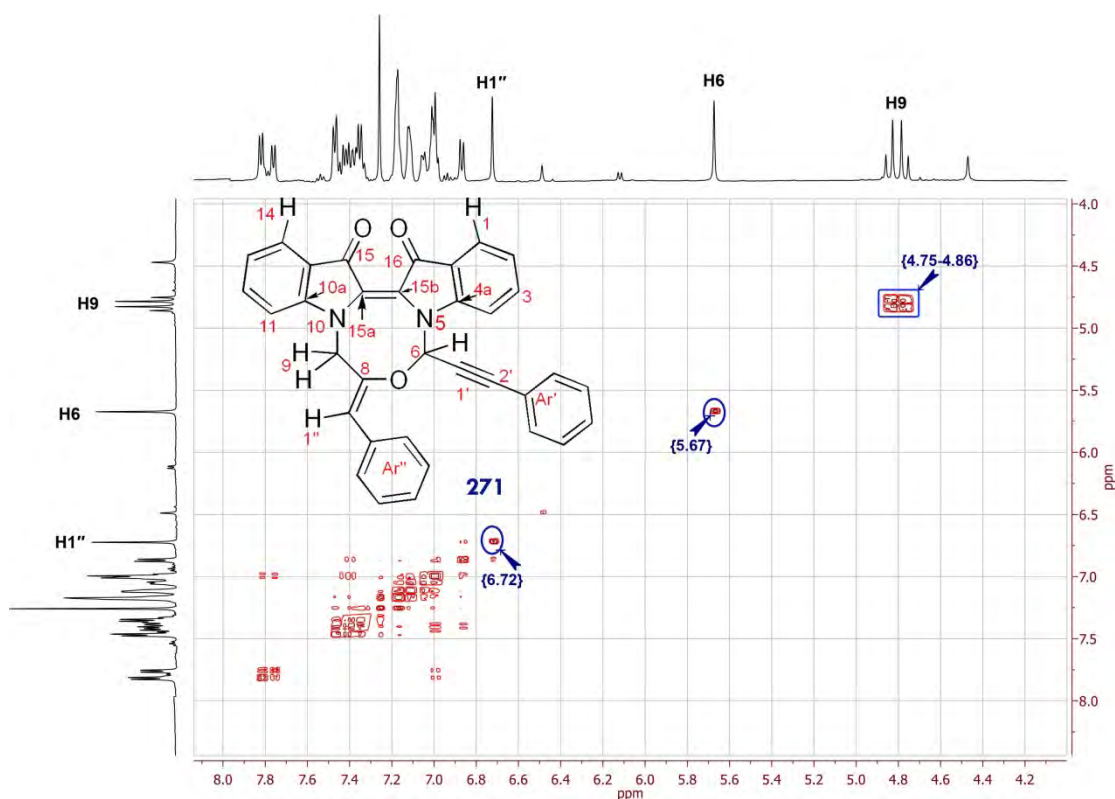
Figure 62: The gCOSY spectrum for the compound **271**.
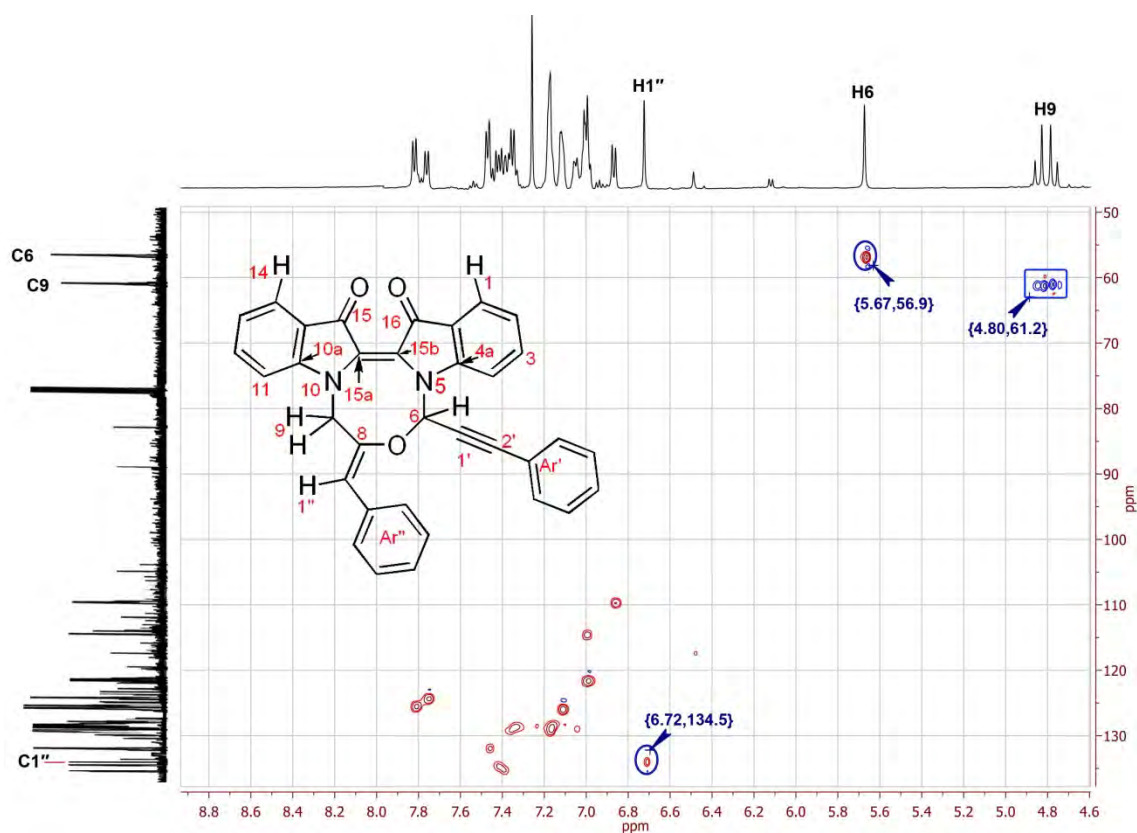
Figure 63: The gHSQC spectrum for compound **271**.

According to the rotating frame NOE (ROESY) spectrum, H6 proton correlates with H1" through the space (Figure 64, red). This suggested the *trans* isomer for the benzylidene pendant. The other noteworthy ROESY correlation was observed between H6 and H4 proton of the aromatic ring of indigo core (Figure 64, blue). The correlation between the H1" and H9 was also observed in this spectrum (Figure 64, green).
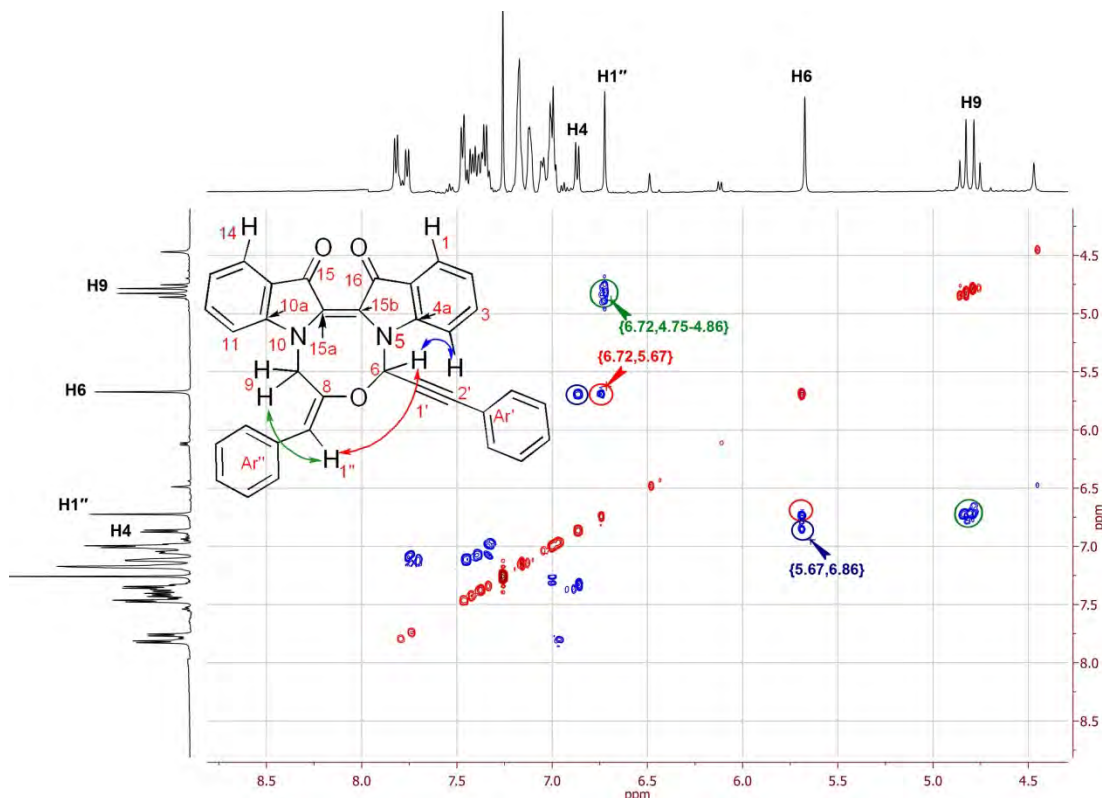
Figure 64: The ROESY spectrum for oxadiazocinodiindole **271** and annotated correlations between H6 and H4, H9 and H1" and H6 and H1".

The gHMBC spectra showed a three bond correlation between the H9 and C1". This was confirmed further by the correlation of H1" and C9 (Figure 65, blue). The weaker signal was observed which was assigned to the correlation of H9 and C1' at 83.0 ppm through the five bonds (red). The other key correlation was noted between the H6 and quaternary 15b at 125.5 ppm which was stronger compare to the signal assigned to the four bond correlation of H6 and C15a at 133.7 ppm (green). The H6 proton showed another weak correlation with the aromatic quaternary Ar'C (orange). The other

noteworthy three bond correlations were observed between H1 at 7.76 ppm and C4a at 148.2 ppm and H14 at 7.82 ppm and C10a at 149.4 ppm (brown). The strong correlation between H1 and the carbonyl group C16, and correlation between H14 and C15 of the other carbonyl indicated that the distance between the coupling proton and carbon nuclei was not further than three bonds (magenta). The three-bond correlation between C2' at 89.0 ppm and the *ortho* proton of the aromatic ring Ar'H was observed and illustrated in Figure 65 (black).
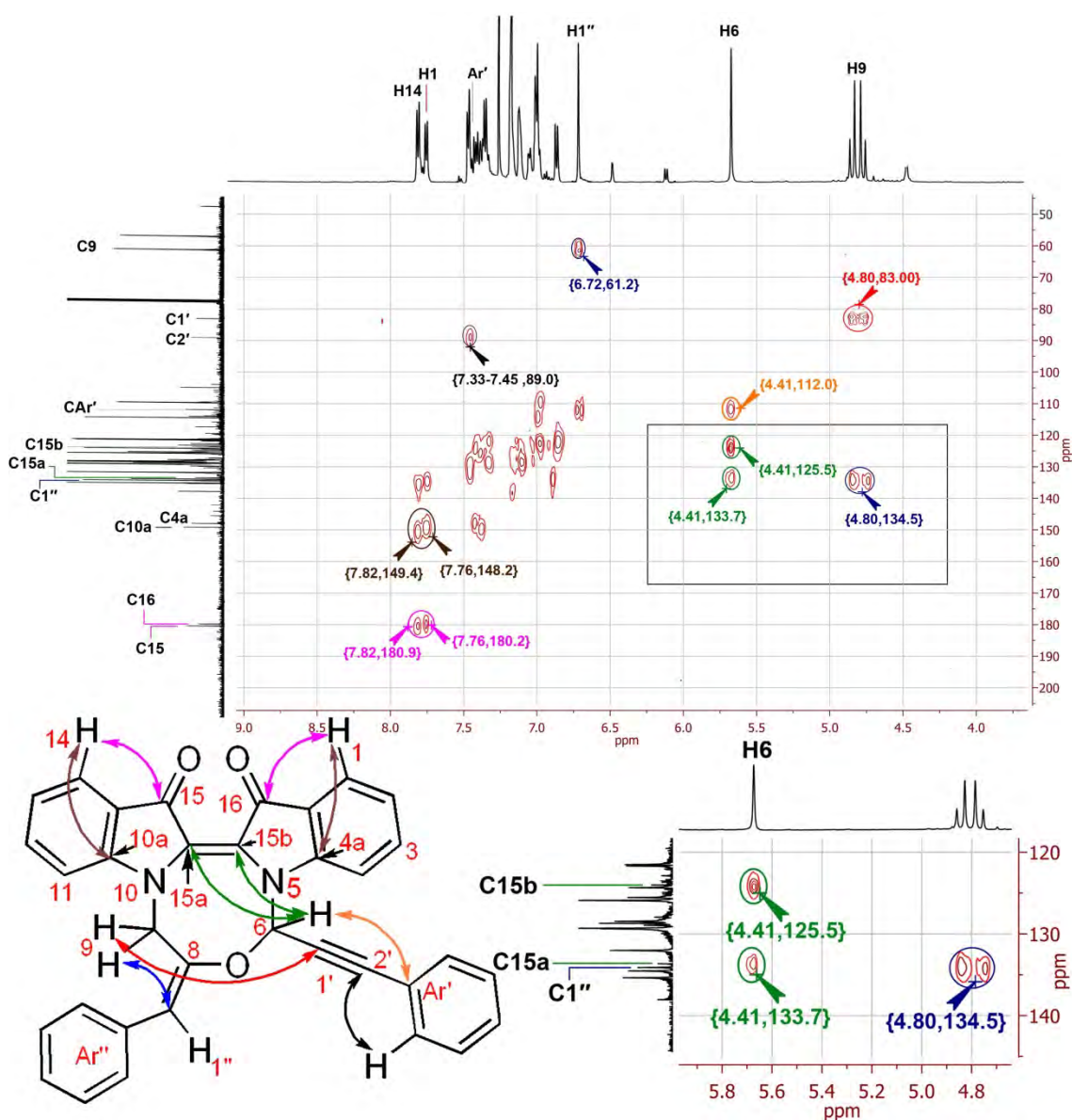
Figure 65: The gHMBC spectrum of **271** and its structure with colour coordinated arrows corresponding to the colour of the pointers on the spectrum.

Long-range or non-standard HMBC correlations, $^{n}J_{C,H}$ n>3: were observed between H9 and C1' (five bonds) and H6 and C15a (four bonds). This could arise from the relaxation delay which is a factor of molecular structure. It is commonly believed that HMBC is only useful to observe short-range correlations between two- or three bonds and observation of long-range HMBC correlations are rather uncommon, without attenuation of the instrument tuning to observe such correlations, and depends to the shape of the scaffold and bond angles. There are a number of reports in which long-range HMBC correlations were observed and considered in characterisation of complex molecules.[150, 151] For example, four-bond correlations are noted in the structural elucidation of distamycin A,[152] or five-bond HMBC correlations have been observed for quinones.[153] The intensity of the HMBC signal is not necessarily dependant to the range of the correlation[154] therefore discrimination of the normal and long-range HMBC signal is not feasible. It is necessary to supplement this HMBC spectrum with more exclusive and restricted experiment such as Heteronuclear 2-Bond Correlation (H2BC) which correlates proton and carbon spins separated by two covalent bonds. Further information could be obtained from ^{1}H-^{15}N HMBC and inadequate NMR experiments.

This ambiguity also emphasises the impact of X-ray crystallography analysis in structural elucidation of the products from these cascade reactions. Attempts to grow X-ray quality crystals from oxadiazocinodiindole **271** and phenylazepinodiindole **270** failed using various solvent systems and techniques.

In another attempt, the above reaction was carried under slightly different conditions in which the reaction mixture was stirred and heated for one hour after the addition of the base, before phenylpropargyl chloride was injected into the reaction mixture. After 10 min, TLC analysis of the reaction showed the complete consumption of the indigo. The reaction mixture was poured into an ice bath and extracted with EtOAc. The organic layer was collected and concentrated under *vacuo*. Fractional recrystallisation of the

filtrate resulted in the isolation of compound **271** in 62% yield with no indication of the formation of **270**.

3.4   Reaction of indigo and propargyl mesylate

In order to investigate the effect of the leaving group on the outcome of the propargylation reaction, indigo was reacted with propargyl mesylate under the standard conditions. The reaction mixture turned to a dark brown solution after 3 min and TLC analysis showed the complete consumption of indigo. The reaction was quenched and extracted by the same protocol and fractional recrystallisation from dichloromethane and pet. spirit yielded 51% of **266**. The mother liquor was concentrated and subjected to preparative plate chromatography which isolated **266** (8%) and **265** (28%) were isolated. In this attempt, compound **263** and **264** were present in the mixture in trace quantities as detected by TLC analysis but were not been isolated (Scheme 70).
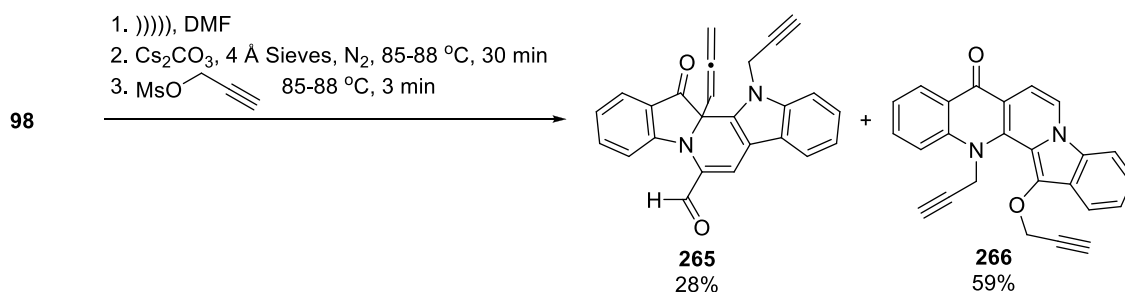
Scheme 70: Reaction of **98** and propargyl mesylate and formation of **265** and **266** with higher yields.

3.5   Reaction of indigo and bromoacetonitrile

To investigate the effect of the polarity of the triple bond on the outcome of the reaction, bromoacetonitrile was reacted with indigo under an identical reaction conditions as used for propargylation reaction. The contents of the flask were poured into ice-water after 5 minutes, and gravity filtered to remove the crushed molecular sieves. The products gradually accumulated on the wall and the bottom of the flask and

the clear liquid layer was decanted a day after. The remaining lumps and amorphous solid were dissolved in CH_2Cl_2 and partitioned in water. After extraction, the organic layer was dried and concentrated to afford shiny brown flakes. Attempts to separate the residue failed and ^{1}H NMR analysis revealed that the brown residue was likely polymeric baseline material. In a separate attempt the reaction was quenched 5 sec after the injection of bromoacetonitrile which was resulted in formation of the navy coloured compound **273**, with a higher R_f value in comparison to indigo (Scheme 71).
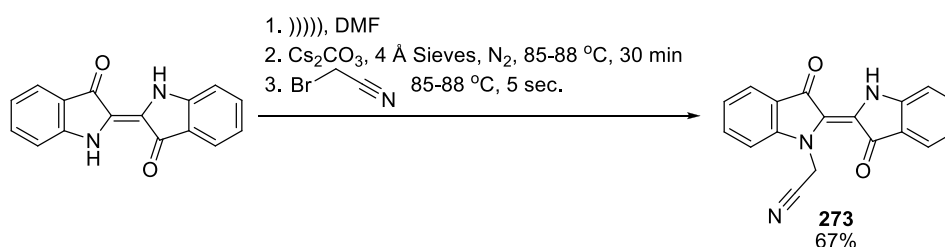
Scheme 71: Reaction of indigo and bromoacetonitrile and formation of **273**.

The peak at *m/z* 301 (M+H^{+}) in the MS (ESI) spectra was assigned to the molecular ion, with the peak at *m/z* 261 assigned to the loss of the acetonitrile unit. The ^{1}H NMR spectrum was lacking the signal at 2.17 ppm of the alkynic proton. The presence of the methylene group of the other propargylic pendant was confirmed by the peak at 5.64 ppm. Additionally there were eight aromatic proton signals, and a singlet at 10.54 ppm, which was assigned to the free NH group. The ^{13}C NMR spectrum lacked a signal at 72.5 ppm corresponding to the terminal carbon of the propargyl pendant. There were eighteen carbon signals present in this spectrum of which the pair at 188.7 and 190.0 were assigned to the carbonyl groups of the structure.

3.6 Mechanistic and reaction discussion

The proposed mechanisms for the propargylation of indigo are summarised in Schemes 77-79 and involve five key pathways.

The pyrazinodiindole **264** is derived from the monopropargylated indigo **263** (blue,

Path I, Scheme 72) after *N*-deprotonation, followed by delocalisation which allows rotation around the central bond to the *cisoid* conformation. A subsequent intramolecular 6-*exo*-dig hydroamination of the propargyl C2 position yields **264**.
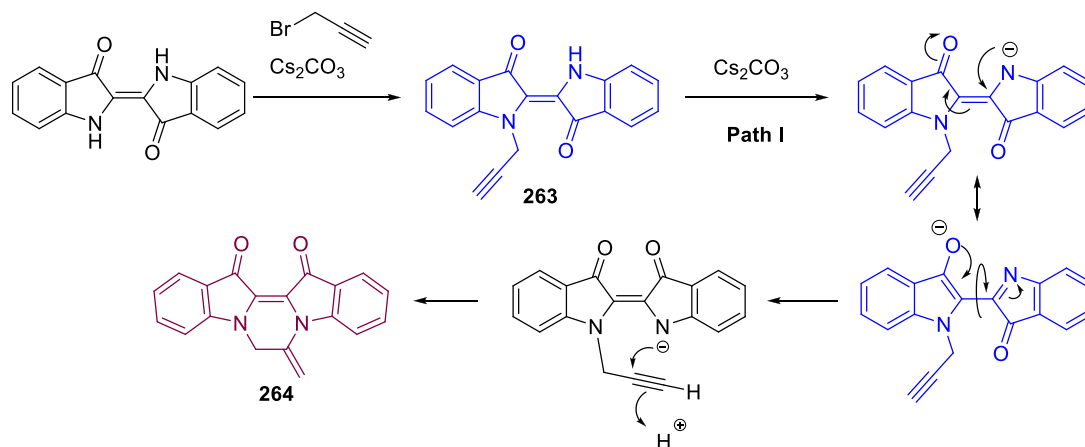
Scheme 72: Proposed mechanism for formation of **263** and **264**. Structures that are coloured indicate common intermediates in the overall mechanism and are the same within Schemes 73 and 74.

Path II starts with the identical key intermediate **263** (blue, Scheme 72) undergoing prototropic tautomerism (**A**) which subsequently *N*-alkylates (**B**) (Scheme 73). Deprotonation of the *N*-methylene generates a stabilised ylid, which allows cyclisation onto the carbonyl, generating an activated cyclic allene intermediate (**C**). Under standard conditions, an 'alkyne nucleophile' is insufficiently strong to attack an electrophilic carbonyl in the absence of a metal (*e.g.* Au, Ru) or an activating influence, however in this instance, the anion from the ylid serves as a formal negative charge, allowing this cyclisation to the 7-ring allene to occur. A comprehensive review on allenes from 1989[155] reported the isolation of an eight-membered carbocyclic allene; however, the corresponding six-membered rings have been plausibly demonstrated as reactive intermediates.[156] Further, with the seven-membered carbocyclic allene, isodesmic reaction energy calculations indicate[157] an allene strain component of 13.5 - 14.3 kcal/mol, consistent with its ready preparation and trapping. Heterocyclic allenes have also been isolated as small as eight-membered rings, with a mixed 'P' and 'B'

heteroatom ylid.[158] Therefore the postulated cyclic allene intermediate **C** (Scheme 73) is reasonable. The cyclic allene could then undergo a ring-expansion reaction, to produce the benzo[*b*]indolo[1,2-*h*][1,7]naphthyridin-8-(13*H*)-one ring structure **D** (Scheme 73). The proposed driving force behind this ring-expansion is relief of ring strain of the 7-membered allenic ring - therefore, there is a favourable energy balance between the 7-membered allenic ring formation, and its subsequent role in providing a driving force for ring expansion. An additional crucial component of this step is the presence of an electrophile (E) - the major product arising from the reaction, **266**, requires $E = H^+$, whereas the minor product **267** requires $E = CO_2$. This, probably generated on the basis of the results noted in Table 1, from carbonic acid decomposition, the acid in turn resulting ultimately from the Cs_2CO_3 base *via* bicarbonate (see below for a greater discussion).
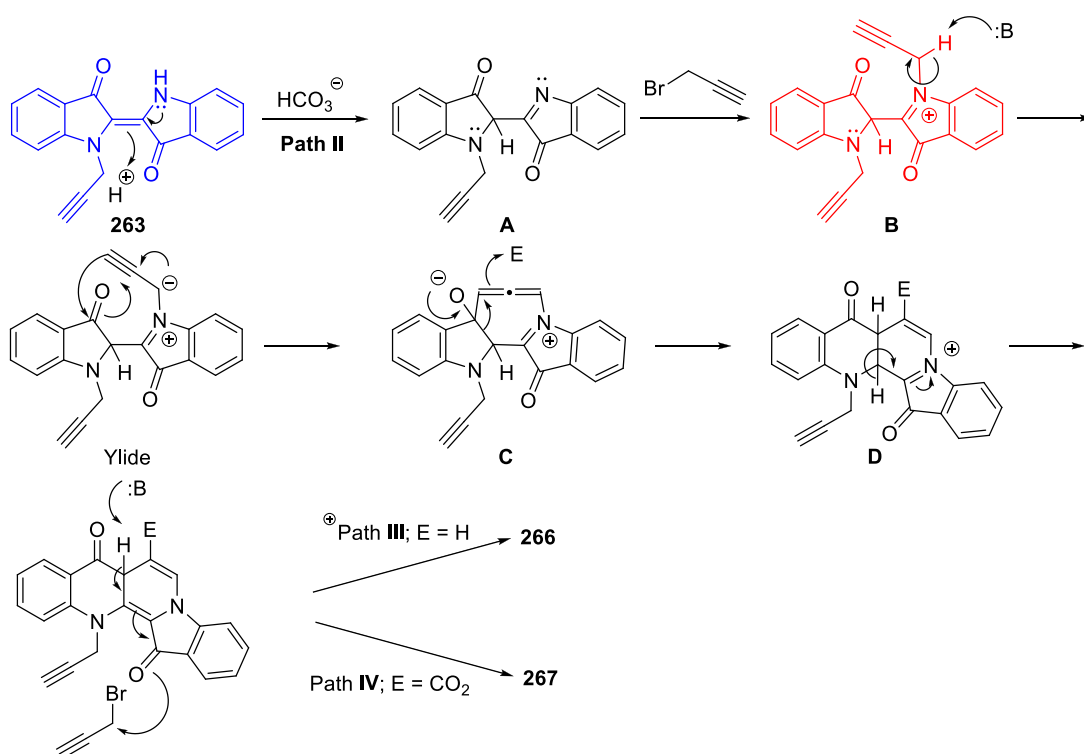
Scheme 73: Proposed mechanism for formation of **266** and **267**

Once the carboxylate unit is incorporated, a further propargyl moiety could be added *via* nucleophilic displacement to produce the ester substituent of **267**. Subsequent

deprotonation, followed by base-induced aromatisation allows for *O*-propargylation in a cascade process, yielding the final products **266** (**Path III**) and **267** (**Path IV**) (Scheme 73).

The addition of a 1-carbon unit is novel and imposes the question as to the origin of this carbon, even though compound **267** is isolated in very low yield. Two possibilities arise and involve either the well-known degradation of DMF[15] to produce a "C=O" fragment that could be incorporated, or it could arise from the generated bicarbonate anion that is present in the solution. Table 1 summarizes experiments to determine the source of the additional carbon atom in **267**. Entry 1 is the standard reaction as previously outlined, whereas entry 2 describes replacing the DMF solvent with DMSO - this resulted in an increase from <1% to a 5% yield suggesting that DMF was not the source of the carboxylate of **267**. Bubbling CO_2 gas through a standard reaction (entry 3) resulted in a 6% yield of **267**, however, the most significant outcome from this reaction is the notably reduced yields of **263**, **264**, **265** and **266**, and a dramatic increase in the production of non-characterisable baseline material. This suggests that the presence of significant quantities of electrophiles could be reacting with different indigo-based nucleophiles as they are being generated resulting in mixtures of products. Entry 4 describes the experiment replacing the Cs_2CO_3 with K_3PO_4 as base, to eliminate the presence of a bicarbonate source. However, the lack of solubility of this base in DMF is the likely reason for the outcome of mostly unreacted indigo being isolated from the reaction.

Table 5: Experiments to probe the source of the ester moiety **267**

	Solvent	Condition	**263**	**264**	**265**	**266**	**267**	BM%	RI%
1	DMF	Cs_2CO_3, N_2	11	21	17	31	1	11	-
2	DMSO	Cs_2CO_3, N_2	-	-	12	13	5	65	-
3	DMF	Cs_2CO_3, CO_2	13	-	7	10	6	61	-
4	DMF	K_3PO_4, N_2	21	-	-	-	-	-	60
5	DMF	Cs_2CO_3, Ar	10	15	14	28	1	*	-

* not isolated, BM = Baseline Material and RI = Recovered Indigo

Path V (Scheme 74) describes a possible mechanism to the allene **265** and diverges from the same intermediate **B** (red, Scheme 73). In this instance it is the iminium indigo moiety that activates the adjacent carbonyl, allowing sufficient electrophilicity to attract the relatively weak nucleophilic alkyne to undergo a cyclisation reaction, promoted by the initial attack of the other indigo nitrogen lone electron pair onto the propargyl C2 in a concerted process yielding the strained fused-aziridine **E**. Carbonate could then act as a nucleophile in a ring-opening of the aziridine and subsequent aromatisation of the central pyridinyl ring to give **F**. *O*-Propargylation of **F** could then afford intermediate **G**. The acidic proton in the CH$_2$OH group α to the iminium ion in **G** may then be removed under the influence of base and further OH proton loss would yield the aldehyde moiety in the intermediate **H**. A Claisen rearrangement of the propargyloxy with the indolic C2-C3 bond could then give rise to product **265**.
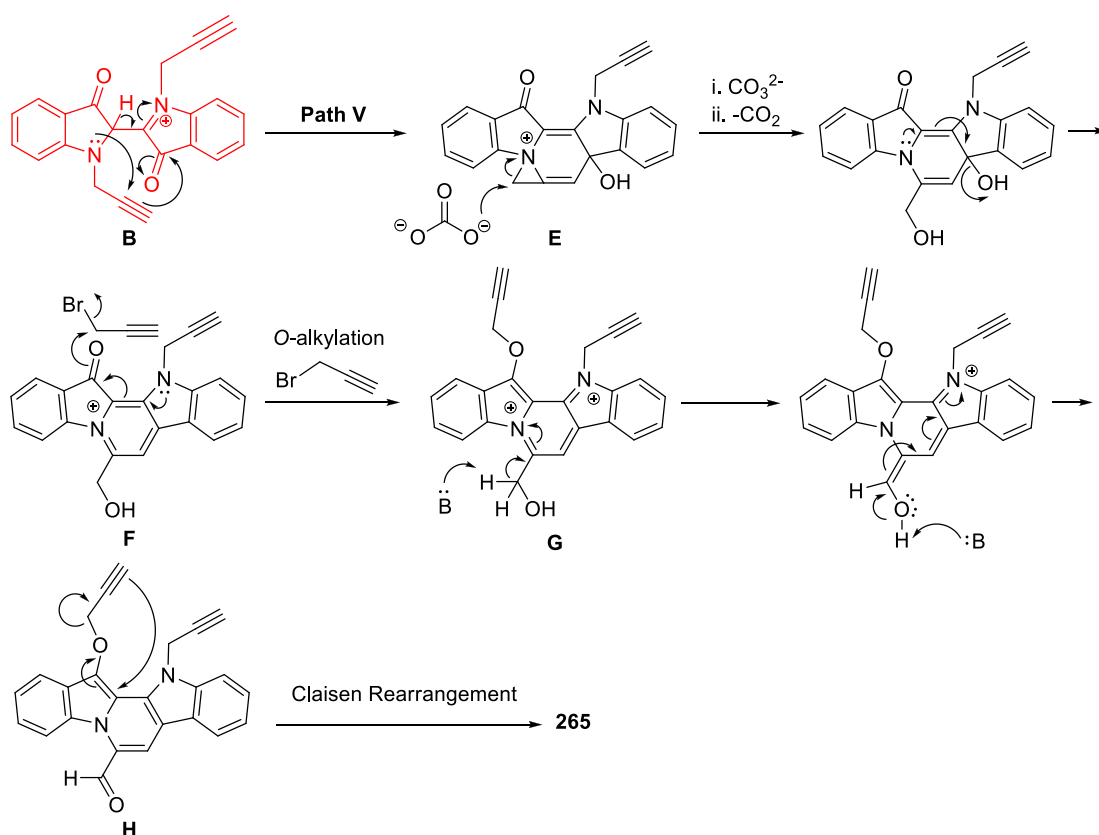
Scheme 74: Proposed mechanism for formation of **265**.

In the case of the reaction of indigo and 4-bromo-2-butyne the mechanism path is

identical with the previously mentioned route in Scheme 72 up to the formation of intermediate **D'**. The presence of methyl group hinders the aromatisation of the ring and subsequently stops enolate formation. The iminium ion is then quenched by the abstraction of the acidic α-proton to furnish **269** (Scheme 75).
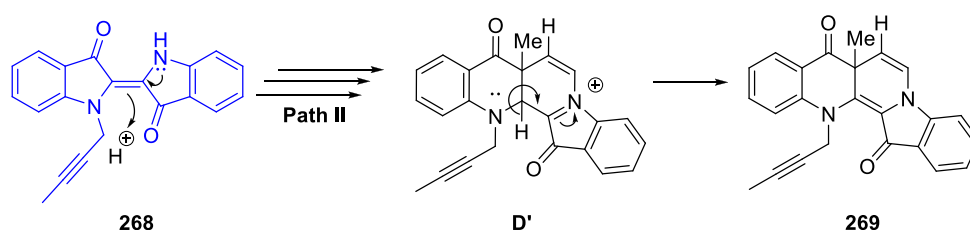
Scheme 75: The proposed mechanism for the formation of **269**.

The reaction of indigo and 3-chloro-1-phenyl-propyne resulted in the formation of two novel structures. A tentative mechanism for the formation of **270** is illustrated in Scheme 76. This starts from deprotonation of the methylene of the phenyl propargyl pendant. Due to the presence of phenyl group and its electron donating nature, the electron-rich alkyne cyclises onto the carbonyl and forms intermediate **C''**. This intermediate rearranges to form **D''** in order to relieve the ring strain of the 7-membered allene ring. The resulting stable enolate is then protonated upon workup, to give **270**.
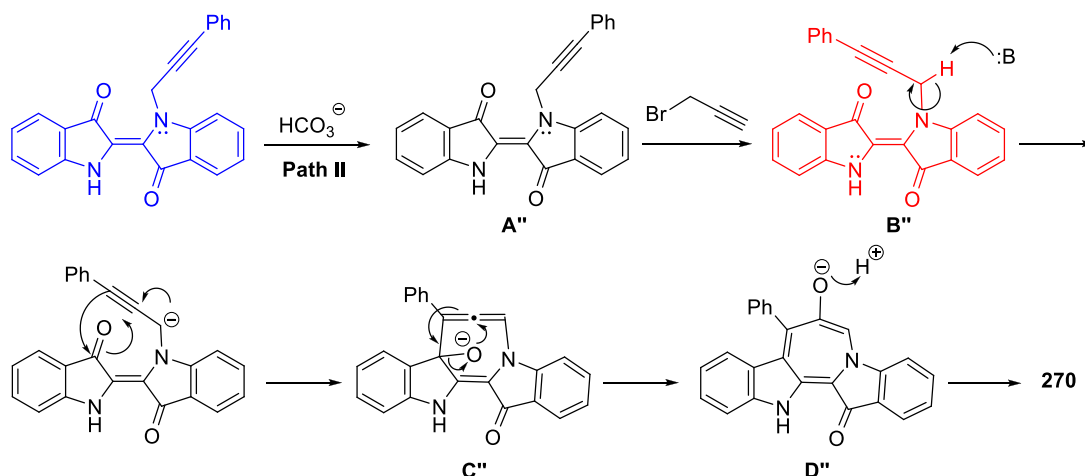
Scheme 76: Proposed mechanism for the formation of **271** form the reaction of indigo and phenylpropargyl chloride.

The presence of the hydroxy group was evidenced by the broad signal at 3282 cm^{-1} in

the IR spectrum. The extended conjugation of the azepine ring prevents tautomerisation and the enol is the preferred form. According to the geometrical and energetic DFT calculations the anti-aromatic azepine ring is planar and stable.[159] Proof of the existence of 1*H*-azepine as a planar seven-membered ring has previously been reported based on the analysis of the ^{1}H and ^{13}C NMR spectroscopy, in which stable *N*-acetyl and *N*-methansulfonyl-1*H*-azepines were synthesised and isolated as pale yellow solids.[160] Computer aided modelling of the **270**, performed with the Wavefunction (Spartan TM) software by optimising the geometry of the molecule using Hartree-Fock theory and the 6-31G level revealed that the azepino diindole unit is planar and the phenyl substituent positioned perpendicularly on the C8 carbon (Figure 66).
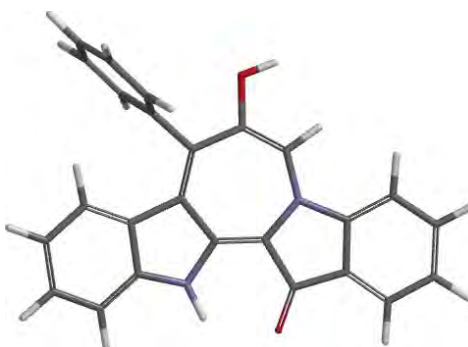
Figure 66: The computer aided model for **270**.

The proposed mechanism for the synthesis of oxadiazocinodiindole **271** includes the generation of phenylpropargyl and aldehyde **E''**. There is no precedent report of this transformation and procedure of this oxidation is under investigation and requires further explanation.[**] Nucleophilic attack from the *N*-phenylpropargyl indigo generates the intermediate **G''**. Concerted addition to the alkynic carbon of the phenylpropargyl pendant forms **H''** and subsequent protonation furnishes **271** (Scheme 77).

Computer aided modelling of the **271** is illustrating the indigo core in a planar position with the eight-membered oxadiazocin ring in a boat-chair conformation. Calculation of

---

[**] One option could be the addition of catalytic amount of water to the reaction mixture and monitor the yield for **271**.

the bond angle was performed by using the Hartree-Fock theory with optimised geometry and the results are summarised in Figure 67.
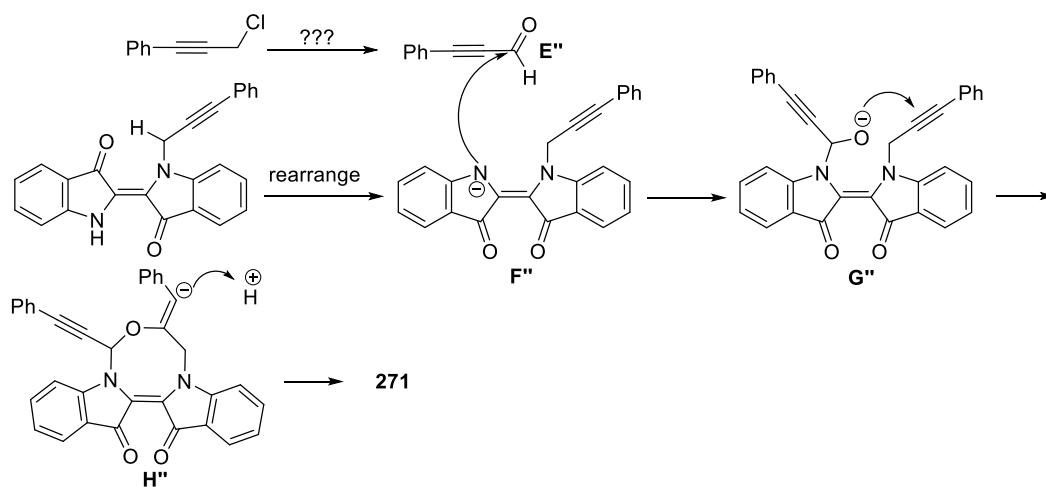
Scheme 77: Proposed mechanism for the generation of oxadiazocinodiindole **271** from the reaction of indigo and phenylpropargyl chloride.
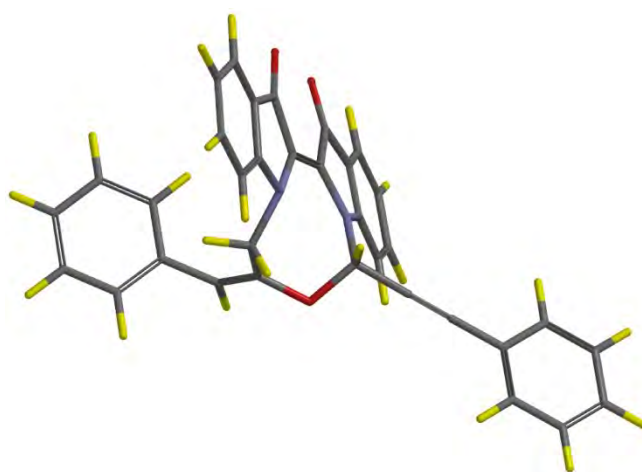
		Bond angle (°)				
Structure	#	α	β	γ	γ	θ
	271	127.4	124.4	112.3	115.5	126.4

Figure 67: Computer aided modelling of structure **271** and the bond angles of the table for oxadiazocin ring bond angles.

The outcomes from these propargylation reactions are repeatable and preliminary investigations also indicate reliable scalability up to at least double quantities. Further, our mechanistic proposals for the formation of **265**-**267** all start from *N*,*N'*-dipropargylated intermediates, rather than an intermediate that had cyclised initially from a *N*-monopropargylated molecule. In support of this proposal were the outcomes from an experiment where a DMF solution of **263** was dripped into a mixture of Cs_2CO_3 and propargyl bromide in DMF over 3 mins before quenching after 2 mins. The result was formation **264** (<3%), **265** (11%), **266** (25%) and **267** (<1%) with complete consumption of the starting material. The poor return of **264** with respect to **265**-**267** suggests that the second *N*-propargylation is a more competitive reaction than cyclisation, and lends support to our proposed dipropargylated compounds as intermediates. This was also confirmed when the propargyl moiety accompanied with a better leaving group such as mesylate, resulted in the formation of **265** (28%) and **266** (59%) (Scheme 70).

It is also relevant to compare the mechanistic outcomes of this propargylation reaction with the outcomes of the corresponding allylation reaction (Scheme 49). Although cyclisation onto the indigo carbonyl of the unsaturated moiety occurred in both instances, reaction onto the indigo C2 position to form a spiro compound only occurs in the case of the alkene. There was no evidence suggesting an equivalent mechanism pathway in the presence of the alkyne. Presumably, the linear alkyne is not able to approach the indigo C2 position whereas the 'bent' nature of the alkene makes this cyclisation reasonable. Further, a significant by-product of the allylation reaction (Scheme 40) was *N*-allylisatin, derived by oxidative cleavage of the central indigo double bond over prolonged reactions. The propargylation reaction went to completion much more rapidly, and as such, under the tested conditions, there was no *N*-

propargylisatin **272** present, as evidenced by TLC analysis, of the reaction mixture against an authentic sample.

A series of simple experiments were undertaken to ascertain whether the reactions are likely to proceed through nucleophilic mechanisms rather than through radical-based sequences. Previous studies have shown that radical reactions with indigo will proceed exceptionally slowly at room temperature and in 4 hours at 100 °C in the presence of oxygen and with irradiation.[131] In contrast, we have repeated our propargylation reaction (as shown in Scheme 65) in the absence of oxygen and light (under argon) with these conditions realizing the same product outcome after 5 mins of reaction at 86 °C. Radical reactions are unlikely to proceed under these conditions, let alone to produce a total yield of 84% of products in 5 mins of reaction time.

Colour is an important qualitative element in the structural elucidation of these polycyclic compounds. The disappearance of the blue and emergence of yellow appears to indicate the loss of H-bonding between the indigo carbonyl and the NH, along with loss of unsaturation in the indigo central bond and the presence of sp^3 hybridised carbon atoms, *e.g.* heterocycles **265**, **266** and **267**. The mono-*N*-propargylated **263**, with both structural elements still present, maintains the deep blue intensity whereas the cyclised structure **264**, which still contains the central double bond but has lost the H-bonding, is a burgundy colour (Scheme 66).

In summary, here we have presented a series of efficient optimised procedures for the synthesis of heterocycles from the reactions of indigo with propargyl halides. Further, it is demonstrated that the presence of terminal substituents not only affects the propensity for the propargylated indigos to undergo one-pot cascade reactions but also in several instances the outcome of these reactions.

Chapter 4: Further Derivatisation Reactions of Cascade Products

Reactions of indigo **98** with allylic and propargylic systems resulted in the formation of a variety of compounds. Amongst these products, some have complex structures such as the spiroindoline-pyridoindolone **227**, fused pyridoindolone **232**, epoxyazepino diindole **253**, pyridodiindole **266** and indolonaphthyridine **267**. A common product between the allylation and propargylation reaction was the variety of *N*-substituted indigos. To expand the scope of generating additional annulated complex systems, candidates of complex and simpler structures were selected to undergo further explorations to probe their synthetic utility.

4.1 Ring-Closing Metathesis of the spiroindoline-pyridoindolone (227)

The previously reported spiro heterocycle **227**, with its pendant allyl substituents, provided an ideal substrate for a metathesis reaction. Therefore, treatment of **227** with Grubbs' 2nd generation catalyst at reflux in CH_2Cl_2 produced not the speculated 9-membered ring **273**, but rather the novel fused heterocycle **274** in 70% isolated yield (Scheme 78).
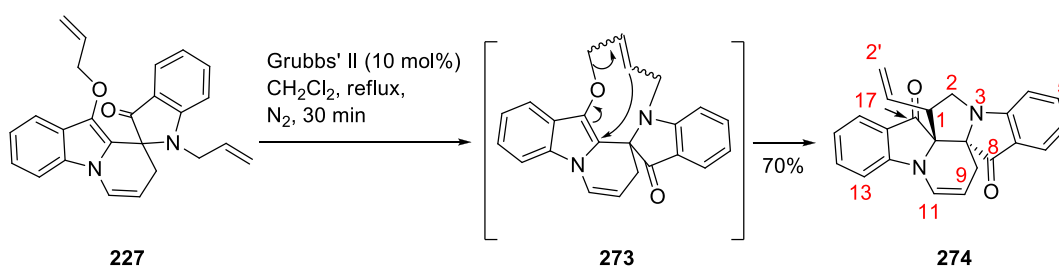
Scheme 78: Reaction of the spiro heterocycle **227** with Grubbs' II ruthenium reagent

The peak at *m/z* 354 in the MS (EI) spectrum was assigned to the molecular ion confirming that a metathesis had taken place with the elimination of an ethylene unit. Both compounds **273** and **274** have three methylene groups. The predicted pattern of

splitting for these methylene groups in **273** consist of three aliphatic methylenes whereas pyrolizino-pyridoindolone **274** has two aliphatic and one terminal olefinic methylene. Analysis of ^{1}H NMR revealed the presence of a multiplet at 4.93 ppm corresponding to the H2'a and 5.10 ppm corresponding to the H2'b. The multiplet at 2.53-2.56 ppm was assigned to the H9a,b and triplet at 3.80 ppm and the multiplet at 3.88 ppm were assigned to the H2a and H2b. From the gHSQC spectrum, the presence of the three positively phased signals (blue) corresponding to the carbons of these methylenes were assigned as C2 at 29.0 ppm, C9 at 49.4 ppm and C2' at 120.2 ppm (Figure 68).
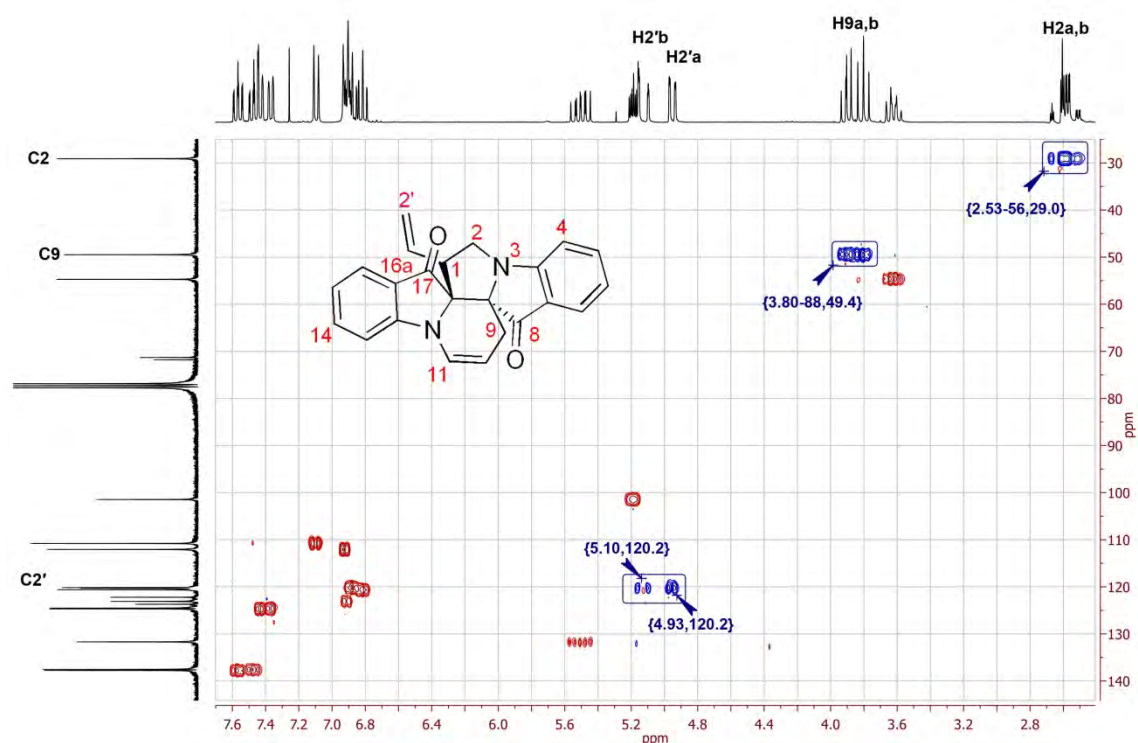
Figure 68: The gHSQC spectrum for **274**

The ^{13}C NMR spectrum showed two signals at 197.9 ppm and 201.0 ppm which were assigned to the C17 and C8 respectively. These two signals confirmed the presence of two unsubstituted carbonyl groups which further confirmed the formation of **274**. The

gHMBC spectrum showed a signal which correlated C8 and C17 to a multiplet between 7.36-7.50 ppm. Two of the protons in this range were assigned to H7 and H16. A three-bond correlation was observed between the C8 and H9 methylene. A strong signal for the protons of the H2 methylene and C8a was suggested that the distance between these two nuclei no further than three bonds. This suggested the formation of the five-membered pyrolizine ring, further confirmed by the observed coupling between the H2 and quaternary C17a at 71.8 ppm. The presence of nine aromatic protons in the ^{1}H NMR spectrum and observed coupling between the C9 nuclei and H11 at 6.96 ppm and correlation of H10 and C8a was confirmed that the spiro six-membered ring is still intact and remained unchanged (Figure 69).
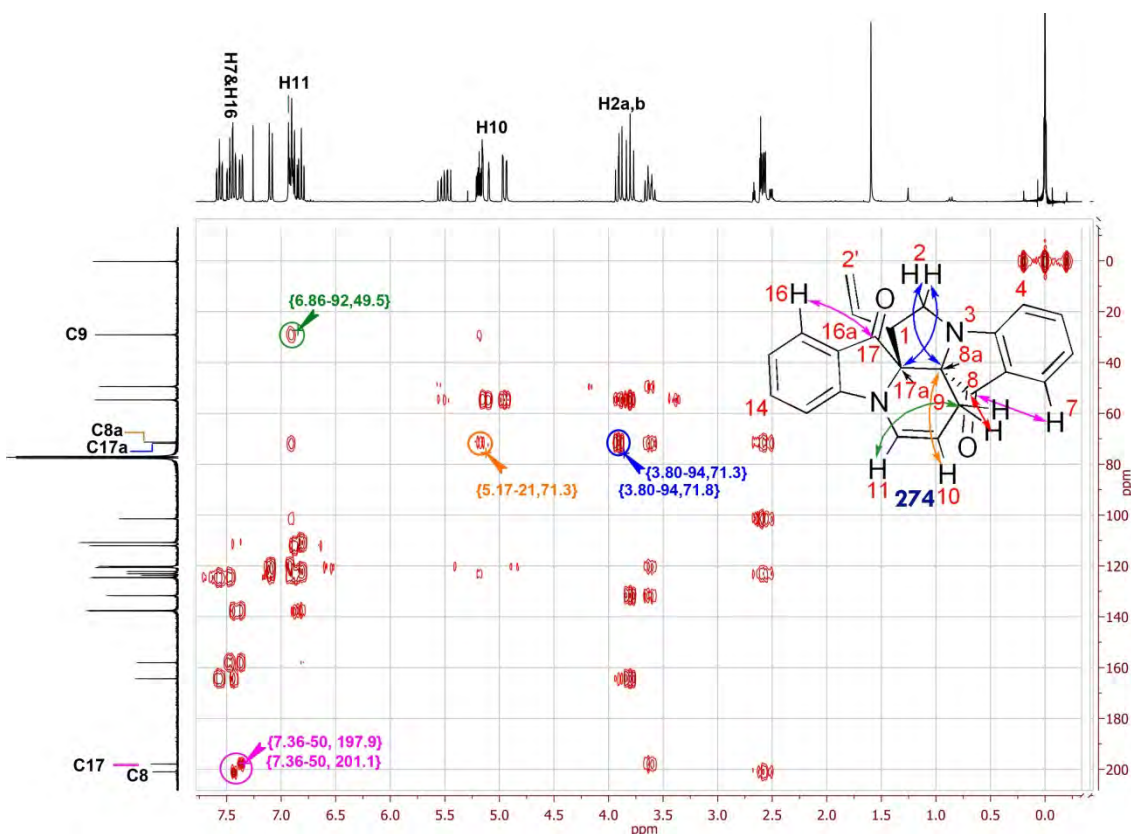
Figure 69: gHMBC spectrum for **274** and the illustration for the key correlations.

X-ray quality crystals were obtained by recrystallisation from a mixture of dichloromethane and petroleum spirit. The X-ray structure of compound **274**, including

relative stereochemistry, is shown in Figure 70 (see Appendix 2 for X-ray crystallographic data).
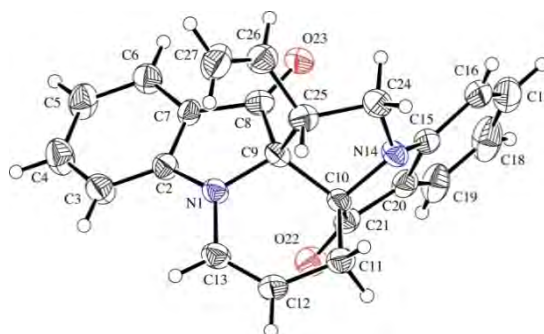
Figure 70 : X-ray crystal structure of the novel product **274**.

The ^{13}C NMR spectrum of **274** showed only one set of peaks for the molecule indicating that only one pair of enantiomers was present, despite the presence of three stereogenic atoms. This is likely to arise from the spiro starting material being racemic, and the subsequent Claisen rearrangement being stereospecific. This structure was formed presumably after initial 9-membered ring production in a typical ring-closing metathesis reaction, followed by an intramolecular Claisen [3,3] rearrangement (Scheme 78).
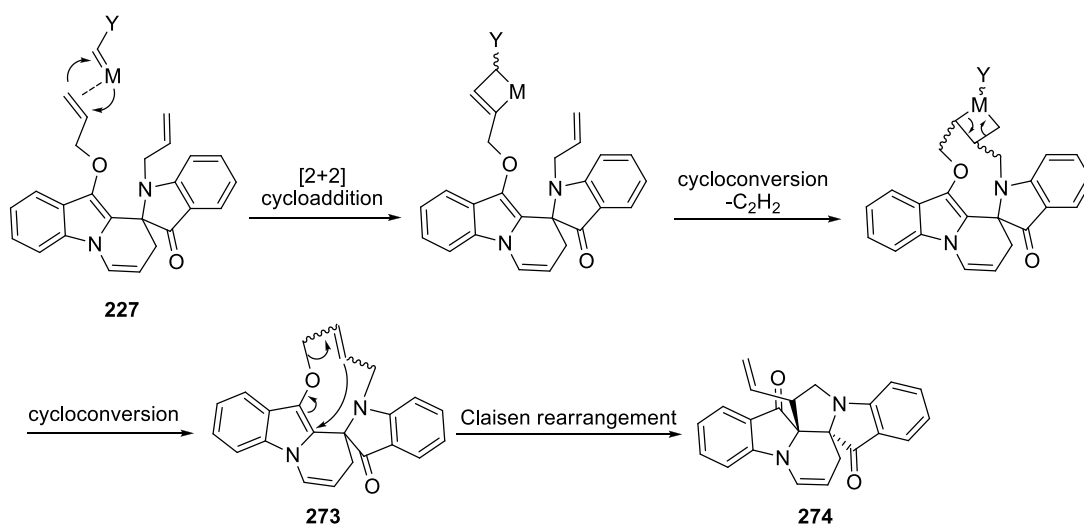
Scheme 79: Tentative mechanism for the RCM of spiroindoline **227** and formation of pyrolizino pyridoindolone **274**.

Attempts to induce a similar Claisen rearrangement starting from the original spiro compound **227** by heating a DMF solution from 40 °C to 110 °C failed, with only decomposition being observed at the higher temperatures. This suggests that the Claisen rearrangement is being catalysed by the Ru present from the Grubbs' reagent. This is not unexpected as there are reports of ruthenium-based species catalysing Claisen rearrangements[161] including a similar RCM/Claisen sequence in 2,2'-bis(allyloxy)-1,1'-binaphthyls and *O,O'*-(but-2-en-1,4-diyl) binaphthols.[162, 163] Additionally, examples of C2 to C3 Claisen rearrangement of 2-allyloxyindoles have been reported by related Pd catalysis.[164]

4.2   Desymmetrisation of bis-indolic system from *N,N'*-dialloc indigo

As explained and illustrated on page 73, Scheme 62, the reaction of the *N,N'*-dialloc indigo with Pd (0) resulted in formation of the *N,N'*-diallyl indigo which was readily converted to **248**.

Immediate protection of the amine groups after abstraction of the allylformates was envisaged as a plausible path in order to activate the central double bond of the *bis*-indolic system to become engaged in nucleophilic addition. Considering the Pd-catalysed C3-selective allylation of indoles[165, 166] and decarboxylative rearrangement of *N*-alloc indoles,[167] Et$_3$B was supposed to be a suitable promoting agent to hinder the *N*-allylation. In the case of the reaction of *N,N'*-dialloc indigo and Pd (0) in presence of Et$_3$B, the reaction progressed much slower than the borane free decarboxylative rearrangements reaction. To circumvent this issue the reaction temperature was boosted to 50 °C and an extra 1% mol of the catalyst was added to the reaction mixture. These changes led to faster progression of the reaction and isolation of the bright yellow solid which was assigned as 2-allyl-2'-ethyl-[2,2'-biindoline]-3,3'-dione (Scheme 79).
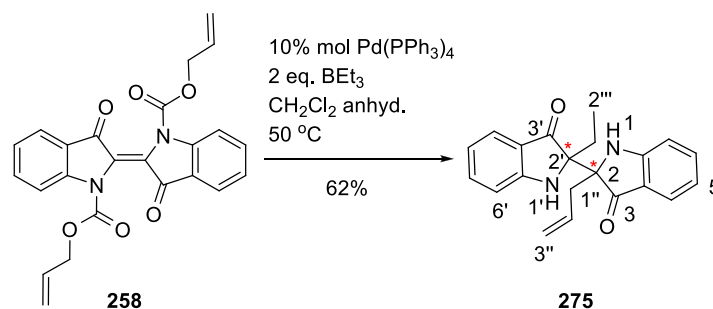
Scheme 80: Decarboxylative rearrangement of **258** and formation of desymmetrised bis-indolic system.

The signal at *m/z* 332 in MS (EI) was assigned as the molecular ion. This was not compatible with our speculated mass of *m/z* 344 corresponding to the sum of the indigo core unit and two allyl groups. The two singlets at 6.02 and 6.07 ppm with the integration of one proton for each were assigned to the two free amine groups, confirmed by the observation that these signals disappeared upon treating the sample with D_2O. This was strong evidence that the core unit of indigo had no substituent on the nitrogens. The ^1H NMR spectrum was also lacking of any deshielded methylene in the range of 4.5-5.5 ppm as it was common for the *N* or *O*-alkylated indigo. A triplet at 0.52 ppm was assigned to the methyl group of the ethyl pendant. A pair of multiplets at 1.34 and 1.37 ppm was assigned to the protons of the H1''' of the ethyl substituent. The other pair of downfield multiplets at 2.10 and 2.60 ppm was assigned to H1'' of the allyl unit. The two doublets at 4.80 and 4.89 ppm were assigned to H3''a and H3''b of the terminal alkene. The gCOSY spectrum showed a correlation between the protons of the methyl (H2''') and H1'''. The spectrum revealed that the H1''' protons have no other correlation and therefore the ethyl pendant has to be positioned on a quaternary carbon. The methylene of the allyl substituent showed a sole gCOSY correlation with the olefinic proton H2''. Considering the chemical shift for H1'' (2.10 – 2.60 ppm), it was concluded that the allylic pendant should be positioned on a quaternary carbon (Figure 71). The gHSQC spectrum revealed three methylene groups (shown in blue) including

one terminal alkene group. The corresponding carbons to these methylene groups were

assigned as C1''' (25.1 ppm), C1'' (36.7 ppm) and C3'' (119.3 ppm) (Figure 72).
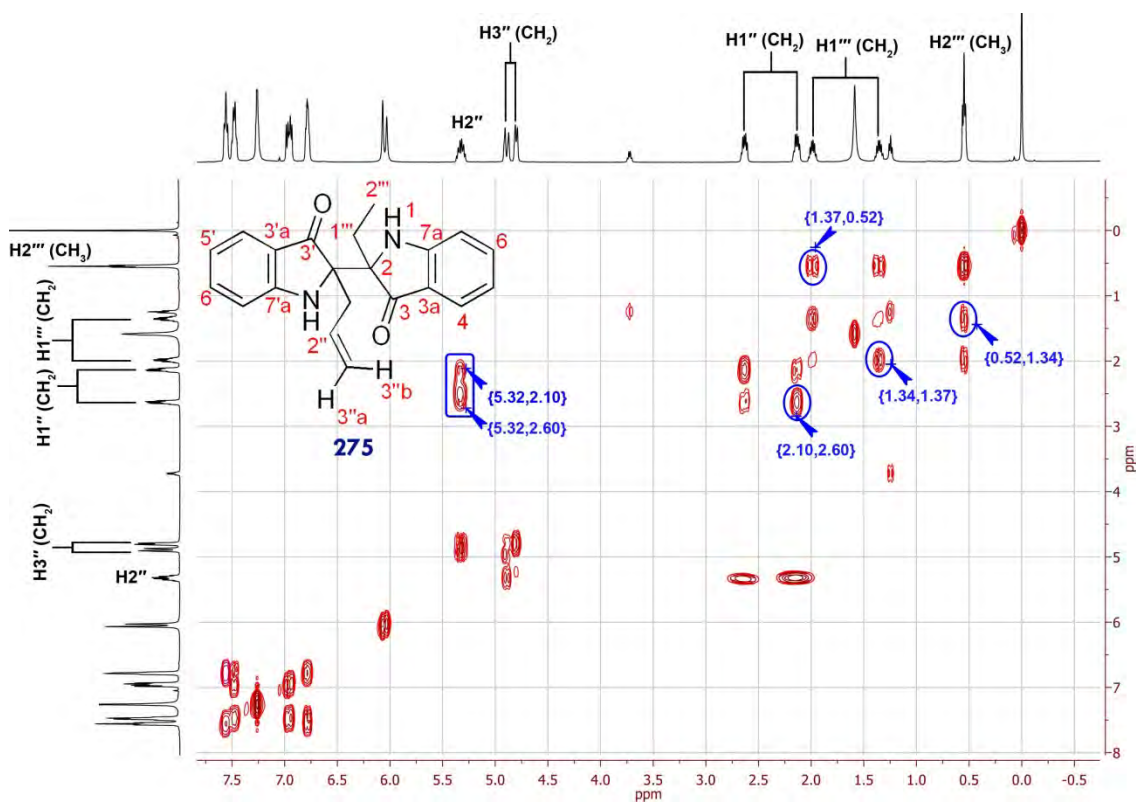
Figure 71: gCOSY spectrum for compound **275**.
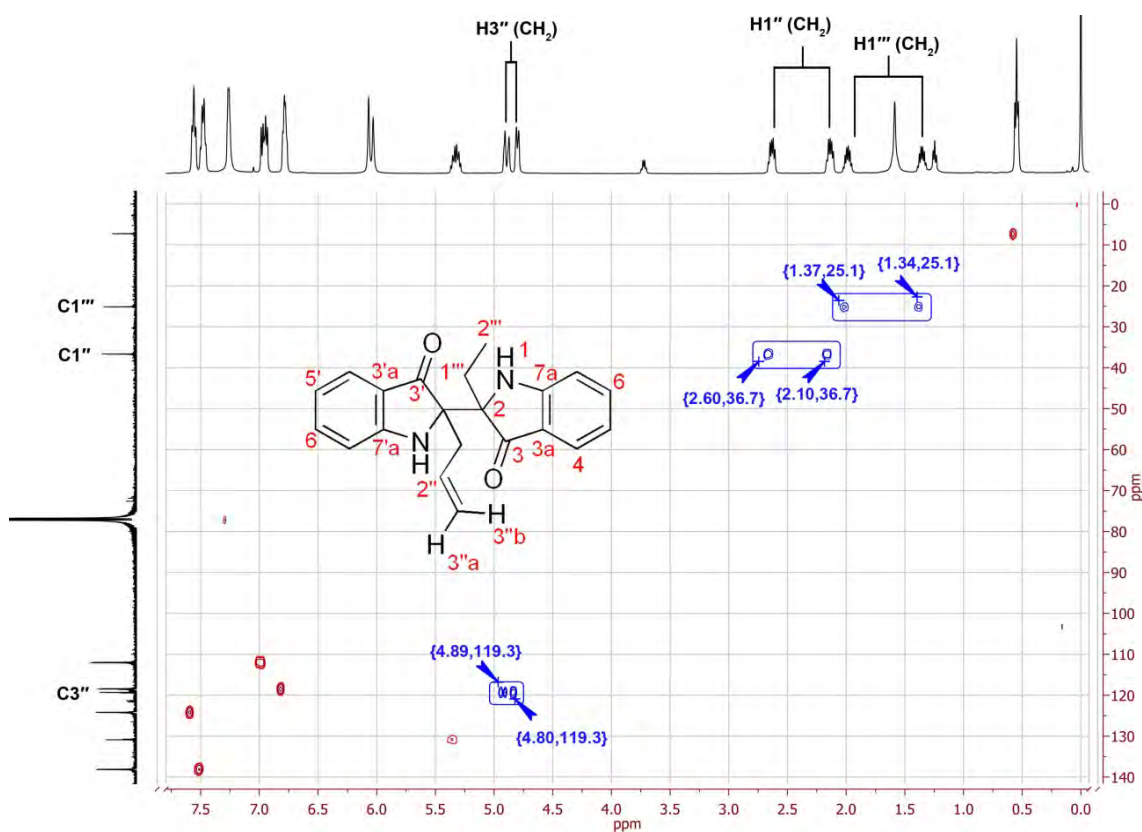
Figure 72: The gHSQC spectrum for biindoline **275** with the CH$_2$ groups highlighted in blue.

The ^{13}C NMR spectrum showed two peaks at 203.8 and 204.1 ppm which were assigned to C3' and C3 respectively.

Key correlations from the gHMBC spectrum included the three bond correlation between the C3' carbonyl group and H1". The same holds for C3 and H1''', confirming the distance between these two nuclei to be no further three bonds (Figure 73, blue). The strong correlation of the quaternary C2' at 71.9 ppm to H1''' and coupling between the H1" and C2 at 72.7 ppm further confirmed the position of the ethyl and allyl pendants on indigo core (Figure 73, orange). A pair of downfield quaternary carbons at 161.8 and 162.1 ppm were assigned to C7a and C7'a showed strong coupling with H6 (7.47 ppm) and H6' (7.56 ppm) (Figure 73, magenta). The other noteworthy correlation was observed between C3 and H4 at 7.47 ppm (Figure 73, green).
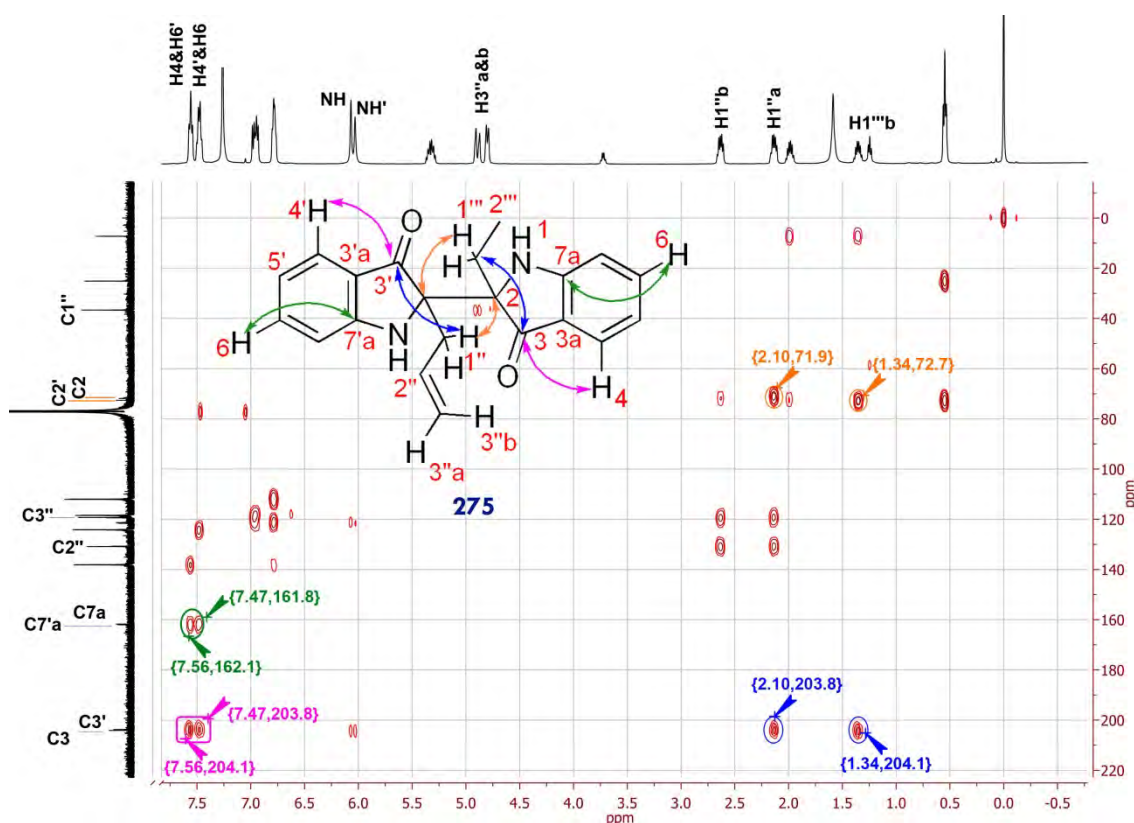
Figure 73: The gHSQC spectrum for biindoline **275**.

Scheme 81 illustrates the tentative mechanism of the formation of **275** from the decarboxylation of **279**. The reaction began with the deallylation and decarboxylation of

the dialloc indigo and then the amine protected by the electrophilic Et$_3$B. At this point formation of the imine **N** induced the central double bond for a nucleophilic attack on the allyl-Pd complex. Nucleophilic attack of the ethyl group to the other side of the central bond resulted in production of **P**. Protonation of the **P** during the workup furnished **275**.
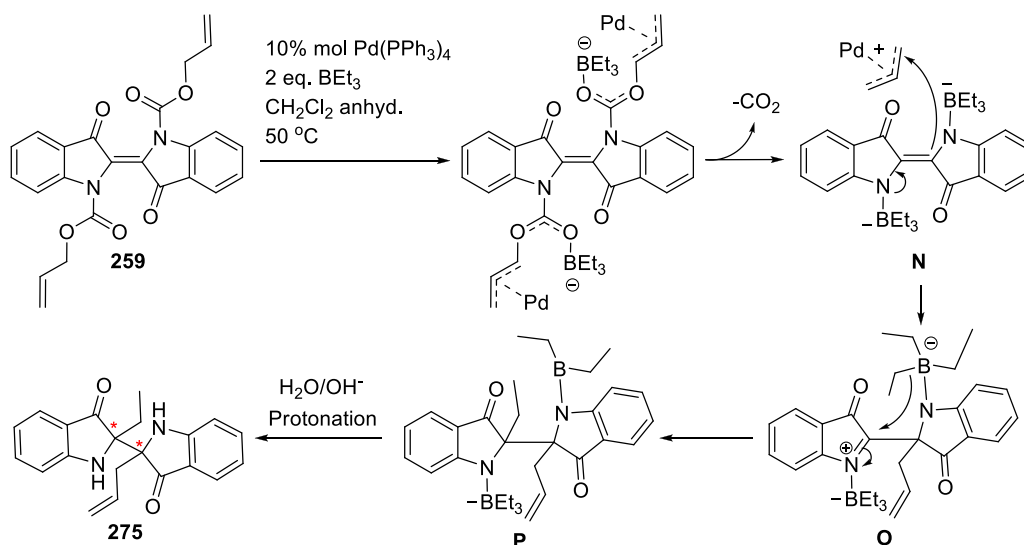
Scheme 81: Proposed mechanism for the formation of **275** from catalytic decarboxylation of **259**.

4.3   Gold-catalysed cyclisation of *mono N*-propargylated indigo

Direct nucleophilic addition of amines onto alkynes is only possible with activated i.e. electron-deficient alkenes or alkynes through the aza-Michael addition or conjugate addition (Figure 74a).[168] In the case of compound **263**, the electron donating effect of the lone pair of the amine deactivates the alkyne and hampers the direct nucleophilic addition (Figure 74b).
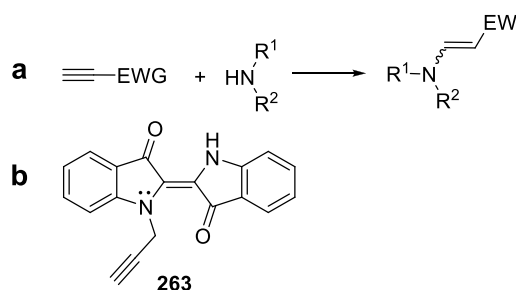
Figure 74: Hydroamination of activated alkyne (**a**) and deactivated propargyl pendant of **263** due to the lone pairs of amine (**b**).

As discussed earlier (Chapter 3, Page 93), base catalysed cyclisation of *N*-propargyl indigo resulted in the formation of **264** in quantitative yield. In a separate attempt and in order to explore the effect of the metal catalysis on the outcome of the intramolecular hydroamination, compound **263** was reacted with gold (I). The reaction was carried in CH$_2$Cl$_2$ under the inert atmosphere at room temperature (Scheme 82).

1) 5% mol Ph$_3$PAuNTf$_2$,
   CH$_2$Cl$_2$,rt, 90 min
2) extra 5% mol Ph$_3$PAuNTf$_2$

263

264
51%

276
32%
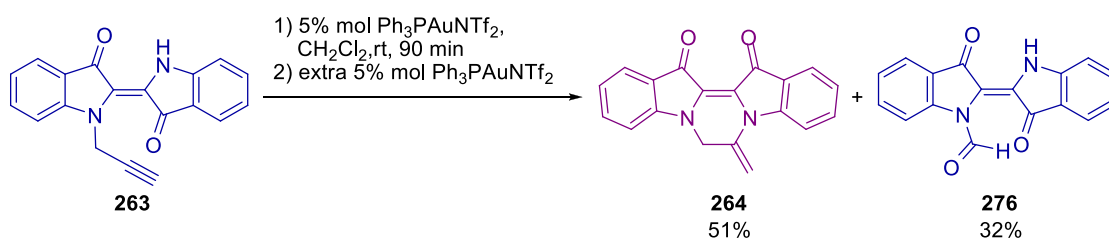
Scheme 82: Gold (I) catalysed intramolecular hydroamination of **263**.

The reaction was monitored by TLC analysis and quenched after 90 mins. At this point the starting material was fully consumed and there were two new spots evident by TLC analysis. The purple spot close to base line corresponded to **264** and the other dark blue spot was a new compound which was elucidated as **276**. *N*-Formylindigo **276** was obtained in 32% as a dark navy solid. The peak at *m/z* 290 (M$^+$) in the MS (EI) spectra was assigned to the molecular ion. This was 10 AMU less than the **263** molecular mass. Analysis of the ^{1}H NMR spectrum showed the absence of the corresponding peak for the alkynic proton at 2.17 ppm. A sharp singlet at 9.98 ppm with the integration of one proton was assigned to H1" proton of the formyl substituent. The aromatic region of the proton NMR revealed the presence of eight aromatic protons and the deshielded doublet at 8.51 ppm was assigned to the H7 proton. The downfield singlet at 10.67 ppm was assigned to the NH (Figure 75). The gCOSY spectrum revealed that the H1" has no correlation with another proton. The gHSQC spectrum lacked any signal with positive phasing and confirmed that there is no methylene group present in the structure. The ^{13}C NMR spectrum showed a peak at 185.8 ppm which was assigned to C1" of the

aldehyde. There were two signals at 188.7 and 189.3 ppm assigned to the C3 and C3' carbonyls.
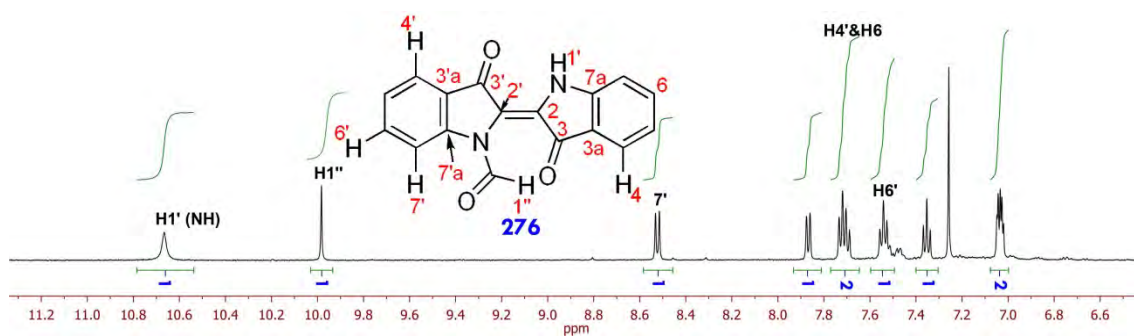
Figure 75: The expansion of the ^{1}H NMR for **276**.

A four bond correlation in the gHMBC spectrum of the quaternary C7'a at 147.0 ppm to proton H1" of the aldehyde further supported the presence of the formyl pendant (Figure 76, green). This quaternary carbon showed strong coupling with H4 and H7 protons of the aromatic ring (Figure 76, orange). The three bond correlation of the carbonyl groups and the aromatic protons H4 and H4 were also noted in the gHMBC spectrum (Figure 76, magenta).
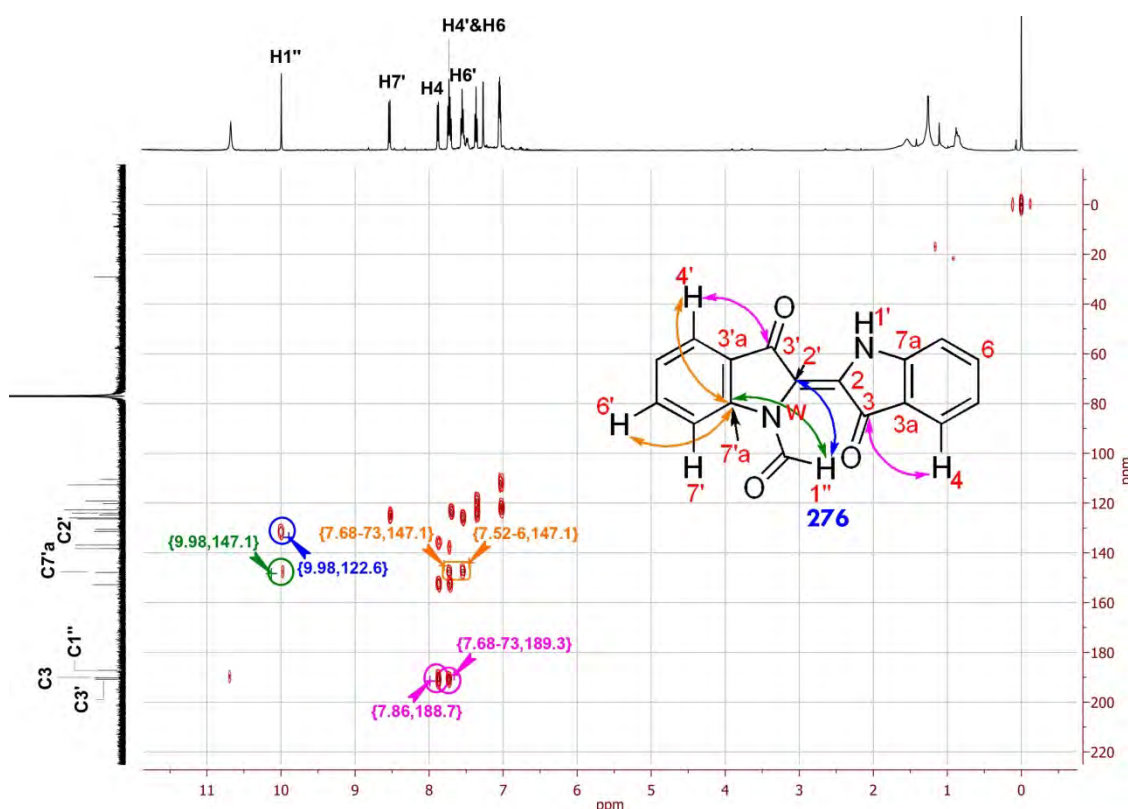
Figure 76: The gHMBC spectrum for **276** and the key correlations with colour coded annotations.

The formation of **276** could be attributed to the oxidative cleavage of alkynyl amine in the presence of molecular oxygen. The precedent for a simultaneous oxidative cleavage of single and triple carbon–carbon bonds using oxygen was reported with aryl-substituted alkynyl ethers using molecular oxygen.[169] The proposed mechanism involves the formation of an allenic intermediate after the interaction of the gold (I) catalyst with the triple bond. Then, formation of the cyclic peroxide lead to the carbon-carbon bond cleavage forming the formyl and ketene gold intermediate which subsequently expels carbon monoxide followed by hydrodeauration (Scheme 83).
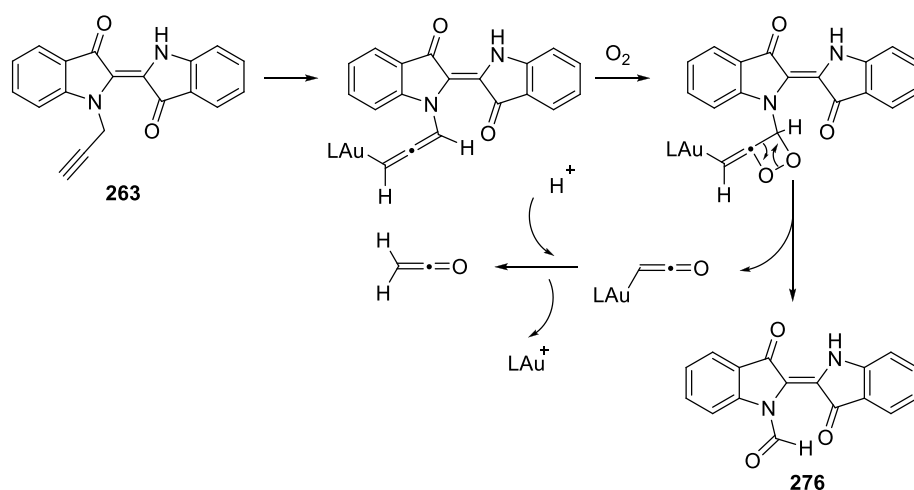
Scheme 83: Possible mechanism for the formation of biindolinylidene carbaldehyde **276**.

As the entire steps of this reaction were carried under the inert atmosphere with the aid of the Schlenk system, the origin of the molecular oxygen could be the dissolved oxygen in the solvent. Therefore, in a separate attempt under similar conditions, the reaction used degassed CH_2Cl_2. TLC analysis of the crude sample along with the ^{1}H NMR and MS analysis showed the absence of **276** and the isolated yield for **264** increased to 79%.

4.4   Click reaction with *N*-propargyl indigo

The presence of the alkynic pendant in *N*-propargyl structure suggested the reaction of the triple bond with an azide under the standard "click reaction" conditions. Benzyl azide and **263** were reacted in the presence of copper acetate and ascorbic acid in *tert*-butanol and water at room temperature. The mixture was stirred for 21 h, and analysis of the reaction showed no progress and the starting material was recovered. Then, the reaction mixture was heated up to 60 ºC but with still no sign of progress (Scheme 84).
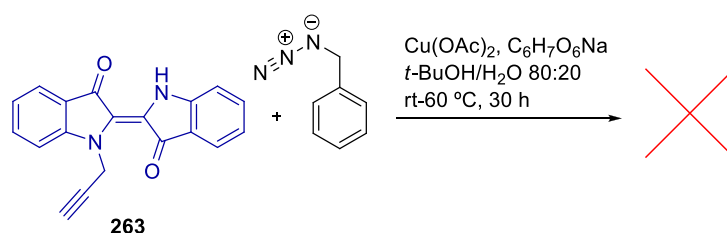
Scheme 84: Reaction of **263** and benzyl azide in *tert*-butanol and water mixture.

The investigation towards the reason of this failure, suggested the lack of solubility of **263** in the mixture of *t*-BuOH and water. Therefore a mixture of DMF and water was selected to repeat the reaction. The reaction carried at the room temperature and showed a slow progress after 5 h. In a separate attempt under the identical conditions, when the reaction was heated up to 40 ºC the reaction was completed in 10 min. Slow recrystallisation of the crude material resulted in isolation of **277** as dark navy solid (Scheme 85).
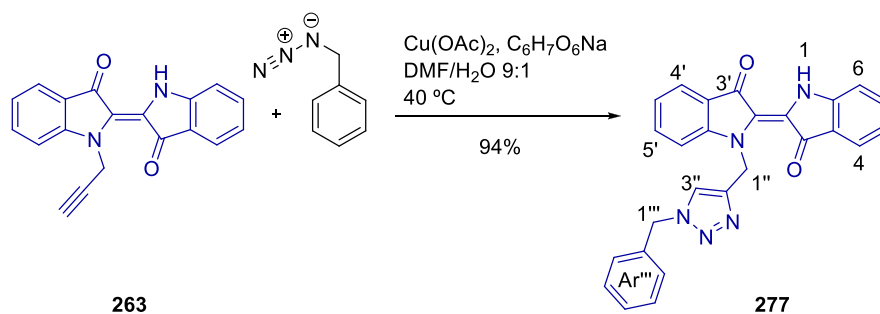
Scheme 85: The formation of the benzyl triazole biindolinylidene **277** from **263**.

A signal at *m/z* 433 MS (EI) assigned to the molecular ion confirmed the addition the benzyl azide to the propargyl indigo. Analysis of the ^{1}H NMR spectrum showed a distinctive singlet at 7.63 ppm, assigned to H3" which was characteristic evidence for formation of the triazole ring. A singlet at 5.62 ppm was assigned to the benzylic proton H1"'. The set of two multiplets from 7.23-7.33 ppm with the integration of 5 protons was assigned to the benzene ring of the benzyl azide. From the ^{13}C NMR spectrum the two signals at 185.9 and 190.1 ppm respectively were assigned to C3 and C3′, confirming the presence of the two carbonyl groups.

In another attempt glycosyl azide **278** was reacted with **263** under the similar reaction condition for the reaction of benzyl azide. The reaction was accomplished after 15 min and compound **279** was isolated with the yield of 83% as dark navy flakes from the slow recrystallisation of the crude material from CH_2Cl_2/MeOH (Scheme 86).
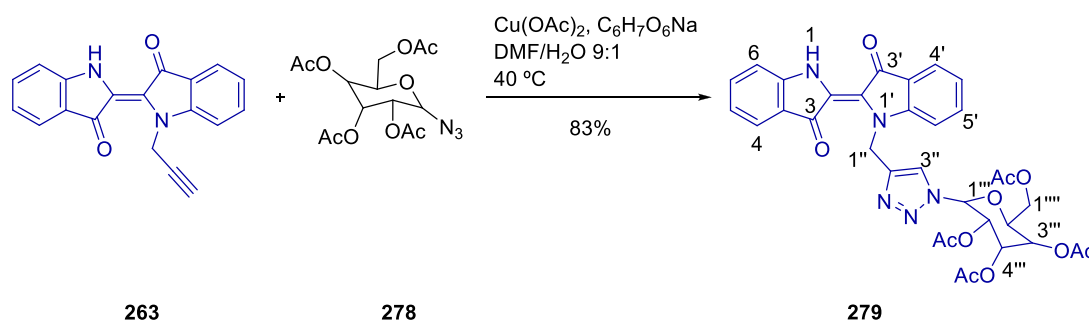
Scheme 86: The Click reaction of **263** and glycosyl azide **279**.

The peak at *m/z* 673 MS (EI) was assigned to the molecular ion from the addition of the glycosyl azide to the **264**. The ^{1}H NMR spectrum showed a singlet at 7.59 ppm corresponding to the H3" of the triazole ring. A singlet at 6.59 ppm was assigned to the H1"' of the glycosyl ring. There were two singlets at 2.02 and 2.18 ppm with the integration of six protons assigned to the methyl groups of the acetate groups. Four triplets at 4.32 – 4.76 ppm were assigned to the methines of the sugar ring. Analysis of the ^{13}C NMR spectrum confirmed the presence of one set of enantiomers and signals at

184.7 and 188.3 ppm confirmed that the carbonyl groups of the indigo core were still intact.

Chapter 5: Biological Activity Testing

5.1   General remarks

While indigo is one of the oldest chemicals, there is no reported biological activity for this heterocycle, however its other isomer, indirubin, is well known for its anticancer activity back to the traditional Chinese medication.[170] Indirubin acts as ATP-competitive inhibitors of the enzyme CDK2.[171-173]
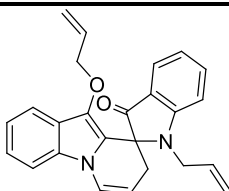
A selection of compounds obtained from the indigo core were assessed for *in vitro* anti-plasmodial (*Plasmodium falciparum*; drug resistant K1 strain) activity,[174] cell-based anti-cancer activity (cell lines: NCI-H187 small cell lung cancer, KB oral cavity cancer, and MCF-7 breast cancer),[175] and *in vitro* anti-tubercular activity (Mycobacterium tuberculosis).
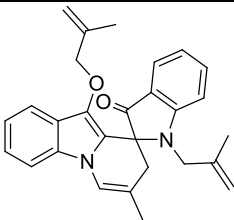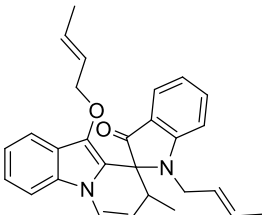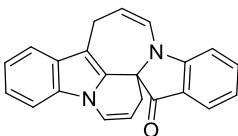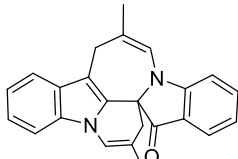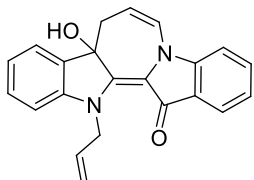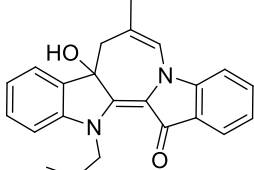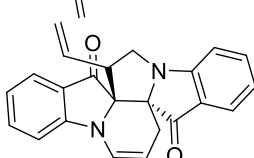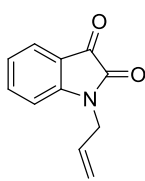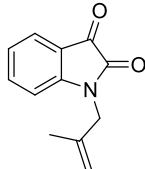
5.2   Anti-cancer, anti-malaria and anti-tuberculosis testing
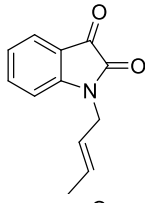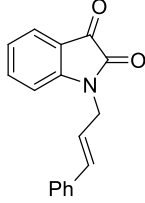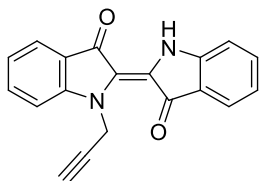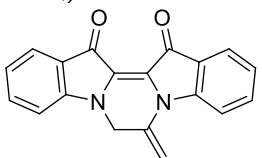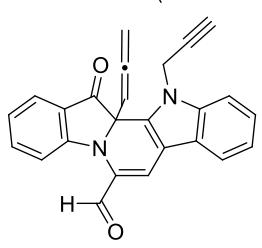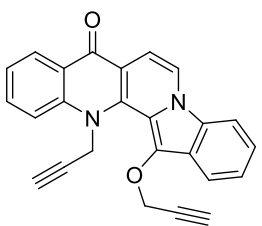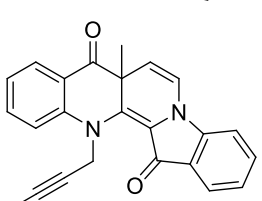
5.2.1   Anti-cancer testing results

The indigo derived compounds were tested against the three cell lines NCI-H187 (small cell lung cancer), KB (oral cavity cancer) and MCF-7 (breast cancer). All derivatives showed cell growth inhibition in micromolar concentrations of at least one cell line. The testing results are summarised in Table 6.

Table 6: *In vitro* anticancer activity of candidate heterocycles derived from indigo

Entry	Compound	#	NCI-H187 IC_{50} μg/mL (μM)[♠]	KB IC_{50} μg/mL (μM)[♣]	MCF-7 IC_{50} μg/mL (μM)[♦]
1		**227**	9.45 (24.7)	-[•]	-

Entry	Compound	#	NCI-H187 IC$_{50}$ μg/mL (μM)[♠]	KB IC$_{50}$ μg/mL (μM)[♣]	MCF-7 IC$_{50}$ μg/mL (μM)[♦]
2		**228**	-	-	-
3		**229**	10.8 (25.5)	11.3 (26.7)	-
4		**232**	3.35 (10.3)	9.71 (30.0)	-
5		**233**	-	-	-
6		**248**	13.1 (35.3)	15.0 (40.6)	5.79 (15.6)
7		**249**	-	24.9 (62.3)	34.7 (93.7)
8		**274**	-	-	-
9		**237**	5.45 (29.1)	-	-
10		**238**	3.23 (16.1)	22.4 (96.4)	-

Entry	Compound	#	NCI-H187 IC$_{50}$ µg/mL (µM)[♠]	KB IC$_{50}$ µg/mL (µM)[♣]	MCF-7 IC$_{50}$ µg/mL (µM)[♦]
11		**239**	4.83 (24.0)	-	-
12		**240**	-	-	-
13		**263**	4.79 (15.9)	8.95 (29.8)	16.49 (43.8)
14		**264**	1.88 (6.24)	1.31 (4.36)	-
15		**265**	4.79 (12.7)	7.81 (20.7)	12.51 (33.2)
16		**266**	17.3 (46.0)	8.44 (22.34)	35.22 (93.7)
17		**269**	16.7 (45.6)	9.25 (25.3)	3.01 (8.21)

● - not active up to 50 µg/mL.

♠ The IC$_{50}$ values of the positive controls ellipticine and doxorubicin are 1.47 µg/mL and 0.077 µg/mL respectively.

♣ The IC$_{50}$ values of the positive controls ellipticine and doxorubicin are 0.737 µg/mL and 0.504 µg/mL respectively.

♦ The IC$_{50}$ values of the positive controls tamoxifen and doxorubicin are 9.47 µg/mL and 8.57 µg/mL respectively.

Modest cytotoxicity against all three cancer cell lines tested was seen with the hydroxyazepino diindole **248** (IC$_{50}$ 5.79-15.6 µg/mL, 15.6-40.6 µM). Similarly **232** showed some activity against the small cell lung and oral cavity cancer cell lines (IC$_{50}$ 3.35 and 9.71 µg/mL, 10.3 and 30.0 µM respectively), but not against the more refractory MCF-7 breast cancer cell line.[164] IC$_{50}$ values of 9.45 and 10.08 µg/mL were obtained against NCI-H187 lung cancer for allylic and crotyl spiroindoline-pyridoindoles **227** and **229** (Entries 1 and 3) while in the case of **228** the presence of methyl substituent at C2 position of the allyl pendant was not tolerated and did not show any activity. Compounds containing a spiro-oxindole core were reported as potent small molecules inhibitor of MDM2 protein which is responsible for tumour regression.[176, 177] As an example MI-17 was found to be active against the LNCaP prostate cancer cell line in a cell growth inhibition assay with IC$_{50}$ = 830 nM (Figure 77).[178] Recently a modified MDM2 inhibitor MI-888 had a K_i value of 0.44 nM with excellent oral bioavailability as highly potent and selective tumour cell growth suppressor (Figure 73).[179] Comparison of these results with the observed biological activity of the indigo derived spiro indoles is not convenient due to the absence of *in-vivo* results for compound **227**-**229**. However this emphasis the necessity of structure-activity relationship (SAR) studies on spiroindolinepyridoindoles derivatives.

MI-17
MDM2 IC$_{50}$=830 nM
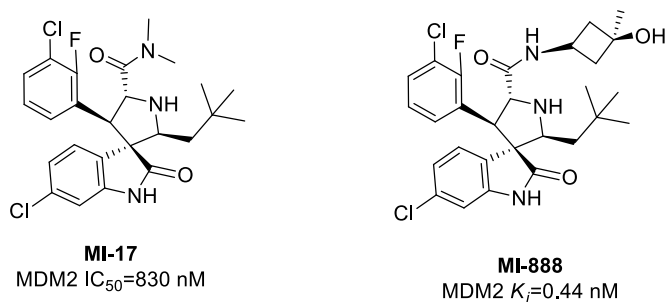
MI-888
MDM2 K_i=0.44 nM

Figure 77: Two examples of MDM2 inhibitors, MI-17 as a potent candidate against LNCaP prostate cancer cell lines (left) and MI-888 a modified version with high tumour cell apoptosis activity

Patchy cytotoxicity was seen with the *N*-substituted isatins **237**, **238**, and **239**. Compounds of this general type, but incorporating *N*-arylmethyl as well as 5,7-dibromo substituents, have given rise to potent anti-cancer compounds with activity probably being mediated, at least in some cases, via microtubule destabilisation and inhibition of tubulin polymerisation.[180-185]

Compounds **263**-**266** and **269** (Entries 13-17) showed notable activity against the KB-oral cavity cell lines. In particular, pyrazinodiindole **264** was equipotent with the positive control ellipticine (Figure 78).

264
1.88 µg/mL

Ellipticine
1.47 µg/mL
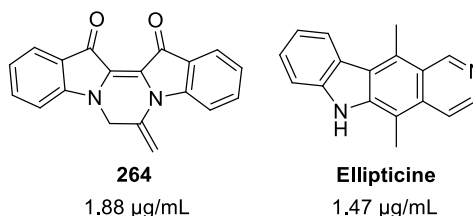
Figure 78: The structure **264** and ellipticine as a positive control for NCI-H187 lung cancer cell line test

The IC_{50} value for compound **263** against NCI-H187 lung cancer, in comparison with *N*-propargyl indirubin (inactive),[186] showed a significant increase to 4.79 µg/mL (Table 6, Entry 11).

Cytotoxicity[174, 180, 181] studies were particularly interesting for **264** and **265**, with the latter being noncytotoxic to normal mammalian cells but the former being toxic to these cells. The other noncytotoxic compound was **269** which showed a selective activity against MCF-7 cell lines (Table 7).

Table 7: Cytotoxicity of compound **264**-**65** and **269** to normal mammalian cells

Entry	Compound	Cytotoxicity vero cell IC_{50} µg/mL (µM)
15	**264**	-
16	**265**	16.4 (43.6)
17	**269**	-

The core unit of compound **265** (Figure 75, highlighted in red) is analogous to the sponge-derived bis-indole alkaloid fascaplysin. The naphthyridine based heterocycles **266**-**267** and **269** are also bearing the core unit of homofascaplysin B (Figure 79, highlighted in orange).
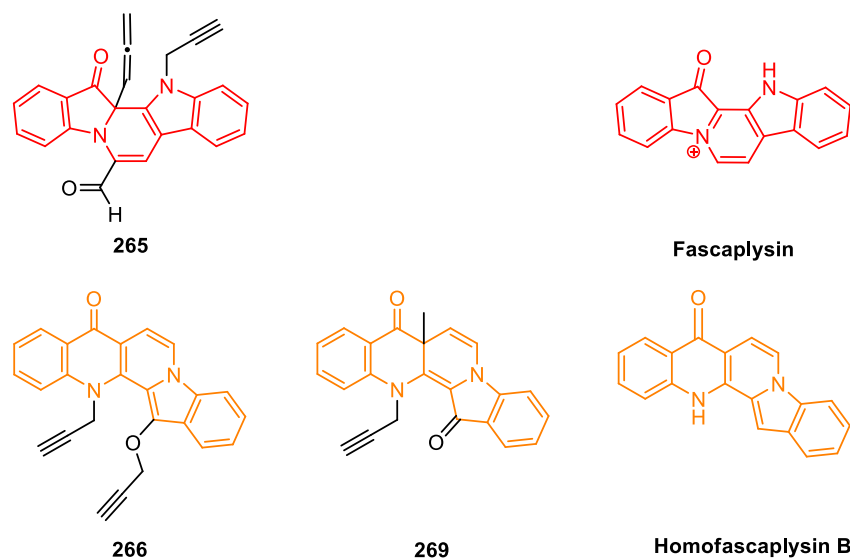
Figure 79: The similarity of the core skeleton of **265** and fascaplysin and comparison of **266** and **269** structure with homofascaplysin

Fascaplysin showed selective cyclin-dependent kinase-4.[187] It had also demonstrated antimicrobial activity against the growth of *Staphylococcus aureus*, *Escherichia coli*, *Candida albicans and Saccharomyces cerevisiae*.[188] Fascaplysin exhibited anti-proliferation against cervical cancer HeLa cells.[189] Fascaplysins have not been administrated as an anti-cancer drug as its flat structure makes it a DNA intercalator with high toxicity. Both **265** and **269** showed that the slight distortion of this planarity results in significant change and makes these compounds noncytotoxic.
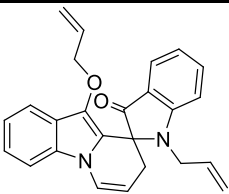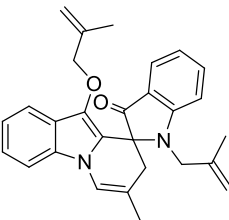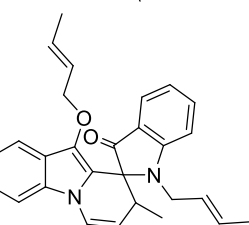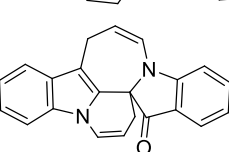
5.2.2   Anti-malaria and anti-tuberculosis testing results
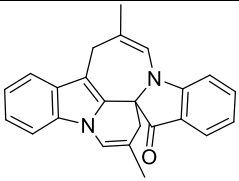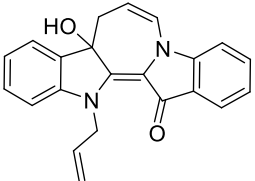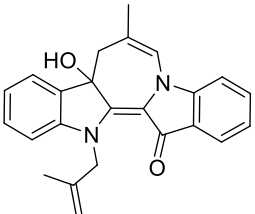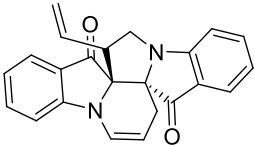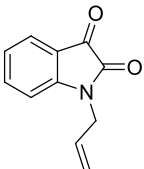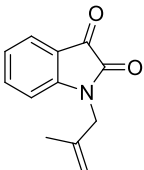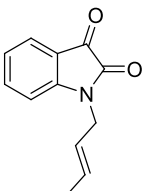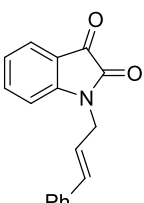
Promising anti-plasmodial activity was seen with the spirocyclic compound **227** (IC$_{50}$ 2.65 µg/mL, 6.25 µM) and with the compound **232** in which the allylic substituents are effectively merged (minus the ether oxygen) and embedded in the 7-membered ring
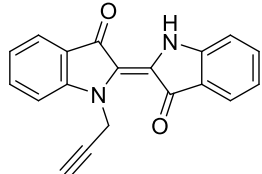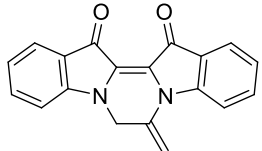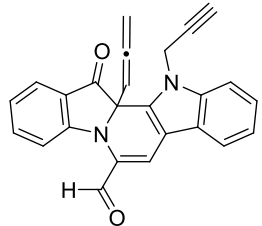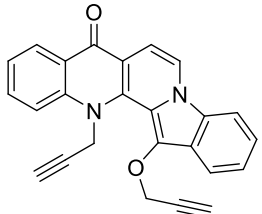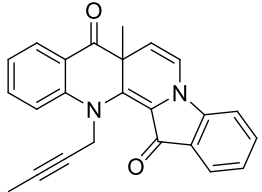
(IC$_{50}$ 3.06 μg/mL, 9.44 μM). While the introduction of methyl substituents in the allylic moieties (**228** and **233**) was detrimental to this activity, other possibilities exist for substituent variation at other sites, for example in the aromatic rings and at the carbonyl group, for future SAR studies. In addition, with compounds in the non-spirocyclic (**248** and **249**) good anti-plasmodial activity was also seen, with **248** the most potent (IC$_{50}$ 1.94 μg/mL, 5.20 μM) of the compounds tested here.

Additionally, **232** exhibited some anti-tubercular activity (MIC 12.5 μg/mL, 38.6 μM), providing a basis for further structural novel lead development of anti-TB compounds. The need for such compounds is a pressing one with the development of major mycobacterial resistance.[180]

Table 8: The IC$_{50}$ values of the indirubin derivatives, tested against tuberculosis (*microbacterium tuberculosis*, H37Ra strain) and malaria (*plasmodium falciparum*, K1 strain)

Entry	Compound	#	TB (tuberculosis, H37Ra strain) IC$_{50}$ µg/mL (µM)	*Plasmodium falciparum* (malaria, K1 Strain) IC$_{50}$ µg/mL (µM)
1		**227**	50.0 (131)	2.65 (6.25)
2		**228**	-	-
3		**229**	-	-
4		**232**	12.5 (38.6)	3.06 (9.44)

Entry	Compound	#	TB (tuberculosis, H37Ra strain) IC$_{50}$ μg/mL (μM)	Plasmodium falciparum (malaria, K1 Strain) IC$_{50}$ μg/mL (μM)
5		**233**	-	-
6		**248**	-	1.94 (5.20)
7		**249**	-	2.97 (8.31)
8		**274**	-	-
9		**237**	nt	nt
10		**238**	50 (248)	-
11		**239**	nt	-
12		**240**	nt	nt

Entry	Compound	#	TB (tuberculosis, H37Ra strain) IC$_{50}$ μg/mL (μM)	*Plasmodium falciparum* (malaria, K1 Strain) IC$_{50}$ μg/mL (μM)
13		**263**	-	0.33 (1.1)
14		**264**	-	0.26 (0.85)
15		**265**	-	3.34 (8.9)
16		**266**	-	3.75 (9.9)
17		**269**	-	2.5 (6.83)

The IC$_{50}$ values of the positive controls rifampicin and streptomycin are 0.0250 μg/mL and 0.625 μg/mL respectively

The IC$_{50}$ values of the positive controls dihydroartemisinine and mefloquine are 0.751 μg/mL and 11.5 μg/mL respectively

In order to further assess selective cytotoxicity, the toxicity of **248** towards Vero cells[175] was attempted but the autofluorescence of **248** precluded a result being obtained. Compounds **227**, **232**, **248**, **249**, **263**-**266** and **269** constitute notable antiplasmodial[181] activity against a drug-resistant strain in the micromolar range, sufficient for all to be considered lead compounds for further development with potentially new modes of action.

Clearly, significant medicinal chemistry studies would need to be undertaken to decrease the toxicity to normal mammalian cells and increase the required selectivity. However, as a random screening process, all these compounds showed activity confirming that they could be considered as new lead compounds for a variety of targets.

Chapter 6: Conclusions and Future Outlook

The search for diversity in new heterocyclic chemical space is increasingly important in areas such as medicinal chemistry and nanotechnology, where novel heterocyclic starting points are urgently required. The newly established cascade chemistry of indigo provides a fertile ground for the discovery of such heterocycles, not readily available by other means and key to this is the ability to produce novel heterocyclic structures in one-pot in reasonable yield.

6.1 The allylation reactions of indigo

6.1.1 Selective synthesis of spiro and fused seven-membered ring products

We report here the optimisation of the synthesis of two heterocycles, the spiro compound **227** (65%) and the fused 7-membered ring product **232** (72%) - both these heterocycles are synthesised in one-pot from a cheap and readily available starting material and represent an exceptionally efficient synthesis of novel polycyclic compounds. Further, we report for the first time the synthesis of derivatives of these heterocycles, including those using the sterically hindered allyl reagents with terminal methyl substituents. The position of the substituents on the allylic bromides appeared to play a role in these syntheses (Scheme 87). When the allylic bromide with no terminal substituent reacted with indigo the major product was the formation of the seven-membered fused ring systems (**232**-**233**) whereas the presence of any terminal substituent resulted in formation of the spiro system (**227**-**231**). The reaction of *N*-methyl indigo with allyl bromide and crotyl bromide resulted in the formation of the seven membered and spiro structures respectively, confirming the observed trend further more.
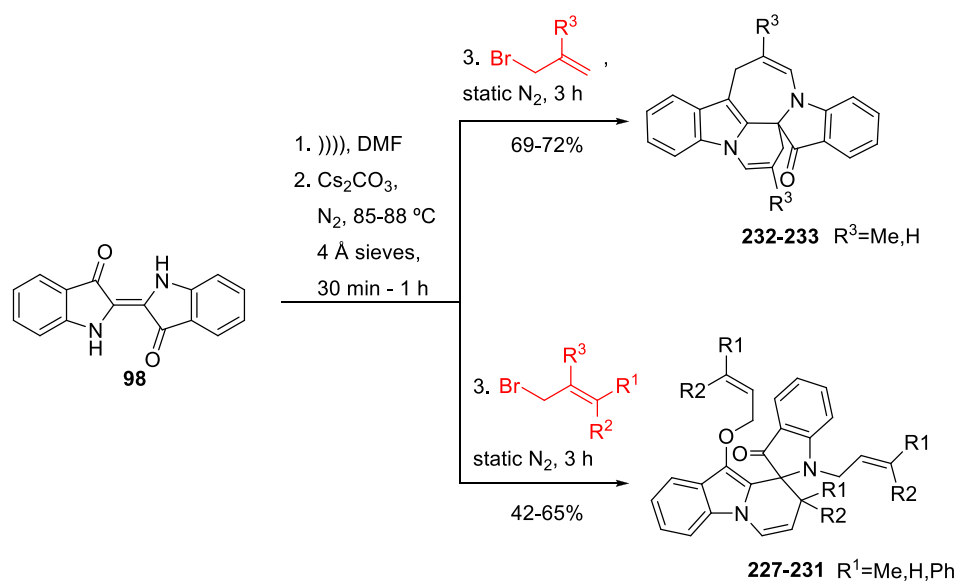
Scheme 87: Controlled allylation of indigo based on the position of substituents on the allylic system

Anti-cancer testing of these compounds revealed inhibitory activity of the spiroindoline–pyridoindolone **227** and **229** with IC_{50} values of 9.45 µg/mL and 10.8 µg/mL against the cell line NCI-H187. Promising *in vitro* anti-plasmodial activity was indicated with a number of the spiro, indoloazepinoindol-17-one while the *in vitro* anti-TB activity of one indoloazepinoindol-17-one compound, **232**, was also of interest. Enhancement of the synthetic scope of the tandem RCM-Claisen chemistry has been established with the production of the new heterocyclic system **274** from the spiro compound **227**. Further application of this tandem methodology offers significant potential in heterocyclic synthesis.

6.1.2 Synthesis of hydroxylated azepino-diindole derivatives

The allylation reaction also provides access to new hydroxylated heterocyclic derivatives of the azepinodiindolo type. These intensely red compounds (**248**-**250**) can be synthesised in one-pot in yields of up to 51% and are presumably also intermediates

in the synthesis the indoloazepinoindol-17-ones. The hydroxy azepino indole **248** inhibited the growth for cell line MCF-7 with an IC_{50} value of 5.79 µg/mL. This compound showed a promising activity against malaria (*Plasmodium falciparum*, K1 Strain) with IC_{50} value of 1.94 µg/mL. One of the more interesting outcomes is the first synthesis of the bridged compound **253**, with a heterocyclic skeleton not likely to be readily accessible by other means. As with all these reactions, the synthesis of **253** is repeatable, and given the reliability of outcome and complexity of structure, a 26% yield is a reasonable achievement.

6.1.3 Alternative pathway for the synthesis of hydroxyazepino diindolones

In order to obtain anti-malaria agents **248**-**253** in higher yields the future exploration may be to alter the synthesis procedure from direct reaction of indigo with allylic bromides in 1 hour time reaction to an alternative pathway of starting from *N,N'*-dialloc derivatives of indigo. This could be achieved by preparing the range of *N,N'*-dialloc derivatives **259'** of indigo and subsequent catalytic decarboxylation (Scheme 88). The procedure resulted in quantitative production of **248** form *N,N'*-dialloc indigo **259** (See Chapter 2 pages 70-71).
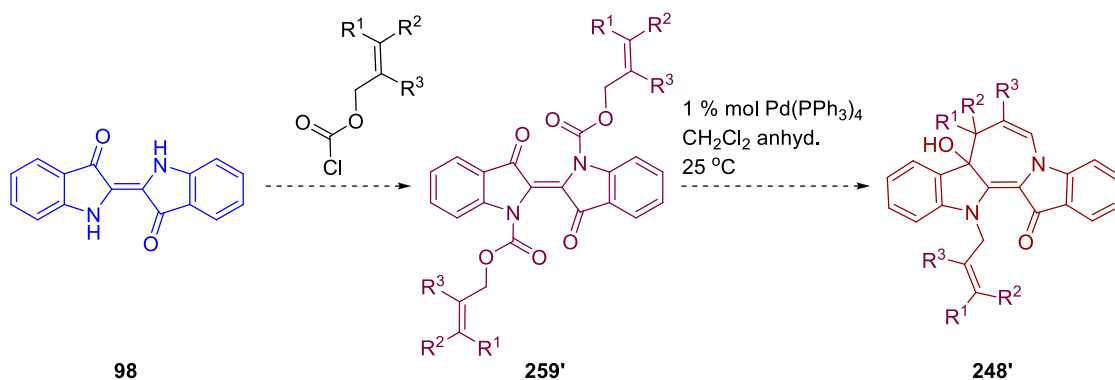
Scheme 88: The proposed synthesis of the hydroxyazepino diindolones via catalytic decarboxylation of *N,N'*-dialloc derivatives of indigo.

6.1.4   Desymmetrisation of the bis-indole system

Reaction of *N,N'*-dialloc indigo and its catalytic decarboxylation in the presence of Et$_3$B resulted in formation of **275** which revealed the possibility of desymmetrisation of the bis-indolic system of indigo. To expand of the scope of this chemistry application of the range of alloc systems and alternate boranes (eg. allyl 9-BBN) to transfer other groups in place of the ethyl could be of interest for future research (Scheme 89).
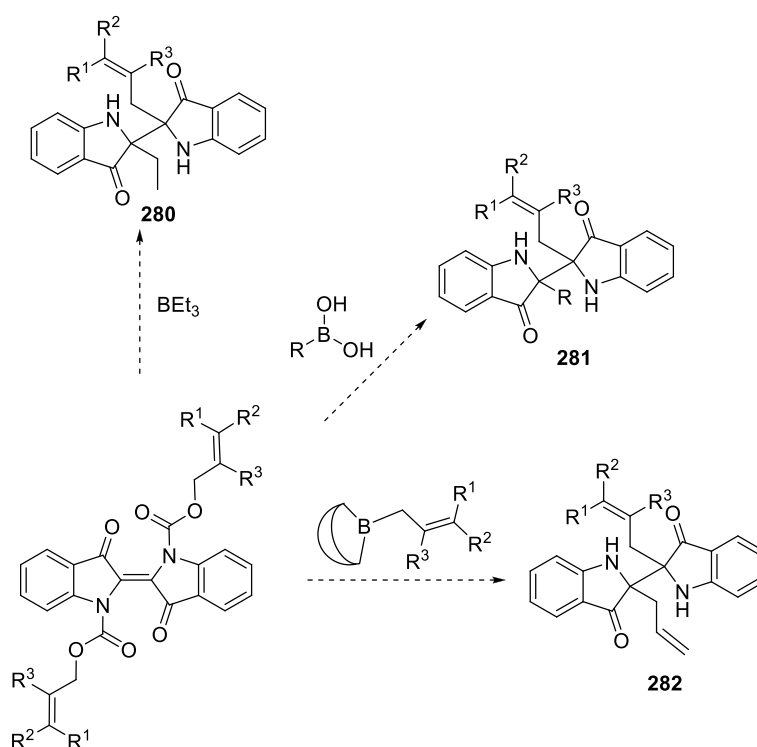
Scheme 89: The possibities to expand the scope of the catalytic decarboxyaltion of *N,N'*-dialloc indigo.

The cascade reactions of indigo with allylic bromides resulted in formation of novel derivatives of indigo and seven types of fused heterocycles (Figure 80). This was a solid proof to show the potential of the application of indigo as an abundant and cheap canvas in the production of diverse and complex heterocycles. However the chemistry and reactivity of this compound still remains widely unexplored.
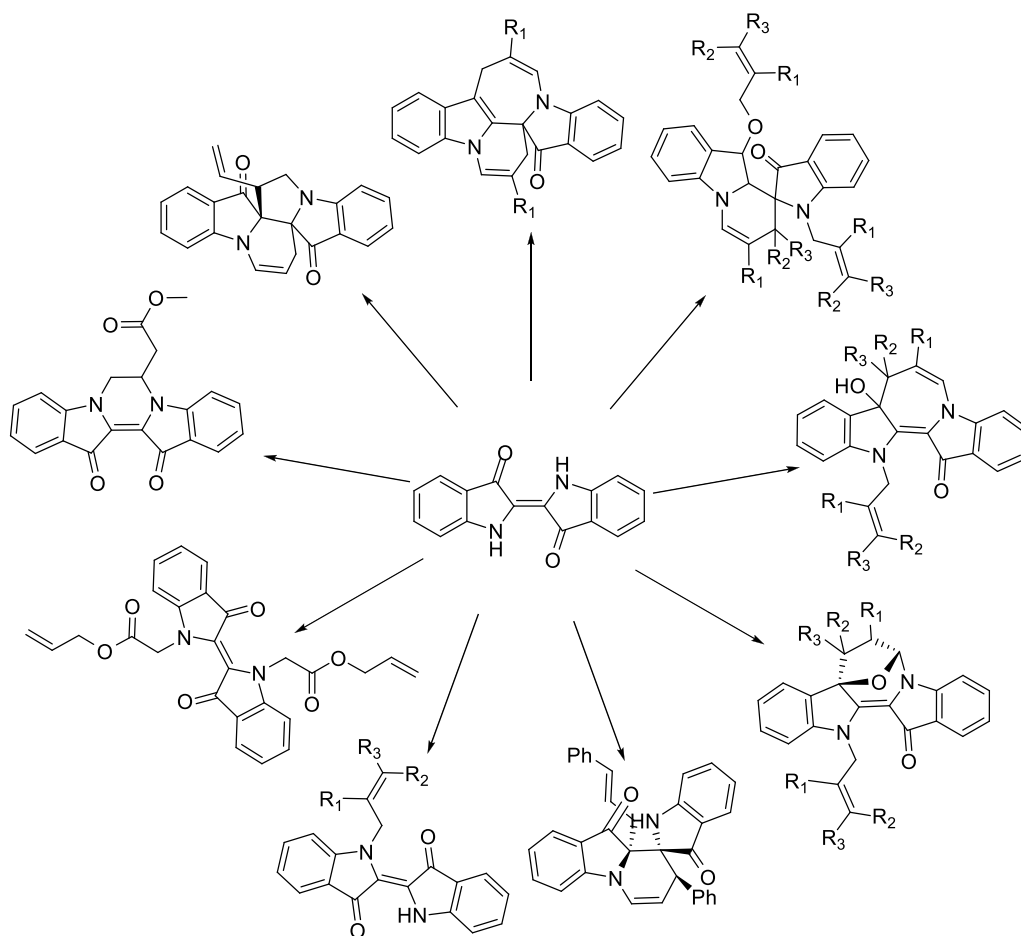
Figure 80: The range of derivatives and fused heterocycles arising from cascade reactions of indigo with allylic bromides.

6.2   The propargylation reaction of indigo

6.2.1   Synthesis of pyridodiindole and benzoindolonaphthyridinone derivatives

The heterocycle **265** is an analogue of the marine natural product fascaplysin, initially isolated from the sponge *Fascaplysinopsis reticulata* and noted for its ATP-competitive inhibitor of Cdk4/D1 (IC$_{50}$ = 0.35 μM)[23,190] activity. As it described earlier (Chapter 5, page 131) compound 265 showed a modest activity against NCH-H187, KB and MCF-7 cell lines. In contrast with fascaplysin, **265** was found as noncytotoxic. The heterocycles **266**-**267** and **269** represent the naphthyridine core of the B-ring homolog of fascaplysin. The reaction of indigo and propargyl mesylate yielded **266** in 59% in a one-pot reaction.

This heterocycle showed IC$_{50}$ value of 8.44 µg/mL against KB oral cancer cell lines. There have been reported syntheses of these natural products including the silver catalysed cascade synthesis of their parent compound and analogs, with this approach involving the initial intermolecular reaction of two components of similar molecular complexity, however, this necessitated the prior synthesis of these two components.[191] Fascaplysin has also been synthesised starting from 4-(1*H*-indol-1-yl)butanoic acid in a 2 step synthesis in a best yield of 42%.[192] Facile synthesis of the benzoindolo[1,2-*h*][1,7]naphthyridine (fascaplysin) heterocyclic skeleton from indigo in the presence of propargylic systems and base provides direct access to this skeleton from exceptionally cheap starting materials and reagents, and provides a convenient access to this system for further elaboration in structure-activity studies. The noncytotoxic methylbenzoindolonaphthyridinedione **267** inhibited the cell line MCF-7 with an IC$_{50}$ value of 3.94 µg/mL.

Considering these results, the SAR studies are desirable for future research to identify the suitable naphthyridine derivatives with distorted planarity. It is also necessary to optimise the yield and selectivity of the reaction. This could be obtained by reaction of *N*-substituted or *N*-Boc protected indigo and propargylic systems (Scheme 90).

R = Me **255**
R = Boc **283**

R = Me **284**
R = Boc **285**
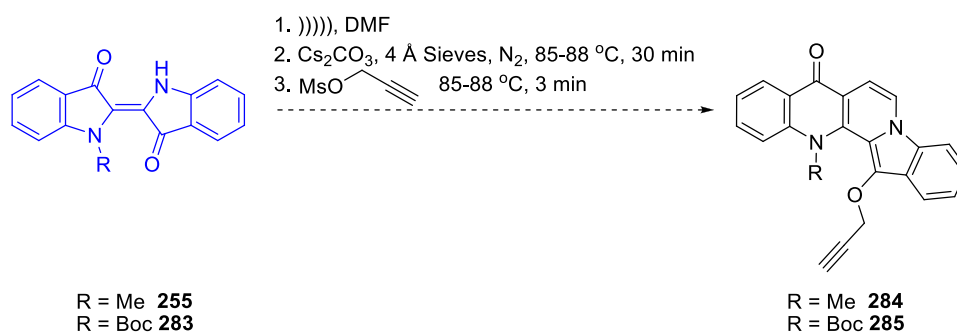
Scheme 90: The proposed method to improve the yield and selectivity of the propargylation cascade reactions in production of naphthyridine based heterocycles.

6.2.2   Synthesis of *N*-propargyl indigo and pyrazinodiindole

In addition to the heterocycles **265**-**267**, the reaction of indigo with propargyl bromide in the presence of base afforded two other derivatives as *N*-propargyl indigo **263** (11%) and pyrazinodiindole **264** (21%). Further elaboration by short time (5 sec) reaction of indigo and propargyl bromide resulted in isolation of **263** (93%). The subsequent base catalysed hydroamination of **263** afforded the pyrazinodiindole **264** quantitatively. These two compound exhibited *antiplasmodial* IC$_{50}$ 0.33 µg/mL, 1.1 µM and IC$_{50}$ 0.256 µg/mL, 0.85 µM values respectively. The click reaction of **263** and glycosyl azide **278** resulted in formation of the **279** in 83% yields. This reaction in particular suggests the possibility of mounting these highly colourful and fluorescent heterocycles on peptide and sugars for live cell imaging applications.

6.2.3   Suggested application of *N*-propargyl indigo in three component coupling reactions with aldehyde and amine

The catalytic coupling of alkyne, aldehyde and amine *via* C-H activation (A^3 coupling)[193] was introduced as an alternative procedure for the synthesis of propargylamines instead of the moisture sensitive nucleophilic attack of Grignard[194] or lithium acetylides[195] on imines. *N*-Propargylindigo could be used in order to produce a variety of propargylamine derivatives of indigo **288-9** by the reaction of amines and aldehyde in presence of Au(I), Au(III) or Cu(I) salts. This proposed procedure could be involved with the protection of the free amine group of the **263** prior to the coupling reaction (Scheme 91).
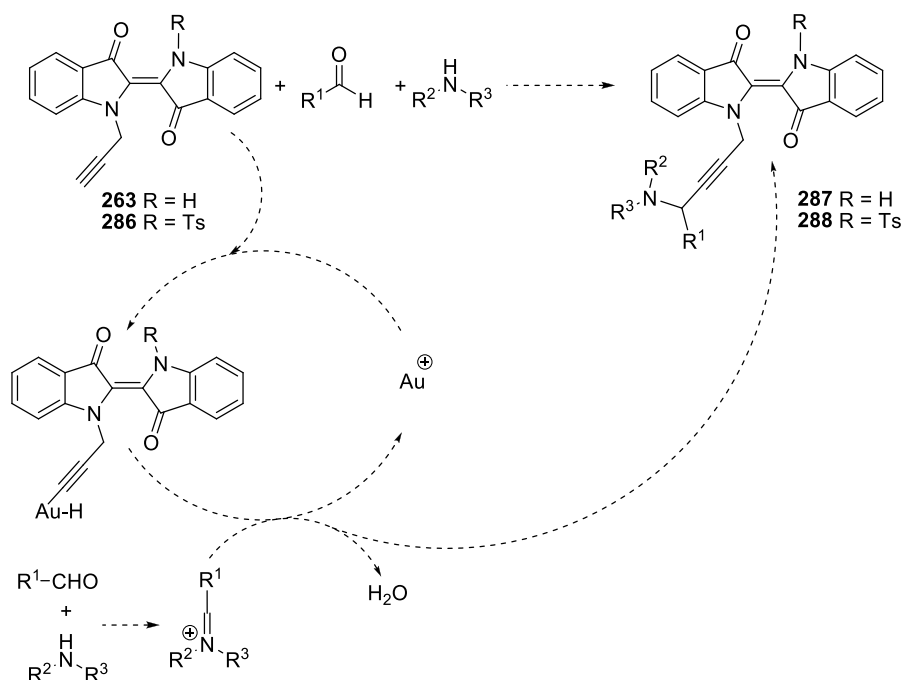
Scheme 91: Proposed procedure for production of propargylamine derivatives of indigo **288**-**289**.

Deprotonation of the **289** and subsequent isomerisation could provide a possibility of base or metal catalysed hydroamination of the amine group of indigo core and the alkyne unit of the propargylamine pendant. This could be implied in generation of pyrazinodiindole derivatives, such as the exocyclic ethylene amine **291** (Scheme 92).
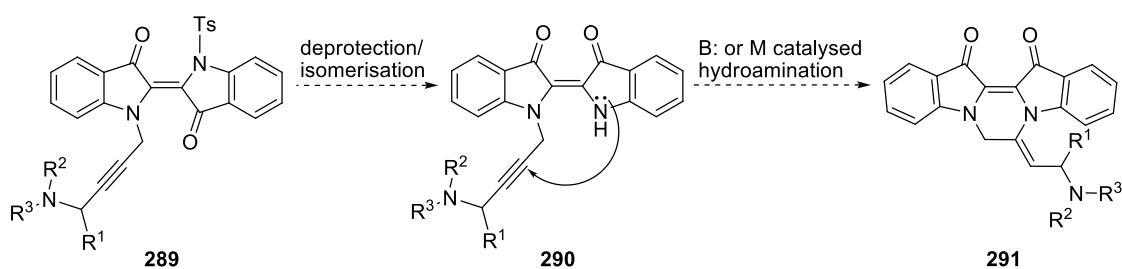
Scheme 92: The proposed base or metal catalysed hydroamination of **289**.

6.2.4 Formation of phenylazepino diindole and oxadiazocino diindole systems from the reaction of indigo and phenylpropargyl chloride

Formation of oxadiazocino diindole **271** was another interesting outcome from the cascade reactions of indigo with propargylic systems. This compound was isolated as a dark navy solid in 35%. The other heterocycle isolated from this reaction mixture was

the phenylazepino diindole **270** as an orange yellow solid in 27%. The optimised condition by extending the time for generation of the indigo anion, resulted in the isolation of **271** in 69%. The structural elucidation for these two heterocycles relies on IR, HRMS and extensive 2D NMR spectroscopy. However attempts for growing crystals suitable for X-ray crystallography failed. This could be done in the future by trying different solvent systems.

Figure 81 illustrates the various product achieved from propargylation reactions of indigo or manipulation of the propargylation products with different chemical means.
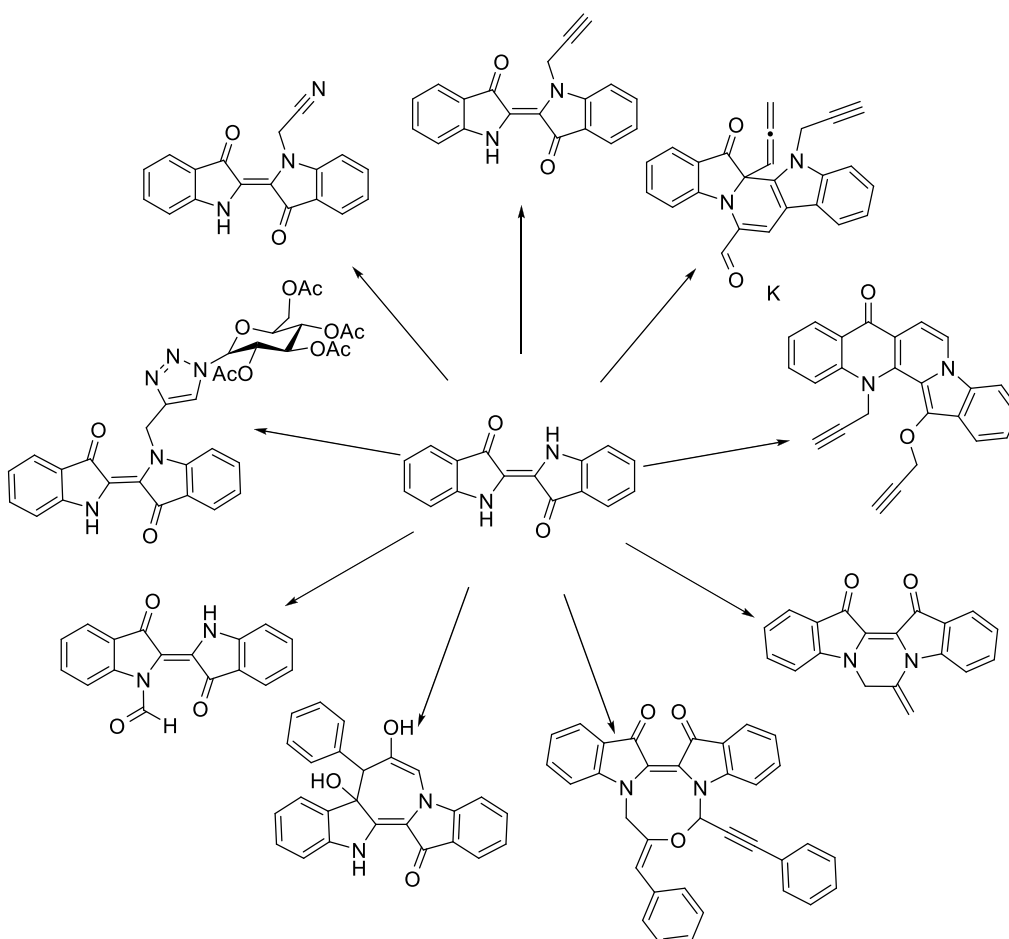
Figure 81: The derivatives and fused heterocycles from cascade reactions of indigo with propargylic halides and their subsequent reactions.

6.3   Suggestions to target the carbonyl of indigo

The nucleophilic cascade reactions of indigo revealed a broad scope in production of complex and annulated structures from this functionalised starting material. The electrophilic sites of indigo i.e. carbonyl groups are less explored in comparison with the nucleophilic sites. Generation of redox complexes by the application of *N,N'*-diaryldiimines (Nindigo)[123] is one of the few examples in which carbonyls of indigo were converted into imines.

6.3.1   Wittig olefination

Wittig olefination[††] is one of the plausible procedures to generate methylene site(s). The major drawback with this olefination is the basicity of the Wittig reaction which could result in the generation of the dianion **293** and recovery of the starting material during the work up.
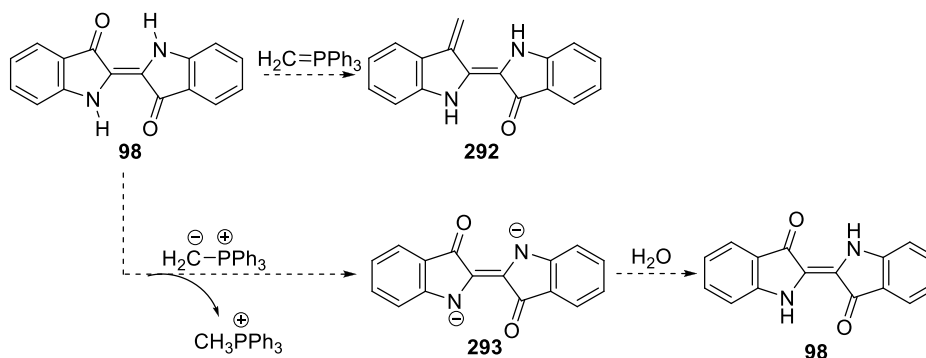
Scheme 93: The Wittig olefination of indigo and expected outcomes.

6.3.2   Methylene indigo from the reaction of 98 and MeMgBr with subsequent dehydration

An alternative procedure could be the treatment of indigo **98** with methyl Grignard and dehydration of the produced 3-hydroxy-3-methyl indigo **178** to afford 3-methylene indigo **292**. The proposed pathway starts with the deprotonation of indigo by the

---

[††] The procedure was proposed by Mr. Nicholas M. Butler and he is currently investigating this chemistry as part of his Honours and subsequent PhD project.

Grignard reagent and results in the dianion **293** which then would lead to the intermediate **294** by resonance. Oxide anion could be stabilised by the cationic effect of the BrMg$^+$ ion and blocks the site from nucleophilic attack. This will force nucleophilic addition to occur on the opposite side and result is the selective formation of the tertiary alcohol **178**. The dehydration of the alcohol will produce the 3-methyleneindigo **292** (Scheme 94). This exocyclic methylene site would be susceptible for further elaborations such as 1,6-conjugate addition.
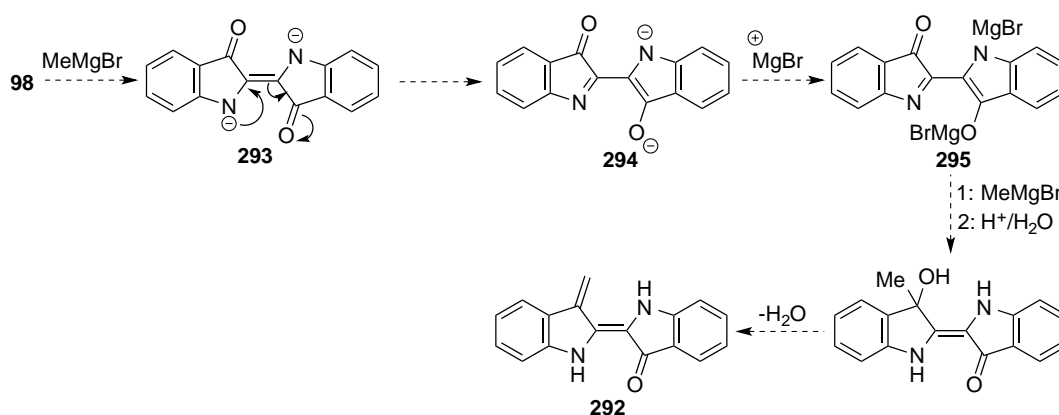
Scheme 94: Proposed pathway for the synthesis of the 3-methylene indigo **292** from the reaction of indigo and methyl Grignard.

6.4 Indigo and its derivatives as processable conjugated polymers

Conjugated polymers are capable of unique physical properties such as high conductivity.[196] Recently bay-annulated[197‡‡] indigo **296** polymers were reported as electron receptors (Figure 82).[198]
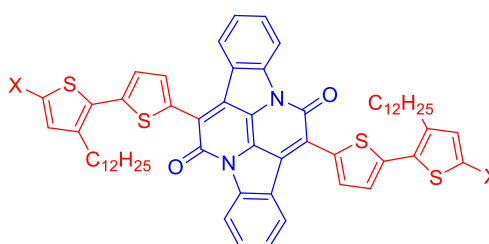
Figure 82: Thiophene Bay-Annulated Indigo (TBIT) as an electron receptor.

---

‡‡ A bay region occurs in a complex ring structure when an angular fused benzene ring is adjacent to an aromatic ring.

The indigo structure with, an extended conjugation and small HOMO-LUMO gap, suggests further exploration in this field. As an example, synthesis of polymeric indigo could be achieved by the formation of Tyrian purple from 6-bromoindole, then through the Ullmann coupling[199] to afford the polymeric indigo **297** (Scheme 95).
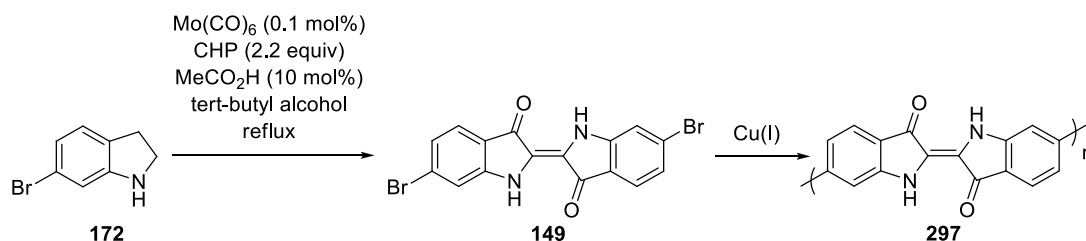
Scheme 95: Proposed procedure for the synthesis of polymeric indigo **297**.

The future research in this area could be involved with the synthesis of the various derivatives of bay-annulated indigo and mounting these derivatives on an amino acid backbone. Photophysical analysis and conductivity evaluation will afford information to narrow the domain of investigation.

6.5   Conclusion

The reaction of indigo with allylic and propargylic systems resulted in the formation of complex heterocycles in one-pot synthesis. This is new science for the indigo moiety and represents an exciting untapped area of heterocyclic chemistry. Our proposed mechanisms (Schemes 49-52 and 72-77) reveal that at different stages of the cascade reaction, the reactivity of different sites on the indigo moiety changes, and additionally, different types of reactivity can occur at different times, including sites acting as nucleophiles or electrophiles, with bond breakage leading to ring expansion and dehydration (Figure 83). A key element to the reactivity is the ability of the indigo heterocycle to tautomerise under different circumstances (*e.g.* upon generation of the *N*-

centered anion with base) to shift reactivity to a different site. This constantly changing reactivity leads to the variety of outcomes as demonstrated. Further, this range of different chemistry all occurs in a tight cluster in the centre of the indigo structure and this combination of properties is the key to the variety of unusual heterocycles that arises. Further, the unexpected outcomes of this initial study not only shows us that there is highly unusual and significant chemistry of indigo, but that there is much yet to be explored in this area.
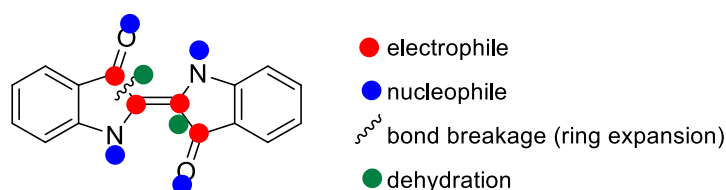
Figure 83: Graphical representation of the changing reactivity of the indigo skeleton with sites of nucleophilicity, electrophilicity, dehydration and bond breakage illustrated. The degree of reactivity at each of these points changes as the molecule(s) progress through the cascade reaction.

<div align="center">**Chapter 7: Experimental**</div>

7.1   Synthesis

7.1.1   General procedure

7.1.1.1   Reagents and solvents

Anhydrous DMF and DMSO were purchased and used without further purification. CH_2Cl_2 for dry reactions were obtained from a solvent purification system or alternatively HPLC grade CH_2Cl_2 was dried over the activated molecular sieves (4 Å) and kept under the N_2 atmosphere. HPLC grade CH_2Cl_2 was used for extractions and column chromatography, while other solvents were purchased reagent grade and used without further purification unless otherwise stated. Indigo (dye content 95%) was used without further purification. Petroleum spirit (pet. spirit) had a bp range of 40−60 °C.

Water for extractions and work-up was obtained from a Millipore purification system. Reactions were carried out under nitrogen which was dried by passing through a 20 cm tube filled with $CaCl_2$ and silica-based drying agent (50:50 W/W%), unless otherwise stated. Solutions such as brine, saturated NH_4Cl, and $NaHCO_3$ were made from the commercial salt. All reagents stated in percentage are dissolved in water and refer to g/100 mL. All other reagents were purchased from commercial sources and used without any further treatment unless otherwise stated.

7.1.1.2   Reactions and purification

All reactions were carried out in standard glassware that was cleaned with domestic detergents, washed with acetone and oven-dried (100 °C), with magnetic stirring in a nitrogen or argon atmosphere unless it was specified that the reaction was performed in the air. Anhydrous and/or air sensitive liquids were added through a rubber septum with a

syringe. Liquid reagents were weighed if stated in g or mg and mixed with the appropriate solvent before being added to the reaction vessel. Air sensitive and/or hygroscopic solid reagents were handled under nitrogen and weighed either directly into the reaction vessel or transferred as a solution in the appropriate solvent. Thermal heating of reactions was carried out with paraffin oil baths. All reactions were quenched immediately by adding water or being poured to an ice bath before work-up. Freezer storage was at -20 °C and fridge recrystallisation at 5 °C. Extracted organic phases were dried over magnesium sulfate or sodium sulfate and gravity filtered. Solvents were removed *in vacuo* on a rotary evaporator and products dried under high vacuum (~1 mbar) at room temperature unless otherwise stated.

Purification by column chromatography was performed using Merck Flash Silica Gel 60 (63-200 mesh) under a positive pressure of air, and, where deactivated silica gel was required, 10% Et$_3$N was added to the eluting solvent. Preparative TLC was performed using Merck Silica Gel F$_{254}$ pre-coated glass plates (20 x 20 cm) with a layer thickness of 500, 1000, 1500 or 2000 μm. Eluents are in volume to volume (v:v) proportions.

7.1.1.3   Analysis and characterisation

Thin Layer chromatography (TLC) was performed using Merck Silica Gel F$_{254}$ pre-coated aluminium plates. Visualisation was accomplished using UV light and/or a phosphomolybdic acid or ninhydrin stain.

Melting points measured on a Buchi Melting Point M-560 apparatus are expressed in degrees Celsius (°C) and are uncorrected.

UV/Vis spectra were obtained using a double beam Cary 100 Bio UV-Vis spectrophotometer, operating between 300 – 1400 nm. All solutions were appropriately

diluted in CH_2Cl_2 prior to analysis to fit within the absorbance limits of the detector, and placed into 1 cm path-length quartz cuvettes. All spectra were collected at room temperature. Sample sizes were between 1.000-2.000 mg, weighted with an accuracy to 6 decimal places using a seven figure balance CAHN C-35. Mono-substituted indigo derivatives were diluted to 50.0 mL, all other derivatives to 25.0 mL and the ε values reported in $M^{-1}cm^{-1}$.

Infrared (IR) spectra were recorded on KBr diluted samples by the Diffuse Reflection Method on a Shimadzu IR Affinity 1 instrument. Neat samples were recorded with the Single Reflection Horizontal Attenuated Total Reflectance (HATR) accessory MIRacle 10, fitted with a 1.5 mm round diamond crystal. IR data were recorded as number of wavelength per unit distance ($\tilde{v}$ or $\frac{1}{\lambda}$) in cm^{-1} with peak intensity assigned as weak (w), medium (m) or strong (s).

Electron impact (EI) mass spectra were performed using a Shimadzu QP-5050 spectrometer with compounds dissolved in CH_2Cl_2. Low resolution mass spectra were obtained by electrospray ionisation (ESI) mass spectrometry on a Micromass Platform LCZ spectrometer by injecting the samples as a solution in MeOH. In some cases 1% formic acid was added to suppress dimerization and or aid in protonation. High resolution mass spectrometry (HRMS) was performed using either electrospray ionisation (ESI) technique on a Waters QTOF Xevo spectrometer or electron impact technique (EI) on a Micromass Autospec Premier spectrometer. Ion mass to charge (m/z) values are stated with their relative abundances as a percentage in parentheses. Peaks assigned to the molecular ion are denoted by M^+ or $[M + H]^+$.

Proton (^1H) and carbon (^{13}C) nuclear magnetic resonance (NMR) spectra were recorded at 500 and 125 MHz respectively on a Varian Inova 500 MHz spectrometer or a

VNMRS PS54 500 MHz spectrometer. Alternatively, ^{1}H and ^{13}C NMR spectra were recorded at 300 and 75 MHz respectively on a Varian Mercury 300 MHz spectrometer. The NMR spectra were acquired in $CDCl_3$ with chemical shifts (δ) reported in parts per million (ppm) relative to TMS (^{1}H: $\delta = 0$ ppm) and $CDCl_3$, ^{13}C: $\delta = 77.0$ ppm). Alternatively, spectra were acquired in $(CD_3)_2SO$ with δ values relative to DMSO (^{1}H: $\delta = 2.50$ ppm) and $(CD_3)_2SO$ (^{13}C: $\delta = 39.5$ ppm). Coupling constants (J) are reported in Hertz (Hz) and refer to the coupling between hydrogen nuclei unless otherwise stated. Multiplicities are reported as singlet (s), broad singlet (bs), doublet (d), doublet of doublet (dd), triplet of doublets (td), triplet (t), doublet of triplet (dt), quartet (q), multiplet (m) or apparent triplet (appt t). The processing of ^{1}H NMR, ^{13}C NMR and two dimensional NMR spectra shown in this work were displayed using MestReNova software (version 8.1.2).

X-ray diffraction data sets were collected on a Nonius Kappa-CCD area-detector diffractometer equipped with IFG capillary X-ray focusing collimators and an Oxford Cryosystems crystal cooling device. Calculations were performed using maXus, Crystals and Reals software packages.

Images from crystals were captured using a Leica MZ 16 A stereo microscope. All the images were obtained from X-ray quality single crystals.

Optical rotations were measured on a Jasco p-2000 polarimeter in CH_2Cl_2 solution at 25 °C. All the compounds with stereogenic centre were characterised as racemates and used with no further isolation of the enantiomers.

7.1.2   Reaction of indigo with allylic bromides

7.1.2.1   Reaction of indigo with allyl bromide

Method A: 5 sec reaction

(*E*)-1-Allyl-[2,2'-biindolinylidene]-3,3'-dione (243)
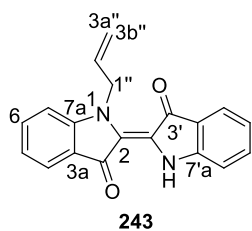
A suspension of indigo (262 mg 1.00 mmol) in anhydrous DMF (40 mL) was sonicated for 30 min and the resulting suspension was transferred to a septum equipped round bottom flask carrying pre-dried Cs_2CO_3 (1.303 g, 4.00 mmol) under N_2 flow. The flask was plunged into a preheated oil bath at 85-88 °C and stirred for 30 min. The N_2 flow was stopped and allyl bromide (605 mg, 5.00 mmol) was added rapidly in one portion by syringe, and after 5 sec, the reaction mixture was poured into an ice bath. The blue-black precipitate was filtered and dissolved in hot CH_2Cl_2 and cooled at 5 °C overnight. The mixture was then filtered to remove the unreacted indigo (36%). The filtrate was concentrated under reduced pressure then recrystallised from pet. spirit/EtOAc (90:10) to furnish **243** (163 mg, 54%) as a dark navy crystalline solid; R_f = 0.68 (CH_2Cl_2/pet. spirit; 7:3), m.p: 170-171 ºC. X-ray quality crystals were obtained by slow recrystallisation from $CHCl_3$ in a small tube while it was placed in another sample tube containing pet. spirit (10 mL). UV-Vis (CH_2Cl_2) λ_{max}/nm (ε, $M^{-1}cm^{-1}$) 289 (22571), 614 (11924). IR (neat) υ_{max} 3290 (m), 1635 (s), 1608 (s), 1462 (s), 1384 (m), 1064 (m), 1027 (s), 921 (m), 748 (m) cm^{-1}. ^1H NMR ($CDCl_3$) δ 5.09-5.16 (3H, m, H2", H3"a, H3"b), 5.90-5.94 (2H, s, H1"), 6.92 (1H, t, *J* = 7.5 Hz, H5'), 6.97 (1H, d, *J* = 8.3 Hz, H7), 7.00 (1H, t, *J* = 7.9 Hz, H5), 7.07 (1H, d, *J* = 7.5 Hz, H7'), 7.44 (1H, t, *J* = 7.5 Hz, H6'), 7.50 (1H, t, *J* = 7.9 Hz, H6), 7.65 (1H, d, *J* = 8.3 Hz, H4), 7.73 (1H, d, *J* = 7.5 Hz, H4'), 10.71 (1H, s, NH). ^{13}C NMR ($CDCl_3$) δ 49.7 (C1"), 111.0 (C7), 111.8 (C5'), 116.8 (C3"), 120.2 (C3'a), 120.6 (C7'), 120.7 (C5), 120.9 (C3a), 122.8 (C2), 124.0 (C4'), 124.7

(C4), 125.6 (C2'), 133.1 (C2''), 135.7 (C6), 136.0 (C6'), 151.4 (C7a), 152.7 (C7'a), 187.1

(C3'), 189.7 (C3). MS (EI): m/z = 302 (66%, M$^+$), 273 (27), 233 (24), 98 (100). HRMS

(ESI): calcd for $C_{19}H_{14}N_2O_2$ [M+H]$^+$ 303.1134; found 303.1143.

13-Allyl-8a-hydroxy-8,13a-dihydroazepino[1,2-*a*:3,4-*b'*]diindol-14(8*H*)-one (248)

248
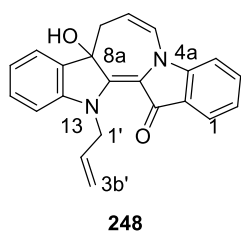
The mother liquor from the recrystallisation above was then dried (Na$_2$SO$_4$), concentrated and subjected to PTLC and developed with CH$_2$Cl$_2$/EtOAc; 9.5:0.5. The selected band was collected and soaked in EtOAc and filtered. The filtrate was concentrated to

afford **5** (30.8 mg, 9%) as a red solid; mp. 163-165 ℃. R_f = 0.20 (CH$_2$Cl$_2$/EtOAc;

9.5:0.5). UV-Vis (CH$_2$Cl$_2$) λ_{max}/nm (ε, M^{-1}cm^{-1}) 306 (14496), 363 (16077), 370

(10096), 498 (11840). IR (neat) υ_{max} 3275 (b), 1608 (m), 1535 (s), 1465 (s), 1419 (m),

1319 (m), 1180 (m), 1111 (m), 748 (s) cm^{-1}. ^{1}H NMR (CDCl$_3$) δ 2.46 (1H, d, J = 17.1

Hz, H8a), 2.97 (1H, dd, J = 12.2, 17.3 Hz, H8b), 4.57 (1H, d, J = 15.3 Hz, 1'a), 4.73

(1H, s, OH), 4.94-5.03 (3H, m, H1'b, H7, H3'a), 5.14 (1H, d, J = 17.3 Hz, H3'b), 5.80-

5.85 (1H, m, H2'), 6.85-6.91 (2H, m, H11, H2), 6.98 (1H, d, J = 8.0 Hz, H4), 7.00 (1H,

d, J = 8.2 Hz, H12), 7.11 (1H, t, J = 7.5 Hz, H10), 7.32 (1H, t, J = 7.5 Hz, H3), 7.49

(1H, d, J = 7.2 Hz, H9), 7.61 (1H, d, J = 7.6 Hz, H1). ^{13}C NMR (CDCl$_3$) δ 38.9 (C8),

52.6 (C1'), 81.3 (C8a), 101.9 (C7), 109.4 (C4), 111.1 (C12), 115.7 (C13b), 117.7 (C3'),

120.2 (C6), 122.6 (C14a), 123.2 (C12), 123.6 (C10), 123.7 (C9), 124.2 (C1), 129.7

(C2'), 133.0 (C11), 134.5 (C3), 136.0 (C8b), 145.1 (C13a), 147.6 (C12a), 156.0 (C4a),

178.5 (C14). MS (EI): m/z = 342 (91%, M$^+$), 324 (100). HRMS (ESI): calcd. for

$C_{22}H_{18}N_2O_2$ [M+H]$^+$ 343.1447; found 343.1440.

Method B: 1 h reaction

13-Allyl-8a-hydroxy-8,13a-dihydroazepino[1,2-*a*:3,4-*b*']diindol-14(8*H*)-one (248)

A mixture of indigo (262 mg, 1.00 mmol) in anhydrous DMF (40.0 mL) was sonicated for 30 min and the resulting suspension was added dropwise into a flask containing 4 Å molecular sieves and pre-dried anhydrous Cs_2CO_3 (1.303 g, 4.00 mmol). The flask was plunged into a pre-heated oil bath at 85-88 °C and the mixture stirred for 30 min under a N_2 flow. The flow was then cut and allyl bromide (600 mg, 5.00 mmol) was added using a syringe and the mixture was stirred and heated at 85-88 ºC for 1 h under a static inert atmosphere (N_2). The crude mixture was then filtered hot (to remove the molecular sieves) into an ice bath. The aqueous mixture was transferred to a conical flask and partitioned in CH_2Cl_2 and washed with brine (2 × 30 mL) and water (5 × 50 mL). The combined organic layers were concentrated under reduced pressure. The residue from the ice bath (thick oily red-orange drops) was dissolved in CH_2Cl_2. This solution was dried over Na_2SO_4 and combined with the collected organic phase from extraction of the aqueous mixture from the ice bath. The filtrate was then concentrated under reduced pressure and adsorbed onto silica (1:1 CH_2Cl_2 : pet. spirit). The silica was then washed and filtered through a sinter with CH_2Cl_2/pet. spirit (9:1) until the filtrate became colourless (filtrate A). The silica was then soaked in EtOAc and filtered. The filtrate was concentrated and the resulting red powder was recrystallised from CH_2Cl_2 giving **248** (140 mg, 41%) as red crystalline flakes.

Filtrate A was concentrated under reduced pressure and subjected to silica gel column chromatography. Elution with 7:3 CH_2Cl_2/pet. spirit resulted in isolation of compound **243** (27.2 mg, 9%) and compound **227** (11.5 mg, 3%).

Method C: 3 h reaction

8*H*,16*H*-Pyrido[1,2,3-*s*,*t*]-indolo[1,2-*a*]azepino[3,4*b*]indol-17-one (232)
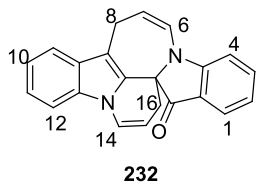
232

A suspension of indigo (262 mg, 1.00 mmol) in DMF was sonicated for 30 min at room temperature and transferred to a septum equipped round bottom flask containing pre-dried and ground Cs_2CO_3 (1.303 g, 4.00 mmol) and molecular sieves under an inert atmosphere. The flask was plunged to a pre-heated oil bath at 85-88 °C and stirred for 30 min. The inert atmosphere flow was then cut and allyl bromide (600 mg, 5.00 mmol) was added, and the mixture was stirred and heated for 1 h under a static inert atmosphere (N_2). Another portion of allyl bromide (2.00 mmol) was added to the mixture and it was stirred for a further 2 h. The colour of solution turned brown-yellow and TLC analysis indicated the complete consumption of indigo. Molecular sieves were filtered from the hot reaction mixture and the filtrate poured into an ice bath and then partitioned between water and CH_2Cl_2, washed with brine (2 × 30 mL) and water (5 × 50 mL) and the combined organic phase were dried (Na_2SO_4) and concentrated under reduced pressure. The residue was subjected to flash silica gel column chromatography and elution with pet. spirit/CH_2Cl_2 (1:3) yielded **232** (221 mg, 72%) as a yellow-brown powder; mp 143-144 °C. X-ray quality crystals were grown through slow crystallization from pet. spirit:CH_2Cl_2 (5:3). R_f = 0.61; IR (neat) υ_{max} 1698 (s), 1614 (s), 1463 (m), 1363 (m), 1020 (m) cm^{-1}. ^{1}H NMR (CDCl$_3$) δ 2.45 (1H, dd, J = 6.5, 6.0 Hz, H16a), 2.75 (1H, dd, J = 4.5, 4.5 Hz, H16b), 3.25 (2H, m, H8), 5.31 (1H, m, H13), 6.34-6.36 (2H, m, H6, H7), 6.85 (1H, appt t, J = 7.5, 7.5 Hz, H2), 6.91 (1H, d, J = 8.5 Hz, H4), 7.13 (1H, dd, J = 7.5, 7.5 Hz, H10), 7.21-7.27 (2H, m, H14, H11), 7.42 (1H, d, J = 8.0 Hz, H9), 7.47 (1H, d, J = 7.5 Hz, H12), 7.52 (1H, dd, J = 7.5, 8.0 Hz, H3), 7.65 (1H, d, J = 8.0 Hz, H1). ^{13}C NMR (CDCl$_3$) δ 20.3 (C8), 29.9 (C16), 67.8 (C16a), 104.3 (C15),

109.7 (C9), 109.8 (C4), 112.6 (C8a), 117.9 (C8b), 118.5 (C12), 119.0 (C2), 120.7 (C10), 123.0 (C14), 124.0 (C11), 125.9 (C1), 127.0 (C7), 128.0 (C4a), 128.6 (C12a), 135.9 (C16b), 136.3 (C6), 137.6 (C3), 150.0 (C17a), 197.5 (C17). MS (EI), *m/z* 324 (100%, M+), HRMS (EI, M+) calcd for $C_{22}H_{16}N_2O$ 324.1263, found 324.1261.

1-Allyl-10'-allyloxy-2'*H*-spiro(indoline-2,1'-pyrido[1,2-*a*]indol)-3-one (227)
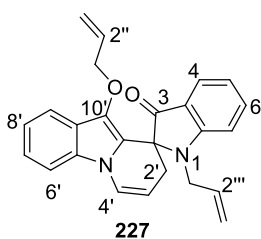
Further elution of the SiO_2 flash column using petroleum spirit : CH_2Cl_2 (3:1) yielded a fraction that was further subjected to gravity column chromatography (pet. spirit : EtOAc, 3:1) followed by PTLC (pet. spirit: EtOAc, 3:2) to yield two products, one of which was 1-allyl-10'-allyloxy-2'*H*-spiro(indoline-2,1'-pyrido[1,2-*a*]indol)-3-one **227** (115 mg, 32%) as an orange solid; mp. 121-122 °C. R_f = 0.51; IR (neat) υ_{max} 1696 (s), 1609 (s), 1481 (s), 1317 (m) cm^{-1}. ^{1}H NMR (CDCl$_3$) δ 2.38 (1H, dd, *J* = 5.7, 17.6 Hz H2'a), 2.80 (1H, dd, *J* = 2.9, 17.6 Hz H2'b), 3.71-3.82 (2H, m, H3'''), 4.11-4.21 (2H, m, H3''), 4.85-4.92 (2H, m, H1'''), 5.04-5.10 (2H, m, H1''), 5.31-5.38 (1H, m, H3'), 5.52-5.63 (2H, m, H2'', H2'''), 6.62 (1H, d, *J* = 7.8 Hz, H7), 6.70 (1H, dd, *J* = 7.2, 7.2 Hz, H6), 7.12-7.18 (2H, m, H8', H4'), 7.32 (1H, d, *J* = 8.1 Hz, H6'), 7.39-7.41 (1H, m, H5), 7.45 (1H, d, *J* = 7.8 Hz, H9'), 7.58 (d, *J* = 7.8 Hz, H4). ^{13}C NMR (CDCl$_3$) δ 31.6 (C2'), 46.8 (C3'''), 66.2 (C1), 74.6 (C3''), 104.6 (C3'), 108.91 (C7), 108.93 (C6'), 116.0 (C1'''), 117.4 (C6), 117.6 (C1''), 118.8 (C9'), 118.9 (C7a), 119.0 (C10a), 120.4 (C7'), 121.3 (C5'a), 121.5 (C4'), 123.1 (C8'), 125.0 (C4), 132.1 (C9'a), 133.5 (C2'''), 133.8 (C2''), 135.9 (C10'), 137.6 (C5), 159.3 (C7a), 200.6 (C3). MS (EI), *m/z* 382 (10%, M$^+$), 341 (100%, M-41). HRMS (EI, M$^+$) calcd for $C_{25}H_{22}N_2O_2$ 382.1681, found 382.1681.

N-Allylisatin (237)
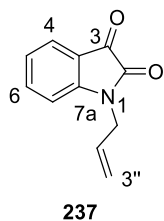
The third product separated from the above column chromatography procedure was crystallised from CDCl$_3$/EtO$_2$ to give *N*-allyisatin[§§] **237** (11.2 mg, 6%) as orange crystals; mp. 87-88 °C (Lit mp 88-89 °C[200]). R_f = 0.51; IR (neat) υ_{max} 1727 (s), 1604 (s), 1469 (s), 1354 (m), 760 (s) cm^{-1}. ^{1}H NMR (CDCl$_3$) δ 4.38 (2H, d, *J* = 6.0 Hz, H3'), 5.32 (2H, dd, *J* = 10.5, 10.5 Hz, H1'), 5.57-5.59 (1H, m, H2'), 6.89 (1H, d, *J* = 8.0 Hz, H7), 7.12 (1H, dd, *J* = 7.5, 7.5 Hz, H5), 7.58 (1H, dd, *J* = 8.0, 8.0 Hz, H6), 7.61-7.63 (1H, d, *J* = 7.5 Hz, H4). ^{13}C NMR (CDCl$_3$) δ 42.5 (C3'), 110. 9 (C7), 117.6 (C3a), 118.7 (C1'), 123.8 (C5), 125.4 (C4), 130.3 (C2'), 138.3 (C6), 150.8 (C7a), 157.9 (C2), 183.2 (C3). MS (ESI) *m/z* 188 (100%, M+H). HRMS (EI, M$^+$) calcd for C$_{11}$H$_9$NO$_2$ 187.0633, found 187.0634

7.1.2.2   Reaction of indigo with 3-bromo-2-methylpropene

Method A: 5 sec reaction

(E)-1-(2-Methylallyl)-[2,2'-biindolinylidene]-3,3'-dione (244)
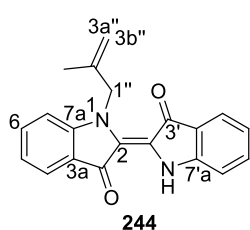
Using Method A, indigo (262 mg, 1.00 mmol) and 3-bromo-2-methylpropene (670 mg, 5.00 mmol) was reacted at 85-88 °C. The reaction mixture was poured onto an ice bath and the dark navy or black precipitate was collected and dissolved in hot CH$_2$Cl$_2$ and cooled at 5 °C overnight. The mixture was then filtered to remove the unreacted indigo (29%). The filtrate was concentrated under reduced pressure then dissolved in hot MeOH/H$_2$O (1:3) then cooled to afford **244** (196 mg, 62%) as a dark navy powder mp.

[§§] *N*-Allylisatin was not isolated from the reaction when additional measures for drying of solvents and reagents was applied.

150-152 °C, R_f = 0.72 (CH$_2$Cl$_2$/pet. spirit; 7:3). UV−Vis (CH$_2$Cl$_2$) λ_{max}/nm (ε, M^{-1}cm^{-1}) 291 (21876), 628 (11669). IR υ_{max} 3271 (m), 1608 (s), 1462 (s), 1388 (m), 1296 (s), 1172 (m), 1072 (s) 1037 (s), 918 (w), 748 (m), 698 (m) cm^{-1}. ^{1}H NMR ((CD$_3$)$_2$SO) δ 1.76 (3H, s, CH$_3$), 4.62 (1H, s, H3"a), 4.83 (1H, d, J = 6.9 Hz, H3"b), 5.11 (2H, s, H1"), 6.93 (1H, t, J = 7.3 Hz, H5'), 6.97-7.04 (3H, m, H7, H7', H5), 7.45 (1H, t, J = 7.7 Hz, H6'), 7.51 (1H, t, J = 7.7 Hz, H6), 7.65 (1H, d, J = 7.7 Hz, H4), 7.58 (1H, d, J = 7.3 Hz, H4'), 10.60 (1H, s, NH). ^{13}C NMR ((CD$_3$)$_2$SO) δ 20.5 (CH$_3$), 52.6 (C1'), 112.1 (C3"), 112.8 (C7), 114.1 (C5'), 120.0 (C3'a), 120.9 (C3a), 121.3 (C7'), 121.8 (C5), 123.4 (C2), 124.3 (C4), 124.8 (C4'), 125.2 (C2'), 136.8 (C6), 136.9 (C6'), 141.3 (C2"), 152.8 (C7a), 153.7 (C7'a), 187.4 (C3'), 189.0 (C3). MS (EI): m/z = 316 (81%), 299 (22), 195 (100). HRMS (ESI): calcd for C$_{20}$H$_{17}$N$_2$O$_2$ [M+H]$^+$ 317.1290; found 371.1298.

8a-Hydroxy-7-methyl-13-(2-methylallyl)-8,13a-dihydroazepino[1,2-*a*:3,4-*b*']diindol-14(8*H*)-one (249)

249
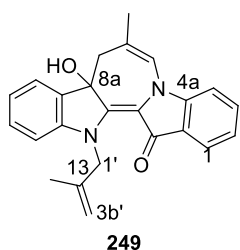
The mother liquor was dried (Na$_2$SO$_4$), concentrated and then subjected to PTLC and developed with CH$_2$Cl$_2$/EtOAc; 9.5:0.5. The selected band was collected and soaked in EtOAc and filtered. The filtrate was concentrated to afford **7** (25.9 mg, 7%) as a red powder; mp. 172-174 ºC. R_f = 0.19 (CH$_2$Cl$_2$/EtOAc; 9.5:0.5). UV−Vis (CH$_2$Cl$_2$) λ_{max}/nm (ε, M^{-1}cm^{-1}) 306 (14007), 377 (10809), 511 (10483). IR υ_{max} 3143 (b), 1651 (s), 1608 (s), 1543 (s), 1465 (s), 1377 (m), 1315 (s), 1192 (m), 1118 (s), 1087 (m), 894 (w), 740 (s) cm^{-1}. ^{1}H NMR (CDCl$_3$) δ 1.50 (3H, s, H1"), 1.90 (3H, s, H1'''), 2.47 (1H, d, J = 17.5 Hz, H8a), 2.90 (1H, d, J = 17.6 Hz, H8b), 4.07 (1H, d, J = 16.8 Hz, H3'a), 4.61 (1H, s, H1'a), 4.75 (1H, s, H1'b), 5.33 (1H, d, J = 15.0 Hz, H3'b), 5.51 (1H, bs, OH), 6.66-6.70 (2H, m, H6, H2), 6.82 (1H, d, J = 7.9 Hz, H12), 7.04 (1H, d, J = 8.3 Hz, H4), 7.11 (2H, t, J = 7.4 Hz, H10), 7.24 (1H, t, J = 8.1 Hz, H3), 7.31 (1H, t, J = 7.9 Hz, H11),

7.38 (1H, d, J = 7.8 Hz, H1), 7.58 (1H, d, J = 7.5 Hz, H9). ^{13}C NMR (CDCl$_3$) δ 19.9 (C1"), 24.8 (C1'''), 43.9 (C8), 54.1 (C3'), 80.6 (C8a), 109.8 (C4), 110.9 (C12), 111.4 (C7), 112.8 (C1'), 116.6 (C13b), 120.1 (C2), 120.9 (C6), 123.0 (C14a), 123.3 (C9,C10), 123.7 (C1), 129.6 (C11), 133.1 (C3), 135.6 (C8b), 139.5 (C2'), 144.8 (C12a), 148.3 (C4a), 154.9 (C13a), 178.4 (C14). MS (EI): m/z = 370 (82%, M$^+$), 353 (30), 315 (71), 299 (32), 195 (100). HRMS (ESI): calcd for C$_{24}$H$_{23}$N$_2$O$_2$ [M+H]$^+$ 371.1760; found 371.1760.

Method B: 1 h reaction

8a-Hydroxy-7-methyl-13-(2-methylallyl)-8,13a-dihydroazepino[1,2-a:3,4-b']diindol-14(8H)-one (249)

Using Method B, indigo (262 mg, 1.00 mmol) and 3-bromo-2-methylpropene (670 mg, 5.00 mmol) was reacted at 85 ºC for 1 h. Upon workup, the filtrate was concentrated under reduced pressure and subjected to a 20 × 1.5 cm silica gel column chromatography. Elution with CH$_2$Cl$_2$ (300 mL) flushed the by-products through (compound **244**, 22.1 mg, 7% and compound **228**, 29.7 mg, 7%), before elution with CH$_2$Cl$_2$/EtOAc (95:5, 300 mL) yielded a red powder which was recrystallized from pet. spirit/EtOAc (9:1) to yield **249** (204 mg, 51%) as shiny ruby crystals with identical spectral characteristics as reported above.

Method C: 3 h reaction

7,15-Dimethyl-8H,16H-pyrido[1,2,3-s,t]-indolo[1,2-a]azepino[3,4-b]indol-17-one (233)

Using Method C, indigo (262 mg, 1.00 mmol) was reacted with 3-bromo-2-methylpropene (680 mg, 5.00 mmol). Upon workup, the residue was dissolved in

233
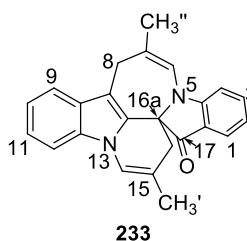
CH$_2$Cl$_2$ (10 mL) and pet. spirit was added gradually while the dark brown mixture turned cloudy. The mixture was heated until it become clear. Crystallisation on cooling overnight deposited the luminescent yellow grains of **233** (183 mg, 52%) mp. 123-124 °C, R_f = 0.58 (CH$_2$Cl$_2$/pet. spirit; 7:3); IR (neat) υ_{max} 1700 (m), 1606 (s), 1451 (s), 1361 (m), 1310 (m), 742 (m) cm^{-1}. ^{1}H NMR (CDCl$_3$) δ 1.90 (3H, s, H″), 1.91 (3H, s, H′), 2.23 (2H, d, J = 16.0 Hz, H16$_a$), 2.74 (1H, d, J = 16.0 Hz, H16$_b$), 2.95 (1H, d, J = 15.0 Hz, H8a), 3.35 (1H, d, J = 15.0 Hz, H8b), 6.03 (1H, s, H6), 6.82 (1H, dd, J = 7.5, 7.5 Hz, H2), 6.91 (1H, d, J = 8.5 Hz, H4), 7.01 (1H, s, H14), 7.10 (1H, dd, J = 7.5, 7.5 Hz, H10), 7.21 (1H, dd, J = 7.8, 7.8 Hz H11), 7.41 (1H, d, J = 8.0 Hz, H9), 7.46-7.51 (2H, m, H6, H12), 7.62 (1H, d, J = 8.0 Hz, H1). ^{13}C NMR (CDCl$_3$) δ 20.1 (C′), 20.6 (C″), 26.3 (C6), 34.7 (C16), 67.8 (C16a), 109.6 (C9), 109.9 (C4), 111.3 (C8a), 114.6 (C15), 118.1 (C8b), 118.2 (C12), 118.3 (C14), 118.7 (C2), 120.0 (C8), 120.2 (C10), 122.5 (C11), 125.8 (C1), 127.1 (C12a), 128.5 (C4a), 135.3 (C13a), 137.6 (C3), 149.1 (C7), 159.9 (C17a), 198.0 (C17). MS (EI), m/z 352 (100%, M$^+$), HRMS (EI, M$^+$) calcd for C$_{24}$H$_{20}$N$_2$O 352.1576, found 352.1573.

3′-Methyl-1-[3-(2-methyl)prop-1-enyl]-10′-[3-(2-methyl)prop-1-enyl]oxy-2′*H*-spiro(indoline-2,1′-pyrido[1,2-*a*]indol)-3-one (228)

228
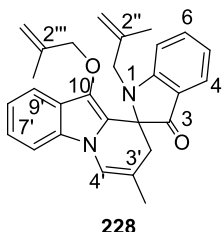
The mother liquor from recrystallisation was concentrated and subjected to flash column chromatography. Elution with CH$_2$Cl$_2$/pet. spirit (70:30) yielded 7,15-dimethyl-8*H*,16*H*-pyrido[1,2,3-*s,t*]-indolo[1,2-*a*]azepino[3,4-*b*]indol-17-one **233** (68.0 mg, 17%). Further elution afforded **228** (63.0 mg, 15%) as a yellow powder; mp. 118-120 °C, R_f = 0.46 (CH$_2$Cl$_2$/pet. spirit; 7:3); IR (neat) υ_{max} 1704 (s), 1613 (m), 1488 (s), 1463 (m), 1320 (m), 710 (m) cm^{-1}. ^{1}H NMR (CDCl$_3$) δ 1.58 (3H, s, C2‴-CH$_3$), 1.63

(3H, s, C2"-CH$_3$), 1.90 (3H, s, C3'-CH$_3$), 2.32 (1H, d, J = 17.0 Hz, H2'a), 2.84 (1H, d, J = 17.0 Hz, H2'b), 3.56 (1H, d, J = 18.0 Hz, H3"a), 3.69 (1H, d, J = 18.0 Hz, H3"b), 4.07 (1H, d, J = 11.5 Hz, H3'''a), 4.16 (1H, d, J = 11.5 Hz, H'''b), 4.73 (2H, d, J = 5.0 Hz, H1"), 4.81 (2H, d, J = 5.0 Hz, H1'''), 6.67 (1H, d, J = 8.0 Hz, H7), 6.75 (1H, dd, J = 7.5, 7.5 Hz, H5), 6.98 (1H, s, H4'), 7.06 (1H, dd, J = 7.5, 7.5 Hz, H8'), 7.22 (1H, dd, J = 8.0, 8.0 Hz, H7'), 7.37 (1H, d, J = 8.5 Hz, H6'), 7.45 (1H, dd, J = 7.5, 8.0 Hz, H6), 7.53 (1H, d, J = 8.5 Hz, H9'), 7.63 (1H, d, J = 7.5 Hz, H4). ^{13}C NMR (CDCl$_3$) δ 19.6 (C2'''-$\underline{\text{C}}$H$_3$), 20.2 (C2"-$\underline{\text{C}}$H$_3$), 20.3 (C3'-$\underline{\text{C}}$H$_3$), 37.6 (C2"), 50.5 (C3"), 67.2 (C2), 77.6 (C3'''), 109.1 (C6'), 109.6 (C7), 110.7 (C1'''), 112.7 (C1"), 114.9 (C3'), 116.5 (C4'), 117.7 (C5), 118.3 (C9'a), 119.0 (C9'), 119.2 (C10'a), 120.1 (C8'), 121.3 (C5'a), 123.0 (C7'), 125.2 (C4), 131.9 (C10'), 135.7 (C3a), 137.9 (C6), 141.5 (C2"), 141.7 (C2'''), 160.2 (C1a), 201.0 (C3). MS (EI), m/z 424 (22%, M$^+$), 369 (100%). HRMS (EI, M$^+$) calcd for C$_{28}$H$_{28}$N$_2$O$_2$ 424.2151, found 424.2146.

7.1.2.3   Reaction of Indigo with 1-bromo-2-butene

Method A: 5 sec reaction

(*E*)-1-((*E*)-But-2-en-1-yl)-[2,2'-biindolinylidene]-3,3'-dione (245)
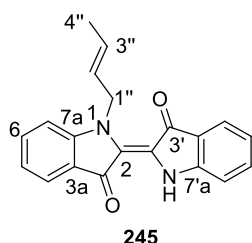
Using Method A, indigo (262 mg, 1.00 mmol) and (*E*)-1-bromobut-2-ene (670 mg, 5 mmol) were reacted at 85-88 ºC for 5 sec. The reaction mix was poured into an ice bath and the dark navy or black precipitate was collected and dissolved in hot CH$_2$Cl$_2$ and cooled at 5 °C overnight. The mixture was then filtered to remove the unreacted indigo (30%). The filtrate was concentrated under reduced pressure then dissolved in hot MeOH/H$_2$O (1:3) and cooled to precipitate **245** (180 mg, 57%) as a dark navy powder, mp. 161-163 ºC. R_f = 0.70 (CH$_2$Cl$_2$:pet. spirit; 7:3). UV−Vis

(CH$_2$Cl$_2$) λ$_{max}$/nm (ε, M^{-1}cm^{-1}) 291 (28583), 632 (16946). IR υ$_{max}$ 3244 (m), 1631(s),

1608 (s), 1465 (s), 1446 (m), 1330 (s), 1180 (s), 1111 (s), 964 (m), 748 (s) cm^{-1}. ^{1}H

NMR (CDCl$_3$) δ 1.62 (3H, d, J = 6.1 Hz, C4'-CH$_3$), 5.06 (2H, d, J = 5.0 Hz, H1''), 5.53-

5.58 (1H, m, H2'') 5.62-5.65 (1H, m, H3''), 6.97 (1H, t, J = 7.5, Hz, H5'), 7.01-7.05 (2H,

m, H7, H5), 7.13 (1H, d, J = 8.0 Hz, H7'), 7.48 (1H, t, J = 7.6 Hz, H6'), 7.54 (1H, t, J =

7.7 Hz, H6), 7.70 (1H, d, J = 7.7 Hz, H4), 7.75 (1H, d, J = 7.6 Hz, H4'), 10.57 (1H, s,

NH). ^{13}C NMR ((CD$_3$)$_2$SO) δ 18.3 (C4''), 49.2 (C1''), 113.0 (C7), 114.1 (C5'), 120.1

(C3'a), 120.6 (C7'), 121.7 (C3a), 121.9 (C5), 123.4 (C2), 124.3 (C4), 124.8 (C4'), 125.2

(C2'), 126.8 (C2''), 129.3 (C3''), 136.8 (C6), 136.9 (C6'), 152.8 (C7a), 153.7 (C7'a),

187.3 (C3'), 189.6 (C3). MS (EI): m/z = 316 (70%, M$^+$), 301 (52), 261 (24), 233 (72),

195 (100), HRMS (ESI): calcd. for C$_{20}$H$_{17}$N$_2$O$_2$ [M+H]$^+$ 317.1290; found 317.1301.

(*E*)-13-(But-2-en-1-yl)-8a-hydroxy-8-methyl-8,13a-dihydroazepino[1,2-*a*:3,4-*b*']diindol-14(8*H*)one (250)
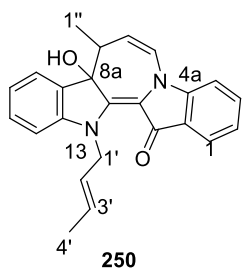
The mother liquor was dried (Na$_2$SO$_4$), concentrated and then subjected to a PTLC plate and developed with CH$_2$Cl$_2$/EtOAc; 9.5:0.5. The selected band was collected and soaked in EtOAc and filtered. The filtrate was concentrated to afford **250** as a red powder (37.0 mg, 10%); mp. 148-150 ℃, R_f = 0.15

(CH$_2$Cl$_2$/EtOAc; 9.5:0.5). UV−Vis (CH$_2$Cl$_2$) λ$_{max}$/nm (ε, M^{-1}cm^{-1}) 306 (13821), 367

(11872), 494 (14637). IR υ$_{max}$ 3278 (b), 1643 (s), 1608 (s), 1465 (s), 1388 (m), 1296

(m), 1168 (m), 1056 (m), 1018 (s), 918 (w), 752 (m) cm^{-1}. ^{1}H NMR (CDCl$_3$) δ 0.67

(3H, d, J = 7.1 Hz, H1''), 1.61 (3H, d, J = 6.1 Hz, H4'), 3.07 (1H, p, J = 7.1 Hz, H8),

3.85 (1H, s, OH), 4.54 (1H, dd, J = 7.7, 5.0 Hz, H1'a), 5.02 (1H, d, J = 7.7 Hz, H1'b),

5.06-5.09 (1H, m, H7), 5.54-5.59 (1H, m, H2'), 5.67-5.74 (1H, m, H3'), 6.87 (1H, d, J =

10.2 Hz, H6), 6.93 (1H, t, J = 7.6 Hz, H2), 7.00 (1H, d, J = 7.6 Hz, H12), 7.10 (1H, t, J

= 7.5 Hz, H4) 7.14 (1H, d, J = 8.1 Hz, H10), 7.30-7.40 (1H, t, J = 7.7 Hz, H3), 7.38 (2H, m, H1, H11), 7.62 (1H, d, J = 7.5 Hz, H9). ^{13}C NMR (CDCl$_3$) δ 17.6 (C1"), 18.7 (C4'), 43.9 (C8), 51.7 (C1'), 84.3 (C8a), 109.4 (C4), 110.0 (C7), 110.1 (C12), 117.4 (C13b), 120.1 (C2), 122.1 (C6) 122.2 (C14a), 122.6 (C9), 123.0 (C10), 123.7 (C1), 123.8 (C13a), 126.3 (C2'), 129.8 (C11), 130.2 (C3'), 133.0 (C3), 133.3 (C8b), 146.1 (C12a), 152.3 (C4a), 178.7 (C14). MS (EI): m/z = 370 (48%, M$^+$), 327 (100), 315 (47), 299 (78), 285 (75), 272 (68). HRMS (ESI): calcd for C$_{24}$H$_{23}$N$_2$O$_2$ [M+H]$^+$ 371.1760; found 371.1747.

Method B: 1 h reaction

(E)-13-(But-2-en-1-yl)-8a-hydroxy-8-methyl-8,13a-dihydroazepino[1,2-a:3,4-b']diindol-14(8H)-one (250)

Using Method B, indigo (262 mg, 1.00 mmol) and (E)-1-bromobut-2-ene (670 mg, 5 mmol) were reacted at 85 ℃. Upon workup, the filtrate was concentrated affording a red powder, which was recrystallized from CH$_2$Cl$_2$ to give **250** as red needle crystals (51.8 mg, 14%).

Two other products were isolated by treatment of the silica washings (see method **B**), as compound **245** (31.6 mg, 10%) and compound **229** (135.7 mg, 32%) with identical spectral characteristics as reported above.

Method C: 3 h reaction

2'-Methyl-1-[1-(but-2-enyl)]-10'-[1-(but-2-enyl)]oxy-2'H-spiro(indoline-2,1'-pyrido[1,2-a]indol)-3-one (229)

Using Method C, indigo (262 mg, 1.00 mmol) and (*E*)-1-bromobut-2-ene (670 mg, 5
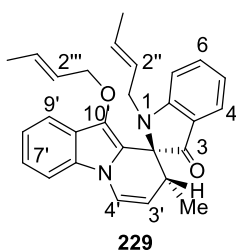
mmol) were reacted at 85-88 ℃. The resulting brown orange

residue was recrystallised from CH_2Cl_2/pet. spirit to give 2'-methyl-

1-[1-(but-2-enyl)]-10'-[1-(but-2-enyl)]oxy-2'*H*-spiro(indoline-2,1'-

pyrido[1,2-*a*]indol)-3-one **229** (169 mg, 40%) as yellow crystals,

mp. 147-148 ℃. R_f = 0.51 (CH_2Cl_2/pet. spirit; 7:3). The X-ray quality crystals were

grown through slow crystallization from pet. spirit : EtOAc (8:2). The mother liquor

was concentrated and subjected to a 30×1.5 cm column of silica gel chromatography

and resulted in separation of an additional 106 mg of **229** (25%); total yield = 65%. IR

(neat) υ_{max} 1689 (m), 1608 (m), 1485 (s), 1468 (m), 1250 (m), 1055 (m) cm^{-1}. ^{1}H NMR

(CDCl$_3$) δ 1.07 (3H, d, *J* = 7.5 Hz, C2'-CH$_3$), 1.55 (3H, d, *J* = 6.5 Hz, H4'''), 1.70 (3H,

d, *J* = 6.0 Hz, H4''), 3.12-3.15 (1H, m, H2'), 3.67 (1H, m, *J* = 7.0, 7.0 Hz, H1''a), 3.94

(1H, dd, *J* = 5.0, 4.5 Hz, H1'''a), 4.10-4.17 (2H, m, H1'''b, H1''b), 5.08-5.12 (1H, m,

H3'''), 5.16 (1H, dd, *J* = 1.5, 2.0 Hz, H3'), 5.27-5.35 (1H, m, H2'''), 5.52-5.58 (1H, m,

H2''), 5.72-5.78 (1H, m, H3''), 6.72 (1H, appt t, *J* = 7.5, 7.5 Hz, H5), 6.87 (1H, d, *J* = 8.5

Hz, H9'), 7.04-7.07 (2H, m, H4', H7), 7.20 (1H, m, H7'), 7.34 (1H, d, *J* = 8.5 Hz, H8'),

7.45-7.50 (2H, m, H8', H6), 7.52 (1H, d, *J* = 7.5, H4). ^{13}C NMR (CDCl$_3$) δ 14.1 (C2'-

CH$_3$), 17.9 (C4'''), 18.0 (C4''), 33.6 (C5'), 46.2 (C1''), 72.8 (C2), 75.1 (C1'''), 109.2 (C9'),

109.3 (C8'), 110.1 (C3'), 117.3 (C5), 118.1 (C9'a), 118.7 (C8'), 119.4 (C10'a), 120.4

(C4'), 120.5 (C7), 122.2 (C5'a), 123.5 (C7'), 125.1 (C4), 126.6 (C3'''), 127.85 (C3''),

127.90 (C2''), 130.9 (C2''), 133.0 (C10'), 136.7 (C3a), 137.5 (C6), 162.2 (C1a), 197.9

(C3). MS (EI), *m/z* 424 (20%, M$^+$), HRMS (ESI, M$^+$) calcd for C$_{28}$H$_{29}$N$_2$O$_2$ 425.2231,

found 425.2229.

7.1.2.4 Reaction of Indigo with 1-bromo-3-methyl-2-butene

Method A: 5 sec reaction

(E)-1-(3-Methylbut-2-en-1-yl)-[2,2'-biindolinylidene]-3,3'-dione (246)
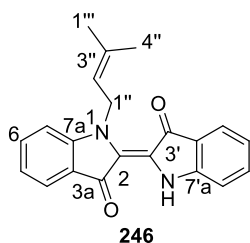
Using Method A, indigo (262 mg, 1.00 mmol) and 1-bromo-3-methylbut-2-ene (810 mg, 5 mmol) were reacted at 85 °C. The reaction mix was poured into an ice bath and the dark navy or black precipitate were collected and dissolved in hot CH_2Cl_2 and cooled at 5 °C overnight. The mixture was then filtered to remove the unreacted indigo (41%). The filtrate was concentrated under reduced pressure then dissolved in hot MeOH/H_2O (1:3) and cooled to precipitate **246** (122 mg, 37%) as a dark navy powder, mp. 98-101 °C, R_f = 0.72 (CH_2Cl_2/pet. spirit; 7:3). UV-Vis (CH_2Cl_2) λmax/nm (ε, $M^{-1}cm^{-1}$) 292 (27415), 639 (16308), 494 (14637). IR υmax 3267 (s), 1627 (s), 1612 (s), 1481 (s), 1462 (s), 1392 (m), 1171 (m), 1130 (m), 1072 (s), 752 (m) cm^{-1}. ^{1}H NMR (CDCl$_3$) δ 1.68 (3H, s, H4"), 1.78 (3H, s, H1'''), 5.12 (2H, bs, H1"), 5.16 (1H, d, J = 4.0 Hz, H2"), 6.94 (1H, t, J = 7.3 Hz, H5'), 6.99-7.02 (2H, m, H7, H7') 7.04 (1H, d, J = 7.9 Hz, H5), 7.45 (1H, t, J = 6.5 Hz, H6'), 7.52 (1H, t, J = 6.5 Hz, H6), 7.68 (1H, d, J = 7.3 Hz, H4), 7.72 (1H, d, J = 7.3 Hz, H4') 10.82 (1H, s, NH). ^{13}C NMR (CDCl$_3$) δ 18.4 (C1'''), 18.9 (C4"), 45.6 (C1"), 112.6 (C7), 113.6 (C5'), 116.4 (C3'a), 119.7 (C7'), 120.3 (C3a), 120.9 (C5), 121.5 (C2), 121.6 (C4), 123.3 (C4'), 123.8 (C2'), 124.3 (C2"), 124.6 (C3"), 136.4 (C6), 136.5 (C6'), 152.4 (C7a), 153.6 (C7'a), 186.6 (C3'), 189.0 (C3). MS (EI): m/z = 330 (20%, M$^+$), 315 (35), 262 (100). HRMS (ESI): calcd for $C_{21}H_{19}N_2O_2$ [M+H]$^+$ 331.1447; found 331.1453. The mother liquor was then dried (Na$_2$SO$_4$), concentrated under reduced pressure and subjected to silica gel column chromatography.

8,8-Dimethyl-13-(3-methylbut-2-en-1-yl)-7,8-dihydro-6H-6,13a-

epoxyazepino[1,2-a:3,4-b']diindol-14(8H)-one (253)
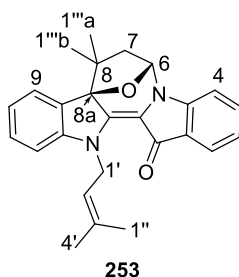
Elution with CH$_2$Cl$_2$/EtOAc; 9.5:0.5 afforded **253** (83.6 mg, 21%) as a red powder; mp. 74-76 ºC, R_f = 0.66 (CH$_2$Cl$_2$/EtOAc (9.5:0.5). UV‑Vis (CH$_2$Cl$_2$) λ_{max}/nm (ε, M^{-1}cm^{-1}) 261 (14848), 311 (7945), 364 (9730), 497 (9114), 528 (12003). IR (neat) υ_{max} 3282 (bm), 1662 (s), 1616 (s), 1562 (s), 1404 (m), 1107 (s), 744 (s) cm^{-1}. ^{1}H NMR (CDCl$_3$) δ 1.08 (3H, s, H1'''b), 1.15 (3H,s, H1'''a), 1.71 (3H, s, H1''), 1.85 (s, 3H, H4'), 2.07 (1H, d, J = 12.7 Hz, H7a), 2.36 (1H, dd, J = 12.6, 5.9 Hz, H7b), 4.94 (1H, dd, J = 15.7, 5.5 Hz, H1'a), 5.28 (1H, bt, J = 5.4 Hz[***], H2'), 5.80 (1H, dd, J = 15.7, 6.7 Hz, H1'a), 6.02 (1H, d, J = 5.7 Hz, H6), 6.79-6.82 (2H, m, H12, H2), 6.87 (1H, d, J = 8.3 Hz, H4), 6.98 (1H, t, J = 7.5 Hz, H10), 7.29-7.39 (3H, m, H9, H11, H3), 7.73 (1H, d, J = 7.7 Hz, H1). ^{13}C NMR (CDCl$_3$) δ 18.3 (C4'-$\underline{C}$H$_3$), 23.6 (C1'''b), 25.7 (C1''), 29.2 (C1'''a), 46.4 (C1'), 49.7 (C8), 49.9 (C7), 83.0 (C6), 92.7 (C8a), 108.2 (C4), 109.9 (C12), 111.2 (C13b), 117.4 (C2), 119.9 (C2'), 121.1 (C10), 122.1 (C14a), 124.4 (C1), 125.4 (C8b), 126.3 (C11), 130.4 (C9), 133.3 (C3), 135.3 (C3'), 145.8 (C4a), 147.3 (C12a), 149.3 (C13a), 177.5 (C14). MS (EI): m/z = 398 (100% M$^+$), 342 (63), 329 (50), 274 (78). HRMS (ESI): calcd for C$_{26}$H$_{27}$N$_2$O$_2$ [M+H]$^+$ 399.2073; found 399.2085.

Method B: 1 h reaction

8a-Hydroxy-8,8-dimethyl-8,13a-dihydroazepino[1,2-a:3,4-b']diindol-

14(8H)one (251)

Using Method B, indigo (262 mg, 1.00 mmol) and 1-bromo-3-methylbut-2-ene (810 mg, 5 mmol) were reacted at 85 ºC. Upon workup, the filtrate was concentrated

---

[***] gCOSY and HMBC confirms the assignment.
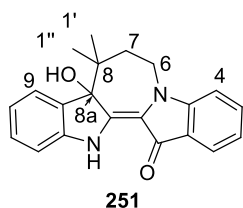
affording a red powder which was recrystallized from pet. spirit/EtOAc (9:1) to deposit orange red crystals of **251** (105 mg, 32%); mp 190-192 ºC, R_f = 0.44 (CH$_2$Cl$_2$/EtOAc; 9.5:0.5).

X-ray quality crystals were grown through slow crystallization from pet. spirit/EtOAc (9:1). UV-Vis (CH$_2$Cl$_2$) λ_{max}/nm (ε, M^{-1}cm^{-1}) 288 (16535), 301 (16077), 371 (13040), 490 (15245). IR υ_{max} 3282 (bs), 1662 (s), 1616 (s), 1562 (s), 1404 (m), 1107 (s), 744 (s) cm^{-1}. ^{1}H NMR (CDCl$_3$) δ 0.80 (3H, s, H1'), 1.63 (3H, s, H1"), 4.82 (1H, d, J = 10.1 Hz, H7), 6.83 (1H, d, J = 10.1 Hz, H6), 6.96 (1H, d, J = 7.9 Hz, H12), 7.01 (2H, t, J = 7.2 Hz, H2, H10), 7.20 (1H, d, J = 8.3 Hz, H4), 7.30 (1H, t, J = 7.9 Hz, H11), 7.40 (1H, t, J = 8.3, H3), 7.60 (1H, d, J = 7.5 Hz, H9), 7.77 (1H, d, J = 7.5 Hz, H1). ^{13}C NMR (CDCl$_3$) δ 26.7 (C1'b), 27.3 (C1'a), 44.3 (C8), 85.8 (C8a), 109.5 (C4), 110.9 (C12), 111.5 (C7), 114.1 (C13b), 120.6 (C6), 120.8 (C2), 121.7 (C10), 122.8 (C14a), 123.7 (C1), 126.6 (C9), 129.6 (C8b), 130.4 (C11), 133.8 (C3), 144.2 (C12a), 146.0 (C4a), 149.5 (C13a), 182.1 (C14). MS (EI): m/z = 330 (75%, M$^+$), 315 (100), 262 (93), HRMS (ESI): calcd for C$_{21}$H$_{19}$N$_2$O$_2$ [M+H]$^+$ 331.1447; found 331.1438.

2',2'-Dimethyl-1-(3-methylbut-2-en-1-yl)-10'-((3-methylbut-2-en-1-yl)oxy)-2'H-spiro[indoline-2,1'-pyrido[1,2-a]indol]-3-one (230)
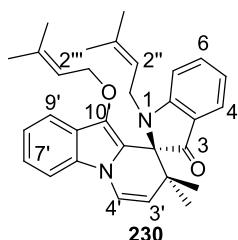
The mother liquor and filtrate from the elution of the silica with CH$_2$Cl$_2$ were combined and subjected to 40 × 1.5 cm silica gel column chromatography. Elution with CH$_2$Cl$_2$/pet. spirit; 9:1, yielded **230** (56 mg, 21%) as a yellow amorphous solid; R_f = 0.96 (CH$_2$Cl$_2$: pet. spirit; 9:1). IR υ_{max} 1701 (m), 1612 (m), 1465 (m), 1261 (m), 1095 (s), 802 (s), 742 (m) cm^{-1}. ^{1}H NMR (CDCl$_3$) δ 1.14 (3H, s, C3"-CH$_3$), 1.22 (3H, s, CH"), 1.42 (3H, s, C3'''-CH$_3$), 1.50 (3H, s, C2'-(CH$_3$)), 1.52 (3H, s, C2'-(CH$_3$)), 1.63 (3H, s,

H4'''), 3.87-3.90 (1H, m, H1''a), 4.06-4.15 (2H, m, H1''b, H1'''a), 4.30-4.33 (1H, m, H1'''b), 5.02 (1H, bs, H2''), 5.08 (1H, t, J = 7.1 Hz, H2'''), 5.21 (1H, d, J = 7.7 Hz, H3'), 6.72 (2H, m, H5, H7), 7.00 (1H, d, J = 7.7 Hz, H4'), 7.06 (1H, t, J = 7.4 Hz, H8'), 7.20 (1H, t, J = 8.2 Hz, H7'), 7.33 (1H, d, J = 8.3 Hz, H6'), 7.40 (1H, t, J = 7.4 Hz, H6), 7.51 (1H, d, J = 7.8 Hz, H9'), 7.58 (1H, d, J = 7.7 Hz, H4). ^{13}C NMR (CDCl$_3$) δ 18.1 (C2'-$\underline{C}$H$_3$a), 18.2 (C2'-$\underline{C}$H$_3$b), 23.8 (C4'''), 24.2 (C3'''), 25.5 (C4''), 26.0 (C3''), 39.4 (C2'), 44.2 (C1''), 71.0 (C1'''), 72.4 (C2), 108.6 (C6'), 109.2 (C5), 117.2 (C7), 117.9 (C2'''), 118.9 (C9'), 119.3 (C3'), 119.4 (C10'), 120.3 (C8'), 120.8 (C4'), 120.9 (C3a), 121.7 (C2''), 122.4 (C10'a), 123.2 (C7'), 124.7 (C4), 132.1 (C9'a), 133.2 (C5'a), 137.3 (C3'''), 137.4 (C6), 137.9 (C3''), 161.3 (C7a), 199.1 (C3). MS (EI): m/z = 466 (12%, M$^+$), 397 (79), 329 (100), HRMS (ESI): calcd for C$_{31}$H$_{35}$N$_2$O$_2$ [M+H]$^+$ 467.2699; found 467.2708.

Further elution with CH$_2$Cl$_2$/EtOAc (95:5) gave **253** (103 mg, 26%).

Method C: 3 h reaction

8',8'-Dimethyl-1-(3-methylbut-2-en-1-yl)-10'-((3-methylbut-2-en-1-yl)oxy)-8'H-spiro[indoline-2,9'-pyrido[1,2-a]indol]-3-one (230)

Using Method C, indigo (262 mg, 1.00 mmol) and 1-bromo-3-methylbut-2-ene (810 mg, 5 mmol) were reacted at 85 ℃ for 3 h. The filtrate was subjected to flash silica gel column chromatography and elution with CH$_2$Cl$_2$/pet. spirit (9:1) yielded **230** (195 mg, 42%) as a yellow amorphous solid. Further elution with CH$_2$Cl$_2$/EtOAc (95:5) gave **253** (103 mg, 26%).

7.1.2.5 Reaction of indigo with 3-bromo-1-phenyl-1-propene

Method A: 5 sec reaction

(2*E*)-1-(3-Phenylallyl)-[2,2'-biindolinylidene]-3,3'-dione (247)
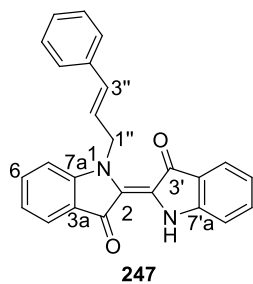
Using Method A, indigo (262 mg, 1.00 mmol) and cinnamyl bromide (980 mg, 5 mmol) were reacted at 85 °C for 5 sec. The reaction was poured into an ice bath and the black precipitate was collected and dissolved in hot CH_2Cl_2 and was cooled at 5 °C overnight. The mixture was then filtered to remove the unreacted indigo (38%). The filtrate was concentrated under reduced pressure and recrystallised from pet. spirit/CH_2Cl_2 (90:10) to furnish **247** (181 mg, 48%) as a navy powder, mp. 192-194 °C, R_f = 0.72 (CH_2Cl_2/pet. spirit; 7:3). UV-Vis (CH_2Cl_2) λ_{max}/nm (ε, $M^{-1}cm^{-1}$) 291 (28197), 628 (15596). IR υ_{max} 3259 (m), 1685 (w), 1639 (s), 1608 (s), 1465 (s), 1388 (s), 1296 (m), 1068 (s), 1018 (s), 918 (m), 748 (s) cm^{-1}. ^{1}H NMR (CDCl$_3$) δ 5.28 (2H, t, *J* = 5.3 Hz, H1"), 6.24-6.30 (1H, m, H2"), 6.48 (1H, d, *J* = 16.1 Hz, H3"), 6.91 (1H, t, *J* = 7.4 Hz, H5), 6.96 (1H, d, *J* = 8.0 Hz, H7), 7.00 (1H, d, *J* = 7.9 Hz, H6), 7.15 (2H, appt t, *J* = 8.2, 7.5 Hz, H7', ArH), 7.21-7.29 (4H, m, ArH), 7.42 (1H, t, *J* = 7.4 Hz, H5'), 7.50 (1H, t, *J* = 7.5 Hz, H6'), 7.65 (1H, d, *J* = 7.7 Hz, H4), 7.73 (1H, d, *J* = 7.7 Hz, H4') 10.70 (1H, s, NH). ^{13}C NMR (CDCl$_3$) δ 49.4 (C1"), 111.2 (C7), 111.9 (C5'), 120.1 (C2), 120.7 (C3"), 120.9 (C7'), 121.1 (C2'), 122.8 (C3a), (ArC), 124.1 (C4'), 124.6 (C5), 124.8 (C4), 125.8 (C3'a), 126.45 (2 × ArC), 127.7 (ArC), 128.5 (2 × ArC), 132.4 (C2"), 135.9 (C6), 136.1 (C6'), 136.4 (ArC), 151.5 (C7a), 152.8 (C7'a), 193.1 (C3'), 196.4 (C3). MS (EI): *m/z* = 378 (100%, M$^+$), HRMS (ESI): calcd for $C_{25}H_{19}N_2O_2$ [M+H]$^+$ 379.1447; found 379.1444.

Method B: 1 h reaction

(8'*R*)-9a'-Cinnamyl-8'-phenyl-8'*H*-spiro[indoline-2,9'-pyrido[1,2-*a*]indole]-3,10'(9a'*H*)-dione (254)
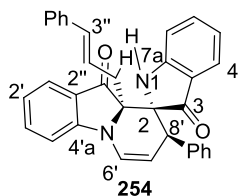
Using Method B, indigo (262 mg, 1.00 mmol) and cinnamyl bromide (980 mg, 5.00 mmol) were reacted at 85 ºC for 1 h. Upon workup, the residue was subjected to a silica gel column chromatography. Elution with CH_2Cl_2/pet. spirit (9:1) yielded a yellow fraction which was concentrated. The residue was dissolved in a minimum volume of CH_2Cl_2 (5-6 mL) and pet. spirit (5-7 mL) was then added dropwise until the solution turned cloudy. The solution was heated in a water-bath and when it became clear, was cooled down to precipitate **254** (79.4 mg, 16%) as a luminous yellow powder, mp. 269-271 ºC, R_f = 0.37 (CH_2Cl_2). X-ray quality crystals were obtained from a DMSO solution by evaporation under stream of N_2. UV−Vis (CH_2Cl_2) λ_{max}/nm (ε, $M^{-1}cm^{-1}$) 285 (15395), 392 (3647). IR (neat) υ_{max} 3356 (m), 3232 (m), 1693 (s), 1662 (s), 1612 (s), 1473 (s), 1233 (m), 752 (s) cm^{-1}. ^1H NMR (($CD_3)_2SO$) δ 2.98-3.10 (2H, m, H1"), 4.12 (1H, s, H8'), 4.98 (1H, d, *J* = 7.7 Hz, H7'), 5.70-5.76 (1H, m, H2"), 6.31 (1H, t, *J* = 7.2 Hz, H5), 6.43 (1H, d, *J* = 15.7 Hz, H3"), 6.73-6.76 (3H, m, H3', H6, H7), 6.99-7.07 (5H, m, Ar"H), 7.13 (1H, d, *J* = 6.9 Hz, H4), 7.02-7.23 (5H, m, Ar'H), 7.26 (1H, d, *J* = 7.7 Hz, H4'), 7.42 (2H, appt t, *J* = 6.4, 8.0 Hz, H6', H1'), 7.52 (1H, t, *J* = 7.4 Hz, H2'), 7.87 (1H, s, N<u>H</u>). ^{13}C NMR (($CD_3)_2SO$) δ 37.1 (C1'), 44.8 (C8'), 68.9 (C2), 69.9 (C9'a), 104.8 (C7'), 110.5 (C1'), 111.5 (C5), 117.0 (C3'), 119.6 (C7), 120.6 (C3a), 122.5 (C4'a), 122.7 (C6), 123.3 (C2'), 123.9 (C4'), 124.7 (C6'), 126.3 (3 × Ar"C), 127.3 (Ar"C), 127.7 (Ar"C), 128.0 (Ar'C), 129.0 (3 × Ar'C), 130.1 (Ar'C), 134.3 (C3"), 136.9 (C4), 137.2 (Ar'C), 137.7 (Ar"C), 138.1 (C2'), 157.2 (C10'a), 161.4 (C7a), 197.5 (C3),

197.8 (C10). MS (EI): m/z = 494 (22%, M$^+$), 377 (100). HRMS (ESI): calcd for

C$_{34}$H$_{27}$N$_2$O$_2$ [M+H]$^+$ 495.2073; found 495.2054.

2'-Phenyl-1-(3-phenylallyl)-10'-((3-phenylallyl)oxy)-2'H-spiro[indoline-2,1'-

pyrido[1,2-a]indol]-3-one (231)

Further elution, yielded **231** (165 mg, 37%) as a yellow crystalline solid mp. 92-93 ºC
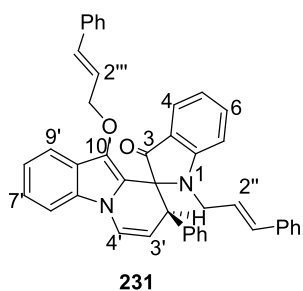
R_{f} = 0.64; IR (neat) $\upsilon_{\max}$ 1699 (m), 1613 (m), 1464 (s), 1349 (m), 1320 (m), 740 (m) cm^{-1}. ^{1}H NMR (CDCl$_3$) δ 3.86 (1H, dd, J = 6.5, 6.5 Hz, H1'''a), 4.33-4.47 (4H, m, H1'''b, H2', H1''a, H1''b), 5.44 (1H, dd, J = 2.0, 2.0 Hz, H3'), 5.81-5.87 (1H, m, H2'''), 6.21 (1H, d, J = 15.5 Hz,

H3'''), 6.55-6.59 (1H, m, H2''), 6.81 (1H, d, J = 15.4 Hz, H3''), 7.10-7.16 (4H, m, H8',

H9', H5, H6), 7.21-7.32 (12H, m, H7', H4', 5 × ArH''', 5 × ArH''), 7.38 (1H, d, J = 7.5

Hz, H7), 7.44 (1H, d, J = 8.5 Hz, H6'), 7.56 (1H, d, J = 7.5 Hz, H4). ^{13}C NMR (CDCl$_3$)

δ 45.4 (C2'), 47.2 (C3''), 73.5 (C2), 74.7 (C6), 108.9 (ArC), 109.2 (C3'), 109.4 (C6'),

117.6 (C2''), 118.6 (C4), 119.5 and 120.6 (ArC), 121.3 (C4'), 122.0 and 123.6 (ArC),

124.5 (C2'''), 124.8, 126.3, 126.62, 126.64, 127.3, 127.6, 127.71, 127.77, 127.84, 128.2,

128.37, 128.41 and 128.44 (ArC), 128.6 (C1''), 129.0, 130.2, 130.38, 130.43 (H7),

131.6, 132.1, 132.9 (ArC), 133.2 (C1'''), 136.4, 136.6 and 137.2 (ArC), 137.7 (C3a),

161.6 (C7a), 197.5 (C3). MS (EI), m/z 310 (12%, M$^+$), 493 (100%, M -117).

Method C: 3 h reaction

8'-Phenyl-1-(3-phenylallyl)-10'-((3-phenylallyl)oxy)-8'H-spiro[indoline-2,9'-

pyrido[1,2-a]indol]-3-one (231)

Using Method C, indigo (262 mg, 1.00 mmol) and 3-bromo-1-phenyl-1-propene

(cinnamyl bromide) (980 mg, 5.00 mmol) were reacted at 85 ºC for 3 h The

concentrated filtrate was subjected to a flash silica gel column chromatography and elution with CH_2Cl_2/pet. spirit (9:1) yielded **231** (226 mg, 37%) as a yellow crystalline solid, with spectral values similar to those reported above.

7.1.2.6 Reaction of indigo with 3-bromocyclohexene

(*E*)-1-(Cyclohex-2-en-1-yl)-[2,2'-biindolinylidene]-3,3'-dione (258)

258
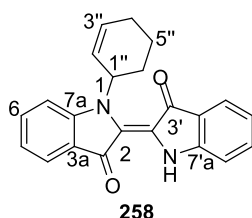
Using Method A, indigo (262 mg, 1.00 mmol) and 3-bromocyclohexene (795 mg, 5.00 mmol) were reacted at 85 ℃ for 5 sec. The reaction was poured into an ice bath and the dark navy precipitate were collected and dissolved in hot CH_2Cl_2 and cooled at 5 °C overnight. The mixture was then filtered to remove the unreacted indigo (38%). The filtrate was concentrated under reduced pressure then dissolved in hot MeOH/H_2O (1:3) and cooled to precipitate **255** (174 mg, 51%) as a dark navy powder, mp. 149-151 ℃, R_f = 0.74 (CH_2Cl_2 : pet. spirit; 7:3). UV−Vis (CH_2Cl_2) λ_{max}/nm (ε, $M^{-1}cm^{-1}$) 249 (135732), 368 (58341). IR (neat) υ_{max} 3278 (bm), 1643 (s), 1462 (s), 1319 (m), 1068 (s), 1045 (s), 748 (s) cm^{-1}. ^{1}H NMR ($CDCl_3$) δ 1.60-2.17 (6H, m, H4", H5", H6"), 5.84 (1H, d, J = 5.9 Hz, H1"), 5.96 (1H, bs, H2"), 6.91-7.01 (3H, m, H3", H7, H5), 7.33 (1H, d, J = 7.4 Hz, H7'), 7.41-7.48 (3H, m, H6', H6, H4), 7.70 (2H, d, J = 7.5 Hz, H4', H5'), 10.73 (1H, s, N<u>H</u>). ^{13}C NMR ($CDCl_3$) δ 22.3 (C4"), 24.9 (C5"), 27.8 (C6"), 57.5 (C1"), 112.0 (C7), 112.1 (C5'), 114.8 (C2"), 120.7 (C3'a), 120.8 (C7'), 120.9 (C5), 124.1 (C3a), 124.4 (C2), 124.8 (C4'), 125.1 (C4), 130.1 (C2'), 135.4 (C2"), 136.0 (C6), 136.3 (C6'), 151.5 (C7a), 151.9 (C7'a), 187.3 (C3'), 190.3 (C3). MS (EI): *m/z* = 342 (43%, M$^+$), 262 (100). HRMS (ESI): calcd for $C_{22}H_{19}N_2O_2$ [M+H]$^+$ 343.1465; found 343.1462.

Optimised procedure of production of monoallylated indigos (243–245)

A suspension of indigo (262 mg 1.00 mmol) in anhydrous DMF (40 mL) was sonicated for 30 min and the resulting suspension was transferred to a septum equipped round bottom flask carrying pre-dried Cs_2CO_3 (1.303 g, 4.00 mmol) under a N_2 flow. The flask was plunged into a preheated oil bath at 85–88 °C and stirred for 1 h. The N_2 flow was stopped and allylic bromide (5.00 mmol) was added rapidly in one portion by syringe, and after 5 s, the reaction mixture was poured into an ice bath. The blue-black precipitate was filtered and dissolved in hot CH_2Cl_2 and cooled at 5 °C overnight. The mixture was then filtered to remove the unreacted indigo (10% >). The filtrate was concentrated under reduced pressure then recrystallised from pet. spirit/EtOAc (90:10) to furnish the monoallylated indigos **243–245** in 83%, 81% and 89% yields, respectively.

Reaction of 13-allyl-8a-hydroxy-8,13a-dihydroazepino[1,2-*a*:3,4-*b*']diindol-14(8*H*)-one (248) with Cs₂CO₃

A solution of **248** (34.2 mg, 0.100 mmol) in DMF (8 mL) was transferred to a septum-equipped round-bottom flask containing pre-dried Cs_2CO_3 (0.200 mmol) under an inert atmosphere. The mixture was heated and stirred for 20 min and then was poured into an ice bath. The cloudy solution was partitioned in CH_2Cl_2 and the combined organic layers were washed with brine (2 × 30 mL) and water (5 × 50 mL), dried (Na_2SO_4) and concentrated under reduced pressure. The residue was subjected to PTLC and elution with pet. spirit/CH_2Cl_2 (1:3) yielded 8*H*,16*H*-pyrido[1,2,3-*s,t*]-indolo[1,2-*a*]azepino[3,4-*b*]indol-17-one **232** (28.6 mg, 89%) as a yellow-brown powder; mp 143-144 °C.

Allylation of (*E*)-1-allyl-[2,2'-biindolinylidene]-3,3'-dione (243)

A solution of **243** (30.2 mg, 0.100 mmol) in DMF (8 mL) was transferred to a septum-equipped round flask containing 4 Å molecular sieves, pre-dried Cs_2CO_3 (0.200 mmol) and allyl bromide (53.6 mg, 0.400 mmol) in DMF (2 mL) under an inert atmosphere. The mixture was heated and stirred for 3 h. The reaction mixture was then filtered into an ice bath. The cloudy solution was partitioned in CH_2Cl_2 (*ca* 10 mL) and the combined organic layers washed with brine (2 × 30 mL) and water (5 × 50 mL), dried (Na_2SO_4) and concentrated under the reduced pressure. The filtrate was subjected to PTLC and elution with pet. spirit/CH_2Cl_2 (1:3) yielded 8*H*,16*H*-pyrido[1,2,3-*s,t*]-indolo[1,2-*a*]azepino[3,4-*b*]indol-17-one **232** (19.1 mg, 59%) as a yellow-brown powder; mp 143-144 °C. X-ray quality crystals were grown through the slow crystallisation from pet. spirit : CH_2Cl_2 (5:3). R_f = 0.61. Results from spectral analysis of the purified compound were compatible with the reported literature values.[146] The other distinctive band was collected and soaked in EtOAc and yielded 1-allyl-10'-allyloxy-2'*H*-spiro(indoline-2,1'-pyrido[1,2-*a*]indol)-3-one **227** (2.30 mg, 8%) as an orange yellow solid; mp. 121-122 ºC. R_f = 0.51. The spectral information was compatible with literature reported values.[146]

(*E*)-1-Methyl-[2,2'-biindolinylidene]-3,3'-dione (255)
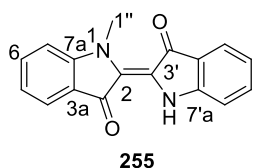
Using Method A, indigo (262 mg, 1.00 mmol) and methyl iodide (709 mg, 5 mmol) were reacted at 85 ºC for 5 sec. The reaction was poured into an ice bath and the black precipitate was collected and dissolved in hot CH_2Cl_2 and was cooled at 5 °C overnight. The mixture was then filtered to remove the unreacted indigo (8%). The filtrate was concentrated under

reduced pressure and recrystallised from pet. spirit/CH$_2$Cl$_2$ (90:10) to furnish **255** (213 mg, 77%) as a navy powder, mp. 167-169 ºC, R_f = 0.76 (CH$_2$Cl$_2$/pet. spirit; 7:3). IR υ_{max} 3260 (m), 1682 (w), 1641 (s), 1611 (s), 1473 (s), 1393 (s), 1295 (m), 1066 (s), 1013 (s), 923 (m), 737 (s) cm^{-1}. ^{1}H NMR (CDCl$_3$) δ 3.47 (3H, s, H1"), 6.78 (1H, t, J = 7.2 Hz, H5'), 6.82 (1H, d, J = 8.2 Hz, H7), 6.98 (1H, t, J = 7.2 Hz, H5), 7.18 (1H, d, J = 8.2 Hz, H7'), 7.28 (1H, t, J = 7.5 Hz, H6'), 7.38 (1H, t, J = 7.5 Hz, H6), 7.68 (1H, d, J = 7.3 Hz, H4), 7.79 (1H, d, J = 7.3 Hz, H4'), 9.47 (1H, s, NH). ^{13}C NMR (CDCl$_3$) δ 34.3 (C1"), 109.9 (C7), 113.6 (C7'), 122.6 (C5), 122.8 (C3'a), 124.4 (C3a), 124.8 (C4'), 125.1 (C5'), 127.7 (C4), 130.9 (C2), 131.0 (C6'), 132.5 (C6), 134.3 (C2'), 152.5 (C7a), 152.7 (C7'a), 186.3 (C3'), 188.6 (C3). MS (EI): m/z = 276 (78%, M$^+$), 261 (100). HRMS (ESI): calcd for C$_{17}$H$_{12}$N$_2$O$_2$ [M+H]$^+$ 277.0899; found 277.0911.

8a-Hydroxy-13-methyl-8a,13-dihydroazepino[1,2-*a*:3,4-*b'*]diindol-14(8*H*)-one (256)

256
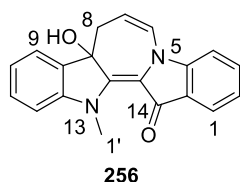
A solution of **255** (55.2 mg, 0.200 mmol) in DMF (10 mL) was transferred to a septum-equipped round flask containing 4 Å molecular sieves, pre-dried Cs$_2$CO$_3$ (0.400 mmol) and allyl bromide (107.2 mg, 0.800 mmol) in DMF (2 mL) under an inert atmosphere. The mixture was heated and stirred for 3 h. The reaction mixture was then filtered into an ice bath. The cloudy solution was partitioned in EtOAc (*ca* 10 mL) and the combined organic layers washed with brine (2 × 30 mL) and water (5 × 50 mL), dried (Na$_2$SO$_4$) and concentrated under the reduced pressure. The filtrate was dissolved in CH$_2$Cl$_2$ (2-3 mL). Dropwise addition of pet. spirit was continued to the stage in which the solution started to became cloudy. The solution was heated in water bath to achieve a clear solution. Then slow recrystallisation of this solution afforded the 8a-hydroxy-13-methyl-8a,13-dihydroazepino[1,2-*a*:3,4-*b'*]diindol-14(8*H*)-one **257** (49.9 mg, 79%) as a

ruby-red crystals; mp 143-145 °C. R_f = 0.19 (CH$_2$Cl$_2$/EtOAc; 9.5:0.5). IR (neat) υ_{max} 3277 (bm), 1611 (m), 1528 (s), 1476 (s), 1412 (m), 1310 (m), 1179 (m), 1101 (m), 743 (s) cm^{-1}. ^{1}H NMR (CDCl$_3$) δ 2.43 (1H, d, J = 2.8 Hz, H8a), 2.97 (1H, dd, J = 2.6, 17.3 Hz, H8b), 3.38 (s, 3H, H1'), 4.90-4.95 (1H, m, H7), 5.67 (1H, bs, OH), 6.76-6.85 (3H, m, H4, H6, H10), 7.01 (1H, t, J = 7.0 Hz, H11), 7.11 (1H, d, J = 7.1 Hz, H12), 7.22 (1H, t, J = 7.2 Hz, H3), 7.35 (1H, t, J = 7.4 Hz, H2), 7.43 (1H, d, J = 7.4 Hz, H9), 7.50 (1H, d, J = 7.5 Hz, H1). ^{13}C NMR (CDCl$_3$) δ 37.2 (C1'), 38.9 (C8), 81.1 (C8a), 101.5 (C7), 109.4 (C4), 114.6 (C7), 117.5 (C13b), 120.1 (C6), 122.6 (C14a), 123.0 (C12), 123.3 (C10), 123.4 (C9), 123.9 (C1), 130.8 (C11), 132.6 (C3), 133.4 (C8b), 135.3 (C13a), 145.7 (C12a), 156.2 (C4a), 178.1 (C14). MS (EI): m/z = 316 (89%, M$^+$), 301 (100), 284 (63). HRMS (ESI): calcd. for C$_{20}$H$_{16}$N$_2$O$_2$ [M+H]$^+$ 317.1212; found 317.1207.

(*E*)-10'-(But-2-en-1-yloxy)-1,8'-dimethyl-8'*H*-spiro[indoline-2,9'-pyrido[1,2-*a*]indole]-3-one (257)

257
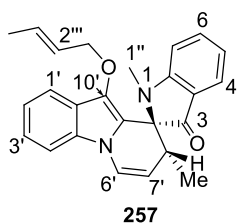
A solution of **255** (50 mg, 0.180 mmol) in DMF (10 mL) was transferred to a septum-equipped round flask containing 4 Å molecular sieves, pre-dried Cs$_2$CO$_3$ (0.400 mmol) and allyl bromide (107.0 mg, 0.800 mmol) in DMF (2 mL) under an inert atmosphere. The mixture was heated and stirred for 3 h. The reaction mixture was then filtered into an ice bath. The cloudy solution was partitioned in CH$_2$Cl$_2$ (*ca* 10 mL) and the combined organic layers washed with brine (2 × 30 mL) and water (5 × 50 mL), dried (Na$_2$SO$_4$) and concentrated under the reduced pressure. The filtrate was dissolved in CH$_2$Cl$_2$ (2-3 ml). Dropwise addition of pet. spirit was continued to the stage in which the solution started to became cloudy. The solution was heated in a water bath to

achieve a clear solution. Then slow recrystallisation of the solution yielded (*E*)-10'-(but-2-en-1-yloxy)-1,8'-dimethyl-8'*H*-spiro[indoline-2,9'-pyrido[1,2-*a*]indole]-3-one   **257** (60.0 mg, 78%) as a yellow-brown powder; mp 127-129 °C R_f = 0.53 (CH$_2$Cl$_2$/pet. spirit; 7:3). The X-ray quality crystals were grown through slow crystallization from pet. spirit : EtOAc (8:2). IR (neat) υ_{max} 1689 (m), 1608 (s), 1485 (s), 1468 (s), 1250 (m), 1055 (m) cm^{-1}. ^{1}H NMR (CDCl$_3$) δ 0.99 (3H, d, *J* = 7.4 Hz, C8'-CH$_3$), 1.53 (3H, d, *J* = 6.5 Hz, H4'''), 3.01 (3H, s, H1''), 3.11-3.14 (1H, m, H2'), 3.67 (1H, dd, *J* = 10.7, 6.9 Hz, H1'''a), 4.16 (1H, dd, *J* = 10.8, 6.7, H1'''b), 5.07-5.13 (1H, m, H3'''), 5.15 (1H, dd, *J* = 1.8, 7.0 Hz, H7'), 5.27-5.34 (1H, m, H2'''), 6.66 (1H, t, *J* = 7.4 Hz, H5), 6.81 (1H, d, *J* = 8.3 Hz H1'), 7.03-7.08 (2H, m, H6',H7), 7.18 (1H, t, *J* = 7.6 Hz, H6), 7.33 (1H, d, *J* = 8.3 Hz, H3'), 7.45-7.52 (2H, m, H4', H4). ^{13}C NMR (CDCl$_3$) δ 13.7 (C8'-$\underline{C}$H$_3$), 17.7 (C4'''), 28.4 (C1a), 32.7 (C8'), 69.6 (C2), 74.9 (C1'''), 108.1 (C4'), 109.0 (C2'), 109.7 (C7'), 116.9 (C5), 117.5 (C9'a), 118.4 (C1'), 119.1 (C10'a), 120.2 (C6'), 120.7 (C7), 122.1 (C4'a), 123.2 (C4), 124.9 (C3'''), 127.5 (C6), 130.5 (C2'''), 133.0 (C10'), 137.5 (C6), 137.7 (C3'a) 161.9 (C7a), 197.7 (C3). MS (EI), *m/z* 384 (28%, M$^+$), 329 (100), HRMS (ESI, M$^+$) calcd for C$_{25}$H$_{24}$N$_2$O$_2$ 385.1916, found 385.1904.

Diallyl (*E*)-3,3'-dioxo-[2,2'-biindolinylidene]-1,1'-dicarboxylate
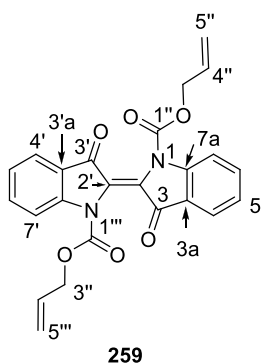
A suspension of indigo (262 mg, 1.00 mmol) in DMF was sonicated for 30 min at room temperature and transferred to a septum equipped round bottom flask containing pre-dried and ground Cs$_2$CO$_3$ (1.303 g, 4.00 mmol) and molecular sieves under an inert atmosphere. The flask was plunged to a pre-heated oil bath at 85-88 °C and stirred for 30 min. The inert atmosphere flow was then cut and allyl chloroformate (600 mg, 5.00 mmol) was added, which

turned the colour of the mixture from green blue to dark purple immediately after the addition. The mixture was stirred and heated for 3 h under a static inert atmosphere (N_2) and TLC analysis indicated the complete consumption of indigo. Molecular sieves were filtered from the hot reaction mixture and the filtrate poured into an ice bath and then partitioned in water and CH_2Cl_2 and washed with brine (2×30 mL) and water (5×50 mL) and the combined organic phases were dried (Na_2SO_4) and concentrated under reduced pressure. The residue was recrystallised from the mixture of pet. spirit/CH_2Cl_2 (8.5:1.5) and yielded **259** (374 mg, 87%) as a dark magenta crystals; mp 188-190 °C. X-ray quality crystals were grown through slow crystallization from pet. spirit : CH_2Cl_2 (5:3). R_f = 0.61; IR (neat) υ_{max} 1752 (s), 1639 (s), 1615 (s), 1457 (s), 1380 (m), 1059 (m), 1031 (s), 925 (m), 743 (m) cm^{-1}. ^{1}H NMR (CDCl$_3$) δ 4.86 (4H, s, H2", H2'''), 5.19 (2H, d, J = 10.4 Hz, H5"a, H5'''a), 5.30 (2H, d, J = 10.4 Hz, H5"b, H5'''b), 5.89-5.97 (2H, m, H4", H4'''), 7.18 (2H, t, J = 8.2 Hz, H5, H5'), 6.85 (2H, t, J = 7.8 Hz, H6, H6'), 7.71 (2H, d, J = 7.6 Hz, H7, H7'), 8.03 (2H, d, J = 8.2, H4, H4'). ^{13}C NMR (CDCl$_3$) δ 68.4 (2C, C2", C2'''), 116.5 (2C, C5", C5'''), 119.1 (2C, C2, C2'), 122.7 (2C, C3a, C3'a), 124.4 (2C, C4, C4'), 124.8 (2C, C5, C5'), 131.6 (2C, C4", C4'''), 136.5 (2C, C6, C6'), 148.8 (2C, C7a, C7'a), 151.7 (2C, C1', C1") 183.7 (2C, C2, C2'). MS (EI), *m/z* 430 (89%, M$^+$), 345 (100) 301 (97), 273(80), HRMS (EI, M$^+$) calcd for $C_{24}H_{18}N_2O$ 430.1160, found 430.1169.

Optimised procedure for the synthesis of 13-allyl-8a-hydroxy-8,13a-dihydroazepino[1,2-*a*:3,4-*b'*]diindol-14(8*H*)-one (248) from (259)

A solution of **259** (45.0 mg, 0.100 mmol) in anhydrous CH_2Cl_2 (10 mL) was stirred under the N_2. The solution was transferred to a septum equipped round bottom flask containing Pd(PPh$_3$)$_4$ and stirred at room temperature (27 °C) for 10 min. The magenta

colour of the solution turned to dark blue and complete conversion of the **259** to a blue compound (R_f = 0.61) was confirmed *via* TLC analysis. The reaction was quenched by addition of the saturated solution of $NaHCO_3$ (5 mL). The solution was partitioned in CH_2Cl_2 (*ca* 10 mL) and washed with brine (2 × 30 mL) and water (5 × 50 mL). The combined organic layers were dried (Na_2SO_4) and mass spectroscopy analysis of the crude was confirmed the mass the presence of a product with mass unit of 342 Da which was assigned to the *N,N'*-diallylindigo. The filtrate was concentrated under reduced pressure. During the concentration of the solution its colour turned to bright red. The filtrate was recrystallised from the mixture of pet. spirit/CH_2Cl_2 (9:1) yielding 13-allyl-8a-hydroxy-8,13a-dihydroazepino[1,2-*a*:3,4-*b'*]diindol-14(8*H*)-one **248** (335 mg, 98%) as dark red crystals.

In a separate attempt the combined organic layers from the extraction were combined in to a flask and plunged to an ice bath and concentrated under the nitrogen. The colour of the solution turned to red after 2 h. Analysis of the solution was confirmed the conversion of the product to **248**.

Methyl-2-(13,14-dioxo-6,7,13,14-tetrahydropyrazino[1,2-*a*:4,3-*a'*]diindol-6-yl)acetate (261)
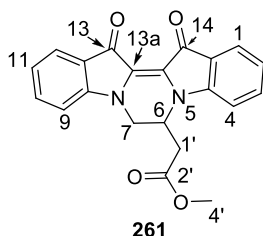
A suspension of indigo (262 mg, 1.00 mmol) in DMF was sonicated for 30 min at room temperature and transferred to a septum equipped round bottom flask containing pre-dried and ground Cs_2CO_3 (1.303 g, 4.00 mmol) and molecular sieves under an inert atmosphere. The flask was plunged to a pre-heated oil bath at 85-88 °C and stirred for 30 min. The inert atmosphere flow was then cut and methyl 4-bromocrotonate (900 mg, 5.00 mmol) was added and the mixture was stirred and heated

for 3 h under a static inert atmosphere (N_2). Molecular sieves were filtered from the hot reaction mixture and the filtrate poured into an ice bath and then partitioned in water and CH_2Cl_2 and washed with brine (2×30 mL) and water (5×50 mL). The combined organic phases were dried (Na_2SO_4) and concentrated under reduced pressure. The residue was recrystallised from pet. spirit/CH_2Cl_2 (9:1) yielding **261** (223 mg, 62%) as a dark purple solid; R_f = 0.51, mp 267−269 °C. IR (neat) υ_{max} 1761 (s), 1709 (m), 1615 (m), 1467 (m), 1292 (m), 1184 (m), 1121 (s), 740 (s) cm^{-1}. ^{1}H NMR ($CDCl_3$) δ 1.61 (1H, s, H1′a), 2.62 (1H, s, H1′b), 3.61 (3H, s, H4), 3.92 (1H, dd, J = 12.4, 3.3 Hz, H7a), 4.17 (1H, d, J = 12.3, H7b), 5.03−5.11 (1H, m, H6), 6.79-6.85 (2H, m, H2, H11), 6.89-6.93 (2H, m, H4, H9), 7.56-7.60 (2H, m, H3, H10), 7.67-7.73 (2H, m, H1, H12). ^{13}C NMR ($CDCl_3$) δ 43.4 (C1'), 50.4 (C7), 50.9 (C6), 51.9 (C4'), 105.0 (C9), 111.2 (C4), 121.8 (C14a), 122.7 (C12a), 124.0 (C2), 124.1 (C11), 127.4 (C1), 128.7 (C12), 133.9 (C10), 133.6 (C13a), 133.8 (C3), 134.25 (C13b), 146.3 (C4a), 148.0 (C8a), 170.3 (C2'), 179.7 (C13), 180.6 (C14). MS (EI), m/z 360 (23%, M^+), 287 (100%). HRMS (ESI) [M + H]$^+$ calcd for $C_{19}H_{13}N_2O_2$, 361.8962; found, 361.8971.

7.1.3   Products from the propargylation of indigo

7.1.3.1   Reaction of indigo and propargyl bromide

A suspension of powdered indigo (262 mg, 1.00 mmol) in anhydrous DMF (40 mL) was sonicated for 30 min and stirred vigorously under N_2 overnight. The resulting suspension was added to pre-dried anhydrous caesium carbonate (1.20 g, 3.40 mmol) and molecular sieves (4 Å) while being stirred and heated to 80−85 °C under a N_2 atmosphere. After 30 min propargyl bromide (595 mg, 5.00 mol) was added and the reaction mixture was heated at 82−85 °C for 5 min. The mixture was filtered hot and

then the solution was concentrated by rotary evaporation and the residue applied to a short plug of silica gel/celite (1:1) and washed consecutively with 4 different solvent mixtures: 1: 70:30 CH_2Cl_2/petroleum spirit (250 mL); 2: CH_2Cl_2; 3: 50:50 CH_2Cl_2/EtOAc and 4: 95:5 EtOAc/MeOH (250 mL). Four fractions were collected from the four different elutions.

(*E*)1-(Prop-2-yn-1-yl)-[2,2′-biindolinylidene]-3,3′-dione
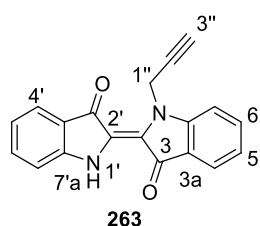
Fraction 1 was concentrated and slowly recrystallised in 9:1 petroleum spirit/EtOAc then filtered to yield 1-(prop-2-yn-1-yl)-[2,2′-biindolinylidene]-3,3′-dione **263** (33.0, mg 11%) as a blue, papery solid. R_f (7:3 CH_2Cl_2/petroleum spirit) = 0.53, mp 267−269 °C; λ_{max}/nm (ε, $M^{-1}cm^{-1}$) 291 (10447), 634 (6381). IR (neat) υ_{max} 3278 (m), 1605 (s), 1463 (s), 1297 (s), 1066 (s), 1027 (s), 927 (m), 743 (m) cm^{-1}. ^1H NMR (CDCl$_3$) δ 2.17 (1H, s, H3″), 5.41 (2H, s, H1″), 6.96 (1H, t, J = 7.1 Hz, H5′), 6.99 (1H, d, J = 8.1 Hz, H7′), 7.09 (1H, t, J = 7.1 Hz, H5), 7.22 (1H, d, J = 8.1 Hz, H7), 7.48 (1H, t, J = 7.5 Hz, H6), 7.60 (1H, t, J = 7.5 Hz, H6′), 7.69 (1H, d, J = 7.5 Hz, H4′), 7.77 (1H, d, J = 7.5 Hz, H4) 10.60 (1H, s, H1). ^{13}C NMR (CDCl$_3$) δ 37.1 (C1″), 72.5 (C3″), 78.4 (C2″), 111.5 (C7′), 111.9 (C7), 120.4 (C3′a), 120.9 (C5′), 121.5 (C5), 122.0 (C2′), 122.4 (C2), 125.0 (C4′), 125.1 (C4), 126.2 (C3a), 135.9 (C6), 136.4 (C6), 151.8 (C7′a), 152.6 (C7a), 187.6 (C3), 189.6 (C3′). MS (EI) *m/z*: 300 (100%, M$^+$), 271 (53), 262 (32). HRMS (ESI) [M + H]$^+$ calcd for $C_{19}H_{13}N_2O_2$, 301.0977; found, 301.0964.

6-Methylene-6,7-dihydropyrazino[1,2-*a*:4,3-*a*′]diindole-13,14-dione (264)
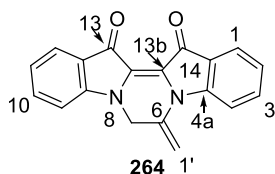
Fraction 4 was purified by preparative TLC using CH_2Cl_2/EtOAc (88:12) as the developing solvent and gave 6-methylene-6,7-dihydropyrazino[1,2-*a*:4,3-*a*′]diindole-13,14-dione **264** was isolated as a dark burgundy powder (63 mg, 21%). R_f (8.5:1.5,

CH$_2$Cl$_2$/EtOAc)= 0.51, mp 280−284 °C. UV−vis (CH$_2$Cl$_2$) λ_{max}/nm (ϵ, M^{-1}cm^{-1}) 324 (13088), 573 (6430). IR (neat) υ_{max} 1701 (m), 1604 (m), 1470 (m), 1298 (m), 1185 (m), 1122 (s), 742 (s) cm^{-1}. ^{1}H NMR (CDCl$_3$) δ 4.41 (2H, s, H7), 5.04 (1H, s, H1'a), 5.38 (1H, s, H1'b), 6.95−7.00 (2H, m, H9, H11), 7.09 (1H, t, J = 7.4 Hz, H2), 7.48−7.55 (3H, m, H3, H4, H10), 7.73 (1H, d, J = 7.5 Hz, H12), 7.82 (1H, d, J = 7.5 Hz, H1). ^{13}C NMR (CDCl$_3$) δ 45.9 (C7), 97.9 (C1'), 109.5 (C9), 112.7 (C4), 121.4 (C13a), 121.8 (C11), 122.7 (C2), 123.0 (C12a), 124.6 (C14a), 125.3 (C1), 125.5 (C12), 125.6 (C6), 131.6 (C13b), 135.1 (C10), 135.5 (C3), 147.0 (C4a), 150.0 (C8a), 179.7 (C14), 180.8 (C13). MS (EI), m/z 300 (14), 207 (100%). HRMS (ESI) [M + H]$^+$ calcd for C$_{19}$H$_{13}$N$_2$O$_2$, 301.0972; found, 301.0960.

13-Oxo-12-(prop-2-yn-1-yl)-12b(propa-1,2-dien-1-yl)-12b,13-dihydro-12H-pyrido[1,2-a:3,4-b']diindole-6-carbaldehyde (265)

The mother liquors from fraction 1 were combined with fraction 2 and then subjected to a silica gel column and elution with 7:3 CH$_2$Cl$_2$/pet. spirit gave 13-oxo-12-(prop-2-yn-1-yl)-12b(propa-1,2-dien-1-yl)-12b,13-dihydro-12H-pyrido[1,2-a:3,4-b']diindole-6-carbaldehyde **265** as yellow−orange crystals (63.92 mg, 17%).

X-ray quality crystals were grown through slow crystallization from pet. spirit/EtOAc (5:3). R_f (CH$_2$Cl$_2$) = 0.26, mp 229−231 °C; UV−vis (CH$_2$Cl$_2$) λ_{max}/nm (ϵ, M^{-1}cm^{-1}) 386 (12825), 244 (34151). IR (neat) υ_{max} 3278 (m), 1604 (s), 1463 (s), 1297 (m), 1065 (s), 1027 (s), 1015 (s), 743 (s) cm^{-1}. ^{1}H NMR (CDCl$_3$) δ 2.33 (1H, s, H3'), 4.79 (2H, d, J = 6.5 Hz, H3"), 5.42 (1H, t, J = 6.5 Hz, H1"), 5.51−5.66 (2H, m, H1'), 6.82 (1H, d, J = 8.4 Hz, H11), 6.94 (1H, t, J = 7.2 Hz, H3), 7.27 (1H, t, J = 7.6 Hz, H2), 7.35 (1H, t, J = 8.0 Hz, H9), 7.49 (1H, t, J = 8.0 Hz, H8), 7.54 (1H, d, J = 8.4 Hz, H10), 7.64−7.68 (2H, m, H1, H4), 7.65 (1H, s, H7), 9.62 (1H, s, H1'''). ^{13}C NMR (CDCl$_3$) δ 36.2 (C1'), 71.3

(C12b), 73.6 (C3'), 77.8 (C2'), 80.4 (C3"), 90.4 (C1"), 110.7 (C7a), 111.1 (C13a), 111.5 (C9), 113.6 (C1), 117.2 (C12a), 118.6 (C11), 121.1 (C3), 122.6 (C8), 124.1 (C10), 124.5 (C11a), 124.9 (C4), 131.8 (C7), 137.7 (C7b), 138.2 (C4a), 138.5 (C2), 158.6 (C6), 185.3 (C1'''), 195.7 (C13), 208.4 (C2"). MS (EI) m/z 376 (5%, M$^+$), 371 (100), 298 (24). HRMS (ESI) [M + H]$^+$ calcd for $C_{25}H_{17}N_2O_2$, 377.1298; found, 377.1285.

13-(Prop-2-yn-1-yl)-14-(prop-2-yn-1-yloxy)benzo[*b*]indolo-[1,2-*h*][1,7] naphthyridine-8-(13*H*)-one (266)

Fraction 3 was recrystallized from CH_2Cl_2/petroleum spirit (1:9) giving 13-(prop-2-yn-1-yl)-14-(prop-2-yn-1-yloxy)benzo[*b*]indolo-[1,2-*h*][1,7]naphthyridin-8-(13*H*)-one **266**

266
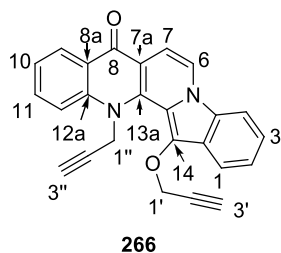
(116.6 mg, 31%) as orange crystals. X-ray quality crystals were grown through slow crystallization from petroleum spirit/ethyl acetate (4:3). R_f (9:1 CH_2Cl_2/EtOAc) = 0.52, mp 218−220 °C; UV−vis (CH_2Cl_2) λ_{max}/nm (ε, $M^{-1}cm^{-1}$) 324 (27663), 441 (10360). IR (neat) υ_{max} 3205 (w), 1588 (m), 1485 (m), 1349 (m), 1260 (m), 1059 (m), 725 (s) cm^{-1}. ^{1}H NMR (CDCl$_3$) δ 2.14 (1H, s, J = 2.4 Hz, H3'), 2.30 (1H, s, J = 2.4 Hz, H3"), 4.74 (2H, d, J = 2.4 Hz, H1'), 5.49 (2H, d, J = 2.4 Hz, H1"), 7.33 (1H, d, J = 7.2 Hz, H7), 7.40-7.47 (3H, m, H1, H2, H3), 7.74−7.77 (1H, m, H11), 7.85−7.90 (3H, m, H4, H10, H12), 8.01 (1H, d, J = 7.3 Hz, H6), 8.71 (1H, dd, J = 8.0, 1.3 Hz, H9). ^{13}C NMR (CDCl$_3$) δ 44.0 (C1″), 63.7 (C1′), 74.5 (C3′), 76.5 (C3″), 78.5 (C2″), 78.6 (C2′), 104.0 (C7), 110.9 (C3), 117.9 (C7a), 118.6 (C12), 118.9 (C13b), 119.1 (C10), 119.9 (C6), 121.6 (C4a), 123.3 (C2), 123.9 (C1, C4), 126.4 (C8a), 126.9 (C9), 129.3 (C14a), 132.6 (C11), 133.2 (C14), 139.1 (C13a), 143.5 (C12a), 91.8 (C8). MS (EI), m/z 376 (6, M$^+$), 337 (100%), 309 (20), 298 (75). HRMS (ESI) [M + H]$^+$ calcd for $C_{25}H_{17}N_2O_2$, 377.1285; found, 377.1302.

Prop-2-yn-1-yl   8-oxo-13-(prop-2-yn-1-yl)-14-(prop-2-yn-1-yloxy)-8,13-dihydrobenzo[*b*]-indolo[1,2-*h*][1,7]naphthyridine-7-carboxylate (267)

The mother liquor from the recrystallisation of **267** was concentrated and then subjected
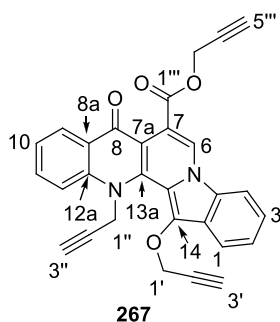
to silica gel column chromatography, and elution with CH$_2$Cl$_2$/EtOAc (92:8) resulted in prop-2-yn-1-yl 8-oxo-13-(prop-2-yn-1-yl)-14-(prop-2-yn-1-yloxy)-8,13-dihydrobenzo[*b*]-indolo[1,2-*h*][1,7]naphthyridine-7-carboxylate **267** (2 mg, <1%) as bright orange crystals. X-ray quality crystals were grown through slow crystallization from chloroform. R_f (9:1, CH$_2$Cl$_2$/EtOAc) = 0.59, mp 258−260 °C; IR (neat) υ_{max} 3278 (m), 2925 (m), 1718 (s), 1595 (s), 1482 (m), 1237 (m), 1062 (m), 964 (m), 749 (s), 643 (s) cm^{-1}. ^{1}H NMR (CDCl$_3$) δ 2.14 (1H, bs, H3″), 2.30 (1H, bs, H5‴), 2.53 (1H, bs, H3′), 4.76 (2H, d, J = 2.0 Hz, H1″), 5.06 (2H, d, J = 1.7 Hz, H1‴), 5.43 (2H, d, J = 1.7 Hz, H1′), 7.43−7.50 (3H, m, H1, H2, H3), 7.75 (1H, t, J = 7.8 Hz, H11), 7.82−7.90 (3H, m, H4, H10, H12), 8.01 (1H, s, H6), 8.48−8.50 (1H, d, J = 7.8, H9). ^{13}C NMR (CDCl$_3$) δ 44.1 (C1‴), 53.4 (C1′), 63.5 (C1″), 74.7 (C3‴), 75.1 (C3′), 76.5 (C3″), 77.9 (C2″), 78.1 (C2′), 78.2 (C2‴), 110.7 (C7a), 110.8 (C7), 112.2 (C3), 115.1 (C13b), 118.1 (C12), 118.7 (C10), 118.8 (C6), 122.0 (C4a), 123.8 (C2), 124.1 (C1), 124.7 (C4), 126.7 (C8a), 126.8 (C9), 130.0 (C14a), 133.6 (C11), 134.5 (C14), 139.2 (C13a), 142.9 (C12a), 167.1 (ester C-O) 174.5 (C8). MS (EI), *m/z* 458 (5, M$^+$), 419 (100%), 380 (10), 375 (5), 337 (20), 298 (45). HRMS (ESI) [M +H]$^+$ calcd for C$_{29}$H$_{19}$N$_2$O$_4$, 459.1345; found, 459.1363.

Optimisation of the synthesis of (*E*)-1-(prop-2-yn-1-yl)-[2,2′-biindolinylidene]-3,3′-dione (263)

A suspension of powdered indigo (262 mg, 1.0 mmol) in anhydrous DMF (50 mL) was sonicated for 60 min and stirred vigorously under N_2 overnight. The resulting suspension was added to pre-dried anhydrous caesium carbonate (2.4 g, 7.42 mmol) and the mixture was stirred and warmed to 80−85 °C under a N_2 atmosphere. After 30 min propargyl bromide (1.90 mg 10.0 mmol) was added and the reaction mixture was heated at 82−85 °C for 5 s. The mixture was then poured into ice water and the resulting precipitate was filtered and recrystallized from pet. spirit/EtOAc (90:10) to furnish (*E*)-1-(prop-2-yn-1-yl)-[2,2′-biindolinylidene]-3,3′-dione **263** (279.00 mg 93%) as a blue, fluffy solid.

Optimisation of the synthesis of 6-methylene-6,7-dihydropyrazino[1,2-*a*:4,3-*a′*]diindole-13,14-dione (264).

A solution of **263** (100 mg, 0.33 mmol) in anhydrous DMF (20 mL) was stirred and warmed to 80−85 °C under a N_2 atmosphere for 20 min. The solution was then added to pre-dried anhydrous caesium carbonate (107 mg, 0.33 mmol) and was stirred and warmed at 80−85 °C under a N_2 atmosphere for 10 min. The mixture was then poured into ice water and the resulting precipitate was separated and subjected to silica gel short column chromatography and eluted with CH_2Cl_2/EtOAc (85:15) to give 6-methylene-6,7-dihydropyrazino[1,2-*a*:4,3-*a′*]diindole-13,14-dione **264** as a dark burgundy powder (98 mg, 98%).

7.1.3.2   Reaction of indigo and propargyl mesylate

A suspension of powdered indigo (262 mg, 1.00 mmol) in anhydrous DMF (40 mL) was sonicated for 30 min and stirred vigorously under N_2 overnight. The resulting suspension was added to pre-dried anhydrous caesium carbonate (1.20 g, 3.4 mmol) and molecular sieves (4 Å) while being stirred and warmed to 80−85 °C under a N_2 atmosphere. After 1 h, propargyl bromide (0.595 mg 5.00 mol) was added and the reaction mixture was heated at 82−85 °C for 5 min. The reaction mixture was filtered hot into an ice bath. Upon leaving to stand overnight, the colloid lumps of the products sank to the bottom of the flask. The clear aqueous layer was decanted out and the remaining crude mixture was partitioned between water and EtOAc and washed with brine (2 × 20 mL) and distilled water (5 × 20 mL). The organic layer was collected and dried and concentrated in the *vacuo*. The residue was recrystallised from CH_2Cl_2/ pet. spirit (1:9) and yielded **266** (51%). The mother liquor was concentrated and subjected to preparative TLC. The two distinctive band were scraped which resulted in the isolation of **266** (8%) and **265** (28%), with spectral values similar to those reported above.

7.1.3.3   Reaction of indigo and bromoacetonitrile

(*E*)-2-(3,3-Dioxo-[2,2′-biindolinylidene]-1yl)acetonitirile
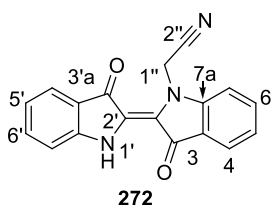
272

A suspension of indigo (262 mg 1.00 mmol) in anhydrous DMF (40 mL) was sonicated for 30 min and the resulting suspension was transferred to a septum equipped round bottom flask carrying pre-dried Cs_2CO_3 (1.303 g, 4.00 mmol) under N_2 flow. The flask was plunged into a preheated oil bath at 85-88 °C and stirred for 30 min. The N_2 flow was stopped and bromoacetonitrile (600 mg, 5.00 mmol) was added rapidly in

one portion by syringe, and after 5 sec, the reaction mixture was poured into an ice bath. The blue-black precipitate was filtered and dissolved in hot CH_2Cl_2 and cooled at 5 °C overnight. The mixture was then filtered to remove the unreacted indigo (21%). The filtrate was concentrated under reduced pressure then recrystallised from pet. spirit/EtOAc (90:10) to furnish **272** (163.6 mg, 54%) as a dark navy crystalline solid; R_f = 0.63 (CH_2Cl_2/pet. spirit; 7:3), m.p: 201-203 °C. IR (neat) υ_{max} 3265 (m), 2198 (m), 1601 (s), 1459 (s), 1299 (s), 1062 (s), 1025 (s), 928 (m), 741 (m) cm^{-1}. ^{1}H NMR (CDCl$_3$) δ 5.64 (2H, s, H1″), 7.00 (1H, t, J = 7.5 Hz, H5′), 7.07 (1H, d, J = 8.3 Hz, H7′), 7.20-7.26 (2H, H5, H7), 7.54 (1H, t, J = 7.5 Hz, H6), 7.69-7.73 (2H, m, H6′, H4′), 7.82 (1H, d, J = 7.6 Hz, H4) 10.54 (1H, s, H1). ^{13}C NMR (CDCl$_3$) δ 38.1 (C1″), 111.6 (C7′), 113.0 (C7), 116.0 (C2″), 121.7 (C3′a), 123.8 (C5′), 124.4 (C3a), 124.8 (C4′), 125.1 (C5), 128.1 (C4) 130.6 (C2), 131.0 (C6′), 132.7 (C6), 133.9 (C2′), 144.5 (C7′a), 145.5 (C7a), 181.2 (C3), 184.0 (C3′). MS (EI) m/z: 301 (100%, M$^+$), 262 (56). HRMS (ESI) [M + H]$^+$ calcd for $C_{18}H_{12}N_2O_2$, 302.1013; found, 302.1018.

7.1.3.4   Reaction of indigo and 1-bromo-2-butyne

A suspension of indigo (262 mg, 1.00 mmol) in DMF (40 mL) in a 100 mL round bottom flask fitted with a septum was sonicated for 30 minutes. The suspension was transferred by a cannula to a septum equipped round bottom flask containing pre-dried caesium carbonate (2.00 g, 6.14 mmol) and activated 4 Å molecular sieves and a stirring bar under a nitrogen atmosphere. The reaction vessel was suspended in an oil bath preheated at 85-87 °C and allowed to react under nitrogen for 30 min, after which the nitrogen input was removed and 1-bromo-2-butyne (665 mg, 5.00 mmol) was injected. After 30 minutes, the content of the vessel was filtered into an ice bath. The mixture

was extracted with CH_2Cl_2 (5 × 20 mL), and the combined organic layers concentrated. The residue was then repeatedly washed with water (10 × 20 mL) and brine (3 × 20 mL), the combined organic layers were dried (Na_2SO_4), and concentrated under the reduced pressure.

(E)-1-(But-2-yn-1-yl)-[2,2'-biindolinylidene]-3,3'-dione (268)
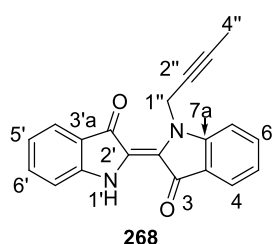
The residue was subjected to a flash silica gel column chromatography and elution with pet. spirit : CH_2Cl_2 (3:7) yielded the (E)-1-(but-2-yn-1-yl)-[2,2'-biindolinylidene]-3,3'-dione **268** (192 mg 62%) as a blue, papery solid. R_f (7:3 CH_2Cl_2/pet. spirit) = 0.58, mp 279-281 °C; IR (neat) υ_{max} 3278 (m), 1608 (s), 1465 (s), 1292 (s), 1061 (s), 1032 (s), 922 (m), 747 (m) cm^{-1}. ^{1}H NMR (CDCl$_3$) δ 1.72 (3H, s, H4″), 5.14 (2H, s, H1″), 6.77 (1H, dd, J = 7.5, 1.6 Hz, H7′[†††]), 6.80 (1H, t, J = 7.5 Hz, H5), 6.90 (1H, dd, J = 7.5, 1.4 Hz, H7), 7.00 (1H, t, J = 7.5 Hz, H5′), 7.30 (1H, t, J = 7.5 Hz, H6′), 7.57 (1H, t, J = 7.5 Hz, H6), 7.68 (1H, d, J = 7.5 Hz, H4′), 8.27 (1H, d, J = 7.4 Hz, H4) 10.49 (1H, s, H1′). ^{13}C NMR (CDCl$_3$) δ 6.9 (C4″), 37.4 (C1″), 73.6 (C3″), 74.3 (C2″), 111.6 (C7), 113.0 (C7′), 121.7 (C3a), 123.8 (C5), 124.4 (C3′a), 124.8 (C4′), 125.1 (C5′), 128.1 (C4), 130.6 (C2), 131.0 (C6′), 132.6 (C6), 133.9 (C2′), 144.5 (C7′a), 152.3 (C7a), 181.6 (C3), 184.0 (C3′). MS (EI) m/z: 314 (100%, M$^+$), 300 (18), 261 (29). HRMS (ESI) [M + H]$^+$ calcd for $C_{20}H_{15}N_2O_2$, 315.1055; found, 315.1063.

13-(But-2-yn-1-yl)-7a-methylbenzo[b]indolo[1,2-h][1,7]naphthyridine-8,14(7aH,13H)-dione (269)
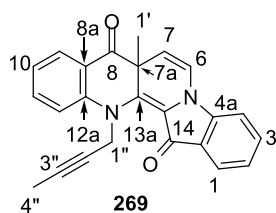
Furthur elution afforded a fraction which recrystallized from EtOAc/pet. spirit (1:9) giving 13-(but-2-yn-1-yl)-7a-methylbenzo[b]indolo[1,2-h][1,7]naphthyridine-8,14(7aH,13H)-

---

[†††] Meta coupling.

dione **269** (117 mg, 31%) as dark red crystals. X-ray quality crystals were grown through slow crystallization from pet. spirit/ethyl acetate (4:3). R_f (9:1 CH_2Cl_2/EtOAc) = 0.53, mp 243−245 °C; IR (neat) υ_{max} 1684 (m), 1599 (m), 1570 (m), 1465 (s), 1329 (s), 1146 (m), 1003 (m), 740 (s) cm^{-1}. ^{1}H NMR (CDCl$_3$) δ 1.65 (3H, s, H1'), 1.74 (3H, s, H4''), 4.66 (1H, d, J = 18.3, Hz, H1''a[‡‡‡]), 4.99 (1H, d, J = 18.3 Hz, H1''b[***]), 5.44 (1H, d, J = 7.9 Hz, H7), 6.81 (1H, d, J = 7.9 Hz, H6), 6.97 (1H, t, J = 7.9 Hz, H10), 7.09-7.15 (2H, m, H2, H12), 7.49-7.57 (2H, m, Hz, H4, H11), 7.71 (1H, d, J = 7.6 Hz, H9), 7.94 (1H, J = 7.7, H1). ^{13}C NMR (CDCl$_3$) δ 3.5 (C4''), 29.3 (C1'), 43.9 (C1''), 48.2 (C7a), 73.7 (C3''), 81.7 (C2''), 103.5 (C7), 108.7 (C3), 116.0 (C12), 119.5 (C13b), 119.8 (C10), 120.5 (C6), 120.7 (C2), 121.4 (C4a), 122.4 (C8a), 124.5 (C1), 128.5 (C4), 130.0 (C9), 135.5 (C11), 138.4 (C14a), 144.2 (C13a), 146.8 (C12a), 178.4 (C14), 193.6 (C8). MS (EI), m/z 366 (23%, M+), 313 (100), 285 (25). HRMS (ESI) [M + H]$^+$ calcd for C$_{24}$H$_{19}$N$_2$O$_2$, 367.1367; found, 367.1382.

7.1.3.5   Reaction of indigo and 3-chloro-1-phenyl-1-propyne (270)

A suspension of indigo (262 mg, 1.00 mmol) in DMF (40 mL) in a 100 mL round bottom flask fitted with a septum was sonicated for 30 minutes. The suspension was transferred by a cannula to a septum equipped round bottom flask containing pre-dried caesium carbonate (2.00 g, 6.14 mmol) and activated 4 Å molecular sieves and a stirring bar under a nitrogen atmosphere. The reaction vessel was suspended in an oil bath preheated at 85-87 ºC and allowed to react under nitrogen for 30 min, after which the nitrogen input was removed and 3-chloro-1-phenyl-1-propyne (753 mg, 5.00 mmol) was injected. After 30 minutes, the content of the vessel was filtered into an ice bath. The mixture was extracted with CH_2Cl_2 (5 × 20 mL), and the combined organic layers

---

[‡‡‡] CH_2(H1''), splits as the presence of terminal alkynic methyl hinders the free rotation across the C-N bond, however the alkynic pendant in naphthyridine **266** rotates freely and CH_2 appears as a singlet.

concentrated. The residue was then repeatedly washed with water (10 × 20 mL) and brine (3 × 20 mL) the combined organic layers were dried (Na₂SO₄), and concentrated under the reduce pressure.

7-Hydroxy-8-phenylazepino[1,2-*a*:3,4-*b*′]diindol-14(13*H*)-one (270)
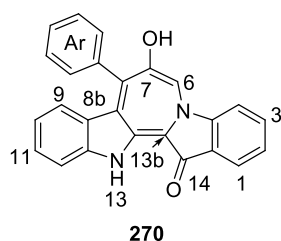
The residue was subjected to a flash silica gel column chromatography and elution with pet. spirit : CH₂Cl₂ (3:7) yielded the 7-hydroxy-8-phenylazepino[1,2-*a*:3,4-*b*′]diindol-14(13*H*)-one (101 mg, 27%) mp 148-150 ℃, R_f = 0.71 (CH₂Cl₂/ pet. spirit; 7:3). IR υ_{max} 3282 (bm), 1656 (s), 1601 (s), 1585 (s), 1394 (m), 1119 (s), 734 (s) cm⁻¹. ¹H NMR (CDCl₃) δ = 6.91 (1H, s, H6), 7.37 (3H, m, ArH), 7.46-7.53 (2H, m, ArH), 7.50 (1H, t, *J* = 7.5 Hz, H11), 7.66-7.73 (2H, m, H2, H10), 7.82-7.85 (1H, t, *J* = 7.9 Hz, H3), 8.03 (1H, dd, *J* = 7.9, 1.4, Hz, H1), 7.60 (1H, d, *J* = 8.0 Hz, H4), 8.22 (1H, d, *J* = 7.6 Hz, H9). ¹³C NMR (CDCl₃) δ = 118.0 (C9), 121.8 (13b), 123.2 (C12), 127.0 (C13b), 127.1 (C11), 127.4 (2×ArC), 128.5 (ArC), 128.8 (ArC), 129.0 (CAr), 129.7 (C1), 130.9 (C2), 133.0 (C3), 133.5 (C4), 133.8 (C10), 135.1 (C13a), 135.7 (C8), 137.8 (C8a), 143.0 (C14a), 144.5 (C8b), 152.2 (C12a), 159.3 (C7), 184.6 (C14). MS (EI): *m/z* = 376 (10%, M⁺), 373 (100), HRMS (ESI): calcd for C₂₅H₁₇N₂O₂ [M+H]⁺ 377.1291; found 377.1290.

(*Z*)-9-((*E*)-Benzylidene)-6-(phenylethynyl)-8,9-dihydro-6*H*-[1,3,6]oxadiazocino[3,4-*a*:6,5-*a*′]diindole-15,16-dione (271)
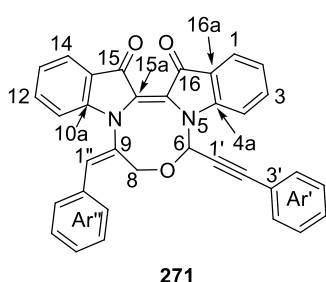
Furthure elution afforded a fraction which recrystallized from EtOAc/petroleum spirit (1:9) giving (*Z*)-9-((*E*)-benzylidene)-6-(phenylethynyl)-8,9-dihydro-6*H*-[1,3,6]oxadiazocino[3,4-*a*:6,5-*a*′]diindole-15,16-dione (177

mg, 35%) as dark navy powder. R_f (9:1, CH_2Cl_2/EtOAc) = 0.51, mp 295-297 °C. IR

(neat) υ_{max} 3076 (m), 1735 (m), 1689 (m), 1459 (m), 1243 (m), 1162 (m), 1102 (s), 761

(s) cm^{-1}. ^{1}H NMR (CDCl$_3$) δ 4.75 (2H, ABq, J = 36.9, 16.0, H8), 5.67 (1H, s, H6), 6.72

(1H, s, H1"), 6.86 (1H, d, J = 8.1 Hz, H4), 6.98-7.17 (10H, m, H2, 4 × Ar'H, 5 × Ar"H),

7.33-7.45 (4H, m, H3, H12, H13, HAr'), 7.46 (1H, d, J = 7.3 Hz, H11), 7.75 (1H, d, J =

7.6 Hz, H1), 7.81 (1H, d, J = 7.5 Hz, H1). ^{13}C NMR (CDCl$_3$) δ 56.8 (C6), 61.2 (C8),

83.0 (C1'), 89.0 (C2'), 109.6 (C4), 114.6 (C2), 117.5 (C9), 121.5 (Ar'C), 121.7 (Ar'C),

122.9 (15a), 123.4 (C14a), 124.4 (C1), 125.6 (C14), 125.9 (3C, 2 × Ar'C, 1 × Ar"C),

128.0 (C16a), 128.5 (Ar"C), 128.7 (Ar'C), 128.95 (C3'), 129.0 (C14a), 129.3 (3 ×

Ar"C), 129.4 (C12), 132.0 (C11), 134.1 (C15b), 134.5 (C1"), 135.4 (C13), 148.24

(C10a), 149.4 (C4a), 180.2 (C16), 180.9 (C15). MS (EI), m/z 506 (M$^+$, 11%), 478 (26),

376 (89), 362 (100). HRMS (ESI) [M + H]$^+$ calcd for $C_{34}H_{23}N_2O_3$, 507.1714; found,

507.1709.

Preparation of 1-(prop-2-yn-1-yl)indoline-2,3-dione (*N*-propargyl isatin) (272)
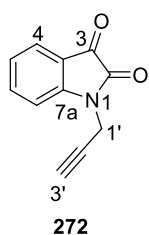
To a solution of isatin (147mg, 1.00 mmol) in dry DMF (40 mL) was

added caesium carbonate (650 mg, 2.00 mmol). The resulting brown

suspension was stirred at 80−85 °C for 30 min and then propargyl

bromide (119 mg, 1.00 mmol) was added under a N$_2$ atmosphere. The

resulting mixture was stirred at 80−85 °C for 30 min, poured into ice

water, and the suspension was partitioned between CH_2Cl_2 (20 mL) and water (20 mL).

The aqueous layer was washed with CH_2Cl_2 (4 × 5 mL), and the combined organic

layers were washed with water (3 × 10 mL), dried (MgSO4), and concentrated. The

residue was recrystallized from chloroform/hexane (1:6) to give *N*-propargylisatin (133

mg, 91%) as an orange solid. ^{1}H NMR (CDCl$_3$) δ 2.32 (2H, d, J = 1.7 Hz, H3'), 4.54

(2H, d, J = 1.9, H1′), 7.16 (2H, m, H5, H7), 7.66 (2H, m, H4, H6). ^{13}C NMR (CDCl$_3$) δ 29.8 (C3′), 73.7 (C2′), 76.0 (C1′), 111.4 (C7), 118.0 (C3a), 124.5 (C5), 125.8 (C4), 138.8 (C6), 149.9 (C7a), 157.5 (C2), 182.9 (C3). MS (EI) m/z 185 (85%, M+), 129 (100%) consistent with literature values.[201]

7.1.4 Elaboration of the products

Ring closing metathesis of 1-allyl-10'-allyloxy-2'H-spiro(indoline-2,1'-pyrido[1,2-a]indol)-3-one (227)
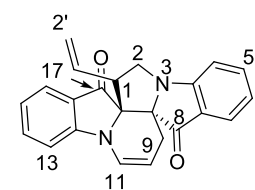
A mixture of the spiro derivative **227** (40.0 mg, 0.95 mmol) and Grubbs' II catalyst (5.00 mg, 10% mmol) in CH$_2$Cl$_2$ (40 mL) was heated at reflux for 1 h. The reaction mixture was then filtered and the filtrate was subjected to flash silica gel column chromatography and elution with pet. spirit/CH$_2$Cl$_2$ (1:9) yielded 1,2-dihydro-1-vinyl-8H,9H,17H-benz[2',3']pyrrolizino-[1',7'a:2,3]pyrido[1,2-a]indole-8,17-dione **274** as a yellow powder (26.0 mg, 70%); mp 229-231 °C, R_f = 0.81 (CH$_2$Cl$_2$: pet. spirit; 9:1). X-ray quality crystals were grown through slow crystallization from pet. spirit : CH$_2$Cl$_2$ (5:3). UV-Vis (CH$_2$Cl$_2$) λ_{max}/nm (ε, M^{-1}cm^{-1}) 286 (8458), 401 (3888). IR (neat) υ_{max} 1685 (s), 1603 (s), 1473 (s), 1318 (m), 1147 (m) cm^{-1}. ^{1}H NMR (CDCl$_3$) δ 2.53-2.65 (2H, m, H9a,b), 3.55-3.58 (1H, m, H1), 3.80 (1H, t, J = 9.6 Hz, H2a), 3.88-3.94 (1H, m, H2b), 4.93 (1H, dd, J = 1.2, 10.0 Hz, H2'a), 5.10 (½H, bs, H2'b†††), 5.15-5.16 (½H, m, H2'b§§§), 5.17-5.21 (1H, m, H10), 5.45-5.56 (1H, m, H1'), 6.79-6.85 (2H, m, H5, H15), 6.86-6.92 (2H, m, H4, H13), 7.08 (1H, d, J = 8.4 Hz, H11), 7.36-7.50 (3H, m, H6, H7, H16), 7.54-7.60 (1H, m, H14). ^{13}C NMR (CDCl3) δ 29.1 (C9), 49.5 (C2), 54.7 (C1), 71.3 (C8a), 71.8 (C17a), 101.5 (C10), 110.8 (C11), 112.1 (C13), 120.2 (C5), 120.3 (C2'), 120.6 (C15), 122.2 (C16a), 123.1 (C4), 123.7 (C7a), 124.5 (C7), 124.7 (C16),

---

§§§ H2'b appears as doublet, half of the signal is merged with the multiplet from H10.

131.7 (C1'), 137.5 (C6), 137.7 (C14), 158.0 (C12a), 164.4 (C3a), 197.9 (C17), 201.0 (C8). MS (EI): m/z = 354 (100%, M$^+$), HRMS (ESI): calcd for $C_{23}H_{19}N_2O_2$ [M+H]$^+$ 355.1447; found 355.1434.

2-Allyl-2'-ethyl-[2,2'-biindole]-3,3'-dione (275)
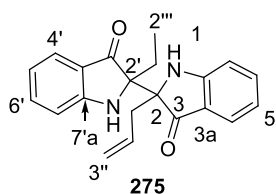
An oven dried round bottom flask equipped with a reflux condenser and magnetic stirrer was purged by dry N$_2$. A solution of N,N'-diallocindigo **259** (43.0 mg 0.1 mmol), Et$_3$B (19.6 mg, 0.2 mmol) and Pd(PPh$_3$)$_4$ (10% mmol) in dry CH$_2$Cl$_2$ (10 mL) was then added and the reaction mixture was heated and stirred at 50 ºC for 1 h. The mixture was diluted with EtOAc and washed by NaHCO$_3$ (2×10 mL), brine (10 mL) and water (3×10 mL). The organic layers were combined and dried (MgSO$_4$). The mixture was concentrated and the residue was subjected to a flash silica gel column chromatography. Elution with a mixture of pet. spirit /CH$_2$Cl$_2$ (1:9) yielded bright yellow fractions. The fractions were collected and combined. After evaporation of the solvent, recrystallisation of the mixture from pet. spirit : EtOAc (9:1) afforded 2-allyl-2'-ethyl-[2,2'-biindole]-3,3'-dione **275** as a bright yellow crystals (23.5 mg, 62%); mp 154-156 °C, R_f = 0.72 (CH$_2$Cl$_2$: pet. spirit; 9:1). IR (neat) υ_{max} 3253 (b), 1696 (s), 1621 (s), 1463 (s), 1319 (m), 1135 (m), 948 (m), 714 (m) cm^{-1}. ^{1}H NMR (CDCl$_3$) δ 0.53 (1H, t, J = 7.2, H2'''), 1.32 (1H, td, J = 14.3, 7.2, H1'''a), 1.95 (1H, td, J = 14.1, 7.1, H1'''b), 2.11 (1H, dt, J = 13.5, 6.7 Hz, H1''a), 2.61 (1H, dt, J = 13.8, 7.0 Hz, H1''b), 4.79 (2H, dd, J = 44.8, 13.4 Hz, H3''a,b), 5.29-5.36 (1H, m, H2''), 6.03 (1H, s, H1, NH), 6.09 (1H, s, H1', NH), 6.72-6.85 (2H, m, H5, H5'), 6.93-6.98 (2H, m, H7, H7'), 7.48 (2H, q, H6, H6'), 7.54 (2H, t, J = 8.0 Hz, H4, H4'). ^{13}C NMR (CDCl$_3$) δ 7.26 (C2'''), 25.1 (C1'''), 36.7 (C1''), 71.9 (C2), 72.6 (C2'), 112.0 (C7), 112.1 (C7'), 118.4 (C5), 118.5 (C5'),

119.3 (C3″), 119.4 (C3′a), 124.1 (C7), 124.2 (C7′), 124.3 (C3a), 130.9 (C3″), 138.1 (C6), 138.2 (C6′), 161.7 (C7a), 162.0 (C7′a), 203.1 (C3′), 204.1 (C3). MS (EI): $m/z =$ 332 (37%, M$^+$), 262 (100%), HRMS (ESI): calcd for $C_{21}H_{21}N_2O_2$ [M+H]$^+$ 333.1527; found 333.1534.

(*E*)-3,3′-Dioxo-[2,2′-biindolinylidene]-1-carbaldehyde (276)
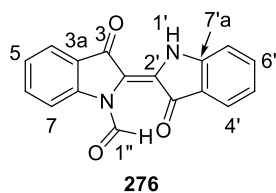
An oven dried Schlenk flask equipped with a magnetic stirrer was purged by dry N_2. A solution of *N*-propargyl indigo **263** (30.0 mg 0.1 mmol) and $Ph_3PAuNTf_2$ (5% mol) in dry CH_2Cl_2 (10 mL) was then added and the reaction mixture was stirred at room temperature (25 °C) for 90 min. Extra $Ph_3PAuNTf_2$ (2% mol) was added and the mixture stirred for a further 90 min. The mixture was diluted with EtOAc and washed with $NaHCO_3$ (2×10 mL), brine (10 mL) and water (3×10 mL). The organic layers were combined and dried ($MgSO_4$). The mixture was concentrated and the residue was dissolved in CH_2Cl_2 (2 mL) and loaded on a preparative layer chromatography (PLC) plate. The plate was placed in a chamber containing (CH_2Cl_2 / EtOAc 9:1) and two distinctive bands were scraped and soaked in separate flasks of EtOAc (20 mL). The first band had a dark purple colour which yielded biindolinylidene carbaldehyde **276** (9.00 mg, 32%); mp 261-263 °C, R_f = 0.49 (CH_2Cl_2 : pet. spirit; 9:1). IR (neat) υ_{max} 3271 (bw), 1723 (s), 1674 (s), 1665 (s), 1482 (s), 1335 (m), 1183 (m), 918 (m), 746 (m) cm^{-1}. ^{1}H NMR (CDCl$_3$) δ 6.99-7.08 (2H, m, H7′, H5), 7.33 (1H, t, *J* = 7.5 Hz, H5′), 7.53 (1H, t, *J* = 7.7 Hz, H6), 7.69-7.73 (2H, m, H4, H6), 7.86 (1H, d, *J* = 7.6 Hz, H4′), 8.51 (1H, d, *J* = 8.3 Hz, H7), 9.98 (1H, s, H1″, CHO), 10.67 (1H, s, H1′, NH). ^{13}C NMR (CDCl$_3$) δ 112.2 (C7), 118.6 (C7′), 119.6 (C3a), 122.1 (C4′), 123.4 (C4), 124.1 (C3′a), 125.3 (C5′), 125.7 (C6′), 129.9 (C2′), 130.7 (C2), 136.1 (C5), 137.4 (C6′), 147.1 (C7a),

155.8 (C7'a), 185.8 (C1"), 188.7 (C3), 189.3 (C3'). MS (EI): m/z = 290 (7%, M$^+$), 262 (100%), HRMS (ESI): calcd for $C_{21}H_{21}N_2O_2$ [M+H]$^+$ 291.1692; found 291.1703.

(*E*)-1-((1-Benzyl-1*H*-1,2,3-triazol-5-yl)methyl)-[2,2'-biindolinylidene]-3,3'-dione (277)
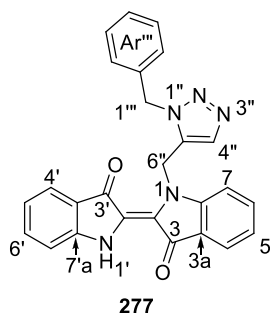
277

An oven dried round bottom flask equipped with magnetic stirrer was purged by dry N$_2$. A solution of *N*-propargyl indigo **263** (30.0 mg 0.1 mmol), Cu(OAc)$_2$ (1 mol%), sodium ascorbate (4 mol%) in DMF/water (8:2) was then added. Benzyl azide (20.0 mg, 0.15 mmol) was injected by a syringe and the reaction mixture was heated and stirred at 40 °C for 10 min. The mixture was quenched with saturated solution of NH$_4$Cl. The mixture was then extracted with CH$_2$Cl$_2$ (2 × 10 mL) and washed with NaHCO$_3$ (2×10 mL), brine (10 mL) and water (3×10 mL). The organic layers were combined and dried (Na$_2$SO$_4$). The mixture was concentrated and the residue was dissolved in hot MeOH/ CH$_2$Cl$_2$ (1:3) and cooled to precipitate (*E*)-1-((1-benzyl-1*H*-1,2,3-triazol-5-yl)methyl)-[2,2'-biindolinylidene]-3,3'-dione (40.7 mg, 94%) as dark navy powder; mp 235-236 °C, R_f = 0.11 (CH$_2$Cl$_2$). IR (neat) υ_{max} 3278 (m), 1605 (s), 1463 (s), 1297 (s), 1066 (s), 1027 (s), 927 (m), 743 (m) cm^{-1}. ^{1}H NMR ((CD$_3$)$_2$SO) δ 5.24 (1H, s, H6"a), 5.43 (2H, d, *J* = 7.3, H1'''), 5.79 (1H, s, H6"b), 6.91 (1H, t, *J* = 8.0 Hz, H5), 6.96 (1H, d, *J* = 7.8 Hz, H7'), 7.13 (1H, t, *J* = 7.7 Hz, H5'), 7.16 (1H, m, Ar'''H), 7.25-7.31 (2H, m, 2 × Ar'''H), 7.35 (1H, d, *J* = 6.3, Ar'''H), 7.46 (1H, t, *J* = 7.7 Hz, H6'), 7.53 (1H, d, *J* = 6.4, Ar'''H), 7.63 (1H, s, H4"), 7.69 (1H, d, *J* = 8.0 Hz, H7), 7.76 (1H, t, *J* = 8.2 Hz, H6), 7.83 (1H, d, *J* = 8.1 Hz, H4), 8.13 (1H, d, *J* = 7.5 Hz, H4'). ^{13}C NMR ((CD$_3$)$_2$SO) δ 38.3 (C6"), 47.9 (C1'''), 111.6 (C7), 113.0 (C7'), 121.7 (C3a), 123.8 (C5), 124.4 (C3'a), 124.8 (C4'), 125.1 (C5'), 126.8

(C5"), 128.1 (C4), 128.2 (2 Ar'"C), 128.4 (Ar'"C), 128.8 (Ar'"C), 130.7 (C6'), 131.2

(C4"), 131.5 (C2), 132.6 (C6), 134.6 (C2'), 135.5 (Ar'"C), 144.5 (C7'a), 145.5 (C7a),

181.3 (C3'), 184.0 (C3). MS (EI): m/z = 433 (63%, M$^+$), 314 (100), 262 (81), HRMS

(ESI): calcd for $C_{26}H_{20}N_2O_2$ [M+H]$^+$ 434.1359; found 434.1367.

(2R,4R,5R,6S)-2-(Acetoxymethyl)-6-(4-(((E)-3,3'-dioxo-[2,2'-biindolinylidene]-1-yl)methyl)-1H-1,2,3-triazol-1-yl)tetrahydro-2H-pyran-3,4,5-triyl triacetate (279)
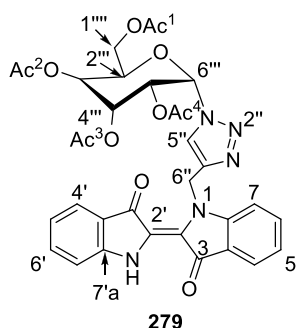
To an oven dried round bottom flask equipped with magnetic stirrer and purged by dry N_2, a solution of N-propargyl indigo **263** (30.0 mg 0.1 mmol), $Cu(OAc)_2$ (1 mol%), sodium ascorbate (4 mol%) and the glycol azide **277** (56 mg, 0.15 mmol) in DMF/water (8:2) was added and the reaction mixture was heated and stirred at 40 °C for 10 min. The mixture was quenched with saturated solution of NH_4Cl. The mixture was then extracted with CH_2Cl_2 (2 × 10 mL) and washed by $NaHCO_3$ (2×10 mL), brine (10 mL) and water (3×10 mL). The organic layers were combined and dried (Na_2SO_4). The mixture was concentrated and the residue was dissolved in hot MeOH/CH_2Cl_2 (1:3) and cooled to precipitate (2R,4R,5R,6S)-2-(acetoxymethyl)-6-(4-(((E)-3,3'-dioxo-[2,2'-biindolinylidene]-1-yl)methyl)-1H-1,2,3-triazol-1-yl)tetrahydro-2H-pyran-3,4,5-triyl triacetate **279** as a papery flakes (56.0 mg, 83%); mp 229-232 °C, R_f = 0.10 (CH_2Cl_2). ^{1}H NMR (($CD_3)_2SO$) δ 1.51 (3H, CH_3, Ac^1), 1.91 (3H, CH_3, Ac^2) 1.94 (3H, CH_3, Ac^3), 1.99 (3H, CH_3, Ac^4) 3.94-4.08 (2H, m, H1''''), 4.23-4.29 (1H, m, H2'''), 5.07 (1H, t, J = 9.7 Hz, H4'''), 5.41 (1H, t, J = 9.5 Hz, H5'''), 5.50 (1H, t, J = 9.4 Hz, H3'''), 5.81 (1H, s, H6"), 6.19 (1H, d, J = 9.2 Hz, H6'''), 6.94 (1H, t, J = 7.4 Hz, H5), 7.05 (1H, t, J = 7.3 Hz, H6'), 7.36 (1H, d, J = 7.7 Hz H7'), 7.46-7.55 (2H, m, H5', H6), 7.58-7.63 (2H, m, H4, H7),

7.64 (1H, d, J = 7.5 Hz, H4'), 8.17 (1H, s, H5''), 10.90 (1H, s, NH). ^{13}C NMR δ

((CD$_3$)$_2$SO) = 19.9 (CH$_3$, Ac^1), 20.7 (CH$_3$, Ac^4), 20.8 (CH$_3$, Ac^2), 20.9 (CH$_3$, Ac^3), 42.2

(C6''), 62.2 (C1''''), 62.8 (C2'''), 70.3 (C4'''), 72.5 (C3'''), 73.7 (C5'''), 84.1 (C6'''), 112.8

(C6), 113.7 (C5'), 119.6 (C3a), 120.9 (C7), 121.5 (C3'a), 121.7 (C7'), 122.9 (C5''), 123.7

(C4'), 124.5 (C4), 125.2 (2 × C, C2,C2'), 136.3 (C6), 136.6 (C6'), 144.0 (C4''), 152.6

(C7a), 153.1 (C7'a), 168.5 (C=O Ac^1), 169.8 (C=O Ac^3), 169.9 (C=O Ac^4), 170.4 (C=O

Ac^2), 187.4 (C3'), 188.5 (C3). MS (EI): m/z = 673 (39%, M$^+$), 342 (100), HRMS (ESI):

calcd for C$_{33}$H$_{32}$N$_5$O$_{11}$ [M+H]$^+$ 674.2029; found 674.2052.

7.2   Biological testing

The biological testing was conducted by Rachada Haritakun at the National Center for

Genetic Engineering and Biotechnology (BIOTEC), 113 Phaholyothin Road, Klong 1,

Klong Luang in Pathumthani 12120, Thailand.

7.2.1   Cancer growth inhibition and *vero cell* toxicity assay.

Cancer growth inhibition assay and the Vero cell assay were performed using the

Resazurin microplate assay (REMA) method as described by O'Brien *et al.*[181] In brief,

cells at a logarithmic growth phase were harvested and diluted to 2.2 × 104 cells/mL for

KB and 3.3 × 104 cells/mL for NCI-H187, in fresh medium. Successively, 5 μL of test

sample diluted in 5% DMSO, and 45 μL of cell suspension were added to 384-well

plates, incubated at 37 °C in 5% CO2 incubator. After the incubation period (3 days for

KB, and 5 days for NCI-H187), 12.5 μL of 62.5 μg/mL resazurin solution was added to

each and the plates were then incubated at 37 °C for 4 h. Fluorescence signal was

measured using SpectraMax M5 multidetection microplate reader (Molecular Devices,

USA) at the excitation and emission wavelengths of 530 and 590 nm. Percent inhibition

of cell growth was calculated by the following equation:

$$\% \text{ Inhibition} = \left[1 - \left(\frac{FU_t}{FU_c}\right)\right] \times 100$$

Where FU_t and FU_c are the mean fluorescent unit from treated and untreated conditions, respectively. Dose−response curves were plotted from 6 concentrations of 3-fold serially diluted test compounds. Sample concentrations that inhibited cell growth by 50% (IC_{50}) were derived using the SOFTMax Pro software (Molecular Devices, USA). Ellipticine and doxorubicin were used as a positive control, and 0.5% DMSO and water were used as a negative control.[174]

7.2.2   Antiplasmodial assay

The compounds and extracts were tested *in vitro* against *Plasmodium falciparum*, K1CB1 (K1), which is a multidrug resistant (chloroquine and antifolate resistant) strain, received as a generous gift from Professor Sodsri Thaithong, Chulalongkorn University, Bangkok, Thailand. The parasites were maintained in human red-blood cells in RPMI 1640 medium supplemented with 25 mM HEPES, 0.2% sodium bicarbonate, and 8% human serum at 37 °C in a 3% carbon dioxide gas incubator.[202] Samples were made up in DMSO solution and the *in vitro* antimalarial activity testing was carried out using the microdilution radioisotope technique. The test sample (25 μL, in the culture medium) was placed in triplicate in a 96-well plate where parasitised erythrocytes (200 μL) with a cell suspension (1.5%) of parasitemia (0.5−1%) were then added to the wells. The ranges of the final concentrations of the samples were varied from 2×10^{-5} to 1×10^{-7} M with 0.1% of the organic solvent. The plates were then cultured under standard conditions for 24 h after which 3*H*-hypoxanthine (25 μL, 0.5 mCi) was added. The culture was incubated for 18-20 h after which the DNA from the parasite was harvested from the culture onto glass fiber filters and a liquid scintillation counter used to

determine the amount of 3*H*-hypoxanthine incorporation.[173] The inhibitory concentration of the sample was determined from its dose−response curves or by calculation.

7.2.3   Anti-mycobacterial assay

The anti-mycobacterial activity was assessed against *M. tuberculosis* H37Ra using the green fluorescent protein microplate assay (GFPMA). Standard drugs, isoniazid (MIC = 0.094 μg/mL), ofloxacin (MIC = 0.391 μg/mL) and ethambutol (MIC = 0.469 μg/mL) were used as reference compounds for the anti-mycobacterial assay. Rifampicin (MIC = 0.0250 μg/mL) and streptomycin (MIC = 0.625 μg/mL) were used as positive controls, while 0.5% DMSO was the negative control. The samples were tested in a final concentration of 50.0 μg/mL.

7.3   Crystallographic studies

X-ray Structure Determination - images were measured on a Nonius Kappa CCD diffractometer (MoKα, graphite monochromator, λ = 0.71073 Å) and data extracted using the DENZO package.[203] Structure solution was by direct methods (SIR92).[204] The structures were refined using the CRYSTALS program package.[205] Atomic coordinates, bond lengths and angles, and displacement parameters for compounds **243**, **248**, **249**, **250**, **251**, **254**, **274**, **265**, **266** and **267** have been deposited at the Cambridge Crystallographic Data Centre (CCDC nos. 986247 – 986253, respectively). These data can be obtained free-of-charge via www.ccdc.cam.ac.uk/data_request/cif, by emailing data_request@ccdc.cam.ac.uk, or by contacting The Cambridge Crystallographic Data Centre, 12 Union Road, Cambridge CB2 1EZ, UK; fax: +44 1223 336033. The entire X-ray crystallography analysis was performed by Dr. Anthony C. Willis at Australian National University Canberra, ACT, Australia.

7.3.1 Crystallographic data for compounds 243, 248, 249, 250, 251, 254, 274, 265, 266 and 267

Compound **243**: $C_{22}H_{18}N_2O_2$, M = 342.40, T = 200 K, monoclinic, space group P21/n, Z = 4, a = 11.888(2), b = 11.667(2), c = 12.5729(17) Å, β = 107.386(11) °; V = 1664.1(5) Å^3, Dx = 1.367 g cm^{-3}, 2915 unique data (2θmax = 50 °), R = 0.095 [for 1849 reflections with I > 2.0σ(I)]; Rw = 0.273 (all data), S = 1.03.

Compound **248**: $C_{19}H_{14}N_2O_2$, M = 302.33, T = 200 K, orthorhombic, space group Pna21, Z = 4, a = 10.0417(3), b = 24.1863(5), c = 5.9097(2) Å; V = 1435.30(7) Å^3, Dx = 1.399 g cm^{-3}, 1799 unique data (2θmax = 55 °), R = 0.040 [for 1359 reflections with I > 2.0σ(I)]; Rw = 0.088 (all data), S = 1.01.

Compound **249**: $C_{24}H_{22}N_2O_2$, M = 370.45, T = 200 K, monoclinic, space group C2/c, Z = 8, a = 45.0292(8), b = 11.1720(3), c = 7.4857(1) Å, β = 99.4875(12) °; V = 3714.29(13) Å^3, Dx = 1.325 g cm^{-3}, 4264 unique data (2θmax = 55 °), R = 0.042 [for 3279 reflections with I > 2.0σ(I)]; Rw = 0.099 (all data), S = 0.98.

Compound **250**: $C_{24}H_{22}N_2O_2$, M = 370.44, T = 200 K, monoclinic, space group P21/n, Z = 4, a = 12.3025(3), b = 10.3191(3), c = 15.2106(3) Å, β = 104.3577(14) °; V = 1870.68(8) Å^3, Dx = 1.315 g cm^{-3}, 4271 unique data (2θmax = 55 °), R = 0.054 [for 3245 reflections with I > 2.0σ(I)]; Rw = 0.141 (all data), S = 0.96.

Compound **251**: $C_{21}H_{18}N_2O_2$, M = 330.39, T = 200 K, monoclinic, space group P21/c, Z = 4, a = 6.2304(2), b = 17.3681(6), c = 14.6545(5) Å, β = 95.602(2) °; V = 1578.19(9)

$Å^3$, Dx = 1.390 g cm^{-3}, 2787 unique data ($2\theta_{max}$ = 50 °), R = 0.043 [for 2321 reflections with I > 2.0σ(I)]; Rw = 0.114 (all data), S = 1.00.

Compound **254**: 2($C_{34}H_{26}N_2O_2$)•C_2H_6OS, M = 1067.32, T = 200 K, triclinic, space group P-1, Z = 2, a = 10.5227(3), b = 12.2715(5), c = 22.4496(9) Å, β = 87.0834(19), β = 88.275(2), ϒ = 75.022(2) °; V = 2796.35(18) $Å^3$, Dx = 1.268 g cm^{-3}, 7798 unique data ($2\theta_{max}$ = 46 °), R = 0.059 [for 4931 reflections with I > 2.0σ(I)]; Rw = 0.157 (all data), S = 0.94.

Compound **274**: $C_{23}H_{18}N_2O_2$, M = 354.41, T = 200 K, orthorhombic, space group Pna21, Z = 8, a = 12.3861(4), b = 10.4051(3), c = 27.6772(2) Å; V = 3567.00(19) $Å^3$, Dx = 1.320 g cm^{-3}, 3221 unique data ($2\theta_{max}$ = 50 °), R = 0.056 [for 2316 reflections with I > 2.0σ(I)]; Rw = 0.140 (all data), S = 1.02.

Compound **265:** $C_{25}H_{16}N_2O_2$, M = 376.41, T = 200 K, monoclinic, space group $P21/n$, Z = 4, a = 8.4251(2), b = 10.9245(3), c = 20.7242(4) Å, β = 100.7475(15) °; V = 1874.00(8) $Å^3$, Dx = 1.334 gcm^{-3}, 4284 unique data ($2\theta_{max}$ = 50 °), R = 0.039 [for 3584 reflections with I > 2.0σ(I)]; Rw = 0.104 (all data), S = 0.99.

Compound 266: $C_{25}H_{16}N_2O_2$, M = 376.41, T = 200 K, monoclinic, space group $P21/n$, Z = 4, a = 8.8893(2), b = 21.6743(3), c = 10.0894(4) Å, β = 106.0180(9) °; V = 1868.45(7) Å3, Dx = 1.338 gcm^{-3}, 4287 unique data ($2\theta_{max}$ = 50 °), R = 0.040 [for 3143 reflections with I > 2.0σ(I)]; Rw = 0.098 (all data), S = 0.96.

Compound 267: $C_{29}H_{18}N_2O_2$, $M = 458.47$, $T = 200$ K, triclinic, space group P-1, $Z = 2$, $a = 7.5927(2)$, $b = 9.4172(3)$, $c = 16.2992(4)$ Å, $\alpha = 76.3835(14)$, $\beta = 88.6282(18)$, $\gamma = 78.0391(19)$ °; $V = 1107.70(6)$ Å3, $Dx = 1.375$ g cm^{-3}, 5070 unique data (2θmax $= 50$ °), $R = 0.046$ [for 4074 reflections with $I > 2.0\sigma(I)$]; $Rw = 0.125$ (all data), $S = 0.99$.

7.4   Computational methods

For all calculations, the Spartan package 2010 (version 1.1.0) was the calculation tool. Geometry Calculations were performed by optimising the geometry of the molecule at the ground state using Hartree-Fock theory and the base 6-31G* were performed by calculate the equilibrium geometry of the molecule at the ground state using density functional theory and the hybrid functional B3LYP with the base 6-31G*. Calculations were performed *in vacuo* unless otherwise stated.

References

1. Kaiser, M.; Wetzel, S.; Kumar, K.; Waldmann, H., *Cell. Mol. Life Sci.* **2008,** 65, 1186-1201.

2. Kirkpatrick, P.; Ellis, C., *Nature* **2004,** 432, 823-865.

3. Dobson, C. M., *Nature* **2004,** 432, 824-828.

4. Bohacek, R. S.; McMartin, C.; Guida, W. C., *Med. Res. Rev.* **1996,** 16, 3-50.

5. Augen, J., *Drug Discov. Today* **2002,** 7, 315-323.

6. Blundell, T. L.; Jhoti, H.; Abell, C., *Nat. Rev. Drug Discov.* **2002,** 1, 45-54.

7. Carr, R.; Hann, M., *Modern Drug Discov.* **2002,** 5, 45-48.

8. Newman, D. J.; Cragg, G. M., *J. Nat. Prod* **2007,** 70, 461-477.

9. van Hattum, H.; Waldmann, H., *J. Am. Chem. Soc.* **2014,** 136 (6), 11583-11589.

10. Schreiber, S. L., *Science* **2000,** 287, 1964-1969.

11. Smith, J. M., *Nature* **1970,** 225, 563-564.

12. Russell, R. B.; Sasieni, P. D.; Sternberg, M. J. E., *J. Mol. Biol.* **1998,** 282, 903-918.

13. Burke, M. D.; Schreiber, S. L., *Angew. Chem. Int. Ed.* **2004,** 43 (1), 46-58.

14. Spring, D. R., *Org. Biomol. Chem.* **2003,** 1, 3867–3870.

15. Burke, M. D.; Schreiber, S. L., *Angew. Chem. Int. Ed.* **2004,** 43 (1), 46-58.

16. Kim, Y.-K.; Arai, M. A.; Arai, T.; O.Lamenzo, J.; Dean, E. F. I.; Patterson, N.; Clemons, P. A.; Schreiber, S. L., *J. Am. Chem. Soc.* **2004,** 126 (45), 14740-14745.

17. Ugi, I.; Meyr, R.; Fetzer, U.; Steinbrückner, C., *Angew. Chem.* **1959,** 71 (11), 386.

18. Lee, D.; Sello, J. K.; Schreiber, S. L., *Org. Lett.* **2000,** 2 (5), 709-712.

19. R.A. Houghten; C. Pinilla; S.E. Blodelle; J. R. Apple; C.T. Dooley; J. H. Cuervo, *Nature* **1991,** 354, 84-86.

20. Dančík, V.; Seiler, K. P.; Young, D. W.; Schreiber, S. L.; Clemons, P. A., *J. Am. Chem. Soc* **2010,** 132 (27), 9259-9261.

21. Shao, Z.; Peng, F. Z., *Curr. Org. Chem.* **2011,** 15 (24), 4144-4160.

22. Anderson, E. A., *Org. Biomol. Chem.* **2011,** 9 (11), 3997-4006.

23. Liu, W.; Khedkar, V.; Baskar, B.; Schermann, M.; Kumar, K., *Angew. Chem. Int. Ed.* **2011,** 50 (30), 6900-6905.

24. Tietze, L. F.; Beifuss, U., *Angew. Chem.* **1993,** 105, 137.

25. Rivera, D. G.; Vercillo, O. E.; Wessjohann, L. A., *Org. Biomol. Chem.* **2008,** 6, 1787-1795.

26. Trost, B. M., *Science* **1991,** 254, 1471-1477.

27. Trost, B. M., *Angew. Chem.* **1995,** 107, 285-307.

28. Trost, B. M., *Angew. Chem. Int. Ed. Engl.* **1995,** 34 (3), 259-281.

29. Robinson, R., *J. Chem. Soc. Trans.* **1917**, 762-768.

30. Johnson, W. S.; Gravestock, M. B.; McCarry, B. E., *J. Am. Chem. Soc.* **1971,** 93 (24), 6696-6698.

31. Stark, A.; Shkumatov, A.; Russell, R. B., *Structure* **2004,** 12, 1405-1412.

32. Ley, S. V.; Brown, D. S.; Clase, J. A.; Fairbanks, A. J.; Lennon, I. C.; Osborn, H. M. I.; Stokes, E. S. E.; Wadsworth, D. J., *J. Chem. Soc. Perkin Trans. 1* **1998**, 2259-2276.

33. Nicolaou, K. C.; Lim, Y. H.; Papageorgiou, C. D.; Piper, J. L., *Angew. Chem. Int. Ed.* **2005,** 44 (48), 7917-7921.

34. Smith III, A. B.; Kim, D. S., *J. Org. Chem.* **2006,** 71 (7), 2547-2557.

35. Mi, Y.; Schreiber, J. V.; Corey, E. J., *J. Am. Chem. Soc.* **2002,** 124 (38), 11290-11291.

36. Nicolaou, K. C.; Simonsen, K. B.; Vassilikogiannakis, G.; S.Baran, P.; Vidali, V. P.; Pitsinos, E. N.; Couladouros, E. A., *Angew. Chem. Int. Ed.* **1999,** 38 (23), 3555-3559.

37. Barnes-Seeman, D.; Corey, E. J., *Org. Lett.* **1999,** 1 (9), 1503-1504.

38. Wenkert, E.; Vankar, Y. D.; Yadav, J. S., *J. Am. Chem. Soc.* **1980,** 102 (27), 7971-7972.

39. Zeng, Y.; Aubé, J., *J. Am. Chem. Soc.* **2005,** 127 (45), 15712-15713.

40. Evans, D. A.; Black, W. C., *J. Am. Chem. Soc.* **1993,** 115 (11), 4497-4513.

41. Vanderwal, C. D.; Vosburg, D. A.; Weiler, S.; Sorensen, E. J., *J. Am. Chem. Soc.* **2003,** 125 (18), 5393-5407.

42. Nicolaou, K. C.; Vassilikogiannakis, G.; Magerlein, W.; Kranich, R., *Angew. Chem. Int. Ed.* **2001,** 40 (13), 2482-2486.

43. Davies, H. M. L.; Dai, X.; Long, M. S., *J. Am. Chem. Soc.* **2006,** 128 (7), 2485-2490.

44. Kakeya, H.; Onose, R.; Koshino, H.; Yoshida, A.; Kobayashi, K.; Kageyama, S. I.; Osada, H., *J. Am. Chem. Soc.* **2002,** 124 (14), 3496-3497.

45. Kerr, D. J.; Willis, A. C.; Flynn, B. L., *Org. Lett.* **2004,** 6 (4), 457-460.

46. Panek, J. S.; Masse, C. E., *J. Org. Chem.* **1997,** 62 (24), 8290-8291.

47. Patil, N. T.; Konala, A.; Sravanti, S.; Singh, A.; Ummannib, R.; Sridharc, B., *Chem. Commun.* **2013,** 49, 10109-10111.

48. Sequin-Frey, M., *J. Chem. Ed.* **1981,** 58, (4), 301.

49. Zelentskii, A. N.; Fomin, G. V.; Kutafina, N. V.; Berlin, A. A., *B. Acad. SCI. USSR. Ch+* **1970,** 19, (5), 1106-1107.

50. Hunt, R. W. G.; Horwood, E., *Measuring Colour*. John Wiley & Sons: New York, 1987.

51. Golding, B. T.; Pierpoint, C., *Edu. Chem.* **1986,** 23 (3), 71-73.

52. Zollinger, H., *Color Chemistry: Syntheses, Properties, and Applications of Organic Dyes*. 3rd ed.; Willey-VCH: Zurich, 2003.

53. de Melo, J. S.; Rondao, R.; Burrows, H. D.; Melo, M. J.; Navaratnam, S.; Edge, E., *ChemPhysChem* **2006,** 7, 2303-2311.

54. Jacquemin, D.; Preat, J.; Wathelet, V.; Perpète, E. A., *J. Chem. Phys.* **2006,** 124 (074104), 1-12.

55. Polette-Niewold, L. A.; Manciu, F. S.; Torres, B.; Alvarado, M.; Chianelli, R. R., *J. Inorg. Biochem.* **2007,** 101 (11-12), 1958-1973.

56. Gribble, G. W.; Pelcman, B., *J. Org. Chem.* **1992,** 57 (13), 3636-3642.

57. Carter, D. S.; Vranken, D. L. V., *J. Org. Chem.* **1999,** 64 (23), 8537-8545.

58. Segraves, N. L.; Robinson, S. J.; Garcia, D.; Said, S. A.; Fu, X.; Schmitz, F. J.; Pietraszkiewicz, H.; Valeriote, F. A.; Crews, P., *J. Nat. Prod.* **2004,** 67 (5), 783-792.

59. Dubovitskii, S. V., *Tetrahedron Lett.* **1996,** 37 (29), 5207-5208.

60. Sasaki, T.; Ohtani, I. I.; Tanaka, J.; Higa, T., *Tetrahedron Lett.* **1999,** 40 (2), 303-306.

61. Bush, J. A.; Long, B. H.; Catino, J. J.; Bradner, W. T.; Tomita, K., *J. Antibiot.* **1987,** 40 (5), 668-678.

62. Plouffe, D.; Brinker, A.; McNamara, C.; Henson, K.; Kato, N.; Kuhen, K.; Nagle, A.; Adrián, F.; Matzen, J. T.; Anderson, P.; Nam, T. G.; Gray, N. S.; Chatterjee, A.; Janen, J.; Yan, S. F.; Trager, R.; Caldwell, J. S.; Schultz, P. G.; Zhou, Y.; Winzeler, E. A., *Proc. Natl. Acad. Sci.* **2008,** 105 (26), 9059-9064.

63.   Ch'ng, J. H.; Kotturi, S. R.; Chong, A. G.; Lear, M. J.; Tan, K. S., *Nature* **2010,** 1 (26), 1-13.

64.   Lawrie, A. M.; Noble, M. E. M.; Tunnah, P.; Brown, N. R.; Johnson, L. N.; Endicott, J. A., *Nat. Struct. Mol. Biol.* **1997**, 4, 796-801.

65.   Bonjouklian, R.; Smitka, T. A.; Doolin, L. E.; Molloy, R. M.; Debono, M.; Shaffer, S. A., *Tetrahedron* **1991,** 47 (37), 7739–7750.

66.   Benkendorff, K.; Bremner, J. B.; Davis, A. R., *J. Chem. Ecol.* **2000,** 26 (4), 1037-1050.

67.   Maskey, R. P.; Grün-Wollny, I.; Fiebig, H. H.; Laatsch, H., *Angew. Chem. Int. Ed.* **2002,** 41, 590-597.

68.   Christie, R. M., *Biotech. Histochem.* **2007,** 82 (2), 51-56.

69.   Baeyer, A.; Emmerling, K., *Ber . Dtsch. Chem. Ges.* **1870,** 3, 514.

70.   Baeyer, A., *Ber . Dtsch. Chem. Ges.* **1879,** 12, 456.

71.   Bayer, A.; Drewson, V., *Ber . Dtsch. Chem. Ges.* **1882,** 15, (2), 2856-2864.

72.   Pfleger, J., *US Patent* **1901,** 680, 1-2.

73.   Heumann, K., *Ber . Dtsch. Chem. Ges.* **1890,** 23, 3431.

74.   Lucius, M.; Brüning, *German Pat.* **1919,** DE204884.

75.   Yamamoto, Y.; Inoue, Y.; Takaki, U.; Suzuki, H., *Bull. Chem. Soc. Jpn.* **2011,** 84, (1), 82-89.

76.   Erdmann, O. L., *J. Prakt. Chem.* **1841,** 24, (1), 1-18.

77.   Erdmann, O. L., *J. Prakt. Chem.* **1840,** 19, (1), 321-362.

78.   van-Alphen, J., *Recl. Trav. Chim.* **1938,** 57, (9), 911-914.

79.   Kalb, L., *Ber. Dtsch. Chem. Ges.* **1909,** 42, (3), 3642-3652.

80.   Sumpter, W. C.; Miler, F. M., *Heterocyclic Compounds Indole Carbazole* Interscience Publishers: New York, **1954**; p 180.

81. Beggiato, G.; Casalboremiceli, G.; Geri, A.; Pietropaolo, D., *Ann. Chim. (Roma)* **1993,** 83, (7-8), 355-363.

82. Berzelius, J. J., *Ann. Phys.* **1827,** 86, (1) 105-136.

83. Grandmougin, E., *J. Prakt. Chem.* **1907,** 76 (1), 124-142.

84. Komorsky-Lovric, S., *J. Electroanal. Chem.* **2000,** 482, 222-225.

85. Bond, A. M., *J. Chem. Soc., Perkin Trans. 2* **1997**, 2 (9), 1735-1742.

86. Vorländer, D.; von Pfeiffer, J., *Ber. Dtsch. Chem. Ges.* **1919,** 52 (2), 325-329.

87. Schützenberger, P., *Comptes. Rendus.* **1877,** 85, 147.

88. Binz, A., *Angew. Chem.* **1906,** 19 (33), 1415-1418.

89. Binz, A.; Kufferath, A., *Justus Lieb. Ann. Chem.* **1902,** 325 (2), 196-204.

90. Bloxam, W. P., *J. Chem. Soc. Trans.* **1905,** 87, 974-987.

91. Friedländer, P.; Schwenk, E., *Ber. Dtsch. Chem. Ges.* **1910,** 43 (2), 1971-1975.

92. Borsche, W.; Meyer, R., *Ber. Deutsch. Chem. Ges.* **1921,** 54 (10), 2854-2856.

93. Thiele, J.; Pickard, R. H., *Ber . Dtsch. Chem. Ges.* **1898,** 31 1252-1253.

94. Madelung, W., *Justus Lieb. Ann. Chem.* **1914,** 405 (1), 58-95.

95. Jensen, L. B., *J. Near Eastern Stud.* **1963,** 22, 104-118.

96. Bruin, F., *Socitis et Campagnies de Commerce en Orient dunsl'Ocean Indien;*. Mollat, M., Ed.; S. E. V. P. E. N.: Paris, 1970.

97. McGovern, P. E.; Michel, R. H., *Acc. Chem. Res.* **1990,** 23 (5), 152-165.

98. Baker, J. T., *Endeavor* **1974,** 33, 11-17.

99. Christophersen, C.; Watjen, F.; Buchardt, O.; Anthoni, U., *Tetrahedron* **1978,** 34 (18), 2779-2781.

100. McGovern, P. E.; Michel, R. H., *Acc. Chem. Res.* **1990,** 23 (5), 152-158.

101. Cooksey, C. J., *Molecules* **2001,** 6, 736-769.

102. Born, W., *Ciba Reu.* **1937,** 1 (106-111), 124-128.

103. Sachs, F.; Kempf, R., *Ber. Dtsch. Chem. Ges.* **1903,** 36 (3), 3299-3303.

104. Imming, P.; Imhof, I.; Zentgraf, M., *Synth. Commun.* **2001,** 31, 153-159.

105. Voss, G.; Gerlach, H., *Chem. Ber.* **1989,** 122, 1199-1201.

106. Cooksey, C. J., *Dyes Hist. Archaeol.* **1995,** 13 7-13.

107. Kröhnke, F., *Angew. Chem. Int. Ed.* **1963,** 2 (7), 380-393.

108. Friedländer, P.; Bruckner, S.; Deutsch, G., *Justus Lieb. Ann. Chem.* **1912,** 388, 23-49.

109. Ettinger, L.; Friedländer, P., *Ber. Deutsch. Chem. Ges.* **1912,** 45 (2), 2074-2080.

110. Claus, A.; Scheulen, M. E., *J. Prakt. Chem.* **1891,** 43, 200-206

111. Waldmann, H., *J. Prakt. Chem.* **1930,** 126, 65-68.

112. Grandmougin, E.; Seyder, P., *Ber. Deutsch. Chem. Ges.* **1914,** 47, 2365-2373.

113. Majima, R.; Kotake, M., *Ber. Dtsch. Chem. Ges.* **1930,** 63B, 2237-2245.

114. Tanoue, Y.; Terada, A.; Sakata, K.; Hashimoto, M.; Morishita, S.; Hamada, M.; Kai, N.; Nagai, T., *Fisheries Sci.* **2001,** 67, 726-729.

115. Darvekar, M.; Ghorpade, B.; Vankar, P. S., *Asian J. Chem.* **2004,** 16 (2), 965-970.

116. Masterson, T. L., *US Patent* **1936,** 2036487, (670512), 2.

117. Kalb, L.; Berrer, D., *Ber . Dtsch. Chem. Ges.* **1924,** 57, 2105.

118. Wolthuis, E.; Nawiasky, P., *US Patent* **1942,** US 22700170 A, 1225-1125.

119. Grandmougin, E., *Ber. Dtsch. Chem. Ges.* **1909,** 42 (3), 4408-4411.

120. Crum, R., *Berz. Jahresb.* **1825,** 4, 189.

121. Vogel, A. I., *Ber. Dtsch. Chem. Ges.* **1878,** 11, 1365.

122. Grandmougin, E., *Comp. Rend.* **1921,** 173, 586.

123. Oakley, S. R.; Nawn, G.; Waldie, K. M.; MacInnis, T. D.; Patrick, B. O.; Hicks, R. G., *Chem. Comm.* **2010,** 46, 6753-6753.

124. Sachs, F.; Kantorowicz, H., *Ber. Dtsch. Chem. Ges.* **1909,** 42 (2), 1565.

125. Kuhn, R.; Trischmann, H., *Chem. Ber.* **1961,** 94 (8), 2258-2263.

126. Kitao, T.; Sestune, J., *Kenkyu Hokoku* **1989,** 55 (73), 73-81.

127. Matsumoto, Y.; Tanaka, H., *Heterocycles* **2003,** 60 (8), 1805-1810.

128. Blanc, J.; Ross, D., *J. Phys. Chem.* **1968,** 72, 2817.

129. Liebermann, C.; Dickhuth, F., *Ber . Dtsch. Chem. Ges.* **1891,** 24 (2), 4130-4136.

130. Kitao, T.; Ishihara, S.; Setsune, J.; Matsukawa, K.; Wakemoto, H.; Yamamoto, R., *J. Chem. Soc., Chem. Commun.* **1982**, (17), 1022-1023.

131. Smith, B. D.; Alonso, D. E.; Bein, J. T.; Metzler, E. C.; Shang, M.; Roosenberg, J. M., *J. Org. Chem.* **1994,** 59, 8011-8014.

132. Pummerer, R., *Ber . Dtsch. Chem. Ges.* **1947,** 80, (3), 242-248.

133. Pummerer, R., *Justus Lieb. Ann. Chem.* **1940,** 544 (1), 206-239.

134. Posner, T.; Zimmermann, W.; Kautz, S., *Ber. Dtsch. Chem. Ges.* **1929,** 62, 2150.

135. Schwartz, R., *J. Prakt. Chem.* **1863,** 91, 382.

136. Hope, E.; Richter, D., *J. Chem. Soc.* **1932**, 2783-2787.

137. Dessoulavy, E., *Ber. Dtsch. Chem. Ges.* **1909,** 42 (3), 3636-3641.

138. Engi, G., *Angew. Chem.* **1914,** 27 (20), 144-148.

139. Posner, T.; Hofmeister, R., *Ber. Dtsch. Chem. Ges.* **1926,** 59 (8), 1827-1835.

140. deDiesbach, H.; Heppner, E., *Helv. Chim. Acta.* **1949,** 32 (3), 687-691.

141. Rihs, G.; Tzikas, A., *Dyes Pigments* **1983,** 4, 163-169.

142. Lucius, F. M.; Höchst, B., *Germ. Pat.* Frdl. **1903,** 7, 637.

143. deDiesbach, H.; Frossard, M., *Helv. Chim. Acta.* **1954,** 37, 701.

144. Rogers, D. Z.; Bruice, T. C., *J. Am. Chem. Soc.* **1979,** 101 (6), 4713-4719.

145. Posner, T.; Kemper, W., *Ber . Dtsch. Chem. Ges.* **1924,** 57 (8), 1311-1315.

146.   Abdel-Hamid, M. K.; Bremner, J. B.; Coates, J.; Keller, P. A.; Miländer, C.; Torkamani, Y. S.; Skelton, B. W.; White, A. H.; Willis, A. C., *Tetrahedron Lett.* **2009,** 50 (50), 6947-6950.

147.   Beesley, R. M.; Ingold, C. K.; Thorpe, J. F., *J. Chem. Soc.* **1915,** 107, 1080-1106.

148.   Jung, M. E.; Piizzi, G.; Zalkow, V., *Chem. Rev.* **2005,** 105, 1735-1766.

149.   Buergi, H. B.; Dunitz, J. D., *Acc. Chem. Res.* **1983,** 16 (5), 153-161.

150.   Araya-Maturana, R.; Delgado-Castro, T.; Cardona, W.; Weiss-López, B., *Curr. Org. Chem.* **2001,** 5, 253-263.

151.   Blinov, K. A.; Buevich, A. V.; Williamsonc, R. T.; Martin, G. E., *Org. Biomol. Chem.* **2014** 12, 9505-9509.

152.   Williamson, D. S.; Smith, R. A.; Nagel, D. L.; Cohen, S. M., *J. Magn. Reson., Ser A* **1989,** 82, 605-612.

153.   Tapia, R. A.; Prieto, Y.; Pautet, F.; Fenet, B.; Fillion, H., *Magn. Reson. Chem.* **2002,** 40, 165-167.

154.   Furrer, J., *Concepts Magn. Reson. Part A* **2012,** 40A, (3), 146-169.

155.   Johnson, R. P., *Chem. Rev.* **1989,** 89, 1111-1124.

156.   Krause, A. N.; Hashmi, S. K., *Modern Allene Chemistry*. 1st ed.; Wiley-VCH: Weinheim, 2004; Vol. 1.

157.   Daoust, K. J.; Hernandez, S. M.; Konrad, K. M.; Mackie, I. D.; Winstanley, J.; Johnson, R. P., *J. Org. Chem.* **2006,** 71, 5708-5714.

158.   Moemming, C. M.; Kehr, G.; Wibbeling, B.; Froehlich, R.; Schirmer, B.; Grimme, S.; Erker, G., *Angew. Chem. Int. Ed.* **2010,** 49, 2414-2417.

159.   Dardonville, C.; Jimeno, M. L.; Alkortaa, I.; Elgueroa, J., *Org. Biomol. Chem.* **2004,** 2, 1587-1591.

160. Vogel, E.; Altenbach, H.-J.; Drossard, J.-M.; Schmickler, H.; Stegelmeier, H., *Angew. Chem. Int. Ed.* **1980,** 19, 1016-1018.

161. Le Nôtre, J.; Touzani, R.; Lavastre, O.; Bruneau, C.; Dixneuf, P. H., *Adv. Synth. Catal.* **2005,** 347, 783-791.

162. Piedra, E.; Francos, J.; Nebra, N.; Suárez, F. J.; Díez, J.; Cadierno, V., *Chem. Commun.* **2011,** 47, 7866-7868.

163. Abraham, M.; Reischl, W.; Kirchner, K. A.; Roller, A.; Veiros, L. F.; Widhalm, M., *Molecules* **2012,** 17, 14531-14554.

164. Linton, E. C.; Kozlowski, M. C., *J. Am. Chem. Soc.* **2008,** 130 (48), 16162-16163.

165. Kimura, M.; Futamata, M.; Mukai, R.; Tamaru, Y., *J. Am. Chem. Soc.* **2005,** 127 (13), 4592-4593.

166. Trost, B. M.; Quancard, J., *J. Am. Chem. Soc.* **2006,** 128 (19), 6314.

167. Chen, J.; Cook, M. J., *Org. Lett.* **2013,** 15 (5), 1088.

168. Müller, T. E.; Beller, M., *Chem.Rev.* **1998,** 98, 675.

169. Das, A.; Chaudhuri, R.; Liu, R.-S., *Chem.Commun.* **2009**, 4046.

170. Xiao, Z., *Leuk. Lymp.* **2002,** 43, 1763-1768.

171. Jautelat, R.; Brumby, T.; Schaefer, M.; Briem, H.; Eisenbrand, G.; Schwahn, S.; Krueger, M.; Luecking, U.; Prien, O.; Siemeister, G., *ChemBioChem* **2005,** 6, 531-540.

172. Choi, S. J.; Lee, J. E.; Jeong, S. Y.; Im, I.; Lee, S. D.; Lee, E. J.; Lee, S. K.; Kwon, S. M.; Ahn, S. G.; Yoon, J. H.; Han, S. Y.; Kim, J. I.; Kim, Y. C., *J. Med. Chem.* **2010**, 3696-3706.

173. Hoessel, R.; Leclerc, S.; Endicott, J. A.; Nobel, M. E. M.; Lawrie, A.; Tunnah, P.; Leost, M.; Damiens, E.; Marie, D.; Marko, D.; Niederberger, E.; Tang, W.; Eisenbrand, G.; Meijer, L., *Nat. Cell Biol.* **1999,** 1, 60-67.

174. Desjardins, R. E.; Canfield, C. J.; Haynes, J. D.; Chulay, J. D., *Antimicrob. Agents Chemother.* **1979,** 16, 710-718.

175. Maheo, K.; Vibet, S.; Steghens, J. P.; Dartigeas, C.; Lehman, M.; Bougnoux, P.; Gore, J., *Free Radic. Biol. Med.* **2005,** 39, 742-751.

176. Vassilev, L. T.; Vu, B. T.; Graves, B.; Carvajal, D.; Podlaski, F.; Filipovic, Z., *Science* **2004,** 303, 844-848.

177. Wang, H.; Ma, X.; Ren, S.; Buolamwini, J. K.; Yan, C., *Mol. Cancer. Ther.* **2011,** 10, 69-79.

178. Ding, K.; Lu, Y. P.; Nikolovska-Coleska, Z.; Wang, G. P.; Qiu, S.; Shangary, S., *J. Med. Chem.* **2006,** 49, 3432-3435.

179. Zhao, Y.; Bernard, D.; Wang, S., *BioDiscovery* **2013,** 8 (4), 1-15.

180. Changsen, C.; Franzblau, S. G.; Palittapongarnpim, P., *Antimicrob. Agents Chemother.* **2003,** 47, 3682-3687.

181. O'Brien, J.; Wilson, I.; Orton, T.; Pognan, F., *Eur. J. Biochem.* **2000,** 267, 5421-5426.

182. Müller, B.; Borrell, S.; Rose, G.; Gagneux, S., *Trends Genet.* **2013,** 29, 160-169.

183. Vine, K. L.; Matesic, L.; Locke, J. M.; Ranson, M.; Skropeta, D., *Anti-Cancer Agents Med. Chem.* **2009,** 9, 397-414.

184. Vine, K. L.; Locke, J. M.; Ranson, M.; Pyne, S. G.; Bremner, J. B., *J. Med. Chem.* **2007,** 50, 5109-5117.

185. Matesic, L.; Locke, J. M.; Bremner, J. B.; Pyne, S. G.; Skropeta, D.; Ranson, M.; Vine, K. L., *Bioorg. Med. Chem.* **2008,** 16, 3118-3124.

186. Sele, A.; Bremner, J. B.; Keller, P. A.; Willis, T., **2013**, *PhD. Thesis,* University of Wollongong, Australia.

187. Soni, R.; Muller, L.; Furet, P.; Schoepfer, J.; Stephan, C.; Zumstein-Mecker, S.; Fretz, H.; Chaudhuri, B., *Biochem. Biophys. Res. Commun.* **2000,** 275, 877-884.

188. Bharate, S. B.; Manda, S.; Mupparapu, N.; Battini, N.; Vishwakarma, R. A., *Mini-Rev. Med. Chem.* **2012,** 12, (6), 1-15.

189. Lu, X.; Zheng, Y.; Chen, H.; Yan, X.; Wang, F.; Xu, W., *Yaoxue Xuebao* **2009,** 44, 980-986.

190. Yan, X.; Chen, H.; Lu, X.; Wang, F.; Xu, W.; Jin, H.; Zhu, P., *Eur. J. Pharm. Sci.* **2011,** 42, 251-259.

191. Waldmann, H.; Eberhardt, L.; Wittstein, K.; Kumar, K., *Chem. Commun.* **2010,** 7, 4622-4624.

192. Baranova, O. V.; Zhidkov, M. E.; Dubovitskii, S. V., *Tetrahedron Lett.* **2011,** 52 (18), 2397-2398.

193. Dyker, G., *Angew. Chem. Int. Ed.* **1999,** 38 (13), 1698-1702.

194. Murai, T.; Mutoh, Y.; Ohta, Y.; Murakami, M., *J. Am. Chem. Soc.* **2004,** 126 (19), 5968-5973.

195. Jung, M. E.; Huang, A., *Org. Lett.* **2000,** 2 (12), 2659-2665.

196. Pron, A.; Rannou, P., *Prog. Polym. Sci.* **2002,** 27, 135-190.

197. Rogers, D. Z.; Bruice, T. C., *J. Am. Chem. Soc.* **1979,** 101 (16), 4713-4719.

198. He, B.; Pun, A. B.; Zherebetskyy, D.; Liu, Y.; Liu, F.; Klivansky, L. M.; McGough, A. M.; Zhang, B. A.; Lo, K.; Russell, T. P.; Wang, L.; Liu, Y., *J. Am. Chem. Soc.* **2014,** 136 (2), 15093-15101.

199. Ullmann, F.; Bielecki, J., *Ber . Dtsch. Chem. Ges.* **1901,** 34 (2), 2174-2185.

200. Aboul-Fadi, T.; Abdel-Hamid, F.; Hassan, E. A., *Arch. Pharm. Res.* **2003,** 26, 778-784.

201. Radul, O. M.; Zhungietu, G. I.; Rekhter, M. A.; Bukhanyuk, S. M., *Khim. Geterotsikl. Soedin.* **1983,** 3, 353-355.

202. Trager, W.; Jensen, J. B., *Science* **1976,** 193 (4254), 673-675.

203. Otwinowski, Z.; Minor, W., Academic Press: New York, 1997; Vol. Part A.

204. Altomare, A.; Cascarano, G.; Giacovazzo, C.; Guagliardi, A.; Burla, M. C.; Polidori, G.; Camalli, M. J., *Appl. Crystallogr.* **1994,** 27, 435-436.

205. Betteridge, P. W.; Carruthers, J. R.; Cooper, R. I.; Prout, K.; Watkin, D. J., *J. Appl. Crystallogr.* **2003,** 36, 1487.

Appendices

9.1 Appendix 1: ^{1}H NMR, ^{13}C NMR and selected 2D NMR

Compound 230
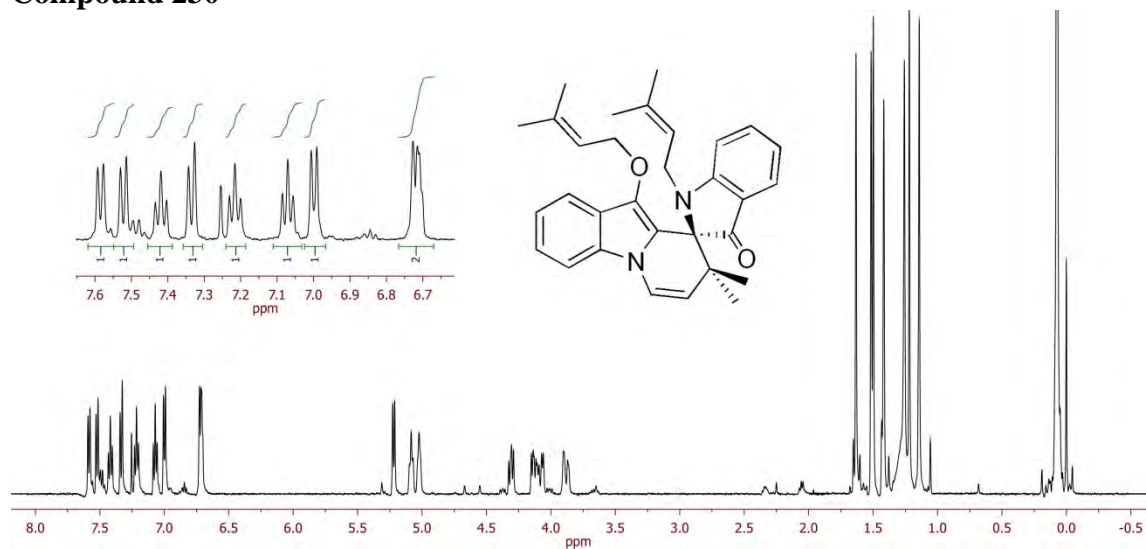
Figure 84: ^{1}H NMR spectrum for compound **230**.
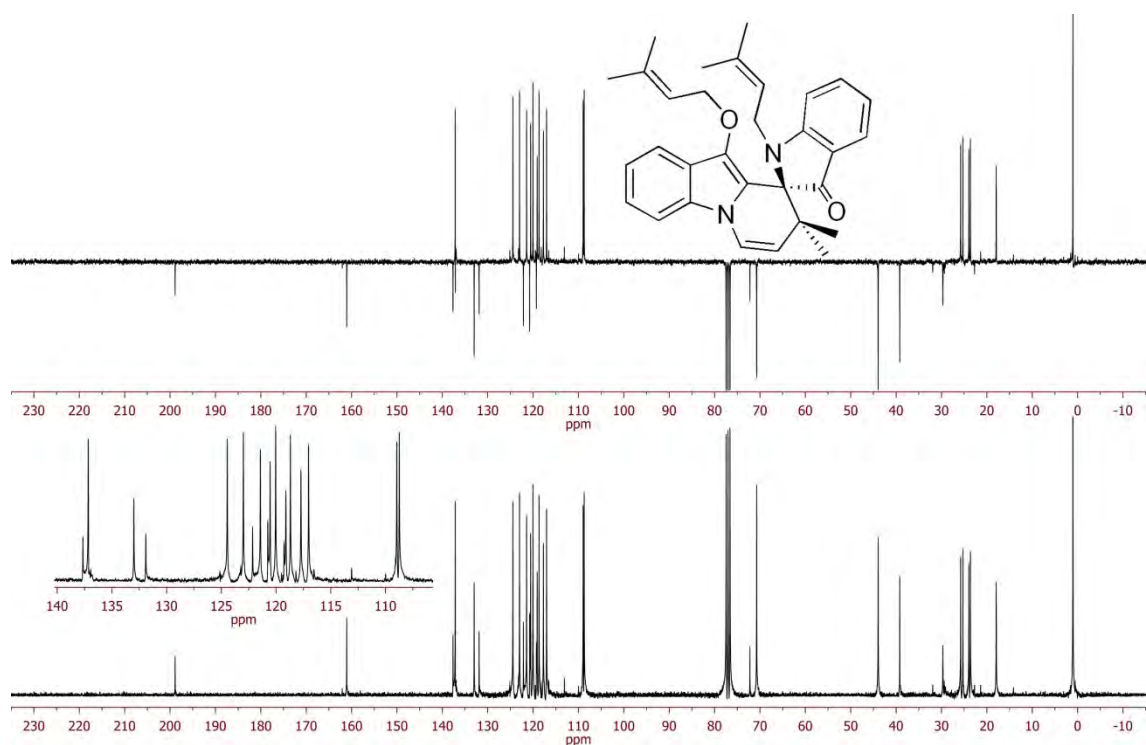
Figure 85: ^{13}C NMR spectrum for compound **230**.
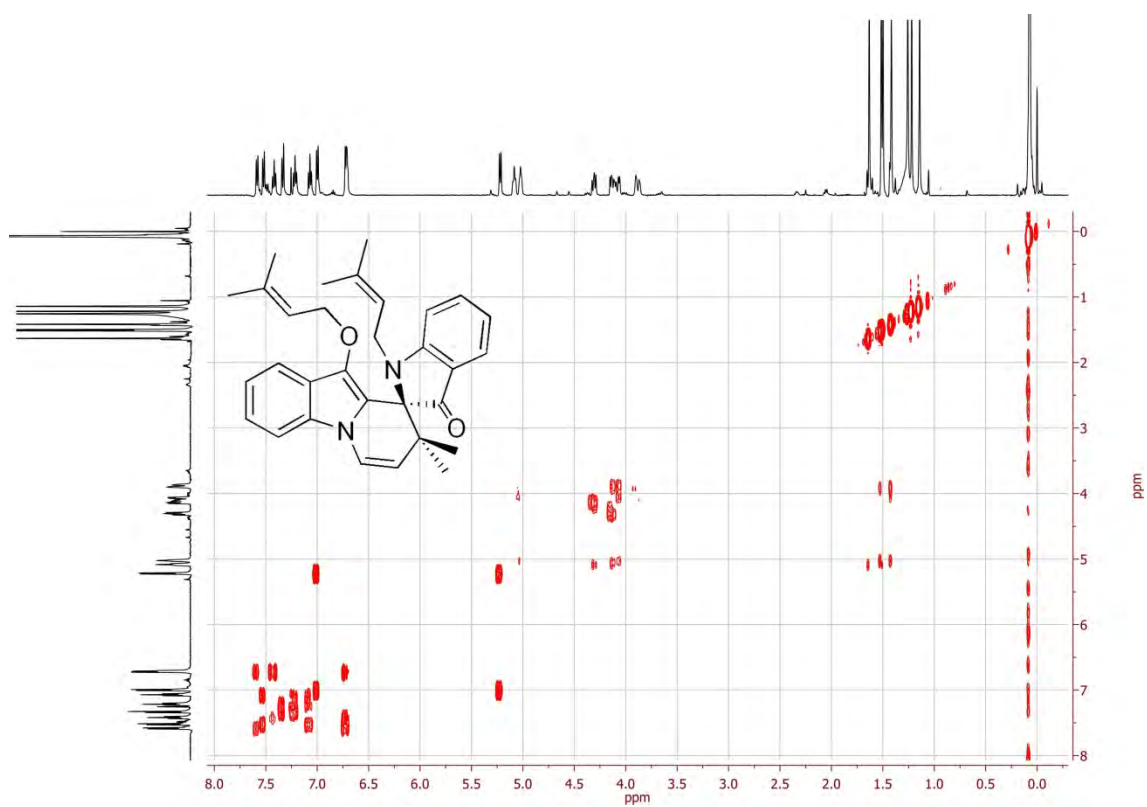
Figure 86: The gCOSY and its expansions for compound **230**.
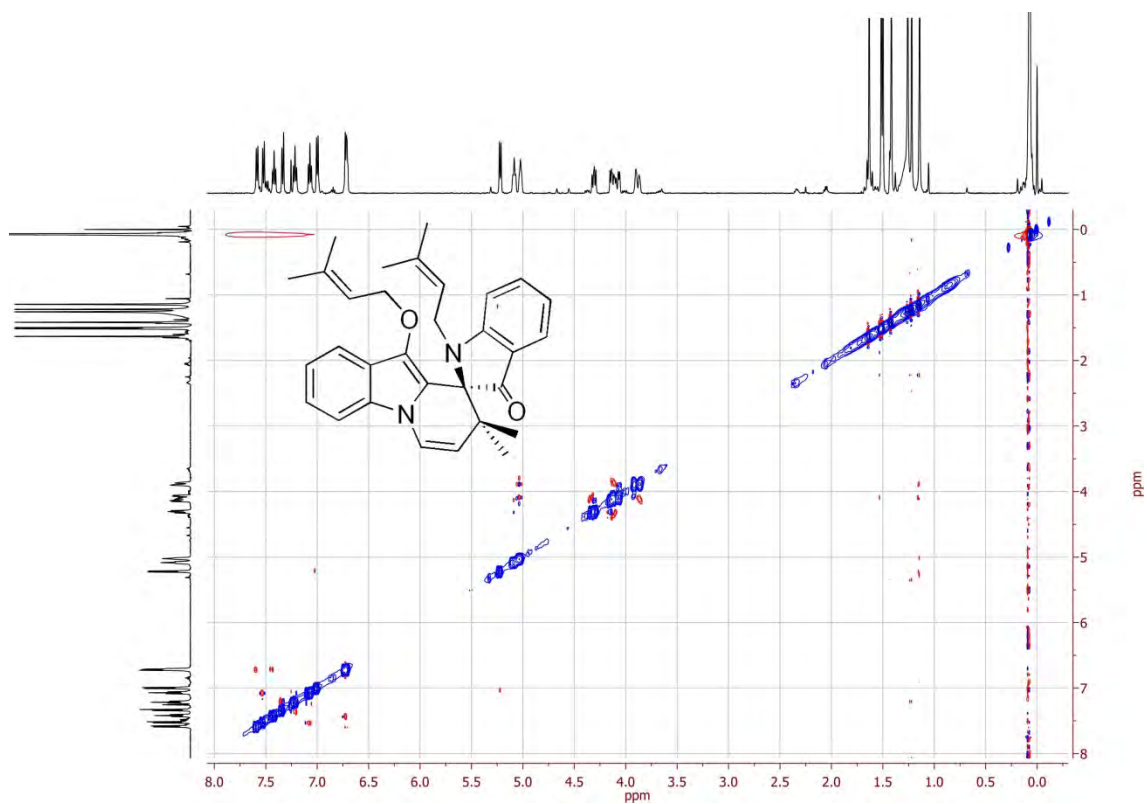
Figure 87 The NOSEY and its expansions for compound **230**.
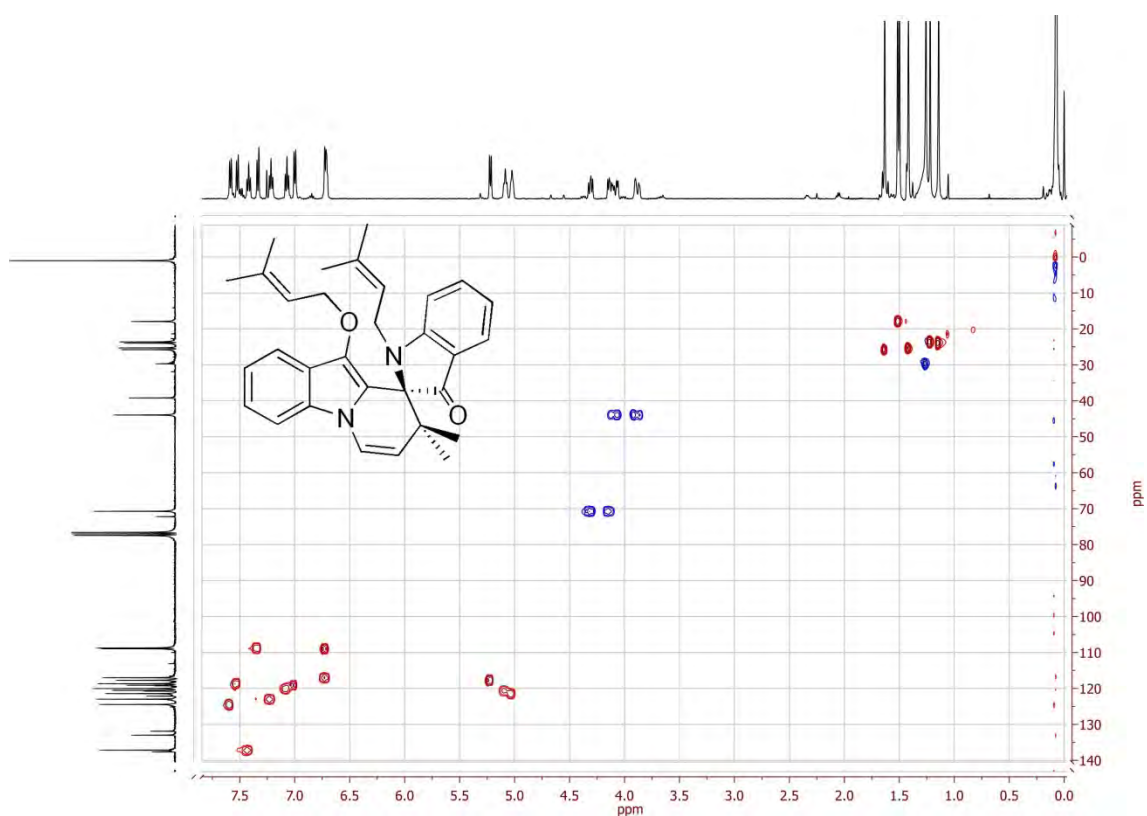
Figure 88: The gHSQC for compound **230**.
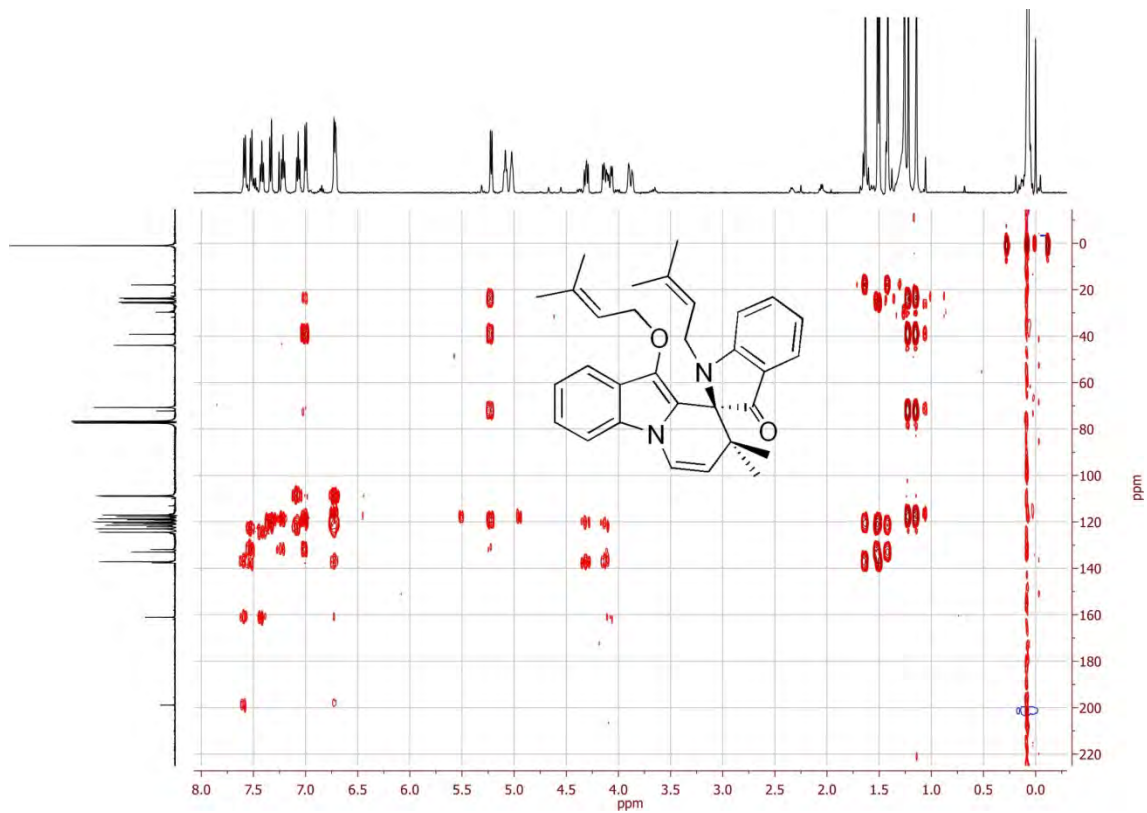
Figure 89: The gHMBC for compound **230**.

Compound 243
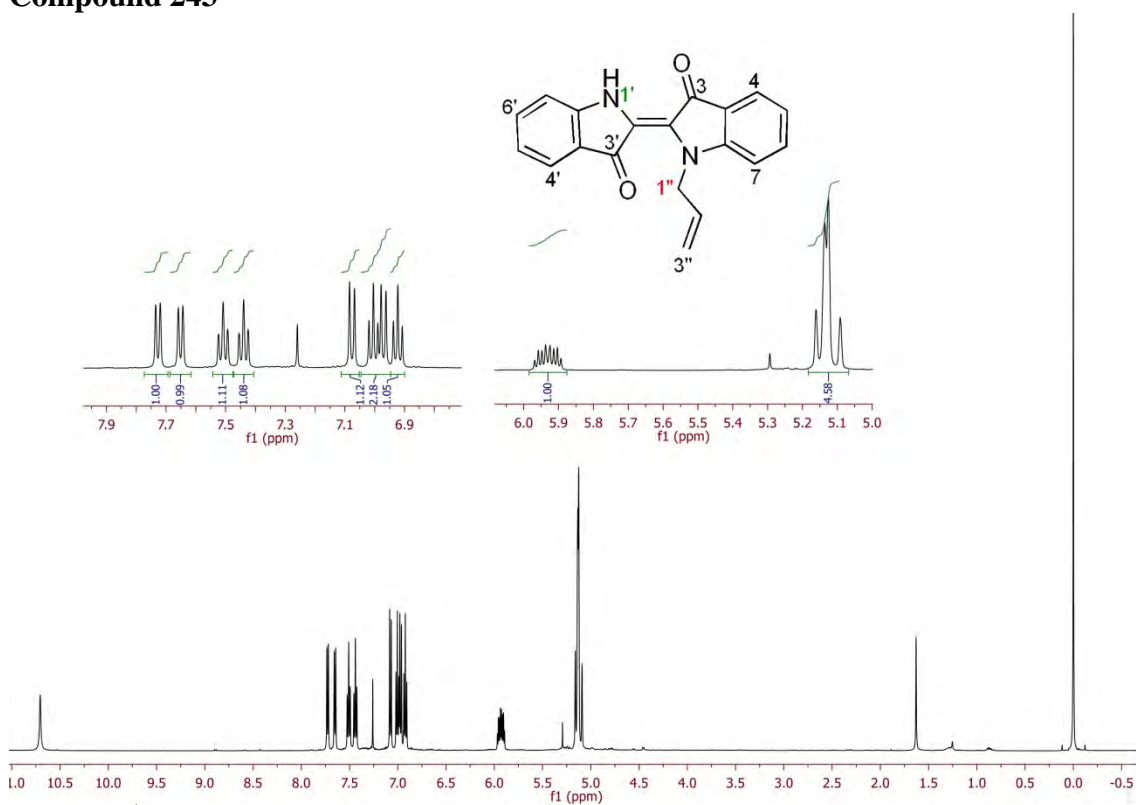
Figure 90: ^{1}H NMR spectrum for compound **243**.
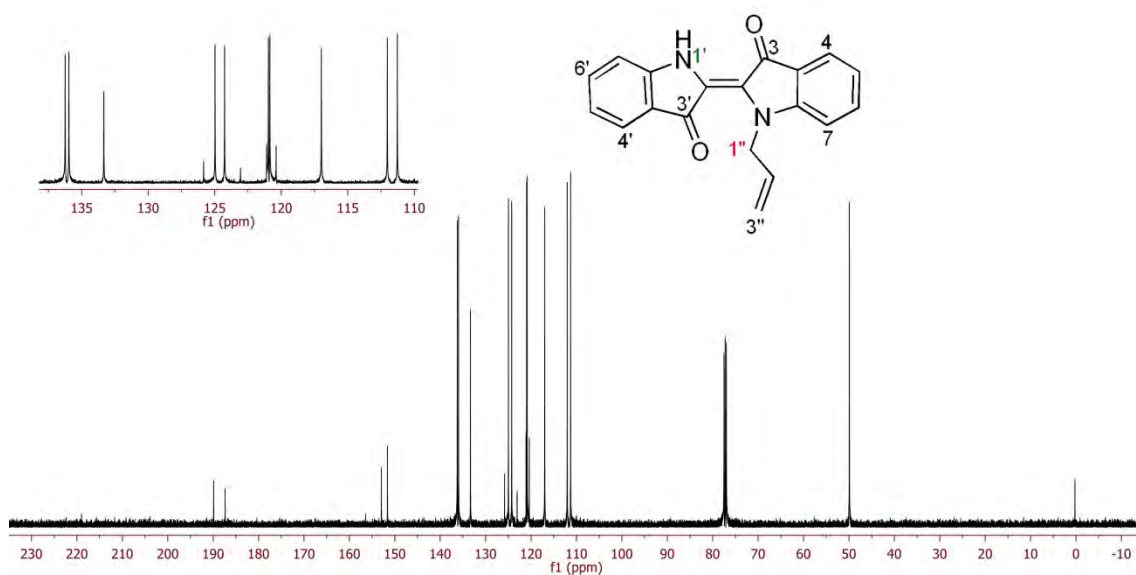
Figure 91: ^{13}C NMR spectrum for compound **243**.

Compound 248
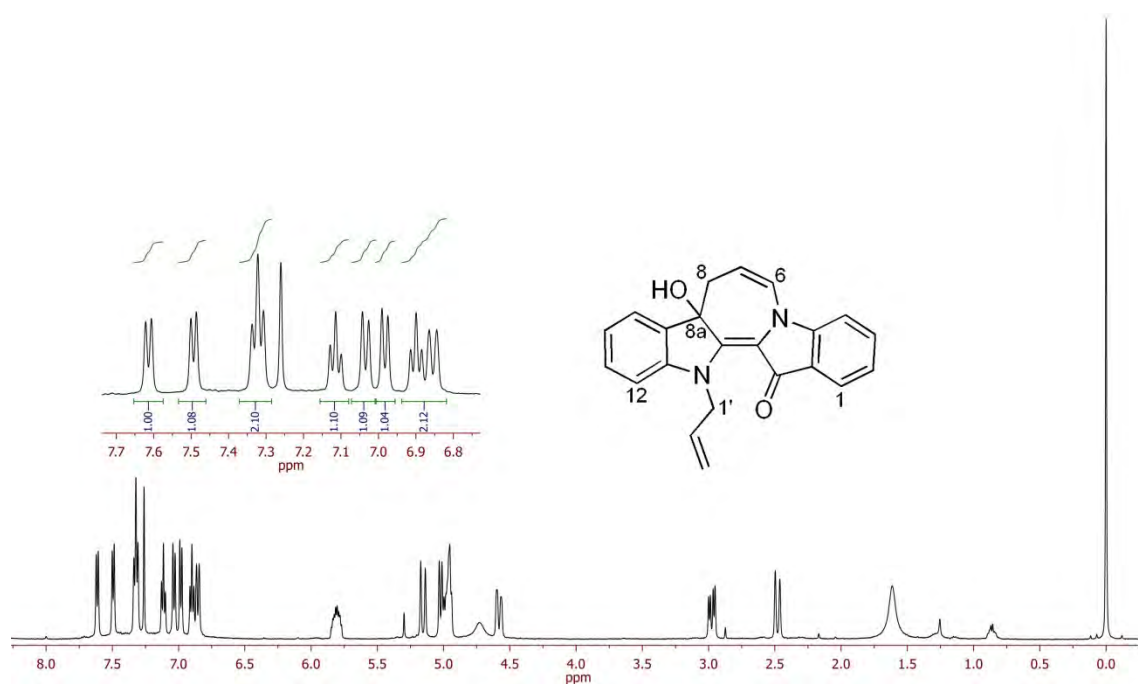
Figure 92: ^{1}H NMR spectrum for compound **248**.
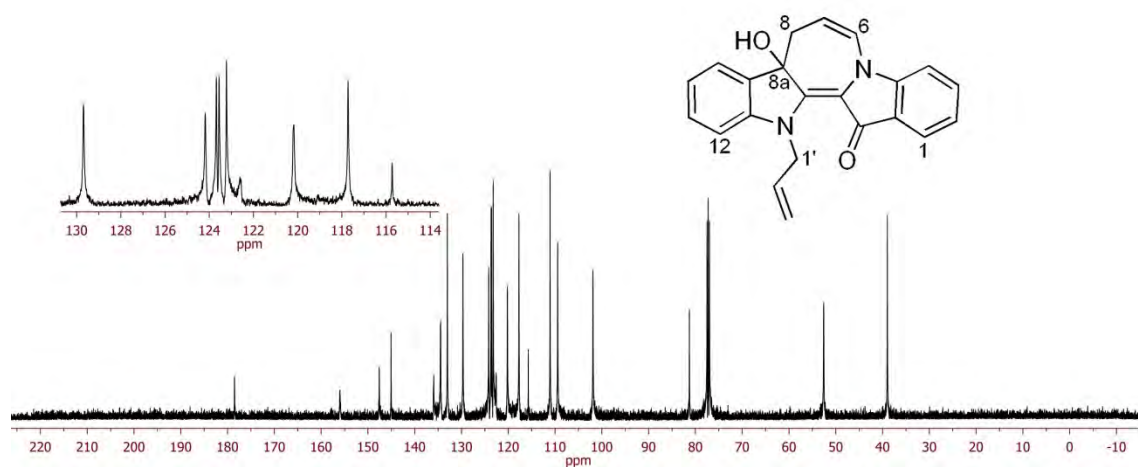
Figure 93: ^{13}C NMR spectrum for compound **248**.
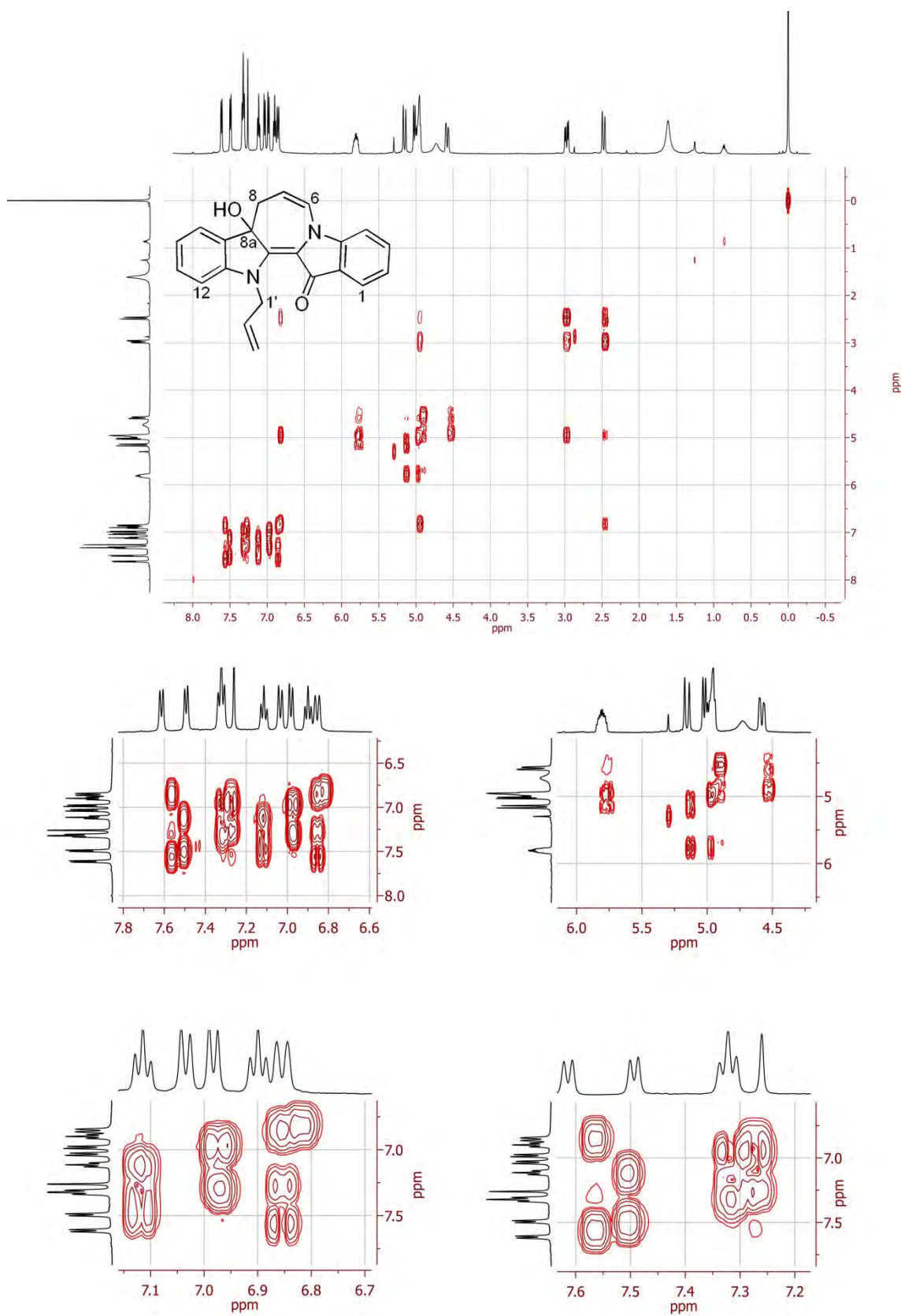
Figure 94: The gCOSY and its expansions for compound **248**.
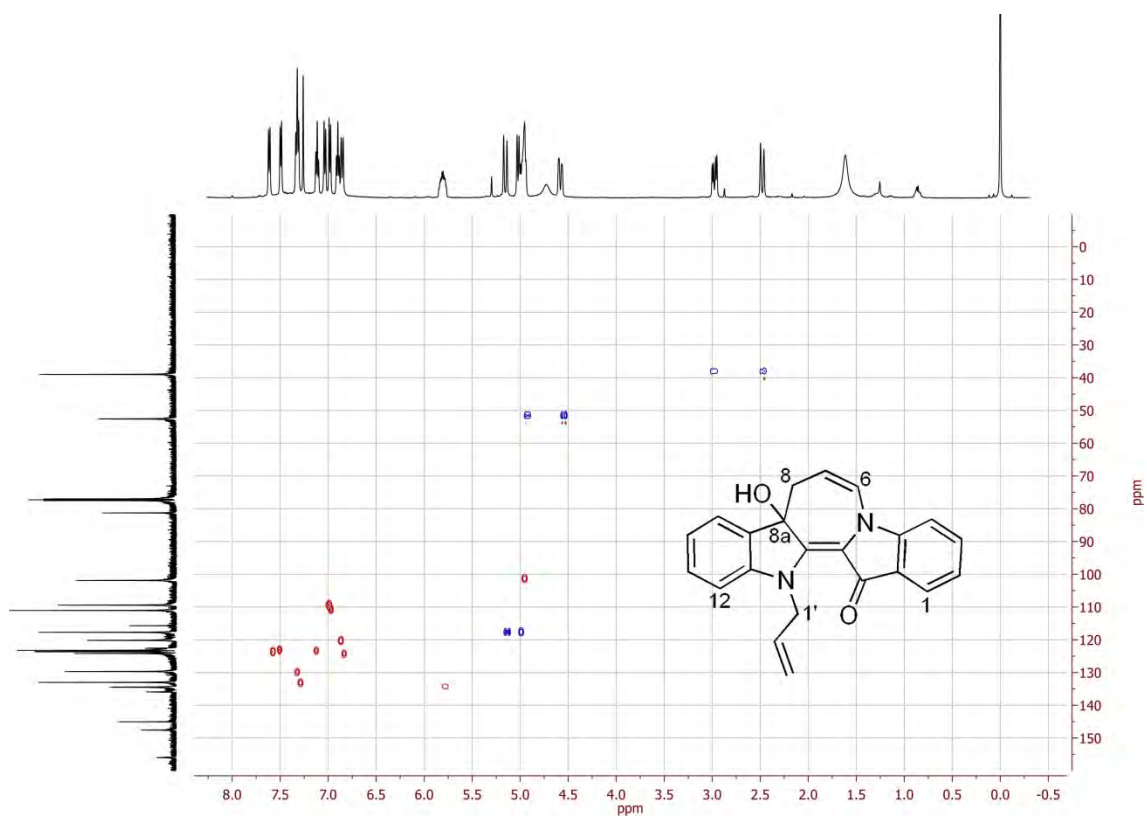
Figure 95: The gHSQC for compound **248**.
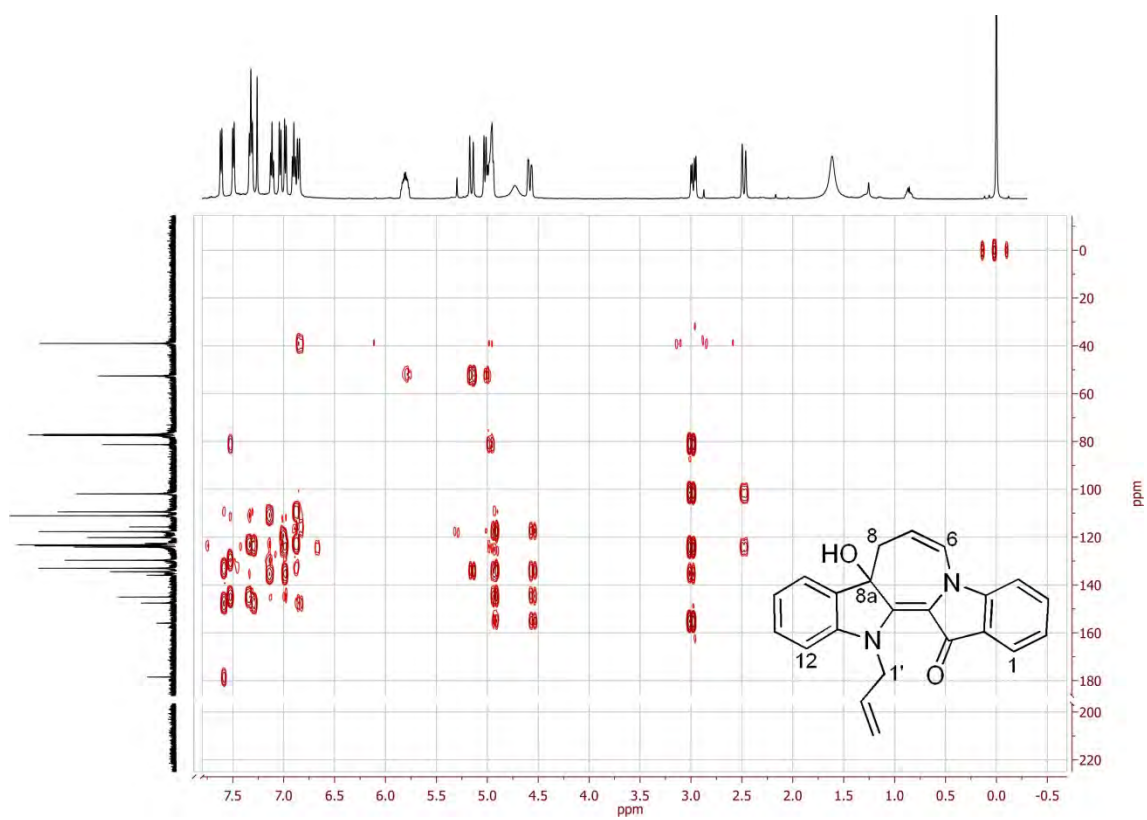
Figure 96: The gHMBC for compound **248**.

Compound 249
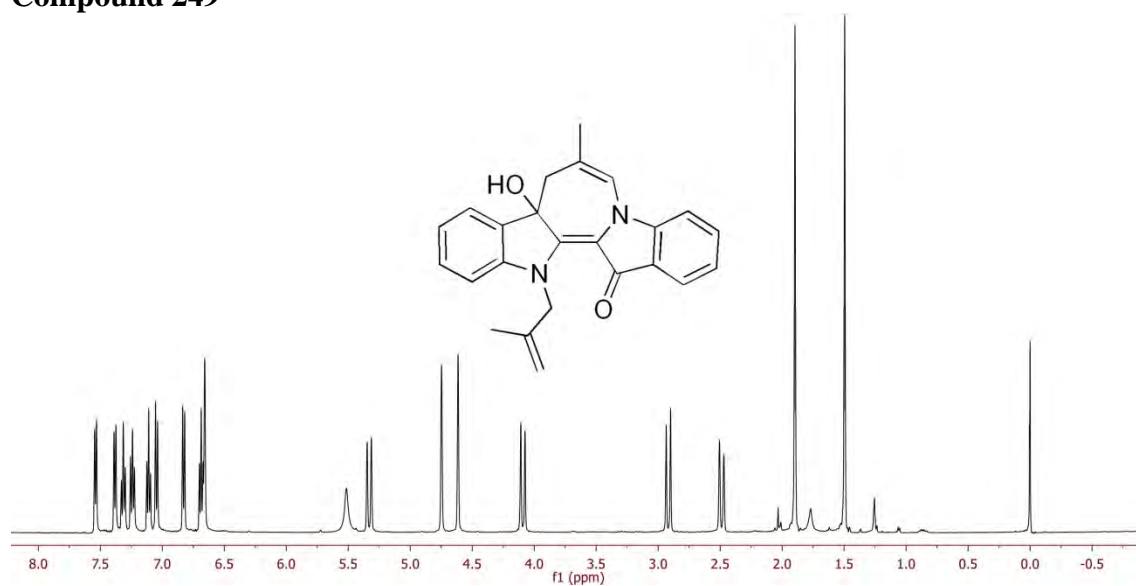
Figure 97: ^{1}H NMR spectrum for compound **249**.
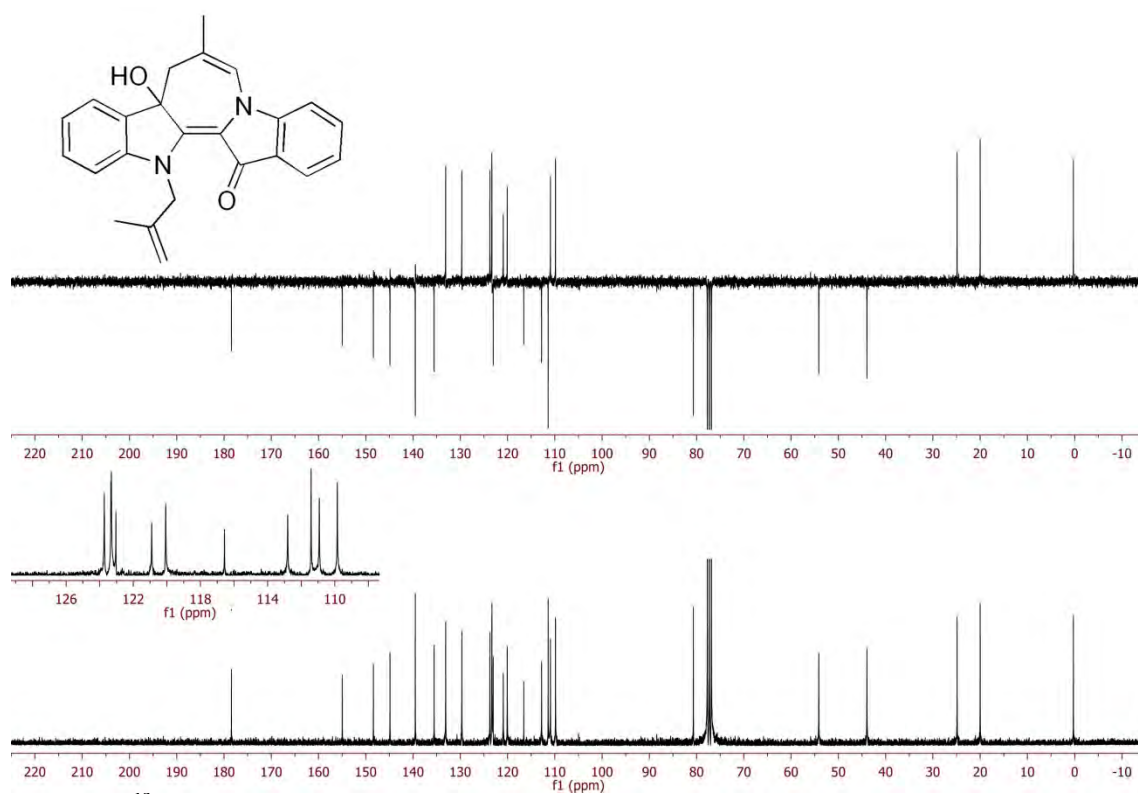
Figure 98: ^{13}C NMR spectrum for compound **249**.
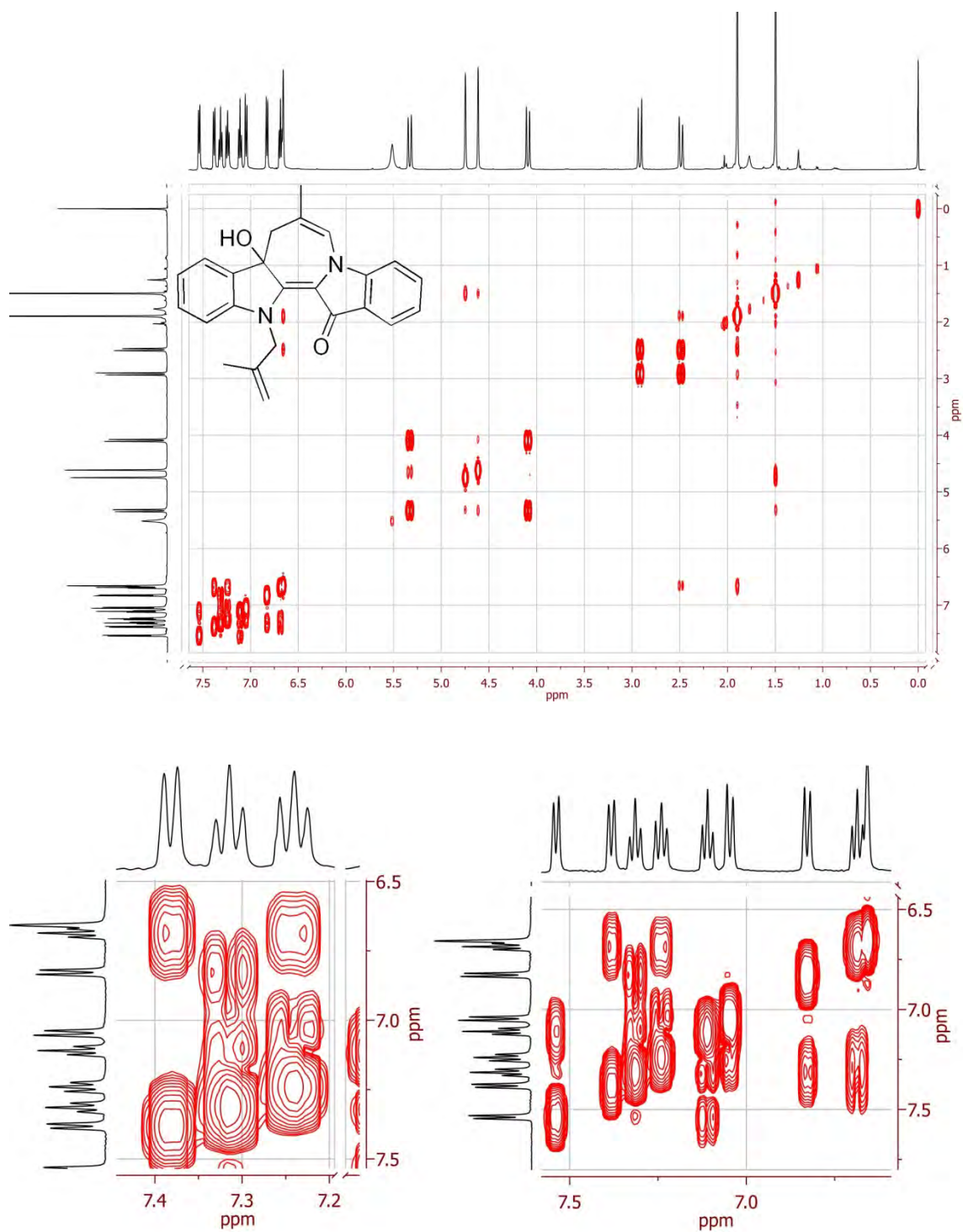
Figure 99: The gCOSY and its expansions for compound **249**.
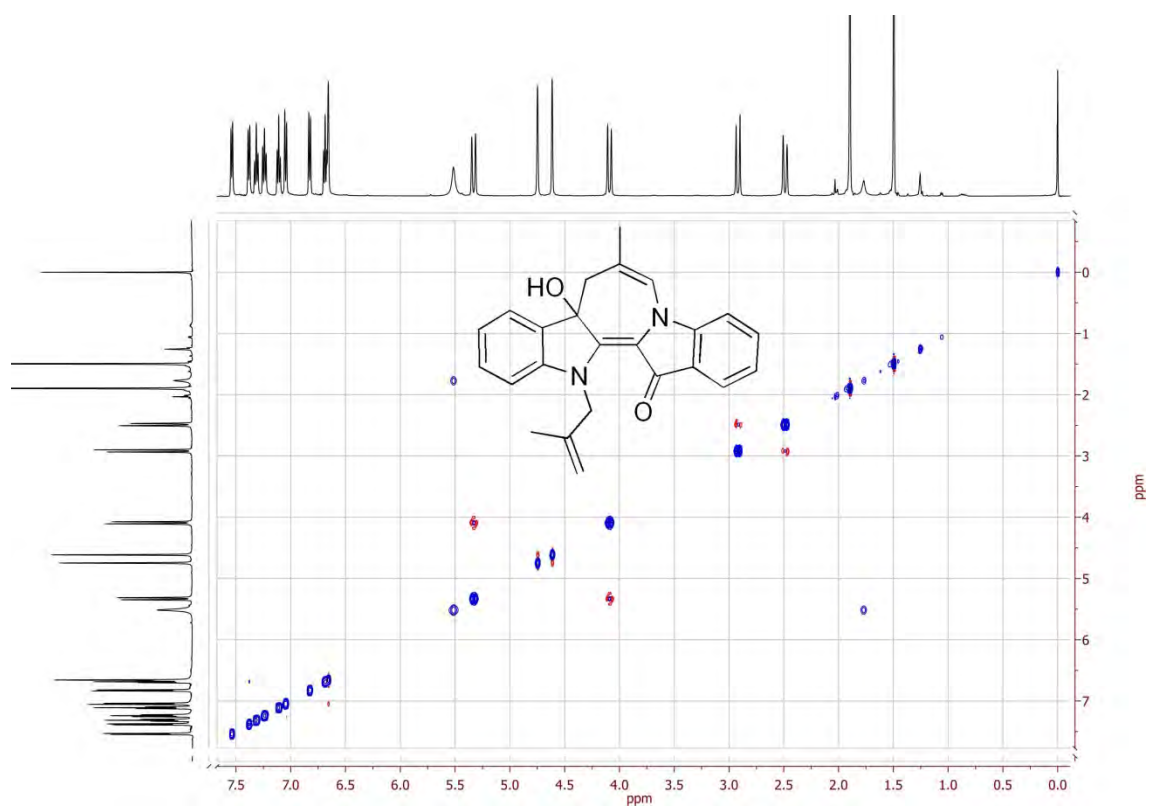
Figure 100: The NOESY for compound **249**.
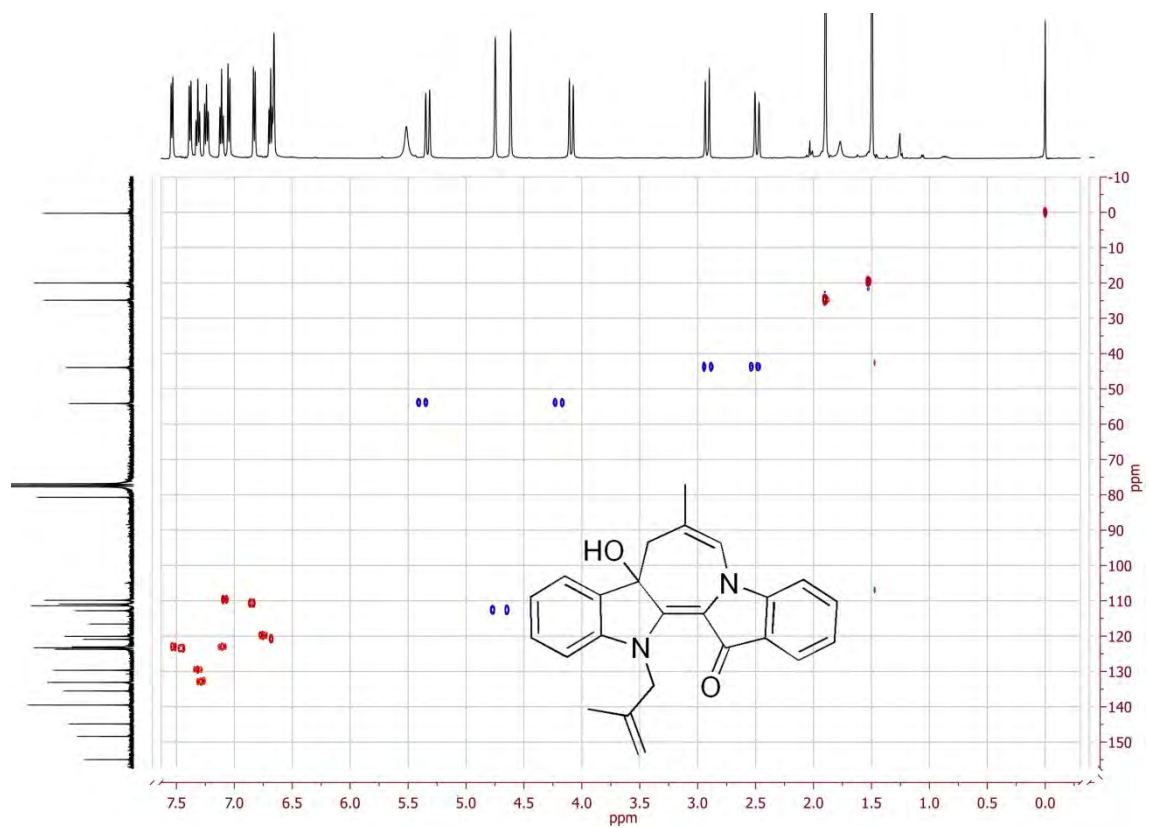
Figure 101: The gHSQC for compound **249**.
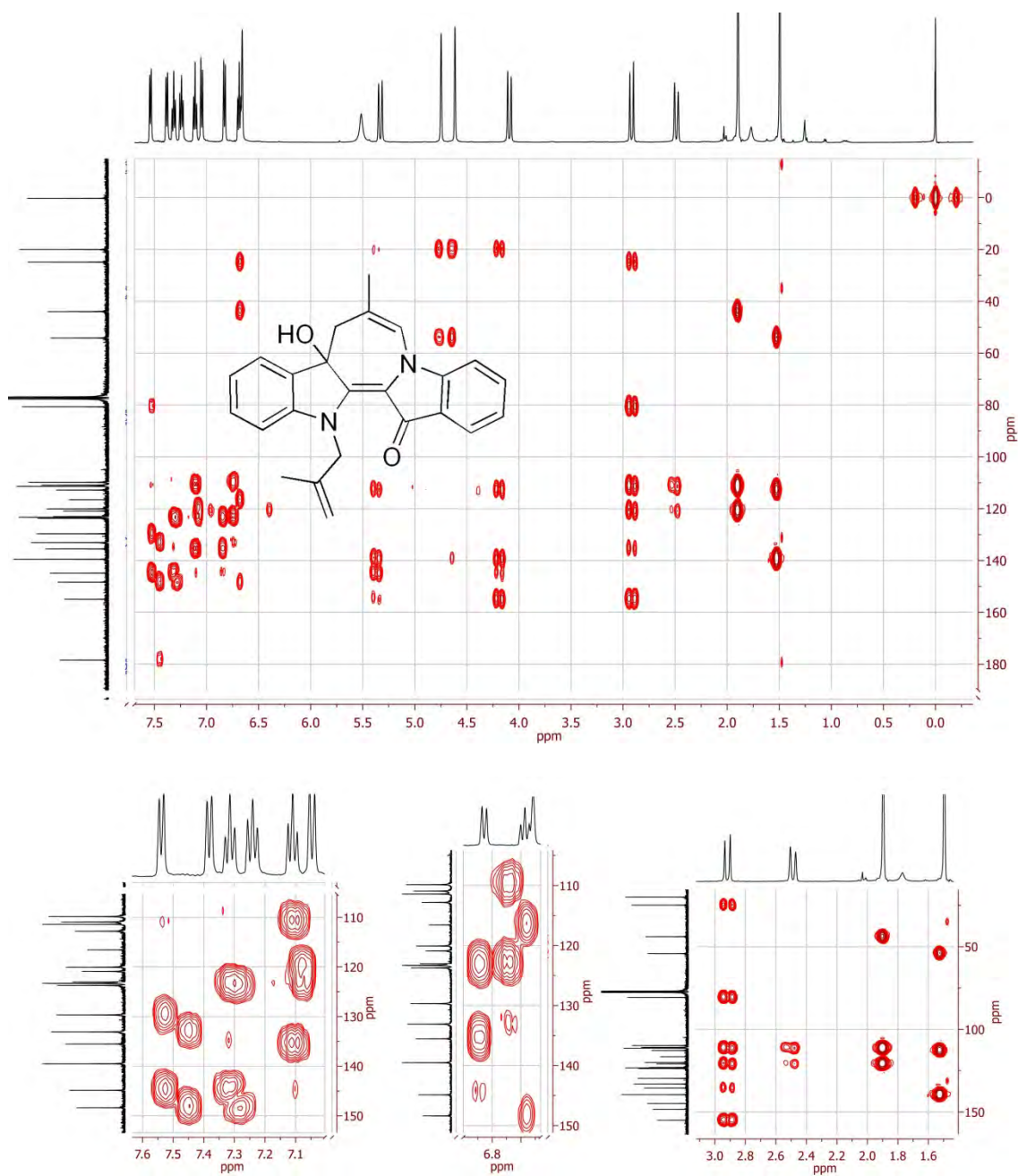
Figure 102: The gHMBC and its expansions for compound **249**.

Compound 250
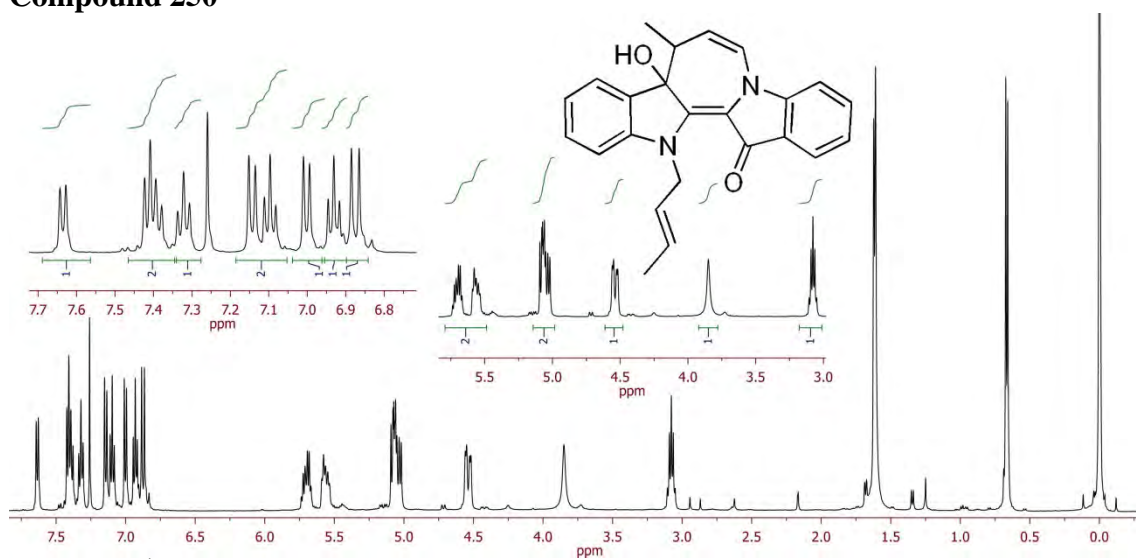
Figure 103: ^{1}H NMR spectrum for compound **250**.
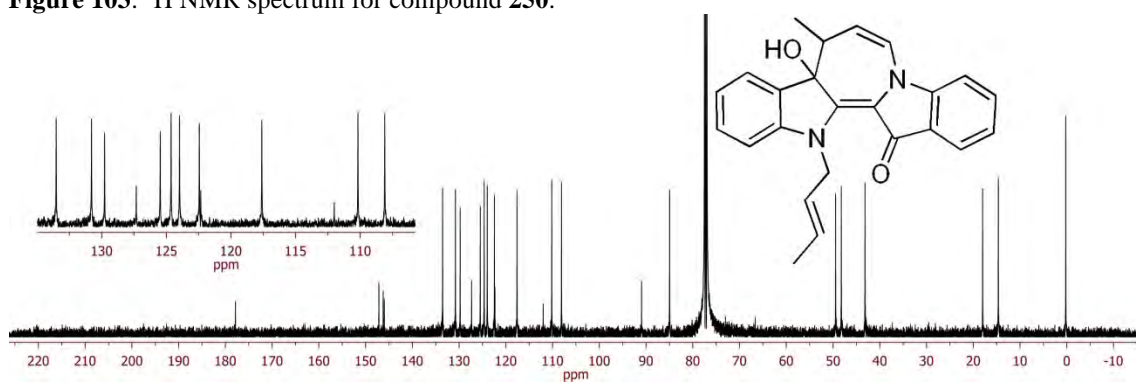
Figure 104: ^{13}C NMR spectrum for compound **250**.
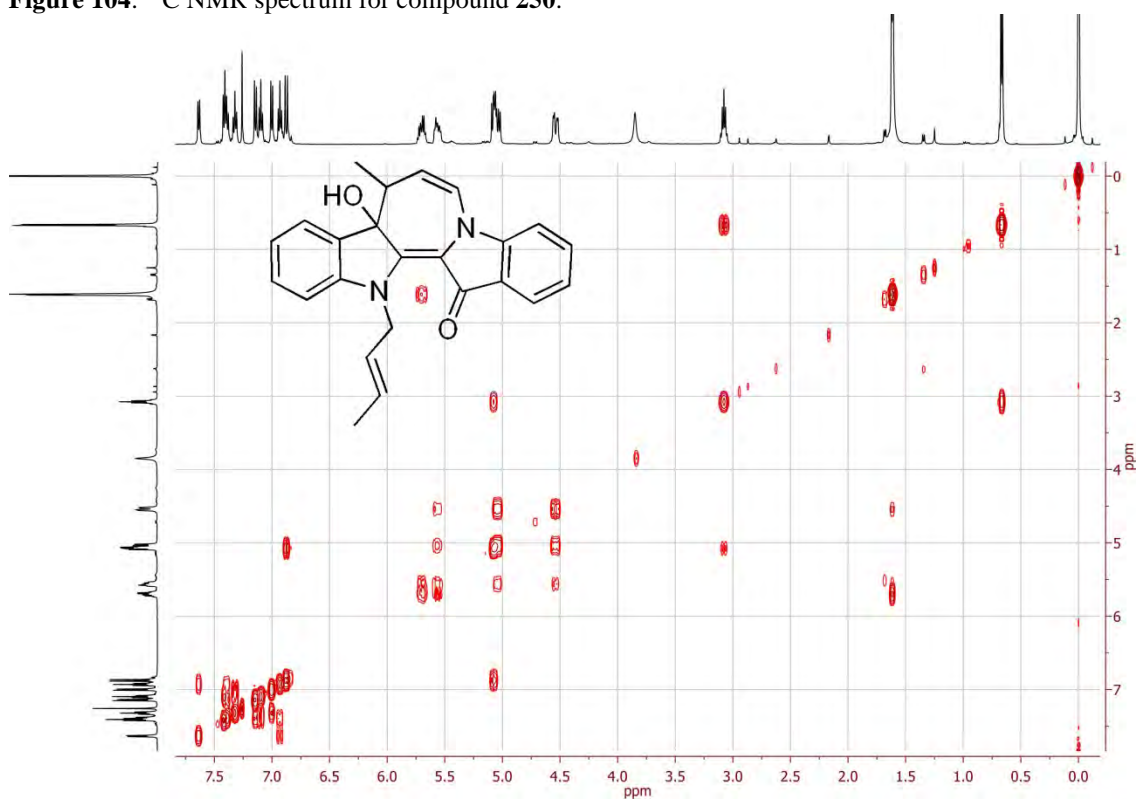
Figure 105: The gCOSY and its expansions for compound **250**.

Compound 251
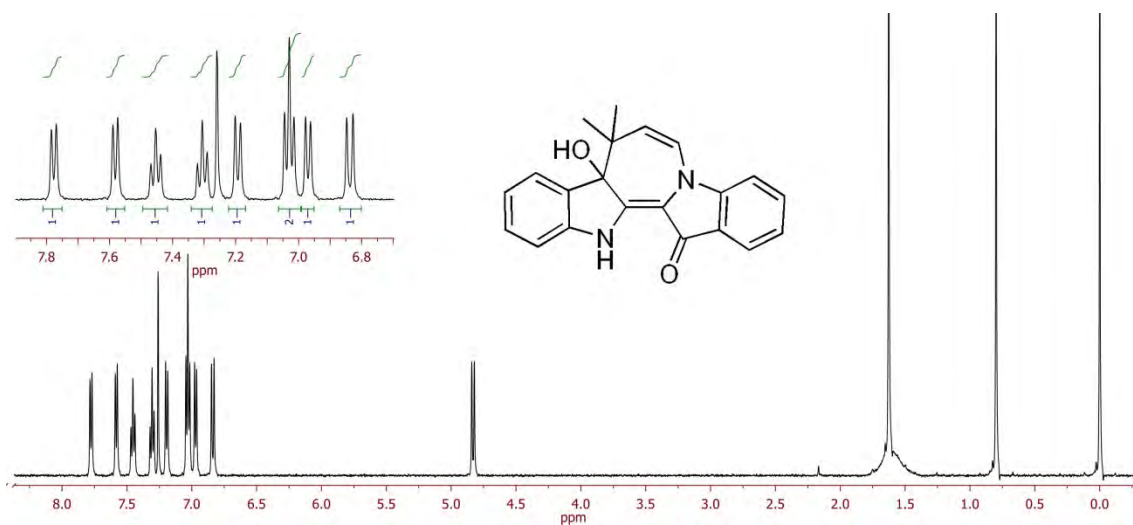
Figure 106: ^{1}H NMR spectrum for compound **251**.
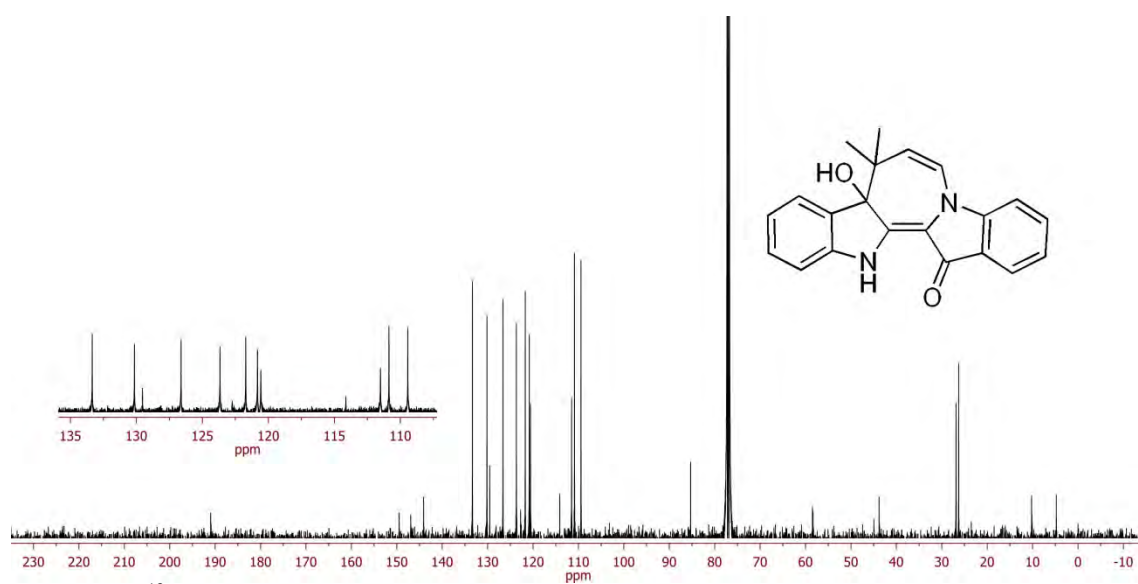
Figure 107: ^{13}C NMR spectrum for compound **251**.
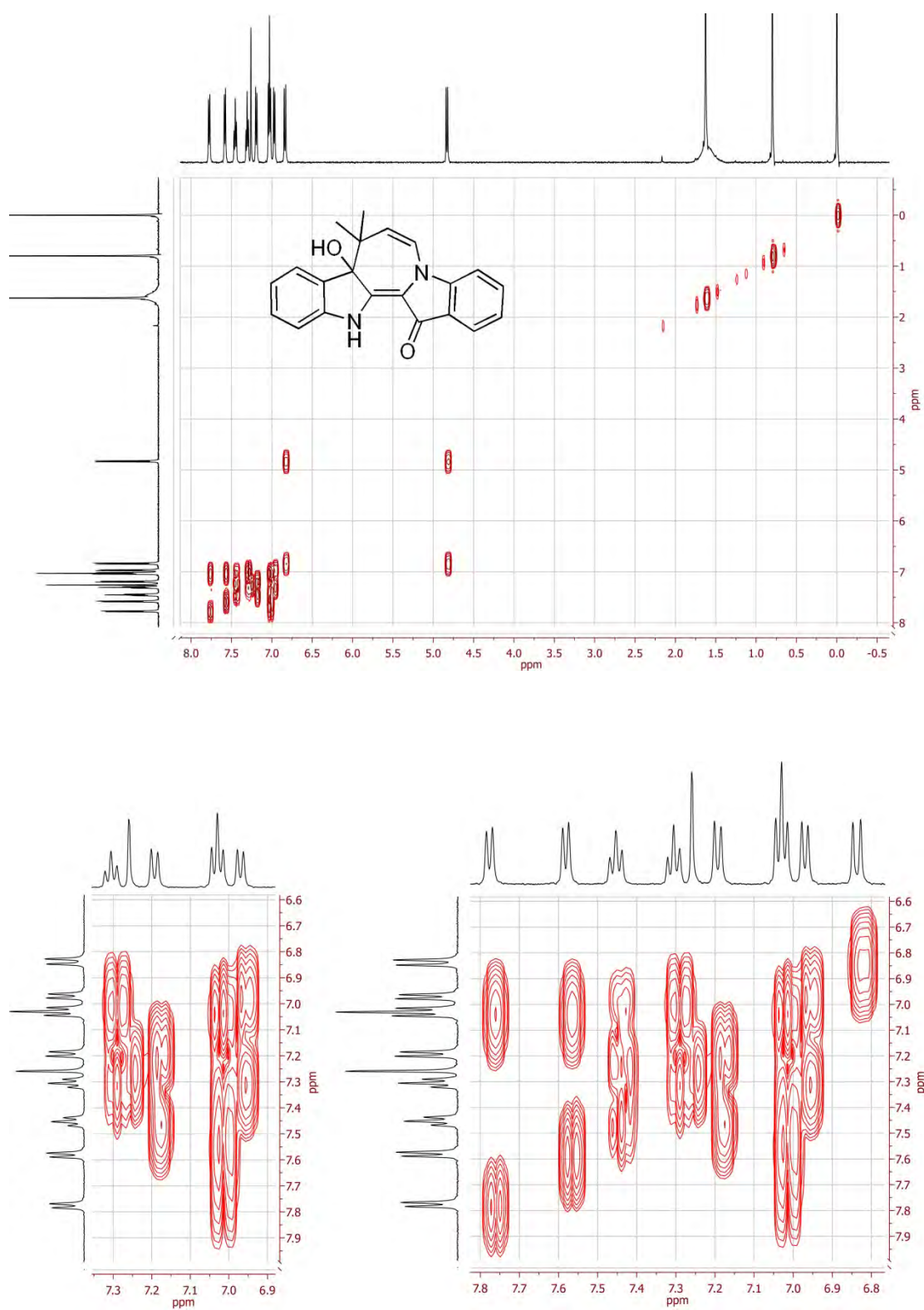
Figure 108: The gCOSY and its expansions for compound **251**.
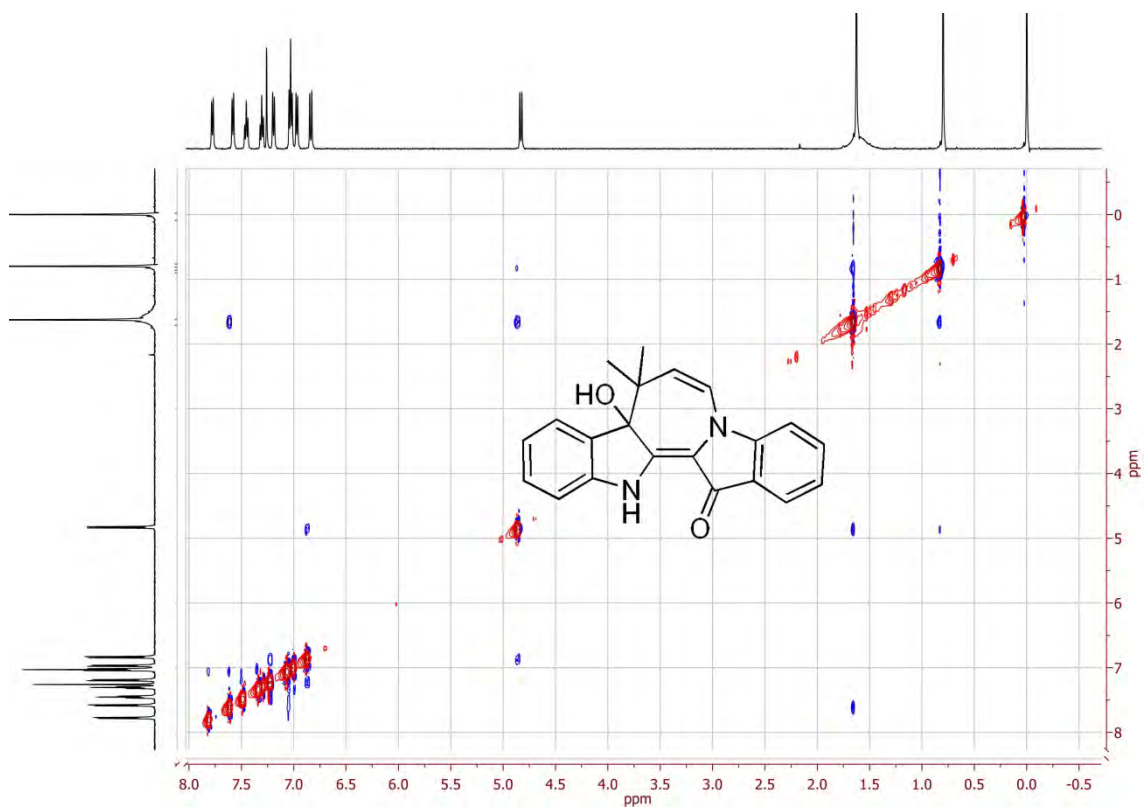
Figure 109: The NOESY for compound **251**.
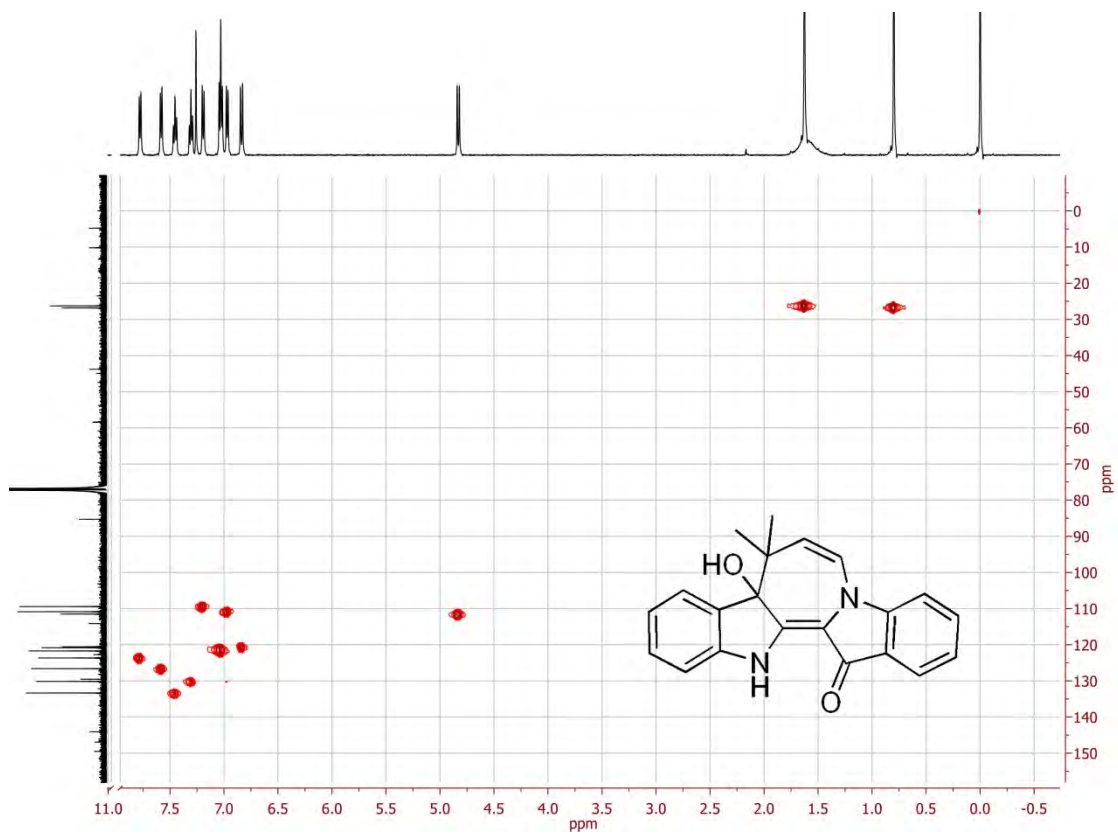
Figure 110: The gHSQC for compound **251**.
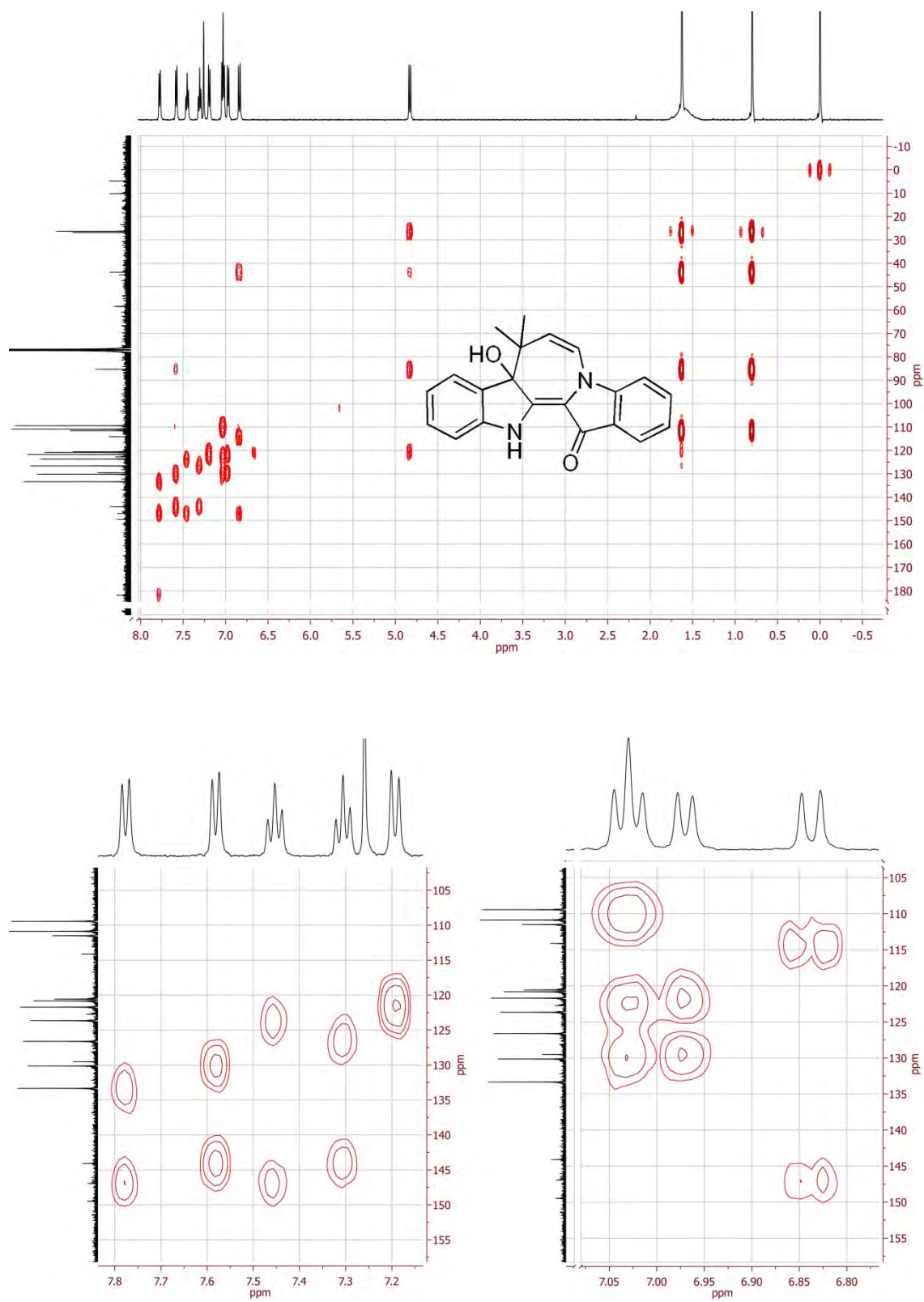
Figure 111: The gHMBC and its expansions for compound **251**.

Compound 253
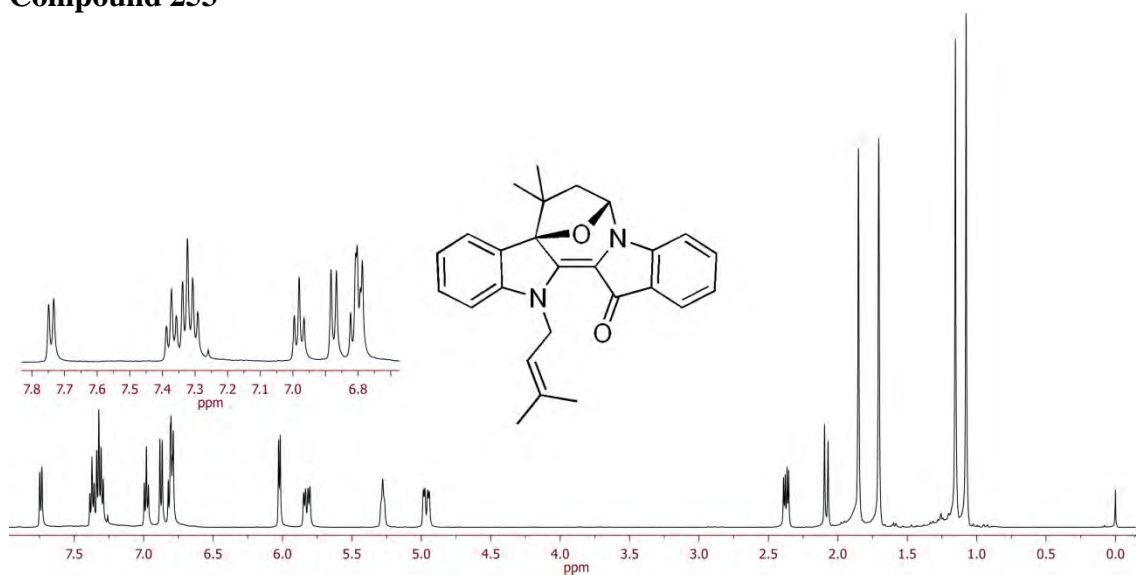
Figure 112: ^{1}H NMR spectrum for compound **253**.
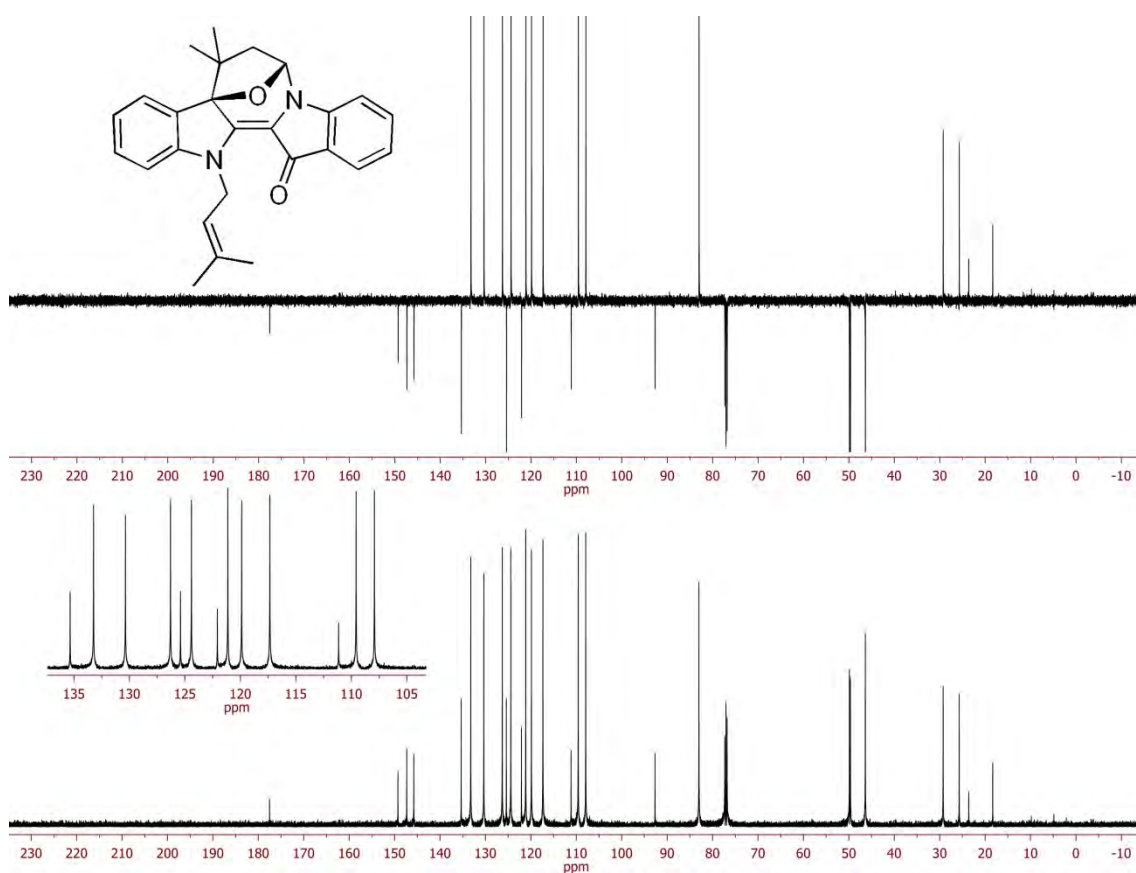
Figure 113: ^{13}C NMR spectrum for compound **253**.
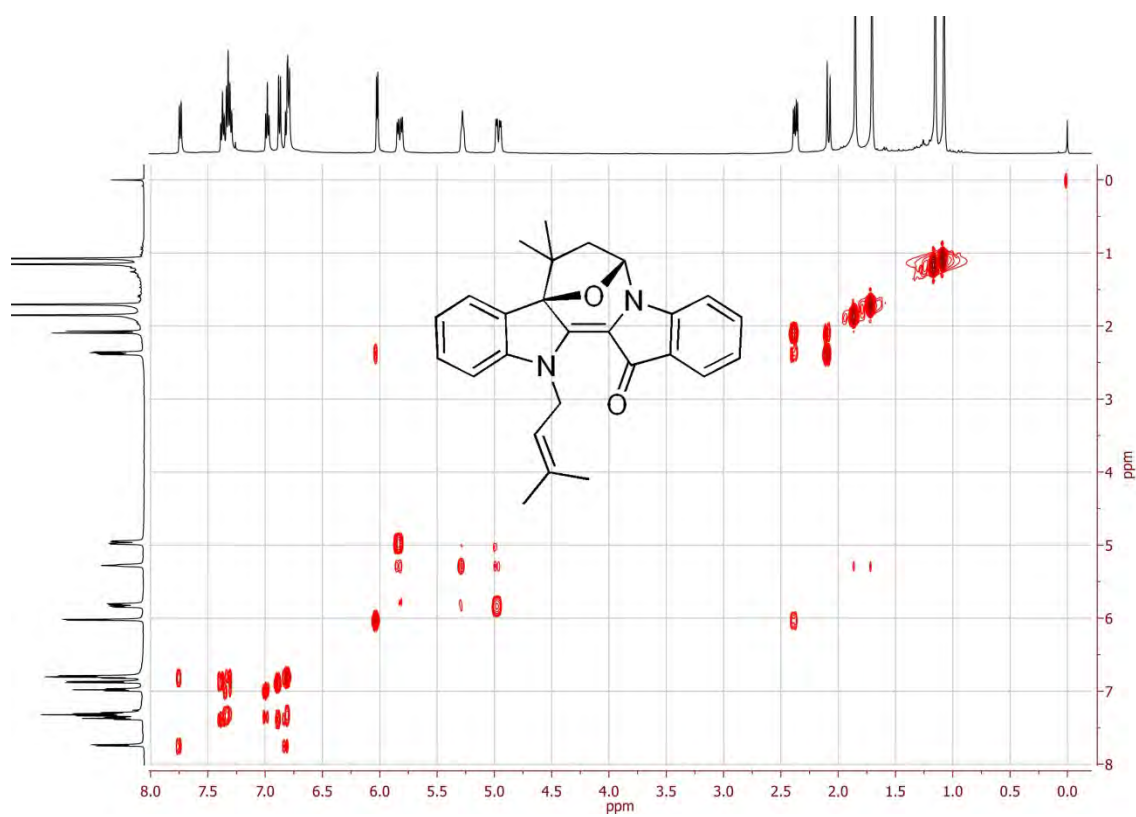
Figure 114: The gCOSY for compound **253**.
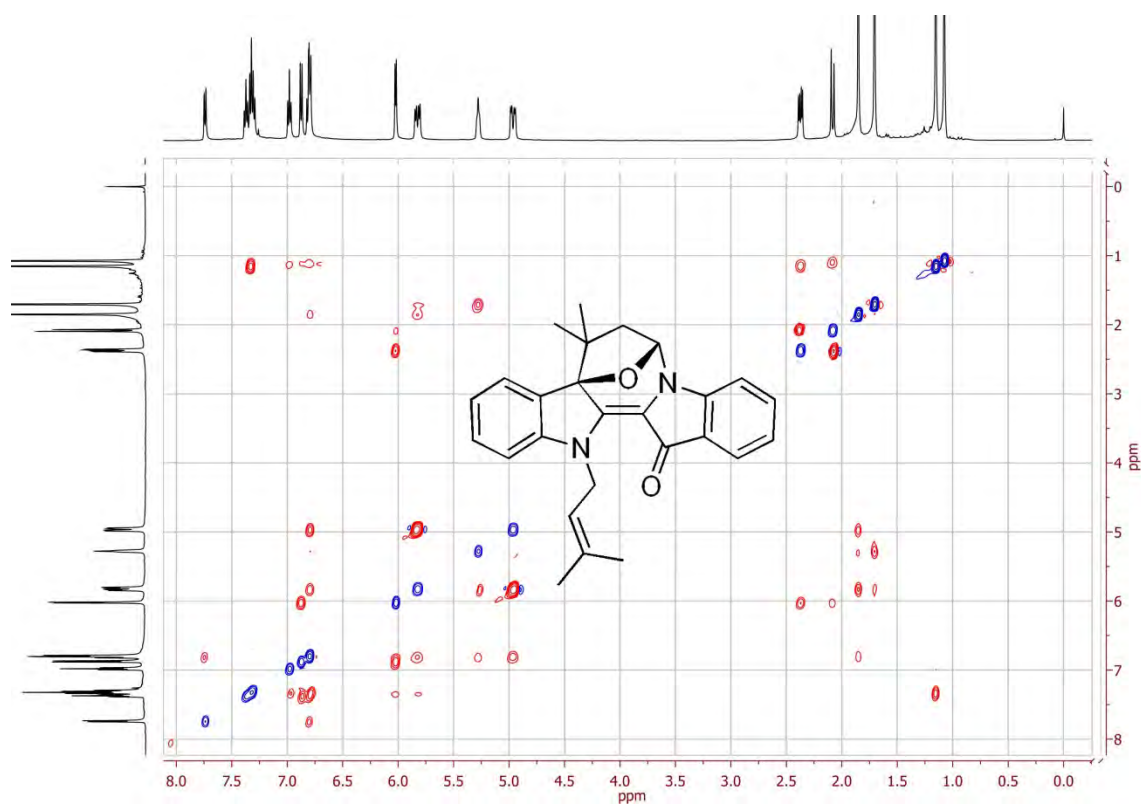
Figure 115: The NOESY for compound **253**.
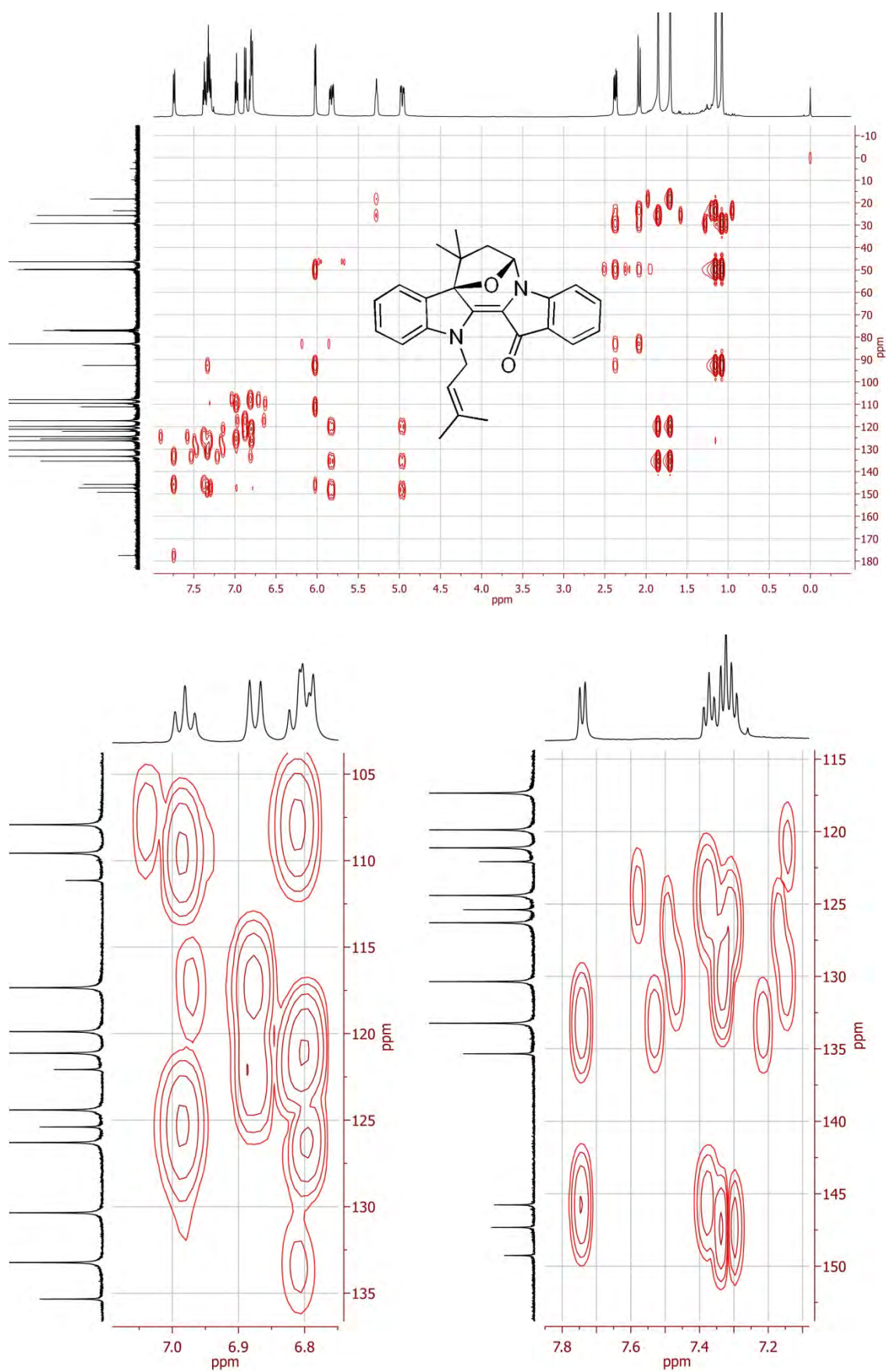
Figure 116: The gHMBC and its expansions for compound **253**.

Compound 254
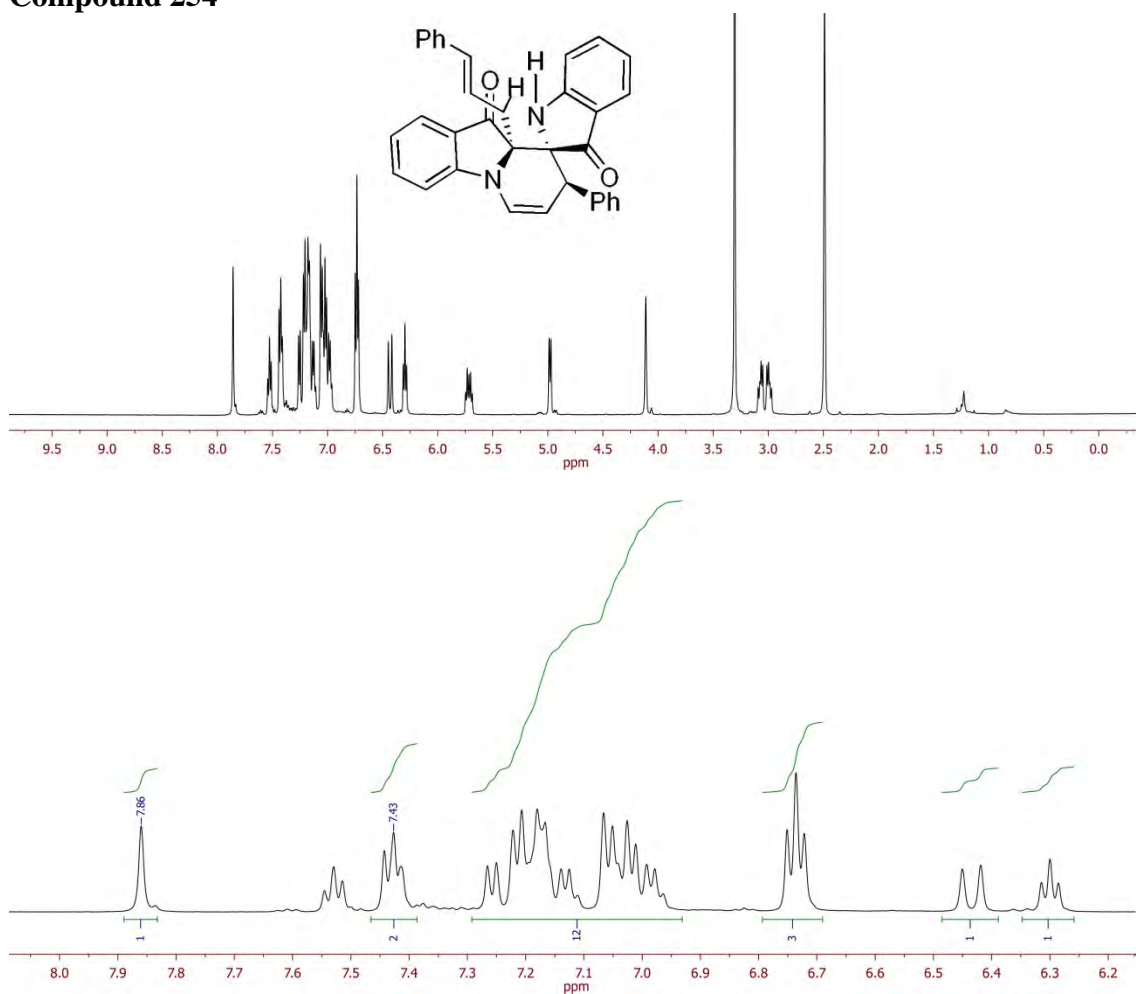
Figure 117: ^{1}H NMR spectrum for compound **254**.
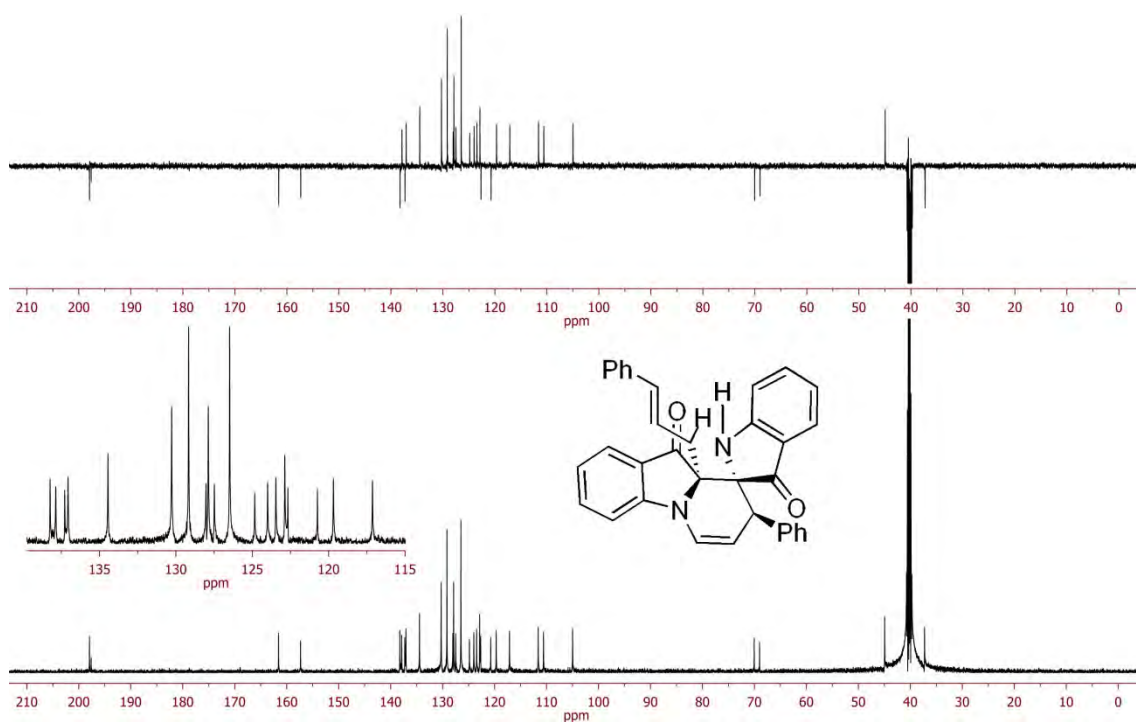
Figure 118: ^{13}C NMR spectrum for compound **254**.
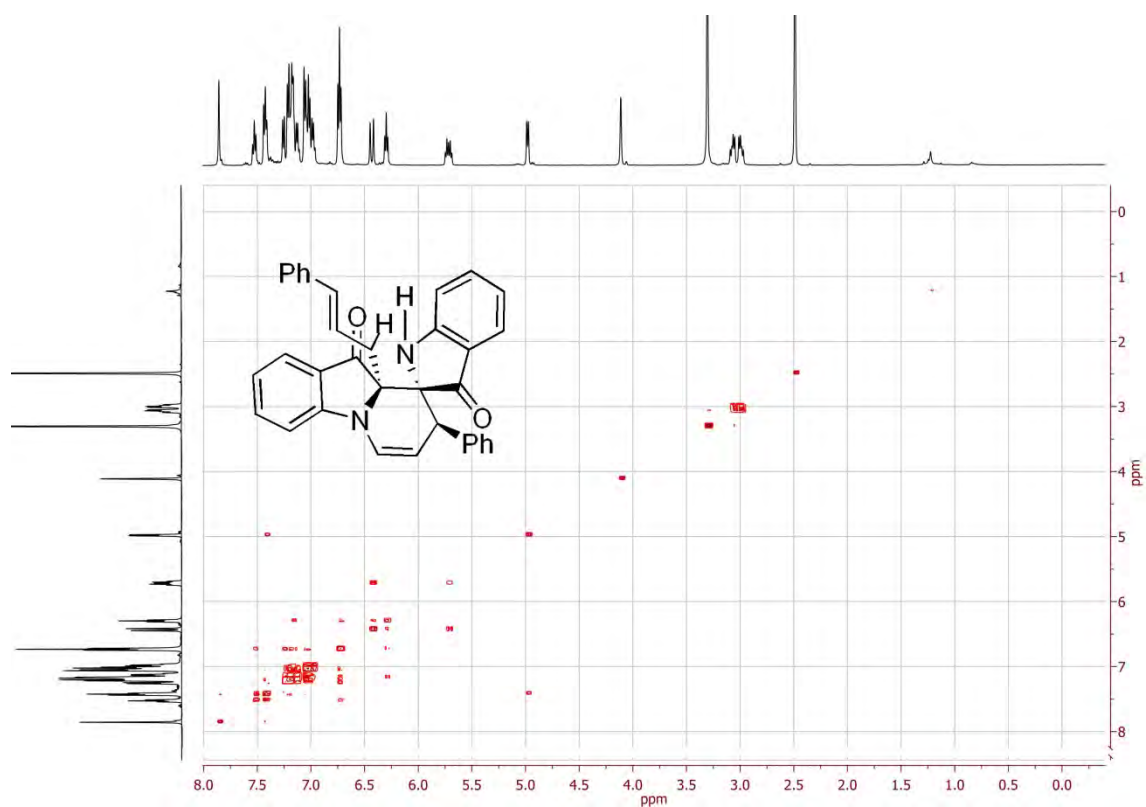
Figure 119: The gCOSY for compound **254**.
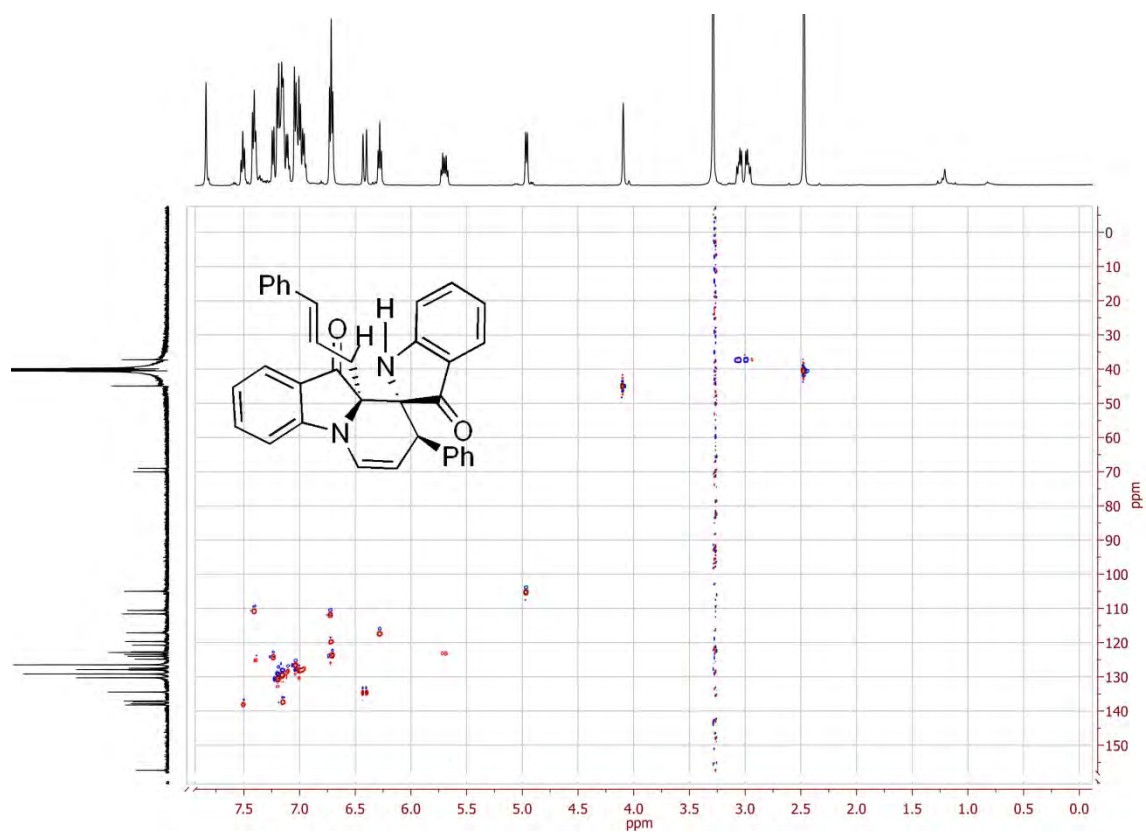
Figure 120: The gHSQC for compound **254**.
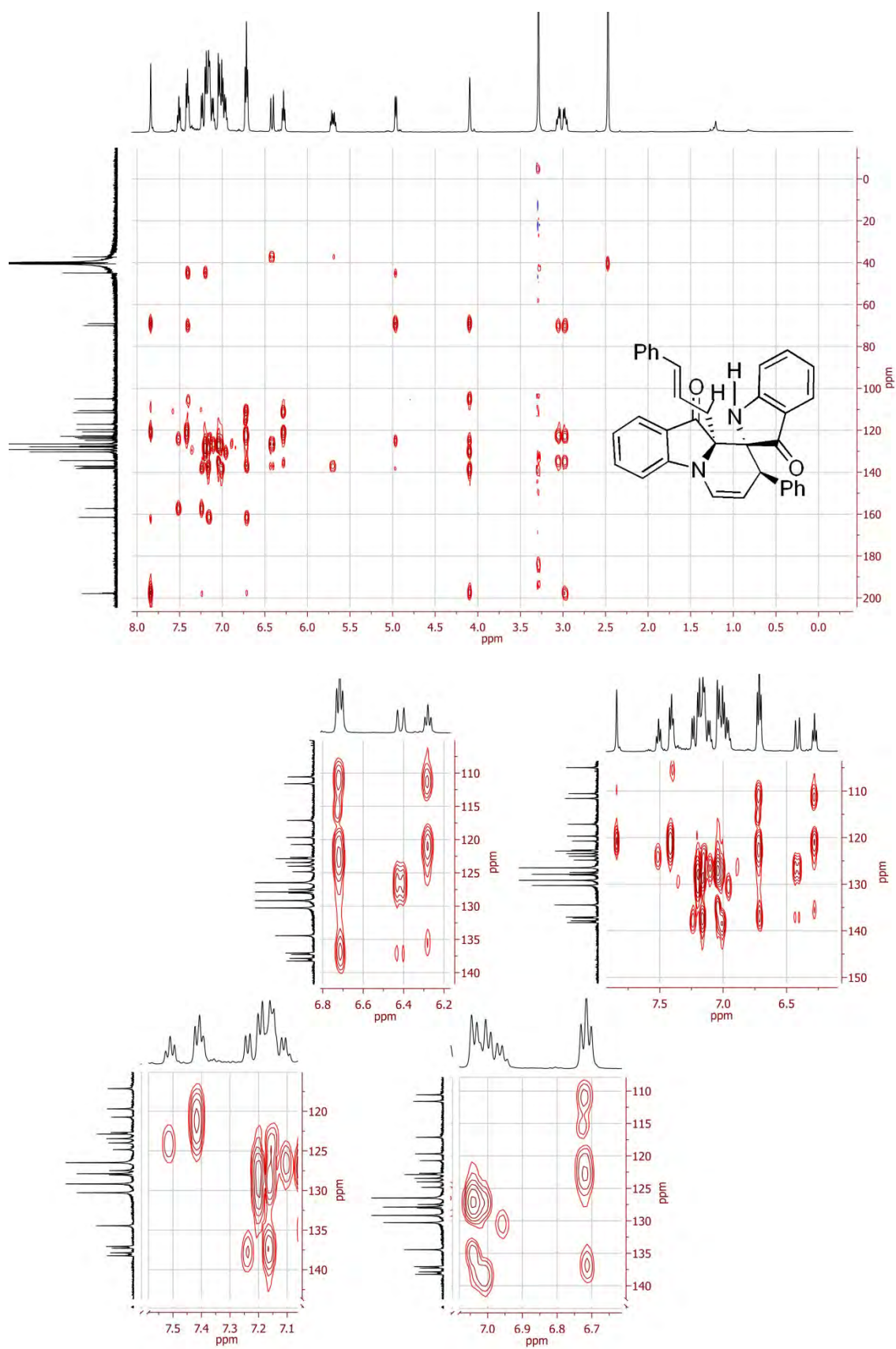
Figure 121: The gHMBC and its expansions for compound **254**.

Compound 256
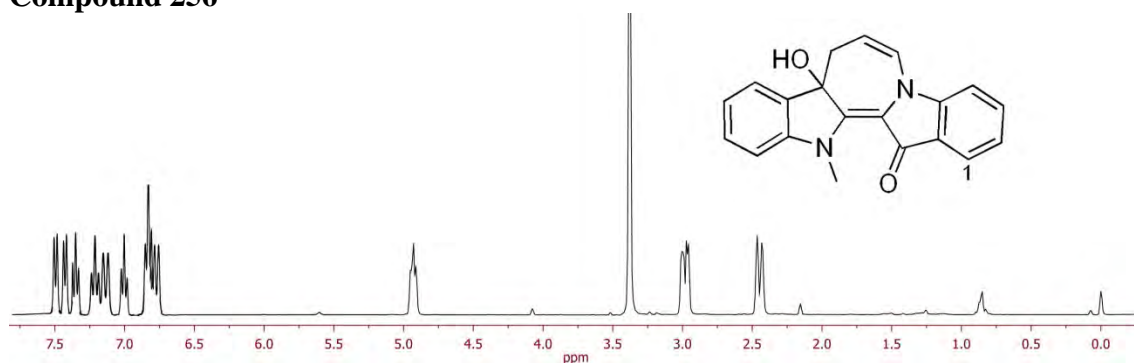
Figure 122: ^{1}H NMR spectrum for compound **256**.
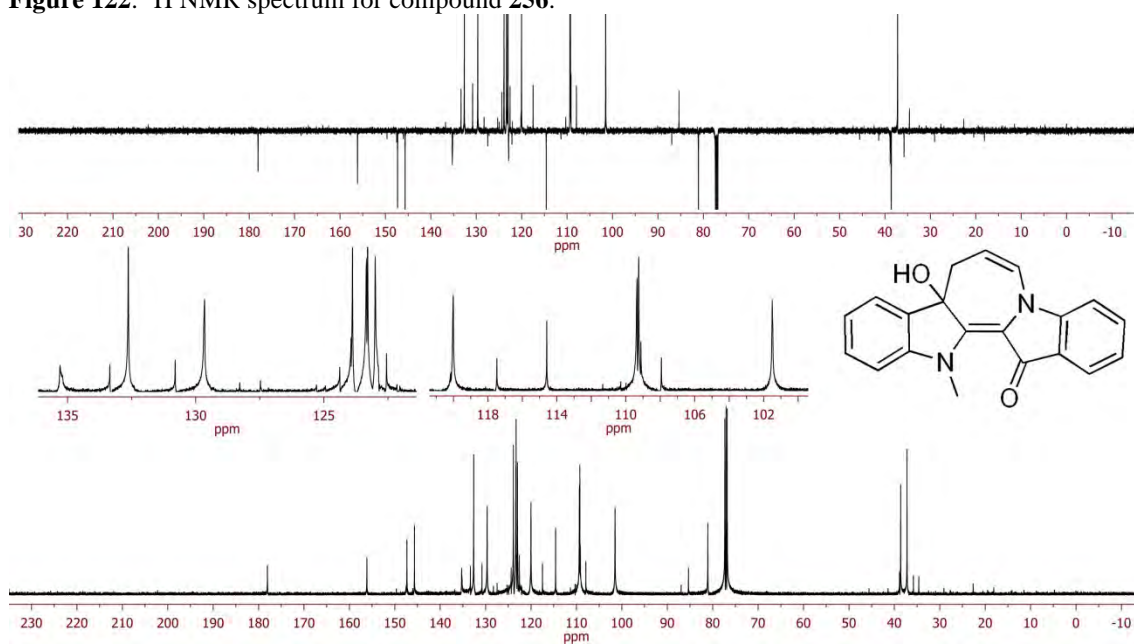
Figure 123: ^{13}C NMR spectrum for compound **256**.
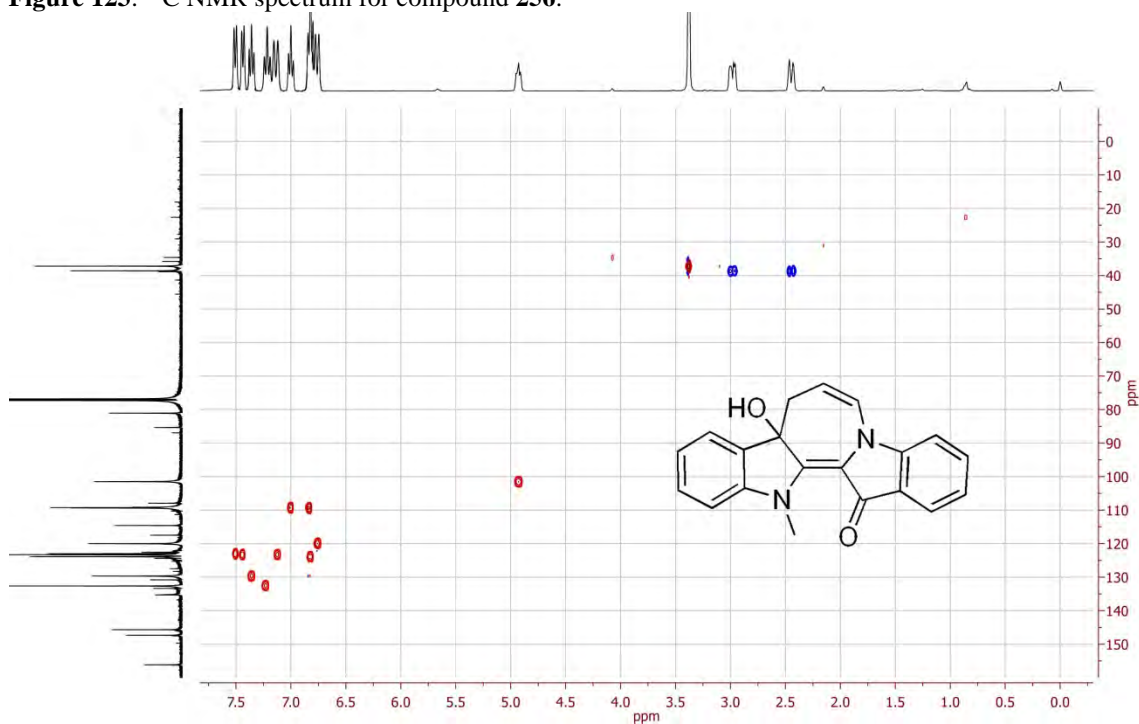
Figure 124: The gHSQC for compound **256**.

Compound 257
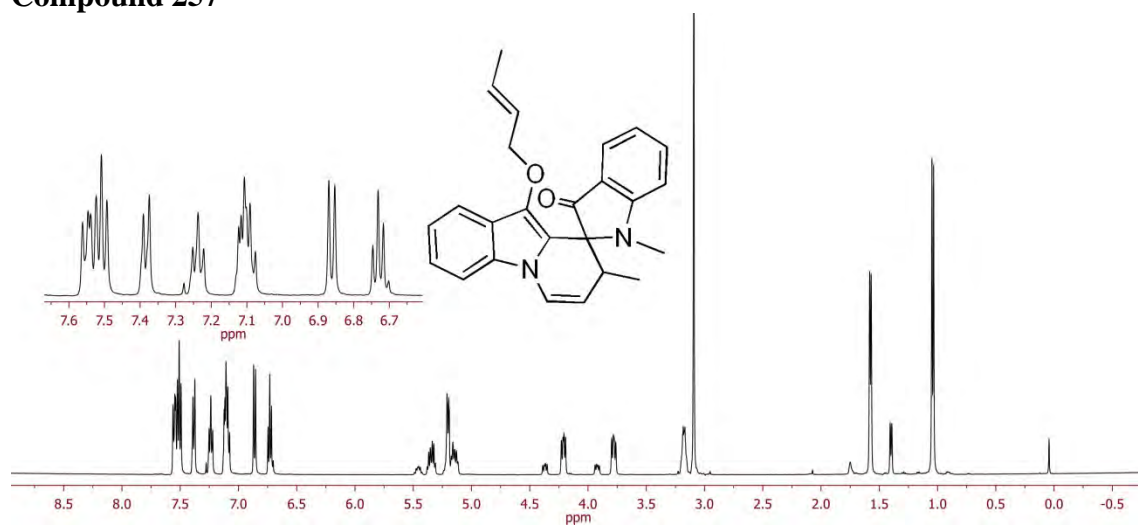
Figure 125: ^{1}H NMR spectrum for compound **257**.
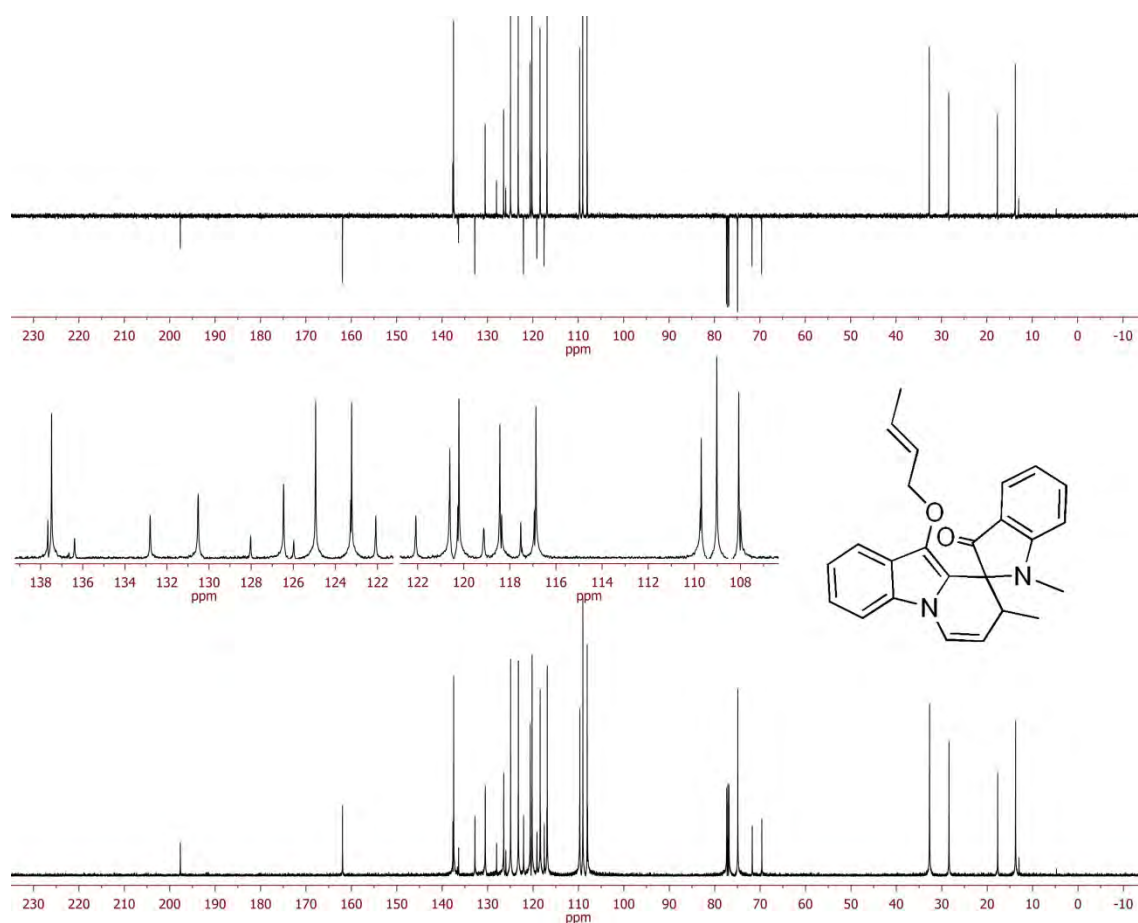
Figure 126: ^{13}C NMR spectrum for compound **257**.

Compound 263
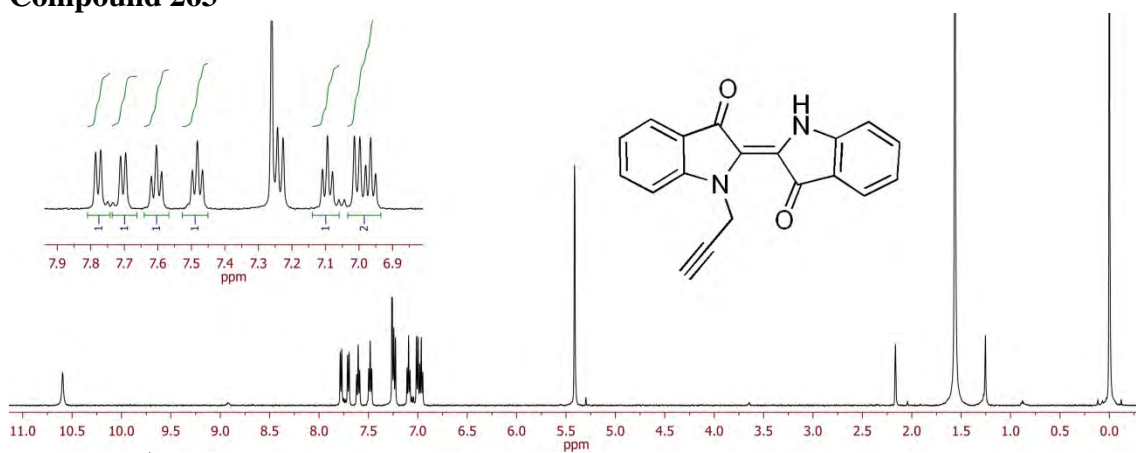
Figure 127: ^{1}H NMR spectrum for compound **263**.
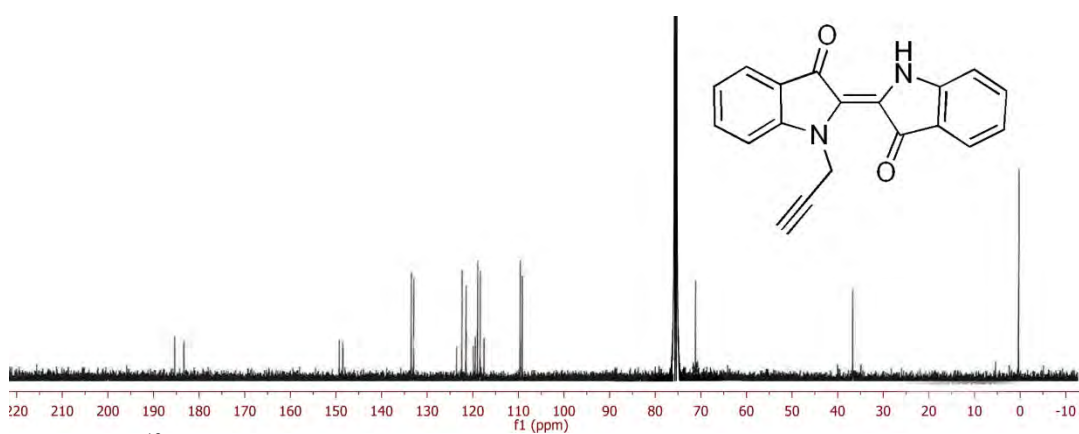
Figure 128: ^{13}C NMR spectrum for compound **263**.
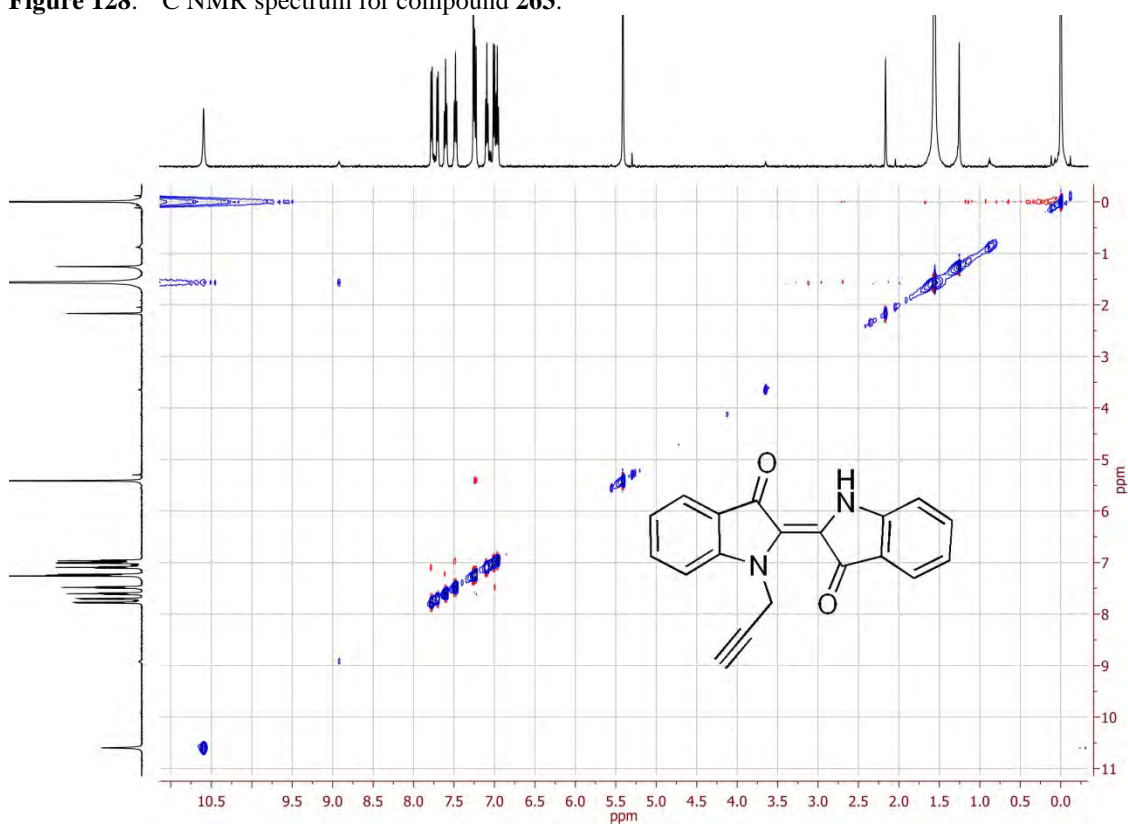
Figure 129: The NOESY for compound **263**.

Compound 264
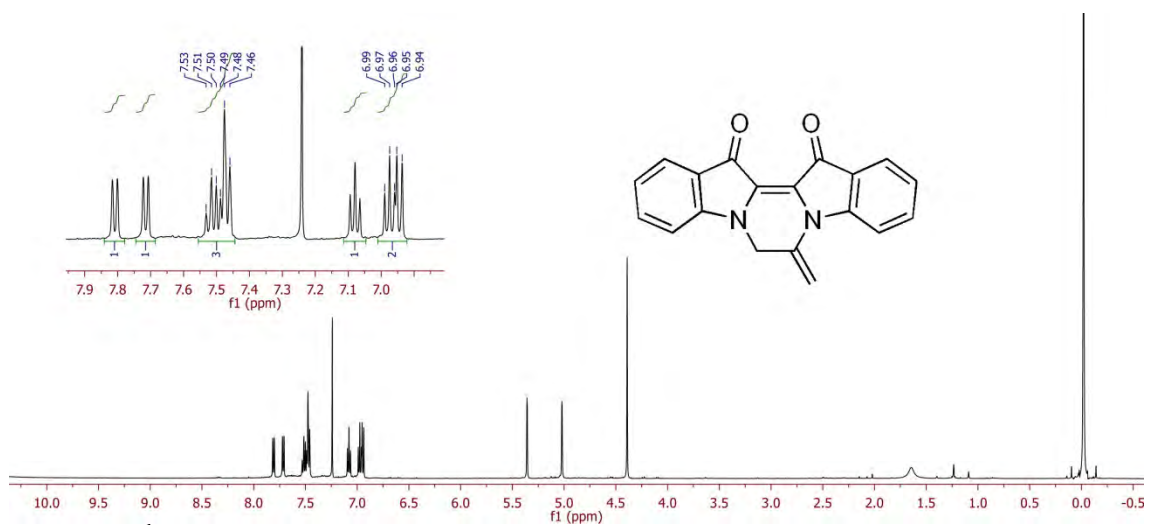
Figure 130: ^{1}H NMR spectrum for compound **264**.
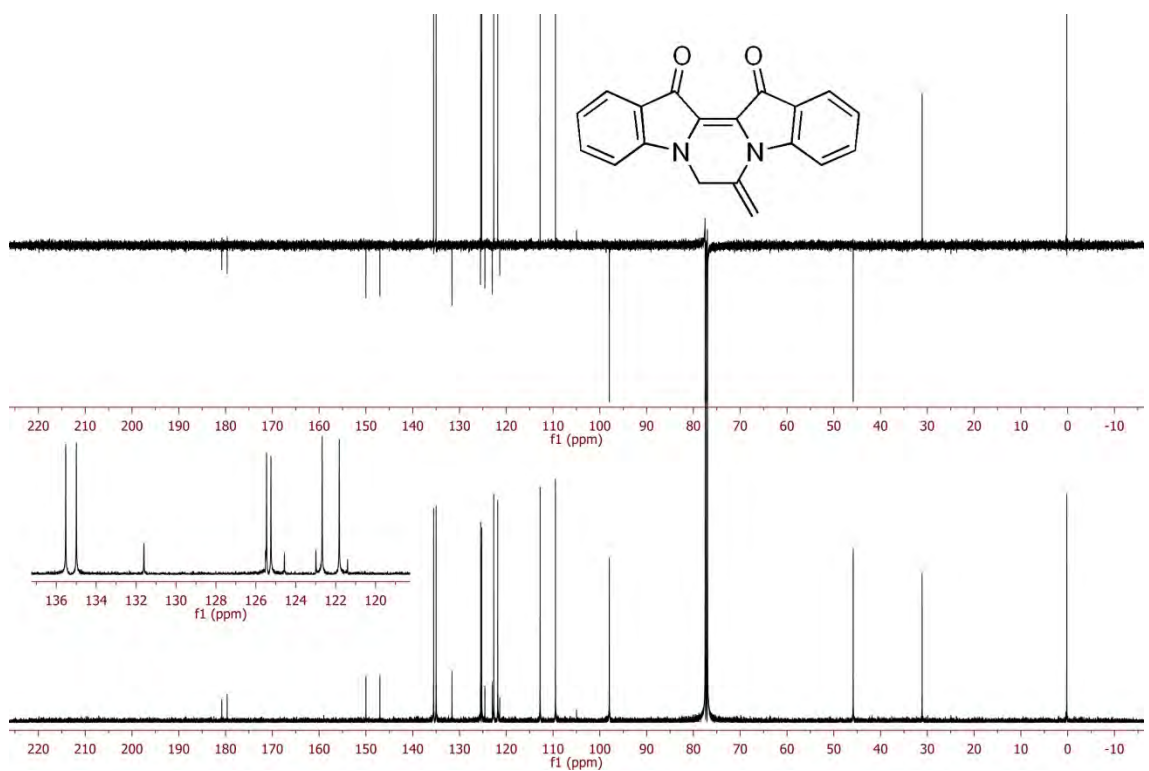
Figure 131: ^{13}C NMR spectrum for compound **264**.
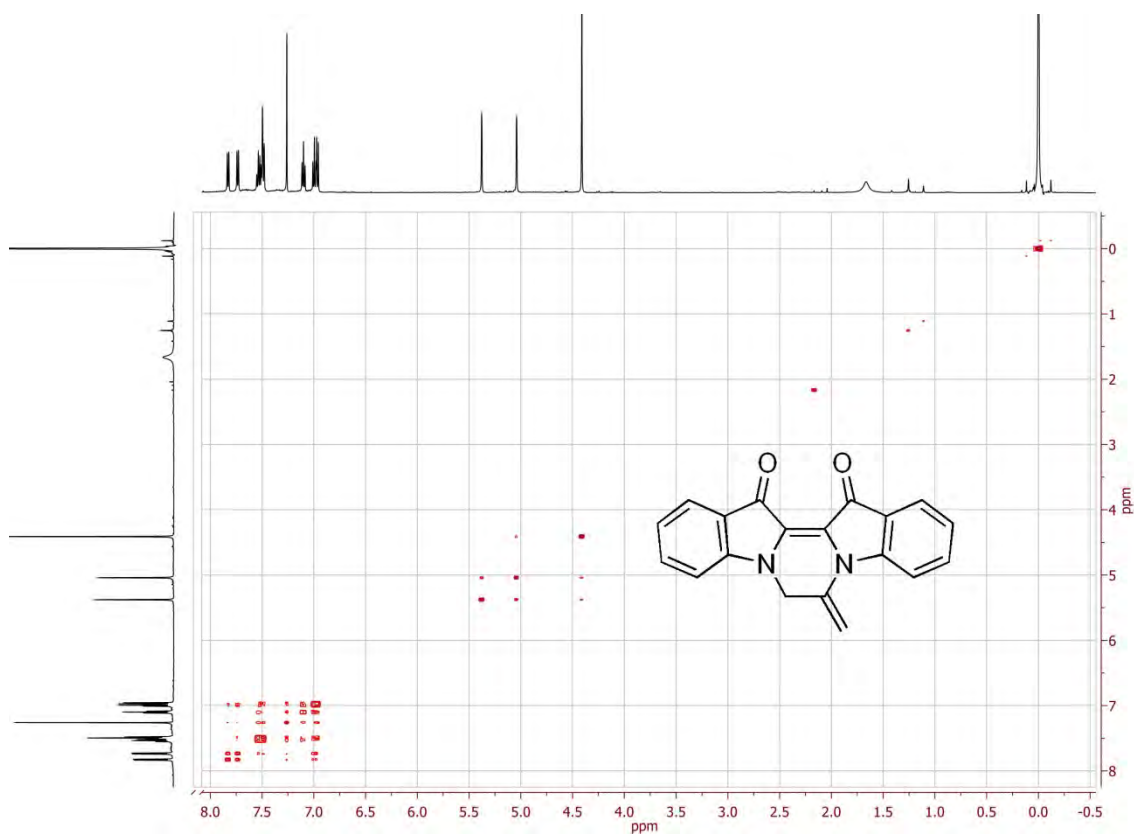
Figure 132: : The gCOSY for compound **264**.
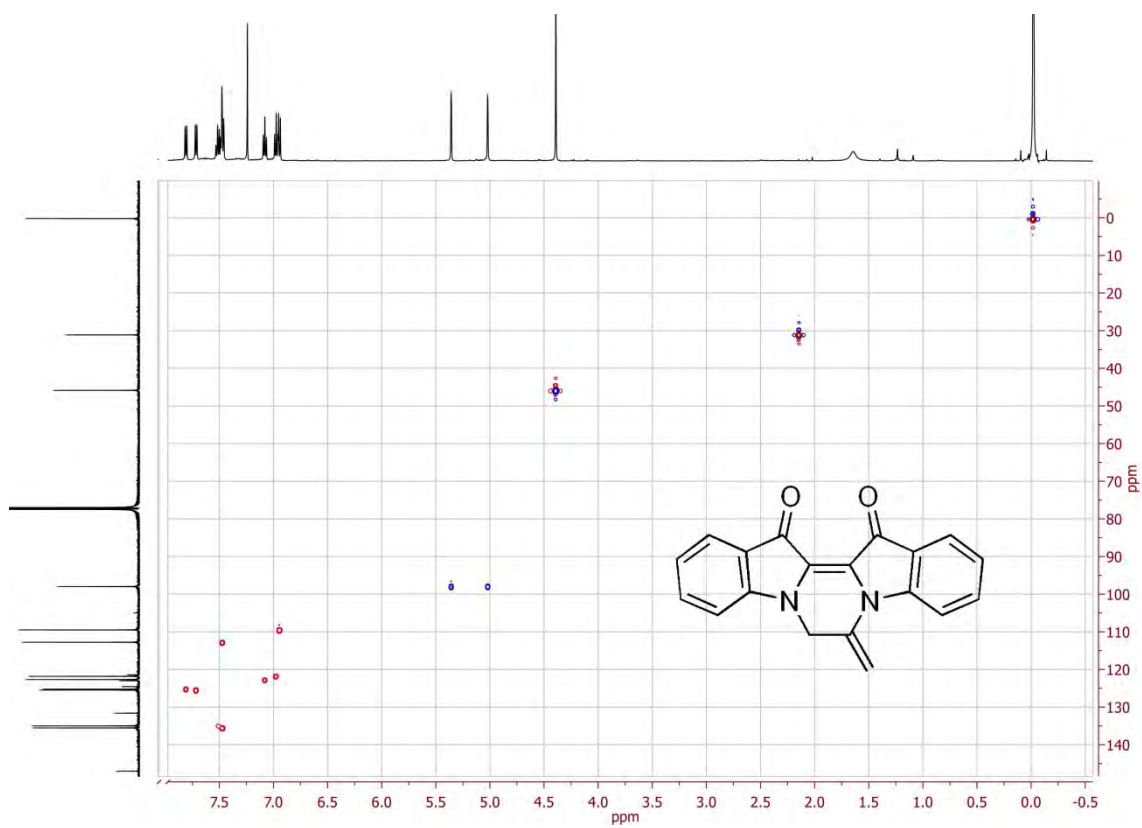
Figure 133: The gHSQC for compound **264**.
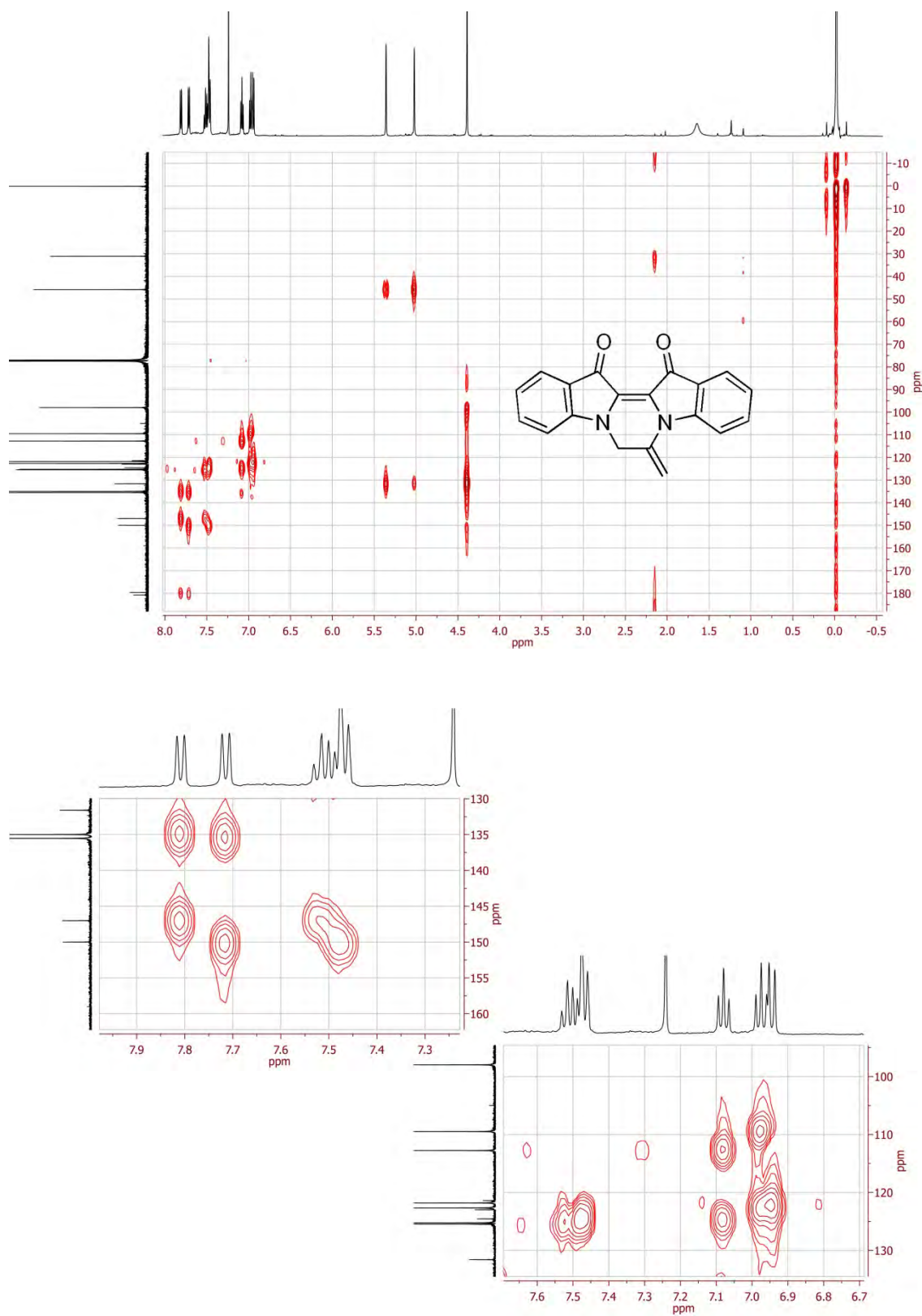
Figure 134: The gHMBC and its expansions for compound **264**.

Compound 265
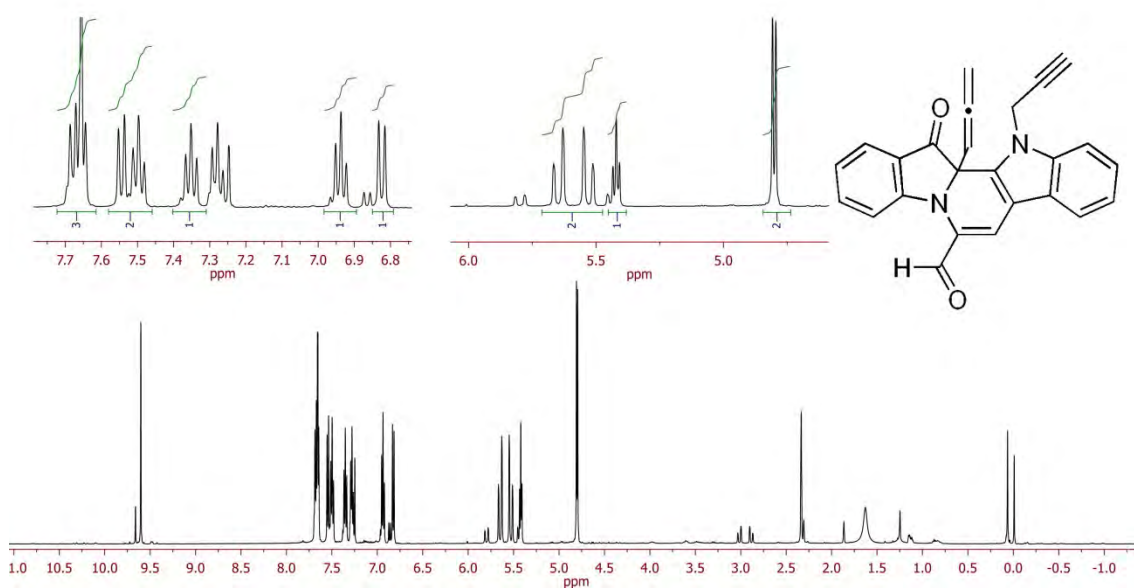
Figure 135: ^{1}H NMR spectrum for compound **265**.
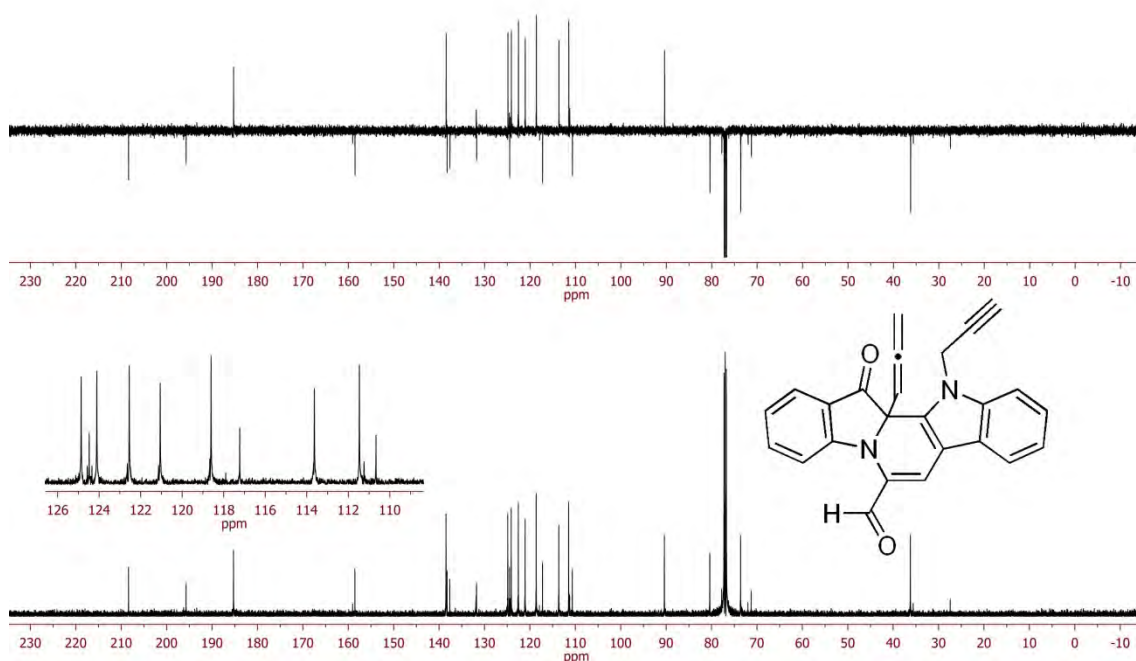
Figure 136: ^{13}C NMR spectrum for compound **265**.
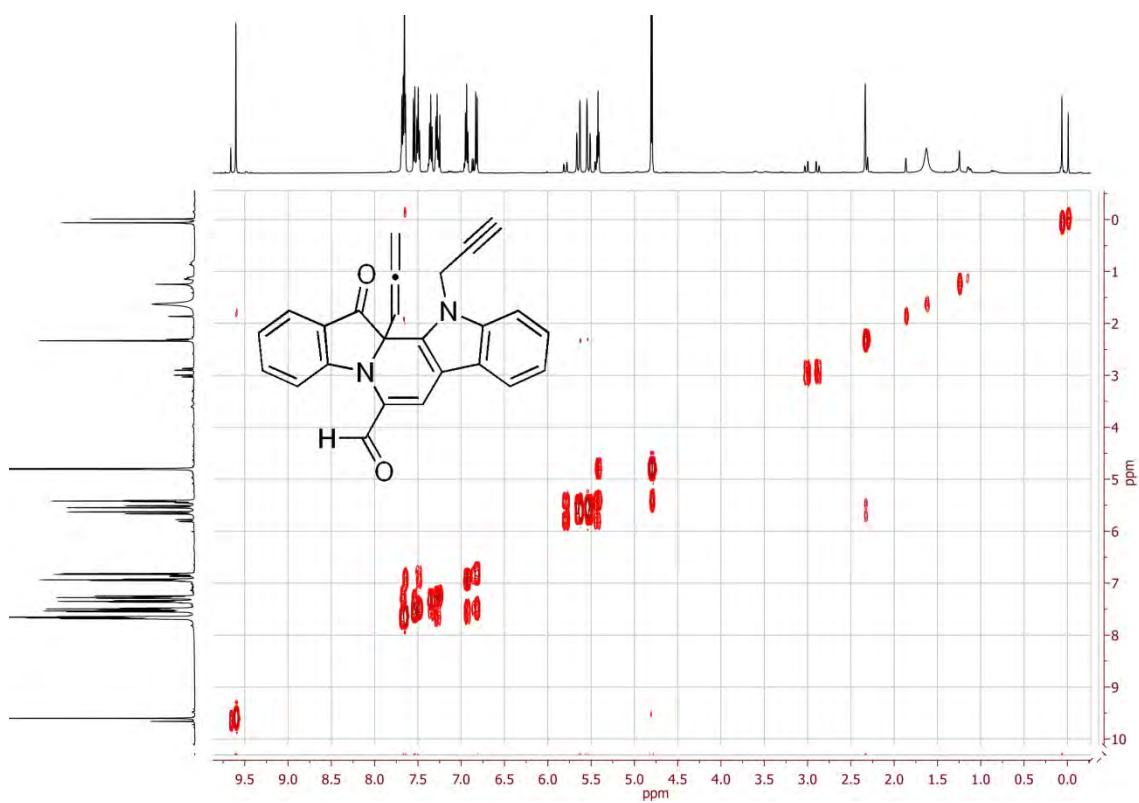
Figure 137: The gCOSY for compound **254**.
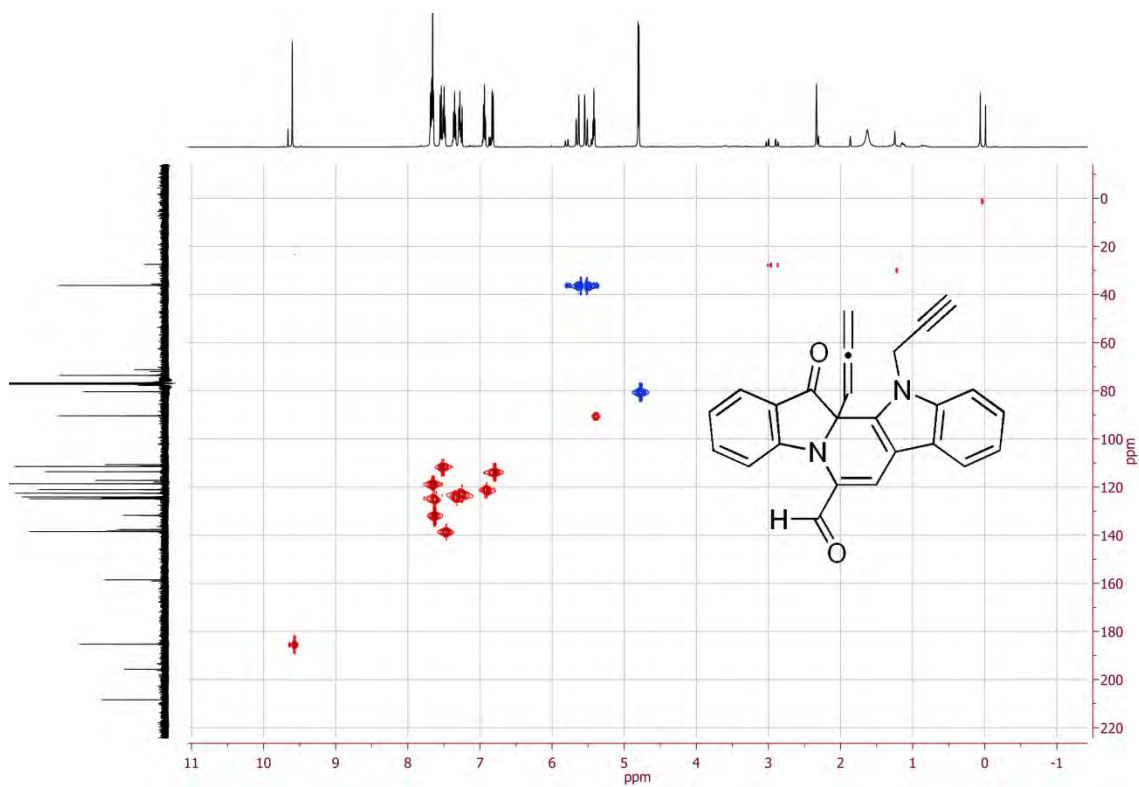
Figure 138: The gHSQC for compound **265**.
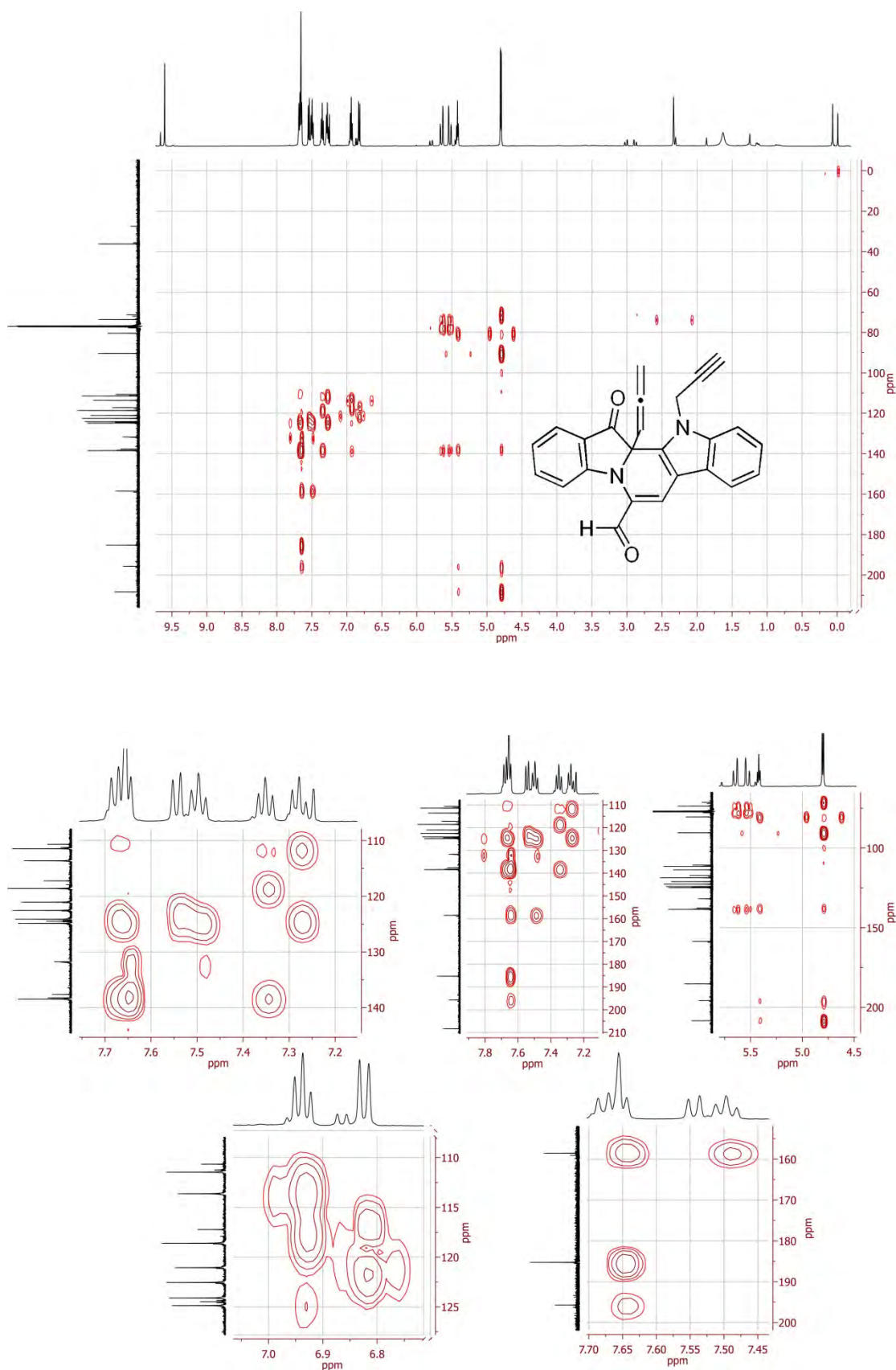
Figure 139: The gHMBC and its expansions for compound **265**.

Compound 266
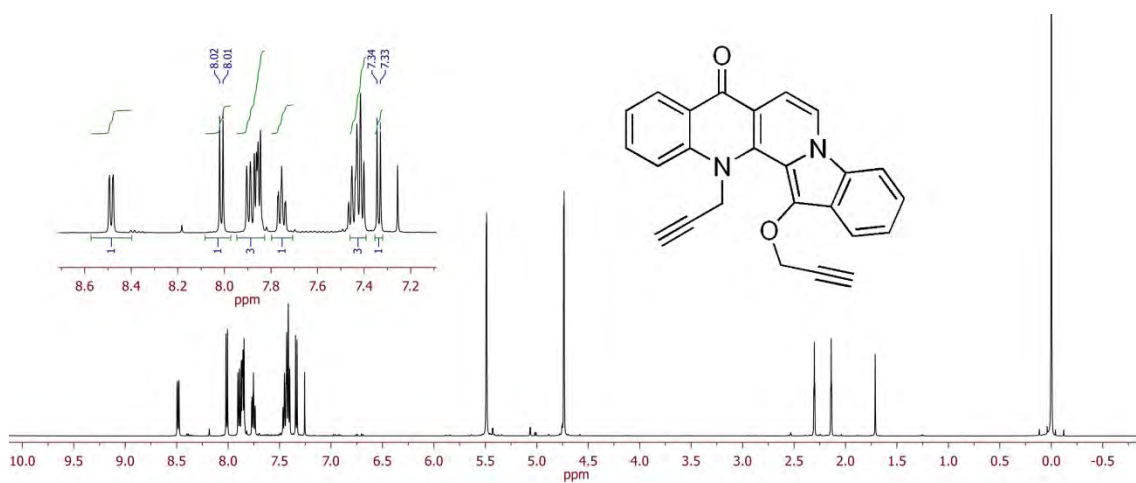
Figure 140: ^{1}H NMR spectrum for compound **266**.
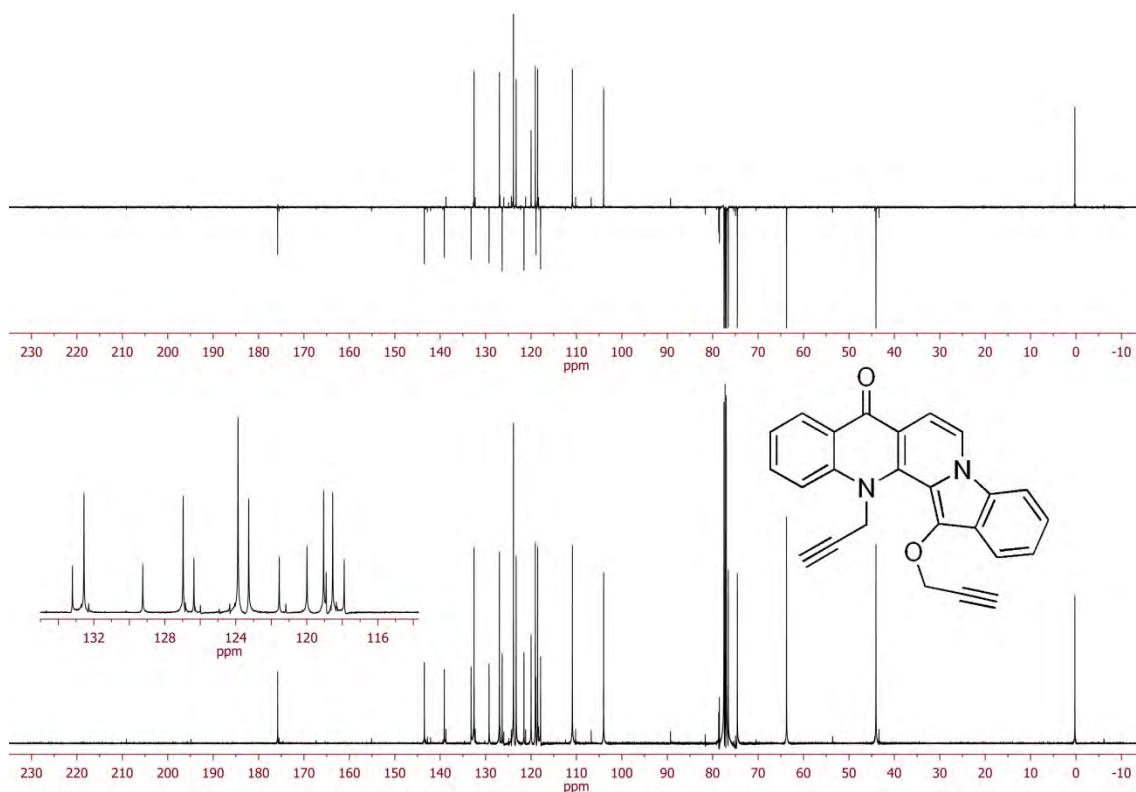
Figure 141: ^{13}C NMR spectrum for compound **266**.
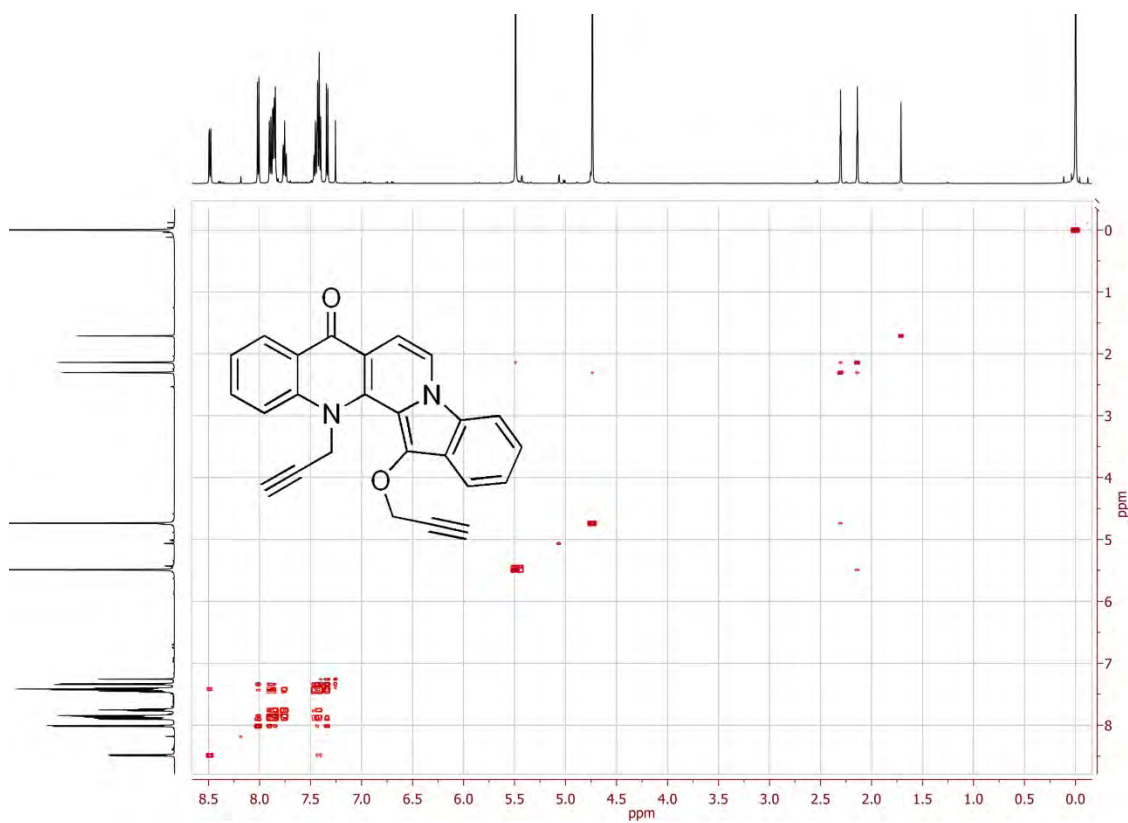
Figure 142: The gCOSY for compound **266**.
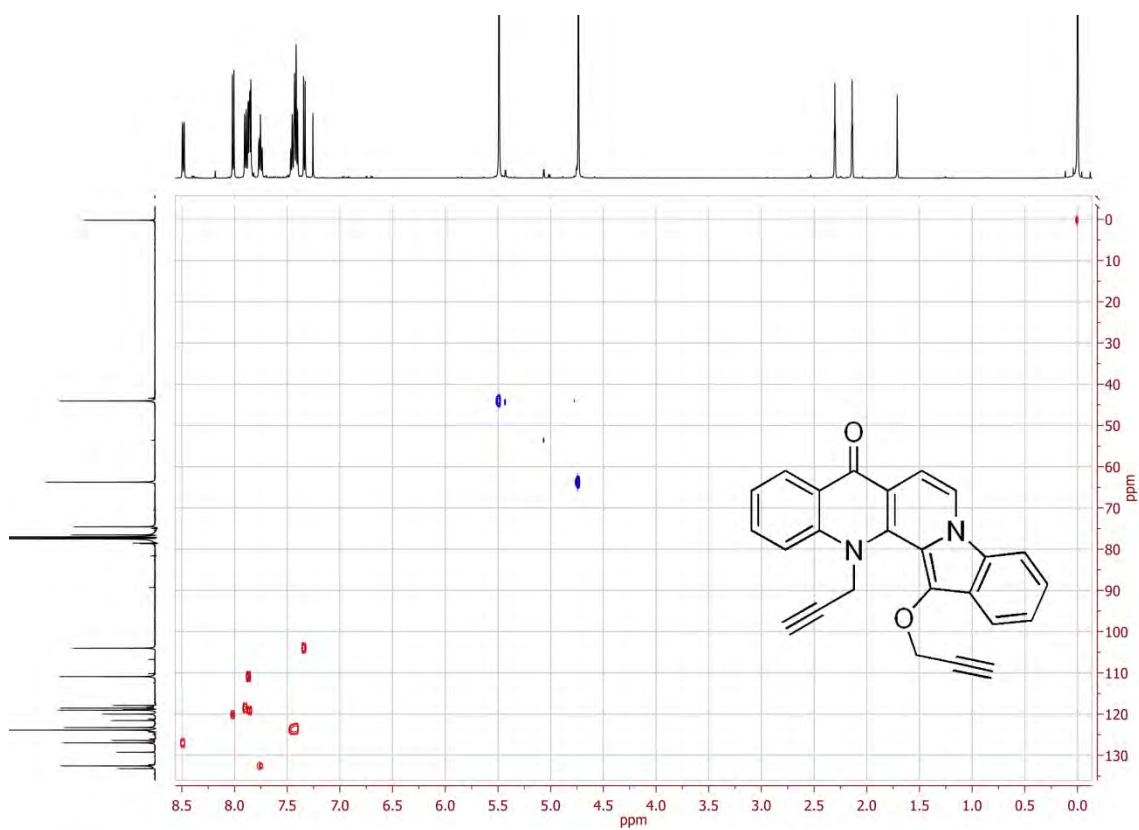
Figure 143: The gHSQC for compound **266**.
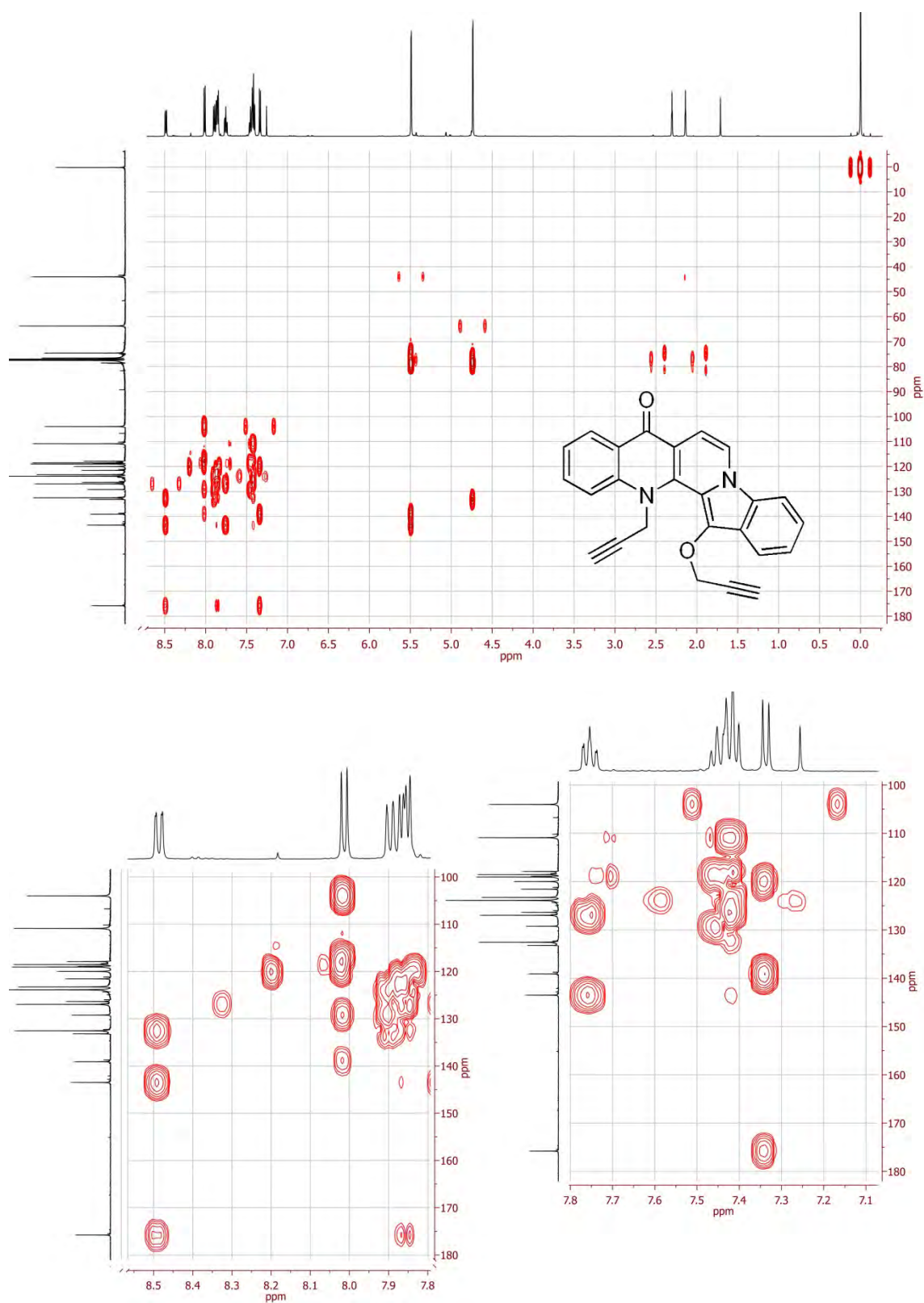
Figure 144: The gHMBC and its expansions for compound **266**.

Compound 269
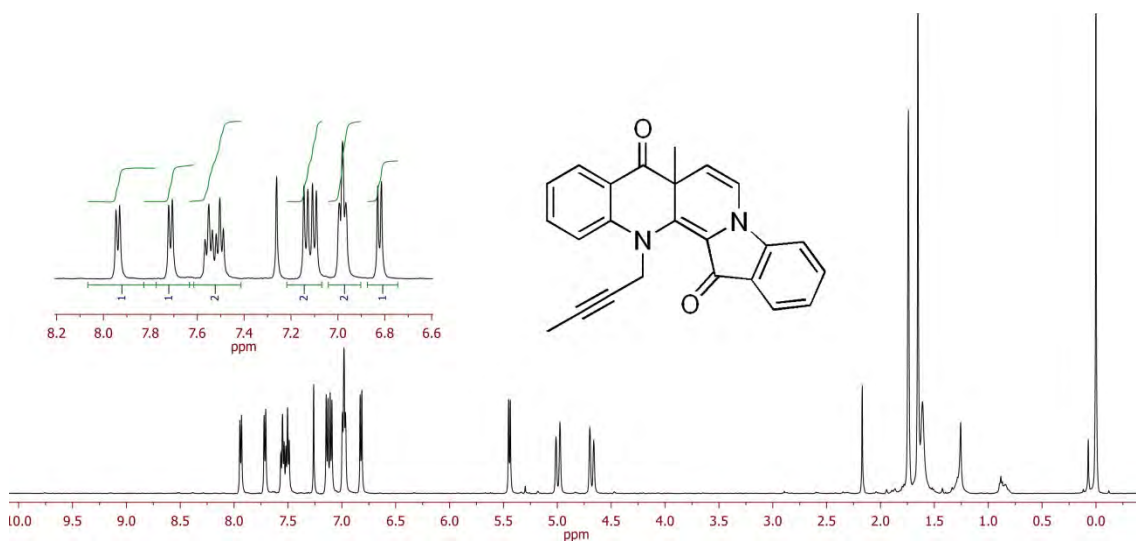
Figure 145: ^{1}H NMR spectrum for compound **269**.
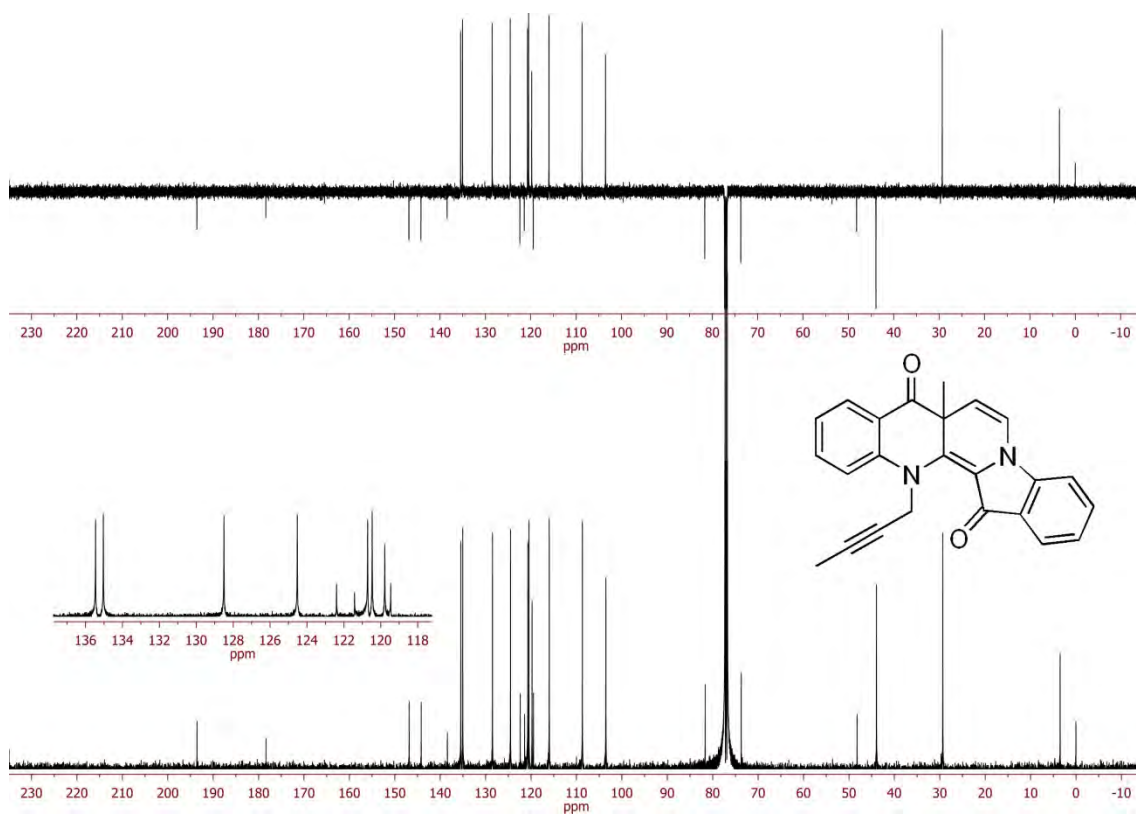
Figure 146: ^{13}C NMR spectrum for compound **269**.
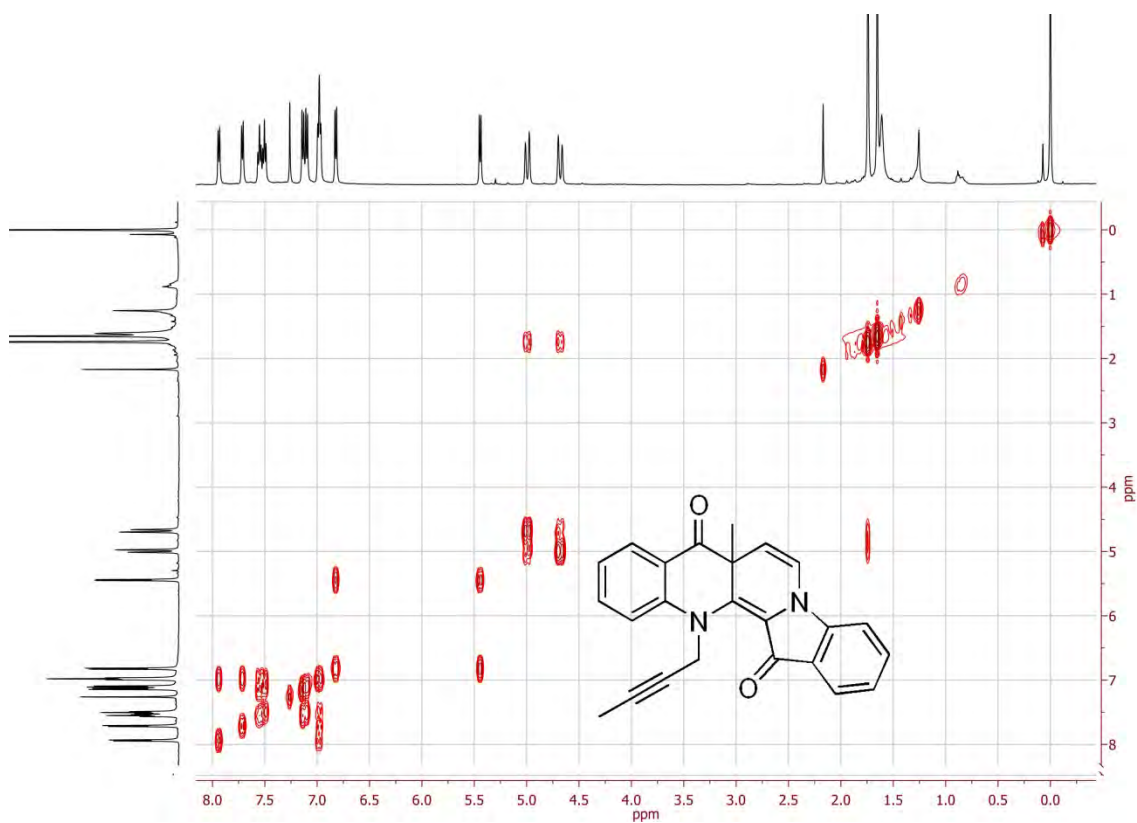
Figure 147: The gCOSY for compound **269**.
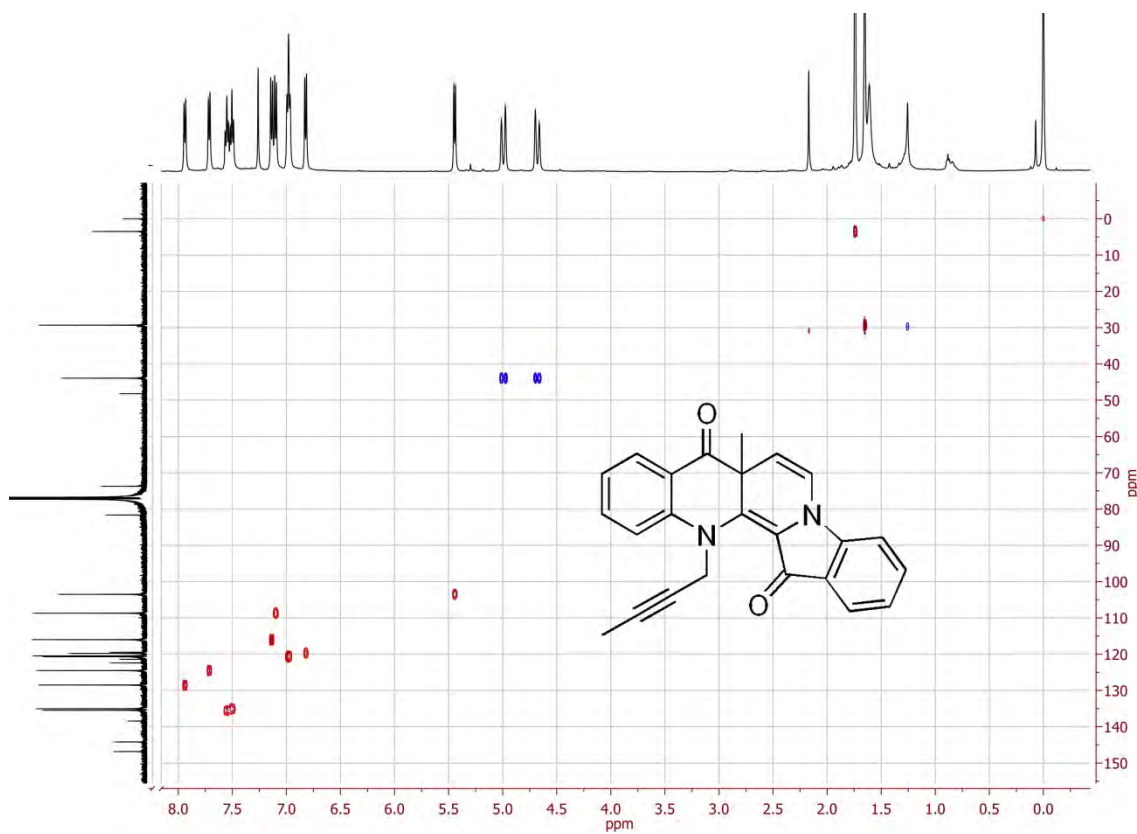
Figure 148: The gHSQC for compound **269**.
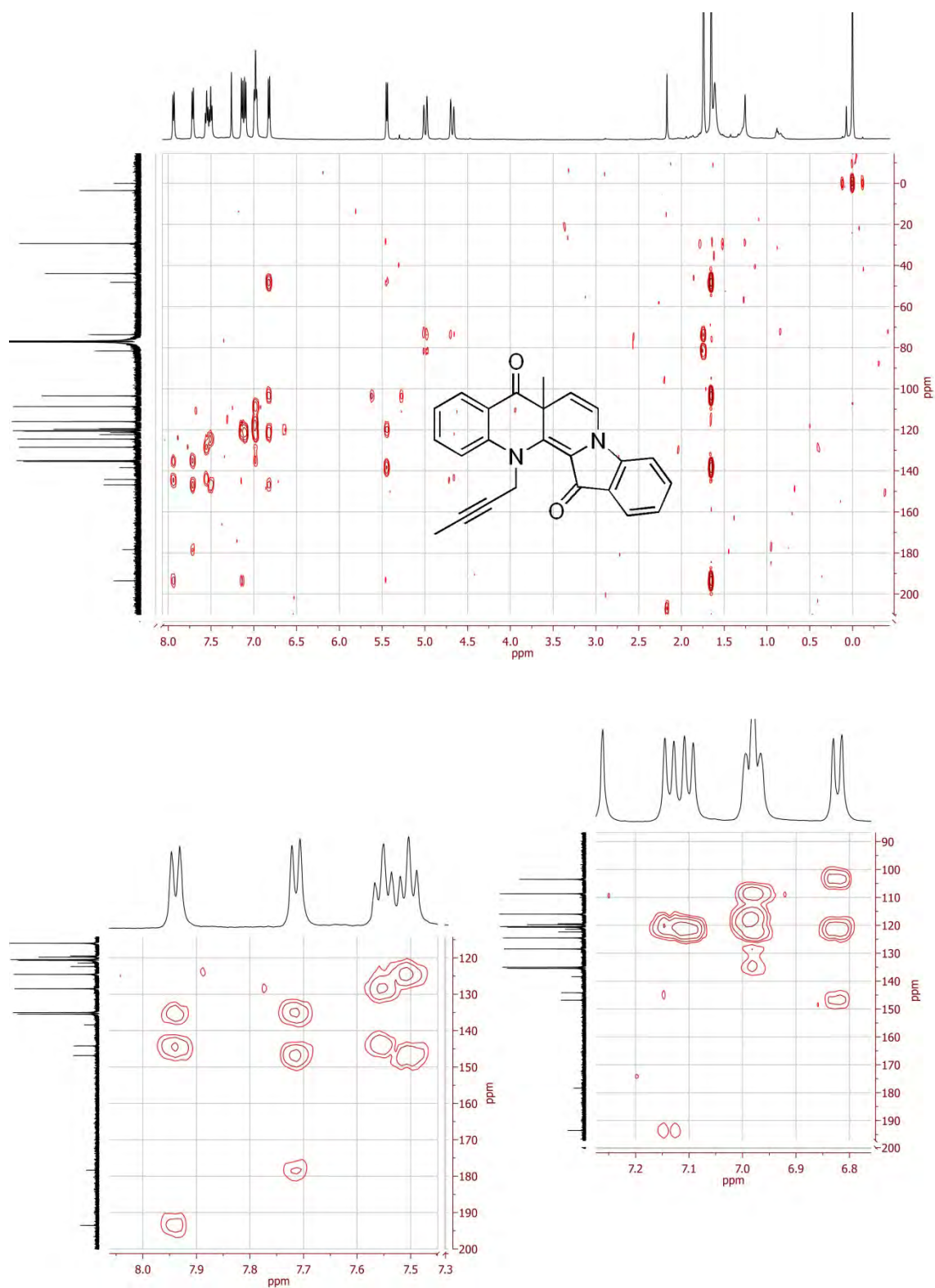
Figure 149: The gHMBC and its expansions for compound **269**.

Compound 270
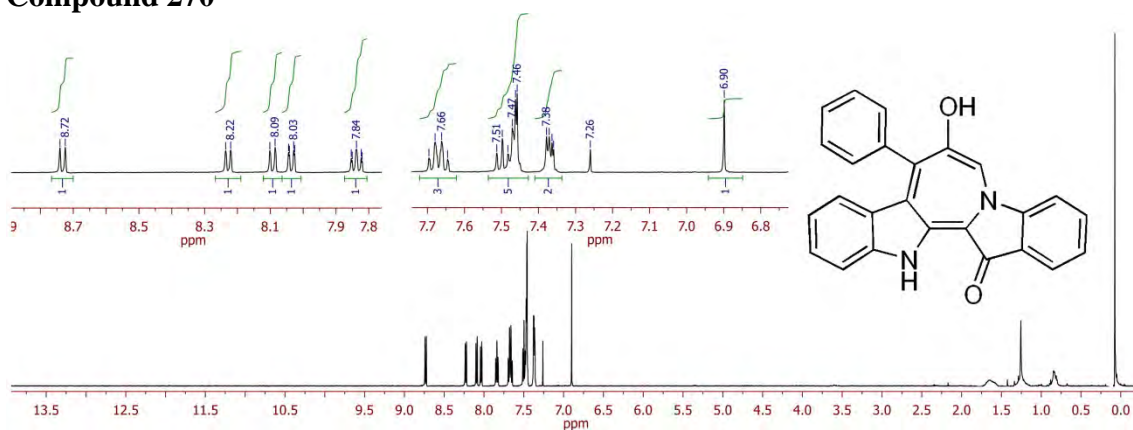
Figure 150: ¹H NMR spectrum for compound **270**.
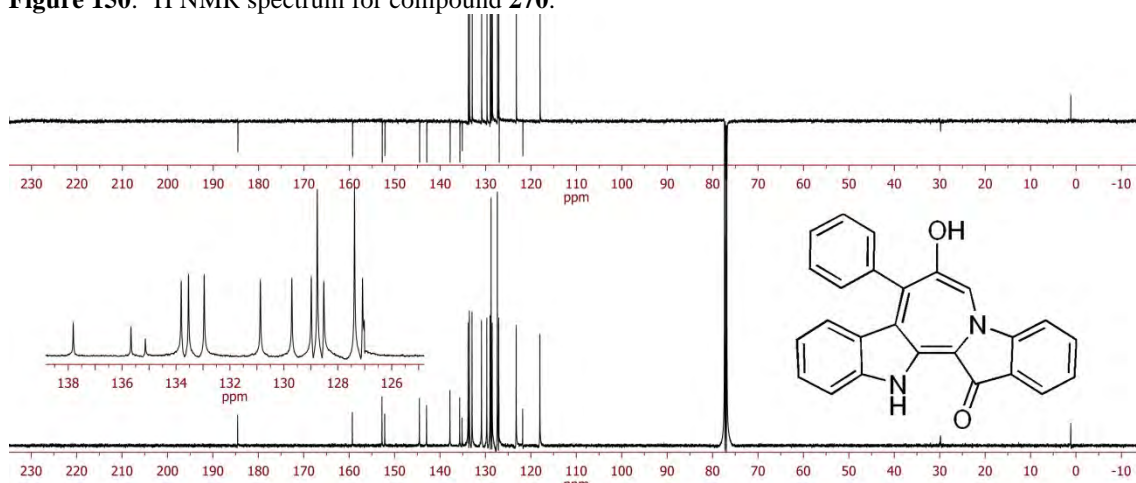
Figure 151: ¹³C NMR spectrum for compound **270**.
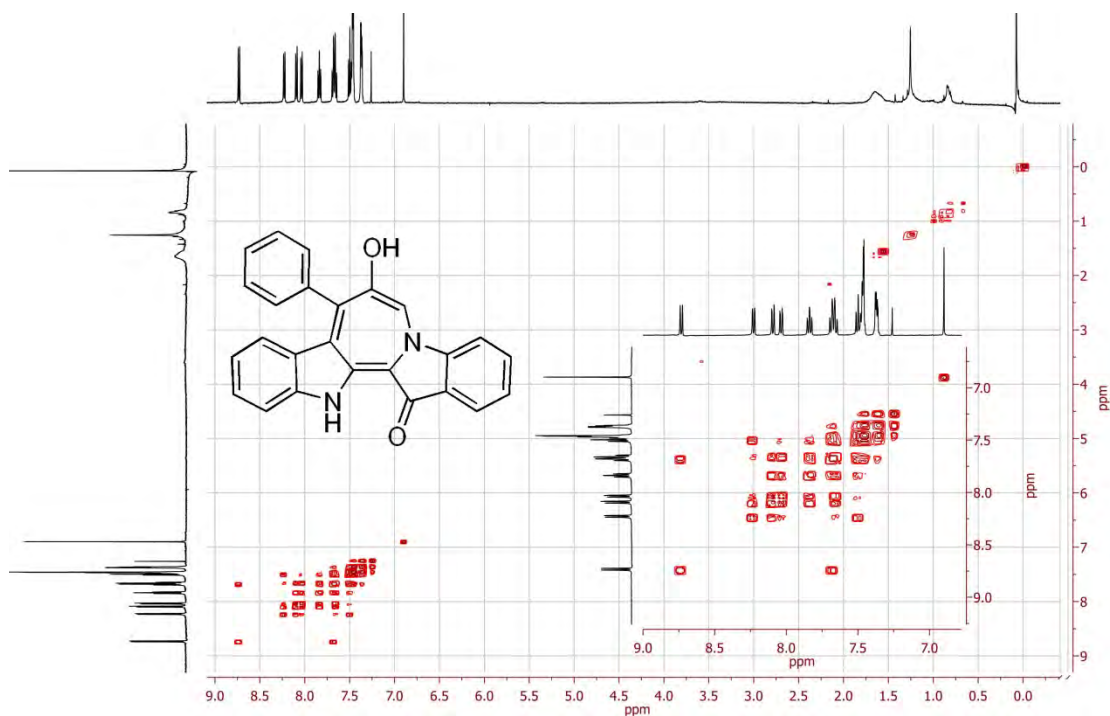
Figure 152 The gCOSY and expansions for compound **270**.
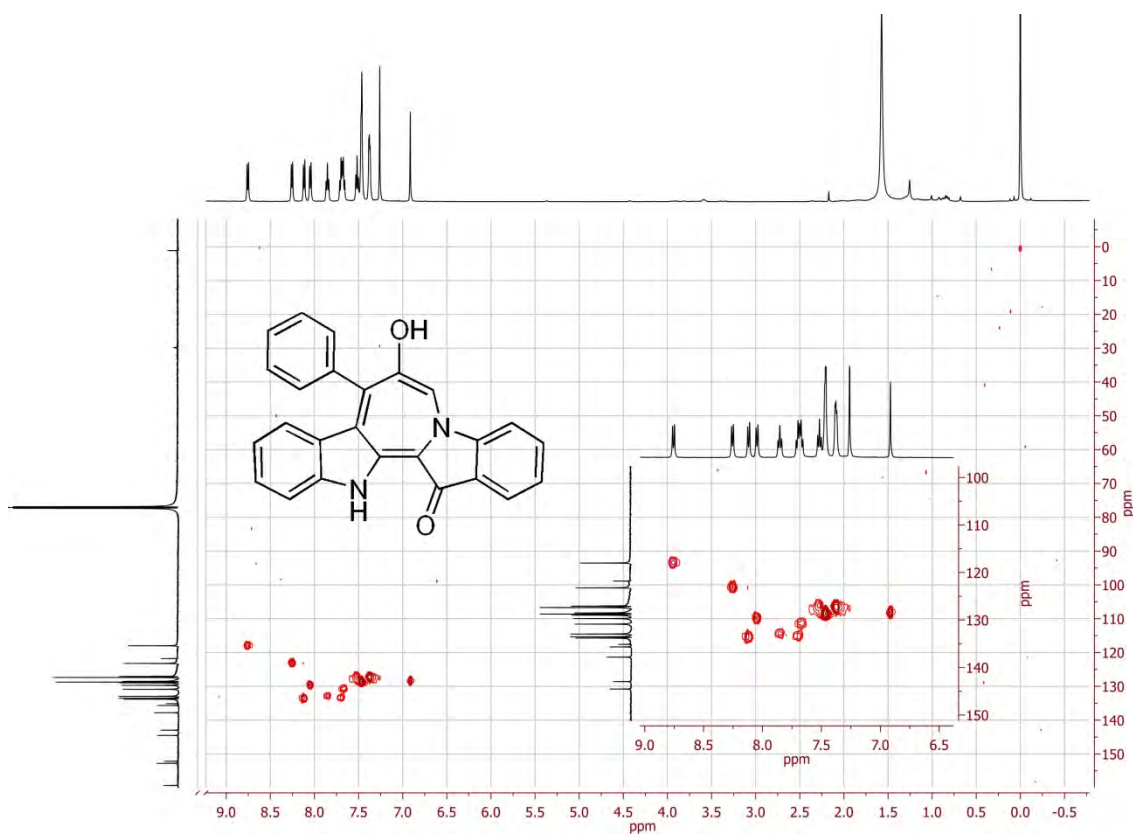
Figure 153: The gHSQC for compound **270**.
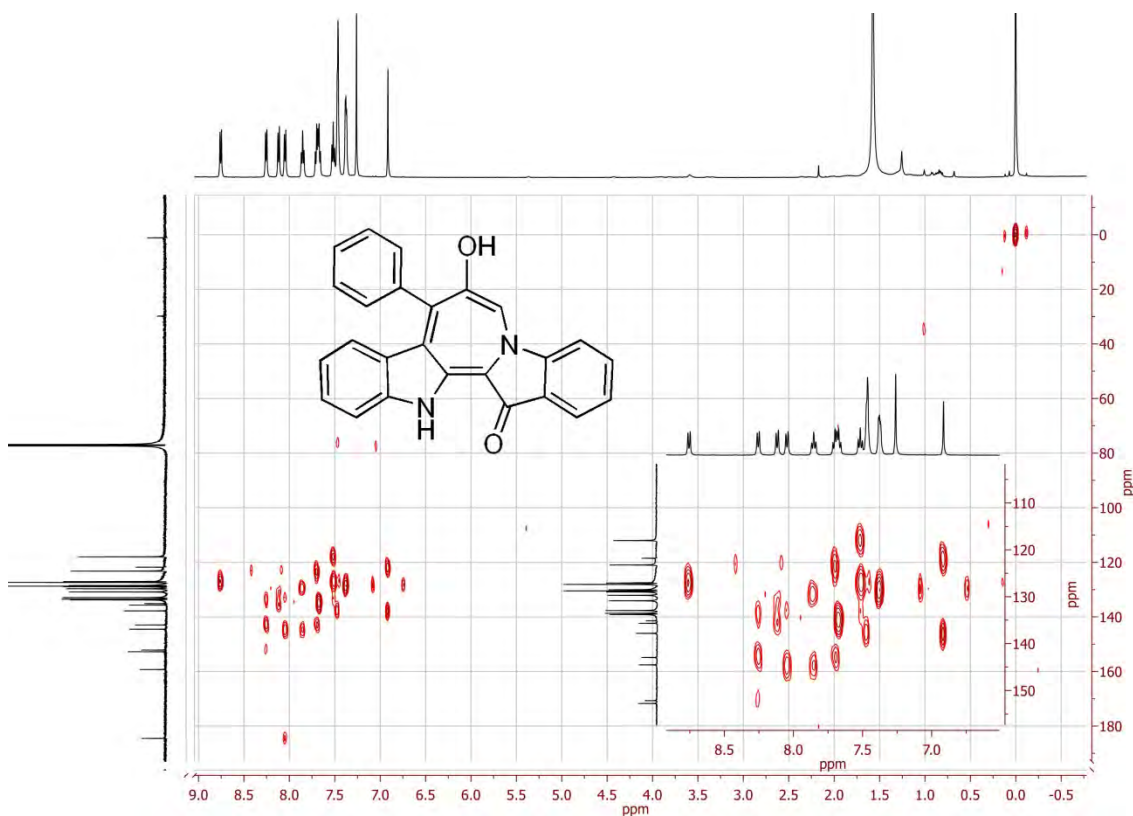
Figure 154: The gHMBC and its expansions for compound **270**.

Compound 271
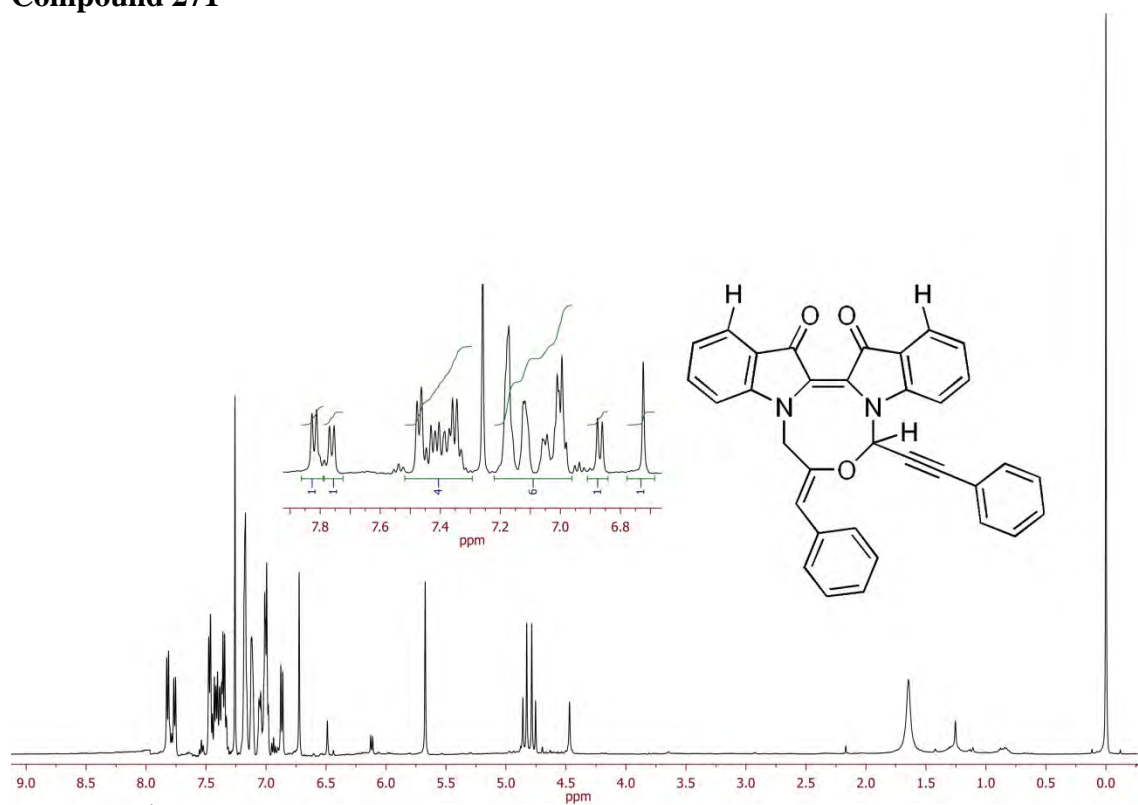
Figure 155: ¹H NMR spectrum for compound **271**.
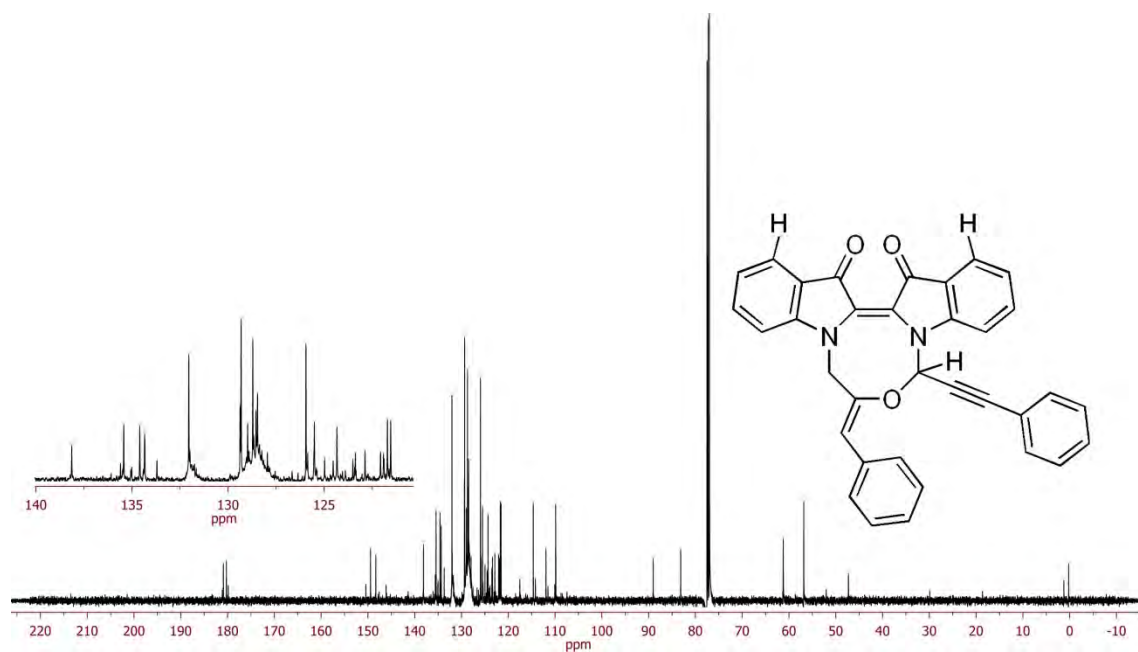
Figure 156: ¹³C NMR spectrum for compound **271**.
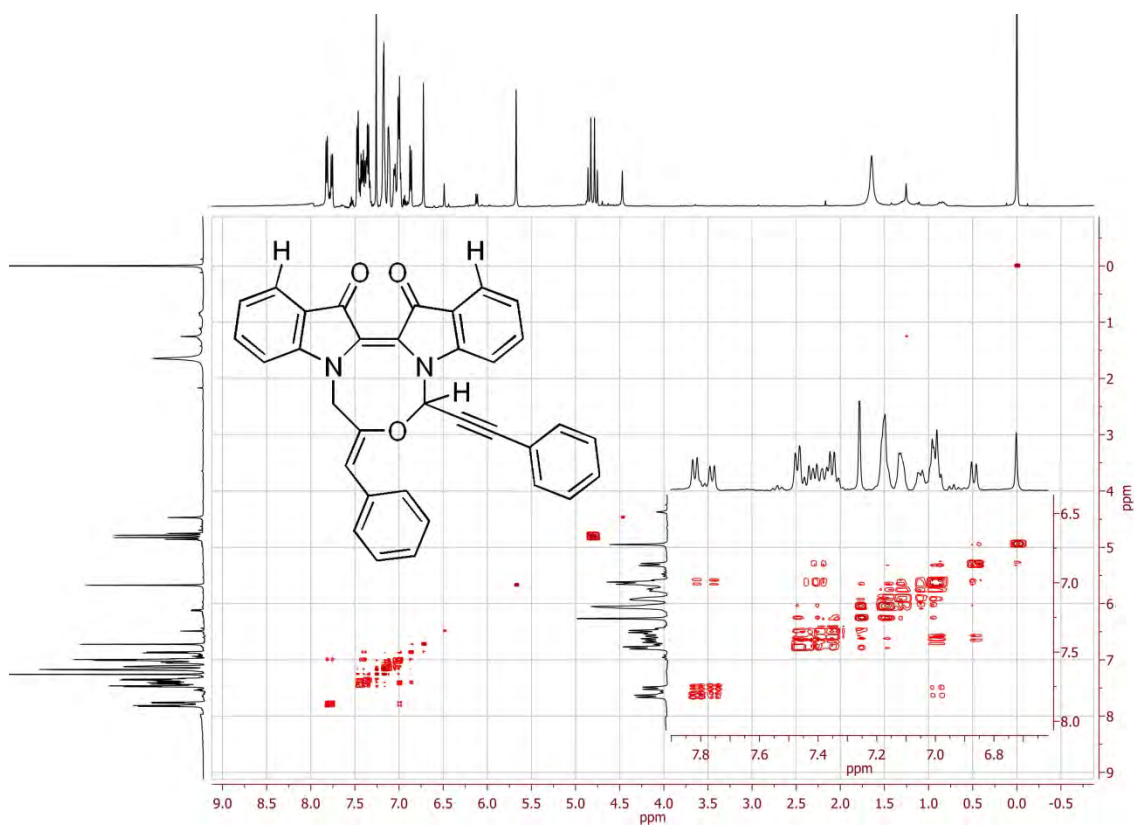
Figure 157: The gCOSY and expansions for compound **271**.
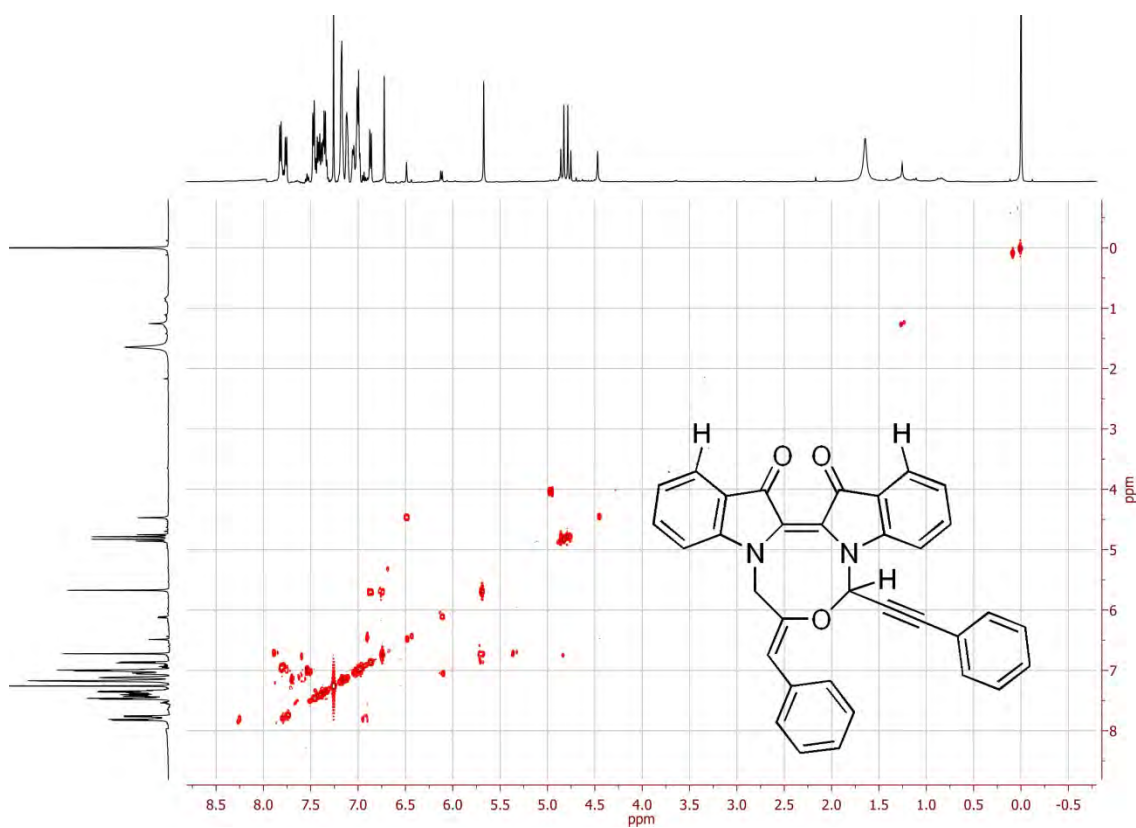
Figure 158: The ROSEY and expansions for compound **271**.
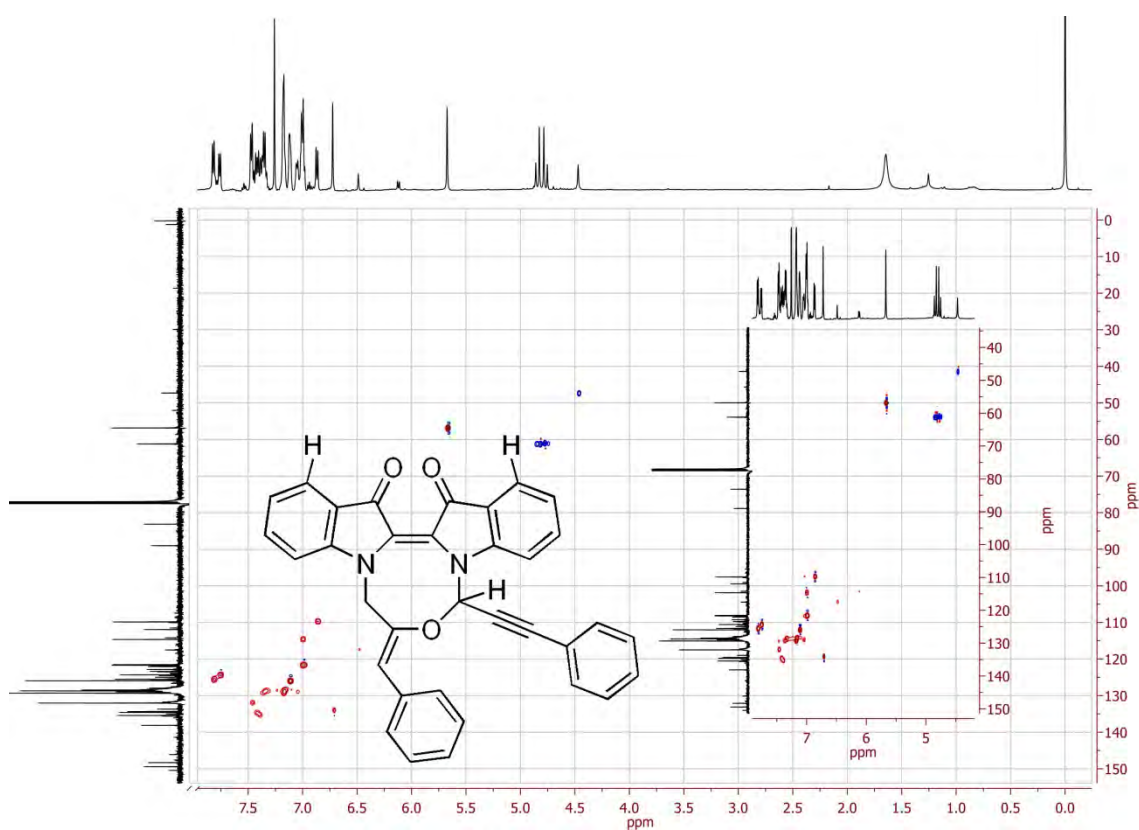
Figure 159: The gHSQC for compound **271**.
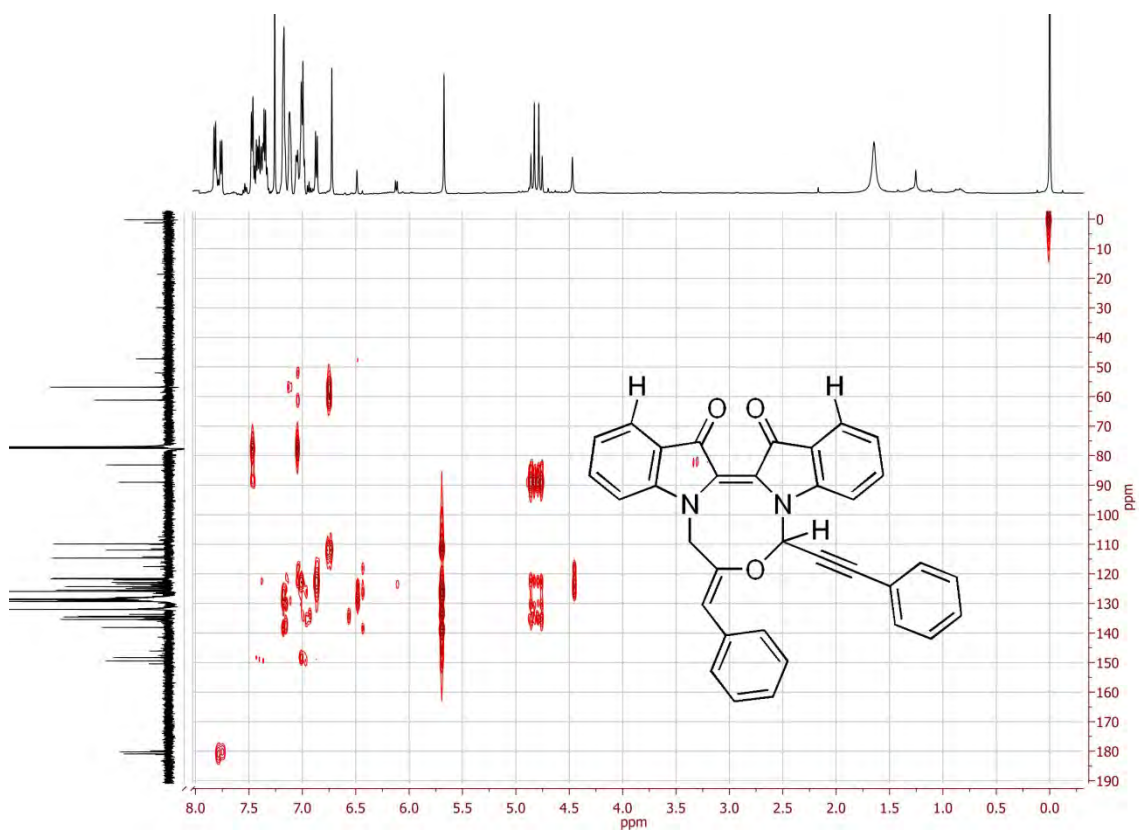
Figure 160: The gHMBC for compound **271**.

Compound 274
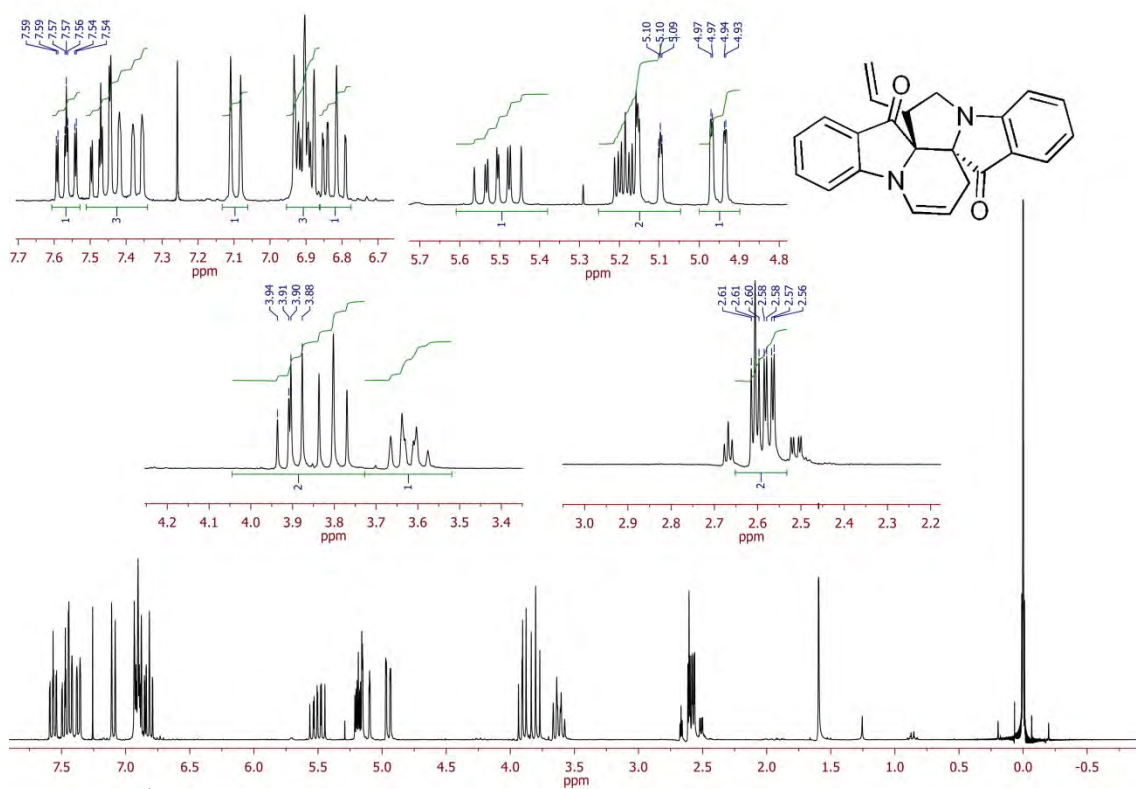
Figure 161: ^{1}H NMR spectrum for compound **274**.
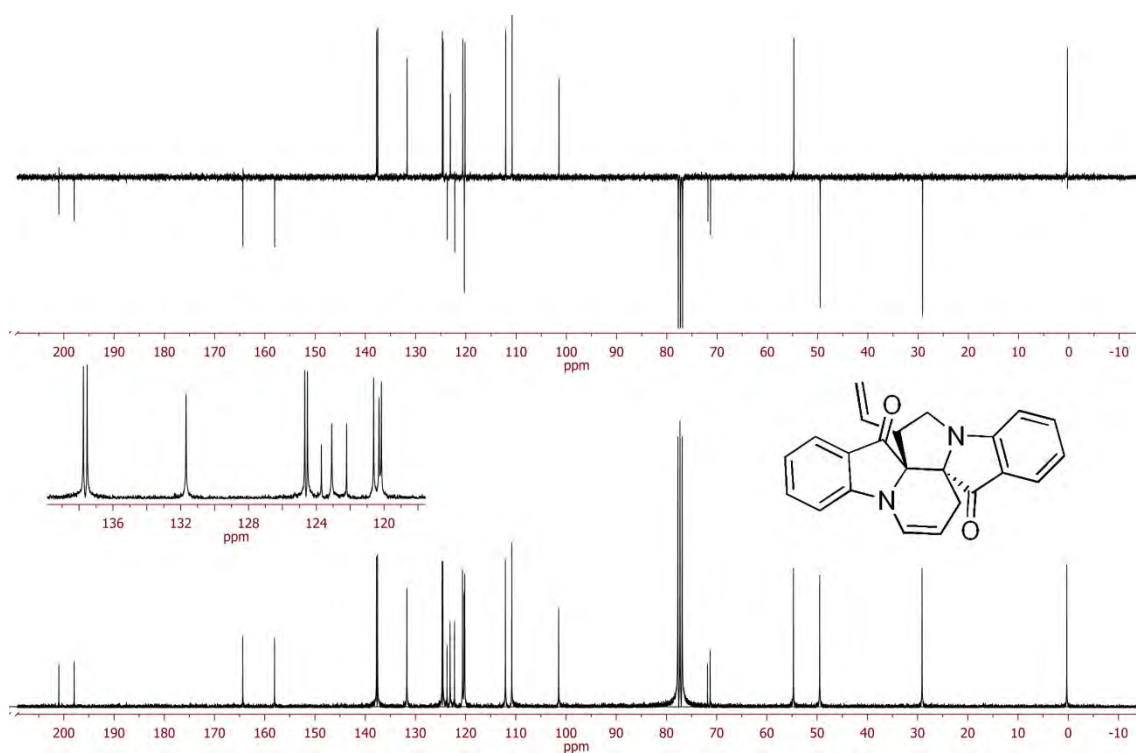
Figure 162: ^{13}C NMR spectrum for compound **274**.
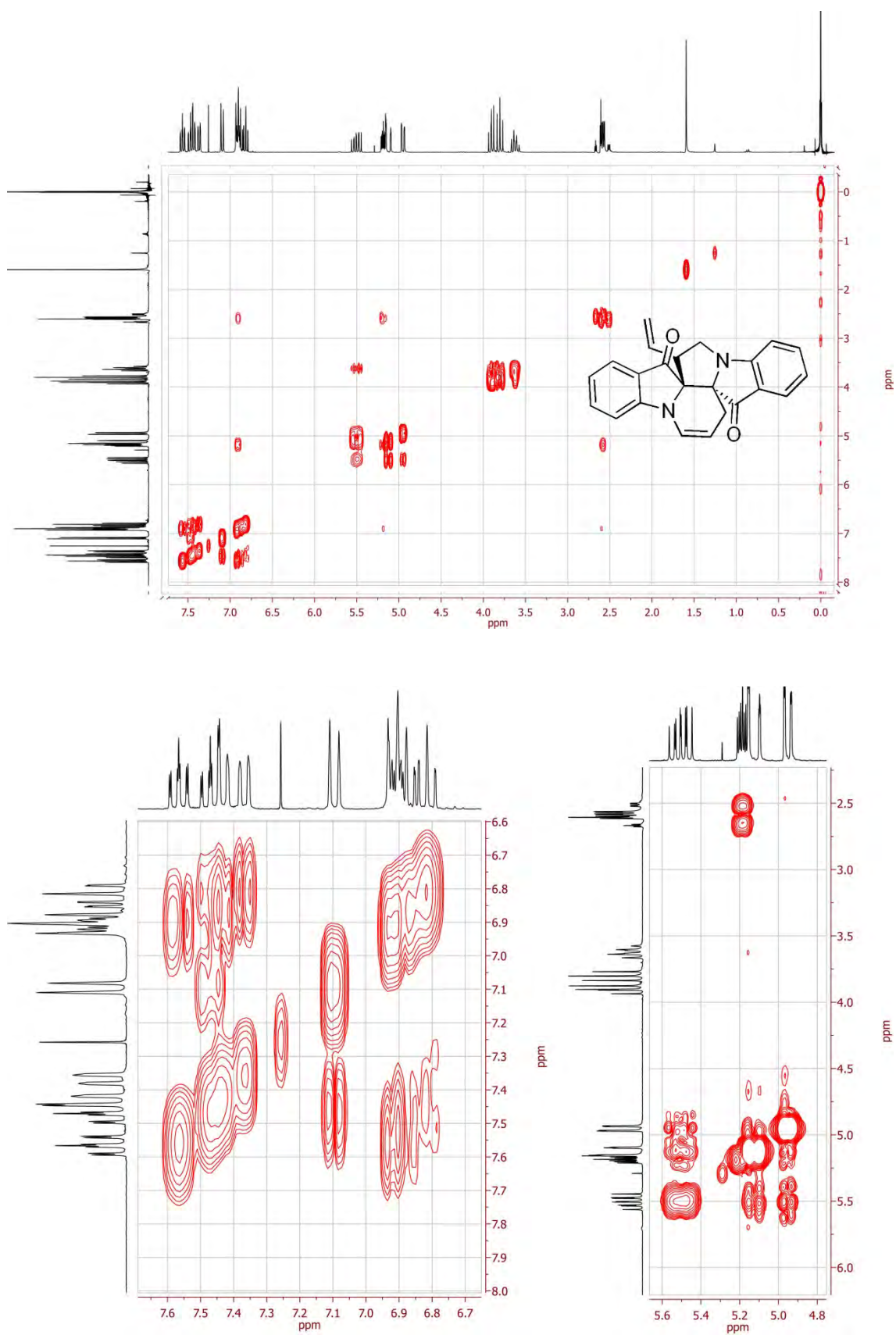
Figure 163: The gCOSY and expansions for compound **274**.
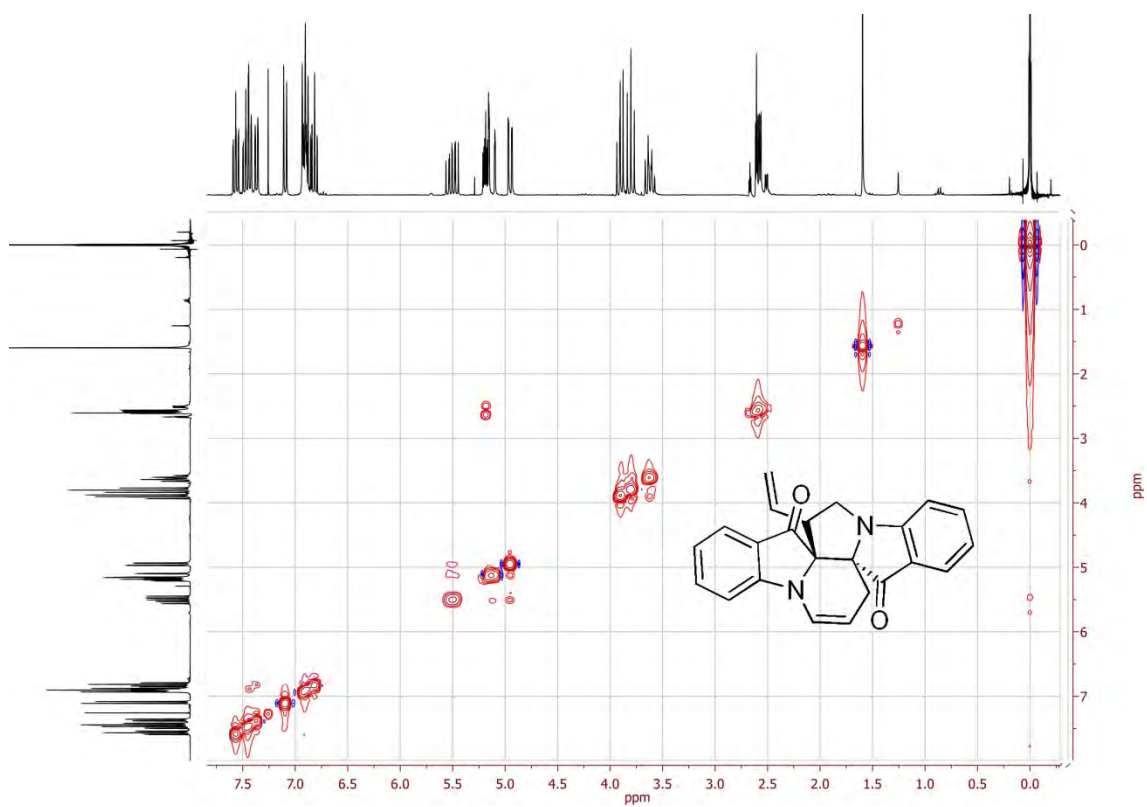
Figure 164: The NOESY for compound **274**.
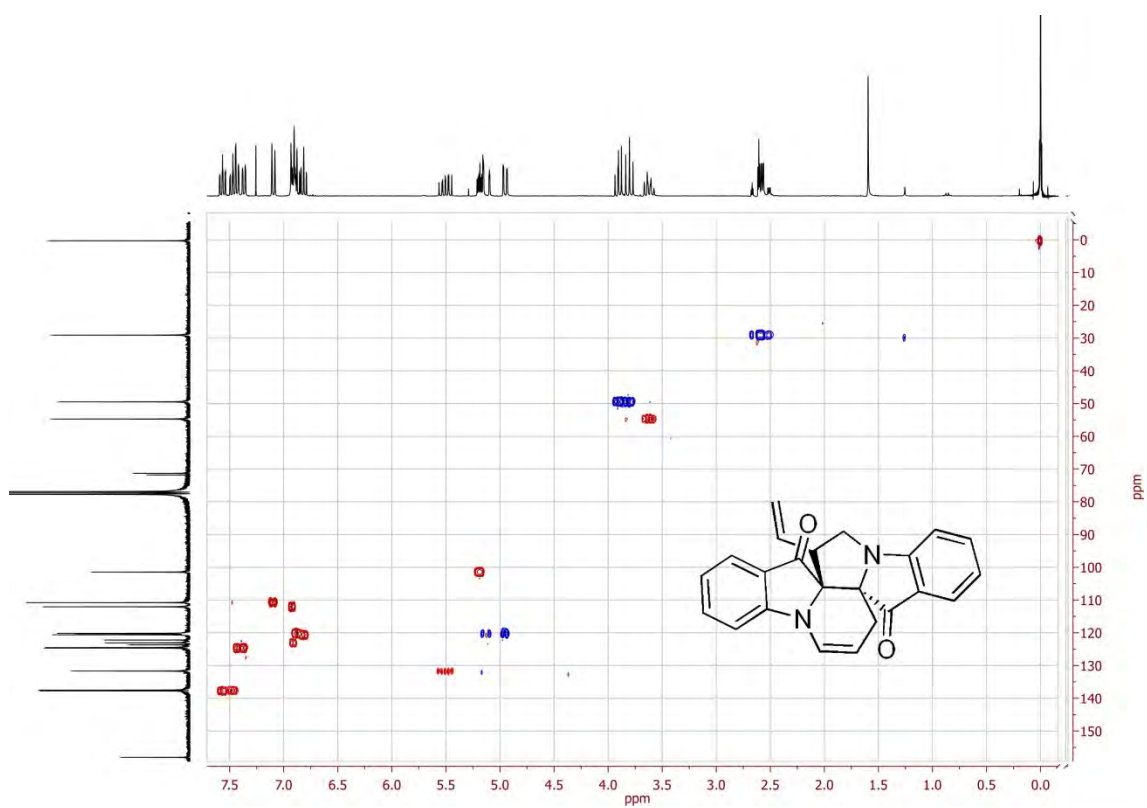
Figure 165: The gHSQC for compound **274**.
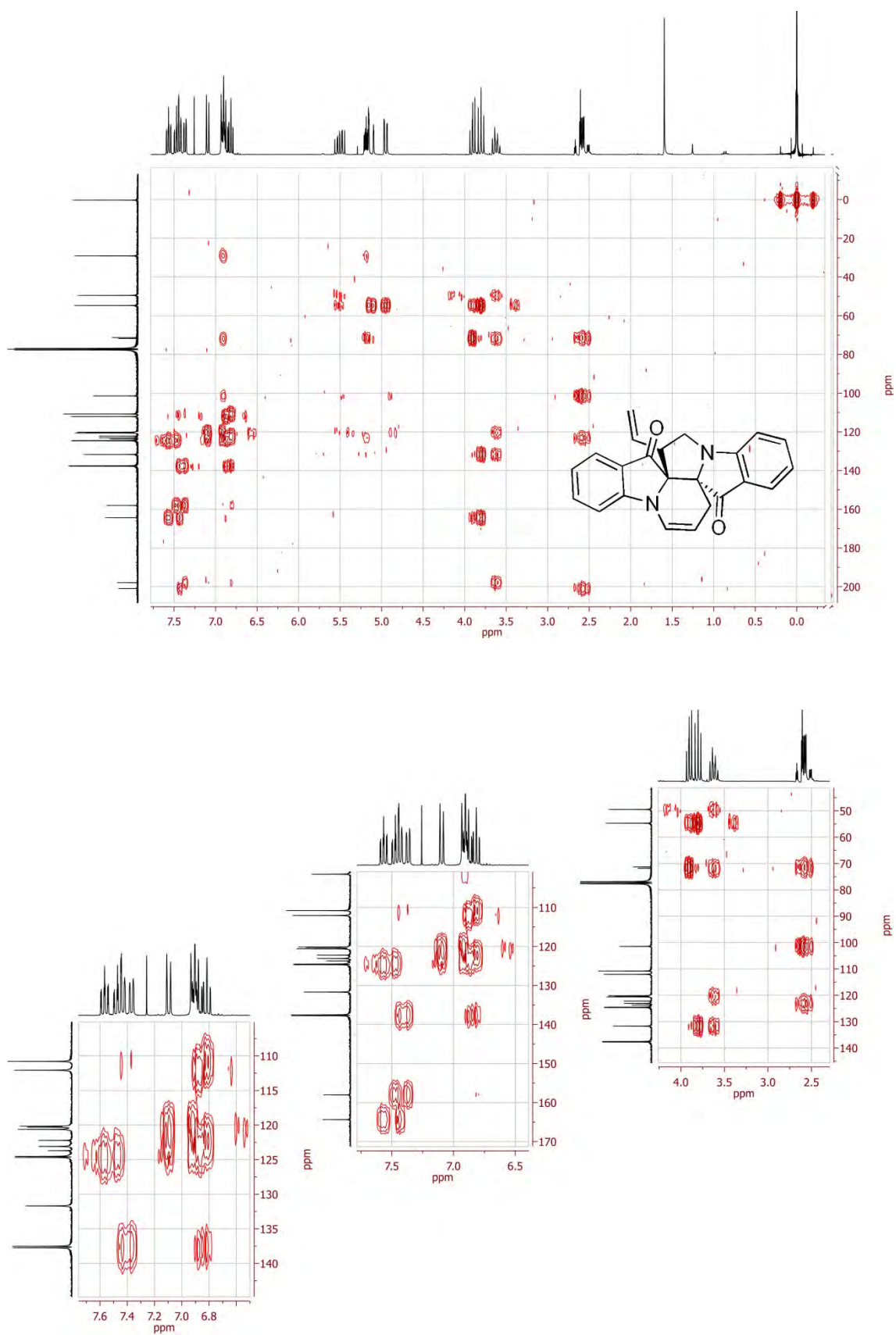
Figure 166: The gHMBC and its expansions for compound **274**.

Compound 275
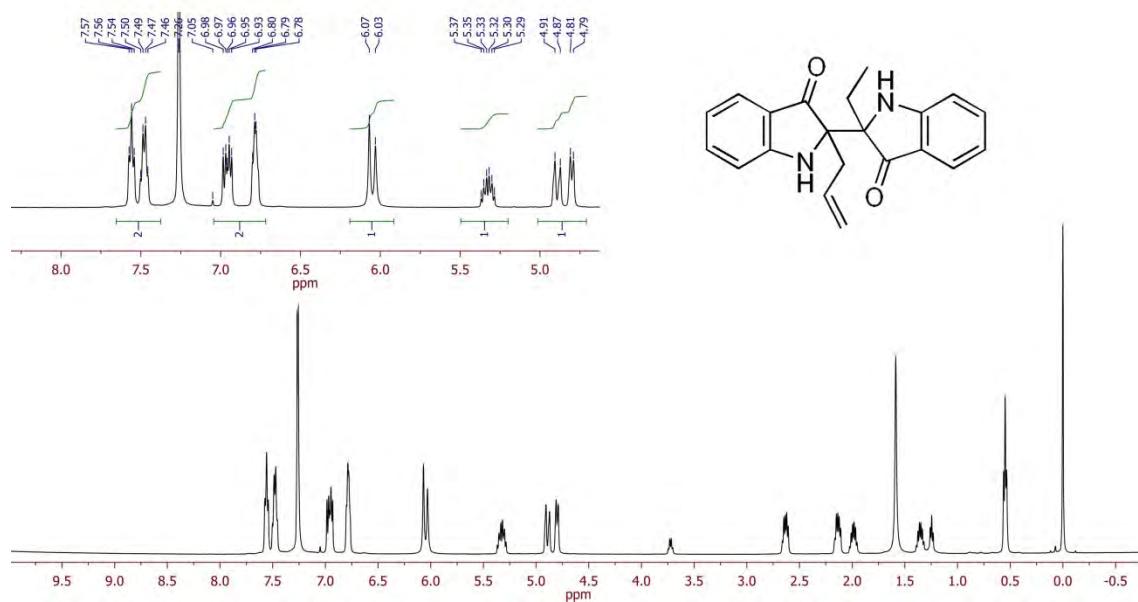
Figure 167: ¹H NMR spectrum for compound **275**.
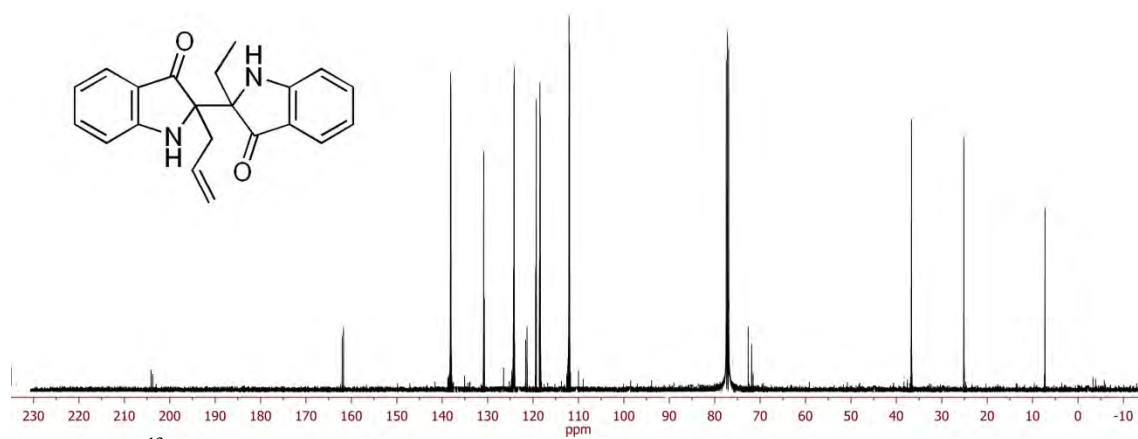
Figure 168: ¹³C NMR spectrum for compound **275**.

Compound 276

Figure 169: ^{1}H NMR spectrum for compound **276**.

Figure 170: ^{13}C NMR spectrum for compound **276**.

Figure 171: The gCOSY and expansions for compound **276**.
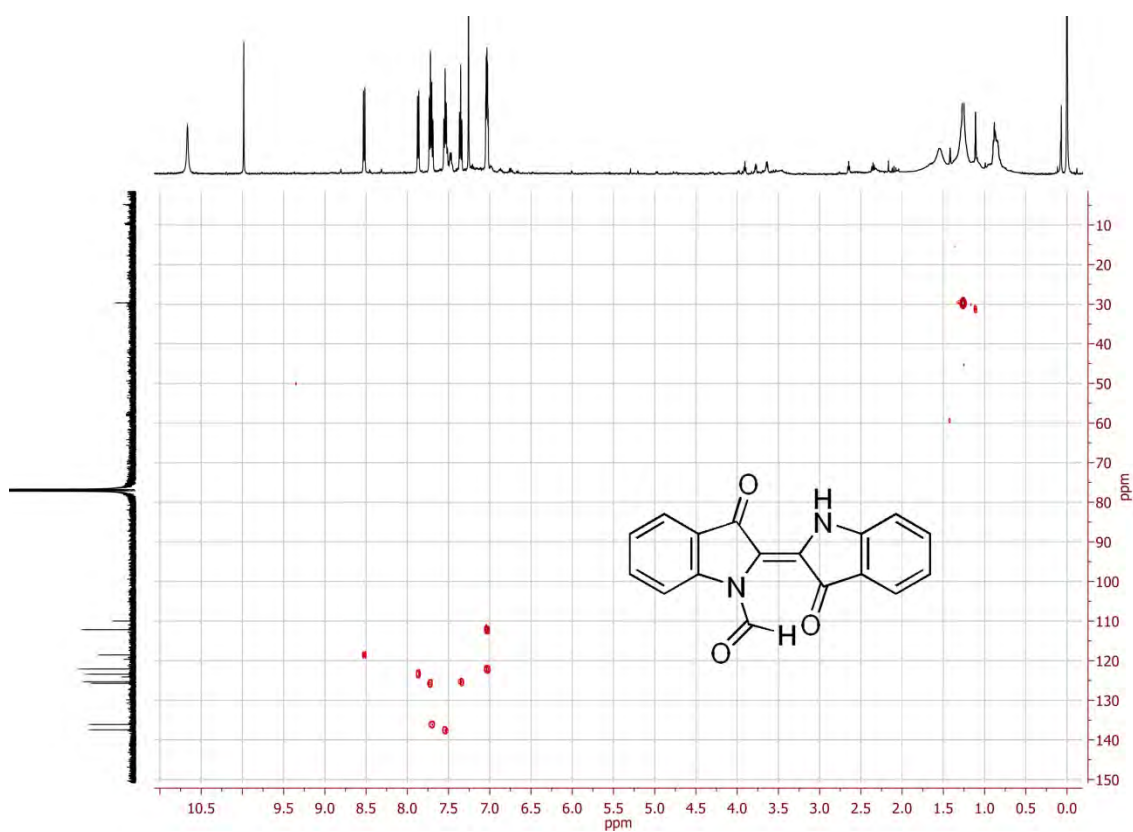
Figure 172: The gHSQC for compound **276**.
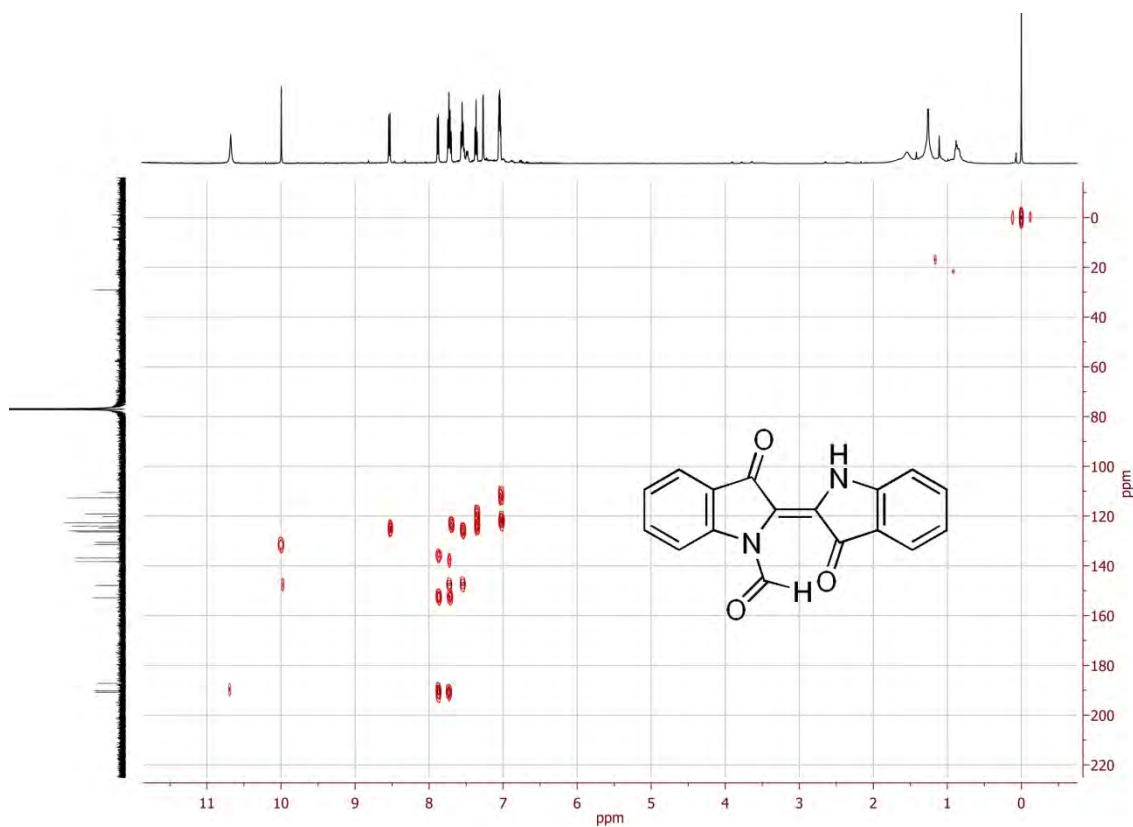
Figure 173: The gHMBC for compound **276**.

9.2   Appendix2: X-Ray Crystallography Data

Compound 243

Crystal data

$C_{19}H_{14}N_2O_2$
$M_r = 302.33$
Orthorhombic, $Pna2_1$
$a = 10.0417$ (3) Å
$b = 24.1863$ (5) Å
$c = 5.9097$ (2) Å
$V = 1435.30$ (7) Å^3
$Z = 4$
$F(000) = 632$

$D_x = 1.399$ Mg m^{-3}
Mo $K\alpha$ radiation, $\lambda = 0.71073$ Å
Cell parameters from 26870 reflections
$\theta = 3$–28°
$\mu = 0.09$ mm^{-1}
$T = 200$ K
Needle, Black
$0.50 \times 0.11 \times 0.04$ mm

Data collection

Nonius KappaCCD
  diffractometer
Graphite monochromator
φ and ω scans with CCD
Absorption correction: Integration
  via Gaussian method (Coppens, 1970) implemented in
  maXus (2000)
$T_{min} = 0.975$, $T_{max} = 0.996$

19627 measured reflections
1800 independent reflections
1359 reflections with $I > 2.0\sigma(I)$
$R_{int} = 0.065$
$\theta_{max} = 27.5°$, $\theta_{min} = 2.6°$
$h = -13 \rightarrow 13$
$k = -31 \rightarrow 31$
$l = -7 \rightarrow 7$

Refinement

Refinement on F^2
Least-squares matrix: Full
$R[F^2 > 2\sigma(F^2)] = 0.040$
$wR(F^2) = 0.088$
$S = 1.01$
1799 reflections
257 parameters
15 restraints
Primary atom site location: Structure-invariant direct
  methods

Hydrogen site location: Inferred from neighbouring
  sites
H atoms treated by a mixture of independent and
  constrained refinement
Method = Modified Sheldrick $w = 1/[\sigma^2(F^2) + (0.05P)^2 + 0.15P]$,
  where $P = (max(F_o^2,0) + 2F_c^2)/3$
$(\Delta/\sigma)_{max} = 0.009$
$\Delta\rho_{max} = 0.31$ e Å^{-3}
$\Delta\rho_{min} = -0.31$ e Å^{-3}

Special details

Refinement. The space group is noncentrosymmetric but the anomalous dispersion terms are very small for all elements in the structure, so the absolute structure of the crystal can not be determined in this experiment. Consequently Friedel-pair reflections have been averaged and the Flack parameter has not been refined. The space group is not enantiomorphic so the compound is present as a racemate within the crystal structure.

Peaks in a difference electron-density map suggested there was disorder in the packing of the —CH$_2$—CH=CH$_2$ group. Alternative sites were introduced for C22 and C23, namely C221 and C231. Restraints were imposed so equivalent bonds and angles should tend towards their mean values, and so the displacement parameters for C22 and C221 would tend to be similar. Even with the restraints, the C21—C22 and C21—C221 distances were still rather different. Consequently C21 was also split over two sites, C21 and C211. The displacement parameters for C21 and C211 were constrained to be identical as they are so close together. Distances restraints were applied to these sites also and now reasonably consistent bond lengths and angles were obtained. The relative occupancies of the disordered sites were refined.

The hydrogen atoms away from the disorder were observed in difference electron-density maps prior to their inclusion. They were included at calculated positions and were initially refined with soft restraints on the bond lengths and angles to regularise their geometry (C—H in the range 0.93–0.98Å; N—H = 0.86Å) and with U$_{iso}$(H) in the range 1.2-1.5 times U$_{eq}$ of the parent atom, after which the positions were refined without constraints and the displacement parameters were held fixed. H atoms within the disorder were included simply at calculated positions and ride on the atom sites to which they are attached.

The largest features in the final difference electron density map are located external to the molecule but seem to have no chemical significance.

Fractional atomic coordinates and isotropic or equivalent isotropic displacement parameters (Å^2)

	x	y	z	U_{iso}*/U_{eq}	Occ. (<1)
N1	0.6903 (2)	0.55609 (7)	0.0489 (4)	0.0413	
C2	0.7767 (2)	0.55333 (9)	−0.1332 (5)	0.0388	
C3	0.7897 (3)	0.51235 (10)	−0.2980 (5)	0.0447	
C4	0.8879 (2)	0.51932 (11)	−0.4586 (5)	0.0491	
C5	0.9712 (3)	0.56551 (11)	−0.4614 (6)	0.0525	
C6	0.9563 (2)	0.60618 (11)	−0.3004 (5)	0.0507	
C7	0.8584 (2)	0.59994 (9)	−0.1363 (5)	0.0426	
C8	0.8173 (2)	0.63614 (9)	0.0481 (5)	0.0462	
C9	0.7080 (2)	0.60528 (8)	0.1679 (5)	0.0383	

C10	0.6327 (2)	0.61759 (9)	0.3548 (5)	0.0377	
C11	0.5245 (2)	0.58007 (9)	0.4355 (5)	0.0400	
C12	0.4624 (2)	0.60853 (9)	0.6247 (5)	0.0426	
C13	0.3563 (3)	0.59429 (12)	0.7650 (6)	0.0561	
C14	0.3194 (3)	0.63076 (11)	0.9325 (6)	0.0600	
C15	0.3873 (3)	0.68096 (11)	0.9582 (5)	0.0540	
C16	0.4937 (3)	0.69553 (10)	0.8221 (5)	0.0464	
C17	0.5304 (2)	0.65865 (9)	0.6540 (5)	0.0407	
N18	0.63284 (18)	0.66341 (7)	0.4959 (4)	0.0415	
O19	0.8582 (2)	0.68267 (7)	0.0866 (5)	0.0737	
O20	0.49540 (17)	0.53457 (6)	0.3532 (4)	0.0485	
C21	0.7376 (12)	0.7051 (4)	0.534 (3)	0.0439	0.664 (9)
C22	0.7049 (5)	0.7621 (2)	0.4512 (10)	0.0413	0.664 (9)
C23	0.5962 (5)	0.7763 (2)	0.3413 (10)	0.0531	0.664 (9)
C211	0.720 (3)	0.7118 (8)	0.494 (5)	0.0439	0.336 (9)
C221	0.6519 (12)	0.7585 (5)	0.378 (2)	0.0542	0.336 (9)
C231	0.6676 (8)	0.8096 (3)	0.4360 (18)	0.0591	0.336 (9)
H11	0.616 (2)	0.5319 (10)	0.067 (5)	0.0495*	
H31	0.731 (3)	0.4788 (11)	−0.297 (5)	0.0537*	
H41	0.903 (2)	0.4915 (11)	−0.584 (5)	0.0589*	
H51	1.041 (3)	0.5680 (10)	−0.574 (5)	0.0630*	
H61	1.012 (3)	0.6410 (10)	−0.296 (6)	0.0609*	
H131	0.312 (3)	0.5584 (12)	0.749 (6)	0.0673*	
H141	0.242 (3)	0.6227 (11)	1.034 (6)	0.0721*	
H151	0.362 (3)	0.7073 (10)	1.073 (6)	0.0648*	
H161	0.538 (2)	0.7324 (10)	0.843 (6)	0.0558*	
H211	0.7539	0.7072	0.6925	0.0524*	0.664
H212	0.8161	0.6930	0.4592	0.0524*	0.664
H221	0.7682	0.7904	0.4806	0.0494*	0.664
H231	0.5837	0.8136	0.2950	0.0634*	0.664
H232	0.5302	0.7493	0.3083	0.0634*	0.664
H2111	0.7407	0.7221	0.6453	0.0524*	0.336
H2112	0.8003	0.7031	0.4160	0.0524*	0.336
H2211	0.5941	0.7504	0.2550	0.0653*	0.336
H2311	0.7247	0.8189	0.5583	0.0715*	0.336
H2312	0.6217	0.8379	0.3562	0.0715*	0.336

Atomic displacement parameters ($\mathring{A}^2$)

	U^{11}	U^{22}	U^{33}	U^{12}	U^{13}	U^{23}
N1	0.0451 (11)	0.0373 (10)	0.0414 (12)	−0.0028 (9)	0.0025 (10)	−0.0013 (10)
C2	0.0407 (12)	0.0393 (11)	0.0365 (13)	0.0058 (10)	−0.0028 (12)	0.0039 (11)
C3	0.0474 (14)	0.0434 (13)	0.0434 (15)	0.0041 (12)	−0.0065 (13)	−0.0029 (13)
C4	0.0510 (15)	0.0542 (15)	0.0421 (15)	0.0132 (12)	−0.0001 (13)	−0.0048 (14)
C5	0.0471 (13)	0.0577 (15)	0.0527 (17)	0.0060 (12)	0.0112 (15)	0.0006 (14)
C6	0.0504 (15)	0.0503 (14)	0.0515 (17)	0.0001 (12)	0.0069 (15)	−0.0005 (13)
C7	0.0444 (13)	0.0409 (12)	0.0424 (14)	0.0011 (10)	0.0036 (13)	0.0027 (12)
C8	0.0523 (14)	0.0402 (12)	0.0461 (15)	−0.0048 (11)	0.0039 (13)	0.0020 (13)
C9	0.0429 (12)	0.0334 (11)	0.0387 (14)	0.0020 (10)	0.0000 (12)	0.0034 (11)
C10	0.0408 (12)	0.0333 (11)	0.0390 (13)	0.0023 (9)	−0.0018 (12)	0.0025 (11)
C11	0.0422 (12)	0.0390 (12)	0.0388 (14)	0.0001 (10)	−0.0022 (11)	0.0044 (12)
C12	0.0456 (13)	0.0427 (12)	0.0394 (13)	0.0009 (11)	0.0025 (12)	0.0032 (12)
C13	0.0574 (17)	0.0541 (16)	0.0567 (19)	−0.0062 (14)	0.0130 (14)	0.0018 (16)
C14	0.0651 (17)	0.0635 (17)	0.0515 (17)	−0.0016 (14)	0.0206 (16)	0.0018 (16)
C15	0.0651 (16)	0.0544 (15)	0.0425 (15)	0.0078 (13)	0.0098 (14)	−0.0015 (14)
C16	0.0562 (15)	0.0430 (13)	0.0402 (14)	0.0031 (12)	0.0036 (13)	−0.0010 (13)
C17	0.0432 (12)	0.0405 (12)	0.0384 (14)	0.0042 (10)	0.0015 (12)	0.0067 (12)
N18	0.0462 (10)	0.0355 (10)	0.0427 (12)	−0.0019 (8)	0.0054 (10)	−0.0011 (9)
O19	0.1027 (15)	0.0490 (10)	0.0695 (14)	−0.0287 (10)	0.0331 (13)	−0.0113 (11)
O20	0.0542 (9)	0.0445 (9)	0.0469 (10)	−0.0087 (8)	0.0050 (9)	−0.0041 (9)
C21	0.051 (3)	0.040 (3)	0.042 (5)	−0.001 (3)	0.004 (2)	0.001 (2)

C22	0.040 (3)	0.041 (3)	0.043 (3)	−0.003 (2)	0.006 (2)	0.001 (2)
C23	0.061 (4)	0.050 (3)	0.048 (3)	0.003 (2)	0.001 (3)	0.006 (2)
C211	0.051 (3)	0.040 (3)	0.042 (5)	−0.001 (3)	0.004 (2)	0.001 (2)
C221	0.046 (9)	0.061 (7)	0.055 (9)	−0.009 (6)	−0.001 (7)	0.021 (7)
C231	0.063 (5)	0.039 (5)	0.075 (6)	−0.006 (4)	0.022 (5)	−0.019 (5)

Geometric parameters (Å, °)

N1—C2	1.384 (3)	C13—H131	0.98 (3)
N1—C9	1.394 (3)	C14—C15	1.401 (4)
N1—H11	0.95 (2)	C14—H141	1.00 (3)
C2—C3	1.396 (3)	C15—C16	1.383 (4)
C2—C7	1.394 (3)	C15—H151	0.96 (3)
C3—C4	1.379 (4)	C16—C17	1.385 (4)
C3—H31	1.00 (3)	C16—H161	1.00 (2)
C4—C5	1.396 (4)	C17—N18	1.395 (3)
C4—H41	1.01 (3)	N18—C21	1.474 (8)
C5—C6	1.377 (4)	N18—C211	1.462 (16)
C5—H51	0.97 (3)	C21—C22	1.500 (9)
C6—C7	1.389 (3)	C21—H211	0.950
C6—H61	1.01 (2)	C21—H212	0.950
C7—C8	1.458 (4)	C22—C23	1.316 (7)
C8—C9	1.504 (3)	C22—H221	0.950
C8—O19	1.219 (3)	C23—H231	0.950
C9—C10	1.371 (3)	C23—H232	0.950
C10—C11	1.494 (3)	C211—C221	1.491 (16)
C10—N18	1.387 (3)	C211—H2111	0.950
C11—C12	1.454 (3)	C211—H2112	0.950
C11—O20	1.238 (3)	C221—C231	1.292 (14)
C12—C13	1.393 (4)	C221—H2211	0.950
C12—C17	1.402 (3)	C231—H2311	0.950
C13—C14	1.377 (4)	C231—H2312	0.950
O19···C23[i]	2.994 (6)	C3···C11[iii]	3.501 (4)
O19···C15[ii]	3.397 (3)	C4···C9[iii]	3.530 (4)
O19···C21[iii]	3.53 (2)	C5···C9[iii]	3.565 (4)
O20···N1[iv]	3.102 (3)	C6···C231[ii]	3.328 (9)
O20···C3[iv]	3.207 (3)	C6···C21[iii]	3.39 (1)
O20···O20[iv]	3.397 (3)	C7···C21[iii]	3.43 (1)
O20···O20[v]	3.397 (3)	C8···C21[iii]	3.56 (2)
O20···C2[iv]	3.463 (3)	C13···C231[vii]	3.574 (9)
O20···C13[v]	3.493 (3)	C15···C231[viii]	3.59 (1)
N18···C7[vi]	3.494 (3)		
C2—N1—C9	110.72 (19)	C13—C14—H141	121.0 (17)
C2—N1—H11	123.0 (16)	C15—C14—H141	118.8 (17)
C9—N1—H11	124.8 (16)	C14—C15—C16	122.3 (3)
N1—C2—C3	129.5 (2)	C14—C15—H151	121.4 (16)
N1—C2—C7	109.9 (2)	C16—C15—H151	116.3 (17)
C3—C2—C7	120.7 (2)	C15—C16—C17	117.3 (2)
C2—C3—C4	117.4 (2)	C15—C16—H161	119.6 (17)
C2—C3—H31	121.2 (16)	C17—C16—H161	123.1 (18)
C4—C3—H31	121.4 (16)	C12—C17—C16	121.1 (2)
C3—C4—C5	122.3 (3)	C12—C17—N18	110.4 (2)
C3—C4—H41	121.8 (15)	C16—C17—N18	128.6 (2)
C5—C4—H41	115.9 (15)	C17—N18—C10	109.66 (17)
C4—C5—C6	119.9 (3)	C17—N18—C21	118.7 (7)
C4—C5—H51	119.4 (16)	C10—N18—C21	129.7 (7)
C6—C5—H51	120.7 (16)	C17—N18—C211	120.9 (15)
C5—C6—C7	118.8 (2)	C10—N18—C211	129.4 (15)
C5—C6—H61	123.7 (17)	N18—C21—C22	114.9 (7)
C7—C6—H61	117.5 (17)	N18—C21—H211	108.1

C2—C7—C6	120.9 (2)	C22—C21—H211	108.1
C2—C7—C8	108.0 (2)	N18—C21—H212	108.1
C6—C7—C8	131.1 (2)	C22—C21—H212	108.1
C7—C8—C9	105.10 (19)	H211—C21—H212	109.5
C7—C8—O19	126.8 (2)	C21—C22—C23	125.7 (6)
C9—C8—O19	128.0 (2)	C21—C22—H221	117.1
C8—C9—N1	106.2 (2)	C23—C22—H221	117.1
C8—C9—C10	132.3 (2)	C22—C23—H231	120.0
N1—C9—C10	121.5 (2)	C22—C23—H232	120.0
C9—C10—C11	121.8 (2)	H231—C23—H232	120.0
C9—C10—N18	131.1 (2)	N18—C211—C221	109.5 (13)
C11—C10—N18	107.10 (19)	N18—C211—H2111	109.4
C10—C11—C12	105.66 (19)	C221—C211—H2111	109.5
C10—C11—O20	125.9 (2)	N18—C211—H2112	109.5
C12—C11—O20	128.5 (2)	C221—C211—H2112	109.5
C11—C12—C13	132.0 (2)	H2111—C211—H2112	109.5
C11—C12—C17	107.2 (2)	C211—C221—C231	123.2 (12)
C13—C12—C17	120.8 (2)	C211—C221—H2211	118.4
C12—C13—C14	118.4 (3)	C231—C221—H2211	118.4
C12—C13—H131	121 (2)	C221—C231—H2311	120.1
C14—C13—H131	121 (2)	C221—C231—H2312	119.9
C13—C14—C15	120.2 (3)	H2311—C231—H2312	120.0
O19—C8—C7—C2	−173.4 (3)	C6—C7—C8—C9	−178.9 (3)
O19—C8—C7—C6	5.0 (5)	C7—C2—N1—C9	2.2 (3)
O19—C8—C9—N1	174.6 (3)	C7—C8—C9—C10	178.7 (3)
O19—C8—C9—C10	−5.2 (5)	C8—C9—C10—C11	177.5 (2)
O20—C11—C10—N18	−178.9 (2)	C9—C10—N18—C17	175.5 (3)
O20—C11—C10—C9	3.2 (4)	C9—C10—N18—C21	−20.8 (9)
O20—C11—C12—C13	−0.1 (5)	C9—C10—N18—C211	−4 (2)
O20—C11—C12—C17	180.0 (3)	C9—C10—C11—C12	−176.2 (2)
N1—C2—C3—C4	−178.1 (2)	C10—N18—C17—C12	1.7 (3)
N1—C2—C7—C6	178.4 (2)	C10—N18—C17—C16	−178.5 (3)
N1—C2—C7—C8	−3.1 (3)	C10—N18—C21—C22	112.6 (8)
N1—C9—C8—C7	−1.5 (3)	C10—N18—C211—C221	99 (2)
N1—C9—C10—N18	−179.6 (2)	C10—C11—C12—C13	179.3 (3)
N1—C9—C10—C11	−2.4 (4)	C10—C11—C12—C17	−0.7 (3)
N18—C10—C9—C8	0.2 (5)	C11—C10—N18—C17	−2.1 (3)
N18—C10—C11—C12	1.7 (3)	C11—C10—N18—C21	161.6 (8)
N18—C17—C12—C11	−0.6 (3)	C11—C10—N18—C211	179 (1)
N18—C17—C12—C13	179.4 (2)	C11—C12—C13—C14	−179.7 (3)
N18—C17—C16—C15	179.9 (3)	C11—C12—C17—C16	179.6 (2)
N18—C21—C22—C23	−3 (2)	C12—C13—C14—C15	0.4 (5)
N18—C211—C221—C231	146 (1)	C12—C17—N18—C21	−164.0 (6)
C2—N1—C9—C8	−0.4 (3)	C12—C17—N18—C211	−179 (1)
C2—N1—C9—C10	179.5 (2)	C12—C17—C16—C15	−0.3 (4)
C2—C3—C4—C5	−0.8 (4)	C13—C12—C17—C16	−0.4 (4)
C2—C7—C6—C5	0.2 (4)	C13—C14—C15—C16	−1.1 (5)
C2—C7—C8—C9	2.7 (3)	C14—C13—C12—C17	0.3 (4)
C3—C2—N1—C9	−178.2 (3)	C14—C15—C16—C17	1.0 (4)
C3—C2—C7—C6	−1.3 (4)	C16—C17—N18—C21	15.8 (7)
C3—C2—C7—C8	177.2 (2)	C16—C17—N18—C211	1 (1)
C3—C4—C5—C6	−0.3 (4)	C17—N18—C21—C22	−85 (1)
C4—C3—C2—C7	1.5 (4)	C17—N18—C211—C221	−80 (2)
C4—C5—C6—C7	0.5 (4)	C22—C21—N18—C211	18 (5)
C5—C6—C7—C8	−177.9 (3)		

Symmetry codes: (i) $x+1/2, -y+3/2, z$; (ii) $x+1/2, -y+3/2, z-1$; (iii) $x, y, z-1$; (iv) $-x+1, -y+1, z+1/2$; (v) $-x+1, -y+1, z-1/2$; (vi) $x, y, z+1$; (vii) $x-1/2, -y+3/2, z$; (viii) $x-1/2, -y+3/2, z+1$.

Hydrogen-bond geometry (Å, °)

D—H⋯A	D—H	H⋯A	D⋯A	D—H⋯A
N1—H11⋯O20	0.95 (2)	2.09 (3)	2.708 (3)	122 (2)
N1—H11⋯O20ᵛ	0.95 (2)	2.33 (3)	3.102 (3)	138 (2)

Symmetry code: (v) $-x+1, -y+1, z-1/2$.

Compound 248

Crystal data

$C_{22}H_{18}N_2O_2$
$M_r = 342.40$
Monoclinic, $P2_1/n$
Hall symbol: -P 2yn
$a = 11.888$ (2) Å
$b = 11.667$ (2) Å
$c = 12.5729$ (17) Å
$\beta = 107.386$ (11)°
$V = 1664.1$ (5) Å^3
$Z = 4$

$F(000) = 720$
$D_x = 1.367$ Mg m^{-3}
Mo $K\alpha$ radiation, $\lambda = 0.71073$ Å
Cell parameters from 148635 reflections
$\theta = 2.6–25°$
$\mu = 0.09$ mm^{-1}
$T = 200$ K
Plate, red
$0.28 \times 0.26 \times 0.09$ mm

Data collection

Nonius KappaCCD
   diffractometer
Graphite monochromator
φ and ω scans with CCD
Absorption correction: multi-scan
   DENZO/SCALEPACK (Otwinowski & Minor, 1997)
$T_{min} = 0.75$, $T_{max} = 0.99$
17695 measured reflections

2918 independent reflections
1849 reflections with $I > 2.0\sigma(I)$
$R_{int} = 0.100$
$\theta_{max} = 25.0°$, $\theta_{min} = 2.7°$
$h = -14 \rightarrow 14$
$k = -13 \rightarrow 13$
$l = -14 \rightarrow 14$

Refinement

Refinement on F^2
Least-squares matrix: full
$R[F^2 > 2\sigma(F^2)] = 0.095$
$wR(F^2) = 0.273$
$S = 1.03$
2915 reflections
235 parameters
0 restraints
Primary atom site location: structure-invariant direct
   methods

Hydrogen site location: inferred from neighbouring
   sites
H-atom parameters constrained
Method = Modified Sheldrick $w = 1/[\sigma^2(F^2) + ($
   $0.07P)^2 + 6.62P]$,
   where $P = (\max(F_o^2, 0) + 2F_c^2)/3$
$(\Delta/\sigma)_{max} = 0.026$
$\Delta\rho_{max} = 0.54$ e Å^{-3}
$\Delta\rho_{min} = -0.57$ e Å^{-3}

Special details

Refinement
Most of the hydrogen atoms were observed in difference electron-density maps prior to their inclusion. Those bonded to C were included at calculated positions. H atoms were initially refined with soft restraints on the bond lengths and angles to regularize their geometry (C—H in the range 0.93–0.98 Å, O—H = 0.82 Å) and with $U_{iso}(H)$ in the range 1.2–1.5 times U_{eq} of the parent atom, after which the positions were refined with riding constraints and the displacement parameters were held fixed.
The largest features in the final difference electron density map are located randomly through the structure.

Fractional atomic coordinates and isotropic or equivalent isotropic displacement parameters (Å^2)

	x	y	z	$U_{iso}*/U_{eq}$
C1	0.5946 (6)	0.6146 (5)	0.1700 (5)	0.0568
N2	0.6875 (5)	0.6356 (4)	0.1315 (4)	0.0585
C3	0.6963 (6)	0.7554 (5)	0.1096 (5)	0.0585
C4	0.7806 (6)	0.8096 (5)	0.0740 (5)	0.0631
C5	0.7669 (7)	0.9288 (6)	0.0591 (5)	0.0689
C6	0.6759 (7)	0.9868 (6)	0.0797 (6)	0.0723
C7	0.5928 (6)	0.9297 (5)	0.1177 (5)	0.0621
C8	0.6044 (6)	0.8117 (5)	0.1326 (5)	0.0603
C9	0.5361 (6)	0.7307 (5)	0.1814 (5)	0.0558
C10	0.5556 (6)	0.7597 (5)	0.3039 (5)	0.0658
C11	0.4938 (7)	0.6818 (6)	0.3630 (5)	0.0722
C12	0.4586 (7)	0.5738 (6)	0.3395 (5)	0.0695
N13	0.4717 (5)	0.5010 (4)	0.2567 (4)	0.0586
C14	0.4332 (6)	0.3871 (5)	0.2526 (5)	0.0594
C15	0.3578 (6)	0.3357 (6)	0.3040 (6)	0.0699
C16	0.3337 (7)	0.2221 (6)	0.2851 (6)	0.0761
C17	0.3826 (6)	0.1572 (6)	0.2178 (6)	0.0685
C18	0.4565 (6)	0.2067 (5)	0.1659 (5)	0.0653
C19	0.4815 (5)	0.3241 (5)	0.1838 (5)	0.0560
C20	0.5599 (6)	0.3967 (5)	0.1439 (5)	0.0568

C21	0.5515 (6)	0.5105 (5)	0.1924 (5)	0.0579
C22	0.7822 (6)	0.5556 (6)	0.1240 (5)	0.0624
C23	0.7776 (7)	0.5318 (6)	0.0071 (6)	0.0697
C24	0.8627 (7)	0.5552 (6)	−0.0350 (7)	0.0827
O25	0.4134 (4)	0.7290 (3)	0.1277 (3)	0.0634
O26	0.6157 (4)	0.3707 (3)	0.0785 (4)	0.0672
H41	0.8440	0.7696	0.0604	0.0747*
H51	0.8228	0.9687	0.0356	0.0818*
H61	0.6690	1.0659	0.0685	0.0848*
H71	0.5320	0.9694	0.1336	0.0750*
H101	0.5258	0.8358	0.3065	0.0790*
H102	0.6403	0.7583	0.3426	0.0790*
H111	0.4783	0.7116	0.4249	0.0880*
H121	0.4185	0.5425	0.3863	0.0839*
H151	0.3253	0.3760	0.3505	0.0830*
H161	0.2833	0.1871	0.3198	0.0910*
H171	0.3652	0.0803	0.2064	0.0829*
H181	0.4897	0.1633	0.1197	0.0788*
H221	0.8579	0.5891	0.1630	0.0749*
H222	0.7739	0.4837	0.1596	0.0748*
H231	0.7083	0.5002	−0.0398	0.0815*
H241	0.9346	0.5830	0.0108	0.0989*
H242	0.8507	0.5435	−0.1124	0.0988*
H251	0.3881	0.7258	0.0597	0.0939*

Atomic displacement parameters (Å²)

	U^{11}	U^{22}	U^{33}	U^{12}	U^{13}	U^{23}
C1	0.071 (4)	0.051 (4)	0.050 (3)	0.003 (3)	0.021 (3)	−0.002 (3)
N2	0.071 (3)	0.053 (3)	0.057 (3)	0.002 (3)	0.027 (3)	0.001 (2)
C3	0.075 (4)	0.046 (3)	0.057 (4)	−0.005 (3)	0.024 (3)	−0.004 (3)
C4	0.069 (4)	0.060 (4)	0.063 (4)	−0.004 (3)	0.024 (3)	−0.003 (3)
C5	0.088 (5)	0.057 (4)	0.061 (4)	−0.010 (4)	0.022 (4)	−0.001 (3)
C6	0.096 (5)	0.053 (4)	0.069 (4)	−0.006 (4)	0.027 (4)	−0.002 (3)
C7	0.073 (4)	0.048 (4)	0.064 (4)	0.002 (3)	0.020 (3)	−0.003 (3)
C8	0.081 (5)	0.049 (4)	0.054 (4)	−0.005 (3)	0.024 (3)	−0.003 (3)
C9	0.067 (4)	0.047 (3)	0.057 (3)	0.006 (3)	0.025 (3)	−0.004 (3)
C10	0.088 (5)	0.052 (4)	0.062 (4)	0.004 (3)	0.029 (4)	−0.008 (3)
C11	0.110 (6)	0.057 (4)	0.061 (4)	0.010 (4)	0.043 (4)	−0.006 (3)
C12	0.095 (5)	0.064 (4)	0.062 (4)	0.006 (4)	0.042 (4)	−0.001 (3)
N13	0.079 (4)	0.047 (3)	0.056 (3)	0.003 (3)	0.031 (3)	−0.002 (2)
C14	0.072 (4)	0.051 (4)	0.056 (3)	0.001 (3)	0.021 (3)	0.003 (3)
C15	0.085 (5)	0.063 (4)	0.070 (4)	0.001 (4)	0.036 (4)	0.002 (3)
C16	0.087 (5)	0.068 (5)	0.083 (5)	−0.005 (4)	0.041 (4)	0.011 (4)
C17	0.079 (5)	0.056 (4)	0.074 (4)	−0.008 (3)	0.028 (4)	0.005 (3)
C18	0.089 (5)	0.048 (4)	0.062 (4)	0.002 (3)	0.028 (4)	0.004 (3)
C19	0.068 (4)	0.051 (4)	0.051 (3)	0.003 (3)	0.021 (3)	0.005 (3)
C20	0.066 (4)	0.053 (4)	0.057 (4)	0.001 (3)	0.027 (3)	0.000 (3)
C21	0.073 (4)	0.050 (4)	0.056 (3)	0.002 (3)	0.028 (3)	−0.001 (3)
C22	0.063 (4)	0.062 (4)	0.066 (4)	0.007 (3)	0.024 (3)	0.001 (3)
C23	0.090 (5)	0.060 (4)	0.067 (4)	0.007 (4)	0.035 (4)	0.004 (3)
C24	0.105 (6)	0.068 (5)	0.090 (5)	0.002 (4)	0.052 (5)	−0.006 (4)
O25	0.075 (3)	0.051 (2)	0.065 (3)	0.006 (2)	0.023 (2)	−0.003 (2)
O26	0.094 (3)	0.052 (3)	0.067 (3)	−0.001 (2)	0.041 (3)	−0.007 (2)

Geometric parameters (Å, º)

C1—N2	1.353 (7)	C12—H121	0.935
C1—C9	1.549 (8)	N13—C14	1.401 (7)
C1—C21	1.380 (8)	N13—C21	1.423 (7)
N2—C3	1.434 (8)	C14—C15	1.388 (9)

C3—C4	1.368 (8)	C15—C16	1.362 (9)
C3—C8	1.378 (9)	C15—H151	0.919
C4—C5	1.406 (9)	C16—C17	1.386 (9)
C4—H41	0.943	C16—H161	0.934
C5—C6	1.365 (9)	C17—C18	1.369 (8)
C5—H51	0.929	C17—H171	0.922
C6—C7	1.390 (9)	C18—C19	1.406 (8)
C6—H61	0.934	C18—H181	0.941
C7—C8	1.391 (8)	C19—C20	1.455 (8)
C7—H71	0.928	C20—C21	1.477 (8)
C8—C9	1.492 (8)	C20—O26	1.239 (7)
C9—C10	1.526 (8)	C22—C23	1.481 (9)
C9—O25	1.413 (7)	C22—H221	0.970
C10—C11	1.499 (9)	C22—H222	0.970
C10—H101	0.960	C23—C24	1.303 (9)
C10—H102	0.979	C23—H231	0.934
C11—C12	1.332 (9)	C24—H241	0.934
C11—H111	0.921	C24—H242	0.950
C12—N13	1.388 (7)	O25—H251	0.818
O25···O26^i	2.767 (6)	C5···C21^{iv}	3.362 (8)
O25···C16^{ii}	3.43 (1)	C5···C17^i	3.548 (9)
O26···C1^i	3.372 (7)	C5···C12^{iv}	3.56 (1)
O26···C9^i	3.437 (7)	C6···C7^v	3.546 (9)
N13···C5^{iii}	3.381 (8)	C7···C22^{iv}	3.468 (8)
C3···C18^i	3.425 (8)	C7···C7^v	3.52 (1)
C4···C18^i	3.464 (8)	C14···C23^i	3.598 (9)
C4···C19^{iv}	3.486 (8)	C24···C24^{vi}	3.37 (2)
C4···C14^{iv}	3.566 (9)		
N2—C1—C9	108.2 (5)	N13—C12—H121	115.1
N2—C1—C21	128.7 (5)	C12—N13—C14	120.0 (5)
C9—C1—C21	123.1 (5)	C12—N13—C21	128.4 (5)
C1—N2—C3	111.1 (5)	C14—N13—C21	108.6 (5)
C1—N2—C22	128.5 (5)	N13—C14—C15	129.9 (6)
C3—N2—C22	119.9 (5)	N13—C14—C19	109.6 (5)
N2—C3—C4	128.0 (6)	C15—C14—C19	120.5 (6)
N2—C3—C8	108.4 (5)	C14—C15—C16	118.1 (6)
C4—C3—C8	123.5 (6)	C14—C15—H151	121.8
C3—C4—C5	115.7 (6)	C16—C15—H151	120.1
C3—C4—H41	122.2	C15—C16—C17	122.3 (7)
C5—C4—H41	122.2	C15—C16—H161	118.3
C4—C5—C6	122.2 (7)	C17—C16—H161	119.4
C4—C5—H51	118.2	C16—C17—C18	120.5 (6)
C6—C5—H51	119.7	C16—C17—H171	120.7
C5—C6—C7	120.9 (6)	C18—C17—H171	118.8
C5—C6—H61	120.0	C17—C18—C19	117.9 (6)
C7—C6—H61	119.1	C17—C18—H181	121.0
C6—C7—C8	117.9 (6)	C19—C18—H181	121.1
C6—C7—H71	120.9	C18—C19—C14	120.7 (6)
C8—C7—H71	121.2	C18—C19—C20	129.6 (6)
C7—C8—C3	119.8 (6)	C14—C19—C20	109.6 (5)
C7—C8—C9	129.6 (6)	C19—C20—C21	104.6 (5)
C3—C8—C9	110.3 (5)	C19—C20—O26	127.7 (6)
C1—C9—C8	101.6 (5)	C21—C20—O26	127.6 (5)
C1—C9—C10	110.6 (5)	C20—C21—N13	107.6 (5)
C8—C9—C10	109.7 (5)	C20—C21—C1	129.2 (5)
C1—C9—O25	111.8 (5)	N13—C21—C1	122.4 (5)
C8—C9—O25	115.0 (5)	N2—C22—C23	112.1 (5)
C10—C9—O25	108.0 (5)	N2—C22—H221	108.8
C9—C10—C11	114.6 (5)	C23—C22—H221	109.3
C9—C10—H101	107.1	N2—C22—H222	109.3

C11—C10—H101	107.7	C23—C22—H222	108.4
C9—C10—H102	108.8	H221—C22—H222	108.8
C11—C10—H102	109.1	C22—C23—C24	124.1 (7)
H101—C10—H102	109.5	C22—C23—H231	117.7
C10—C11—C12	129.2 (6)	C24—C23—H231	118.2
C10—C11—H111	116.2	C23—C24—H241	120.1
C12—C11—H111	114.6	C23—C24—H242	119.2
C11—C12—N13	130.3 (6)	H241—C24—H242	120.8
C11—C12—H121	114.5	C9—O25—H251	120.3
O25—C9—C1—N2	128.7 (5)	C3—C8—C7—C6	−0.1 (8)
O25—C9—C1—C21	−48.9 (8)	C3—C8—C9—C10	110.5 (6)
O25—C9—C8—C3	−127.4 (5)	C4—C3—N2—C22	4.6 (8)
O25—C9—C8—C7	58.2 (8)	C4—C3—C8—C7	1.3 (9)
O25—C9—C10—C11	55.5 (7)	C4—C3—C8—C9	−173.7 (5)
O26—C20—C19—C14	−177.8 (6)	C4—C5—C6—C7	1 (1)
O26—C20—C19—C18	5 (1)	C5—C4—C3—C8	−1.5 (8)
O26—C20—C21—N13	176.2 (5)	C5—C6—C7—C8	−0.8 (9)
O26—C20—C21—C1	6 (1)	C6—C7—C8—C9	173.8 (6)
N2—C1—C9—C8	5.5 (6)	C7—C8—C9—C10	−63.8 (8)
N2—C1—C9—C10	−110.9 (6)	C8—C3—N2—C22	−174.2 (5)
N2—C1—C21—N13	164.7 (5)	C8—C9—C1—C21	−172.1 (5)
N2—C1—C21—C20	−26 (1)	C8—C9—C10—C11	−178.4 (6)
N2—C3—C4—C5	179.9 (5)	C9—C1—N2—C22	169.2 (5)
N2—C3—C8—C7	−179.8 (5)	C9—C1—C21—C20	150.8 (6)
N2—C3—C8—C9	5.2 (6)	C9—C10—C11—C12	25 (1)
N2—C22—C23—C24	119.5 (8)	C10—C9—C1—C21	71.5 (7)
N13—C12—C11—C10	2 (1)	C11—C12—N13—C14	176.0 (7)
N13—C14—C15—C16	179.4 (6)	C11—C12—N13—C21	18 (1)
N13—C14—C19—C18	179.9 (5)	C12—N13—C14—C15	16.2 (9)
N13—C14—C19—C20	2.7 (6)	C12—N13—C14—C19	−164.6 (5)
N13—C21—C1—C9	−18.2 (8)	C12—N13—C21—C20	161.5 (5)
N13—C21—C20—C19	0.1 (6)	C14—N13—C21—C20	1.5 (6)
C1—N2—C3—C4	177.4 (6)	C14—C15—C16—C17	1 (1)
C1—N2—C3—C8	−1.4 (6)	C14—C19—C18—C17	0.5 (8)
C1—N2—C22—C23	114.0 (7)	C14—C19—C20—C21	−1.7 (6)
C1—C9—C8—C3	−6.4 (6)	C15—C14—N13—C21	178.2 (6)
C1—C9—C8—C7	179.2 (6)	C15—C14—C19—C18	−0.9 (8)
C1—C9—C10—C11	−67.1 (8)	C15—C14—C19—C20	−178.1 (5)
C1—C21—N13—C12	−27.4 (9)	C15—C16—C17—C18	−1 (1)
C1—C21—N13—C14	172.6 (5)	C16—C15—C14—C19	0.4 (9)
C1—C21—C20—C19	−170.2 (6)	C16—C17—C18—C19	0.5 (9)
C3—N2—C1—C9	−2.8 (6)	C17—C18—C19—C20	177.0 (6)
C3—N2—C1—C21	174.6 (6)	C18—C19—C20—C21	−178.5 (5)
C3—N2—C22—C23	−74.6 (7)	C19—C14—N13—C21	−2.6 (6)
C3—C4—C5—C6	0.5 (9)	C21—C1—N2—C22	−13.4 (9)

Symmetry codes: (i) −x+1, −y+1, −z; (ii) −x+1/2, y+1/2, −z+1/2; (iii) −x+3/2, y−1/2, −z+1/2; (iv) −x+3/2, y+1/2, −z+1/2; (v) −x+1, −y+2, −z; (vi) −x+2, −y+1, −z.

Hydrogen-bond geometry (Å, º)

D—H⋯A	D—H	H⋯A	D⋯A	D—H⋯A
O25—H251⋯O26ⁱ	0.82	2.06	2.767 (10)	145

Symmetry code: (i) −x+1, −y+1, −z.

Compound 249

Crystal data

$C_{24}H_{22}N_2O_2$	$F(000) = 1568$
$M_r = 370.45$	$D_x = 1.325$ Mg m^{-3}
Monoclinic, $C2/c$	Mo $K\alpha$ radiation, $\lambda = 0.71073$ Å
$a = 45.0292\ (8)$ Å	Cell parameters from 21124 reflections
$b = 11.1720\ (3)$ Å	$\theta = 2.6–27.5°$
$c = 7.4857\ (1)$ Å	$\mu = 0.09$ mm^{-1}
$\beta = 99.4875\ (12)°$	$T = 200$ K
$V = 3714.29\ (13)$ Å^3	Lath, Red
$Z = 8$	$0.40 \times 0.11 \times 0.03$ mm

Data collection

Nonius KappaCCD diffractometer	3279 reflections with $I > 2.0\sigma(I)$
graphite	$R_{int} = 0.051$
φ & ω scans	$\theta_{max} = 27.5°,\ \theta_{min} = 2.8°$
Absorption correction: Integration via Gaussian method (Coppens, 1970) implemented in *maXus* (2000)	$h = -58 \rightarrow 58$
$T_{min} = 0.975,\ T_{max} = 0.998$	$k = -14 \rightarrow 14$
27569 measured reflections	$l = -9 \rightarrow 9$
4264 independent reflections	

Refinement

Refinement on F^2	Primary atom site location: Structure-invariant direct methods
Least-squares matrix: Full	Hydrogen site location: Inferred from neighbouring sites
$R[F^2 > 2\sigma(F^2)] = 0.042$	H atoms treated by a mixture of independent and constrained refinement
$wR(F^2) = 0.099$	Method = Modified Sheldrick $w = 1/[\sigma^2(F^2) + (0.05P)^2 + 1.35P]$, where $P = (\max(F_o^2,0) + 2F_c^2)/3$
$S = 0.98$	$(\Delta/\sigma)_{max} = 0.001$
4264 reflections	$\Delta\rho_{max} = 0.30$ e Å^{-3}
257 parameters	$\Delta\rho_{min} = -0.27$ e Å^{-3}
0 restraints	

Special details

Refinement. The crystal is twinned. Application of a twinning correction within CRYSTALS to allow for overlapping reflections arising from a 180° rotation about the (1 0 1) direct axis gave a very significant improvement in agreement factors [the R-factor, using unit weights and all reflections, was reduced from 0.133 to 0.063]. Twin elements refined to final values of 0.880 (1):0.120 (1).

The H of the alcohol group was included at the position where it was observed in a difference electron density map, the other H atoms were included at geometrically determined positions. H atoms were then refined with soft restraints on the bond lengths and angles to regularise their geometry (C—H in the range 0.93–0.98Å, O—H = 0.82 Å) and with U_{iso}(H) in the range 1.2-1.5 times U_{eq} of the parent atom after which the positions were refined with riding constraints, except for H241 which was allowed to refine freely.

The largest features in the final difference electron density map are located half-way along existing bonds or external to the molecule.

Fractional atomic coordinates and isotropic or equivalent isotropic displacement parameters (Å^2)

	x	y	z	$U_{iso}*/U_{eq}$
N1	0.58896 (3)	0.16132 (11)	0.42102 (17)	0.0301
C2	0.56895 (3)	0.24351 (14)	0.4832 (2)	0.0301
C3	0.53776 (3)	0.24416 (15)	0.4517 (2)	0.0351
C4	0.52339 (4)	0.33735 (15)	0.5281 (2)	0.0383

C5	0.53947 (4)	0.42540 (14)	0.6317 (2)	0.0379
C6	0.57092 (4)	0.42237 (14)	0.6633 (2)	0.0352
C7	0.58541 (3)	0.33106 (13)	0.5886 (2)	0.0297
C8	0.61869 (3)	0.30440 (13)	0.6027 (2)	0.0298
C9	0.61808 (3)	0.18684 (13)	0.4977 (2)	0.0291
C10	0.64288 (3)	0.11740 (13)	0.4912 (2)	0.0294
N11	0.67278 (3)	0.16110 (11)	0.54787 (19)	0.0329
C12	0.69212 (3)	0.06285 (14)	0.5694 (2)	0.0323
C13	0.72332 (4)	0.05953 (16)	0.6261 (2)	0.0401
C14	0.73691 (4)	−0.05150 (17)	0.6431 (2)	0.0435
C15	0.72086 (4)	−0.15788 (17)	0.6049 (3)	0.0443
C16	0.69011 (4)	−0.15453 (15)	0.5474 (2)	0.0387
C17	0.67597 (3)	−0.04304 (14)	0.5298 (2)	0.0316
C18	0.64439 (3)	−0.01263 (13)	0.4762 (2)	0.0295
O19	0.62274 (2)	−0.08360 (9)	0.44030 (16)	0.0355
C20	0.57980 (3)	0.08100 (14)	0.2654 (2)	0.0325
C21	0.55952 (4)	0.14083 (16)	0.1130 (2)	0.0384
C22	0.53461 (4)	0.0851 (2)	0.0355 (3)	0.0591
C23	0.56975 (5)	0.25683 (19)	0.0491 (3)	0.0578
O24	0.63378 (2)	0.29539 (10)	0.78366 (15)	0.0329
C25	0.63509 (3)	0.40120 (14)	0.5113 (2)	0.0346
C26	0.66843 (3)	0.38261 (14)	0.5229 (2)	0.0330
C27	0.68317 (3)	0.27899 (14)	0.5394 (2)	0.0339
C28	0.68589 (4)	0.49734 (16)	0.5168 (3)	0.0412
H241	0.6274 (4)	0.2262 (19)	0.835 (3)	0.0503*
H31	0.5264	0.1832	0.3788	0.0409*
H41	0.5018	0.3396	0.5081	0.0470*
H51	0.5290	0.4881	0.6849	0.0453*
H61	0.5823	0.4814	0.7366	0.0421*
H131	0.7348	0.1317	0.6530	0.0488*
H141	0.7582	−0.0539	0.6844	0.0519*
H151	0.7311	−0.2327	0.6190	0.0526*
H161	0.6784	−0.2267	0.5204	0.0450*
H201	0.5986	0.0571	0.2222	0.0376*
H202	0.5700	0.0093	0.3030	0.0394*
H221	0.5293	0.0070	0.0852	0.0717*
H222	0.5221	0.1197	−0.0672	0.0718*
H231	0.5576	0.2804	−0.0633	0.0877*
H232	0.5908	0.2554	0.0356	0.0863*
H233	0.5688	0.3214	0.1387	0.0873*
H251	0.6314	0.4793	0.5705	0.0399*
H252	0.6254	0.4064	0.3824	0.0409*
H271	0.7044	0.2810	0.5465	0.0409*
H281	0.7073	0.4819	0.5164	0.0611*
H282	0.6841	0.5475	0.6224	0.0612*
H283	0.6779	0.5445	0.4091	0.0603*

Atomic displacement parameters ($Å^2$)

	U^{11}	U^{22}	U^{33}	U^{12}	U^{13}	U^{23}
N1	0.0265 (6)	0.0292 (6)	0.0341 (7)	0.0015 (5)	0.0037 (5)	−0.0038 (5)
C2	0.0294 (8)	0.0282 (8)	0.0330 (8)	0.0027 (6)	0.0060 (6)	0.0022 (6)
C3	0.0286 (8)	0.0360 (8)	0.0403 (9)	−0.0001 (7)	0.0050 (7)	−0.0006 (7)
C4	0.0307 (8)	0.0401 (9)	0.0451 (10)	0.0059 (7)	0.0096 (7)	0.0045 (8)
C5	0.0389 (9)	0.0316 (8)	0.0456 (10)	0.0096 (7)	0.0138 (7)	0.0025 (7)
C6	0.0387 (8)	0.0273 (8)	0.0396 (9)	0.0033 (7)	0.0061 (7)	0.0003 (7)
C7	0.0319 (8)	0.0251 (7)	0.0318 (8)	0.0007 (6)	0.0044 (6)	0.0028 (6)
C8	0.0294 (8)	0.0258 (7)	0.0333 (8)	0.0009 (6)	0.0023 (6)	0.0002 (6)

C9	0.0290 (8)	0.0263 (7)	0.0319 (8)	−0.0011 (6)	0.0050 (6)	0.0009 (6)
C10	0.0262 (7)	0.0280 (8)	0.0339 (8)	−0.0005 (6)	0.0044 (6)	−0.0014 (6)
N11	0.0264 (6)	0.0288 (7)	0.0427 (8)	0.0001 (5)	0.0036 (6)	−0.0011 (6)
C12	0.0296 (8)	0.0343 (8)	0.0330 (8)	0.0037 (6)	0.0053 (6)	−0.0009 (7)
C13	0.0300 (8)	0.0461 (10)	0.0427 (10)	0.0002 (7)	0.0018 (7)	−0.0012 (8)
C14	0.0289 (8)	0.0542 (11)	0.0462 (10)	0.0079 (8)	0.0024 (7)	0.0021 (8)
C15	0.0386 (9)	0.0440 (10)	0.0492 (11)	0.0142 (8)	0.0036 (8)	0.0030 (8)
C16	0.0373 (9)	0.0347 (9)	0.0428 (10)	0.0064 (7)	0.0030 (7)	−0.0006 (7)
C17	0.0301 (8)	0.0316 (8)	0.0330 (8)	0.0034 (6)	0.0051 (7)	−0.0016 (7)
C18	0.0292 (7)	0.0283 (7)	0.0309 (8)	0.0013 (6)	0.0046 (6)	−0.0021 (6)
O19	0.0315 (6)	0.0271 (5)	0.0473 (7)	−0.0005 (5)	0.0046 (5)	−0.0033 (5)
C20	0.0331 (8)	0.0300 (8)	0.0340 (8)	−0.0013 (7)	0.0040 (7)	−0.0034 (7)
C21	0.0394 (9)	0.0410 (9)	0.0345 (9)	0.0091 (7)	0.0048 (7)	−0.0064 (7)
C22	0.0430 (10)	0.0732 (14)	0.0555 (12)	0.0137 (10)	−0.0083 (9)	−0.0228 (11)
C23	0.0729 (14)	0.0513 (12)	0.0522 (12)	0.0168 (10)	0.0194 (10)	0.0148 (9)
O24	0.0360 (6)	0.0280 (6)	0.0329 (6)	−0.0032 (5)	0.0007 (5)	0.0005 (5)
C25	0.0363 (8)	0.0273 (8)	0.0396 (9)	−0.0002 (7)	0.0048 (7)	0.0037 (7)
C26	0.0345 (8)	0.0309 (8)	0.0335 (9)	−0.0040 (7)	0.0050 (7)	0.0020 (7)
C27	0.0281 (8)	0.0344 (8)	0.0393 (9)	−0.0056 (7)	0.0056 (7)	−0.0005 (7)
C28	0.0414 (9)	0.0364 (9)	0.0452 (10)	−0.0088 (8)	0.0051 (8)	0.0052 (8)

Geometric parameters (Å, º)

N1—C2	1.4178 (19)	C14—H141	0.959
N1—C9	1.3720 (19)	C15—C16	1.381 (2)
N1—C20	1.474 (2)	C15—H151	0.952
C2—C3	1.385 (2)	C16—C17	1.395 (2)
C2—C7	1.391 (2)	C16—H161	0.967
C3—C4	1.397 (2)	C17—C18	1.453 (2)
C3—H31	0.965	C18—O19	1.2507 (18)
C4—C5	1.381 (2)	C20—C21	1.496 (2)
C4—H41	0.960	C20—H201	0.993
C5—C6	1.397 (2)	C20—H202	0.978
C5—H51	0.965	C21—C22	1.330 (3)
C6—C7	1.378 (2)	C21—C23	1.481 (3)
C6—H61	0.952	C22—H221	0.992
C7—C8	1.515 (2)	C22—H222	0.957
C8—C9	1.528 (2)	C23—H231	0.962
C8—O24	1.4154 (19)	C23—H232	0.969
C8—C25	1.533 (2)	C23—H233	0.991
C9—C10	1.367 (2)	O24—H241	0.93 (2)
C10—N11	1.4292 (19)	C25—C26	1.503 (2)
C10—C18	1.460 (2)	C25—H251	1.005
N11—C12	1.3939 (19)	C25—H252	0.992
N11—C27	1.403 (2)	C26—C27	1.330 (2)
C12—C13	1.399 (2)	C26—C28	1.508 (2)
C12—C17	1.395 (2)	C27—H271	0.950
C13—C14	1.380 (2)	C28—H281	0.978
C13—H131	0.962	C28—H282	0.983
C14—C15	1.396 (3)	C28—H283	0.980
O19···O24^{i}	2.723 (2)	O19···C8^{i}	3.515 (2)
O19···C23^{ii}	3.278 (2)	O24···C16^{ii}	3.340 (2)
O19···C20^{ii}	3.349 (2)	O24···C18^{ii}	3.472 (2)
O19···C21^{ii}	3.376 (2)	O24···C28^{iii}	3.545 (2)
O19···C9^{i}	3.482 (2)	C6···C23^{iv}	3.437 (3)
C2—N1—C9	110.07 (12)	C16—C15—H151	120.0
C2—N1—C20	122.93 (12)	C15—C16—C17	118.18 (16)
C9—N1—C20	125.49 (12)	C15—C16—H161	121.9

N1—C2—C3	128.96 (14)	C17—C16—H161	119.9
N1—C2—C7	109.49 (12)	C16—C17—C12	121.55 (14)
C3—C2—C7	121.55 (14)	C16—C17—C18	130.21 (14)
C2—C3—C4	117.32 (15)	C12—C17—C18	108.23 (13)
C2—C3—H31	121.3	C10—C18—C17	105.50 (12)
C4—C3—H31	121.3	C10—C18—O19	127.09 (13)
C3—C4—C5	121.71 (15)	C17—C18—O19	127.13 (14)
C3—C4—H41	118.8	N1—C20—C21	112.74 (13)
C5—C4—H41	119.5	N1—C20—H201	106.1
C4—C5—C6	120.02 (15)	C21—C20—H201	108.6
C4—C5—H51	120.2	N1—C20—H202	110.6
C6—C5—H51	119.8	C21—C20—H202	109.7
C5—C6—C7	118.94 (15)	H201—C20—H202	109.0
C5—C6—H61	121.0	C20—C21—C22	119.23 (17)
C7—C6—H61	120.1	C20—C21—C23	117.00 (15)
C2—C7—C6	120.45 (14)	C22—C21—C23	123.63 (19)
C2—C7—C8	109.25 (12)	C21—C22—H221	119.0
C6—C7—C8	130.29 (14)	C21—C22—H222	120.3
C7—C8—C9	101.50 (12)	H221—C22—H222	120.7
C7—C8—O24	113.19 (12)	C21—C23—H231	111.1
C9—C8—O24	113.34 (12)	C21—C23—H232	112.4
C7—C8—C25	111.98 (12)	H231—C23—H232	109.8
C9—C8—C25	110.24 (13)	C21—C23—H233	111.6
O24—C8—C25	106.67 (12)	H231—C23—H233	108.1
C8—C9—N1	109.20 (12)	H232—C23—H233	103.6
C8—C9—C10	124.07 (13)	C8—O24—H241	108.9 (12)
N1—C9—C10	126.66 (13)	C8—C25—C26	115.24 (13)
C9—C10—N11	122.05 (13)	C8—C25—H251	106.7
C9—C10—C18	128.04 (13)	C26—C25—H251	109.4
N11—C10—C18	108.02 (12)	C8—C25—H252	108.0
C10—N11—C12	107.79 (12)	C26—C25—H252	109.7
C10—N11—C27	127.76 (13)	H251—C25—H252	107.5
C12—N11—C27	122.53 (12)	C25—C26—C27	127.15 (14)
N11—C12—C13	129.26 (15)	C25—C26—C28	113.67 (13)
N11—C12—C17	110.44 (13)	C27—C26—C28	119.18 (14)
C13—C12—C17	120.28 (14)	N11—C27—C26	131.00 (14)
C12—C13—C14	117.36 (16)	N11—C27—H271	111.1
C12—C13—H131	121.4	C26—C27—H271	117.9
C14—C13—H131	121.3	C26—C28—H281	111.7
C13—C14—C15	122.68 (15)	C26—C28—H282	110.4
C13—C14—H141	117.4	H281—C28—H282	108.2
C15—C14—H141	119.9	C26—C28—H283	111.1
C14—C15—C16	119.95 (16)	H281—C28—H283	108.6
C14—C15—H151	120.0	H282—C28—H283	106.7
O19—C18—C10—N11	175.6 (2)	C4—C5—C6—C7	0.4 (2)
O19—C18—C10—C9	11.2 (3)	C5—C6—C7—C8	−178.8 (1)
O19—C18—C17—C12	−175.7 (2)	C6—C7—C8—C9	176.4 (2)
O19—C18—C17—C16	2.9 (3)	C6—C7—C8—C25	−66.0 (2)
O24—C8—C7—C2	−124.4 (1)	C7—C2—N1—C9	5.7 (2)
O24—C8—C7—C6	54.6 (2)	C7—C2—N1—C20	−161.0 (1)
O24—C8—C9—N1	127.7 (1)	C7—C8—C9—C10	−171.2 (1)
O24—C8—C9—C10	−49.5 (2)	C7—C8—C25—C26	178.7 (1)
O24—C8—C25—C26	54.4 (2)	C8—C9—N1—C20	158.9 (1)
N1—C2—C3—C4	−179.2 (1)	C8—C9—C10—C18	147.9 (2)
N1—C2—C7—C6	179.3 (1)	C8—C25—C26—C27	26.8 (2)
N1—C2—C7—C8	−1.6 (2)	C8—C25—C26—C28	−152.3 (1)
N1—C9—C8—C7	6.0 (2)	C9—N1—C20—C21	−124.3 (2)

N1—C9—C8—C25	−112.8 (1)	C9—C8—C25—C26	−69.1 (1)
N1—C9—C10—N11	168.8 (1)	C9—C10—N11—C12	164.9 (1)
N1—C9—C10—C18	−28.8 (3)	C9—C10—N11—C27	−30.8 (2)
N1—C20—C21—C22	−132.8 (2)	C9—C10—C18—C17	−163.1 (2)
N1—C20—C21—C23	51.3 (2)	C10—N11—C12—C13	−178.7 (2)
N11—C10—C9—C8	−14.5 (2)	C10—N11—C12—C17	−0.3 (2)
N11—C10—C18—C17	1.2 (2)	C10—N11—C27—C26	19.2 (3)
N11—C12—C13—C14	177.3 (2)	C10—C9—N1—C20	−24.0 (2)
N11—C12—C17—C16	−177.7 (1)	C10—C9—C8—C25	70.0 (2)
N11—C12—C17—C18	1.1 (2)	C10—C18—C17—C12	−1.4 (2)
N11—C27—C26—C25	1.1 (3)	C10—C18—C17—C16	177.2 (2)
N11—C27—C26—C28	−179.8 (2)	C12—N11—C10—C18	−0.6 (2)
C2—N1—C9—C8	−7.4 (2)	C12—N11—C27—C26	−178.6 (2)
C2—N1—C9—C10	169.7 (2)	C12—C13—C14—C15	0.5 (3)
C2—N1—C20—C21	40.3 (2)	C12—C17—C16—C15	−0.3 (2)
C2—C3—C4—C5	−0.3 (2)	C13—C12—N11—C27	16.0 (3)
C2—C7—C6—C5	0.1 (2)	C13—C12—C17—C16	0.8 (2)
C2—C7—C8—C9	−2.5 (2)	C13—C12—C17—C18	179.6 (1)
C2—C7—C8—C25	115.0 (1)	C13—C14—C15—C16	0.0 (3)
C3—C2—N1—C9	−174.2 (2)	C14—C13—C12—C17	−0.9 (2)
C3—C2—N1—C20	19.1 (2)	C14—C15—C16—C17	−0.2 (3)
C3—C2—C7—C6	−0.8 (2)	C15—C16—C17—C18	−178.7 (2)
C3—C2—C7—C8	178.3 (1)	C17—C12—N11—C27	−165.6 (1)
C3—C4—C5—C6	−0.4 (2)	C18—C10—N11—C27	163.7 (2)
C4—C3—C2—C7	0.8 (2)		

Symmetry codes: (i) x, $-y$, $z-1/2$; (ii) x, $-y$, $z+1/2$; (iii) x, $-y+1$, $z+1/2$; (iv) x, y, $z+1$.

Hydrogen-bond geometry (Å, °)

D—H···A	D—H	H···A	D···A	D—H···A
O24—H241···O19[ii]	0.93 (2)	1.81 (2)	2.723 (2)	168.8 (17)

Symmetry code: (ii) x, $-y$, $z+1/2$.

Compound 250

Crystal data

$C_{24}H_{22}N_2O_2$
$M_r = 370.44$
Monoclinic, $P2_1/n$
Hall symbol: -P 2yn
$a = 12.3025$ (3) Å
$b = 10.3191$ (3) Å
$c = 15.2106$ (3) Å
$\beta = 104.3577$ (14)°
$V = 1870.68$ (8) Å^3
$Z = 4$

$F(000) = 783.967$
$D_x = 1.315$ Mg m^{-3}
Mo $K\alpha$ radiation, $\lambda = 0.71073$ Å
Cell parameters from 25826 reflections
$\theta = 3$–27.5°
$\mu = 0.08$ mm^{-1}
$T = 200$ K
Block, red
$0.31 \times 0.24 \times 0.21$ mm

Data collection

Nonius KappaCCD
   diffractometer
Graphite monochromator
φ and ω scans with CCD
Absorption correction: integration
   via Gaussian method (Coppens, 1970) implemented in
   maXus (2000)
$T_{min} = 0.979$, $T_{max} = 0.990$

39404 measured reflections
4273 independent reflections
3245 reflections with $I > 2.0\sigma(I)$
$R_{int} = 0.053$
$\theta_{max} = 27.5°$, $\theta_{min} = 2.6°$
$h = -15 \rightarrow 15$
$k = -13 \rightarrow 13$
$l = -19 \rightarrow 19$

Refinement

Refinement on F^2
Least-squares matrix: full
$R[F^2 > 2\sigma(F^2)] = 0.054$
$wR(F^2) = 0.141$
$S = 0.96$
4271 reflections
284 parameters
23 restraints
Primary atom site location: structure-invariant direct
   methods

Hydrogen site location: difference Fourier map
H atoms treated by a mixture of independent and
   constrained refinement
Method = Modified Sheldrick $w = 1/[\sigma^2(F^2) + ($
   $0.06P)^2 + 1.18P]$,
   where $P = (\max(F_o^2,0) + 2F_c^2)/3$
$(\Delta/\sigma)_{max} = 0.020$
$\Delta\rho_{max} = 0.58$ e Å^{-3}
$\Delta\rho_{min} = -0.41$ e Å^{-3}

Special details

Refinement
There is disorder in the packing of the —CH$_2$—CH=CH—CH$_3$ group. There are two sites for each of C23, C24 and C25. Restraints were applied to distances, angles and displacement parameters of the minor sites C231, C241 and C251. The relative occupancies of disordered atom sites were refined appropriately.
Most of the hydrogen atoms were observed in difference electron-density maps prior to their inclusion. Those bonded to C away from the disorder were included at calculated positions. H atoms were initially refined with soft restraints on the bond lengths and angles to regularize their geometry (C—H in the range 0.93–0.98 Å, O—H = 0.82 Å) and with U_{iso}(H) in the range 1.2–1.5 times U_{eq} of the parent atom, after which the positions were refined with riding constraints and the displacement parameters were held fixed. The exception was the H on O26 which was allowed to refine freely. H atoms within the disorder were included at calculated positions and ride on the atom site to which they are bonded.
The two largest peaks in the final difference electron density map are located bridging C9 and C12 and might indicate an alternative configuration of the 7-membered ring. Their occupancy, even if so, was estimated at <0.06, and not worth pursuing further. The next largest peaks in the difference map are generally between existing atoms.

Fractional atomic coordinates and isotropic or equivalent isotropic displacement parameters (Å^2)

	x	y	z	U_{iso}*/U_{eq}	Occ. (<1)
C1	0.37938 (13)	0.39811 (16)	0.60105 (11)	0.0285	
N2	0.44984 (11)	0.29749 (13)	0.63282 (9)	0.0312	
C3	0.48694 (13)	0.30285 (16)	0.72867 (11)	0.0316	
C4	0.55850 (15)	0.21897 (18)	0.78704 (13)	0.0396	
C5	0.58364 (17)	0.2485 (2)	0.87890 (13)	0.0468	
C6	0.53915 (18)	0.3556 (2)	0.91072 (13)	0.0504	
C7	0.46637 (17)	0.4380 (2)	0.85175 (12)	0.0442	
C8	0.44080 (14)	0.40989 (17)	0.76009 (11)	0.0337	
C9	0.36088 (14)	0.47576 (16)	0.68171 (11)	0.0326	
C10	0.24000 (15)	0.4635 (2)	0.69228 (13)	0.0411	
C11	0.15811 (16)	0.5328 (2)	0.61889 (14)	0.0475	
C12	0.16225 (16)	0.5572 (2)	0.53439 (15)	0.0474	
N13	0.24387 (12)	0.52598 (14)	0.48857 (10)	0.0373	

C14	0.22617 (16)	0.55460 (18)	0.39674 (13)	0.0428	
C15	0.1448 (2)	0.6350 (2)	0.34194 (16)	0.0577	
C16	0.1441 (2)	0.6420 (2)	0.25059 (17)	0.0674	
C17	0.2179 (2)	0.5735 (3)	0.21325 (16)	0.0656	
C18	0.29872 (19)	0.4962 (2)	0.26711 (13)	0.0544	
C19	0.30262 (16)	0.48767 (19)	0.35985 (12)	0.0413	
C20	0.37551 (15)	0.41245 (17)	0.43171 (11)	0.0347	
C21	0.33409 (14)	0.43463 (16)	0.51238 (11)	0.0310	
C22	0.46944 (17)	0.18238 (18)	0.58132 (13)	0.0418	
C23	0.3683 (2)	0.0969 (2)	0.55321 (19)	0.0438	0.828 (6)
C24	0.3721 (3)	−0.0303 (3)	0.5663 (2)	0.0508	0.828 (6)
C25	0.2752 (3)	−0.1185 (4)	0.5321 (4)	0.0609	0.828 (6)
O26	0.38464 (11)	0.60974 (12)	0.67425 (9)	0.0402	
C27	0.20517 (18)	0.3233 (2)	0.69875 (17)	0.0567	
O28	0.46026 (11)	0.34982 (13)	0.42583 (8)	0.0420	
C231	0.4078 (13)	0.0670 (11)	0.6035 (9)	0.0668	0.172 (6)
C241	0.3301 (15)	0.0057 (14)	0.5405 (12)	0.0794	0.172 (6)
C251	0.315 (2)	−0.1348 (16)	0.552 (2)	0.0806	0.172 (6)
H41	0.5894	0.1455	0.7646	0.0466*	
H51	0.6316	0.1928	0.9211	0.0555*	
H61	0.5576	0.3719	0.9739	0.0581*	
H71	0.4336	0.5114	0.8724	0.0519*	
H101	0.2397	0.5053	0.7520	0.0478*	
H111	0.0934	0.5628	0.6356	0.0566*	
H121	0.0978	0.6032	0.4964	0.0564*	
H151	0.0957	0.6824	0.3680	0.0664*	
H161	0.0901	0.6967	0.2129	0.0791*	
H171	0.2115	0.5804	0.1483	0.0774*	
H181	0.3519	0.4504	0.2428	0.0637*	
H271	0.1285	0.3206	0.7064	0.0837*	
H272	0.2545	0.2796	0.7490	0.0838*	
H273	0.2028	0.2724	0.6423	0.0820*	
H261	0.445 (2)	0.621 (2)	0.6410 (16)	0.0602*	
H221	0.5289	0.1334	0.6182	0.0492*	0.828
H222	0.4903	0.2105	0.5283	0.0492*	0.828
H223	0.5475	0.1639	0.5961	0.0492*	0.172
H224	0.4444	0.2001	0.5182	0.0492*	0.172
H231	0.2983	0.1356	0.5250	0.0543*	0.828
H241	0.4409	−0.0674	0.5992	0.0627*	0.828
H251	0.2122	−0.0693	0.5007	0.0756*	0.828
H252	0.2576	−0.1619	0.5819	0.0756*	0.828
H253	0.2939	−0.1804	0.4921	0.0756*	0.828
H2311	0.4245	0.0363	0.6643	0.0753*	0.172
H2411	0.2877	0.0515	0.4892	0.0909*	0.172
H2511	0.3644	−0.1651	0.6068	0.0878*	0.172
H2512	0.2397	−0.1482	0.5547	0.0878*	0.172
H2513	0.3293	−0.1808	0.5021	0.0878*	0.172

Atomic displacement parameters ($Å^2$)

	U^{11}	U^{22}	U^{33}	U^{12}	U^{13}	U^{23}
C1	0.0258 (7)	0.0275 (8)	0.0329 (8)	−0.0021 (6)	0.0087 (6)	−0.0027 (7)
N2	0.0336 (7)	0.0268 (7)	0.0331 (7)	0.0027 (6)	0.0082 (6)	−0.0042 (6)
C3	0.0284 (8)	0.0320 (8)	0.0336 (9)	−0.0016 (7)	0.0061 (7)	−0.0003 (7)
C4	0.0344 (9)	0.0359 (10)	0.0467 (10)	0.0042 (7)	0.0067 (8)	0.0036 (8)
C5	0.0406 (10)	0.0516 (12)	0.0429 (11)	0.0031 (9)	0.0004 (8)	0.0096 (9)
C6	0.0527 (12)	0.0634 (14)	0.0303 (9)	−0.0029 (10)	0.0014 (8)	−0.0006 (9)
C7	0.0504 (11)	0.0469 (11)	0.0346 (9)	0.0031 (9)	0.0092 (8)	−0.0063 (8)
C8	0.0345 (9)	0.0334 (9)	0.0323 (9)	0.0003 (7)	0.0067 (7)	−0.0023 (7)
C9	0.0373 (9)	0.0299 (8)	0.0317 (8)	0.0045 (7)	0.0102 (7)	−0.0024 (7)
C10	0.0370 (9)	0.0471 (11)	0.0427 (10)	0.0058 (8)	0.0165 (8)	0.0035 (8)
C11	0.0351 (10)	0.0541 (12)	0.0547 (12)	0.0139 (9)	0.0139 (9)	0.0058 (10)

C12	0.0379 (10)	0.0453 (11)	0.0573 (12)	0.0095 (8)	0.0086 (9)	0.0044 (9)
N13	0.0374 (8)	0.0327 (8)	0.0397 (8)	0.0022 (6)	0.0053 (6)	0.0023 (6)
C14	0.0451 (10)	0.0362 (10)	0.0409 (10)	−0.0090 (8)	−0.0009 (8)	0.0073 (8)
C15	0.0570 (13)	0.0438 (12)	0.0619 (14)	−0.0042 (10)	−0.0051 (11)	0.0118 (10)
C16	0.0768 (17)	0.0543 (14)	0.0538 (14)	−0.0173 (13)	−0.0166 (12)	0.0250 (12)
C17	0.0731 (16)	0.0729 (17)	0.0417 (12)	−0.0311 (14)	−0.0026 (11)	0.0170 (12)
C18	0.0588 (13)	0.0639 (14)	0.0370 (10)	−0.0284 (11)	0.0054 (9)	0.0069 (10)
C19	0.0447 (10)	0.0415 (10)	0.0346 (9)	−0.0162 (8)	0.0036 (8)	0.0041 (8)
C20	0.0383 (9)	0.0336 (9)	0.0317 (9)	−0.0131 (7)	0.0080 (7)	−0.0052 (7)
C21	0.0303 (8)	0.0284 (8)	0.0334 (9)	−0.0030 (6)	0.0064 (6)	−0.0023 (7)
C22	0.0527 (11)	0.0315 (9)	0.0439 (10)	0.0078 (8)	0.0171 (9)	−0.0051 (8)
C23	0.0521 (15)	0.0363 (14)	0.0417 (15)	−0.0005 (11)	0.0092 (11)	−0.0076 (11)
C24	0.0529 (17)	0.0380 (16)	0.0586 (19)	0.0056 (12)	0.0081 (14)	−0.0065 (13)
C25	0.063 (2)	0.0423 (17)	0.078 (3)	−0.0029 (15)	0.0180 (19)	−0.0072 (16)
O26	0.0509 (8)	0.0277 (6)	0.0458 (7)	0.0023 (6)	0.0191 (6)	−0.0042 (5)
C27	0.0416 (11)	0.0601 (14)	0.0715 (15)	−0.0033 (10)	0.0198 (10)	0.0139 (11)
O28	0.0453 (7)	0.0454 (8)	0.0394 (7)	−0.0047 (6)	0.0181 (6)	−0.0055 (6)
C231	0.089 (8)	0.050 (7)	0.059 (7)	0.009 (6)	0.014 (6)	−0.012 (6)
C241	0.102 (9)	0.038 (7)	0.080 (8)	0.025 (7)	−0.012 (7)	−0.012 (6)
C251	0.091 (10)	0.062 (8)	0.095 (9)	0.008 (8)	0.034 (8)	0.010 (7)

Geometric parameters (Å, °)

C1—N2	1.362 (2)	C16—H161	0.949
C1—C9	1.529 (2)	C17—C18	1.376 (3)
C1—C21	1.378 (2)	C17—H171	0.974
N2—C3	1.417 (2)	C18—C19	1.402 (3)
N2—C22	1.475 (2)	C18—H181	0.953
C3—C4	1.387 (2)	C19—C20	1.454 (3)
C3—C8	1.380 (2)	C20—C21	1.459 (2)
C4—C5	1.388 (3)	C20—O28	1.249 (2)
C4—H41	0.949	C22—C23	1.498 (3)
C5—C6	1.373 (3)	C22—C231	1.495 (8)
C5—H51	0.950	C22—H221	0.950
C1—C9—C8	101.59 (13)	C22—C23—C24	122.9 (3)
C1—C9—C10	112.37 (14)	C22—C23—H231	118.5
C8—C9—C10	109.76 (14)	C24—C23—H231	118.6
C1—C9—O26	111.76 (14)	C23—C24—C25	123.9 (3)
C8—C9—O26	113.25 (14)	C23—C24—H241	118.1
C10—C9—O26	108.10 (14)	C25—C24—H241	118.0
C9—C10—C11	111.96 (16)	C24—C25—H251	109.4
C9—C10—C27	112.34 (16)	C24—C25—H252	109.3
C11—C10—C27	110.90 (17)	H251—C25—H252	109.5
C9—C10—H101	106.2	C24—C25—H253	109.6
C11—C10—H101	108.6	H251—C25—H253	109.5
C27—C10—H101	106.6	H252—C25—H253	109.5
C10—C11—C12	129.67 (18)	C9—O26—H261	110.1 (14)
C10—C11—H111	114.4	C10—C27—H271	109.3
C12—C11—H111	115.9	C10—C27—H272	111.4
C11—C12—N13	130.34 (18)	H271—C27—H272	109.2
C11—C12—H121	116.4	C10—C27—H273	113.2
N13—C12—H121	113.3	H271—C27—H273	105.2
C12—N13—C14	119.99 (16)	H272—C27—H273	108.3
C12—N13—C21	129.38 (15)	C22—C231—C241	121.9 (11)
C14—N13—C21	108.19 (15)	C22—C231—H2311	119.1
N13—C14—C15	129.3 (2)	C241—C231—H2311	119.0
N13—C14—C19	110.25 (16)	C231—C241—C251	117.8 (14)
C15—C14—C19	120.5 (2)	C231—C241—H2411	120.3
C14—C15—C16	116.8 (2)	C251—C241—H2411	121.9
C14—C15—H151	119.7	C241—C251—H2511	111.0
C16—C15—H151	123.4	C241—C251—H2512	107.5
C15—C16—C17	122.9 (2)	H2511—C251—H2512	109.5

C15—C16—H161	117.8	C241—C251—H2513	110.0
C17—C16—H161	119.3	H2511—C251—H2513	109.5
C16—C17—C18	120.3 (2)	H2512—C251—H2513	109.5
C16—C17—H171	119.0		
O26—C9—C1—N2	126.6 (1)	C3—C8—C7—C6	−0.1 (3)
O26—C9—C1—C21	−50.2 (2)	C3—C8—C9—C10	113.2 (2)
O26—C9—C8—C3	−125.9 (2)	C4—C3—N2—C22	11.0 (3)
O26—C9—C8—C7	57.5 (3)	C4—C3—C8—C7	1.0 (3)
O26—C9—C10—C11	53.2 (2)	C4—C3—C8—C9	−175.9 (2)
O26—C9—C10—C27	178.7 (2)	C4—C5—C6—C7	0.5 (3)
O28—C20—C19—C14	−173.0 (2)	C5—C4—C3—C8	−1.1 (3)
O28—C20—C19—C18	9.1 (3)	C5—C6—C7—C8	−0.6 (3)
O28—C20—C21—N13	172.3 (2)	C6—C7—C8—C9	176.1 (2)
O28—C20—C21—C1	3.2 (3)	C7—C8—C9—C10	−63.4 (2)
N2—C1—C9—C8	5.5 (2)	C8—C3—N2—C22	−169.4 (2)
N2—C1—C9—C10	−111.7 (2)	C8—C9—C1—C21	−171.2 (2)
N2—C1—C21—N13	167.1 (2)	C8—C9—C10—C11	177.1 (2)
N2—C1—C21—C20	−25.2 (3)	C8—C9—C10—C27	−57.3 (2)
N2—C3—C4—C5	178.4 (2)	C9—C1—N2—C22	164.7 (2)
N2—C3—C8—C7	−178.6 (2)	C9—C1—C21—C20	150.8 (2)
N2—C3—C8—C9	4.4 (2)	C9—C10—C11—C12	28.7 (3)
N2—C22—C23—C24	−131.2 (3)	C10—C9—C1—C21	71.6 (2)
N2—C22—C231—C241	119 (1)	C11—C12—N13—C14	175.6 (2)
N13—C12—C11—C10	−0.1 (4)	C11—C12—N13—C21	15.6 (3)
N13—C14—C15—C16	−177.6 (2)	C12—N13—C14—C15	13.6 (3)
N13—C14—C19—C18	177.3 (2)	C12—N13—C14—C19	−165.1 (2)
N13—C14—C19—C20	−0.8 (2)	C12—N13—C21—C20	164.6 (2)
N13—C21—C1—C9	−16.9 (3)	C12—C11—C10—C27	−97.7 (3)
N13—C21—C20—C19	−3.2 (2)	C14—N13—C21—C20	2.7 (2)
C1—N2—C3—C4	179.7 (2)	C14—C15—C16—C17	0.6 (3)
C1—N2—C3—C8	−0.7 (2)	C14—C19—C18—C17	0.6 (3)
C1—N2—C22—C23	−66.2 (2)	C14—C19—C20—C21	2.5 (2)
C1—N2—C22—C231	−102.1 (6)	C15—C14—N13—C21	177.5 (2)
C1—C9—C8—C3	−5.9 (2)	C15—C14—C19—C18	−1.6 (3)
C1—C9—C8—C7	177.5 (2)	C15—C14—C19—C20	−179.7 (2)
C1—C9—C10—C11	−70.6 (2)	C15—C16—C17—C18	−1.6 (4)
C1—C9—C10—C27	54.9 (2)	C16—C15—C14—C19	0.9 (3)
C1—C21—N13—C12	−25.3 (3)	C16—C17—C18—C19	1.0 (4)
C1—C21—N13—C14	172.9 (2)	C17—C18—C19—C20	178.2 (2)
C1—C21—C20—C19	−172.2 (2)	C18—C19—C20—C21	−175.4 (2)
C3—N2—C1—C9	−3.3 (2)	C19—C14—N13—C21	−1.2 (2)
C3—N2—C1—C21	173.2 (2)	C21—C1—N2—C22	−18.8 (3)
C3—N2—C22—C23	100.6 (2)	C22—C23—C24—C25	−174.6 (4)
C3—N2—C22—C231	64.7 (6)	C22—C231—C241—C251	150 (2)
C3—C4—C5—C6	0.4 (3)		

Symmetry codes: (i) −x+1, −y+1, −z+1; (ii) x, y+1, z; (iii) −x+1/2, y+1/2, −z+3/2; (iv) −x+1/2, y−1/2, −z+1/2; (v) −x+1, −y, −z+1; (vi) x+1/2, −y+1/2, z+1/2.

Hydrogen-bond geometry (Å, °)

D—H⋯A	D—H	H⋯A	D⋯A	D—H⋯A
O26—H261⋯O28[i]	1.00 (2)	1.75 (2)	2.752 (2)	174 (2)

Symmetry code: (i) −x+1, −y+1, −z+1.

Compound 251

Crystal data

$C_{21}H_{18}N_2O_2$
$M_r = 330.39$
Monoclinic, $P2_1/c$
Hall symbol: -P 2ybc
$a = 6.2304 (2)$ Å
$b = 17.3681 (6)$ Å
$c = 14.6545 (5)$ Å
$\beta = 95.602 (2)°$
$V = 1578.19 (9)$ Å^3
$Z = 4$

$F(000) = 696$
$D_x = 1.390$ Mg m^{-3}
Mo $K\alpha$ radiation, $\lambda = 0.71073$ Å
Cell parameters from 22977 reflections
$\theta = 3–25°$
$\mu = 0.09$ mm^{-1}
$T = 200$ K
Rod, red
$0.45 \times 0.08 \times 0.06$ mm

Data collection

Nonius KappaCCD
  diffractometer
Graphite monochromator
φ and ω scans with CCD
Absorption correction: multi-scan
  DENZO/SCALEPACK (Otwinowski & Minor, 1997)
$T_{min} = 0.65$, $T_{max} = 0.99$
21442 measured reflections

2787 independent reflections
2321 reflections with $I > 2.0\sigma(I)$
$R_{int} = 0.082$
$\theta_{max} = 25.0°$, $\theta_{min} = 2.7°$
$h = -7 \rightarrow 7$
$k = -20 \rightarrow 20$
$l = -17 \rightarrow 17$

Refinement

Refinement on F^2
Least-squares matrix: full
$R[F^2 > 2\sigma(F^2)] = 0.043$
$wR(F^2) = 0.114$
$S = 1.00$
2787 reflections
280 parameters
0 restraints

Primary atom site location: structure-invariant direct
  methods
Hydrogen site location: difference Fourier map
Only H-atom coordinates refined
Method = Modified Sheldrick $w = 1/[\sigma^2(F^2) + (0.06P)^2 + 0.6P]$,
  where $P = (max(F_o^2,0) + 2F_c^2)/3$
$(\Delta/\sigma)_{max} = 0.020$
$\Delta\rho_{max} = 0.22$ e Å^{-3}
$\Delta\rho_{min} = -0.28$ e Å^{-3}

Special details

Refinement
The H atoms were all located in a difference map, but those attached to carbon atoms were repositioned geometrically. H atoms were initially refined with soft restraints on the bond lengths and angles to regularize their geometry (C—H in the range 0.93–0.98 Å, O—H = 0.82 Å, N—H = 0.86 Å,) and with U_{iso}(H) in the range 1.2–1.5 times U_{eq} of the parent atom, after which the positions were refined without restraints and the displacement parameters were held fixed.
The largest peaks in the final difference electron density map are located randomly through the structure.

Fractional atomic coordinates and isotropic or equivalent isotropic displacement parameters (Å^2)

	x	y	z	U_{iso}*/U_{eq}
C1	0.5384 (2)	0.54046 (10)	0.62238 (11)	0.0303
N2	0.3682 (2)	0.49217 (8)	0.60807 (10)	0.0334
C3	0.4180 (3)	0.41792 (9)	0.64054 (12)	0.0320
C4	0.2887 (3)	0.35295 (10)	0.63264 (13)	0.0363
C5	0.3781 (3)	0.28423 (11)	0.66646 (13)	0.0390
C6	0.5915 (3)	0.28116 (11)	0.70500 (13)	0.0391
C7	0.7202 (3)	0.34650 (10)	0.71051 (12)	0.0367
C8	0.6317 (3)	0.41632 (10)	0.67930 (12)	0.0323
C9	0.7326 (3)	0.49516 (10)	0.66792 (12)	0.0312
C10	0.8284 (3)	0.53708 (10)	0.75718 (12)	0.0354
C11	0.9460 (3)	0.60912 (11)	0.73184 (13)	0.0383
C12	0.8819 (3)	0.66599 (10)	0.67499 (13)	0.0362
N13	0.6865 (2)	0.67341 (8)	0.62044 (10)	0.0343
C14	0.6057 (3)	0.74365 (10)	0.58605 (12)	0.0341
C15	0.7024 (3)	0.81619 (11)	0.59142 (13)	0.0413
C16	0.5829 (4)	0.87748 (12)	0.55352 (14)	0.0466
C17	0.3729 (4)	0.86826 (11)	0.51100 (14)	0.0465
C18	0.2792 (3)	0.79658 (11)	0.50549 (13)	0.0409
C19	0.3968 (3)	0.73386 (10)	0.54341 (12)	0.0335
C20	0.3415 (3)	0.65329 (10)	0.54962 (11)	0.0317

C21	0.5256 (3)	0.61660 (10)	0.60010 (12)	0.0312
O22	0.90018 (17)	0.49096 (7)	0.60845 (8)	0.0346
C23	0.6472 (3)	0.55682 (13)	0.81726 (14)	0.0443
C24	0.9909 (3)	0.48460 (12)	0.81301 (15)	0.0448
O25	0.17021 (18)	0.62067 (7)	0.51803 (8)	0.0360
H21	0.237 (4)	0.5087 (11)	0.5915 (14)	0.0419*
H41	0.141 (3)	0.3547 (11)	0.6032 (13)	0.0430*
H51	0.290 (3)	0.2346 (12)	0.6595 (13)	0.0456*
H61	0.652 (3)	0.2306 (12)	0.7256 (14)	0.0462*
H71	0.872 (3)	0.3415 (11)	0.7334 (14)	0.0440*
H111	1.100 (3)	0.6155 (12)	0.7613 (14)	0.0465*
H121	0.973 (3)	0.7111 (11)	0.6673 (13)	0.0424*
H151	0.849 (4)	0.8242 (12)	0.6232 (15)	0.0498*
H161	0.646 (4)	0.9304 (13)	0.5561 (15)	0.0552*
H171	0.295 (4)	0.9136 (13)	0.4874 (15)	0.0547*
H181	0.135 (4)	0.7884 (12)	0.4771 (15)	0.0490*
H221	0.861 (3)	0.4511 (13)	0.5658 (16)	0.0524*
H231	0.703 (4)	0.5794 (13)	0.8758 (18)	0.0660*
H232	0.542 (4)	0.5964 (14)	0.7874 (16)	0.0655*
H233	0.562 (4)	0.5090 (14)	0.8298 (17)	0.0639*
H241	1.062 (4)	0.5163 (14)	0.8634 (18)	0.0668*
H242	1.100 (4)	0.4627 (14)	0.7741 (17)	0.0659*
H243	0.913 (4)	0.4400 (14)	0.8392 (17)	0.0656*

Atomic displacement parameters (Å²)

	U^{11}	U^{22}	U^{33}	U^{12}	U^{13}	U^{23}
C1	0.0246 (8)	0.0332 (9)	0.0329 (8)	−0.0007 (7)	0.0014 (6)	−0.0026 (7)
N2	0.0234 (7)	0.0310 (8)	0.0445 (9)	−0.0002 (6)	−0.0026 (6)	0.0022 (6)
C3	0.0284 (8)	0.0326 (9)	0.0349 (9)	0.0014 (7)	0.0024 (7)	−0.0001 (7)
C4	0.0285 (9)	0.0357 (9)	0.0444 (10)	−0.0029 (7)	0.0027 (8)	0.0001 (8)
C5	0.0387 (10)	0.0337 (10)	0.0448 (10)	−0.0033 (8)	0.0054 (8)	0.0018 (8)
C6	0.0420 (10)	0.0332 (10)	0.0418 (10)	0.0038 (8)	0.0024 (8)	0.0050 (8)
C7	0.0329 (9)	0.0368 (10)	0.0393 (10)	0.0042 (7)	−0.0015 (8)	0.0023 (8)
C8	0.0293 (8)	0.0336 (9)	0.0336 (9)	0.0003 (7)	0.0005 (7)	−0.0014 (7)
C9	0.0249 (8)	0.0321 (9)	0.0361 (9)	0.0004 (7)	−0.0001 (7)	−0.0010 (7)
C10	0.0322 (9)	0.0361 (9)	0.0363 (9)	0.0021 (7)	−0.0052 (7)	−0.0033 (7)
C11	0.0285 (9)	0.0392 (10)	0.0453 (11)	−0.0018 (7)	−0.0065 (8)	−0.0061 (8)
C12	0.0274 (8)	0.0360 (10)	0.0443 (10)	−0.0049 (7)	−0.0014 (7)	−0.0059 (8)
N13	0.0291 (8)	0.0315 (8)	0.0410 (8)	−0.0044 (6)	−0.0030 (6)	0.0002 (6)
C14	0.0370 (9)	0.0311 (9)	0.0341 (9)	−0.0019 (7)	0.0034 (7)	−0.0015 (7)
C15	0.0441 (11)	0.0372 (10)	0.0417 (10)	−0.0081 (8)	−0.0005 (8)	0.0001 (8)
C16	0.0589 (13)	0.0340 (10)	0.0464 (11)	−0.0065 (9)	0.0018 (9)	0.0020 (8)
C17	0.0586 (13)	0.0335 (10)	0.0461 (11)	0.0034 (9)	−0.0020 (9)	0.0051 (8)
C18	0.0430 (11)	0.0380 (10)	0.0406 (10)	0.0041 (8)	−0.0005 (8)	0.0020 (8)
C19	0.0338 (9)	0.0336 (9)	0.0330 (9)	0.0002 (7)	0.0033 (7)	−0.0004 (7)
C20	0.0285 (8)	0.0349 (9)	0.0319 (9)	0.0004 (7)	0.0028 (7)	−0.0023 (7)
C21	0.0262 (8)	0.0318 (9)	0.0351 (9)	−0.0029 (6)	0.0001 (7)	−0.0012 (7)
O22	0.0253 (6)	0.0369 (7)	0.0415 (7)	−0.0023 (5)	0.0025 (5)	−0.0054 (5)
C23	0.0465 (11)	0.0457 (11)	0.0406 (11)	0.0019 (9)	0.0040 (9)	−0.0051 (9)
C24	0.0431 (11)	0.0427 (11)	0.0454 (11)	0.0048 (9)	−0.0121 (9)	−0.0017 (9)
O25	0.0281 (6)	0.0371 (7)	0.0414 (7)	−0.0014 (5)	−0.0027 (5)	−0.0022 (5)

Geometric parameters (Å, º)

C1—N2	1.353 (2)	C12—H121	0.98 (2)
C1—C9	1.540 (2)	N13—C14	1.395 (2)
C1—C21	1.363 (2)	N13—C21	1.418 (2)
N2—C3	1.399 (2)	C14—C15	1.396 (3)
N2—H21	0.88 (2)	C14—C19	1.398 (2)
C3—C4	1.385 (2)	C15—C16	1.384 (3)

C3—C8	1.396 (2)	C15—H151	0.99 (2)
C4—C5	1.388 (3)	C16—C17	1.403 (3)
C4—H41	0.98 (2)	C16—H161	1.00 (2)
C5—C6	1.394 (3)	C17—C18	1.374 (3)
C5—H51	1.02 (2)	C17—H171	0.97 (2)
C6—C7	1.387 (3)	C18—C19	1.397 (3)
C6—H61	0.99 (2)	C18—H181	0.97 (2)
C7—C8	1.391 (2)	C19—C20	1.446 (2)
C7—H71	0.98 (2)	C20—C21	1.450 (2)
C8—C9	1.522 (2)	C20—O25	1.256 (2)
C9—C10	1.564 (2)	O22—H221	0.95 (2)
C9—O22	1.426 (2)	C23—H231	0.98 (3)
C10—C11	1.514 (3)	C23—H232	1.02 (3)
C10—C23	1.537 (3)	C23—H233	1.01 (3)
C10—C24	1.538 (3)	C24—H241	0.99 (3)
C11—C12	1.328 (3)	C24—H242	1.01 (3)
C11—H111	1.02 (2)	C24—H243	1.01 (3)
C12—N13	1.395 (2)		
O22···O25^i	2.688 (2)	O25···C9^i	3.487 (2)
O22···N2^{ii}	2.917 (2)	O25···C7^i	3.529 (2)
O22···O25^{ii}	3.178 (2)	O25···C11^{iv}	3.559 (2)
O22···C4^{ii}	3.401 (2)	N2···C1^i	3.528 (2)
O22···N2^i	3.452 (2)	C3···C20^i	3.515 (2)
O22···C3^{ii}	3.456 (2)	C5···C19^i	3.517 (3)
O22···O22^{iii}	3.539 (2)	C6···C14^{vi}	3.470 (3)
O25···C12^{iv}	3.153 (2)	C6···C18^i	3.532 (3)
O25···C8^i	3.316 (2)	C8···C20^i	3.585 (2)
O25···C4^v	3.468 (2)	C12···C20^{ii}	3.557 (3)
N2—C1—C9	108.74 (14)	N13—C12—H121	110.0 (11)
N2—C1—C21	122.53 (15)	C12—N13—C14	123.48 (14)
C9—C1—C21	128.70 (15)	C12—N13—C21	128.01 (15)
C1—N2—C3	111.98 (14)	C14—N13—C21	108.04 (13)
C1—N2—H21	122.3 (13)	N13—C14—C15	129.08 (16)
C3—N2—H21	124.4 (13)	N13—C14—C19	110.04 (15)
N2—C3—C4	127.92 (16)	C15—C14—C19	120.86 (16)
N2—C3—C8	109.14 (14)	C14—C15—C16	117.36 (18)
C4—C3—C8	122.83 (16)	C14—C15—H151	121.6 (12)
C3—C4—C5	117.43 (16)	C16—C15—H151	121.0 (12)
C3—C4—H41	121.8 (12)	C15—C16—C17	122.17 (18)
C5—C4—H41	120.8 (12)	C15—C16—H161	119.8 (13)
C4—C5—C6	120.76 (17)	C17—C16—H161	118.0 (13)
C4—C5—H51	119.9 (11)	C16—C17—C18	120.15 (18)
C6—C5—H51	119.3 (11)	C16—C17—H171	118.4 (13)
C5—C6—C7	121.01 (17)	C18—C17—H171	121.4 (13)
C5—C6—H61	118.4 (12)	C17—C18—C19	118.66 (18)
C7—C6—H61	120.6 (12)	C17—C18—H181	122.1 (13)
C6—C7—C8	119.08 (16)	C19—C18—H181	119.2 (13)
C6—C7—H71	118.9 (12)	C14—C19—C18	120.80 (16)
C8—C7—H71	122.0 (12)	C14—C19—C20	107.84 (15)
C3—C8—C7	118.86 (16)	C18—C19—C20	131.35 (17)
C3—C8—C9	108.98 (14)	C19—C20—C21	106.02 (14)
C7—C8—C9	131.73 (15)	C19—C20—O25	127.75 (16)
C1—C9—C8	101.06 (13)	C21—C20—O25	126.23 (15)
C1—C9—C10	110.13 (13)	C20—C21—N13	108.02 (14)
C8—C9—C10	117.07 (14)	C20—C21—C1	125.02 (15)
C1—C9—O22	110.63 (13)	N13—C21—C1	126.96 (15)
C8—C9—O22	110.85 (13)	C9—O22—H221	106.4 (13)
C10—C9—O22	107.02 (13)	C10—C23—H231	111.9 (14)
C9—C10—C11	109.50 (14)	C10—C23—H232	112.4 (13)
C9—C10—C23	109.96 (14)	H231—C23—H232	105.5 (19)

C11—C10—C23	110.87 (15)	C10—C23—H233	110.4 (13)
C9—C10—C24	110.30 (15)	H231—C23—H233	109 (2)
C11—C10—C24	108.12 (15)	H232—C23—H233	107.8 (19)
C23—C10—C24	108.06 (16)	C10—C24—H241	106.9 (14)
C10—C11—C12	130.18 (16)	C10—C24—H242	111.7 (14)
C10—C11—H111	116.4 (11)	H241—C24—H242	111 (2)
C12—C11—H111	113.4 (11)	C10—C24—H243	109.9 (14)
C11—C12—N13	128.32 (17)	H241—C24—H243	110 (2)
C11—C12—H121	121.7 (11)	H242—C24—H243	108 (2)
O22—C9—C1—N2	114.7 (2)	C3—C8—C7—C6	−2.1 (3)
O22—C9—C1—C21	−66.8 (2)	C3—C8—C9—C10	122.6 (2)
O22—C9—C8—C3	−114.2 (2)	C4—C3—C8—C7	0.7 (3)
O22—C9—C8—C7	57.9 (2)	C4—C3—C8—C9	174.0 (2)
O22—C9—C10—C11	47.7 (2)	C4—C5—C6—C7	−0.1 (3)
O22—C9—C10—C23	169.8 (1)	C5—C4—C3—C8	1.0 (3)
O22—C9—C10—C24	−71.1 (2)	C5—C6—C7—C8	1.8 (3)
O25—C20—C19—C14	−178.3 (2)	C6—C7—C8—C9	−173.6 (2)
O25—C20—C19—C18	2.7 (3)	C7—C8—C9—C10	−65.2 (3)
O25—C20—C21—N13	178.1 (2)	C8—C9—C1—C21	175.8 (2)
O25—C20—C21—C1	−1.2 (3)	C8—C9—C10—C11	172.8 (2)
N2—C1—C9—C8	−2.8 (2)	C8—C9—C10—C23	−65.1 (2)
N2—C1—C9—C10	−127.2 (2)	C8—C9—C10—C24	53.9 (2)
N2—C1—C21—N13	173.2 (2)	C9—C1—C21—C20	174.1 (2)
N2—C1—C21—C20	−7.6 (3)	C9—C10—C11—C12	50.2 (3)
N2—C3—C4—C5	176.7 (2)	C10—C9—C1—C21	51.3 (2)
N2—C3—C8—C7	−175.7 (2)	C11—C12—N13—C14	158.9 (2)
N2—C3—C8—C9	−2.4 (2)	C11—C12—N13—C21	−12.2 (3)
N13—C12—C11—C10	−2.0 (4)	C12—N13—C14—C15	5.5 (3)
N13—C14—C15—C16	−178.0 (2)	C12—N13—C14—C19	−173.0 (2)
N13—C14—C19—C18	178.4 (2)	C12—N13—C21—C20	173.5 (2)
N13—C14—C19—C20	−0.8 (2)	C12—C11—C10—C23	−71.3 (3)
N13—C21—C1—C9	−5.2 (3)	C12—C11—C10—C24	170.4 (2)
N13—C21—C20—C19	−1.7 (2)	C14—N13—C21—C20	1.3 (2)
C1—N2—C3—C4	−175.7 (2)	C14—C15—C16—C17	−0.1 (3)
C1—N2—C3—C8	0.5 (2)	C14—C19—C18—C17	−0.1 (3)
C1—C9—C8—C3	3.1 (2)	C14—C19—C20—C21	1.5 (2)
C1—C9—C8—C7	175.2 (2)	C15—C14—N13—C21	178.2 (2)
C1—C9—C10—C11	−72.6 (2)	C15—C14—C19—C18	−0.3 (3)
C1—C9—C10—C23	49.5 (2)	C15—C14—C19—C20	−179.4 (2)
C1—C9—C10—C24	168.5 (1)	C15—C16—C17—C18	−0.3 (3)
C1—C21—N13—C12	−7.1 (3)	C16—C15—C14—C19	0.4 (3)
C1—C21—N13—C14	−179.4 (2)	C16—C17—C18—C19	0.4 (3)
C1—C21—C20—C19	178.9 (2)	C17—C18—C19—C20	178.8 (2)
C3—N2—C1—C9	1.6 (2)	C18—C19—C20—C21	−177.5 (2)
C3—N2—C1—C21	−177.1 (2)	C19—C14—N13—C21	−0.3 (2)
C3—C4—C5—C6	−1.3 (3)		

Symmetry codes: (i) −x+1, −y+1, −z+1; (ii) x+1, y, z; (iii) −x+2, −y+1, −z+1; (iv) x−1, y, z; (v) −x, −y+1, −z+1; (vi) −x+1, y−1/2, −z+3/2.

Hydrogen-bond geometry (Å, °)

D—H···A	D—H	H···A	D···A	D—H···A
N2—H21···O22[iv]	0.88 (2)	2.16 (2)	2.917 (3)	144.1 (18)
N2—H21···O25	0.88 (2)	2.24 (2)	2.815 (3)	122.7 (16)
O22—H221···O25[i]	0.95 (2)	1.75 (2)	2.688 (3)	171 (2)

Symmetry codes: (i) −x+1, −y+1, −z+1; (iv) x−1, y, z.

Compound 254

Crystal data

2($C_{34}H_{26}N_2O_2$)·C_2H_6OS
$M_r = 1067.32$
Triclinic, $P\bar{1}$
Hall symbol: -P 1
$a = 10.5227\ (3)$ Å
$b = 12.2715\ (5)$ Å
$c = 22.4496\ (9)$ Å
$\alpha = 87.0834\ (19)°$
$\beta = 88.275\ (2)°$
$\gamma = 75.022\ (2)°$
$V = 2796.35\ (18)$ Å^3

$Z = 2$
$F(000) = 1124$
$D_x = 1.268$ Mg m^{-3}
Mo $K\alpha$ radiation, $\lambda = 0.71073$ Å
Cell parameters from 45984 reflections
$\theta = 3–25°$
$\mu = 0.12$ mm^{-1}
$T = 200$ K
Plate, yellow
$0.30 \times 0.17 \times 0.04$ mm

Data collection

Nonius KappaCCD
  diffractometer
Graphite monochromator
φ and ω scans with CCD
Absorption correction: multi-scan
  DENZO/SCALEPACK (Otwinowski & Minor, 1997)
$T_{min} = 0.92$, $T_{max} = 1.00$
38034 measured reflections

7799 independent reflections
4931 reflections with $I > 2.0\sigma(I)$
$R_{int} = 0.070$
$\theta_{max} = 23.0°$, $\theta_{min} = 2.6°$
$h = -11 \rightarrow 11$
$k = -12 \rightarrow 13$
$l = -24 \rightarrow 24$

Refinement

Refinement on F^2
Least-squares matrix: full
$R[F^2 > 2\sigma(F^2)] = 0.059$
$wR(F^2) = 0.157$
$S = 0.94$
7798 reflections
731 parameters
24 restraints
Primary atom site location: structure-invariant direct
  methods

Hydrogen site location: inferred from neighbouring
  sites
H-atom parameters constrained
Method = Modified Sheldrick $w = 1/[\sigma^2(F^2) + ($
  $0.07P)^2 + 2.62P]$,
  where $P = (max(F_o{}^2, 0) + 2F_c{}^2)/3$
$(\Delta/\sigma)_{max} = 0.012$
$\Delta\rho_{max} = 0.62$ e Å^{-3}
$\Delta\rho_{min} = -0.60$ e Å^{-3}

Special details

Refinement
The dimethylsulfoxide molecule is located in a large interstice in the lattice and is disordered. The present model has two overlapping images of a dimethylsulfoxide molecule, with the C and O atoms being coincident but with the S sites on opposite sides of this plane. The relative occupancies of the S sites were refined. Restraints were imposed on bonded distances and angles for each image and upon the anisotropic displacement parameters of adjacent sites.
Hydrogen atoms were included at calculated positions and ride on the atom sites to which they are attached.
Intensity data had been collected to $2\theta = 50°$, but the outer shell had hardly any observable data and just created noise in the refinement. Data was therefore reprocessed using a maximum value of $2\theta = 48°$. The R-factor for data with $F^2 > 2\sigma(F^2)$ dropped from 0.086 to 0.059, vindicating this decision.
High values for the anisotropic displacement parameters of the solvate molecule could indicate a more complex disordering than we have modelled here or could infer that the site has an occupancy of less than unity.
The largest features in the final difference electron density map are located within the disorder or adjacent to atoms of the $C_{34}H_{26}N_2O_2$ molecules but seem to have no chemical significance.

Fractional atomic coordinates and isotropic or equivalent isotropic displacement parameters (Å^2)

	x	y	z	U_{iso}*/U_{eq}	Occ. (<1)
N1	0.8400 (3)	−0.2220 (2)	0.32414 (13)	0.0455	
C2	0.9589 (3)	−0.1975 (3)	0.32749 (14)	0.0399	
C3	1.0847 (3)	−0.2731 (3)	0.32727 (15)	0.0459	
C4	1.1902 (4)	−0.2280 (4)	0.33092 (16)	0.0566	
C5	1.1778 (3)	−0.1120 (3)	0.33476 (16)	0.0513	
C6	1.0551 (3)	−0.0392 (3)	0.33440 (15)	0.0461	
C7	0.9448 (3)	−0.0817 (3)	0.33054 (14)	0.0380	
C8	0.8053 (3)	−0.0276 (3)	0.32884 (14)	0.0353	
C9	0.7336 (3)	−0.1212 (3)	0.32471 (15)	0.0391	
C10	0.6542 (3)	−0.1027 (3)	0.26546 (15)	0.0414	
C11	0.7346 (4)	−0.0768 (3)	0.21033 (16)	0.0453	
C12	0.6727 (4)	0.0374 (3)	0.18939 (15)	0.0452	
C13	0.7079 (4)	0.1034 (4)	0.14268 (18)	0.0614	

C14	0.6334 (5)	0.2127 (4)	0.13337 (19)	0.0672
C15	0.5242 (4)	0.2539 (3)	0.16932 (19)	0.0644
C16	0.4862 (4)	0.1903 (3)	0.21555 (18)	0.0556
C17	0.5631 (3)	0.0796 (3)	0.22539 (16)	0.0436
N18	0.5474 (3)	0.0007 (2)	0.26868 (13)	0.0431
O19	0.7503 (2)	0.07388 (19)	0.32884 (10)	0.0449
O20	0.8289 (3)	−0.1457 (2)	0.18993 (11)	0.0662
C21	0.4755 (3)	0.0249 (3)	0.32154 (18)	0.0499
C22	0.5110 (3)	−0.0334 (3)	0.37209 (18)	0.0500
C23	0.6369 (3)	−0.1257 (3)	0.37871 (15)	0.0447
C24	0.6972 (3)	−0.1290 (3)	0.43923 (16)	0.0442
C25	0.7380 (3)	−0.2286 (3)	0.47155 (18)	0.0537
C26	0.7867 (4)	−0.2315 (4)	0.5288 (2)	0.0645
C27	0.7960 (4)	−0.1332 (4)	0.55353 (19)	0.0626
C28	0.7570 (4)	−0.0327 (4)	0.52080 (18)	0.0608
C29	0.7069 (3)	−0.0289 (3)	0.46496 (17)	0.0523
C30	0.5988 (4)	−0.2042 (3)	0.25490 (18)	0.0554
C31	0.5276 (4)	−0.1945 (3)	0.19789 (19)	0.0610
C32	0.3996 (4)	−0.1664 (3)	0.19394 (19)	0.0634
C33	0.3218 (4)	−0.1511 (4)	0.1396 (2)	0.0641
C34	0.3727 (5)	−0.1868 (6)	0.0856 (2)	0.1109
C35	0.2982 (9)	−0.1670 (8)	0.0350 (3)	0.1454
C36	0.1697 (10)	−0.1124 (7)	0.0395 (4)	0.1352
C37	0.1136 (7)	−0.0795 (5)	0.0916 (4)	0.1211
C38	0.1895 (5)	−0.0976 (4)	0.1424 (3)	0.0890
N101	0.8710 (3)	0.2534 (2)	0.34647 (12)	0.0384
C102	0.8760 (3)	0.2798 (3)	0.40478 (15)	0.0371
C103	0.8794 (3)	0.2100 (3)	0.45575 (16)	0.0465
C104	0.8868 (4)	0.2549 (3)	0.51015 (17)	0.0548
C105	0.8904 (4)	0.3663 (4)	0.51491 (18)	0.0578
C106	0.8864 (3)	0.4359 (3)	0.46507 (17)	0.0483
C107	0.8786 (3)	0.3921 (3)	0.40955 (15)	0.0376
C108	0.8653 (3)	0.4449 (3)	0.35050 (16)	0.0394
C109	0.8501 (3)	0.3542 (3)	0.30733 (15)	0.0375
C110	0.9538 (3)	0.3402 (3)	0.25562 (14)	0.0387
C111	1.0955 (3)	0.3301 (3)	0.27627 (16)	0.0431
C112	1.1357 (3)	0.4259 (3)	0.24865 (16)	0.0441
C113	1.2545 (4)	0.4566 (3)	0.25196 (19)	0.0565
C114	1.2679 (4)	0.5512 (4)	0.2199 (2)	0.0702
C115	1.1632 (5)	0.6158 (4)	0.1870 (2)	0.0760
C116	1.0438 (4)	0.5897 (3)	0.18413 (19)	0.0626
C117	1.0332 (3)	0.4912 (3)	0.21506 (16)	0.0460
N118	0.9262 (3)	0.4445 (2)	0.21747 (12)	0.0437
O119	0.8649 (2)	0.5420 (2)	0.33447 (11)	0.0520
O120	1.1597 (2)	0.2507 (2)	0.30635 (11)	0.0547
C121	0.7967 (4)	0.4999 (3)	0.20426 (17)	0.0554
C122	0.6947 (4)	0.4738 (3)	0.23202 (17)	0.0541
C123	0.7081 (3)	0.3840 (3)	0.28109 (16)	0.0455
C124	0.6042 (3)	0.4124 (3)	0.33044 (16)	0.0460
C125	0.5604 (4)	0.5208 (3)	0.35110 (19)	0.0613
C126	0.4736 (4)	0.5415 (4)	0.3994 (2)	0.0825
C127	0.4302 (4)	0.4545 (5)	0.4269 (2)	0.0919
C128	0.4713 (4)	0.3481 (4)	0.4064 (2)	0.0831
C129	0.5566 (3)	0.3271 (3)	0.35774 (19)	0.0610
C130	0.9515 (4)	0.2385 (3)	0.21816 (16)	0.0494
C131	1.0576 (4)	0.2131 (3)	0.17144 (18)	0.0594
C132	1.0393 (4)	0.2296 (4)	0.1142 (2)	0.0678
C133	1.1396 (4)	0.1981 (4)	0.06561 (19)	0.0638
C134	1.2721 (5)	0.1559 (4)	0.0761 (2)	0.0812
C135	1.3606 (5)	0.1229 (5)	0.0283 (3)	0.0987
C136	1.3142 (7)	0.1320 (5)	−0.0291 (3)	0.1027
C137	1.1844 (7)	0.1749 (5)	−0.0391 (2)	0.0912

C138	1.0983 (5)	0.2083 (4)	0.0079 (2)	0.0790	
S201	0.7009 (9)	0.5237 (8)	0.0309 (3)	0.2537	0.696 (10)
S202	0.7576 (16)	0.4459 (10)	−0.0039 (8)	0.2596	0.304 (10)
O203	0.6799 (14)	0.4172 (8)	0.0436 (5)	0.3589	
C204	0.8710 (14)	0.5127 (11)	0.0221 (9)	0.3727	
C205	0.6712 (15)	0.5458 (11)	−0.0466 (5)	0.3271	
H11	0.8299	−0.2898	0.3220	0.0546*	
H1011	0.8793	0.1855	0.3345	0.0462*	
H31	1.0959	−0.3520	0.3247	0.0552*	
H41	1.2760	−0.2777	0.3308	0.0681*	
H51	1.2537	−0.0844	0.3376	0.0616*	
H61	1.0449	0.0397	0.3368	0.0553*	
H131	0.7819	0.0736	0.1177	0.0738*	
H141	0.6570	0.2597	0.1023	0.0808*	
H151	0.4733	0.3292	0.1619	0.0774*	
H161	0.4109	0.2203	0.2397	0.0669*	
H211	0.3981	0.0854	0.3213	0.0598*	
H221	0.4545	−0.0163	0.4060	0.0602*	
H231	0.6129	−0.1949	0.3766	0.0538*	
H251	0.7331	−0.2969	0.4548	0.0644*	
H261	0.8137	−0.3015	0.5509	0.0777*	
H271	0.8288	−0.1349	0.5926	0.0753*	
H281	0.7650	0.0350	0.5372	0.0730*	
H291	0.6784	0.0414	0.4434	0.0627*	
H301	0.6699	−0.2702	0.2546	0.0666*	
H302	0.5396	−0.2111	0.2868	0.0666*	
H311	0.5783	−0.2098	0.1621	0.0733*	
H321	0.3513	−0.1544	0.2305	0.0762*	
H341	0.4629	−0.2267	0.0827	0.1331*	
H351	0.3365	−0.1916	−0.0025	0.1752*	
H361	0.1181	−0.0970	0.0046	0.1626*	
H371	0.0221	−0.0438	0.0941	0.1452*	
H381	0.1498	−0.0730	0.1796	0.1070*	
H1031	0.8766	0.1337	0.4532	0.0559*	
H1041	0.8896	0.2082	0.5454	0.0658*	
H1051	0.8956	0.3946	0.5531	0.0694*	
H1061	0.8890	0.5123	0.4682	0.0580*	
H1131	1.3240	0.4129	0.2759	0.0678*	
H1141	1.3485	0.5724	0.2201	0.0844*	
H1151	1.1744	0.6814	0.1654	0.0913*	
H1161	0.9727	0.6364	0.1622	0.0753*	
H1211	0.7807	0.5588	0.1741	0.0666*	
H1221	0.6087	0.5141	0.2202	0.0649*	
H1231	0.6977	0.3181	0.2636	0.0547*	
H1251	0.5900	0.5810	0.3321	0.0736*	
H1261	0.4441	0.6157	0.4135	0.0989*	
H1271	0.3713	0.4688	0.4602	0.1102*	
H1281	0.4414	0.2884	0.4256	0.0997*	
H1291	0.5828	0.2533	0.3430	0.0732*	
H1301	0.9609	0.1738	0.2444	0.0593*	
H1302	0.8690	0.2542	0.1991	0.0593*	
H1311	1.1452	0.1825	0.1844	0.0713*	
H1321	0.9522	0.2657	0.1021	0.0815*	
H1341	1.3035	0.1491	0.1157	0.0976*	
H1351	1.4520	0.0947	0.0354	0.1186*	
H1361	1.3733	0.1080	−0.0615	0.1233*	
H1371	1.1525	0.1819	−0.0787	0.1097*	
H1381	1.0076	0.2393	0.0000	0.0951*	
H2041	0.8839	0.5857	0.0135	0.4377*	0.696
H2042	0.9143	0.4817	0.0580	0.4377*	0.696
H2043	0.9062	0.4652	−0.0097	0.4377*	0.696
H2044	0.9227	0.5318	−0.0102	0.4377*	0.304

H2045	0.8252	0.5794	0.0411	0.4377*	0.304
H2046	0.9266	0.4633	0.0501	0.4377*	0.304
H2051	0.6834	0.6173	−0.0596	0.3621*	0.696
H2052	0.7308	0.4882	−0.0676	0.3621*	0.696
H2053	0.5835	0.5437	−0.0541	0.3621*	0.696
H2054	0.7255	0.5636	−0.0782	0.3621*	0.304
H2055	0.6360	0.6109	−0.0243	0.3621*	0.304
H2056	0.6013	0.5212	−0.0626	0.3621*	0.304

Atomic displacement parameters (Å²)

	U^{11}	U^{22}	U^{33}	U^{12}	U^{13}	U^{23}
N1	0.0484 (18)	0.0271 (16)	0.062 (2)	−0.0109 (14)	−0.0001 (15)	−0.0072 (14)
C2	0.044 (2)	0.041 (2)	0.035 (2)	−0.0104 (18)	0.0034 (15)	−0.0047 (16)
C3	0.045 (2)	0.044 (2)	0.046 (2)	−0.0062 (18)	0.0036 (17)	−0.0055 (17)
C4	0.040 (2)	0.073 (3)	0.049 (2)	0.000 (2)	0.0050 (17)	−0.009 (2)
C5	0.041 (2)	0.062 (3)	0.051 (2)	−0.014 (2)	0.0045 (17)	−0.010 (2)
C6	0.047 (2)	0.051 (2)	0.045 (2)	−0.0197 (19)	0.0042 (17)	−0.0061 (17)
C7	0.040 (2)	0.037 (2)	0.038 (2)	−0.0123 (16)	0.0007 (15)	−0.0019 (16)
C8	0.040 (2)	0.032 (2)	0.0340 (19)	−0.0085 (16)	0.0028 (15)	−0.0037 (15)
C9	0.0372 (19)	0.0314 (19)	0.050 (2)	−0.0104 (16)	−0.0001 (16)	−0.0024 (16)
C10	0.045 (2)	0.0296 (19)	0.051 (2)	−0.0116 (16)	−0.0044 (17)	−0.0029 (16)
C11	0.048 (2)	0.043 (2)	0.044 (2)	−0.0083 (19)	0.0003 (17)	−0.0130 (18)
C12	0.058 (2)	0.043 (2)	0.038 (2)	−0.0189 (19)	−0.0036 (18)	−0.0029 (18)
C13	0.073 (3)	0.060 (3)	0.055 (3)	−0.022 (2)	−0.002 (2)	−0.004 (2)
C14	0.098 (3)	0.055 (3)	0.053 (3)	−0.031 (3)	−0.007 (3)	0.010 (2)
C15	0.084 (3)	0.044 (2)	0.060 (3)	−0.008 (2)	−0.018 (2)	0.005 (2)
C16	0.063 (2)	0.044 (2)	0.055 (3)	−0.004 (2)	−0.011 (2)	−0.006 (2)
C17	0.044 (2)	0.038 (2)	0.049 (2)	−0.0090 (17)	−0.0098 (18)	−0.0038 (18)
N18	0.0379 (16)	0.0420 (18)	0.0489 (19)	−0.0096 (14)	0.0005 (14)	−0.0013 (15)
O19	0.0472 (14)	0.0305 (14)	0.0577 (16)	−0.0104 (11)	−0.0033 (11)	−0.0039 (11)
O20	0.0732 (19)	0.0621 (18)	0.0536 (17)	0.0004 (15)	0.0081 (14)	−0.0098 (14)
C21	0.035 (2)	0.049 (2)	0.064 (3)	−0.0092 (17)	0.0020 (19)	−0.003 (2)
C22	0.037 (2)	0.057 (2)	0.056 (3)	−0.0128 (18)	0.0080 (18)	−0.003 (2)
C23	0.045 (2)	0.041 (2)	0.051 (2)	−0.0183 (17)	0.0067 (17)	−0.0020 (17)
C24	0.0374 (19)	0.050 (2)	0.046 (2)	−0.0143 (17)	0.0047 (16)	0.0027 (19)
C25	0.046 (2)	0.051 (3)	0.064 (3)	−0.0122 (19)	0.002 (2)	0.005 (2)
C26	0.047 (2)	0.076 (3)	0.066 (3)	−0.013 (2)	0.002 (2)	0.019 (3)
C27	0.051 (2)	0.089 (4)	0.050 (3)	−0.022 (2)	0.0032 (19)	0.003 (3)
C28	0.066 (3)	0.071 (3)	0.050 (3)	−0.027 (2)	0.009 (2)	−0.007 (2)
C29	0.055 (2)	0.056 (3)	0.049 (3)	−0.0192 (19)	0.0035 (19)	−0.003 (2)
C30	0.065 (2)	0.042 (2)	0.065 (3)	−0.0212 (19)	−0.015 (2)	−0.0030 (19)
C31	0.069 (3)	0.056 (3)	0.064 (3)	−0.026 (2)	−0.002 (2)	−0.009 (2)
C32	0.073 (3)	0.066 (3)	0.059 (3)	−0.033 (2)	0.003 (2)	−0.003 (2)
C33	0.066 (3)	0.069 (3)	0.068 (3)	−0.037 (2)	−0.005 (2)	0.003 (2)
C34	0.088 (4)	0.201 (7)	0.065 (4)	−0.072 (4)	−0.001 (3)	−0.022 (4)
C35	0.133 (6)	0.256 (10)	0.074 (4)	−0.096 (6)	−0.016 (4)	−0.006 (5)
C36	0.148 (8)	0.161 (8)	0.126 (7)	−0.097 (6)	−0.058 (6)	0.049 (6)
C37	0.093 (5)	0.088 (4)	0.183 (8)	−0.026 (3)	−0.059 (6)	0.034 (5)
C38	0.083 (4)	0.062 (3)	0.122 (5)	−0.020 (3)	−0.019 (3)	0.008 (3)
N101	0.0494 (17)	0.0224 (15)	0.0440 (19)	−0.0100 (12)	0.0044 (13)	−0.0038 (13)
C102	0.0359 (18)	0.035 (2)	0.042 (2)	−0.0113 (15)	0.0027 (15)	−0.0022 (17)
C103	0.052 (2)	0.041 (2)	0.048 (2)	−0.0164 (17)	0.0065 (17)	0.0021 (19)
C104	0.065 (3)	0.058 (3)	0.042 (2)	−0.017 (2)	0.0052 (19)	0.003 (2)
C105	0.064 (3)	0.065 (3)	0.044 (2)	−0.014 (2)	0.0055 (19)	−0.013 (2)
C106	0.050 (2)	0.043 (2)	0.054 (3)	−0.0141 (17)	0.0044 (18)	−0.011 (2)
C107	0.0347 (18)	0.034 (2)	0.043 (2)	−0.0065 (15)	0.0024 (15)	−0.0052 (17)
C108	0.0327 (19)	0.032 (2)	0.055 (2)	−0.0109 (15)	0.0050 (16)	−0.0053 (18)
C109	0.0386 (19)	0.0302 (19)	0.044 (2)	−0.0103 (15)	0.0013 (16)	−0.0013 (16)
C110	0.046 (2)	0.0295 (19)	0.041 (2)	−0.0112 (15)	0.0036 (16)	0.0007 (16)
C111	0.044 (2)	0.041 (2)	0.041 (2)	−0.0064 (18)	0.0054 (17)	−0.0053 (18)

C112	0.043 (2)	0.038 (2)	0.050 (2)	−0.0083 (18)	0.0115 (17)	−0.0057 (18)
C113	0.045 (2)	0.045 (2)	0.078 (3)	−0.0076 (19)	0.013 (2)	−0.012 (2)
C114	0.053 (3)	0.055 (3)	0.105 (4)	−0.019 (2)	0.021 (3)	−0.012 (3)
C115	0.079 (3)	0.048 (3)	0.105 (4)	−0.028 (3)	0.032 (3)	0.003 (3)
C116	0.062 (3)	0.045 (2)	0.077 (3)	−0.012 (2)	0.011 (2)	0.012 (2)
C117	0.047 (2)	0.038 (2)	0.053 (2)	−0.0128 (18)	0.0107 (18)	−0.0003 (18)
N118	0.0449 (18)	0.0386 (17)	0.0448 (18)	−0.0074 (14)	0.0010 (14)	0.0064 (14)
O119	0.0603 (16)	0.0303 (15)	0.0668 (17)	−0.0153 (12)	0.0054 (13)	−0.0008 (12)
O120	0.0479 (15)	0.0547 (17)	0.0552 (17)	−0.0048 (13)	0.0004 (12)	0.0110 (14)
C121	0.054 (3)	0.054 (2)	0.053 (2)	−0.006 (2)	−0.0059 (19)	0.0154 (19)
C122	0.039 (2)	0.062 (3)	0.057 (3)	−0.0075 (19)	−0.0068 (19)	0.006 (2)
C123	0.042 (2)	0.047 (2)	0.049 (2)	−0.0130 (17)	−0.0024 (17)	0.0020 (18)
C124	0.0370 (19)	0.045 (2)	0.055 (2)	−0.0102 (18)	−0.0009 (17)	0.0027 (19)
C125	0.052 (2)	0.051 (3)	0.075 (3)	−0.005 (2)	0.003 (2)	0.003 (2)
C126	0.061 (3)	0.076 (3)	0.093 (4)	0.012 (3)	0.013 (3)	−0.008 (3)
C127	0.058 (3)	0.103 (4)	0.096 (4)	0.008 (3)	0.035 (3)	0.006 (3)
C128	0.053 (3)	0.085 (4)	0.100 (4)	−0.006 (3)	0.028 (3)	0.021 (3)
C129	0.041 (2)	0.058 (3)	0.082 (3)	−0.0115 (19)	0.010 (2)	0.003 (2)
C130	0.063 (2)	0.044 (2)	0.043 (2)	−0.0182 (18)	0.0057 (18)	−0.0015 (17)
C131	0.075 (3)	0.056 (3)	0.050 (3)	−0.022 (2)	0.003 (2)	−0.011 (2)
C132	0.070 (3)	0.072 (3)	0.066 (3)	−0.026 (2)	0.003 (2)	−0.008 (2)
C133	0.075 (3)	0.069 (3)	0.056 (3)	−0.035 (2)	0.017 (2)	−0.013 (2)
C134	0.091 (4)	0.104 (4)	0.058 (3)	−0.040 (3)	0.008 (3)	−0.013 (3)
C135	0.081 (3)	0.126 (5)	0.096 (4)	−0.038 (3)	0.027 (3)	−0.027 (4)
C136	0.126 (5)	0.122 (5)	0.072 (4)	−0.053 (4)	0.040 (4)	−0.027 (3)
C137	0.125 (5)	0.094 (4)	0.061 (3)	−0.041 (4)	0.015 (3)	−0.010 (3)
C138	0.099 (4)	0.079 (3)	0.066 (3)	−0.035 (3)	0.010 (3)	−0.010 (3)
S201	0.418 (9)	0.234 (7)	0.157 (4)	−0.179 (7)	−0.059 (5)	0.075 (4)
S202	0.424 (14)	0.110 (8)	0.241 (13)	−0.066 (8)	−0.081 (9)	0.058 (8)
O203	0.67 (2)	0.249 (9)	0.234 (9)	−0.261 (13)	−0.061 (10)	0.082 (8)
C204	0.389 (13)	0.184 (12)	0.56 (3)	−0.093 (14)	−0.04 (2)	−0.003 (15)
C205	0.48 (2)	0.296 (16)	0.197 (9)	−0.104 (14)	−0.118 (13)	0.133 (11)

Geometric parameters (Å, °)

N1—C2	1.366 (4)	C105—C106	1.367 (5)
N1—C9	1.438 (4)	C105—H1051	0.950
N1—H11	0.870	C106—C107	1.395 (5)
C2—C3	1.406 (5)	C106—H1061	0.950
C2—C7	1.395 (5)	C107—C108	1.440 (5)
C3—C4	1.369 (5)	C108—C109	1.554 (5)
C3—H31	0.950	C108—O119	1.227 (4)
C4—C5	1.402 (5)	C109—C110	1.554 (4)
C4—H41	0.950	C109—C123	1.570 (4)
C5—C6	1.368 (5)	C110—C111	1.547 (5)
C5—H51	0.950	C110—N118	1.472 (4)
C6—C7	1.396 (5)	C110—C130	1.546 (5)
C6—H61	0.950	C111—C112	1.454 (5)
C7—C8	1.447 (4)	C111—O120	1.218 (4)
C8—C9	1.537 (5)	C112—C113	1.400 (5)
C8—O19	1.230 (4)	C112—C117	1.384 (5)
C9—C10	1.567 (5)	C113—C114	1.372 (6)
C9—C23	1.567 (5)	C113—H1131	0.950
C10—C11	1.544 (5)	C114—C115	1.387 (6)
C10—N18	1.465 (4)	C114—H1141	0.950
C10—C30	1.537 (5)	C115—C116	1.379 (6)
C11—C12	1.446 (5)	C115—H1151	0.950
C11—O20	1.220 (4)	C116—C117	1.391 (5)
C12—C13	1.392 (5)	C116—H1161	0.950
C12—C17	1.388 (5)	C117—N118	1.387 (4)
C13—C14	1.376 (6)	N118—C121	1.390 (4)
C13—H131	0.950	C121—C122	1.327 (5)

C14—C15	1.383 (6)	C121—H1211	0.950
C14—H141	0.950	C122—C123	1.501 (5)
C15—C16	1.379 (6)	C122—H1221	0.950
C15—H151	0.950	C123—C124	1.521 (5)
C16—C17	1.400 (5)	C123—H1231	0.950
C16—H161	0.950	C124—C125	1.389 (5)
C17—N18	1.374 (4)	C124—C129	1.382 (5)
N18—C21	1.391 (5)	C125—C126	1.386 (6)
C21—C22	1.320 (5)	C125—H1251	0.950
C21—H211	0.950	C126—C127	1.378 (7)
C22—C23	1.509 (5)	C126—H1261	0.950
C22—H221	0.950	C127—C128	1.364 (7)
C23—C24	1.511 (5)	C127—H1271	0.950
C23—H231	0.950	C128—C129	1.385 (6)
C24—C25	1.365 (5)	C128—H1281	0.950
C24—C29	1.411 (5)	C129—H1291	0.950
C25—C26	1.394 (6)	C130—C131	1.492 (5)
C25—H251	0.950	C130—H1301	0.950
C26—C27	1.380 (6)	C130—H1302	0.950
C26—H261	0.950	C131—C132	1.303 (5)
C27—C28	1.376 (6)	C131—H1311	0.950
C27—H271	0.950	C132—C133	1.488 (6)
C28—C29	1.369 (5)	C132—H1321	0.950
C28—H281	0.950	C133—C134	1.379 (6)
C29—H291	0.950	C133—C138	1.368 (6)
C30—C31	1.487 (5)	C134—C135	1.405 (6)
C30—H301	0.950	C134—H1341	0.950
C30—H302	0.950	C135—C136	1.381 (7)
C31—C32	1.305 (5)	C135—H1351	0.950
C31—H311	0.950	C136—C137	1.352 (7)
C32—C33	1.468 (6)	C136—H1361	0.950
C32—H321	0.950	C137—C138	1.378 (7)
C33—C34	1.357 (6)	C137—H1371	0.950
C33—C38	1.378 (6)	C138—H1381	0.950
C34—C35	1.377 (8)	S201—O203	1.395 (10)
C34—H341	0.950	S201—C204	1.766 (14)
C35—C36	1.348 (10)	S201—C205	1.773 (10)
C35—H351	0.950	S202—O203	1.410 (17)
C36—C37	1.326 (10)	S202—C204	1.741 (17)
C36—H361	0.950	S202—C205	1.614 (13)
C37—C38	1.389 (8)	C204—H2041	0.950
C37—H371	0.950	C204—H2042	0.950
C38—H381	0.950	C204—H2043	0.950
N101—C102	1.370 (4)	C204—H2044	0.950
N101—C109	1.453 (4)	C204—H2045	0.950
N101—H1011	0.870	C204—H2046	0.950
C102—C103	1.390 (5)	C205—H2051	0.950
C102—C107	1.395 (4)	C205—H2052	0.950
C103—C104	1.377 (5)	C205—H2053	0.950
C103—H1031	0.950	C205—H2054	0.950
C104—C105	1.388 (5)	C205—H2055	0.950
C104—H1041	0.950	C205—H2056	0.950
O1···C3^{i}	3.57 (1)	O21···C8	3.293 (8)
O4···O21^{ii}	2.717 (6)	O21···C14	3.318 (9)
O7···C6^{iii}	3.57 (1)	O21···C5^{iv}	3.335 (9)
O10···O10	2.700 (4)	O21···C16	3.351 (8)
O10···O10	2.700 (4)	O21···C14^{i}	3.564 (9)
O10···C9	3.323 (9)	O21···C17	3.565 (8)
O10···O12	3.324 (6)	C9···C13^{iii}	3.50 (1)
O12···C16^{iii}	3.444 (9)	C13···C16^{iii}	3.49 (1)
O12···C14^{iii}	3.484 (9)	C17···C20^{i}	3.50 (1)

O15···O21	2.618 (8)	C17···C19^{i}	3.53 (1)
O15···O21^{iii}	2.825 (8)	C18···C20^{i}	3.56 (1)
C2—N1—C9	111.3 (3)	C105—C106—C107	118.4 (3)
C2—N1—H11	124.4	C105—C106—H1061	120.8
C9—N1—H11	124.4	C107—C106—H1061	120.8
N1—C2—C3	127.9 (3)	C102—C107—C106	121.0 (3)
N1—C2—C7	111.7 (3)	C102—C107—C108	107.7 (3)
C3—C2—C7	120.5 (3)	C106—C107—C108	131.3 (3)
C2—C3—C4	117.1 (3)	C107—C108—C109	107.0 (3)
C2—C3—H31	121.4	C107—C108—O119	129.1 (3)
C4—C3—H31	121.4	C109—C108—O119	123.9 (3)
C3—C4—C5	123.2 (3)	C108—C109—N101	102.2 (3)
C3—C4—H41	118.4	C108—C109—C110	111.4 (3)
C5—C4—H41	118.4	N101—C109—C110	111.9 (2)
C4—C5—C6	119.1 (4)	C108—C109—C123	111.1 (3)
C4—C5—H51	120.4	N101—C109—C123	110.3 (3)
C6—C5—H51	120.4	C110—C109—C123	109.7 (3)
C5—C6—C7	119.5 (3)	C109—C110—C111	113.9 (3)
C5—C6—H61	120.3	C109—C110—N118	109.0 (2)
C7—C6—H61	120.3	C111—C110—N118	102.5 (3)
C6—C7—C2	120.6 (3)	C109—C110—C130	111.1 (3)
C6—C7—C8	132.4 (3)	C111—C110—C130	109.9 (3)
C2—C7—C8	107.0 (3)	N118—C110—C130	110.0 (3)
C7—C8—C9	107.3 (3)	C110—C111—C112	106.7 (3)
C7—C8—O19	128.3 (3)	C110—C111—O120	124.1 (3)
C9—C8—O19	124.4 (3)	C112—C111—O120	129.0 (3)
C8—C9—N1	102.8 (2)	C111—C112—C113	130.3 (3)
C8—C9—C10	109.5 (3)	C111—C112—C117	108.9 (3)
N1—C9—C10	111.5 (3)	C113—C112—C117	120.8 (3)
C8—C9—C23	112.9 (3)	C112—C113—C114	118.4 (4)
N1—C9—C23	111.1 (3)	C112—C113—H1131	120.8
C10—C9—C23	108.9 (3)	C114—C113—H1131	120.8
C9—C10—C11	113.2 (3)	C113—C114—C115	119.7 (4)
C9—C10—N18	109.1 (3)	C113—C114—H1141	120.1
C11—C10—N18	102.5 (3)	C115—C114—H1141	120.1
C9—C10—C30	111.0 (3)	C114—C115—C116	123.3 (4)
C11—C10—C30	110.3 (3)	C114—C115—H1151	118.3
N18—C10—C30	110.4 (3)	C116—C115—H1151	118.4
C10—C11—C12	106.8 (3)	C115—C116—C117	116.4 (4)
C10—C11—O20	123.2 (3)	C115—C116—H1161	121.8
C12—C11—O20	129.9 (3)	C117—C116—H1161	121.8
C11—C12—C13	130.5 (4)	C116—C117—C112	121.4 (3)
C11—C12—C17	108.5 (3)	C116—C117—N118	127.6 (3)
C13—C12—C17	121.0 (3)	C112—C117—N118	111.0 (3)
C12—C13—C14	118.8 (4)	C110—N118—C117	110.8 (3)
C12—C13—H131	120.6	C110—N118—C121	119.5 (3)
C14—C13—H131	120.6	C117—N118—C121	126.6 (3)
C13—C14—C15	119.8 (4)	N118—C121—C122	122.7 (3)
C13—C14—H141	120.1	N118—C121—H1211	118.7
C15—C14—H141	120.1	C122—C121—H1211	118.7
C14—C15—C16	122.7 (4)	C121—C122—C123	123.4 (3)
C14—C15—H151	118.6	C121—C122—H1221	118.3
C16—C15—H151	118.6	C123—C122—H1221	118.3
C15—C16—C17	117.3 (4)	C109—C123—C122	110.4 (3)
C15—C16—H161	121.4	C109—C123—C124	110.9 (3)
C17—C16—H161	121.3	C122—C123—C124	114.1 (3)
C16—C17—C12	120.4 (4)	C109—C123—H1231	107.0
C16—C17—N18	128.4 (3)	C122—C123—H1231	107.0
C12—C17—N18	111.2 (3)	C124—C123—H1231	107.0
C10—N18—C17	110.9 (3)	C123—C124—C125	121.9 (3)
C10—N18—C21	119.9 (3)	C123—C124—C129	119.2 (3)

C17—N18—C21	125.0 (3)	C125—C124—C129	118.8 (4)
N18—C21—C22	122.3 (3)	C124—C125—C126	120.2 (4)
N18—C21—H211	118.8	C124—C125—H1251	119.9
C22—C21—H211	118.9	C126—C125—H1251	119.9
C21—C22—C23	123.4 (3)	C125—C126—C127	120.0 (4)
C21—C22—H221	118.3	C125—C126—H1261	120.0
C23—C22—H221	118.3	C127—C126—H1261	120.0
C9—C23—C22	111.1 (3)	C126—C127—C128	120.2 (4)
C9—C23—C24	114.5 (3)	C126—C127—H1271	119.9
C22—C23—C24	112.3 (3)	C128—C127—H1271	120.0
C9—C23—H231	106.1	C127—C128—C129	120.1 (4)
C22—C23—H231	106.1	C127—C128—H1281	119.9
C24—C23—H231	106.1	C129—C128—H1281	120.0
C23—C24—C25	120.5 (3)	C128—C129—C124	120.6 (4)
C23—C24—C29	121.0 (3)	C128—C129—H1291	119.7
C25—C24—C29	118.4 (3)	C124—C129—H1291	119.7
C24—C25—C26	120.9 (4)	C110—C130—C131	114.0 (3)
C24—C25—H251	119.5	C110—C130—H1301	108.3
C26—C25—H251	119.6	C131—C130—H1301	108.3
C25—C26—C27	120.2 (4)	C110—C130—H1302	108.3
C25—C26—H261	119.9	C131—C130—H1302	108.3
C27—C26—H261	119.9	H1301—C130—H1302	109.5
C26—C27—C28	119.1 (4)	C130—C131—C132	125.0 (4)
C26—C27—H271	120.5	C130—C131—H1311	117.5
C28—C27—H271	120.4	C132—C131—H1311	117.5
C27—C28—C29	121.0 (4)	C131—C132—C133	127.3 (4)
C27—C28—H281	119.5	C131—C132—H1321	116.4
C29—C28—H281	119.5	C133—C132—H1321	116.4
C24—C29—C28	120.4 (4)	C132—C133—C134	123.0 (4)
C24—C29—H291	119.8	C132—C133—C138	118.6 (4)
C28—C29—H291	119.9	C134—C133—C138	118.3 (4)
C10—C30—C31	113.8 (3)	C133—C134—C135	120.0 (5)
C10—C30—H301	108.4	C133—C134—H1341	120.0
C31—C30—H301	108.3	C135—C134—H1341	120.0
C10—C30—H302	108.4	C134—C135—C136	119.7 (5)
C31—C30—H302	108.4	C134—C135—H1351	120.1
H301—C30—H302	109.5	C136—C135—H1351	120.2
C30—C31—C32	124.0 (4)	C135—C136—C137	119.9 (5)
C30—C31—H311	118.0	C135—C136—H1361	120.0
C32—C31—H311	118.0	C137—C136—H1361	120.1
C31—C32—C33	127.5 (4)	C136—C137—C138	120.1 (5)
C31—C32—H321	116.3	C136—C137—H1371	119.9
C33—C32—H321	116.2	C138—C137—H1371	120.0
C32—C33—C34	123.6 (4)	C137—C138—C133	122.0 (5)
C32—C33—C38	119.2 (5)	C137—C138—H1381	119.0
C34—C33—C38	117.2 (5)	C133—C138—H1381	119.0
C33—C34—C35	122.1 (6)	O203—S201—C204	110.0 (9)
C33—C34—H341	118.9	O203—S201—C205	103.1 (7)
C35—C34—H341	118.9	C204—S201—C205	93.6 (8)
C34—C35—C36	118.7 (7)	O203—S202—C204	110.7 (13)
C34—C35—H351	120.6	O203—S202—C205	110.8 (12)
C36—C35—H351	120.7	C204—S202—C205	100.5 (9)
C35—C36—C37	121.6 (7)	S201—C204—H2041	109.2
C35—C36—H361	119.2	S201—C204—H2042	109.4
C37—C36—H361	119.2	H2041—C204—H2042	109.5
C36—C37—C38	119.5 (7)	S201—C204—H2043	109.9
C36—C37—H371	120.3	H2041—C204—H2043	109.5
C38—C37—H371	120.2	H2042—C204—H2043	109.5
C37—C38—C33	120.7 (6)	S202—C204—H2044	109.9
C37—C38—H381	119.6	S202—C204—H2045	109.2
C33—C38—H381	119.7	S202—C204—H2046	109.3
C102—N101—C109	110.7 (3)	H2044—C204—H2045	109.5

C102—N101—H1011	124.6	H2044—C204—H2046	109.5
C109—N101—H1011	124.6	H2045—C204—H2046	109.5
N101—C102—C103	128.2 (3)	S201—C205—H2051	109.3
N101—C102—C107	111.6 (3)	S201—C205—H2052	109.6
C103—C102—C107	120.1 (3)	H2051—C205—H2052	109.5
C102—C103—C104	118.0 (3)	S201—C205—H2053	109.5
C102—C103—H1031	121.0	H2051—C205—H2053	109.5
C104—C103—H1031	121.0	H2052—C205—H2053	109.5
C103—C104—C105	121.9 (4)	S202—C205—H2054	109.3
C103—C104—H1041	119.1	S202—C205—H2055	109.9
C105—C104—H1041	119.1	S202—C205—H2056	109.2
C104—C105—C106	120.6 (4)	H2054—C205—H2055	109.5
C104—C105—H1051	119.7	H2054—C205—H2056	109.5
C106—C105—H1051	119.7	H2055—C205—H2056	109.5
O1—C2—C3—O4	21 (1)	C2—C20—C19—C13	−175.6 (8)
O1—C2—C3—C6	149.2 (7)	C2—C20—C19—C18	3 (2)
O1—C2—C20—C11	−172.0 (7)	C3—C2—C20—C11	10 (1)
O1—C2—C20—C19	3 (1)	C3—C2—C20—C19	−174.5 (8)
O4—C3—C2—C20	−161.3 (6)	C3—C6—O7—C8	130.1 (6)
O4—C3—C6—O7	−61.9 (8)	C3—C6—C9—C11	−44.7 (9)
O4—C3—C6—C9	−179.5 (7)	C5—O4—C3—C6	−63.6 (9)
O7—C6—C3—C2	169.7 (6)	C6—C3—C2—C20	−32.9 (9)
O7—C6—C9—O10	78.7 (7)	C6—C9—C11—C20	24 (1)
O7—C6—C9—C11	−160.9 (6)	C8—O7—C6—C9	−109.1 (6)
O10—C9—C6—C3	−165.0 (6)	C9—C11—O12—C13	−177.7 (6)
O10—C9—C11—O12	−37.8 (8)	C9—C11—C20—C19	177.4 (7)
O10—C9—C11—C20	144.3 (7)	C11—O12—C13—C14	−174.2 (7)
O12—C11—C9—C6	−158.3 (6)	C11—O12—C13—C19	−0.3 (8)
O12—C11—C20—C2	175.9 (6)	C11—C20—C19—C13	0.4 (8)
O12—C11—C20—C19	−0.6 (8)	C11—C20—C19—C18	179.2 (9)
O12—C13—C14—O15	−5 (1)	C13—O12—C11—C20	0.5 (8)
O12—C13—C14—C16	178.8 (7)	C13—C14—C16—C17	−3 (1)
O12—C13—C19—C18	−179.1 (7)	C13—C19—C18—C17	2 (1)
O12—C13—C19—C20	−0.1 (8)	C14—C13—C19—C18	−5 (1)
O15—C14—C13—C19	−178.3 (7)	C14—C13—C19—C20	174.0 (7)
O15—C14—C16—C17	−179.4 (7)	C14—C16—C17—C18	1 (1)
C2—C3—O4—C5	66.1 (7)	C16—C14—C13—C19	5 (1)
C2—C3—C6—C9	52.2 (9)	C16—C17—C18—C19	−1 (1)
C2—C20—C11—C9	−6 (1)	C17—C18—C19—C20	−176.3 (8)

Symmetry codes: (i) $x+1, y, z$; (ii) $-x, -y+1, -z$; (iii) $x-1, y, z$; (iv) $-x, -y+1, -z-1$.

Hydrogen-bond geometry (Å, º)

D—H···A	D—H	H···A	D···A	D—H···A
N1—H11···O119[v]	0.87	2.01	2.837 (6)	159
N101—H1011···O19	0.87	2.17	2.861 (6)	136

Symmetry code: (v) $x, y-1, z$.

Compound 265

Crystal data

$C_{25}H_{16}N_2O_2$
$M_r = 376.41$
Monoclinic, $P2_1/n$
$a = 8.4251\ (2)$ Å
$b = 10.9245\ (3)$ Å
$c = 20.7242\ (4)$ Å
$\beta = 100.7475\ (15)°$
$V = 1874.00\ (8)$ Å^3
$Z = 4$

$F(000) = 784$
$D_x = 1.334$ Mg m^{-3}
Mo $K\alpha$ radiation, $\lambda = 0.71073$ Å
Cell parameters from 70629 reflections
$\theta = 3–27.5°$
$\mu = 0.09$ mm^{-1}
$T = 200$ K
Plate, Yellow
$0.42 \times 0.36 \times 0.10$ mm

Data collection

Nonius KappaCCD diffractometer
graphite
φ and ω scans with CCD
Absorption correction: Multi-scan
DENZO/SCALEPACK (Otwinowski & Minor, 1997)
$T_{min} = 0.71$, $T_{max} = 0.99$
35059 measured reflections
4284 independent reflections

3584 reflections with $I > 2.0\sigma(I)$
$R_{int} = 0.055$
$\theta_{max} = 27.5°$, $\theta_{min} = 2.7°$
$h = 10\rightarrow10$
$k = 14\rightarrow14$
$l = -26\rightarrow26$

Refinement

Refinement on F^2
Least-squares matrix: Full
$R[F^2 > 2\sigma(F^2)] = 0.039$

$wR(F^2) = 0.104$

$S = 0.99$
4284 reflections
310 parameters
0 restraints

Primary atom site location: Structure-invariant direct methods
Hydrogen site location: Inferred from neighbouring sites
Only H-atom coordinates refined
Method = Modified Sheldrick $w = 1/[\sigma^2(F^2) + (0.05P)^2 + 0.54P]$, where $P = (\max(F_o^2,0) + 2F_c^2)/3$
$(\Delta/\sigma)_{max} = 0.004$
$\Delta\rho_{max} = 0.23$ e Å^{-3}
$\Delta\rho_{min} = -0.24$ e Å^{-3}

Special details

Refinement. All hydrogen atoms were observed in difference electron-density maps prior to their inclusion. They were included at calculated positions and were initially refined with soft restraints on the bond lengths and angles to regularise their geometry (C—H in the range 0.93–0.98Å) and with U$_{iso}$(H) in the range 1.2-1.5 times U$_{eq}$ of the parent atom, after which the positions were refined without restraints but the displacement parameters were held fixed.

The largest features in the final difference electron density map are located midway between bonded atoms.

Fractional atomic coordinates and isotropic or equivalent isotropic displacement parameters (Å^2)

	x	y	z	$U_{iso}*/U_{eq}$
N1	0.56607 (13)	0.32416 (9)	0.69523 (4)	0.0351
C2	0.48221 (14)	0.40634 (11)	0.72709 (6)	0.0366
C3	0.46820 (17)	0.40899 (15)	0.79350 (7)	0.0472
C4	0.38190 (19)	0.50451 (17)	0.81378 (8)	0.0571
C5	0.30846 (19)	0.59574 (16)	0.77102 (8)	0.0572
C6	0.31760 (17)	0.59128 (14)	0.70540 (8)	0.0479
C7	0.40348 (15)	0.49491 (12)	0.68381 (6)	0.0378
C8	0.42544 (14)	0.46510 (11)	0.61799 (6)	0.0348
C9	0.53245 (14)	0.34739 (10)	0.62365 (5)	0.0322
C10	0.45370 (14)	0.23239 (10)	0.59158 (5)	0.0309

C10	0.45370 (14)	0.23239 (10)	0.59158 (5)	0.0309
C11	0.48090 (14)	0.11939 (11)	0.62212 (5)	0.0330
C12	0.58519 (15)	0.10833 (12)	0.68455 (6)	0.0374
C13	0.62843 (15)	0.21021 (11)	0.72071 (6)	0.0375
N14	0.36170 (12)	0.21721 (9)	0.53013 (4)	0.0328
C15	0.32353 (14)	0.09329 (11)	0.52157 (6)	0.0340
C16	0.22837 (17)	0.03534 (13)	0.46783 (7)	0.0439
C17	0.21027 (18)	−0.08969 (13)	0.47219 (7)	0.0489
C18	0.28423 (17)	−0.15532 (13)	0.52773 (7)	0.0462
C19	0.37799 (16)	−0.09764 (12)	0.58061 (7)	0.0400
C20	0.39802 (14)	0.02941 (11)	0.57772 (6)	0.0334
O21	0.37764 (12)	0.52057 (8)	0.56699 (4)	0.0440
C22	0.68643 (15)	0.37969 (11)	0.59819 (6)	0.0369
C23	0.82852 (16)	0.38258 (12)	0.63577 (7)	0.0444
C24	0.9699 (2)	0.3850 (2)	0.67269 (11)	0.0738
C25	0.74583 (18)	0.20421 (14)	0.78139 (7)	0.0474
O26	0.80433 (14)	0.29135 (10)	0.81423 (5)	0.0577
C27	0.32466 (16)	0.30494 (12)	0.47600 (6)	0.0373
C28	0.15554 (17)	0.34428 (13)	0.46383 (7)	0.0456
C29	0.0201 (2)	0.37869 (16)	0.45320 (9)	0.0635
H31	0.5177 (19)	0.3446 (16)	0.8240 (8)	0.0559*
H41	0.373 (2)	0.5077 (16)	0.8606 (9)	0.0678*
H51	0.248 (2)	0.6617 (17)	0.7874 (9)	0.0689*
H61	0.266 (2)	0.6554 (16)	0.6736 (8)	0.0572*
H121	0.6285 (17)	0.0282 (14)	0.7006 (7)	0.0458*
H161	0.1777 (19)	0.0829 (15)	0.4286 (8)	0.0532*
H171	0.142 (2)	−0.1332 (16)	0.4363 (8)	0.0592*
H181	0.2702 (19)	−0.2465 (16)	0.5295 (7)	0.0545*
H191	0.4297 (18)	−0.1442 (14)	0.6192 (8)	0.0483*
H221	0.6703 (17)	0.4015 (14)	0.5516 (7)	0.0460*
H241	1.039 (3)	0.305 (2)	0.6775 (10)	0.0894*
H242	1.010 (3)	0.464 (2)	0.6944 (10)	0.0879*
H251	0.7762 (19)	0.1168 (15)	0.7956 (8)	0.0564*
H271	0.3485 (18)	0.2637 (14)	0.4376 (8)	0.0449*
H272	0.3951 (18)	0.3762 (14)	0.4863 (7)	0.0445*
H291	−0.091 (2)	0.4129 (18)	0.4471 (9)	0.0778*

Atomic displacement parameters (Å^2)

	U^{11}	U^{22}	U^{33}	U^{12}	U^{13}	U^{23}
N1	0.0447 (6)	0.0333 (5)	0.0259 (5)	0.0000 (4)	0.0027 (4)	−0.0004 (4)
C2	0.0372 (6)	0.0376 (6)	0.0350 (6)	−0.0086 (5)	0.0066 (5)	−0.0064 (5)
C3	0.0484 (7)	0.0586 (9)	0.0353 (7)	−0.0097 (7)	0.0093 (6)	−0.0081 (6)
C4	0.0521 (8)	0.0768 (11)	0.0458 (8)	−0.0123 (8)	0.0182 (7)	−0.0201 (8)
C5	0.0465 (8)	0.0627 (10)	0.0652 (10)	−0.0028 (7)	0.0175 (7)	−0.0261 (8)
C6	0.0415 (7)	0.0442 (8)	0.0582 (8)	−0.0015 (6)	0.0093 (6)	−0.0127 (6)
C7	0.0357 (6)	0.0370 (6)	0.0404 (6)	−0.0054 (5)	0.0066 (5)	−0.0058 (5)
C8	0.0361 (6)	0.0295 (6)	0.0377 (6)	−0.0042 (5)	0.0039 (5)	−0.0005 (5)
C9	0.0386 (6)	0.0299 (6)	0.0267 (5)	−0.0005 (5)	0.0026 (4)	0.0003 (4)
C10	0.0338 (6)	0.0304 (6)	0.0278 (5)	−0.0003 (4)	0.0042 (4)	−0.0009 (4)
C11	0.0375 (6)	0.0304 (6)	0.0304 (5)	−0.0003 (5)	0.0044 (4)	0.0009 (4)
C12	0.0437 (7)	0.0338 (6)	0.0331 (6)	0.0015 (5)	0.0026 (5)	0.0044 (5)
C13	0.0429 (7)	0.0382 (6)	0.0294 (6)	0.0002 (5)	0.0016 (5)	0.0031 (5)
N14	0.0386 (5)	0.0302 (5)	0.0273 (5)	−0.0016 (4)	0.0004 (4)	0.0008 (4)
C15	0.0367 (6)	0.0310 (6)	0.0339 (6)	−0.0023 (5)	0.0051 (5)	−0.0027 (4)
C16	0.0478 (7)	0.0407 (7)	0.0389 (7)	−0.0036 (6)	−0.0033 (6)	−0.0055 (5)
C17	0.0497 (8)	0.0414 (7)	0.0518 (8)	−0.0076 (6)	−0.0003 (6)	−0.0124 (6)
C18	0.0506 (8)	0.0317 (7)	0.0565 (8)	−0.0059 (6)	0.0105 (6)	−0.0056 (6)
C19	0.0447 (7)	0.0316 (6)	0.0440 (7)	−0.0010 (5)	0.0090 (5)	0.0005 (5)

C20	0.0363 (6)	0.0307 (6)	0.0334 (6)	−0.0012 (5)	0.0075 (5)	−0.0012 (4)
O21	0.0532 (5)	0.0352 (5)	0.0417 (5)	0.0047 (4)	0.0038 (4)	0.0066 (4)
C22	0.0417 (6)	0.0340 (6)	0.0349 (6)	−0.0042 (5)	0.0067 (5)	−0.0009 (5)
C23	0.0445 (7)	0.0382 (7)	0.0509 (7)	−0.0034 (6)	0.0097 (6)	0.0037 (6)
C24	0.0464 (9)	0.0822 (14)	0.0860 (13)	−0.0093 (9)	−0.0053 (8)	0.0167 (11)
C25	0.0526 (8)	0.0494 (8)	0.0357 (6)	0.0005 (6)	−0.0030 (6)	0.0044 (6)
O26	0.0643 (7)	0.0620 (7)	0.0390 (5)	−0.0071 (5)	−0.0107 (5)	−0.0046 (5)
C27	0.0437 (7)	0.0363 (6)	0.0293 (6)	−0.0015 (5)	0.0000 (5)	0.0048 (5)
C28	0.0484 (8)	0.0390 (7)	0.0452 (7)	−0.0029 (6)	−0.0023 (6)	0.0099 (6)
C29	0.0472 (8)	0.0567 (10)	0.0815 (12)	0.0013 (7)	−0.0011 (8)	0.0195 (8)

Geometric parameters (Å, °)

N1—C2	1.3838 (16)	N14—C15	1.3951 (15)
N1—C9	1.4795 (14)	N14—C27	1.4642 (15)
N1—C13	1.4145 (16)	C15—C16	1.3968 (16)
C2—C3	1.4034 (17)	C15—C20	1.4009 (16)
C2—C7	1.3995 (18)	C16—C17	1.379 (2)
C3—C4	1.381 (2)	C16—H161	0.991 (16)
C3—H31	0.985 (17)	C17—C18	1.400 (2)
C4—C5	1.399 (3)	C17—H171	0.975 (17)
C4—H41	0.989 (18)	C18—C19	1.3781 (19)
C5—C6	1.377 (2)	C18—H181	1.004 (17)
C5—H51	0.979 (19)	C19—C20	1.4008 (17)
C6—C7	1.3974 (19)	C19—H191	0.979 (15)
C6—H61	1.005 (17)	C22—C23	1.3011 (18)
C7—C8	1.4475 (17)	C22—H221	0.980 (15)
C8—C9	1.5623 (16)	C23—C24	1.290 (2)
C8—O21	1.2197 (14)	C24—H241	1.04 (2)
C9—C10	1.5152 (16)	C24—H242	1.00 (2)
C9—C22	1.5300 (17)	C25—O26	1.2196 (17)
C10—C11	1.3868 (16)	C25—H251	1.018 (17)
C10—N14	1.3718 (14)	C27—C28	1.4644 (19)
C11—C12	1.4271 (16)	C27—H271	0.968 (16)
C11—C20	1.4355 (16)	C27—H272	0.978 (15)
C12—C13	1.3532 (17)	C28—C29	1.183 (2)
C12—H121	0.982 (15)	C29—H291	0.995 (19)
C13—C25	1.4492 (17)		
O21···C27[i]	3.399 (2)	C4···C20[vi]	3.559 (2)
O21···C29[ii]	3.477 (2)	C5···C11[vi]	3.596 (2)
O21···C22[i]	3.537 (2)	C11···C17[v]	3.549 (2)
O26···C19[iii]	3.348 (2)	C15···C19[v]	3.577 (2)
O26···C27[iv]	3.487 (2)	C16···C20[v]	3.523 (2)
O26···C12[iii]	3.585 (2)	C23···C29[i]	3.564 (2)
N14···C18[v]	3.483 (2)	C29···C29[ii]	3.339 (4)
C4···C19[vi]	3.552 (2)		
C2—N1—C9	110.35 (10)	C12—C13—C25	120.86 (12)
C2—N1—C13	125.45 (10)	C10—N14—C15	108.19 (9)
C9—N1—C13	120.90 (9)	C10—N14—C27	129.41 (10)
N1—C2—C3	128.68 (12)	C15—N14—C27	121.78 (10)
N1—C2—C7	111.47 (10)	N14—C15—C16	128.72 (11)
C3—C2—C7	119.85 (12)	N14—C15—C20	108.71 (10)
C2—C3—C4	117.34 (15)	C16—C15—C20	122.56 (11)
C2—C3—H31	120.8 (10)	C15—C16—C17	116.78 (13)
C4—C3—H31	121.8 (10)	C15—C16—H161	120.7 (9)
C3—C4—C5	122.76 (14)	C17—C16—H161	122.5 (9)

C3—C4—H41	117.8 (11)	C16—C17—C18	121.56 (13)
C5—C4—H41	119.4 (11)	C16—C17—H171	119.4 (10)
C4—C5—C6	120.05 (14)	C18—C17—H171	119.1 (10)
C4—C5—H51	120.1 (11)	C17—C18—C19	121.39 (13)
C6—C5—H51	119.8 (11)	C17—C18—H181	120.0 (9)
C5—C6—C7	118.06 (15)	C19—C18—H181	118.6 (9)
C5—C6—H61	121.7 (10)	C18—C19—C20	118.35 (12)
C7—C6—H61	120.2 (10)	C18—C19—H191	120.9 (9)
C2—C7—C6	121.84 (12)	C20—C19—H191	120.7 (9)
C2—C7—C8	108.65 (11)	C11—C20—C15	106.28 (10)
C6—C7—C8	129.50 (13)	C11—C20—C19	134.36 (11)
C7—C8—C9	106.73 (10)	C15—C20—C19	119.35 (11)
C7—C8—O21	128.71 (12)	C9—C22—C23	122.95 (12)
C9—C8—O21	124.51 (11)	C9—C22—H221	115.2 (9)
C8—C9—N1	102.50 (9)	C23—C22—H221	121.8 (9)
C8—C9—C10	116.75 (9)	C22—C23—C24	179.54 (18)
N1—C9—C10	106.49 (9)	C23—C24—H241	118.5 (12)
C8—C9—C22	107.39 (9)	C23—C24—H242	118.9 (12)
N1—C9—C22	111.67 (10)	H241—C24—H242	122.6 (17)
C10—C9—C22	111.72 (9)	C13—C25—O26	126.04 (13)
C9—C10—C11	121.08 (10)	C13—C25—H251	112.8 (9)
C9—C10—N14	129.26 (10)	O26—C25—H251	121.1 (9)
C11—C10—N14	109.44 (10)	N14—C27—C28	112.68 (11)
C10—C11—C12	120.70 (11)	N14—C27—H271	106.2 (9)
C10—C11—C20	107.32 (10)	C28—C27—H271	109.9 (9)
C12—C11—C20	131.82 (11)	N14—C27—H272	108.7 (8)
C11—C12—C13	119.28 (11)	C28—C27—H272	109.6 (8)
C11—C12—H121	120.7 (8)	H271—C27—H272	109.8 (12)
C13—C12—H121	120.0 (8)	C27—C28—C29	178.28 (15)
N1—C13—C12	118.31 (10)	C28—C29—H291	175.2 (12)
N1—C13—C25	120.64 (11)		
O21—C8—C7—C2	−178.8 (1)	C7—C2—N1—C13	−165.5 (1)
O21—C8—C7—C6	2.7 (2)	C7—C8—C9—C10	114.0 (1)
O21—C8—C9—N1	175.6 (1)	C7—C8—C9—C22	−119.7 (1)
O21—C8—C9—C10	−68.5 (2)	C8—C9—N1—C13	165.3 (1)
O21—C8—C9—C22	57.8 (1)	C8—C9—C10—C11	−139.2 (1)
O26—C25—C13—N1	−2.3 (2)	C8—C9—C22—C23	113.2 (1)
O26—C25—C13—C12	172.6 (2)	C9—N1—C13—C12	−32.2 (2)
N1—C2—C3—C4	177.4 (1)	C9—N1—C13—C25	142.8 (1)
N1—C2—C7—C6	−176.8 (1)	C9—C10—N14—C15	176.8 (1)
N1—C2—C7—C8	4.6 (1)	C9—C10—N14—C27	5.8 (2)
N1—C9—C8—C7	−1.9 (1)	C9—C10—C11—C12	−0.5 (2)
N1—C9—C10—N14	160.5 (1)	C9—C10—C11—C20	−176.5 (1)
N1—C9—C10—C11	−25.5 (2)	C10—N14—C15—C16	177.8 (1)
N1—C9—C22—C23	1.6 (2)	C10—N14—C15—C20	−2.2 (1)
N1—C13—C12—C11	0.8 (2)	C10—N14—C27—C28	−109.9 (1)
N14—C10—C9—C8	46.8 (2)	C10—C9—N1—C13	42.1 (1)
N14—C10—C9—C22	−77.3 (2)	C10—C9—C22—C23	−117.5 (1)
N14—C10—C11—C12	174.6 (1)	C10—C11—C12—C13	14.9 (2)
N14—C10—C11—C20	−1.4 (1)	C10—C11—C20—C15	0.0 (1)
N14—C15—C16—C17	179.9 (1)	C10—C11—C20—C19	−178.8 (1)
N14—C15—C20—C11	1.3 (1)	C11—C10—N14—C15	2.2 (1)
N14—C15—C20—C19	−179.7 (1)	C11—C10—N14—C27	−168.8 (1)
C2—N1—C9—C8	4.7 (1)	C11—C10—C9—C22	96.7 (1)
C2—N1—C9—C10	−118.4 (1)	C11—C12—C13—C25	−174.2 (1)
C2—N1—C9—C22	119.4 (1)	C11—C20—C15—C16	−178.7 (1)
C2—N1—C13—C12	125.3 (1)	C11—C20—C19—C18	178.4 (1)

C2—N1—C13—C25	−59.7 (2)	C12—C11—C20—C15	−175.4 (1)
C2—C3—C4—C5	0.7 (2)	C12—C11—C20—C19	5.8 (3)
C2—C7—C6—C5	−1.6 (2)	C13—N1—C9—C22	−80.1 (1)
C2—C7—C8—C9	−1.4 (1)	C13—C12—C11—C20	−170.2 (1)
C3—C2—N1—C9	173.4 (1)	C15—N14—C27—C28	80.2 (1)
C3—C2—N1—C13	14.0 (2)	C15—C16—C17—C18	−0.2 (2)
C3—C2—C7—C6	3.7 (2)	C15—C20—C19—C18	−0.3 (2)
C3—C2—C7—C8	−174.9 (1)	C16—C15—N14—C27	−10.4 (2)
C3—C4—C5—C6	1.4 (2)	C16—C15—C20—C19	0.3 (2)
C4—C3—C2—C7	−3.1 (2)	C16—C17—C18—C19	0.2 (2)
C4—C5—C6—C7	−0.9 (2)	C17—C16—C15—C20	−0.1 (2)
C5—C6—C7—C8	176.7 (1)	C17—C18—C19—C20	0.0 (2)
C6—C7—C8—C9	−179.9 (1)	C20—C15—N14—C27	169.6 (1)
C7—C2—N1—C9	−6.0 (1)		

Symmetry codes: (i) −x+1, −y+1, −z+1; (ii) −x, −y+1, −z+1; (iii) −x+3/2, y+1/2, −z+3/2; (iv) x+1/2, −y+1/2, z+1/2; (v) −x+1, −y, −z+1; (vi) −x+1/2, y+1/2, −z+3/2.

Compound 266

Crystal data

$C_{25}H_{16}N_2O_2$
$M_r = 376.41$
Monoclinic, $P2_1/n$
$a = 8.8893$ (2) Å
$b = 21.6743$ (4) Å
$c = 10.0894$ (2) Å
$\beta = 106.0180$ (9)°
$V = 1868.45$ (7) Å^3
$Z = 4$

$F(000) = 784$
$D_x = 1.338$ Mg m^{-3}
Mo $K\alpha$ radiation, $\lambda = 0.71073$ Å
Cell parameters from 22246 reflections
$\theta = 2.6$–27.5°
$\mu = 0.09$ mm^{-1}
$T = 200$ K
Block, Yellow
$0.37 \times 0.19 \times 0.16$ mm

Data collection

Nonius KappaCCD
  diffractometer
Graphite monochromator
φ and ω scans with CCD
Absorption correction: Integration
  via Gaussian method (Coppens, 1970) implemented in
  maXus (2000)
$T_{min} = 0.976$, $T_{max} = 0.990$

36338 measured reflections
4287 independent reflections
3143 reflections with $I > 2.0\sigma(I)$
$R_{int} = 0.042$
$\theta_{max} = 27.5°$, $\theta_{min} = 2.8°$
$h = -11 \rightarrow 11$
$k = -28 \rightarrow 27$
$l = -13 \rightarrow 13$

Refinement

Refinement on F^2
Least-squares matrix: Full
$R[F^2 > 2\sigma(F^2)] = 0.040$
$wR(F^2) = 0.098$
$S = 0.96$
4287 reflections
262 parameters
0 restraints
Primary atom site location: Structure-invariant direct
  methods

Hydrogen site location: Inferred from neighbouring
  sites
H-atom parameters constrained
Method = Modified Sheldrick $w = 1/[\sigma^2(F^2) + (0.05P)^2 + 0.4P]$,
  where $P = (\max(F_o^2,0) + 2F_c^2)/3$
$(\Delta/\sigma)_{max} = 0.001$
$\Delta\rho_{max} = 0.34$ e Å^{-3}
$\Delta\rho_{min} = -0.28$ e Å^{-3}

Special details

Refinement. The hydrogen atoms were observed in difference electron-density maps prior to their inclusion. They were included at calculated positions and were initially refined with soft restraints on the bond lengths and angles to regularise their geometry (C—H in the range 0.93–0.98Å) and with U$_{iso}$(H) in the range 1.2-1.5 times U$_{eq}$ of the parent atom, after which the positions were refined with riding constraints and the displacement parameters were held fixed.
The largest features in the final difference electron density map are located randomly through the structure, including midway between bonded atoms.

Fractional atomic coordinates and isotropic or equivalent isotropic displacement parameters (Å²)

	x	y	z	$U_{iso}*/U_{eq}$
N1	0.31637 (11)	0.58293 (5)	0.74109 (10)	0.0328
C2	0.35144 (14)	0.64483 (6)	0.77638 (12)	0.0344
C3	0.24318 (16)	0.69170 (6)	0.71968 (14)	0.0429
C4	0.27974 (18)	0.75226 (7)	0.75395 (15)	0.0511
C5	0.42286 (19)	0.76858 (7)	0.84485 (16)	0.0538
C6	0.52916 (17)	0.72345 (6)	0.90081 (14)	0.0456
C7	0.49516 (14)	0.66095 (6)	0.86846 (13)	0.0355
C8	0.60712 (14)	0.61365 (6)	0.93346 (12)	0.0349
C9	0.57134 (13)	0.55167 (6)	0.88234 (12)	0.0323
C10	0.68130 (14)	0.50292 (6)	0.93645 (12)	0.0354
C11	0.65502 (14)	0.44533 (6)	0.89046 (12)	0.0363
N12	0.52453 (12)	0.43254 (5)	0.78143 (11)	0.0350
C13	0.50125 (15)	0.38050 (6)	0.69821 (14)	0.0397
C14	0.58789 (17)	0.32587 (7)	0.71324 (18)	0.0530
C15	0.5453 (2)	0.28365 (7)	0.6077 (2)	0.0648
C16	0.4203 (2)	0.29482 (8)	0.4902 (2)	0.0640
C17	0.33404 (17)	0.34814 (7)	0.47549 (16)	0.0505
C18	0.37491 (15)	0.39230 (6)	0.58175 (14)	0.0392
C19	0.32131 (13)	0.45289 (6)	0.59688 (12)	0.0337
C20	0.41268 (13)	0.47782 (6)	0.71961 (12)	0.0316
C21	0.43170 (13)	0.53834 (6)	0.78327 (12)	0.0307

C22	0.14868 (13)	0.56506 (6)	0.69577 (13)	0.0364
C23	0.06206 (14)	0.58639 (6)	0.79144 (13)	0.0379
C24	−0.01267 (16)	0.60177 (7)	0.86634 (15)	0.0462
O25	0.72994 (10)	0.62662 (5)	1.02458 (10)	0.0468
O26	0.20053 (9)	0.48110 (4)	0.50061 (8)	0.0356
C27	0.25427 (15)	0.51943 (7)	0.40649 (14)	0.0446
C28	0.12143 (15)	0.55427 (6)	0.32289 (13)	0.0397
C29	0.01329 (17)	0.58130 (7)	0.25306 (15)	0.0464
H31	0.1421	0.6811	0.6564	0.0494*
H41	0.2068	0.7840	0.7153	0.0613*
H51	0.4470	0.8121	0.8687	0.0649*
H61	0.6280	0.7337	0.9642	0.0556*
H101	0.7746	0.5132	1.0073	0.0424*
H111	0.7240	0.4112	0.9250	0.0435*
H141	0.6733	0.3188	0.7947	0.0638*
H151	0.6042	0.2455	0.6144	0.0778*
H161	0.3939	0.2643	0.4190	0.0766*
H171	0.2474	0.3559	0.3954	0.0592*
H221	0.0988	0.5813	0.6024	0.0431*
H222	0.1441	0.5198	0.6905	0.0440*
H241	−0.0740	0.6150	0.9258	0.0564*
H271	0.3359	0.5480	0.4610	0.0553*
H272	0.3020	0.4924	0.3488	0.0552*
H291	−0.0774	0.6013	0.1964	0.0594*

Atomic displacement parameters (Å²)

	U^{11}	U^{22}	U^{33}	U^{12}	U^{13}	U^{23}
N1	0.0249 (5)	0.0369 (6)	0.0350 (5)	0.0013 (4)	0.0054 (4)	0.0035 (4)
C2	0.0317 (6)	0.0387 (7)	0.0330 (6)	0.0015 (5)	0.0091 (5)	0.0032 (5)
C3	0.0379 (7)	0.0442 (8)	0.0420 (7)	0.0051 (6)	0.0033 (6)	0.0059 (6)
C4	0.0553 (9)	0.0421 (8)	0.0513 (8)	0.0094 (7)	0.0070 (7)	0.0071 (7)
C5	0.0644 (10)	0.0396 (8)	0.0525 (9)	−0.0013 (7)	0.0077 (8)	0.0010 (7)
C6	0.0452 (8)	0.0460 (8)	0.0421 (7)	−0.0048 (6)	0.0061 (6)	−0.0016 (6)
C7	0.0328 (6)	0.0414 (7)	0.0322 (6)	−0.0009 (5)	0.0088 (5)	0.0004 (5)
C8	0.0269 (6)	0.0488 (8)	0.0295 (6)	0.0007 (5)	0.0083 (5)	−0.0016 (5)
C9	0.0261 (6)	0.0431 (7)	0.0281 (6)	0.0024 (5)	0.0081 (5)	0.0033 (5)
C10	0.0273 (6)	0.0484 (8)	0.0293 (6)	0.0037 (5)	0.0060 (5)	0.0047 (6)
C11	0.0294 (6)	0.0452 (8)	0.0335 (6)	0.0061 (5)	0.0071 (5)	0.0102 (6)
N12	0.0298 (5)	0.0368 (6)	0.0377 (6)	0.0018 (4)	0.0078 (4)	0.0070 (5)
C13	0.0347 (7)	0.0356 (7)	0.0493 (8)	−0.0015 (5)	0.0127 (6)	0.0043 (6)
C14	0.0426 (8)	0.0398 (8)	0.0738 (10)	0.0029 (6)	0.0113 (7)	0.0059 (8)
C15	0.0540 (10)	0.0402 (9)	0.0980 (14)	0.0051 (7)	0.0172 (10)	−0.0066 (9)
C16	0.0582 (10)	0.0479 (10)	0.0836 (12)	−0.0043 (8)	0.0155 (9)	−0.0179 (9)
C17	0.0452 (8)	0.0463 (8)	0.0581 (9)	−0.0048 (7)	0.0110 (7)	−0.0070 (7)
C18	0.0341 (7)	0.0382 (7)	0.0459 (7)	−0.0040 (6)	0.0120 (6)	0.0017 (6)
C19	0.0270 (6)	0.0386 (7)	0.0350 (6)	−0.0011 (5)	0.0077 (5)	0.0051 (5)
C20	0.0255 (6)	0.0373 (7)	0.0325 (6)	0.0014 (5)	0.0087 (5)	0.0073 (5)
C21	0.0251 (6)	0.0386 (7)	0.0290 (6)	0.0018 (5)	0.0084 (5)	0.0072 (5)
C22	0.0241 (6)	0.0467 (8)	0.0367 (7)	0.0018 (5)	0.0054 (5)	0.0004 (6)
C23	0.0278 (6)	0.0434 (7)	0.0397 (7)	0.0020 (5)	0.0048 (5)	0.0031 (6)
C24	0.0367 (7)	0.0580 (9)	0.0454 (8)	0.0050 (6)	0.0137 (6)	0.0011 (7)
O25	0.0332 (5)	0.0575 (6)	0.0432 (5)	0.0030 (4)	−0.0004 (4)	−0.0106 (5)
O26	0.0277 (4)	0.0449 (5)	0.0326 (4)	−0.0009 (4)	0.0059 (4)	0.0053 (4)
C27	0.0329 (7)	0.0591 (9)	0.0422 (7)	0.0031 (6)	0.0108 (6)	0.0161 (7)
C28	0.0377 (7)	0.0444 (8)	0.0364 (7)	−0.0008 (6)	0.0094 (6)	0.0037 (6)
C29	0.0428 (8)	0.0488 (8)	0.0437 (8)	0.0057 (6)	0.0053 (6)	0.0047 (7)

Geometric parameters (Å, º)

N1—C2	1.4009 (16)	C13—C18	1.4068 (18)

N1—C21	1.3876 (15)	C14—C15	1.376 (2)
N1—C22	1.4850 (15)	C14—H141	0.965
C2—C3	1.4077 (18)	C15—C16	1.405 (2)
C2—C7	1.4008 (17)	C15—H151	0.970
C3—C4	1.373 (2)	C16—C17	1.372 (2)
C3—H31	0.975	C16—H161	0.957
C4—C5	1.393 (2)	C17—C18	1.408 (2)
C4—H41	0.952	C17—H171	0.965
C5—C6	1.369 (2)	C18—C19	1.4195 (18)
C5—H51	0.982	C19—C20	1.3892 (17)
C6—C7	1.4066 (19)	C19—O26	1.3764 (14)
C6—H61	0.960	C20—C21	1.4498 (17)
C7—C8	1.4530 (17)	C22—C23	1.4657 (18)
C8—C9	1.4427 (18)	C22—H221	0.989
C8—O25	1.2500 (14)	C22—H222	0.983
C9—C10	1.4407 (17)	C23—C24	1.1835 (18)
C9—C21	1.3924 (16)	C24—H241	0.959
C10—C11	1.3296 (18)	O26—C27	1.4389 (15)
C10—H101	0.960	C27—C28	1.4583 (18)
C11—N12	1.3886 (16)	C27—H271	0.997
C11—H111	0.962	C27—H272	0.999
N12—C13	1.3871 (17)	C28—C29	1.1789 (18)
N12—C20	1.4136 (15)	C29—H291	0.954
C13—C14	1.3978 (19)		
O25⋯C29^i	3.069 (2)	C10⋯C21^{vi}	3.372 (2)
O25⋯C24^{ii}	3.177 (2)	C11⋯C28^v	3.308 (2)
O25⋯C4^{iii}	3.446 (2)	C11⋯C27^v	3.398 (2)
O26⋯C22^{iv}	3.342 (1)	C11⋯C23^{vi}	3.556 (2)
O26⋯C23^{iv}	3.532 (1)	C11⋯C24^{vi}	3.587 (2)
N12⋯C27^v	3.256 (2)	C11⋯C21^{vi}	3.599 (2)
N12⋯C8^{vi}	3.536 (2)	C13⋯C27^v	3.437 (2)
N12⋯C28^v	3.595 (2)	C20⋯C27^v	3.531 (2)
C5⋯C29^{iii}	3.536 (2)	C22⋯C28^{iv}	3.499 (2)
C8⋯C11^{vi}	3.536 (2)	C22⋯C29^{iv}	3.579 (2)
C9⋯C11^{vi}	3.443 (2)	C23⋯C28^{iv}	3.500 (2)
C9⋯C10^{vi}	3.472 (2)		
C2—N1—C21	119.69 (10)	C13—C14—H141	120.5
C2—N1—C22	117.52 (10)	C15—C14—H141	122.5
C21—N1—C22	120.44 (10)	C14—C15—C16	121.56 (15)
N1—C2—C3	120.57 (11)	C14—C15—H151	119.0
N1—C2—C7	120.38 (11)	C16—C15—H151	119.4
C3—C2—C7	119.06 (12)	C15—C16—C17	121.65 (15)
C2—C3—C4	119.98 (13)	C15—C16—H161	119.1
C2—C3—H31	120.0	C17—C16—H161	119.2
C4—C3—H31	120.1	C16—C17—C18	118.13 (14)
C3—C4—C5	121.20 (13)	C16—C17—H171	122.0
C3—C4—H41	120.0	C18—C17—H171	119.9
C5—C4—H41	118.8	C17—C18—C13	119.42 (13)
C4—C5—C6	119.42 (14)	C17—C18—C19	133.40 (13)
C4—C5—H51	120.2	C13—C18—C19	107.02 (12)
C6—C5—H51	120.4	C18—C19—C20	108.94 (11)
C5—C6—C7	120.85 (13)	C18—C19—O26	123.69 (11)
C5—C6—H61	120.7	C20—C19—O26	127.34 (11)
C7—C6—H61	118.5	N12—C20—C19	106.88 (11)
C6—C7—C2	119.49 (12)	N12—C20—C21	116.80 (10)
C6—C7—C8	119.88 (12)	C19—C20—C21	135.63 (11)
C2—C7—C8	120.60 (11)	C20—C21—C9	118.53 (10)
C7—C8—C9	116.08 (10)	C20—C21—N1	120.56 (10)
C7—C8—O25	121.58 (12)	C9—C21—N1	120.83 (11)
C9—C8—O25	122.28 (11)	N1—C22—C23	112.34 (10)
C8—C9—C10	119.20 (11)	N1—C22—H221	110.4

C8—C9—C21	120.98 (11)	C23—C22—H221	109.6
C10—C9—C21	119.81 (12)	N1—C22—H222	107.4
C9—C10—C11	121.38 (11)	C23—C22—H222	109.2
C9—C10—H101	117.9	H221—C22—H222	107.7
C11—C10—H101	120.7	C22—C23—C24	177.17 (14)
C10—C11—N12	119.46 (11)	C23—C24—H241	178.7
C10—C11—H111	124.2	C19—O26—C27	112.69 (9)
N12—C11—H111	116.3	O26—C27—C28	108.50 (10)
C11—N12—C13	126.47 (11)	O26—C27—H271	108.6
C11—N12—C20	122.89 (11)	C28—C27—H271	110.3
C13—N12—C20	109.15 (10)	O26—C27—H272	108.5
N12—C13—C14	129.60 (13)	C28—C27—H272	111.9
N12—C13—C18	108.01 (11)	H271—C27—H272	109.0
C14—C13—C18	122.25 (13)	C27—C28—C29	178.40 (15)
C13—C14—C15	116.99 (15)	C28—C29—H291	177.1
O25—C8—C7—C2	−173.8 (1)	C7—C2—N1—C21	−8.3 (2)
O25—C8—C7—C6	4.5 (2)	C7—C2—N1—C22	154.4 (1)
O25—C8—C9—C10	−0.8 (2)	C7—C8—C9—C10	176.6 (1)
O25—C8—C9—C21	178.3 (1)	C7—C8—C9—C21	−4.3 (2)
O26—C19—C18—C13	178.4 (1)	C8—C9—C10—C11	−178.6 (1)
O26—C19—C18—C17	3.4 (3)	C8—C9—C21—C20	170.2 (1)
O26—C19—C20—N12	−178.1 (1)	C9—C21—N1—C22	−149.2 (1)
O26—C19—C20—C21	−8.4 (3)	C9—C21—C20—C19	−156.9 (2)
N1—C2—C3—C4	−179.3 (1)	C10—C9—C21—C20	−10.6 (2)
N1—C2—C7—C6	179.0 (1)	C10—C11—N12—C13	161.7 (1)
N1—C2—C7—C8	−2.7 (2)	C10—C11—N12—C20	−2.8 (2)
N1—C21—C9—C8	−6.5 (2)	C11—N12—C13—C14	9.9 (3)
N1—C21—C9—C10	172.6 (1)	C11—N12—C13—C18	−165.8 (1)
N1—C21—C20—N12	−171.3 (1)	C11—N12—C20—C19	166.5 (1)
N1—C21—C20—C19	19.8 (2)	C11—N12—C20—C21	−5.4 (2)
N12—C11—C10—C9	4.6 (2)	C11—C10—C9—C21	2.3 (2)
N12—C13—C14—C15	−174.5 (2)	C13—N12—C20—C19	−0.4 (2)
N12—C13—C18—C17	175.5 (1)	C13—N12—C20—C21	−172.3 (1)
N12—C13—C18—C19	−0.4 (2)	C13—C14—C15—C16	−0.1 (3)
N12—C20—C19—C18	0.2 (2)	C13—C18—C17—C16	−0.0 (2)
N12—C20—C21—C9	12.0 (2)	C13—C18—C19—C20	0.1 (2)
C2—N1—C21—C9	13.0 (2)	C14—C13—N12—C20	176.1 (2)
C2—N1—C21—C20	−163.7 (1)	C14—C13—C18—C17	−0.5 (2)
C2—N1—C22—C23	−50.2 (1)	C14—C13—C18—C19	−176.4 (1)
C2—C3—C4—C5	−0.2 (3)	C14—C15—C16—C17	−0.5 (3)
C2—C7—C6—C5	0.8 (2)	C15—C14—C13—C18	0.6 (2)
C2—C7—C8—C9	8.8 (2)	C15—C16—C17—C18	0.5 (3)
C3—C2—N1—C21	171.5 (1)	C16—C17—C18—C19	174.5 (2)
C3—C2—N1—C22	−25.8 (2)	C17—C18—C19—C20	−174.9 (2)
C3—C2—C7—C6	−0.9 (2)	C18—C13—N12—C20	0.5 (2)
C3—C2—C7—C8	177.4 (1)	C18—C19—O26—C27	−95.0 (1)
C3—C4—C5—C6	0.1 (3)	C18—C19—C20—C21	169.8 (1)
C4—C3—C2—C7	0.6 (2)	C19—O26—C27—C28	−171.5 (1)
C4—C5—C6—C7	−0.5 (3)	C20—C19—O26—C27	83.0 (2)
C5—C6—C7—C8	−177.5 (1)	C20—C21—N1—C22	34.1 (2)
C6—C7—C8—C9	−172.9 (1)	C21—N1—C22—C23	112.3 (1)

Symmetry codes: (i) $x+1$, y, $z+1$; (ii) $x+1$, y, z; (iii) $x+1/2$, $−y+3/2$, $z+1/2$; (iv) $−x$, $−y+1$, $−z+1$; (v) $−x+1$, $−y+1$, $−z+1$; (vi) $−x+1$, $−y+1$, $−z+2$.

Compound 267

Crystal data

$C_{29}H_{18}N_2O_4$	$Z = 2$
$M_r = 458.47$	$F(000) = 476$
Triclinic, $P\bar{1}$	$D_x = 1.375$ Mg m^{-3}
$a = 7.5927$ (2) Å	Mo $K\alpha$ radiation, $\lambda = 0.71073$ Å
$b = 9.4172$ (3) Å	Cell parameters from 17260 reflections
$c = 16.2992$ (5) Å	$\theta = 2.6–27.5°$
$\alpha = 76.3835$ (14)°	$\mu = 0.09$ mm^{-1}
$\beta = 88.6282$ (18)°	$T = 200$ K
$\gamma = 78.0391$ (19)°	Plate, Pale yellow
$V = 1107.70$ (6) Å^3	$0.51 \times 0.24 \times 0.06$ mm

Data collection

Nonius KappaCCD diffractometer	4074 reflections with $I > 2.0\sigma(I)$
graphite	$R_{int} = 0.040$
φ and ω scans with CCD	$\theta_{max} = 27.5°$, $\theta_{min} = 2.6°$
Absorption correction: Integration via Gaussian method (Coppens, 1970) implemented in *maXus* (2000)	$h = -9 \rightarrow 9$
$T_{min} = 0.969$, $T_{max} = 0.994$	$k = -12 \rightarrow 12$
23182 measured reflections	$l = -21 \rightarrow 21$
5070 independent reflections	

Refinement

Refinement on F^2	Primary atom site location: Structure-invariant direct methods
Least-squares matrix: Full	Hydrogen site location: Inferred from neighbouring sites
$R[F^2 > 2\sigma(F^2)] = 0.046$	H-atom parameters constrained
$wR(F^2) = 0.125$	Method = Modified Sheldrick $w = 1/[\sigma^2(F^2) + (0.06P)^2 + 0.46P]$, where $P = (max(F_o^2,0) + 2F_c^2)/3$
$S = 0.99$	$(\Delta/\sigma)_{max} = 0.001$
5070 reflections	$\Delta\rho_{max} = 0.47$ e Å^{-3}
316 parameters	$\Delta\rho_{min} = -0.27$ e Å^{-3}
0 restraints	

Special details

Refinement. All hydrogen atoms were observed in difference electron-density maps prior to their inclusion. They were included at calculated positions and were initially refined with soft restraints on the bond lengths and angles to regularise their geometry (C—H in the range 0.93–0.98Å) and with U_{iso}(H) in the range 1.2-1.5 times U_{eq} of the parent atom, after which the positions were refined with riding constraints but the displacement parameters were held fixed.

The largest features in the final difference electron density map are located adjacent to C33, C34 and C35 and possibly indicate an alternative packing of this group. An attempt to model this suggested its relative occupancy, compared with that of the main orientation of the group, as 0.07:0.93, and so not worth pursuing. Other peaks are situated in gaps between molecules or adjacent to other peripheral groups.

Fractional atomic coordinates and isotropic or equivalent isotropic displacement parameters (Å^2)

	x	y	z	$U_{iso}*/U_{eq}$
N1	0.11689 (17)	0.26129 (14)	0.34464 (8)	0.0334
C2	−0.0641 (2)	0.30181 (17)	0.36439 (9)	0.0344
C3	−0.1488 (2)	0.1977 (2)	0.41846 (11)	0.0438
C4	−0.3238 (2)	0.2411 (2)	0.44071 (11)	0.0487

C4	−0.3238 (2)	0.2411 (2)	0.44071 (11)	0.0487
C5	−0.4204 (2)	0.3861 (2)	0.41054 (11)	0.0468
C6	−0.3404 (2)	0.48781 (19)	0.35640 (10)	0.0403
C7	−0.1610 (2)	0.44732 (17)	0.33225 (9)	0.0334
C8	−0.07573 (19)	0.55747 (16)	0.27601 (9)	0.0320
C9	0.09525 (19)	0.49653 (16)	0.24286 (9)	0.0307
C10	0.1786 (2)	0.59215 (16)	0.17710 (9)	0.0323
C11	0.3523 (2)	0.55044 (16)	0.15915 (9)	0.0340
N12	0.44742 (16)	0.41020 (13)	0.19686 (8)	0.0323
C13	0.6187 (2)	0.34433 (17)	0.17642 (10)	0.0346
C14	0.7461 (2)	0.40925 (19)	0.12680 (11)	0.0417
C15	0.9067 (2)	0.3151 (2)	0.11699 (12)	0.0488
C16	0.9386 (2)	0.1621 (2)	0.15515 (12)	0.0505
C17	0.8123 (2)	0.0978 (2)	0.20304 (11)	0.0433
C18	0.6466 (2)	0.19094 (17)	0.21372 (9)	0.0357
C19	0.4866 (2)	0.16415 (16)	0.25583 (9)	0.0342
C20	0.3659 (2)	0.29967 (16)	0.24841 (9)	0.0314
C21	0.18952 (19)	0.35290 (16)	0.27964 (9)	0.0301
C22	0.2343 (2)	0.15000 (17)	0.41153 (9)	0.0360
C23	0.2165 (2)	0.18879 (18)	0.49380 (10)	0.0371
C24	0.2159 (2)	0.2125 (2)	0.56153 (11)	0.0473
O25	−0.14477 (14)	0.69270 (12)	0.25819 (7)	0.0391
C26	0.0786 (2)	0.73591 (16)	0.12384 (9)	0.0346
O27	0.13360 (16)	0.85049 (13)	0.10729 (8)	0.0476
O28	−0.07264 (15)	0.71983 (12)	0.08924 (7)	0.0387
C29	−0.1876 (2)	0.85735 (18)	0.04479 (11)	0.0441
C30	−0.3402 (3)	0.82102 (19)	0.00774 (11)	0.0461
C31	−0.4655 (3)	0.7964 (2)	−0.02167 (13)	0.0640
O32	0.46256 (16)	0.02647 (12)	0.29973 (7)	0.0413
C33	0.4191 (3)	−0.0688 (2)	0.25010 (12)	0.0496
C34	0.3080 (2)	−0.1631 (2)	0.30266 (13)	0.0493
C35	0.2224 (3)	−0.2376 (3)	0.34730 (16)	0.0687
H31	−0.0858	0.0988	0.4375	0.0528*
H41	−0.3785	0.1703	0.4772	0.0580*
H51	−0.5397	0.4130	0.4281	0.0563*
H61	−0.4042	0.5886	0.3331	0.0482*
H111	0.4137	0.6138	0.1194	0.0406*
H141	0.7247	0.5119	0.1014	0.0500*
H151	0.9996	0.3542	0.0828	0.0585*
H161	1.0518	0.1005	0.1481	0.0613*
H171	0.8341	−0.0052	0.2279	0.0511*
H221	0.3594	0.1461	0.3949	0.0429*
H222	0.2085	0.0495	0.4165	0.0427*
H241	0.2151	0.2340	0.6145	0.0586*
H291	−0.2291	0.9199	0.0843	0.0530*
H292	−0.1201	0.9098	0.0011	0.0540*
H311	−0.5646	0.7748	−0.0450	0.0781*
H331	0.5310	−0.1320	0.2345	0.0572*
H332	0.3512	−0.0099	0.1995	0.0608*
H351	0.1563	−0.2955	0.3826	0.0831*

Atomic displacement parameters (Å²)

	U^{11}	U^{22}	U^{33}	U^{12}	U^{13}	U^{23}
N1	0.0336 (6)	0.0323 (6)	0.0298 (6)	−0.0078 (5)	−0.0029 (5)	0.0031 (5)
C2	0.0336 (7)	0.0386 (8)	0.0295 (7)	−0.0128 (6)	−0.0036 (6)	−0.0002 (6)
C3	0.0399 (9)	0.0439 (9)	0.0412 (9)	−0.0154 (7)	−0.0058 (7)	0.0091 (7)
C4	0.0397 (9)	0.0596 (11)	0.0425 (9)	−0.0242 (8)	−0.0029 (7)	0.0090 (8)

C5	0.0331 (8)	0.0611 (11)	0.0448 (9)	−0.0167 (8)	0.0036 (7)	−0.0038 (8)
C6	0.0332 (8)	0.0450 (9)	0.0403 (8)	−0.0091 (7)	0.0002 (6)	−0.0047 (7)
C7	0.0329 (7)	0.0367 (8)	0.0299 (7)	−0.0107 (6)	−0.0008 (6)	−0.0034 (6)
C8	0.0338 (7)	0.0323 (7)	0.0285 (7)	−0.0070 (6)	−0.0013 (6)	−0.0044 (6)
C9	0.0333 (7)	0.0284 (7)	0.0294 (7)	−0.0083 (6)	0.0005 (6)	−0.0031 (6)
C10	0.0362 (8)	0.0263 (7)	0.0325 (7)	−0.0071 (6)	0.0027 (6)	−0.0028 (6)
C11	0.0392 (8)	0.0278 (7)	0.0336 (7)	−0.0084 (6)	0.0046 (6)	−0.0035 (6)
N12	0.0344 (6)	0.0279 (6)	0.0335 (6)	−0.0068 (5)	0.0028 (5)	−0.0052 (5)
C13	0.0336 (7)	0.0362 (8)	0.0352 (8)	−0.0056 (6)	0.0011 (6)	−0.0121 (6)
C14	0.0414 (9)	0.0410 (9)	0.0458 (9)	−0.0119 (7)	0.0081 (7)	−0.0143 (7)
C15	0.0411 (9)	0.0549 (11)	0.0552 (11)	−0.0124 (8)	0.0136 (8)	−0.0216 (9)
C16	0.0393 (9)	0.0535 (11)	0.0592 (11)	0.0002 (8)	0.0053 (8)	−0.0232 (9)
C17	0.0428 (9)	0.0406 (9)	0.0441 (9)	0.0022 (7)	−0.0020 (7)	−0.0142 (7)
C18	0.0393 (8)	0.0352 (8)	0.0319 (7)	−0.0038 (6)	−0.0025 (6)	−0.0096 (6)
C19	0.0407 (8)	0.0297 (7)	0.0298 (7)	−0.0043 (6)	−0.0028 (6)	−0.0045 (6)
C20	0.0362 (8)	0.0292 (7)	0.0274 (7)	−0.0079 (6)	−0.0012 (6)	−0.0026 (5)
C21	0.0334 (7)	0.0295 (7)	0.0270 (7)	−0.0093 (6)	−0.0009 (5)	−0.0031 (5)
C22	0.0383 (8)	0.0342 (8)	0.0301 (7)	−0.0058 (6)	−0.0033 (6)	0.0017 (6)
C23	0.0313 (7)	0.0404 (8)	0.0352 (8)	−0.0092 (6)	−0.0019 (6)	0.0017 (6)
C24	0.0449 (9)	0.0606 (11)	0.0354 (9)	−0.0114 (8)	−0.0012 (7)	−0.0087 (8)
O25	0.0387 (6)	0.0325 (6)	0.0425 (6)	−0.0043 (4)	0.0068 (5)	−0.0050 (5)
C26	0.0393 (8)	0.0293 (7)	0.0333 (8)	−0.0074 (6)	0.0060 (6)	−0.0037 (6)
O27	0.0484 (7)	0.0308 (6)	0.0583 (8)	−0.0116 (5)	0.0002 (6)	0.0028 (5)
O28	0.0436 (6)	0.0299 (5)	0.0378 (6)	−0.0050 (5)	−0.0049 (5)	−0.0004 (4)
C29	0.0547 (10)	0.0302 (8)	0.0422 (9)	−0.0047 (7)	−0.0071 (7)	−0.0008 (7)
C30	0.0571 (11)	0.0353 (9)	0.0386 (9)	−0.0036 (8)	−0.0055 (8)	0.0011 (7)
C31	0.0787 (14)	0.0582 (12)	0.0505 (11)	−0.0130 (11)	−0.0266 (10)	−0.0020 (9)
O32	0.0568 (7)	0.0285 (5)	0.0355 (6)	−0.0077 (5)	−0.0050 (5)	−0.0017 (4)
C33	0.0666 (12)	0.0393 (9)	0.0451 (10)	−0.0157 (8)	−0.0002 (8)	−0.0102 (7)
C34	0.0431 (9)	0.0496 (10)	0.0593 (11)	−0.0116 (8)	−0.0025 (8)	−0.0186 (9)
C35	0.0576 (12)	0.0837 (16)	0.0803 (15)	−0.0368 (12)	0.0161 (11)	−0.0319 (13)

Geometric parameters (Å, º)

N1—C2	1.399 (2)	C15—H151	0.967
N1—C21	1.3818 (18)	C16—C17	1.370 (3)
N1—C22	1.4844 (18)	C16—H161	0.953
C2—C3	1.406 (2)	C17—C18	1.409 (2)
C2—C7	1.399 (2)	C17—H171	0.941
C3—C4	1.373 (2)	C18—C19	1.420 (2)
C3—H31	0.938	C19—C20	1.389 (2)
C4—C5	1.389 (3)	C19—O32	1.3716 (18)
C4—H41	0.941	C20—C21	1.454 (2)
C5—C6	1.372 (2)	C22—C23	1.467 (2)
C5—H51	0.945	C22—H221	0.977
C6—C7	1.409 (2)	C22—H222	0.990
C6—H61	0.964	C23—C24	1.177 (2)
C7—C8	1.462 (2)	C24—H241	0.931
C8—C9	1.453 (2)	C26—O27	1.2065 (18)
C8—O25	1.2399 (18)	C26—O28	1.3428 (19)
C9—C10	1.4524 (19)	O28—C29	1.4436 (18)
C9—C21	1.392 (2)	C29—C30	1.456 (3)
C10—C11	1.342 (2)	C29—H291	0.977
C10—C26	1.488 (2)	C29—H292	0.967
C11—N12	1.3738 (19)	C30—C31	1.164 (3)
C11—H111	0.955	C31—H311	0.930
N12—C13	1.3886 (19)	O32—C33	1.430 (2)
N12—C20	1.4150 (18)	C33—C34	1.467 (3)

C13—C14	1.392 (2)	C33—H331	0.996
C13—C18	1.402 (2)	C33—H332	0.969
C14—C15	1.381 (2)	C34—C35	1.170 (3)
C14—H141	0.939	C35—H351	0.913
C15—C16	1.401 (3)		
O25···C24^i	3.268 (2)	C5···C20^v	3.470 (3)
O25···C35^{ii}	3.422 (3)	C6···C13^v	3.551 (3)
O25···C33^{iii}	3.581 (2)	C7···C13^v	3.497 (2)
O27···C16^{iii}	3.261 (2)	C7···C14^v	3.553 (2)
O27···C29^{iv}	3.330 (2)	C8···C14^v	3.497 (3)
O27···C34^{ii}	3.442 (2)	C9···C15^v	3.462 (3)
O27···C33^{ii}	3.529 (3)	C10···C35^{ii}	3.569 (3)
O28···C14^v	3.407 (2)	C13···C31^{ix}	3.439 (3)
O32···C24^{vi}	3.425 (2)	C15···C21^{vii}	3.578 (2)
N12···C6^{vii}	3.388 (2)	C18···C31^{ix}	3.415 (3)
N12···C5^{vii}	3.590 (2)	C24···C35^{viii}	3.597 (3)
C4···C35^{viii}	3.549 (3)		
C2—N1—C21	119.86 (12)	C15—C16—H161	119.3
C2—N1—C22	116.17 (12)	C17—C16—H161	118.7
C21—N1—C22	120.89 (12)	C16—C17—C18	117.92 (16)
N1—C2—C3	120.30 (14)	C16—C17—H171	121.6
N1—C2—C7	120.24 (13)	C18—C17—H171	120.5
C3—C2—C7	119.44 (14)	C17—C18—C13	119.18 (15)
C2—C3—C4	119.70 (16)	C17—C18—C19	133.50 (15)
C2—C3—H31	119.4	C13—C18—C19	107.31 (13)
C4—C3—H31	120.9	C18—C19—C20	108.82 (13)
C3—C4—C5	121.40 (15)	C18—C19—O32	124.39 (14)
C3—C4—H41	118.7	C20—C19—O32	126.71 (14)
C5—C4—H41	119.9	N12—C20—C19	106.67 (13)
C4—C5—C6	119.45 (16)	N12—C20—C21	115.92 (12)
C4—C5—H51	119.3	C19—C20—C21	137.41 (14)
C6—C5—H51	121.2	C20—C21—C9	119.07 (12)
C5—C6—C7	120.71 (16)	C20—C21—N1	120.14 (13)
C5—C6—H61	121.8	C9—C21—N1	120.79 (13)
C7—C6—H61	117.5	N1—C22—C23	112.78 (13)
C6—C7—C2	119.28 (14)	N1—C22—H221	108.2
C6—C7—C8	120.29 (14)	C23—C22—H221	107.7
C2—C7—C8	120.41 (13)	N1—C22—H222	110.1
C7—C8—C9	115.00 (13)	C23—C22—H222	110.1
C7—C8—O25	122.25 (13)	H221—C22—H222	107.8
C9—C8—O25	122.75 (13)	C22—C23—C24	174.50 (17)
C8—C9—C10	119.52 (13)	C23—C24—H241	178.5
C8—C9—C21	120.71 (13)	C10—C26—O27	124.43 (15)
C10—C9—C21	119.39 (13)	C10—C26—O28	111.83 (12)
C9—C10—C11	120.45 (13)	O27—C26—O28	123.42 (14)
C9—C10—C26	123.27 (13)	C26—O28—C29	115.01 (12)
C11—C10—C26	116.22 (13)	O28—C29—C30	108.40 (13)
C10—C11—N12	119.96 (13)	O28—C29—H291	109.4
C10—C11—H111	122.6	C30—C29—H291	110.3
N12—C11—H111	117.4	O28—C29—H292	109.3
C11—N12—C13	126.41 (12)	C30—C29—H292	110.3
C11—N12—C20	122.73 (12)	H291—C29—H292	109.1
C13—N12—C20	109.30 (12)	C29—C30—C31	177.8 (2)
N12—C13—C14	129.34 (14)	C30—C31—H311	178.9
N12—C13—C18	107.78 (13)	C19—O32—C33	116.04 (12)
C14—C13—C18	122.86 (14)	O32—C33—C34	106.55 (15)
C13—C14—C15	116.65 (16)	O32—C33—H331	110.3
C13—C14—H141	122.0	C34—C33—H331	110.1

C15—C14—H141	121.4	O32—C33—H332	110.3
C14—C15—C16	121.32 (17)	C34—C33—H332	109.6
C14—C15—H151	120.1	H331—C33—H332	109.9
C16—C15—H151	118.6	C33—C34—C35	177.4 (2)
C15—C16—C17	122.04 (16)	C34—C35—H351	179.3
O25—C8—C7—C2	−167.0 (2)	C6—C7—C8—C9	−168.7 (2)
O25—C8—C7—C6	11.3 (3)	C7—C2—N1—C21	−14.1 (2)
O25—C8—C9—C10	−9.0 (2)	C7—C2—N1—C22	146.3 (2)
O25—C8—C9—C21	163.9 (2)	C7—C8—C9—C10	171.1 (1)
O27—C26—O28—C29	−13.1 (2)	C7—C8—C9—C21	−16.1 (2)
O27—C26—C10—C9	135.1 (2)	C8—C9—C10—C11	164.6 (2)
O27—C26—C10—C11	−47.4 (2)	C8—C9—C10—C26	−18.1 (2)
O28—C26—C10—C9	−51.1 (2)	C8—C9—C21—C20	−175.8 (2)
O28—C26—C10—C11	126.3 (2)	C9—C21—N1—C22	−148.4 (2)
O32—C19—C18—C13	179.9 (2)	C9—C21—C20—C19	−166.5 (2)
O32—C19—C18—C17	0.9 (3)	C10—C9—C21—C20	−2.9 (2)
O32—C19—C20—N12	−179.5 (1)	C10—C11—N12—C13	170.7 (2)
O32—C19—C20—C21	1.8 (3)	C10—C11—N12—C20	6.5 (2)
N1—C2—C3—C4	176.7 (2)	C10—C26—O28—C29	173.1 (1)
N1—C2—C7—C6	−176.8 (2)	C11—N12—C13—C14	13.4 (3)
N1—C2—C7—C8	1.6 (2)	C11—N12—C13—C18	−165.1 (2)
N1—C21—C9—C8	4.6 (3)	C11—N12—C20—C19	163.8 (1)
N1—C21—C9—C10	177.4 (2)	C11—N12—C20—C21	−17.2 (2)
N1—C21—C20—N12	−165.5 (1)	C11—C10—C9—C21	−8.3 (3)
N1—C21—C20—C19	13.1 (3)	C13—N12—C20—C19	−2.8 (2)
N12—C11—C10—C9	6.7 (3)	C13—N12—C20—C21	176.3 (1)
N12—C11—C10—C26	−170.8 (1)	C13—C14—C15—C16	0.1 (3)
N12—C13—C14—C15	−179.7 (2)	C13—C18—C17—C16	−0.9 (3)
N12—C13—C18—C17	−179.5 (2)	C13—C18—C19—C20	−3.1 (2)
N12—C13—C18—C19	1.3 (2)	C14—C13—N12—C20	179.4 (2)
N12—C20—C19—C18	3.6 (2)	C14—C13—C18—C17	1.9 (3)
N12—C20—C21—C9	14.8 (2)	C14—C13—C18—C19	−177.3 (2)
C2—N1—C21—C9	11.0 (2)	C14—C15—C16—C17	0.8 (3)
C2—N1—C21—C20	−168.6 (2)	C15—C14—C13—C18	−1.4 (3)
C2—N1—C22—C23	−49.8 (2)	C15—C16—C17—C18	−0.4 (3)
C2—C3—C4—C5	0.4 (3)	C16—C17—C18—C19	178.0 (2)
C2—C7—C6—C5	−0.3 (3)	C17—C18—C19—C20	177.9 (2)
C2—C7—C8—C9	13.0 (2)	C18—C13—N12—C20	0.9 (2)
C3—C2—N1—C21	167.6 (2)	C18—C19—O32—C33	−79.8 (2)
C3—C2—N1—C22	−32.1 (2)	C18—C19—C20—C21	−175.1 (2)
C3—C2—C7—C6	1.6 (3)	C19—O32—C33—C34	−149.8 (1)
C3—C2—C7—C8	179.9 (2)	C20—C19—O32—C33	103.7 (2)
C3—C4—C5—C6	0.9 (3)	C20—C21—N1—C22	32.0 (2)
C4—C3—C2—C7	−1.6 (3)	C21—N1—C22—C23	110.3 (2)
C4—C5—C6—C7	−1.0 (3)	C21—C9—C10—C26	169.0 (2)
C5—C6—C7—C8	−178.6 (2)	C26—O28—C29—C30	177.3 (1)

Symmetry codes: (i) −x, −y+1, −z+1; (ii) x, y+1, z; (iii) x−1, y+1, z; (iv) −x, −y+2, −z; (v) x−1, y, z; (vi) −x+1, −y, −z+1; (vii) x+1, y, z; (viii) −x, −y, −z+1; (ix) −x, −y+1, −z.

Compound 269

Crystal data

C$_{24}$H$_{18}$N$_2$O$_2$
M_r = 366.42
Monoclinic, *C2/c*
a = 15.5385 (5) Å
b = 8.8840 (3) Å
c = 27.3267 (9) Å
β = 104.0916 (15)°
V = 3658.8 (2) Å^3
Z = 8

$F(000)$ = 1536
D_x = 1.330 Mg m^{-3}
Mo *K*α radiation, λ = 0.71073 Å
Cell parameters from 70395 reflections
θ = 2.6–25°
μ = 0.09 mm^{-1}
T = 200 K
Plate, Dark red
0.40 × 0.20 × 0.07 mm

Data collection

Nonius KappaCCD
diffractometer
Graphite monochromator
φ and ω scans with CCD
Absorption correction: Multi-scan
DENZO/SCALEPACK (Otwinowski & Minor, 1997)
T_{min} = 0.71, T_{max} = 0.99
27989 measured reflections
3238 independent reflections

2149 reflections with $I > 2.0\sigma(I)$
R_{int} = 0.081
θ_{max} = 25.0°, θ_{min} = 2.7°
$h = -18 \rightarrow 18$
$k = -10 \rightarrow 10$
$l = -32 \rightarrow 31$

Refinement

Refinement on F^2

Least-squares matrix: Full
$R[F^2 > 2\sigma(F^2)]$ = 0.051

$wR(F^2)$ = 0.139

S = 1.00
3238 reflections
253 parameters
0 restraints

Primary atom site location: Structure-invariant direct methods
Hydrogen site location: Inferred from neighbouring sites
H-atom parameters constrained
Method = Modified Sheldrick $w = 1/[\sigma^2(F^2) + (0.05P)^2 + 5.35P]$,
where $P = (\max(F_o^2, 0) + 2F_c^2)/3$
$(\Delta/\sigma)_{max}$ = 0.001
$\Delta\rho_{max}$ = 0.43 e Å^{-3}
$\Delta\rho_{min}$ = −0.42 e Å^{-3}

Special details

Refinement. Most of the hydrogen atoms were observed in difference electron-density maps prior to their inclusion. They were included at calculated positions and were initially refined with soft restraints on the bond lengths and angles to regularise their geometry (C—H in the range 0.93–0.98Å) and with U$_{iso}$(H) in the range 1.2-1.5 times U$_{eq}$ of the parent atom, after which the positions were refined with riding constraints and the displacement parameters were held fixed.

The largest features in the final difference electron density map are located midway between bonded atoms.

Fractional atomic coordinates and isotropic or equivalent isotropic displacement parameters (Å^2)

	x	*y*	*z*	$U_{iso}*/U_{eq}$
N1	0.44813 (13)	0.2278 (2)	0.55399 (7)	0.0473
C2	0.39983 (16)	0.1164 (3)	0.52330 (9)	0.0448
C3	0.33406 (18)	0.1316 (3)	0.47906 (10)	0.0548
C4	0.2952 (2)	0.0007 (4)	0.45694 (11)	0.0618
C5	0.3208 (2)	−0.1406 (4)	0.47694 (11)	0.0600
C6	0.38660 (18)	−0.1550 (3)	0.52049 (10)	0.0524
C7	0.42731 (17)	−0.0255 (3)	0.54376 (9)	0.0452
C8	0.49818 (16)	−0.0040 (3)	0.58946 (9)	0.0443
C9	0.50991 (16)	0.1621 (3)	0.59464 (9)	0.0432
C10	0.57160 (16)	0.2449 (3)	0.62615 (9)	0.0437
C11	0.58526 (17)	0.4100 (3)	0.61673 (9)	0.0462
C12	0.51752 (18)	0.4648 (3)	0.57111 (10)	0.0553
C13	0.45483 (18)	0.3791 (3)	0.54313 (10)	0.0523
N14	0.63195 (13)	0.1830 (2)	0.66777 (7)	0.0460
C15	0.72118 (16)	0.2217 (3)	0.67532 (9)	0.0437
C16	0.78659 (17)	0.1466 (3)	0.71089 (10)	0.0513

C17	0.87485 (18)	0.1776 (3)	0.71469 (11)	0.0567
C18	0.90139 (18)	0.2833 (3)	0.68406 (10)	0.0549
C19	0.83695 (17)	0.3605 (3)	0.65014 (10)	0.0500
C20	0.74678 (16)	0.3340 (3)	0.64526 (9)	0.0419
C21	0.68029 (17)	0.4266 (3)	0.61073 (10)	0.0462
O22	0.54144 (12)	−0.1010 (2)	0.61734 (7)	0.0530
C23	0.58102 (19)	0.5056 (3)	0.66346 (11)	0.0597
C24	0.60138 (18)	0.0914 (3)	0.70532 (9)	0.0515
C25	0.62300 (17)	0.1641 (3)	0.75508 (11)	0.0521
C26	0.64477 (19)	0.2214 (3)	0.79526 (11)	0.0573
C27	0.6737 (2)	0.2894 (4)	0.84528 (11)	0.0734
O28	0.69896 (13)	0.5167 (2)	0.58099 (7)	0.0606
H31	0.3153	0.2284	0.4654	0.0653*
H41	0.2499	0.0073	0.4264	0.0735*
H51	0.2903	−0.2265	0.4613	0.0714*
H61	0.4034	−0.2507	0.5347	0.0621*
H121	0.5214	0.5692	0.5628	0.0652*
H131	0.4106	0.4171	0.5152	0.0629*
H161	0.7714	0.0726	0.7321	0.0617*
H171	0.9190	0.1237	0.7390	0.0679*
H181	0.9628	0.3028	0.6867	0.0663*
H191	0.8530	0.4344	0.6287	0.0602*
H231	0.5937	0.6106	0.6570	0.0890*
H232	0.6256	0.4719	0.6937	0.0892*
H233	0.5216	0.5003	0.6700	0.0898*
H241	0.6277	−0.0127	0.7069	0.0617*
H242	0.5363	0.0821	0.6934	0.0615*
H271	0.6350	0.3693	0.8497	0.1108*
H272	0.6759	0.2160	0.8716	0.1105*
H273	0.7339	0.3307	0.8503	0.1105*

Atomic displacement parameters ($Å^2$)

	U^{11}	U^{22}	U^{33}	U^{12}	U^{13}	U^{23}
N1	0.0449 (13)	0.0474 (13)	0.0466 (12)	0.0002 (10)	0.0054 (10)	0.0042 (10)
C2	0.0430 (15)	0.0503 (16)	0.0433 (14)	−0.0014 (12)	0.0149 (12)	−0.0006 (13)
C3	0.0537 (17)	0.0622 (18)	0.0468 (15)	−0.0028 (14)	0.0089 (13)	0.0037 (14)
C4	0.0598 (19)	0.078 (2)	0.0445 (16)	−0.0037 (16)	0.0061 (14)	−0.0007 (16)
C5	0.066 (2)	0.0607 (19)	0.0529 (17)	−0.0112 (15)	0.0148 (15)	−0.0103 (15)
C6	0.0566 (17)	0.0468 (16)	0.0580 (17)	−0.0015 (13)	0.0222 (14)	−0.0024 (14)
C7	0.0420 (14)	0.0504 (16)	0.0467 (14)	−0.0012 (12)	0.0174 (12)	−0.0001 (13)
C8	0.0401 (14)	0.0482 (16)	0.0480 (15)	0.0015 (12)	0.0174 (12)	0.0064 (13)
C9	0.0412 (14)	0.0472 (15)	0.0416 (14)	0.0000 (12)	0.0106 (12)	0.0041 (12)
C10	0.0401 (14)	0.0493 (15)	0.0431 (14)	0.0012 (12)	0.0127 (12)	0.0056 (12)
C11	0.0460 (15)	0.0444 (15)	0.0480 (15)	0.0004 (12)	0.0114 (12)	0.0010 (12)
C12	0.0543 (17)	0.0453 (16)	0.0624 (18)	0.0023 (14)	0.0068 (14)	0.0091 (14)
C13	0.0533 (17)	0.0474 (16)	0.0532 (16)	0.0053 (13)	0.0073 (13)	0.0096 (13)
N14	0.0395 (12)	0.0541 (13)	0.0441 (12)	−0.0035 (10)	0.0097 (10)	0.0111 (10)
C15	0.0401 (14)	0.0497 (15)	0.0426 (14)	−0.0030 (12)	0.0126 (12)	0.0022 (12)
C16	0.0447 (16)	0.0585 (17)	0.0511 (15)	−0.0029 (13)	0.0126 (13)	0.0107 (14)
C17	0.0432 (16)	0.0640 (18)	0.0619 (17)	0.0036 (14)	0.0106 (13)	0.0102 (15)
C18	0.0394 (15)	0.0601 (18)	0.0671 (18)	−0.0028 (13)	0.0167 (14)	0.0062 (15)
C19	0.0486 (16)	0.0492 (16)	0.0562 (16)	−0.0026 (13)	0.0208 (13)	0.0048 (13)
C20	0.0451 (15)	0.0384 (13)	0.0437 (14)	−0.0009 (11)	0.0134 (12)	0.0017 (11)
C21	0.0516 (16)	0.0395 (14)	0.0486 (15)	−0.0050 (12)	0.0141 (13)	−0.0024 (13)
O22	0.0517 (11)	0.0477 (11)	0.0608 (11)	0.0026 (9)	0.0156 (9)	0.0107 (9)
C23	0.0584 (18)	0.0596 (18)	0.0625 (18)	0.0045 (14)	0.0176 (14)	−0.0091 (15)
C24	0.0467 (16)	0.0593 (17)	0.0484 (15)	−0.0074 (13)	0.0111 (12)	0.0115 (13)
C25	0.0455 (16)	0.0613 (18)	0.0498 (17)	−0.0044 (13)	0.0122 (13)	0.0134 (15)
C26	0.0543 (18)	0.0644 (19)	0.0540 (18)	−0.0022 (14)	0.0148 (14)	0.0104 (16)
C27	0.088 (2)	0.072 (2)	0.0578 (19)	0.0025 (18)	0.0132 (17)	−0.0003 (16)
O28	0.0634 (13)	0.0528 (11)	0.0676 (12)	−0.0037 (10)	0.0200 (10)	0.0171 (10)

Geometric parameters (Å, º)

N1—C2	1.392 (3)	N14—C15	1.394 (3)
N1—C9	1.406 (3)	N14—C24	1.476 (3)
N1—C13	1.386 (3)	C15—C16	1.393 (3)
C2—C3	1.387 (4)	C15—C20	1.410 (3)
C2—C7	1.403 (4)	C16—C17	1.378 (4)
C3—C4	1.380 (4)	C16—H161	0.944
C3—H31	0.955	C17—C18	1.386 (4)
C4—C5	1.388 (4)	C17—H171	0.958
C4—H41	0.953	C18—C19	1.371 (4)
C5—C6	1.373 (4)	C18—H181	0.956
C5—H51	0.945	C19—C20	1.395 (3)
C6—C7	1.390 (4)	C19—H191	0.952
C6—H61	0.945	C20—C21	1.469 (4)
C7—C8	1.463 (4)	C21—O28	1.225 (3)
C8—C9	1.490 (4)	C23—H231	0.979
C8—O22	1.236 (3)	C23—H232	0.986
C9—C10	1.341 (3)	C23—H233	0.982
C10—C11	1.514 (4)	C24—C25	1.469 (4)
C10—N14	1.399 (3)	C24—H241	1.007
C11—C12	1.503 (4)	C24—H242	0.988
C11—C21	1.532 (4)	C25—C26	1.182 (4)
C11—C23	1.548 (4)	C26—C27	1.462 (4)
C12—C13	1.323 (4)	C27—H271	0.956
C12—H121	0.961	C27—H272	0.966
C13—H131	0.955	C27—H273	0.983
O22⋯C18[i]	3.324 (4)	C5⋯C21[v]	3.489 (4)
O22⋯C19[i]	3.522 (4)	C8⋯C19[i]	3.535 (4)
O28⋯C27[ii]	3.450 (4)	C12⋯C13[iii]	3.536 (4)
O28⋯C3[iii]	3.508 (3)	C17⋯C23[vi]	3.575 (4)
C5⋯C5[iv]	3.400 (7)	C19⋯C26[ii]	3.519 (4)
C2—N1—C9	110.2 (2)	C10—N14—C24	121.1 (2)
C2—N1—C13	128.2 (2)	C15—N14—C24	120.65 (19)
C9—N1—C13	119.9 (2)	N14—C15—C16	121.0 (2)
N1—C2—C3	129.1 (2)	N14—C15—C20	120.0 (2)
N1—C2—C7	109.4 (2)	C16—C15—C20	118.9 (2)
C3—C2—C7	121.5 (2)	C15—C16—C17	120.1 (2)
C2—C3—C4	116.8 (3)	C15—C16—H161	120.9
C2—C3—H31	121.3	C17—C16—H161	119.1
C4—C3—H31	121.9	C16—C17—C18	121.8 (3)
C3—C4—C5	122.4 (3)	C16—C17—H171	119.0
C3—C4—H41	118.9	C18—C17—H171	119.2
C5—C4—H41	118.7	C17—C18—C19	118.1 (3)
C4—C5—C6	120.5 (3)	C17—C18—H181	121.1
C4—C5—H51	119.2	C19—C18—H181	120.8
C6—C5—H51	120.2	C18—C19—C20	122.1 (2)
C5—C6—C7	118.6 (3)	C18—C19—H191	120.2
C5—C6—H61	120.9	C20—C19—H191	117.7
C7—C6—H61	120.5	C15—C20—C19	118.9 (2)
C2—C7—C6	120.1 (2)	C15—C20—C21	121.1 (2)
C2—C7—C8	108.4 (2)	C19—C20—C21	120.0 (2)
C6—C7—C8	131.5 (2)	C11—C21—C20	115.0 (2)
C7—C8—C9	105.1 (2)	C11—C21—O28	121.6 (2)
C7—C8—O22	128.2 (2)	C20—C21—O28	123.3 (2)
C9—C8—O22	126.7 (2)	C11—C23—H231	108.9
C8—C9—N1	107.0 (2)	C11—C23—H232	111.2
C8—C9—C10	131.0 (2)	H231—C23—H232	108.0
N1—C9—C10	121.6 (2)	C11—C23—H233	110.7
C9—C10—C11	122.0 (2)	H231—C23—H233	108.5
C9—C10—N14	122.7 (2)	H232—C23—H233	109.5
C11—C10—N14	115.2 (2)	N14—C24—C25	111.2 (2)

C10—C11—C12	110.8 (2)	N14—C24—H241	109.9
C10—C11—C21	106.8 (2)	C25—C24—H241	111.4
C12—C11—C21	112.3 (2)	N14—C24—H242	107.1
C10—C11—C23	110.8 (2)	C25—C24—H242	109.0
C12—C11—C23	110.2 (2)	H241—C24—H242	108.1
C21—C11—C23	105.8 (2)	C24—C25—C26	176.7 (3)
C11—C12—C13	124.2 (3)	C25—C26—C27	178.5 (3)
C11—C12—H121	115.9	C26—C27—H271	111.4
C13—C12—H121	119.9	C26—C27—H272	111.4
N1—C13—C12	121.2 (2)	H271—C27—H272	108.5
N1—C13—H131	115.9	C26—C27—H273	110.5
C12—C13—H131	122.9	H271—C27—H273	108.1
C10—N14—C15	118.0 (2)	H272—C27—H273	106.7
O22—C8—C7—C2	−177.6 (3)	C6—C7—C8—C9	−178.6 (3)
O22—C8—C7—C6	3.3 (5)	C7—C2—N1—C9	1.4 (3)
O22—C8—C9—N1	178.5 (3)	C7—C2—N1—C13	166.3 (3)
O22—C8—C9—C10	6.5 (5)	C7—C8—C9—C10	−171.7 (3)
O28—C21—C11—C10	144.1 (2)	C8—C9—N1—C13	−167.4 (2)
O28—C21—C11—C12	22.3 (4)	C8—C9—C10—C11	164.1 (3)
O28—C21—C11—C23	−97.8 (3)	C9—N1—C13—C12	−1.5 (4)
O28—C21—C20—C15	−173.8 (3)	C9—C10—N14—C15	132.9 (3)
O28—C21—C20—C19	8.7 (4)	C9—C10—N14—C24	−52.9 (4)
N1—C2—C3—C4	−178.2 (3)	C9—C10—C11—C12	4.1 (4)
N1—C2—C7—C6	178.1 (3)	C9—C10—C11—C21	−118.5 (3)
N1—C2—C7—C8	−1.1 (3)	C9—C10—C11—C23	126.8 (3)
N1—C9—C8—C7	0.4 (3)	C10—N14—C15—C16	−169.6 (2)
N1—C9—C10—N14	177.9 (2)	C10—N14—C15—C20	7.6 (3)
N1—C9—C10—C11	−6.9 (4)	C10—N14—C24—C25	−116.0 (2)
N1—C13—C12—C11	−1.0 (5)	C10—C9—N1—C13	5.6 (4)
N14—C10—C9—C8	−11.0 (5)	C10—C11—C12—C13	−0.2 (4)
N14—C10—C11—C12	179.6 (2)	C10—C11—C21—C20	−39.5 (3)
N14—C10—C11—C21	57.0 (3)	C11—C10—N14—C15	−42.5 (3)
N14—C10—C11—C23	−57.7 (3)	C11—C10—N14—C24	131.7 (2)
N14—C15—C16—C17	174.4 (2)	C11—C21—C20—C15	9.8 (4)
N14—C15—C20—C19	−173.8 (2)	C11—C21—C20—C19	−167.6 (2)
N14—C15—C20—C21	8.7 (4)	C12—C11—C21—C20	−161.3 (2)
C2—N1—C9—C8	−1.1 (3)	C13—C12—C11—C21	119.2 (3)
C2—N1—C9—C10	171.9 (3)	C13—C12—C11—C23	−123.2 (3)
C2—N1—C13—C12	−165.1 (3)	C15—N14—C24—C25	58.0 (3)
C2—C3—C4—C5	−1.1 (5)	C15—C16—C17—C18	0.4 (4)
C2—C7—C6—C5	1.3 (4)	C15—C20—C19—C18	−1.6 (4)
C2—C7—C8—C9	0.5 (3)	C16—C15—N14—C24	16.1 (4)
C3—C2—N1—C9	−178.6 (3)	C16—C15—C20—C19	3.5 (4)
C3—C2—N1—C13	−13.7 (5)	C16—C15—C20—C21	−174.0 (2)
C3—C2—C7—C6	−2.0 (4)	C16—C17—C18—C19	1.6 (4)
C3—C2—C7—C8	178.8 (3)	C17—C16—C15—C20	−3.0 (4)
C3—C4—C5—C6	0.4 (5)	C17—C18—C19—C20	−1.0 (4)
C4—C3—C2—C7	1.8 (4)	C18—C19—C20—C21	176.0 (3)
C4—C5—C6—C7	−0.5 (5)	C20—C15—N14—C24	−166.6 (2)
C5—C6—C7—C8	−179.8 (3)	C20—C21—C11—C23	78.6 (3)

Symmetry codes: (i) $x-1/2$, $y-1/2$, z; (ii) $-x+3/2$, $y+1/2$, $-z+3/2$; (iii) $-x+1$, $-y+1$, $-z+1$; (iv) $-x+1/2$, $-y-1/2$, $-z+1$; (v) $-x+1$, $-y$, $-z+1$; (vi) $-x+3/2$, $y-1/2$, $-z+3/2$.

Compound 274

Crystal data

$C_{23}H_{18}N_2O_2$	$D_x = 1.320$ Mg m^{-3}
$M_r = 354.41$	Mo $K\alpha$ radiation, $\lambda = 0.71073$ Å
Orthorhombic, $Pna2_1$	Cell parameters from 148086 reflections
$a = 12.3861$ (4) Å	$\theta = 3$–25°
$b = 10.4051$ (3) Å	$\mu = 0.09$ mm^{-1}
$c = 27.6772$ (8) Å	$T = 200$ K
$V = 3567.00$ (19) Å^3	Block, Yellow
$Z = 8$	$0.13 \times 0.09 \times 0.09$ mm
$F(000) = 1488$	

Data collection

Nonius KappaCCD diffractometer	2316 reflections with $I > 2.0\sigma(I)$
graphite	$R_{int} = 0.060$
φ and ω scans with CCD	$\theta_{max} = 25.0°$, $\theta_{min} = 2.6°$
Absorption correction: Multi-scan *DENZO/SCALEPACK* (Otwinowski & Minor, 1997)	$h = -11 \rightarrow 14$
$T_{min} = 0.82$, $T_{max} = 0.99$	$k = -12 \rightarrow 8$
36972 measured reflections	$l = -32 \rightarrow 32$
3221 independent reflections	

Refinement

Refinement on F^2	Primary atom site location: Structure-invariant direct methods
Least-squares matrix: Full	Hydrogen site location: Inferred from neighbouring sites
$R[F^2 > 2\sigma(F^2)] = 0.056$	H-atom parameters constrained
$wR(F^2) = 0.140$	Method = Modified Sheldrick $w = 1/[\sigma^2(F^2) + (0.07P)^2 + 1.65P]$, where $P = (\max(F_o^2,0) + 2F_c^2)/3$
$S = 1.02$	$(\Delta/\sigma)_{max} = 0.031$
3221 reflections	$\Delta\rho_{max} = 0.42$ e Å^{-3}
500 parameters	$\Delta\rho_{min} = -0.47$ e Å^{-3}
8 restraints	

Special details

Refinement. Crystals of this compound were poorly formed and gave diffuse diffraction patterns. Eventually a very small fragment was found which gave sharp spots, but they were rather weak. Very long exposure times were used to collect the intensity data. There were no detectable data beyond 2θ 50°.

The space group is noncentrosymmetric but the anomolous dispersion terms are very small for all elements in the structure, so the absolute structure of the crystal can not be determined in this experiment. Consequently Friedel-pair reflections have been averaged and the Flack parameter has not been refined. The space group is not enantiomorphic so the compound is present as a racemate within the crystal structure.

There is conformational disorder of the vinyl group in one of the molecules. The major sites for these carbon atoms are C126 and C127 and the minor sites are C226 and C227. The relative occupancies were refined. The displacement parameters for C126 and C226 were

constrained to be identical as these sites are close together. Restraints were placed on distances and angles for disordered sites so they would tend to match the values found in the other, non-disordered, molecule.

Hydrogen atoms within the disordered section of the molecule were included at calculated positions and ride on the atom to which they are attached. The other hydrogen atoms were included at calculated positions and were initially refined with soft restraints on the bond lengths and angles to regularise their geometry (C—H in the range 0.93–0.98Å) and with U_{iso}(H) in the range 1.2-1.5 times U_{eq} of the parent atom, after which the positions were refined with riding constraints and the displacement parameters were held fixed.

The largest features in the final difference electron density map are located randomly through the structure.

Fractional atomic coordinates and isotropic or equivalent isotropic displacement parameters (Å²)

	x	y	z	$U_{iso}*/U_{eq}$	Occ. (<1)
O22	0.3012 (3)	0.3091 (4)	0.54908 (14)	0.0645	
O23	0.2136 (3)	0.1506 (4)	0.67798 (13)	0.0597	
O122	0.4549 (3)	0.7892 (4)	0.46061 (13)	0.0575	
O123	0.5483 (3)	0.6515 (4)	0.32831 (14)	0.0605	
N1	0.3654 (3)	0.0000 (4)	0.58576 (16)	0.0480	
N14	0.4319 (4)	0.2763 (4)	0.66225 (15)	0.0498	
N101	0.3920 (3)	0.4889 (4)	0.41598 (16)	0.0493	
N114	0.3301 (3)	0.7778 (5)	0.34527 (15)	0.0533	
C2	0.2623 (4)	−0.0501 (5)	0.57850 (19)	0.0481	
C3	0.2281 (5)	−0.1335 (6)	0.5431 (2)	0.0646	
C4	0.1219 (5)	−0.1695 (7)	0.5430 (2)	0.0760	
C5	0.0488 (5)	−0.1248 (6)	0.5780 (2)	0.0719	
C6	0.0833 (5)	−0.0425 (6)	0.6135 (2)	0.0602	
C7	0.1918 (4)	−0.0038 (5)	0.61325 (19)	0.0452	
C8	0.2480 (4)	0.0871 (5)	0.64364 (19)	0.0485	
C9	0.3659 (4)	0.0893 (5)	0.62626 (17)	0.0450	
C10	0.4126 (4)	0.2244 (5)	0.61363 (18)	0.0436	
C11	0.5186 (4)	0.2102 (6)	0.58505 (19)	0.0541	
C12	0.5181 (5)	0.1008 (6)	0.5503 (2)	0.0584	
C13	0.4470 (4)	0.0064 (6)	0.5506 (2)	0.0554	
C15	0.3640 (4)	0.3780 (6)	0.6694 (2)	0.0552	
C16	0.3470 (5)	0.4473 (6)	0.7127 (2)	0.0679	
C17	0.2820 (6)	0.5529 (8)	0.7102 (3)	0.0844	
C18	0.2320 (6)	0.5921 (7)	0.6674 (4)	0.0933	
C19	0.2447 (5)	0.5232 (6)	0.6259 (3)	0.0729	
C20	0.3104 (4)	0.4141 (6)	0.6273 (2)	0.0514	
C21	0.3336 (4)	0.3177 (5)	0.5906 (2)	0.0474	
C24	0.4544 (5)	0.1749 (5)	0.6972 (2)	0.0617	
C25	0.4429 (4)	0.0498 (5)	0.6682 (2)	0.0548	
C26	0.4054 (5)	−0.0647 (6)	0.6961 (2)	0.0661	
C27	0.4422 (6)	−0.1806 (7)	0.6882 (3)	0.0868	
C102	0.4958 (4)	0.4412 (5)	0.4236 (2)	0.0501	
C103	0.5294 (5)	0.3552 (5)	0.4595 (2)	0.0644	
C104	0.6383 (5)	0.3215 (6)	0.4601 (3)	0.0746	
C105	0.7095 (5)	0.3676 (7)	0.4259 (3)	0.0816	
C106	0.6762 (5)	0.4523 (6)	0.3906 (2)	0.0655	
C107	0.5687 (4)	0.4898 (5)	0.39076 (19)	0.0509	
C108	0.5132 (4)	0.5854 (5)	0.36081 (18)	0.0486	
C109	0.3934 (4)	0.5842 (5)	0.37701 (18)	0.0458	
C110	0.3471 (4)	0.7158 (6)	0.39210 (18)	0.0489	
C111	0.2398 (4)	0.6998 (6)	0.4200 (2)	0.0528	
C112	0.2431 (5)	0.5928 (6)	0.4547 (2)	0.0597	
C113	0.3138 (4)	0.4974 (6)	0.4523 (2)	0.0556	
C115	0.3965 (4)	0.8845 (6)	0.34177 (19)	0.0537	
C116	0.4119 (6)	0.9676 (7)	0.3032 (2)	0.0711	
C117	0.4752 (6)	1.0765 (7)	0.3116 (3)	0.0842	
C118	0.5214 (6)	1.1050 (7)	0.3556 (3)	0.0793	
C119	0.5095 (5)	1.0201 (6)	0.3931 (2)	0.0654	
C120	0.4480 (4)	0.9104 (5)	0.38587 (19)	0.0485	
C121	0.4246 (4)	0.8047 (5)	0.4190 (2)	0.0476	
C124	0.3135 (5)	0.6831 (6)	0.3068 (2)	0.0644	
C125	0.3210 (5)	0.5522 (6)	0.33270 (19)	0.0587	
C126	0.3556 (19)	0.4303 (12)	0.3068 (5)	0.0652	0.651 (16)
C127	0.3767 (8)	0.4257 (10)	0.2593 (3)	0.0714	0.651 (16)
C226	0.355 (4)	0.456 (2)	0.2963 (13)	0.0652	0.349 (16)
C227	0.3067 (19)	0.345 (2)	0.2933 (11)	0.1181	0.349 (16)

H31	0.2755	−0.1650	0.5196	0.0770*
H41	0.0963	−0.2248	0.5187	0.0909*
H51	−0.0228	−0.1499	0.5765	0.0860*
H61	0.0361	−0.0125	0.6372	0.0714*
H111	0.5776	0.2006	0.6079	0.0648*
H112	0.5286	0.2903	0.5674	0.0650*
H121	0.5728	0.0994	0.5262	0.0699*
H131	0.4497	−0.0579	0.5274	0.0658*
H161	0.3788	0.4218	0.7413	0.0806*
H171	0.2703	0.6015	0.7383	0.1007*
H181	0.1909	0.6673	0.6672	0.1118*
H191	0.2109	0.5486	0.5974	0.0871*
H241	0.5266	0.1824	0.7109	0.0740*
H242	0.4013	0.1754	0.7236	0.0737*
H251	0.5133	0.0267	0.6537	0.0657*
H261	0.3519	−0.0518	0.7199	0.0793*
H271	0.4144	−0.2511	0.7060	0.1040*
H272	0.4970	−0.1945	0.6651	0.1041*
H1031	0.4810	0.3222	0.4821	0.0770*
H1041	0.6646	0.2659	0.4838	0.0890*
H1051	0.7816	0.3425	0.4271	0.0976*
H1061	0.7231	0.4835	0.3672	0.0789*
H1111	0.2240	0.7803	0.4363	0.0627*
H1112	0.1845	0.6832	0.3962	0.0625*
H1121	0.1918	0.5937	0.4802	0.0716*
H1131	0.3123	0.4313	0.4754	0.0671*
H1161	0.3813	0.9502	0.2734	0.0846*
H1171	0.4874	1.1334	0.2861	0.1010*
H1181	0.5604	1.1813	0.3599	0.0951*
H1191	0.5414	1.0362	0.4231	0.0778*
H1241	0.3705	0.6894	0.2830	0.0768*
H1242	0.2443	0.6944	0.2914	0.0767*
H1251	0.2510	0.5353	0.3452	0.0703*	0.651
H1252	0.2512	0.5296	0.3440	0.0703*	0.349
H1261	0.3633	0.3538	0.3251	0.0773*	0.651
H1271	0.3696	0.5009	0.2401	0.0860*	0.651
H1272	0.3984	0.3471	0.2447	0.0860*	0.651
H2261	0.4126	0.4762	0.2747	0.0773*	0.349
H2271	0.2496	0.3252	0.3149	0.1402*	0.349
H2272	0.3288	0.2844	0.2697	0.1402*	0.349

Atomic displacement parameters (Å²)

	U^{11}	U^{22}	U^{33}	U^{12}	U^{13}	U^{23}
O22	0.062 (2)	0.080 (3)	0.051 (2)	−0.006 (2)	−0.015 (2)	0.014 (2)
O23	0.060 (2)	0.068 (2)	0.051 (2)	−0.006 (2)	0.0123 (19)	−0.008 (2)
O122	0.062 (2)	0.074 (2)	0.037 (2)	0.003 (2)	−0.0097 (18)	0.0017 (19)
O123	0.059 (2)	0.070 (3)	0.053 (2)	0.002 (2)	0.0121 (19)	0.008 (2)
N1	0.042 (2)	0.060 (3)	0.042 (2)	−0.004 (2)	0.004 (2)	−0.007 (2)
N14	0.057 (3)	0.056 (3)	0.036 (2)	0.001 (2)	−0.008 (2)	−0.002 (2)
N101	0.043 (2)	0.058 (3)	0.047 (2)	−0.001 (2)	0.003 (2)	0.000 (2)
N114	0.056 (3)	0.069 (3)	0.034 (2)	0.014 (3)	−0.005 (2)	0.000 (2)
C2	0.044 (3)	0.052 (3)	0.048 (3)	−0.002 (3)	0.000 (3)	−0.003 (3)
C3	0.055 (4)	0.081 (4)	0.058 (4)	−0.004 (3)	0.001 (3)	−0.013 (3)
C4	0.063 (4)	0.086 (5)	0.080 (4)	−0.006 (4)	−0.009 (4)	−0.025 (4)
C5	0.043 (3)	0.078 (4)	0.094 (5)	−0.009 (3)	0.000 (3)	−0.017 (4)
C6	0.053 (3)	0.062 (4)	0.066 (4)	0.003 (3)	0.008 (3)	−0.010 (3)
C7	0.043 (3)	0.045 (3)	0.048 (3)	−0.010 (2)	−0.004 (3)	0.000 (2)

C8	0.046 (3)	0.054 (3)	0.046 (3)	0.005 (3)	0.000 (3)	0.008 (3)
C9	0.045 (3)	0.053 (3)	0.037 (3)	0.002 (2)	−0.001 (2)	−0.005 (2)
C10	0.041 (3)	0.054 (3)	0.035 (3)	−0.008 (3)	0.000 (2)	−0.005 (2)
C11	0.050 (3)	0.064 (3)	0.049 (3)	−0.006 (3)	0.004 (3)	0.002 (3)
C12	0.054 (3)	0.067 (4)	0.054 (3)	−0.007 (3)	0.013 (3)	−0.002 (3)
C13	0.051 (3)	0.066 (4)	0.048 (3)	0.001 (3)	0.009 (3)	−0.006 (3)
C15	0.053 (3)	0.059 (4)	0.053 (3)	−0.014 (3)	0.015 (3)	−0.009 (3)
C16	0.072 (4)	0.066 (4)	0.066 (4)	−0.021 (4)	0.021 (3)	−0.012 (3)
C17	0.070 (4)	0.077 (5)	0.106 (6)	−0.019 (4)	0.031 (4)	−0.034 (4)
C18	0.062 (4)	0.063 (4)	0.155 (8)	0.004 (3)	0.008 (5)	−0.030 (5)
C19	0.053 (4)	0.056 (4)	0.110 (5)	−0.001 (3)	−0.006 (4)	−0.011 (4)
C20	0.042 (3)	0.052 (4)	0.060 (3)	−0.007 (3)	0.001 (3)	−0.001 (3)
C21	0.040 (3)	0.053 (4)	0.049 (3)	−0.010 (2)	−0.004 (3)	0.007 (3)
C24	0.070 (4)	0.071 (4)	0.044 (3)	−0.009 (3)	−0.014 (3)	0.005 (3)
C25	0.047 (3)	0.066 (4)	0.051 (3)	−0.001 (3)	−0.006 (3)	0.007 (3)
C26	0.067 (4)	0.073 (4)	0.058 (4)	−0.008 (3)	−0.007 (3)	0.008 (3)
C27	0.102 (5)	0.066 (4)	0.093 (5)	−0.020 (4)	−0.014 (4)	0.011 (4)
C102	0.048 (3)	0.055 (3)	0.048 (3)	−0.002 (3)	−0.005 (3)	−0.002 (3)
C103	0.067 (4)	0.060 (4)	0.066 (4)	−0.002 (3)	−0.002 (3)	0.016 (3)
C104	0.054 (4)	0.074 (4)	0.096 (5)	0.010 (3)	−0.014 (4)	0.027 (4)
C105	0.046 (3)	0.077 (5)	0.121 (6)	0.006 (3)	−0.007 (4)	0.025 (5)
C106	0.048 (3)	0.064 (4)	0.085 (5)	−0.002 (3)	0.005 (3)	0.011 (3)
C107	0.047 (3)	0.057 (3)	0.048 (3)	−0.008 (3)	−0.001 (3)	0.002 (3)
C108	0.054 (3)	0.051 (3)	0.041 (3)	−0.001 (3)	0.005 (3)	−0.004 (3)
C109	0.046 (3)	0.055 (4)	0.037 (3)	0.001 (3)	0.000 (2)	0.000 (3)
C110	0.046 (3)	0.068 (4)	0.033 (3)	0.002 (3)	−0.001 (2)	−0.003 (3)
C111	0.045 (3)	0.063 (4)	0.051 (3)	0.004 (3)	−0.006 (3)	−0.003 (3)
C112	0.055 (3)	0.066 (4)	0.057 (3)	−0.008 (3)	0.011 (3)	−0.001 (3)
C113	0.050 (3)	0.065 (4)	0.052 (3)	−0.006 (3)	0.004 (3)	0.005 (3)
C115	0.052 (3)	0.061 (4)	0.048 (3)	0.017 (3)	0.004 (3)	0.006 (3)
C116	0.088 (5)	0.080 (5)	0.045 (3)	0.028 (4)	0.008 (3)	0.012 (3)
C117	0.111 (6)	0.062 (4)	0.080 (5)	0.014 (4)	0.031 (5)	0.022 (4)
C118	0.085 (5)	0.062 (4)	0.091 (5)	0.001 (4)	0.021 (4)	0.005 (4)
C119	0.062 (4)	0.060 (4)	0.074 (4)	0.004 (3)	0.006 (3)	0.009 (3)
C120	0.047 (3)	0.046 (3)	0.053 (3)	0.007 (3)	0.003 (3)	0.005 (3)
C121	0.040 (3)	0.057 (3)	0.045 (3)	0.009 (2)	0.003 (2)	0.000 (3)
C124	0.066 (4)	0.080 (4)	0.047 (3)	0.008 (3)	−0.013 (3)	−0.002 (3)
C125	0.056 (3)	0.076 (4)	0.044 (3)	0.002 (3)	−0.005 (3)	−0.009 (3)
C126	0.065 (4)	0.074 (7)	0.057 (9)	0.010 (6)	−0.006 (6)	−0.006 (7)
C127	0.087 (7)	0.077 (7)	0.049 (6)	0.023 (6)	−0.013 (5)	−0.017 (5)
C226	0.065 (4)	0.074 (7)	0.057 (9)	0.010 (6)	−0.006 (6)	−0.006 (7)
C227	0.087 (16)	0.100 (15)	0.17 (3)	−0.015 (12)	−0.025 (17)	−0.040 (19)

Geometric parameters (Å, °)

O22—C21	1.222 (6)	C26—C27	1.307 (9)
O23—C8	1.233 (6)	C26—H261	0.945
O122—C121	1.221 (6)	C27—H271	0.949
O123—C108	1.213 (6)	C27—H272	0.945
N1—C2	1.393 (6)	C102—C103	1.402 (7)
N1—C9	1.455 (6)	C102—C107	1.378 (7)
N1—C13	1.406 (6)	C103—C104	1.393 (9)
N14—C10	1.470 (6)	C103—H1031	0.932
N14—C15	1.366 (7)	C104—C105	1.379 (9)
N14—C24	1.458 (7)	C104—H1041	0.933
N101—C102	1.394 (7)	C105—C106	1.380 (9)
N101—C109	1.465 (7)	C105—H1051	0.931
N101—C113	1.398 (7)	C106—C107	1.387 (8)

N114—C110	1.463 (7)	C106—H1061	0.929
N114—C115	1.384 (7)	C107—C108	1.466 (8)
N114—C124	1.466 (7)	C108—C109	1.550 (7)
C2—C3	1.376 (8)	C109—C110	1.542 (8)
C2—C7	1.386 (7)	C109—C125	1.555 (7)
C3—C4	1.367 (8)	C110—C111	1.546 (7)
C3—H31	0.936	C110—C121	1.527 (8)
C4—C5	1.406 (9)	C111—C112	1.472 (8)
C4—H41	0.939	C111—H1111	0.972
C5—C6	1.372 (8)	C111—H1112	0.965
C5—H51	0.925	C112—C113	1.325 (8)
C6—C7	1.402 (8)	C112—H1121	0.950
C6—H61	0.932	C113—H1131	0.941
C7—C8	1.445 (7)	C115—C116	1.386 (8)
C8—C9	1.537 (7)	C115—C120	1.403 (8)
C9—C10	1.560 (7)	C116—C117	1.397 (10)
C9—C25	1.558 (7)	C116—H1161	0.926
C10—C11	1.540 (7)	C117—C118	1.379 (10)
C10—C21	1.518 (8)	C117—H1171	0.934
C11—C12	1.489 (8)	C118—C119	1.370 (9)
C11—H111	0.971	C118—H1181	0.936
C11—H112	0.973	C119—C120	1.387 (9)
C12—C13	1.319 (8)	C119—H1191	0.936
C12—H121	0.952	C120—C121	1.461 (8)
C13—H131	0.928	C124—C125	1.542 (8)
C15—C16	1.414 (8)	C124—H1241	0.967
C15—C20	1.392 (8)	C124—H1242	0.964
C16—C17	1.364 (10)	C125—C126	1.519 (12)
C16—H161	0.924	C125—C226	1.480 (17)
C17—C18	1.397 (11)	C125—H1251	0.950
C17—H171	0.939	C125—H1252	0.950
C18—C19	1.363 (10)	C126—C127	1.341 (13)
C18—H181	0.933	C126—H1261	0.950
C19—C20	1.398 (9)	C127—H1271	0.950
C19—H191	0.932	C127—H1272	0.950
C20—C21	1.455 (8)	C127—H2261	0.811
C24—C25	1.535 (8)	C226—C227	1.306 (18)
C24—H241	0.975	C226—H2261	0.950
C24—H242	0.982	C227—H2271	0.950
C25—C26	1.493 (8)	C227—H2272	0.950
C25—H251	0.989		
O22···C113	3.322 (7)	C6···C15^{i}	3.564 (8)
O22···C104^{i}	3.462 (8)	C17···C27^{iv}	3.46 (1)
O23···C127^{ii}	3.43 (1)	C18···C27^{iv}	3.56 (1)
O23···C124^{ii}	3.597 (7)	C26···C117^{vi}	3.52 (1)
O23···N14^{i}	3.598 (6)	C106···C115^{v}	3.487 (8)
O122···C4^{iii}	3.321 (7)	C112···C119^{vii}	3.558 (9)
O122···C13^{iv}	3.365 (7)	C117···C227^{iv}	3.52 (2)
O123···N114^{v}	3.598 (5)		
C2—N1—C9	110.7 (4)	H271—C27—H272	119.7
C2—N1—C13	125.2 (4)	N101—C102—C103	127.5 (5)
C9—N1—C13	120.0 (4)	N101—C102—C107	112.0 (5)
C10—N14—C15	108.5 (4)	C103—C102—C107	120.5 (5)
C10—N14—C24	111.9 (4)	C102—C103—C104	117.1 (6)
C15—N14—C24	125.5 (5)	C102—C103—H1031	121.4
C102—N101—C109	110.0 (4)	C104—C103—H1031	121.5
C102—N101—C113	123.6 (5)	C103—C104—C105	121.6 (6)
C109—N101—C113	119.6 (4)	C103—C104—H1041	120.1

C5—C4—H41	118.6	C107—C108—C109	106.3 (4)
C4—C5—C6	120.0 (5)	O123—C108—C109	124.2 (5)
C4—C5—H51	119.5	C108—C109—N101	103.3 (4)
C6—C5—H51	120.5	C108—C109—C110	115.3 (4)
C5—C6—C7	118.3 (5)	N101—C109—C110	113.4 (4)
C5—C6—H61	121.2	C108—C109—C125	109.0 (4)
C7—C6—H61	120.5	N101—C109—C125	115.4 (4)
C6—C7—C2	120.5 (5)	C110—C109—C125	100.9 (4)
C6—C7—C8	130.3 (5)	C109—C110—N114	101.8 (4)
C2—C7—C8	109.1 (5)	C109—C110—C111	111.1 (5)
C7—C8—O23	129.3 (5)	N114—C110—C111	111.4 (4)
C7—C8—C9	106.6 (5)	C109—C110—C121	115.9 (4)
O23—C8—C9	124.2 (5)	N114—C110—C121	104.8 (5)
C8—C9—N1	103.2 (4)	C111—C110—C121	111.2 (4)
C8—C9—C10	115.8 (4)	C110—C111—C112	112.5 (5)
N1—C9—C10	113.8 (4)	C110—C111—H1111	108.2
C8—C9—C25	110.2 (4)	C112—C111—H1111	110.7
N1—C9—C25	114.1 (4)	C110—C111—H1112	106.8
C10—C9—C25	100.2 (4)	C112—C111—H1112	109.3
C9—C10—N14	100.8 (4)	H1111—C111—H1112	109.3
C9—C10—C11	110.2 (4)	C111—C112—C113	123.4 (5)
N14—C10—C11	111.5 (4)	C111—C112—H1121	117.4
C9—C10—C21	115.6 (4)	C113—C112—H1121	119.2
N14—C10—C21	104.7 (4)	N101—C113—C112	122.9 (5)
C11—C10—C21	113.3 (4)	N101—C113—H1131	117.2
C10—C11—C12	113.6 (4)	C112—C113—H1131	120.0
C10—C11—H111	108.5	N114—C115—C116	129.5 (5)
C12—C11—H111	110.1	N114—C115—C120	111.3 (5)
C10—C11—H112	106.5	C116—C115—C120	119.1 (6)
C12—C11—H112	109.4	C115—C116—C117	117.1 (6)
H111—C11—H112	108.6	C115—C116—H1161	120.4
C11—C12—C13	124.7 (5)	C117—C116—H1161	122.4
C11—C12—H121	117.5	C116—C117—C118	123.6 (6)
C13—C12—H121	117.8	C116—C117—H1171	118.7
N1—C13—C12	121.2 (5)	C118—C117—H1171	117.7
N1—C13—H131	118.1	C117—C118—C119	119.0 (7)
C12—C13—H131	120.7	C117—C118—H1181	120.5
N14—C15—C16	127.6 (6)	C119—C118—H1181	120.4
N14—C15—C20	112.4 (5)	C118—C119—C120	118.8 (7)
C16—C15—C20	120.0 (6)	C118—C119—H1191	120.8
C15—C16—C17	117.1 (7)	C120—C119—H1191	120.4
C15—C16—H161	121.1	C115—C120—C119	122.2 (5)
C17—C16—H161	121.8	C115—C120—C121	108.1 (5)
C16—C17—C18	122.7 (7)	C119—C120—C121	129.7 (5)
C16—C17—H171	118.9	C110—C121—C120	105.9 (4)
C18—C17—H171	118.4	C110—C121—O122	125.0 (5)
C17—C18—C19	120.6 (7)	C120—C121—O122	129.0 (5)
C17—C18—H181	119.4	N114—C124—C125	104.3 (4)
C19—C18—H181	120.0	N114—C124—H1241	110.2
C18—C19—C20	118.1 (7)	C125—C124—H1241	109.4
C18—C19—H191	120.9	N114—C124—H1242	111.4
C20—C19—H191	121.0	C125—C124—H1242	111.5
C19—C20—C15	121.3 (6)	H1241—C124—H1242	109.9
C19—C20—C21	130.9 (6)	C124—C125—C109	102.3 (4)
C15—C20—C21	107.7 (5)	C124—C125—C126	122.3 (7)
C10—C21—C20	106.0 (4)	C109—C125—C126	112.9 (10)
C10—C21—O22	124.0 (5)	C124—C125—C226	107.2 (15)
C20—C21—O22	130.0 (5)	C109—C125—C226	121 (2)
N14—C24—C25	104.5 (4)	C124—C125—H1251	106.1

C25—C24—H241	110.8	C126—C125—H1251	106.0
N14—C24—H242	111.2	C124—C125—H1252	108.5
C25—C24—H242	109.3	C109—C125—H1252	108.5
H241—C24—H242	108.9	C226—C125—H1252	108.7
C24—C25—C9	102.9 (4)	C125—C126—C127	123.3 (11)
C24—C25—C26	115.8 (5)	C125—C126—H1261	118.4
C9—C25—C26	113.9 (4)	C127—C126—H1261	118.4
C24—C25—H251	109.7	C126—C127—H1271	119.9
C9—C25—H251	107.6	C126—C127—H1272	120.1
C26—C25—H251	106.8	H1271—C127—H1272	120.0
C25—C26—C27	122.8 (6)	C227—C226—H2261	119.8
C25—C26—H261	117.7	C226—C227—H2271	120.0
C27—C26—H261	119.4	C226—C227—H2272	120.0
C26—C27—H271	120.0	H2271—C227—H2272	120.0
C26—C27—H272	120.3		
O22—C21—C10—N14	177.2 (5)	C10—N14—C24—C25	−2.7 (6)
O22—C21—C10—C9	−73.0 (6)	C10—C9—N1—C13	32.6 (6)
O22—C21—C10—C11	55.4 (7)	C10—C9—C25—C24	41.3 (5)
O22—C21—C20—C15	177.7 (5)	C10—C9—C25—C26	167.4 (4)
O22—C21—C20—C19	0 (1)	C10—C11—C12—C13	−15.0 (8)
O23—C8—C7—C2	178.8 (5)	C10—C21—C20—C15	−3.7 (6)
O23—C8—C7—C6	2 (1)	C10—C21—C20—C19	179.0 (6)
O23—C8—C9—N1	179.9 (5)	C11—C10—N14—C15	129.2 (5)
O23—C8—C9—C10	−55.1 (7)	C11—C10—N14—C24	−88.1 (6)
O23—C8—C9—C25	57.7 (7)	C11—C10—C9—C25	75.8 (5)
O122—C121—C110—N114	176.5 (5)	C11—C10—C21—C20	−123.2 (5)
O122—C121—C110—C109	−72.2 (7)	C12—C11—C10—C21	−93.8 (6)
O122—C121—C110—C111	55.9 (7)	C13—N1—C9—C25	−81.6 (6)
O122—C121—C120—C115	179.1 (5)	C15—N14—C10—C21	6.3 (5)
O122—C121—C120—C119	−1 (1)	C15—N14—C24—C25	132.3 (5)
O123—C108—C107—C102	178.9 (5)	C15—C16—C17—C18	1 (1)
O123—C108—C107—C106	2 (1)	C15—C20—C19—C18	−1.7 (9)
O123—C108—C109—N101	179.0 (5)	C16—C15—N14—C24	36.3 (9)
O123—C108—C109—C110	−56.8 (7)	C16—C15—C20—C19	4.1 (9)
O123—C108—C109—C125	55.8 (7)	C16—C15—C20—C21	−173.5 (5)
N1—C2—C3—C4	−179.7 (6)	C16—C17—C18—C19	1 (1)
N1—C2—C7—C6	−179.2 (5)	C17—C16—C15—C20	−3.7 (9)
N1—C2—C7—C8	3.4 (6)	C17—C18—C19—C20	−1 (1)
N1—C9—C8—C7	1.5 (5)	C18—C19—C20—C21	175.4 (6)
N1—C9—C10—N14	−164.2 (4)	C20—C15—N14—C24	−145.5 (5)
N1—C9—C10—C11	−46.4 (5)	C21—C10—N14—C24	149.0 (4)
N1—C9—C10—C21	83.6 (5)	C21—C10—C9—C25	−154.2 (4)
N1—C9—C25—C24	163.4 (4)	C24—C25—C26—C27	−142.6 (6)
N1—C9—C25—C26	−70.6 (6)	C102—N101—C109—C108	1.5 (5)
N1—C13—C12—C11	−1.8 (9)	C102—N101—C109—C110	−124.0 (5)
N14—C10—C9—C8	76.4 (5)	C102—N101—C109—C125	120.3 (5)
N14—C10—C9—C25	−42.0 (4)	C102—N101—C113—C112	144.3 (6)
N14—C10—C11—C12	148.3 (5)	C102—C103—C104—C105	−2.0 (9)
N14—C10—C21—C20	−1.5 (5)	C102—C107—C106—C105	−2.5 (9)
N14—C15—C16—C17	174.4 (6)	C102—C107—C108—C109	−3.6 (6)
N14—C15—C20—C19	−174.2 (5)	C103—C102—N101—C109	175.5 (5)
N14—C15—C20—C21	8.2 (6)	C103—C102—N101—C113	24.9 (8)
N14—C24—C25—C9	−24.7 (5)	C103—C102—C107—C106	2.6 (8)
N14—C24—C25—C26	−149.6 (5)	C103—C102—C107—C108	−174.8 (5)
N101—C102—C103—C104	−179.7 (5)	C103—C104—C105—C106	2 (1)
N101—C102—C107—C106	−177.9 (5)	C104—C103—C102—C107	−0.3 (8)
N101—C102—C107—C108	4.7 (6)	C104—C105—C106—C107	0 (1)
N101—C109—C108—C107	1.3 (5)	C105—C106—C107—C108	174.2 (6)

|			
N101—C109—C110—N114	−164.9 (4)	C106—C107—C108—C109	179.3 (5)
N101—C109—C110—C111	−46.1 (5)	C107—C102—N101—C109	−4.0 (6)
N101—C109—C110—C121	82.0 (5)	C107—C102—N101—C113	−154.6 (5)
N101—C109—C125—C124	163.9 (4)	C107—C108—C109—C110	125.5 (5)
N101—C109—C125—C126	−62.8 (9)	C107—C108—C109—C125	−121.9 (5)
N101—C109—C125—C226	−77 (2)	C108—C109—N101—C113	153.4 (4)
N101—C113—C112—C111	−0.6 (9)	C108—C109—C110—C111	−164.9 (4)
N114—C110—C109—C108	76.3 (5)	C108—C109—C110—C121	−36.8 (6)
N114—C110—C109—C125	−40.9 (5)	C108—C109—C125—C124	−80.5 (5)
N114—C110—C111—C112	154.5 (5)	C108—C109—C125—C126	52.8 (9)
N114—C110—C121—C120	−0.7 (5)	C108—C109—C125—C226	39 (2)
N114—C115—C116—C117	173.0 (6)	C109—N101—C113—C112	−3.7 (8)
N114—C115—C120—C119	−172.9 (5)	C109—C110—N114—C115	−115.9 (5)
N114—C115—C120—C121	7.4 (6)	C109—C110—N114—C124	26.2 (5)
N114—C124—C125—C109	−26.1 (5)	C109—C110—C111—C112	41.7 (6)
N114—C124—C125—C126	−154 (1)	C109—C110—C121—C120	110.6 (5)
N114—C124—C125—C226	−155 (2)	C109—C125—C126—C127	−126 (2)
C2—N1—C9—C8	0.4 (5)	C109—C125—C226—C227	109 (4)
C2—N1—C9—C10	−125.9 (4)	C110—N114—C115—C116	176.1 (6)
C2—N1—C9—C25	119.9 (5)	C110—N114—C115—C120	−8.0 (6)
C2—N1—C13—C12	147.6 (6)	C110—N114—C124—C125	0.1 (6)
C2—C3—C4—C5	−0.7 (9)	C110—C109—N101—C113	28.0 (6)
C2—C7—C6—C5	−1.3 (8)	C110—C109—C125—C124	41.3 (5)
C2—C7—C8—C9	−3.0 (6)	C110—C109—C125—C126	174.6 (8)
C3—C2—N1—C9	177.6 (5)	C110—C109—C125—C226	160 (2)
C3—C2—N1—C13	20.4 (9)	C110—C111—C112—C113	−19.8 (8)
C3—C2—C7—C6	0.8 (8)	C110—C121—C120—C115	−3.9 (6)
C3—C2—C7—C8	−176.6 (5)	C110—C121—C120—C119	176.5 (6)
C3—C4—C5—C6	0 (1)	C111—C110—N114—C115	125.6 (5)
C4—C3—C2—C7	0.2 (9)	C111—C110—N114—C124	−92.3 (5)
C4—C5—C6—C7	0.9 (9)	C111—C110—C109—C125	77.9 (5)
C5—C6—C7—C8	175.4 (6)	C111—C110—C121—C120	−121.3 (5)
C6—C7—C8—C9	180.0 (5)	C112—C111—C110—C121	−88.9 (6)
C7—C2—N1—C9	−2.4 (6)	C113—N101—C109—C125	−87.7 (6)
C7—C2—N1—C13	−159.5 (5)	C115—N114—C110—C121	5.1 (5)
C7—C8—C9—C10	126.6 (5)	C115—N114—C124—C125	135.1 (5)
C7—C8—C9—C25	−120.6 (5)	C115—C116—C117—C118	−0 (1)
C8—C9—N1—C13	159.0 (4)	C115—C120—C119—C118	−0.9 (9)
C8—C9—C10—C11	−165.7 (4)	C116—C115—N114—C124	40.2 (9)
C8—C9—C10—C21	−35.8 (6)	C116—C115—C120—C119	3.5 (8)
C8—C9—C25—C24	−81.2 (5)	C116—C115—C120—C121	−176.2 (5)
C8—C9—C25—C26	44.8 (6)	C116—C117—C118—C119	3 (1)
C9—N1—C13—C12	−7.6 (8)	C117—C116—C115—C120	−2.7 (9)
C9—C10—N14—C15	−114.0 (4)	C117—C118—C119—C120	−2 (1)
C9—C10—N14—C24	28.8 (5)	C118—C119—C120—C121	178.6 (6)
C9—C10—C11—C12	37.3 (6)	C120—C115—N114—C124	−143.9 (5)
C9—C10—C21—C20	108.3 (5)	C121—C110—N114—C124	147.2 (4)
C9—C25—C26—C27	98.5 (7)	C121—C110—C109—C125	−154.0 (4)
C10—N14—C15—C16	172.6 (5)	C124—C125—C126—C127	−4 (2)
C10—N14—C15—C20	−9.2 (6)	C124—C125—C226—C227	−134 (3)

Symmetry codes: (i) $x-1/2$, $-y+1/2$, z; (ii) $-x+1/2$, $y-1/2$, $z+1/2$; (iii) $x+1/2$, $-y+1/2$, z; (iv) x, $y+1$, z; (v) $x+1/2$, $-y+3/2$, z; (vi) $-x+1$, $-y+1$, $z+1/2$; (vii) $x-1/2$, $-y+3/2$, z.

9.3 Appendix 3: Images

Compound 243   Compound 248   Compound 249

Compound 250   Compound 251   Compound 254

Compound 265   Compound 266   Compound 267
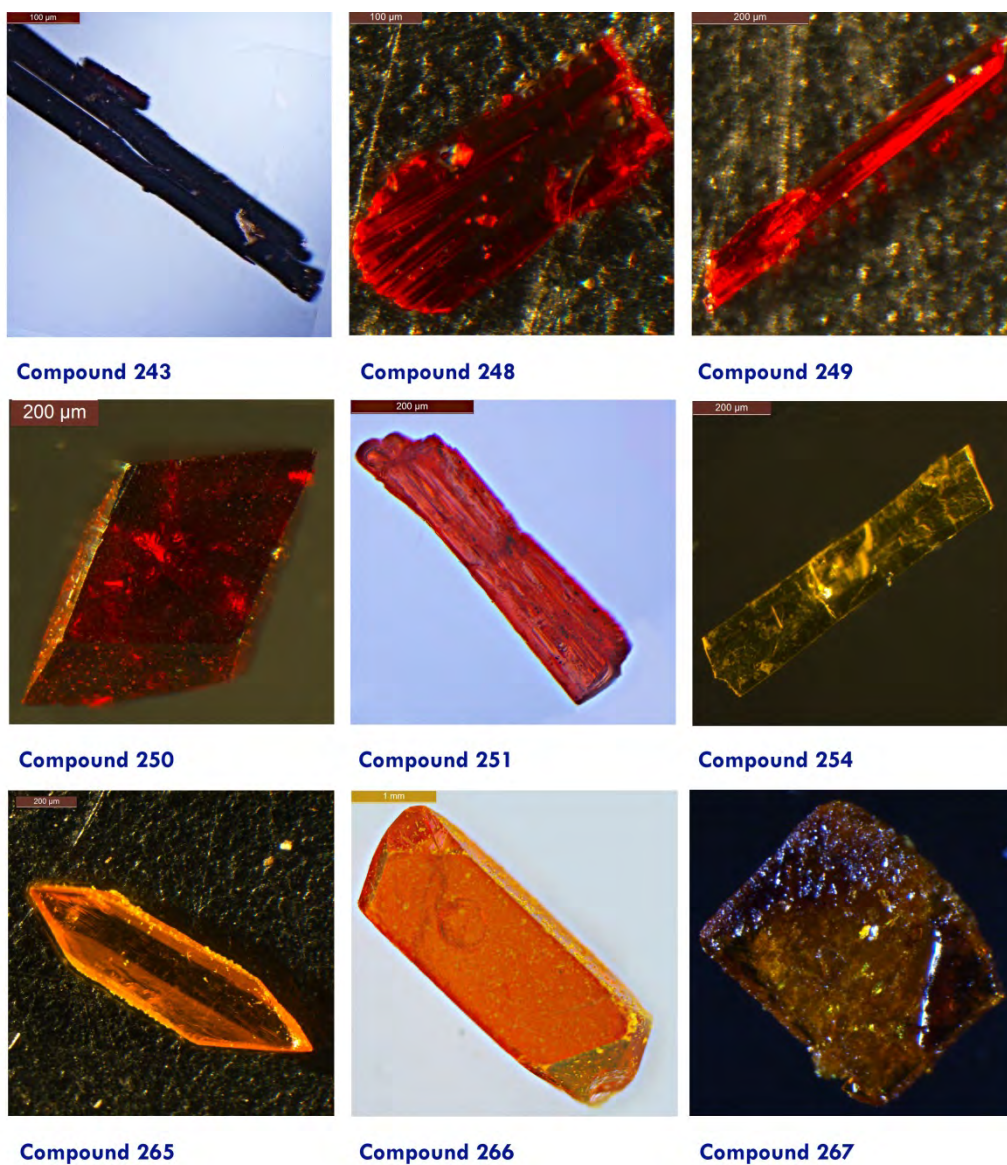
Figure 174: Microscopic photos of the X-ray crystals captured by Leica MZ 16 A stereo microscope.

A   B   C
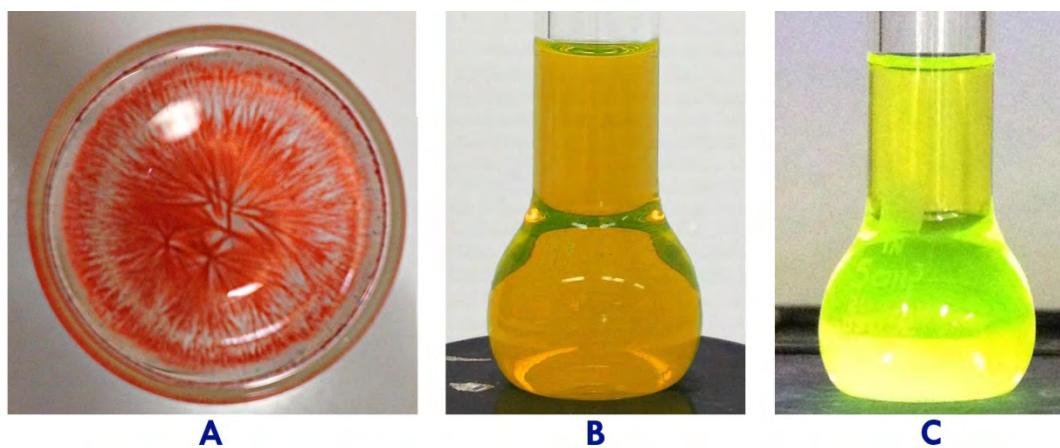
Figure 175: Hydroxyazepino **252**, crystals (A), solution in CH_2Cl_2 under the visible light (B) and the UV light (C).

Figure 176: Fluorescent emission of naphtiridine **266** (left) and **267** (right).